Dual-mode cholinesterase inhibitors targeting muscarinic receptors

Dissertation

zur

Erlangung des Doktorgrades (Dr. rer. nat.)

der Mathematisch-Naturwissenschaftlichen Fakultät

der Rheinischen Friedrich-Wilhelms-Universität

vorgelegt von

Paul Wilhelm Elsinghorst

aus

Lengerich (Westfalen)

Bonn, October 2006

This thesis was prepared with permission of the Faculty of Mathematics and Science at the University of Bonn.

It has been published electronically at http://hss.ulb.uni-bonn.de/diss_online in 2007.

1. Referee: Prof. Dr. Michael Gütschow
2. Referee: Priv.-Doz. Dr. Daniela Gündisch

Oral examination: 26.01.2007

Science cannot solve the ultimate mystery of nature. And that is because, in the last analysis, we ourselves are part of the mystery that we are trying to solve.

Max Planck

To Julia, for her patience and unfailing support.

Contents

Abbreviations

Aβ	amyloid β
A1E	(5R)-5-((10-(1,2,3,4-tetrahydroacridin-9-ylamino)decyl)amino)-5,6,7,8-tetrahydroquinolin-2(1*H*)-one
Ac	acetyl
ACh	acetylcholine
AChE	acetylcholinesterase
AICD	APP intracellular domain
APH-1	presenilin enhancer 1
APP	amyloid β precursor protein
ASCh	acetylthiocholine
BACE	β-site APP cleaving enzyme
BChE	butyrylcholinesterase
bmim	1-butyl-3-methylimidazolium
Bn	benzyl
Boc	*tert*-butyloxycarbonyl
BSCh	butyrylthiocholine
Bu	butyl
Bz	benzoyl
ColQ	collagene queue
CTF	carboxy-terminal fragment
DCM	dichloromethane
DIEA	*N,N*-diisopropylethylamine
DMF	*N,N*-dimethylformamide
DPPA	diphenylphosphoryl azide
DTNB	5,5'-dithiobis-(2-nitrobenzoic acid)
e.g.	for example (exempli gratia)
EC	enzyme code
Ee	Electrophorus electricus
emim	1-ethyl-3-methylimidazolium
eq.	molar equivalents
Et	ethyl
et al.	and coworkers (et alii)
FCA	Friedel-Crafts acylation
gallamine triethiodide	2-(2,3-bis(2-triethylammonioethoxy)phenoxy)ethyl-*N,N,N*-triethyl-ammonium triiodide
GPCR	G protein-coupled receptor
GPI	glycosylphosphatidylinositol
GSK-3	glycogen synthase kinase-3
Hs	Homo sapiens
i.e.	that is (id est)
ICD	intracellular domain
mAChR	muscarinic acetylcholine receptor
Me	methyl
MNB	5-mercapto-2-nitrobenzoic acid

mRNA	messenger ribonucleic acid
nAChR	nicotinic acetylcholine receptor
NCT	nicastrin
NMM	*N*-methylmorpholine
NMR	nuclear magnetic resonance
[³H]NMS	tritiated *N*-methyl scopolamine
NTF	amino-terminal fragment
OXC	oxalylchloride
PAS	peripheral anionic site
PEN-2	presenilin enhancer 2
Ph	phenyl
PHF	paired helical filaments
PRAD	proline rich attachment domain
PRiMA	proline rich membrane anchor
PS1	presenilin 1
PS2	presenilin 2
Py	pyridine
RMSD	root mean square deviation
RP	reversed phase
SCh	thiocholine
SEM	standard error of the mean
tacrine	9-amino-1,2,3,4-tetrahydroacridine
Tc	Torpedo californica
THF	tetrahydrofurane
TMD	transmembrane domain

1 Introduction

1.1 Alzheimer's disease

Historical outline

It was in 1906 that the psychiatrist Alois Alzheimer defined for the first time the clinico-pathological syndrome that was later on called Alzheimer's disease. Looking at his patient, Auguste D., a woman in her early 50s, Alzheimer described her symptoms as a rare dementia occuring in a presenile period, *i.e.* before the age of 65. Neither he nor his colleagues recognized the disorder to be indistinguishable from the commonly known senile dementia. Alzheimer already exemplified several symptomatic hallmarks of the disorder, that are still observed in most patients today: a progressive memory impairment, a disordered cognitive function, an altered behavior including paranoia, delusions and loss of social appropriateness and, finally, a progressive decline in language function[1]. It was not until the 1960s that the development of electron microscopy led to the discovery of those striking histological changes underlying this disorder: neuritic plaques and neurofibrillary tangles. Their formation was further clarified during the mid 1970s, as neurons synthesizing and releasing acetylcholine were found to undergo variable but usually severe degeneration. The observations leading to this concerned those enzymes directly connected to acetylcholine. A decrease in amount and activity of cholin acetyltransferase and its opponent acetylcholinesterase in the limbic and cerebral cortices was associated with a loss of cholinergic neurons in those subcortical nuclei projecting there. Hence the pharmacological research focused mainly on attempts to elevate the levels of acetylcholine in the synaptic cleft, primarily by inhibiting its degradation by acetylcholinesterase. These efforts finally led to those compounds that are used today for the symptomatic treatment of Alzheimer's disease: tacrine (Cognex[R]), donepezil (Aricept[R]), rivastigmine (Exelon[R]) and galanthamine (Razadyne[R]).

Neuritic plaques

Biochemical and immunohistochemical methods were subsequently applied to investigate the plaques observed *post mortem*. They were found to contain extracellular deposits of amyloid β peptides (Aβ) that usually occur in star-shaped clusters of amyloid fibrils. These amyloid β peptides differ with respect to their C-termini and thus in overall length. Prominent representatives are Aβ1-40 and Aβ1-42, the main subjective of recent research. Using supersaturated solutions of the model peptides Aβ26-40 and Aβ26-42 it was found that Aβ26-42 was prone to crystallize, while Aβ26-40 was stable within solution[2]. This led to the hypothesis, that Aβ1-42 could seed the aggregation of Aβ1-40 *in vivo.* As selective antibodies became available for Aβ1-40 and Aβ1-42, two types of plaques were identified, that had already been distinguished by classical staining. Diffuse plaques, also called preamyloid, were found throughout the brain consisting solely of Aβ1-42, while the former senile plaques comprised both Aβ peptides[3]. The common precursor of the Aβ-peptides, the amyloid β precursor protein (APP) is encoded on chromosome 21. Patients suffering from trisomy 21 (Down's syndrome) show histological changes related to those in patients with Alzheimer's disease, as the APP overexpression leads to raised levels of Aβ peptides. In a histological study[4] of brain tissue from 29 patients affected by trisomy 21 it was found, that a stable level of diffuse, Aβ1-42 containing plaques was already established at the age of 12. Until the age of 29 no neuritic plaques were observed, though a steady increase was seen from there on. Obviously, this cannot be directly transferred to patients with Alzheimer's disease, but there is a physiological occurrence of Aβ peptides and Aβ1-42 will trigger the aggregation of Aβ1-40 once a critical concentration has been reached.
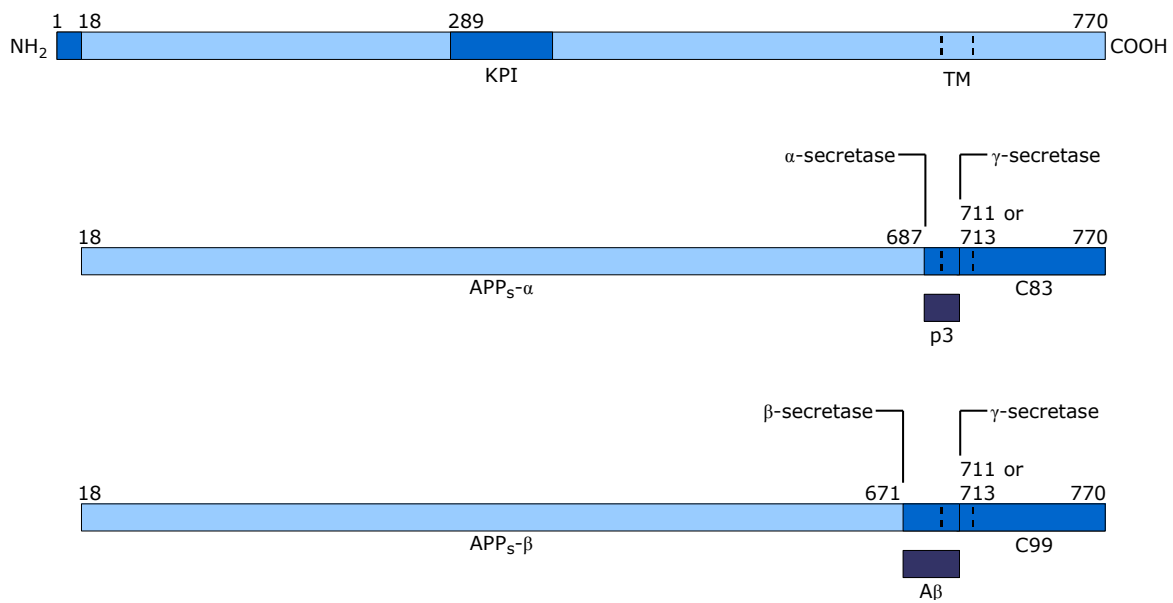
Figure 1: Metabolic processing of the amyloid β precursor protein (APPₛ-α/APPₛ-β = soluble APP fragments, TM = transmembrane domain, KPI = Kunitz-type serine protease inhibitor domain).

Neurofibrillary tangles

Next to neuritic plaques another histological symptom is often observed with patients suffering from Alzheimer's disease. The formation of neurofibrillary tangles, also called paired helical filaments (PHF), is not necessarily linked to the occurrence of neuritic plaques, but in most cases both of them are observed. These tangles were found to consist of the τ protein, physiologically associated with microtubules[5]. The τ protein promotes the assembly of tubulin into microtubules and maintains the microtubule structure. It is a phosphoprotein and precisely regulated by its degree of phosphorylation. An abnormal hyperphosphorylation forces the τ protein to detach from the microtubules into the cytosol. Reaching critical concentration it polymerizes into PHF[6]. Various kinases have been shown to be capable of phosphorylating τ at various sites, but during the last ten years a major focus has been on glycogen synthase kinase-3 (GSK-3)[7,8].

APP – the amyloid β precursor protein

As mentioned above APP is the precursor protein of Aβ. APP is an ubiquitously expressed polypeptide with a molecular weight of 100 to 140 kDa resulting from alternative splicing and posttranslational modifications[1]. The predominant isoforms contain 770, 751 or 695 amino acids, depending on the inclusion of a 19 or 56 amino acid motif (KPI, Figure 1). This motif is homologous to the Kunitz-type serine protease inhibitors[9] indicating one of the physiological functions of APP: the KPI-containing forms of APP are found in human platelets, where they serve as inhibitors of factor XIa, a serine protease involved in the blood coagulation cascade. It was subsequently discovered that APP is a member of a large gene family, that was therefore called the amyloid precursor-like proteins, APLPs.

The APP leaves the endoplasmatic reticulum as a single transmembrane polypeptide guided by an 18 amino acid signal peptide as can be seen in Figure 1. Most of the APP is then subjected to proteolytic cleavage by α-secretase, leaving a 83-residue (C83) carboxy-terminal fragment anchored inside the membrane. Alternatively β-secretase may cleave a slightly smaller ectodomain fragment from APP leading to a 99-residue carboxy-terminal (C99) remnant. Both peptides remaining inside the membrane can be additionally cleaved by γ-secretase, either behind residue 711 or 713. The cleavage of C99 finally leads to Aβ1-40 and Aβ1-42 that were identified as major constituents of neuritic plaques.

β-secretase

In 1999, after almost 10 years of research, β-secretase was identified as a novel member of the pepsin family of aspartic proteases showing less than 30 % sequence identity with other human pepsin family members[13]. Following its enzymatic classification it was renamed BACE, standing for β-site APP cleaving enzyme, and the discovery of a second 64 % sequence homologue led to the two designations BACE-1 and BACE-2. Until today there is no evidence that BACE-2 is involved into APP processing and research related to Alzheimers' disease focusses on BACE-1. To prevent the formation of Aβ1-40 and Aβ1-42 research went for selective inhibitors of BACE-1. After first approaches towards peptidomimetic transition state inhibitors also nonpeptidic lead compounds were identified[14] (Figure 2).

γ-secretase

Opposed to β-secretase, the characterization of γ-secretase was a fairly tough case for the researchers involved. Because of its ability to catalyse proteolysis inside a hydrophobic environment, for example the cleavage of APP inside transmembrane region, it has attracted not only the interest of scientists involved in Alzheimer's disease, but also those with a general biological interest[15]. Though its identity remained enigmatic for a long time, genetic and biochemical studies revealed that γ-secretase is a complex of at least four integral membrane proteins: presenilin (PS1/2), nicastrin (NCT), presenilin enhancer 1 (APH-1) and presenilin enhancer 2 (PEN-2)[16].

The presenilin subunit can be either of two isoforms called PS1 or PS2, that are believed to include eight transmembrane domains (TMD). It is synthesized as a holoprotein and endoproteolytically split between TMD6 and TMD7 into a carboxy-terminal (CTF) and an amino-terminal fragment (NTF), that remain physically associated[15] (Figure 3). The heterodimer of the NTF and CTF acts as an aspartyl protease with the two aspartic residues needed for catalysis located opposed on TMD6 and TMD7. Next to presenilin three other proteins were found inside the γ-secretase complex, but little is knwon so far about their function. Nicastrin, a type I transmembrane glycoprotein that is heavily glycosylated during protein maturation, is thought to be involved in substrate recognition. The γ-secretase cleaves substrates of less than 50 amino acids very efficiently and it is suggested that the glycosylated ectodomain of the associated NCT functions as a molecular ruler for substrate length. Almost none is known about APH-1 and PEN-2, except for their necessity that was demonstrated in several knockout experiments.

Not onyl for β-secretase, but also for γ-secretase, inhibitors were developed as potential drug targets for Alzheimer's disease. Looking at the γ-secretase complex one has to keep in mind that it does not solely catalyse the cleavage of APP,
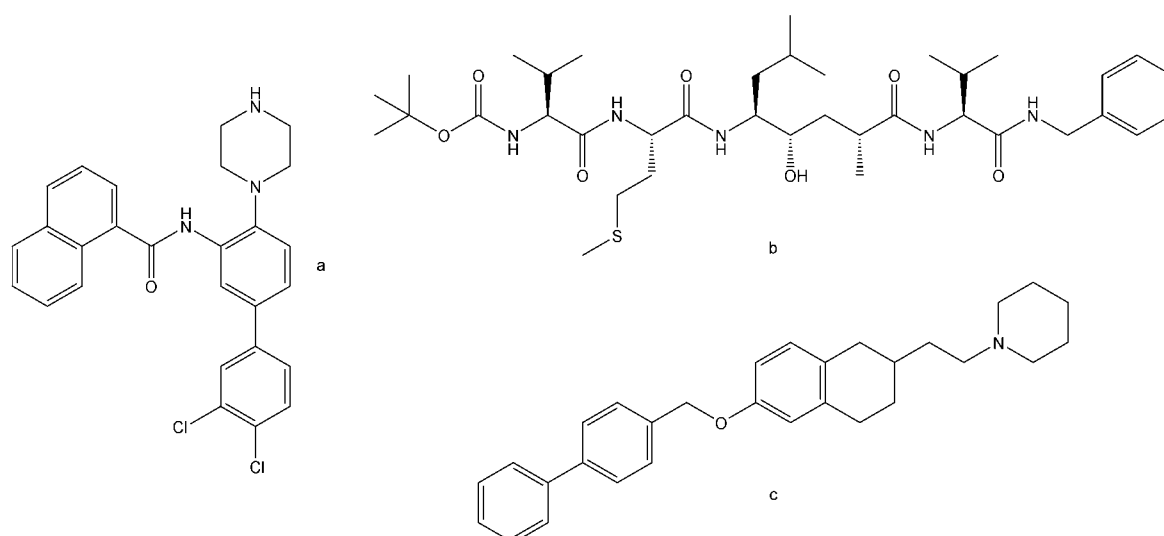
Figure 2: BACE-1 inhibitors: a) $IC_{50} < 3\,\mu M$[10], b) $IC_{50} = 2.5\,nM$[11], c) $IC_{50} = 349\,nM$[12].
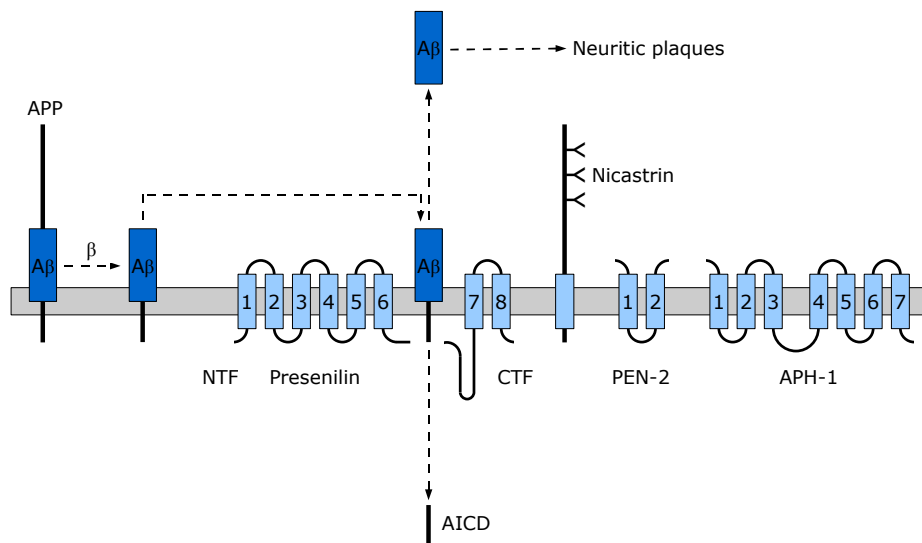
Figure 3: γ-secretase complex: APP is processed by β-secretase and subsequently forwarded to the γ-secretase complex where it is cleaved by the presenilin subunit.

but is also involved in the prosessing of several other transmembrane proteins, like Notch-1 and CD44. It was found that their intracellular domains (ICD) translocate to the nucleus after cleavage by γ-secretase and act as transcription factors of their corresponding target genes[17]. Thus it will be a challenging task to find a therapeutic window for Aβ1-42 reduction maintaining sufficient ICD generation to avoid side effects.

1.2 Cholinesterases

The cholinesterases are characterized according to their specifity for substrates and inhibitors. At first, acetylcholinesterase will be discussed, followed by butyrylcholinesterase. mRNA processing, that leads to different isoforms, and possible oligomers formed subsequently apply likewise to both cholinesterases.

Acetylcholinesterase

Signal transmission at the synaptical cleft and the neuromuscular junction relies particularly on acetylcholine. Emitted at the presynaptic neuron acetylcholine crosses the synaptic cleft to reach postsynaptic acetylcholine receptors which will be illustrated later on. The essential termination of excitation is accomplished by acetylcholinesterase, an enzyme that catalyses the hydrolysis of acetylcholine into acetic acid and choline. Vertebrate acetylcholinesterase (AChE, EC 3.1.1.7) is encoded on a single gene, but alternative splicing leads to a variety of isoforms with distinct properties. The different nomenclatures that have gradually evolved can be summarized as follows.

With respect to their carboxy-terminals, that are responsible for the final localization, a *synaptic* (AChE-S), an *erythrocytic* (AChE-E) and a so called *readthrough* acetylcholinesterase (AChE-R) were identified[19] (Figure 4). The latter refers to a hypothetical splicing form, keeping the intronic region that follows the exon encoding the catalytic domain. The corresponding enzyme is monomeric and thus soluble, but it is only observed following stress situations. These stress situations, *e.g.* exposure to AChE inhibitors or pathophysiological conditions like *Myasthenia gravis*[20], lead to a shift in the splicing pattern from AChE-S to AChE-R. Unfortunately the AChE-S term is sometimes misleadingly used to refer to a soluble isoform, that has to be carefully distinguished from the synaptic isoform. This sol-

uble form is found in several snake venoms, but little is known so far about its specific function in poisoning.

While this nomenclature is based on a more genetic perspective, there is also a way to classify the different isoforms on a protein basis. Following this, one distinguishes between *hydrophobic* (AChE-H) and so called *tailed* isoforms (AChE-T). The inclusion of the hydrophobic subunit leads to a carboxy-terminal region, called the H peptide, that contains three distinct elements. One or two cysteine residues that cause dimerization by disulfide bonds, a sequence encoding for the addition of a glycosylphosphatidylinositol (GPI) anchor and an appropiate ω cleavage site[21]. This ω cleavage site is used to introduce the ethanolamine moiety that connects AChE to GPI. Alternatively, another subunit may be inserted by alternative splicing which results in a so called T peptide. This T peptide refers to the *tail* that comprises again a cysteine and additionally a series of conserved aromatic residues. While the cysteine is needed for disulfide bonds to form AChE di- or tetramers, the conserved aromatic residues allow the binding to a so called *proline rich attachment domain* (PRAD). This PRAD is either part of a special collagen type, ColQ, or a hydrophobic protein, PRiMA. These quaternary interactions may lead either to globular (G1, G2, G4) or asymmetric (A4, A8, A12) associates, the trailing number indicating the number of catalytic subunits (Figure 4).

Referring to physiological properties that do not rest upon acetylcholine hydrolysis, several *non-classical* functions of acetylcholinesterase have been investigated. It was shown that AChE is involved in development and maintenance of the synaptic cleft[22], the bone matrix[23] and the formation of AChE-R modulates haematopoesis[24]. Most important with respect to Alzheimer's disease is the ability of acetylcholinesterase to promote the formation of Aβ-peptides. This feature of AChE is linked to the *peripheral* binding site (PAS), as can be concluded from AChE inhibitors binding to the PAS, that can significantly reduce the Aβ-peptide aggregation[25]. Additionally, it has been shown that the complexes formed by AChE and Aβ-peptides exhibit enhanced neurotoxicity compared to fibrils containing solely Aβ[26].

Butyrylcholinesterase

Butyrylcholinesterase (BChE, EC 3.1.1.8), sometimes also referred to as pseudocholinesterase, is a close relative of AChE, that lacks the substrate specifity for acetylcholine. BChE hydrolyses a variety of choline esters, like butyrylcholine,
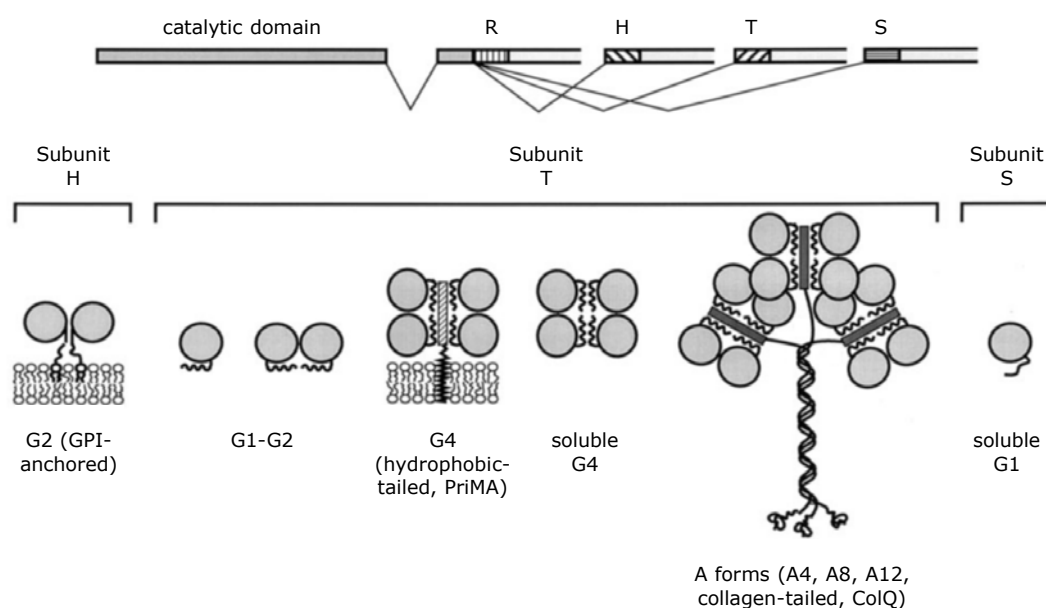
Figure 4: Alternative splicing leads to several cholinesterase isoforms (adapted from Massoulié *et al.*[18]).

acetylcholine and succinylcholine. It was succinylcholine, that brought BChE into the focus of anaesthesia, because BChE terminates its muscle-paralyzing effect and patients with unusual variants of BChE suffered from prolonged, life-threatening apnoea.

Initially most of the cholinesterase research, especially brain related investigations, was devoted to AChE, while BChE played a minor role. However recent findings related to Alzheimer's disease changed this view on BChE[27] and subsequently several functions of BChE have been proposed. Among these, a participation in neurite growth and Alzheimer's disease need to be mentioned. In contrast to the depletion of cholinergic neurons and the concurrent loss of acetylcholine and AChE, levels of BChE are significantly increased in association with neuritic plaques and neurofibrillary tangles.

Both cholinesterases are glycoproteins, but differ with respect to their degree of glycosylation. While human AChE incorporates three glycosylation sites[28], BChE has even nine[29] and the glycosylation pattern of both enzymes can differ depending on the tissue[30]. The high degree of glycosylation was the major impairment towards the final crystal structure of BChE[31] that was obtained more than ten years after the first AChE[32] structure.

Physiological occurence of cholinesterases

AChE and BChE do both exist in a water-soluble form that is secreted into various body fluids. Human plasma butyrylcholinesterase is certainly the most studied soluble form. 95 % of the plasma activity relates to BChE in G4 tetramers (Figure 4), that are believed to orginate from the liver. The plasma AChE is found to 54 % as G4 tetramers, while 44 % are in G1 or G2 state. It is suggested that the AChE tetramers are released from neuromuscular junctions or the central nervous system, the dimers might be liberated from erythrocytes. All oligomers of BChE and AChE are membrane bound before they are secreted into the blood. Based on the H peptide, the AChE G2 dimer is bound to a GPI, that anchors it inside the erythrocyte membrane. The membrane bound G4 tetramers of AChE and BChE are linked to the PRiMA, that fixates them to mammalian brain

cells, but differs entirely from the GPI[30]. The asymmetric oligomers of AChE and BChE, mainly the A12 associates, are the sole form observed at the neuromuscular junction. They differ with respect to their collagen tail and may even exist as mixed oligomers containing both enzymes AChE and BChE[35].

Catalytic mechanism

Both enzymes, acetylcholinesterase and butyrylcholinesterase, belong to the class of α/β-hydrolases representing a subfamily that carries a glutamate residue as part of the catalytic triade instead of an aspartate[36]. While the α/β-hydrolase fold refers to structural elements of the protein, the main emphasis in the following will be put on the catalytic mechanism and not the subsidiary protein backbone.

In Figure 5 I the *catalytic triade* of both cholinesterases is shown as a charge-relay system of $Ser^{203/198}$, $His^{447/438}$ and $Glu^{334/325}$ (numbering: HsAChE/HsBChE)[37,38]. The *charge relay* describes the catalytic function of the histidine imidazole, that easily abstracts a proton from the serine side chain hydroxyl. The additional electron relay from the adjacent glutamate onto the serine hydroxyl oxygen turns it into a nucleophil, that readily attacks the ester carbonyl of a suitable substrate, *e.g.* acetyl- or butyrylcholine.

This nucleophilic attack results in a tetrahedral transition state that is stabilized by three backbone amide nitrogens as depicted in Figure 5 II. The moiety formed by two glycines and one alanine is therefore refered to as the *oxyanion hole*. This three-pronged oxyanion hole is another remarkable difference to most other serine and cysteine proteases, that use only two hydrogen bond donators to stabilize the transition state[39].

The release of choline leads to the intermediate stage of an acyl enzyme (Figure 5 III). This acyl enzyme is characterized through the acyl group that has been transferred onto the active site serine. The space requirement of this acyl residue is of vital importance towards the substrate selectivity of the cholinesterases. Figure 6 illustrates the so called acyl pocket of AChE and BChE, the moiety of the enzyme, that will host the substrate acyl group during hydrolysis. One can eas-
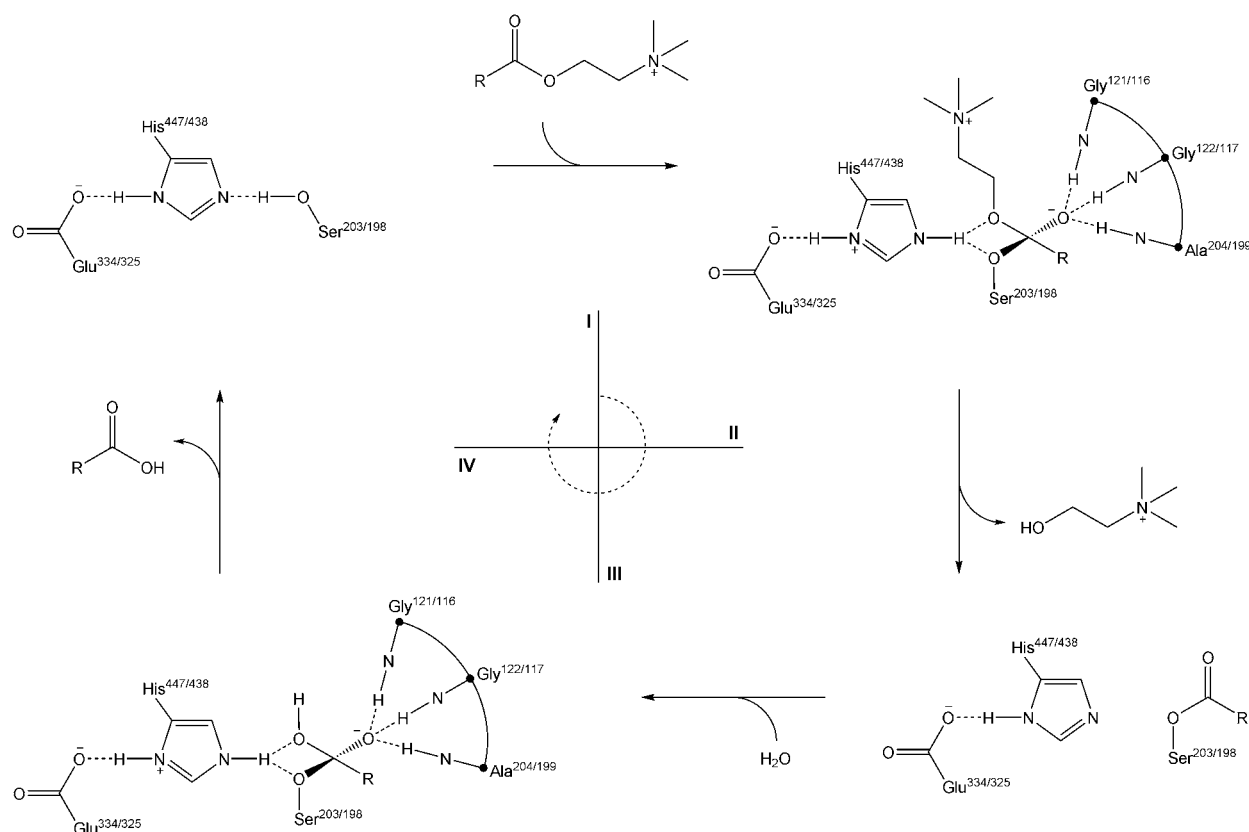
Figure 5: Catalytic mechanism of cholinesterases: residue numbers are given for AChE/BChE, R = methyl or butyl.

ily observe, that the acyl pocket of AChE offers considerably less space than the one of BChE. The AChE residues Phe[295] and Phe[297] are replaced by the aliphatic amino acids Leu[286] and Val[288] of BChE. This allows the accomodation of the bigger butyryl residue, whereas AChE ensures its substrate specifity towards the smaller acetyl function[40]. Final reactivation of the enzyme is accomplished through the nucleophilic attack of a water molecule (Figure 5 IV). Again a tetrahedral transition state is passed and the substrate

corresponding carboxylic acid is released to reestablish the catalytic triade. The remarkable activity of AChE with a turnover of 25000 molecules acetylcholine per second is not only due to this efficient mechanism of catalysis. AChE shows very high on- and off-rates for its substrate, which implies that the in and out of the substrate along the 20 Å deep gorge proceeds within very short time. Aromatic residues of the gorge and the anionic binding site at its bottom (Trp[84]) are thought to facilitate this entry[32]. On the other hand, this

a   b   c
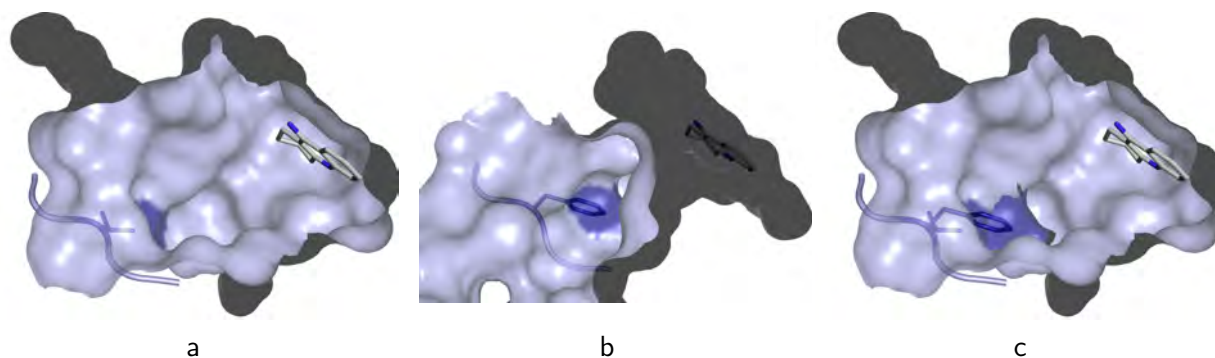
Figure 6: Active site and acyl pocket of human AChE[33] and BChE[34] with tacrine inserted for comparison: a) Val[288] (only two methyl groups are visible) ending the acyl pocket of BChE. b) Phe[297] forming the smaller acyl pocket of AChE. c) Size comparison of both acyl pockets.

would impair the exit of acetylcholine after hydrolysis and the existance of a *back door* was proposed[44]. This back door refers to a channel between the gorge bottom, *i.e.* Trp[84], and the outer surface located near Glu[445], that has been suggested by molecular docking studies[45].

Cholinesterase inhibitors

As pointed out in the beginning, two different strategies for the treatment of Alzheimer's disease have to be separated. Several approaches towards a causal therapy of Alzheimer's disease, *e.g.* β- and γ-secretase inhibitors, have been outlined above. The crucial point for a causal treatment of Alzheimer's disease remains the diagnosis. Only the early intervention can stop the formation of neuritic plaques and neurofibrillary tangles, that, if untreated, will lead to severe depletion of cholinergic neurons.

Supposing that diagnosis occurs at a point where a substantial loss of cholinergic neurons has already taken place, the treatment changes to a palliative strategy. The established *cholinergic hypothesis*[49] associates low levels of acetyl-

choline with cognitive, functional and behavioral symptoms experienced by patients suffering from Alzheimer's disease. The obvious drawback of this symptomatic treatment is that it does not stop the disease progress. Typically, improvements last only a short term (6 to 12 months) and only one third of the treated patients experiences long-term profits (1 to 4 years). Acetylcholinesterase inibition does not only relate to Alzheimer's disease. Reversible inhibitors like neostigmine, pyridostigmine or physostigmine are used to alleviate symptoms of Myasthenia gravis, glaucoma and for termination of paralysis. Irreversible inhibitors, especially organophosphates and -phosphonates, are widely used as insecticides and have been stockpiled as chemical warfare agents.

Both reversible and irreversible inhibitors (Figure 7) of cholinesterases target the catalytic serine residue. The reversible inhibitors comprise a group of carbamates, that lead to a carbamylation of $Ser^{203/198}$, that can subsequently be cleaved by the described mechanism (Figure 5). Because of the intermediate serine-carbamate being less prone to hydrolysis due to π-electron donation from its nitrogen, an actual cholinesterase inhib-

		IC$_{50}$ HsAChE [nM]	IC$_{50}$ HsBChE [nM]
a	rivastigmine	48000	54000
b	phenyletyhlnorcymserine	30000	6
c	soman	3	
d	dichlorvos	13	
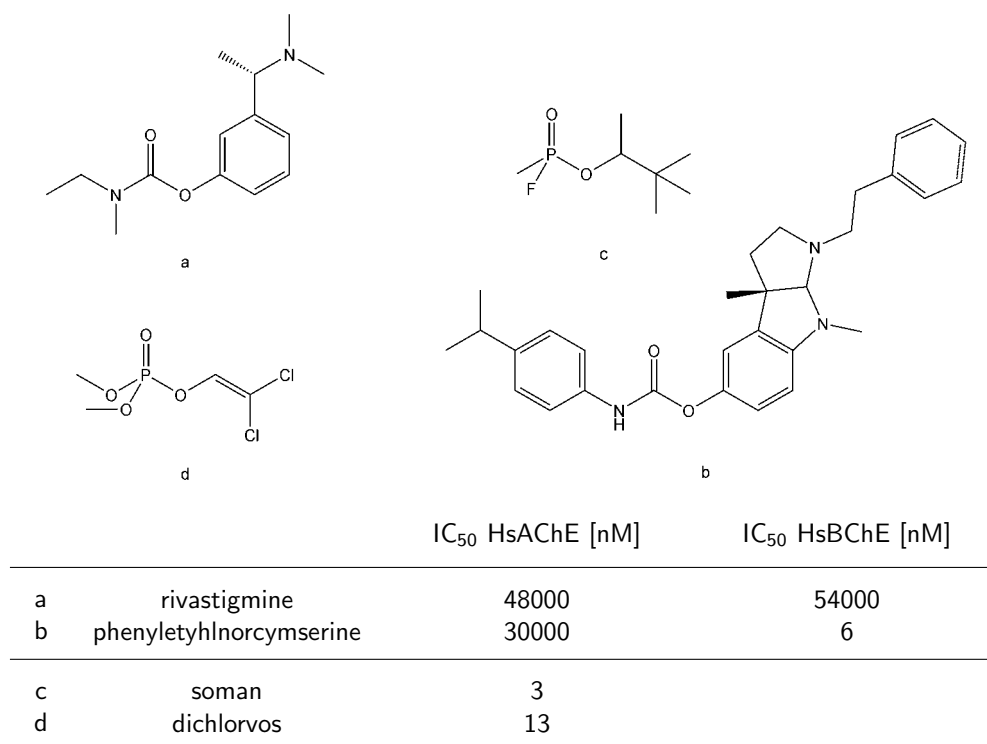
Figure 7: Irreversible and reversible cholinesterase inhibitors: rivastigmine, a drug for Alzheimer's disease; phenethylnorcymserine, a selective BChE inhibitor; soman, a nerve agent; dichlorvos, an important insecticide. IC$_{50}$ values: Yu *et al.*[41,42] and Erhard *et al.*[43].
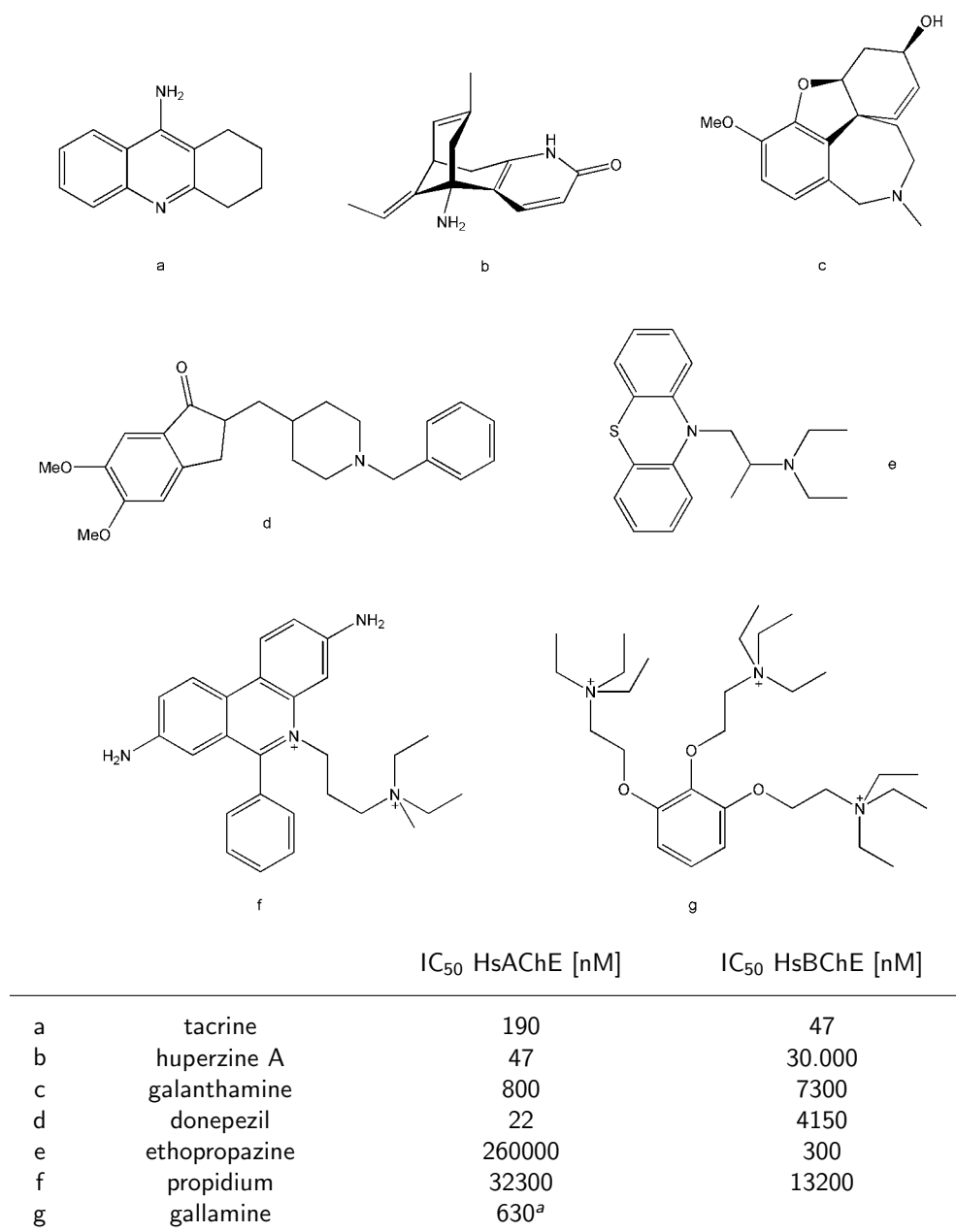
Figure 8: Competitive cholinesterase inhibitors. IC_{50} values: Yu *et al.*[42], Bolognesi *et al.*[46], Al-Jafari[47] and Giacobini[48]. *a*) Camel retina AChE

		IC_{50} HsAChE [nM]	IC_{50} HsBChE [nM]
a	tacrine	190	47
b	huperzine A	47	30.000
c	galanthamine	800	7300
d	donepezil	22	4150
e	ethopropazine	260000	300
f	propidium	32300	13200
g	gallamine	630[a]	

tion is observed. The irreversible inhibitors lead to a phosphorylation of the catalytic serine that cannot be reversed by the catalytic mechanism. Several antidotes, that are characterized by an oxime moiety, have been developed that facilitate its reactivation.

A variety of competitive inhibitors for both, acetyl- and butyrylcholinesterase, have been identified until know. Their classification relies on their specific binding site, where inhibitors that bind to the active site are distinguished from those, that are attracted to the peripheral bind-ing site or target both binding sites simultaneously. Three of the four AChE inhibitors approved for the treatment of Alzheimer's disease belong to the class of competitive inhibitors (Figure 8). Tacrine and galanthamine were found to bind to the active site, while donepezil was the first inhibitor to reach both, the active and the peripheral binding site. Recently also huperzine A, the active principle of the Chinese remedy *Huperzia serrata, Lycopodiaceae*, has been identified as an active site ligand of AChE. Selectivity towards butyrylcholinesterase is established by bulkier residues, that can only be accommodated

by its larger active site. Ethopropazine, an anti-dyskinetic, was found as a very selective active site inhibitor of BChE. Most of these inhibitors contain a basic nitrogen as part or close to a π-system, that anchors them at the anionic binding site by π-π or π-cation interactions. The peripheral binding site of AChE utilizes also π-π or π-cation interactions, whereas BChE is restricted to hydrophobic contacts at this point. Several ligands of the PAS have been identified, of which propidium and gallamine are depicted in Figure 8.

After the discovery, that the PAS of AChE is involved in Aβ-peptide aggregation[25], research went for compounds that would simultaneously bind to the active and peripheral binding site. These compounds were suggested to raise levels of acetylcholine by binding to the active site and to prevent Aβ-peptide aggregation by occupying the PAS. Most of these hybrid substances are based on at least one tacrine moiety (Figure 9) that is directed to the peripheral binding site. The PAS directed part of these dimers differs from
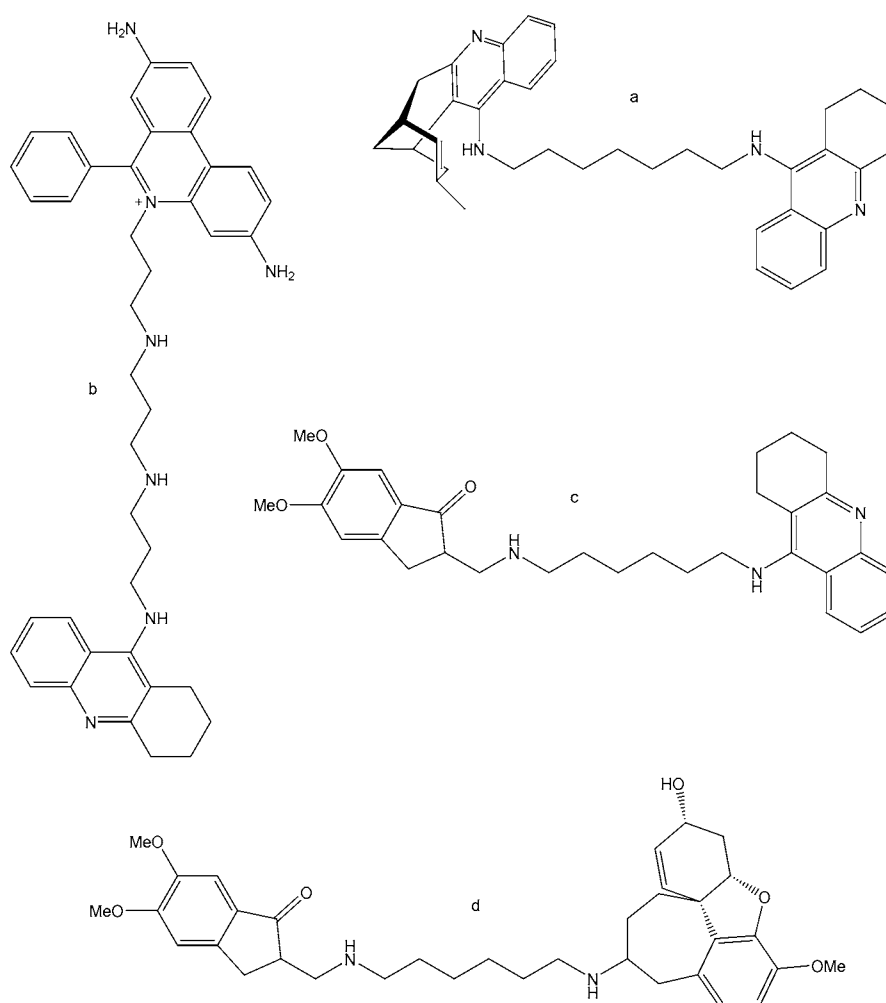
		IC$_{50}$ HsAChE [nM]	IC$_{50}$ HsBChE [nM]
a	tacrine-huprine	0.34	6.70
b	tacrine-propidium	1.55	63.7
c	tacrine-dimethoxyindanone	100	500
d	galanthamine-dimethoxyindanone	5.2	240

Figure 9: Hybrid inhibitors of cholinesterases. IC$_{50}$ values: Camps *et al.*[50], Bolognesi *et al.*[46], Martinez *et al.*[51] and Jordis *et al.*[52].

simply another tacrine to donepezil analogues or complex structures as huprine, a chimera derived from tacrine and huperzine A. The linker used to connect the two binding parts typically comprises a simple alkyl chain that can be interrupted by an additional amine function that facilitates mid-gorge interactions. In general these hybrid inhibitors show enhanced inhibition profiles compared to their contributing monomers. The an-

ticipated selectivity towards AChE due to π-π and π-cation interactions at the PAS was found for most of the hybrid inhibitors developed. Recently, a class of tacrine homodimers has been described that show surprising selectivity towards BChE[53] and gives rise to a more complex look on ligand interactions at cholinesterases. Particularly mid-gorge contacts of sophisticated linkers replacing simple alkyl tethers have gained special attention.

1.3 Acetylcholine receptors

Acetylcholine receptors are found throughout the human body where they mediate a variety nerve responses. They can be divided into two classes, the *nicotinic* and *muscarinic* acetylcholine receptors, their names being historically derived from those substances that were used to differentiate them, nicotine and muscarine.

Nicotinic acetylcholine receptors

The nicotinic acetylcholine receptors (nAChR) comprise a group of ligand-gated ion channels, that are responsible for nerve responses of rapid onset, short duration and generally, excitatory effect.

They consist of five subunits, each encoding a protein with four transmembrane domains, that are used to classify them. Divided into α and β subunits several of them have been located inside the human brain (α3, α4, α5 and α7; β2, β3, and β4). Of these at least three populations of receptors containing either α3, α4β2 or α7 nicotinic receptor subtypes are found in the cerebral cor-

tex. These three subtypes of nicotinic receptors appear to be reduced in Alzheimer's disease, although levels of the α4 subunit are reduced more extensively in the cortex of Alzheimer's disease patients[60].

Especially the α7 nicotinic receptor was found to be associated with Aβ1-42 in neuritic plaques of patients suffering from Alzheimer's disease[61]. It was shown that nicotinic ligands can suppress this association and that Aβ1-42 can actually inhibit the activation of α7 nicotinic receptors. This inhibition of activation may contribute to the neuronal degeneration observed with Alzheimer's disease[62].

Over the past several years, numerous nicotinic agonists have been identified with improved CNS activity and reduced propensity for interacting with peripheral nicotinic receptors located in the neuromuscular junction and the autonomic ganglia. During this research a main focus was put on the identification of compounds that lack the addictive properties of nicotine[60]. Figure 10 shows three compounds, that have been clinically investigated for the treatment of Alzheimer's dis-
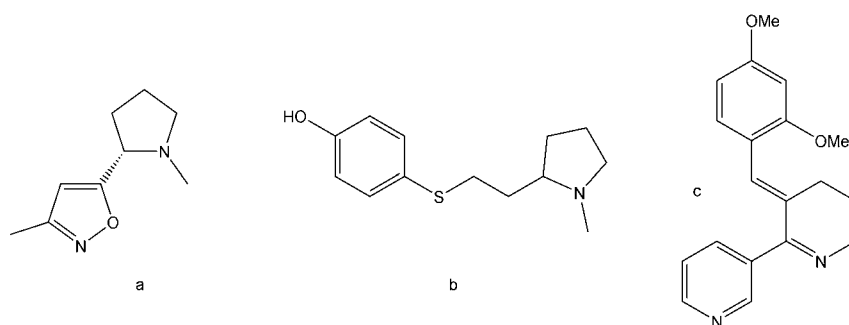
Figure 10: nAChR ligands in Alzheimer's disease: a) ABT-418[54], b) SIB-1553A[55], c) GTS-21[56].

ease. All of them were found to improve learning and memory in either rodents, primates or humans and to produce only little adverse effects. From their different selectivity patterns it was concluded, that the clinical utility of nicotinic agonists may depend on the development of compounds with enhanced activity and selectivity on $\alpha 7$ and $\beta 4$ containing nicotinic receptors[60].

Muscarinic acetylcholine receptors

The muscarinic acetylcholine receptors belong to the superfamily of G protein-coupled receptors (GPCR) and mediate nerve responses in the central and peripheral nervous system. In contrast to nAChR the muscarinic acetylcholine receptors mediate responses that are typically of slow onset, long duration and can be either excitatory or inhibitory.

Molecular cloning studies identified five muscarinic receptor subtypes (M_1-M_5 receptors), each of them displaying a unique amino acid sequence and tissue distribution. M_1 receptors are found in the central nervous system, especially in the cerebral cortex and hippocampus, and in the stomach where they mediate gastric acid secretion. M_2 receptors are autoreceptors in the brain, regulating acetylcholine release, and inhibit smooth muscle contraction, most notably in the heart. M_3 receptors are also found in the central nervous system and in smooth muscle and exocrine glands. M_4 receptors are found in the central nervous system, particularly in the neostriatum and in the spinal cord. Finally, M_5 receptors are found in dopamine neurons in the midbrain and in the cerebral blood vessels[60].

As many G protein-coupled receptors, also the muscarinic acetylcholine receptors are sensitive to allosteric modulation, where most of the allosteric modulators show a selectivity for the M_2 receptor. A closer look on the allosteric modulation reveales two classes of allosteric modulators, referred to as the *typical* like gallamine or the *atypcical* like tacrine (Figure 8), that differ with respect to the slope of their concentration-effect curves[63]. The identification of the allosteric binding sites on the M_2 receptor is a subject of ongoing research and has not been clarified until today[64].

Based on the localization of M_1 receptors in brain regions associated with learning and memory function, drug development efforts focused on the synthesis and biological characterization of M_1 agonists. Figure 11 shows four orthosteric ligands that have been clinically investigated for the treatment of Alzheimer's disease. Because of either lack in M_1 selectivity or their metabolism leading to dose-limiting side effects, all compounds were removed from clinical trial, except for CDD-0102. The high conservation of the orthosteric binding site throughout all mAChR subtypes may explain, why no M_1 selective agonist has been found yet.

Allosteric modulators might become a valuable alternative, as the allosteric binding sites of muscarinic acetylcholine receptors differ with respect to their amino acids. They might enhance or impair the binding of the endogeneous ligand acetylcholine (ACh) and thus regulate pathophysiological imbalances, *i.e.* an allosteric modulator might enhance the binding of ACh to M_1 receptors and improve cognitive functioning or it may impair binding of ACh to M_2 receptors and indirectly raise synaptical levels of ACh.

At this point it should also be mentioned that several non-cholinergic functions of muscarinic receptors have been discovered. It was found that
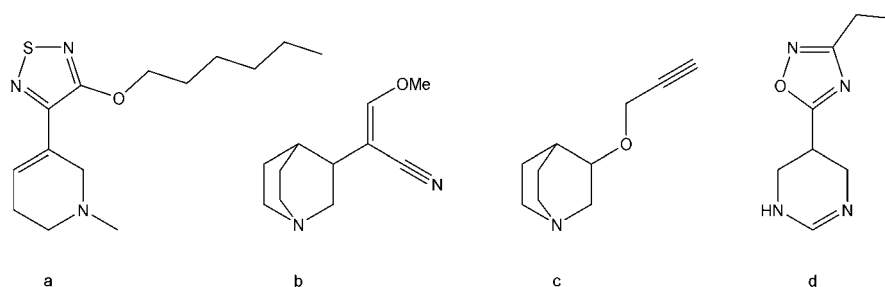
Figure 11: mAChR ligands in Alzheimer's disease: a) xanomeline[57], b) sabcomeline[58], c) talsaclidine[58], d) CDD-0102[59].

M_1 receptors promote α-secretase activity which results in the secretion of non-toxic peptide fragments of APP and thus decreased Aβ deposition. Muscarinic agonists may also have neuroprotective activity as they inhibit the hyperphosphorylation of τ proteins, a key component of neurofibrillary tangle formation in Alzheimers disease, thereby inhibiting apoptosis and promoting cell survival. Thus muscarinic agonists could be useful in preventing the formation of neuritic plaques and neurofibrillary tangles[60].

1.4 Objective of the dissertation

The aim of the presented studies was to establish a synthetic access to hybrid inhibitors of cholinesterases that comprise a gallamine and a tacrine moiety (Figure 12). The way towards these compounds was paved by preliminary investigations using a 3,4,5-trimethoxybenzene moiety representing gallamine and in some part also donepezil. The linker to be introduced was primarily selected because of chemical considerations and an incremental search was aspired to identify its optimal length. The inhibitory potential of the final compounds was to be determined by kinetic investigations based on an established assay. These findings were intended to be reinforced by profound molecular docking investigations following appropriate literature reports. Additionally these hybrid inhibitors were designed to act as allosteric modulators of muscarinic receptors, especially the M_2 receptor. Investigations of receptor binding though were beyond this dissertation and are reported to illustrate the versatile potential of these compounds.
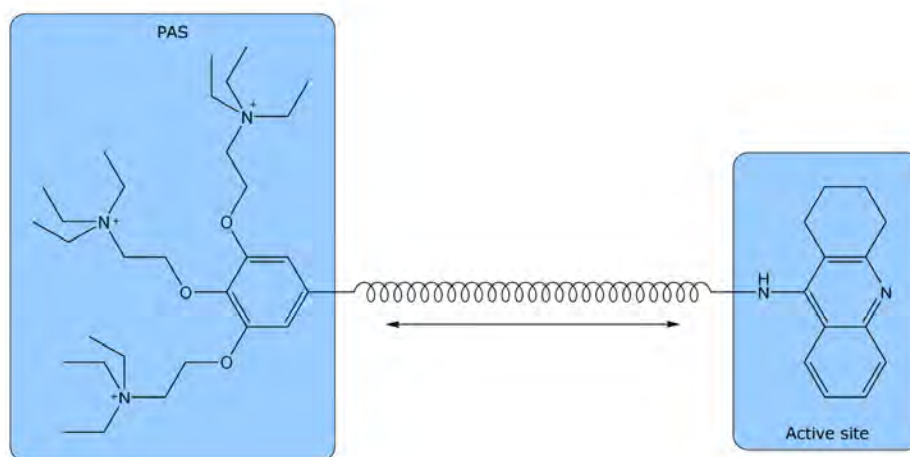
Figure 12: The target structures.

2 Synthesis

2.1 The tacrine moiety

Starting compound for the introduction of the tacrine moiety was 1,3,4,10-tetrahydro-9(2*H*)-acridinone (Scheme 1). To facilitate a nucleophilic substitution at C9 it was readily converted by phosphorus(V) oxychloride into 9-chloro-1,2,3,4-tetrahydroacridine (**1**) following the procedure of Michalson *et al.*[65]. The hydrazine analogue **4** of 9-amino-1,2,3,4-tetrahydroacridine was synthesized by subsequent reaction with aqueous hydrazine. The nucleophilic substitution still required high reaction temperatures and was therefore carried out in small glass reactors. Bielavsky[66] reported a synthesis of 9-hydrazino-1,2,3,4-tetrahydroacridine using phenol as a solvent and suggested an intermediate phenol ether to be the electrophilic species. Nevertheless the use of the less acidic ethanol, that would presumably not result in an intermediate ether, allowed the reaction to proceed and indicates that there is no ether formation required for the nucleophilic substitution. Both, the hydrochloride and the free base of the hydrazine analogue, proved to be very hygroscopic and sensitive to light. 6,9-Dichloro-1,2,3,4-tetrahydroacridine (**2**) was prepared by a Friedländer-type condensation of 2-amino-4-chloro-benzoic acid and cyclohexanone as described by Recanatini *et al.*[67].
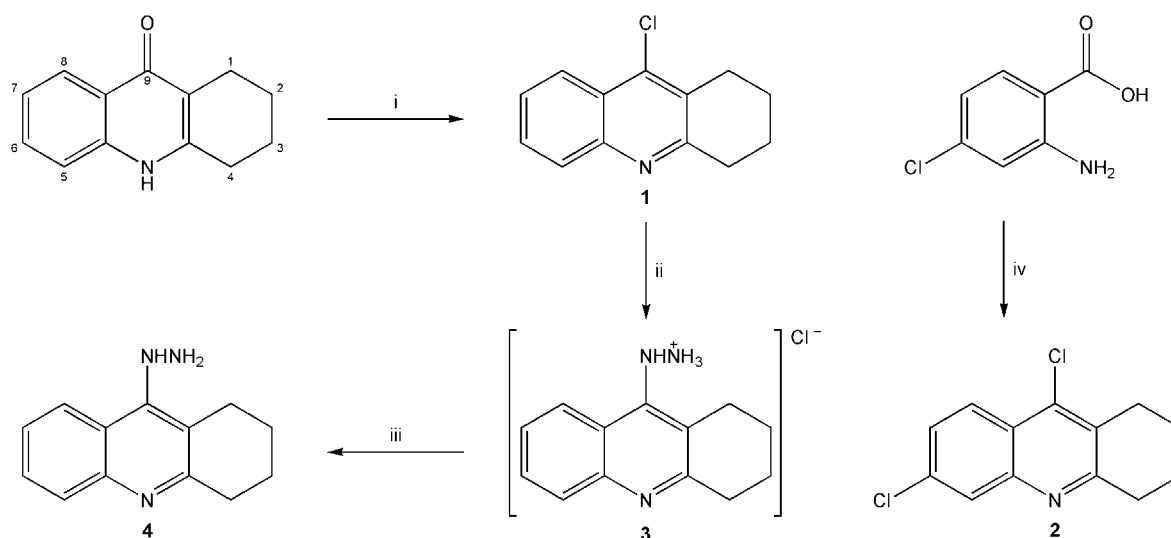
Scheme 1: Analogues of tacrine: i) POCl$_3$. ii) N$_2$H$_4$, EtOH. iii) NaOH, H$_2$O. iv) cyclohexanone, POCl$_3$.

2.2 The ω-aminocarboxylic acid precursors

Aminoacetic acid, 3-aminopropanoic acid and 4-aminobutanoic acid were purchased as hydrochlorides of the corresponding ethyl esters and were directly used in the following synthetic step. For the ω-amino analogues of pentanoic, hexanoic, heptanoic and octanoic acid the ω-aminocarboxylic acids were purchased and converted into the hydrochlorides of their ethyl esters. The synthesis is depicted in Scheme 2 and was carried out as follows. According to Temple
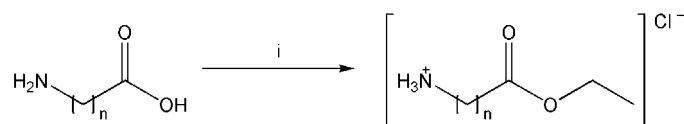
Scheme 2: Synthesis of ethyl ω-aminocarboxylic esters. n = 4-7
i) SOCl$_2$, EtOH.

et al.[68] 1.5 equivalents of thionyl chloride were added dropwise to anhydrous ethanol while stirring. The drop speed was kept at a level that keeps the ethanol at about room temperature. Subsequently, the ω-aminocarboxylic acids were added in portions and the reaction mixture was stirred over night. The solvent was removed by evaporation and the resulting foam was recrystallized from ethyl acetate. The hydrochlorides were collected by suction filtration in excellent yields and stored protected from moisture. Unfortunately, 9-aminononanoic acid was commercialy unavailable and in analogy to Leone-Bay *et*

al.[69] a synthesis towards ethyl 9-aminononanoate hydrochloride was considered. The first step of a four step sequence (Scheme 3) was the formation of ethyl 10-azido-10-oxodecanoate from the corresponding monoester using diphenylphosphoryl azide. Subsequent Curtius rearrangement gave ethyl 9-isocyanatononanoate that was directly reacted with *tert*-butanol to yield the Boc-protected ethyl 9-aminononanoate. Simple deprotection using hydrogen chloride in anhydrous ethyl acetate precipitated the target ethyl 9-aminononanoate hydrochloride that was recovered by suction filtration in good yield.
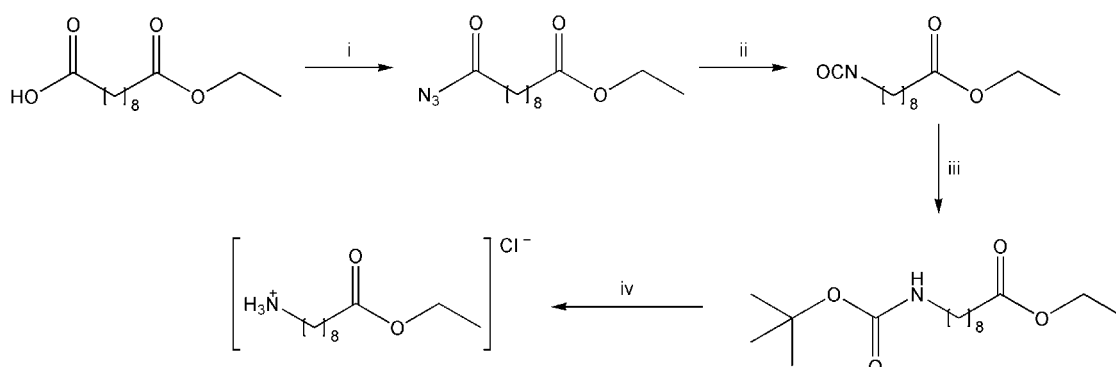
Scheme 3: Synthesis of ethyl 9-aminononanoate. i) DPPA, Et$_3$N, PhMe. ii) ΔT. iii) *tert*-BuOH. iv) HCl, EtOAc.

2.3 The donepezil-like compounds

The synthesis of the compounds containing a donepezil-derived moiety will be exemplified with the butanoic acid derivative. Differences from the standard procedure will be stated where applicable and the synthesis of the truncated homologues will be explained by the end of this section. First step of the multistep synthesis reported here was the activation of 3,4,5-trimethoxybenzoic or 3-(3,4,5-trimethoxyphenyl)propionic acid to facilitate the amide formation with ethyl 4-aminobutanoate giving **17** and **53**. At first the mixed-anhydride procedure known from peptide

chemistry was used but it soon became impractical. As depicted in Scheme 4 the carboxylic acid is first converted to the corresponding *iso*-butyl carbonate followed by regioselective attack of the ω-aminocarboxylic ester. The selectivity results from the reaction temperature of approximately -25 °C and the formation of carbon dioxide and *iso*-butanol. Alternatively, the classical activation as an acyl chloride, formed by oxalyl chloride, was applied and gave comparable results. To avoid the effort associated with low temperature chemistry the classical route was therefore estab-
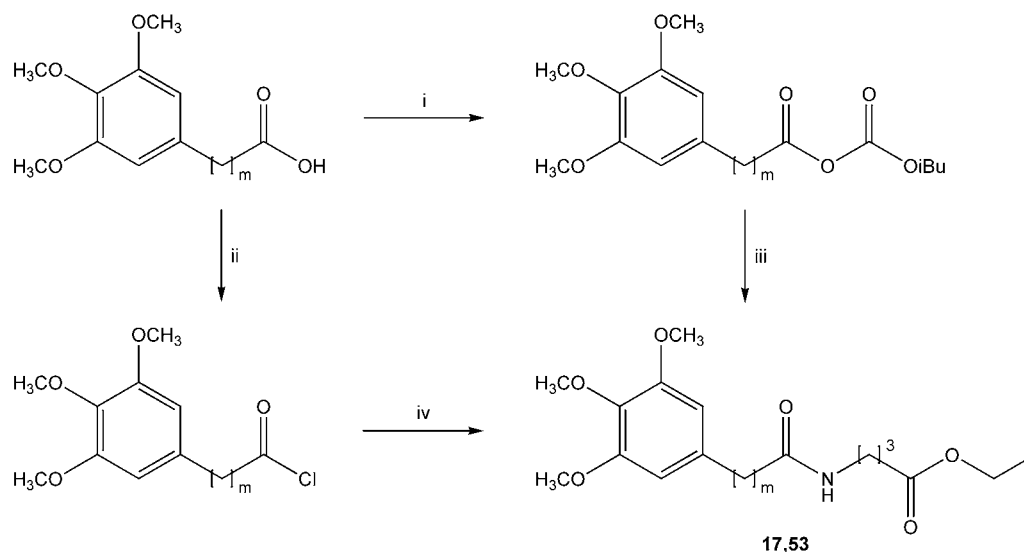
Scheme 4: Amide bond formation utilizing the mixed-anhydride or acyl chloride procedure. m = 0,2
i) isobutyl chloroformiate, NMM, THF. ii) OXC, DCM. iii) ethyl 4-aminobutanoate HCl,
DCM, DIEA. iv) ethyl 4-aminobutanoate HCl, DIEA, THF.

lished. During the next stage of synthesis it was attempted to couple the first step intermediates with the tacrine moiety utilizing the chemistry already established. Therefore the carboxylic esters **17** and **53** had to be hydrolized without cleaving the just formed amide bond (Scheme 5). Using diluted sulfuric acid in an acetone–water system was found to be the most convenient method to achieve selective ester cleavage. The thus obtained carboxylic acids **87** and **88** were again converted into their corresponding acyl chlorides

by reaction with oxalyl chloride. For testing purposes it was then tried to couple these acyl chlorides with 2-methyl-4-quinolinamine serving as a tacrine analogue. Unfortunately, workup produced a complex mixture of compounds with one side product in notable quantity and NMR spectra showed that a cyclization had occured resulting in *N*-acylpyrrolidin-2-ones **89** and **90**. A second try without 2-methyl-4-quinolinamine gave comparable results. Probably the proton scavenger *N,N*-diisopropylethylamine facilitates this nucle-
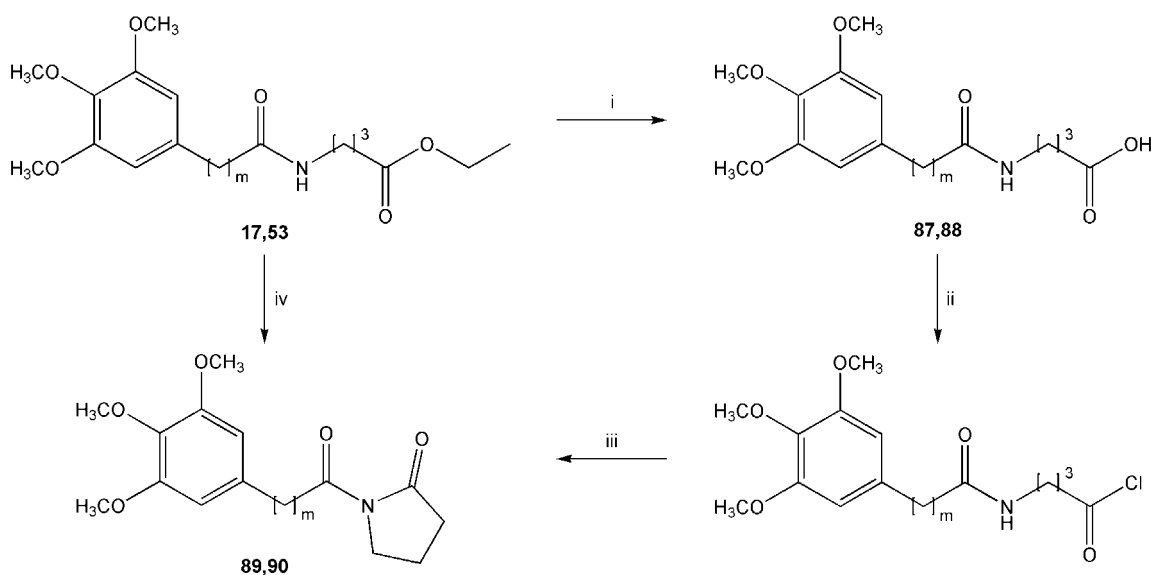
Scheme 5: Unexpected cyclization forming *N*-acylpyrrolidin-2-ones. m = 0,2 i) H$^+$/H$_2$O, Me$_2$CO. ii) OXC,
DCM. iii) DIEA, DCM. iv) NaH, DMF.
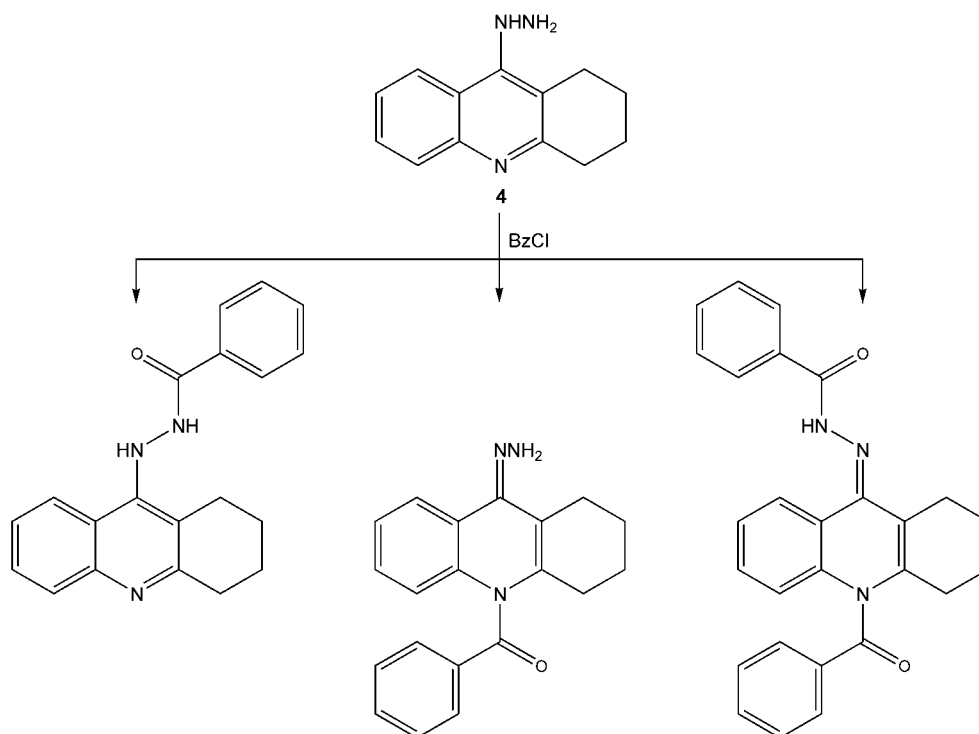
Scheme 6: Possible benzoylation products of 9-hydrazino-1,2,3,4-tetrahydroacridine.

ophilic substitution by abstracting the amide proton. This hypothesis was further affirmed since a direct cyclization of compounds **17** and **53** occured in DMF using sodium hydride to activate the amide[70].

In a separate setup, the acylation capabilities of 9-hydrazino-1,2,3,4-tetrahydroacridine (**4**) were investigated using benzoyl chloride. However, no selectivity for the primary amine nitrogen could be established and a range of acylation products was obtained that were not separated (Scheme 6). So, as the intended coupling of 4-((3,4,5-trimethoxybenzoyl)amino)butanoic acid (**87**) and 9-hydrazino-1,2,3,4-tetrahydroacridine (**4**) using the activated carboxylic acid failed, a new strategy was worked out. A first attempt to link both parts by a hydrazide formation, where the primary amine nitrogen of 9-hydrazino-1,2,3,4-tetrahydroacridine (**4**) was supposed to attack the ester carbonyl of ethyl 4-((3,4,5-trimethoxybenzoyl)amino)butanoate (**17**), did not succeed (Scheme 7). To circumvent this situation, where the nucleophilicity of the mono-substituted hydrazine derivate is too low to attack the ester carbonyl, the synthesis was turned to the opposite direction. Now the carboxylic ester was converted into the hydrazide **18** that

was intended to attack the 9-chloro-1,2,3,4-tetrahydroacridine (**1**). Applying the same reaction conditions, the nucleophilicity of the mono-substituted hydrazide was now high enough to facilitate a substitution of the chlorine in 9-chloro-1,2,3,4-tetrahydroacridine (**1**) (Scheme 7).

The hydrazide formation from **17** to **18** required some optimization. Having in mind that mono-substituted hydrazides are formed when reacting carboxylic esters and hydrazine as opposed to di-substituted hydrazides that result from the more reactive acyl chlorides, the reaction conditions still had to be optimized. Several runs, each raising the reaction temperature and amount of hydrazine equivalents, finally led to refluxing ethanol and a tenfold excess of hydrazine. Worth mentioning at this point is the excellent crystallizability of all hydrazides synthesized for the two series (Scheme 8).

As already outlined in Scheme 7 the final introduction of the tacrine moiety was established using 9-chloro-1,2,3,4-tetrahydroacridine (**1**) and the hydrazides **18** and **54** recovered from the previous reaction step. Carlier *et al.*[71,72,73] reported the nucleophilic substitution of 9-chloro-1,2,3,4-tetrahydroacridine (**1**) by primary amines such as 1,7-diaminoheptane in refluxing pen-
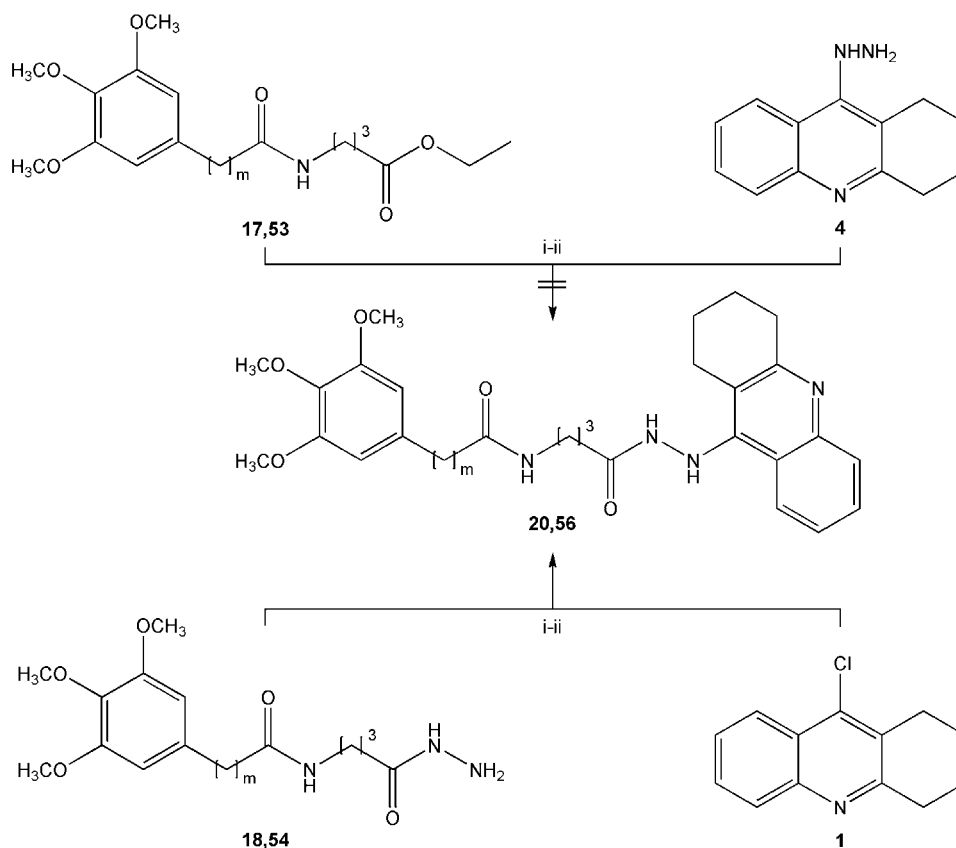
Scheme 7: Turning the coupling strategy: i) EtOH, 140 °C. ii) OH⁻/H₂O.

tanol and, as already mentioned, the synthesis of 9-hydrazino-1,2,3,4-tetrahydroacridine (**4**) was first achieved using refluxing phenol. To avoid these high boiling solvents that are difficult to remove during workup, different reaction conditions were searched for. To allow low boiling solvents to be heated to temperatures above their boiling point small glass reactors were used. These glass reactors were equipped with a bursting membrane that allowed the pressure to raise up to 15 bar. In these glass reactors an ethanolic solution of the reaction partners was heated to 140 °C, a reaction temper-

ature where yields beyond 90 % were reached within 24 hours. The following tables list all compounds that were obtained by these conditions (Scheme 7). The were usually first recovered as their hydrochlorides and subsequently converted into their corresponding bases. Three derivatives from 3,4,5-trimethoxybenzoic acid (**32**), (**36**) and (**44**) were additionally obtained by reaction with 6,9-dichloro-1,2,3,4-tetrahydroacridine (**2**). Compounds **31**, **35** and **39** (Table 2) were not recovered as their hydrochlorides because recrystallization always produced oily residues. Instead the crude products were directly treated
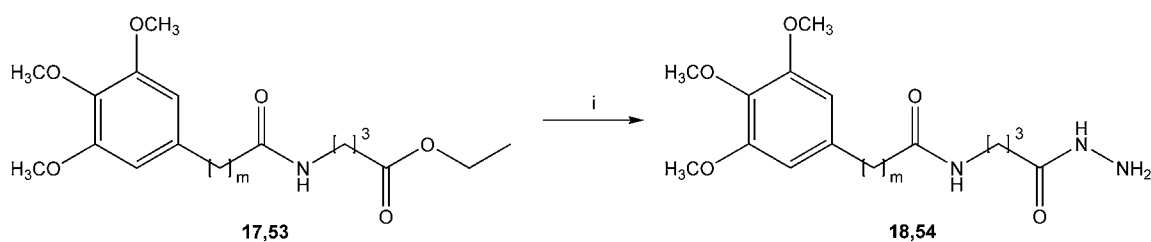
Scheme 8: Hydrazide formation: i) 10 eq. N₂H₄, EtOH, ΔT.

with aqueous sodium hydroxide and the oily layer formed upon was boiled up in ethyl acetate producing solid precipitates of high purity. The truncated homologues **8** and **44** (Table 1, Table 2) were synthesized to complete both series as depicted in Scheme 9. The starting compounds, 3,4,5-trimethoxybenzoic and 3-(3,4,5-trimethoxyphenyl)propionic acid, were converted into their methyl esters and subsequently into their hydrazides. The tacrine moiety was introduced as shown in Scheme 7 to yield the final compounds.
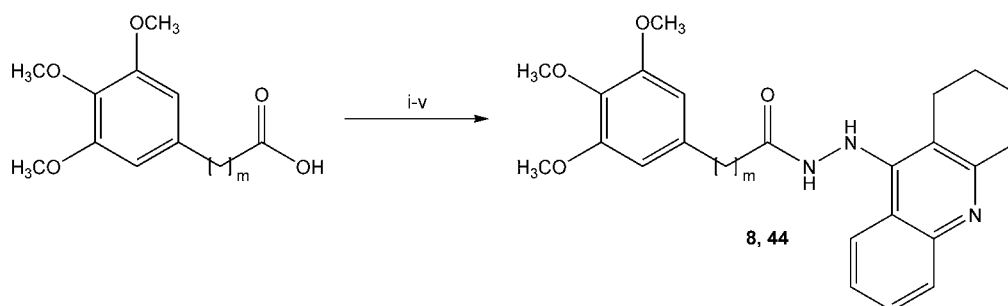
Scheme 9: Synthesis of the truncated homologues. m = 0,2 i) OXC, DCM ii) NaOMe iii) 10 eq. N_2H_4, EtOH, ΔT. iv) 9-chloro-1,2,3,4-tetrahydroacridine, EtOH, 140 °C. v) OH^-/H_2O.

Table 1: Final compounds derived from 3-(3,4,5-trimethoxyphenyl)propionic acid.

Compound	Structure	Formula	MW [$\frac{g}{mol}$]	Yield^a [%]
44		$C_{25}H_{29}N_3O_4$	435.52	42
48		$C_{27}H_{32}N_4O_5$	492.57	16
52		$C_{28}H_{34}N_4O_5$	506.60	56
56		$C_{29}H_{36}N_4O_5$	520.63	28
60		$C_{30}H_{38}N_4O_5$	534.66	31
64		$C_{31}H_{40}N_4O_5$	548.68	42

a Total yield for all steps.

Table 2: Final compounds derived from 3,4,5-trimethoxybenzoic acid.

Compound	Structure	Formula	MW [$\frac{g}{mol}$]	Yield[a] [%]
8		$C_{23}H_{25}N_3O_4$	407.48	49
12		$C_{25}H_{28}N_4O_5$	464.52	35
16		$C_{26}H_{30}N_4O_5$	479.32	54
20		$C_{27}H_{32}N_4O_5$	493.34	32
24		$C_{28}H_{34}N_4O_5$	506.60	22
28		$C_{29}H_{36}N_4O_5$	520.63	25
31		$C_{30}H_{38}N_4O_5$	534.66	33
32		$C_{30}H_{38}Cl_2N_4O_5$	605.56	45
35		$C_{31}H_{40}N_4O_5$	548.68	40
36		$C_{31}H_{40}Cl_2N_4O_5$	619.59	47
39		$C_{32}H_{42}N_4O_5$	562.71	34
40		$C_{32}H_{42}Cl_2N_4O_5$	633.61	54

[a] Total yield for all steps.
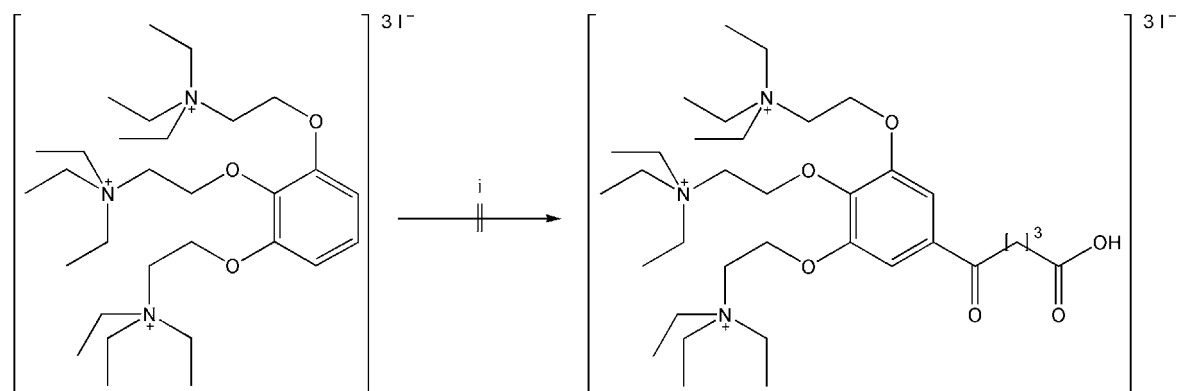
Scheme 10: Unsuccessful FCA of gallamine: i) glutaric anhydride, [bmim][PF$_6$], ZnCl$_2$.

2.4 The gallamine-like compounds

The first attempt to introduce the gallamine moiety into the desired compounds was undertaken by a Friedel-Crafts acylation. Due to the ionic nature of gallamine triethiodide a compatible solvent had to be found. Following Boon *et al.*[74], who reported Friedel-Crafts reactions to proceed in chloroaluminate ionic liquids like [emim][Cl]–AlCl$_3$, an ionic liquid was considered a potential solvent. From the miscibility characteristics published by Koel[75], [bmim][PF$_6$] was chosen for its immiscibility with water that would allow the extraction of gallamine triethiodide and possible acylation products. The chloroaluminate catalyst AlCl$_3$, however, was replaced by the less reactive ZnCl$_2$. Zink chloride is applied throughout conventional Friedel-Crafts acylations and was supposed to precipitate due to the introduction of hydrogen sulfide. This was anticipated to allow the separation of the gallamine triethiodide derived compounds from the catalyst as they would

both be extracted into water from the ionic liquid. Unfortunately and for unknown reasons, iodine formed after a few minutes when reacting gallamine triethiodide with glutaric anhydride under anhydrous conditions in [bmim][PF$_6$] containing 5 equivalents of ZnCl$_2$ (Scheme 10). So, as chloride might replace iodide the approach was dropped because the stochiometric composition of the intended product was changed irreversible.

As the introduction of a complete gallamine moiety by Friedel-Crafts acylation failed, the classical synthesis as depicted in Scheme 11 was considered. Fourneau[76] and Bovet *et al.*[77] reported the successful alkylation of 1,2,3-trihydroxybenzene by 2-(diethylamino)ethyl chloride followed by quaternization with ethyl iodide. Both groups used an aqueous solution of alkali hydroxide to facilitate the ether formation accepting the drawback due to oxidation processes. The ease of sep-
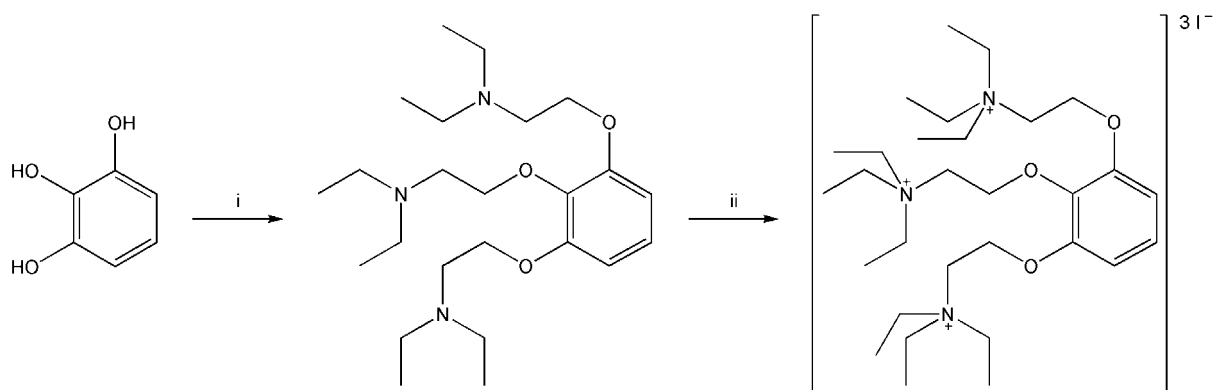
Scheme 11: Classical synthesis of gallamine: i) Et$_2$NCH$_2$CH$_2$Cl, KOH, H$_2$O, ΔT. ii) EtI.
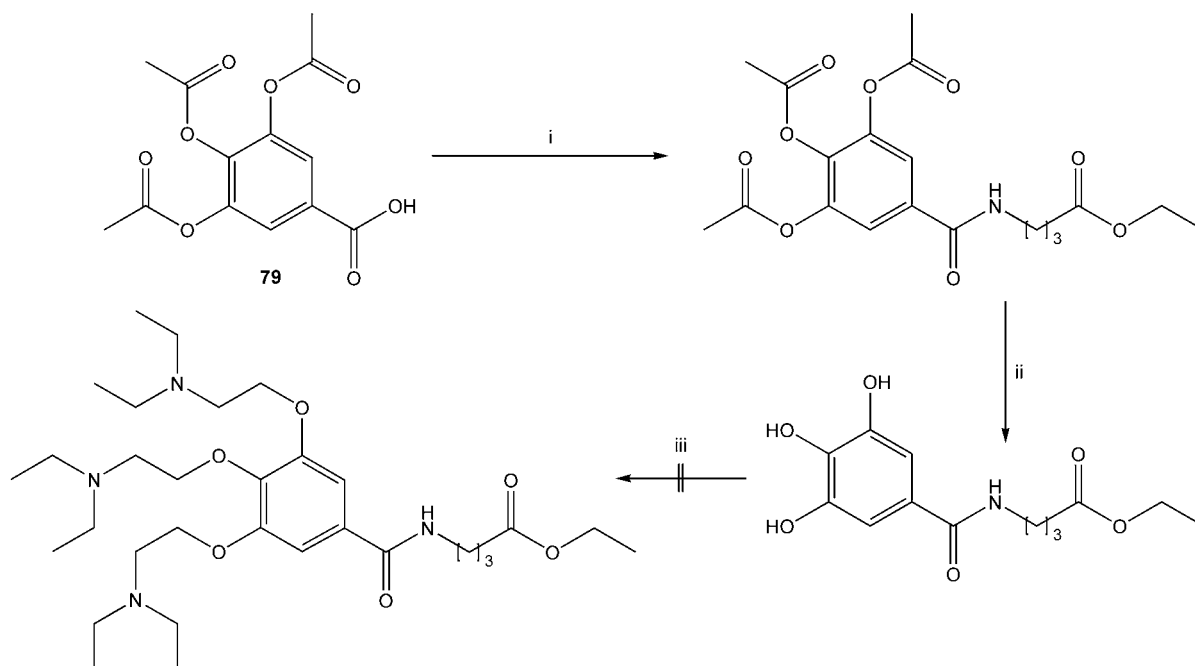
Scheme 12: Applying the classical route. i) OXC, DCM, DIEA, ethyl 4-aminobutanoate HCl. ii) K_2CO_3, MeOH. iii) THF, NaH, $Et_2NCH_2CH_2Cl$.

aration as the peralkylated intermediate formes an oily layer is the reason why oxidation processes during the alkylation can be ignored.

Due to the basic conditions used for alkylation, the synthesis of a gallamine analogue from benzoic acid seemed unapplicable because the product would not separate as in the classical synthesis. Therefore the amide bond with the ω-aminocarboxylic acid linker was established first, using acetyl-protected 3,4,5-trihydroxybenzoic acid **79**, that was subsequently deprotected. The following alkylation step was carried out with sodium hydride under argon protection to activate the phenolic groups while avoiding oxidative side reactions (Scheme 12). It was hereby intended that the activated phenolic groups would rather react with the alkylation reagent than with the ethyl ester of the linker.

Unfortunately, the alkylation reagent tends to react with itself and the already alkylated 3,4,5-trihydroxybenzamide. This resulted in a very diverse dendrimer formation of quaternary compounds and it was impossible to separate the non-quaternary compounds by column chromatography as they proved to be very basic substances.

So, neither the direct use of gallamine triethiodide, nor the application of the classical synthesis was possible and the whole gallamine moiety had to be set up from scratch by a new synthetic route. Applying part of the chemistry already depicted in Scheme 12 the synthesis was planned to start with the amide bond formation between the benzoic acid moiety and the ω-aminocarboxylic acid linker. In order to utilize the acyl chloride procedure the phenolic groups had to be protected by an acid-stable group and the

R^1	H	OH	OH
R^2	OH	H	OH
	65	**72**	**79**
R^1	H	OAc	OAc
R^2	OAc	H	OAc
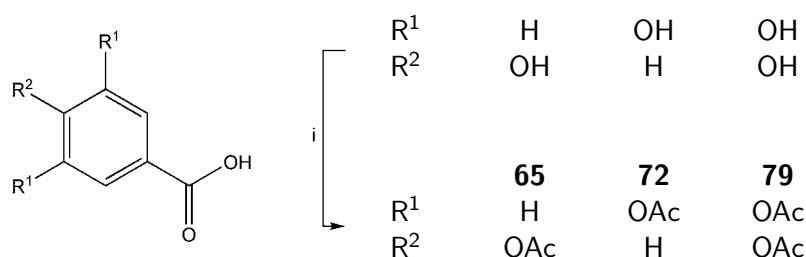
Scheme 13: Acetyl protection: i) Ac_2O, Py.
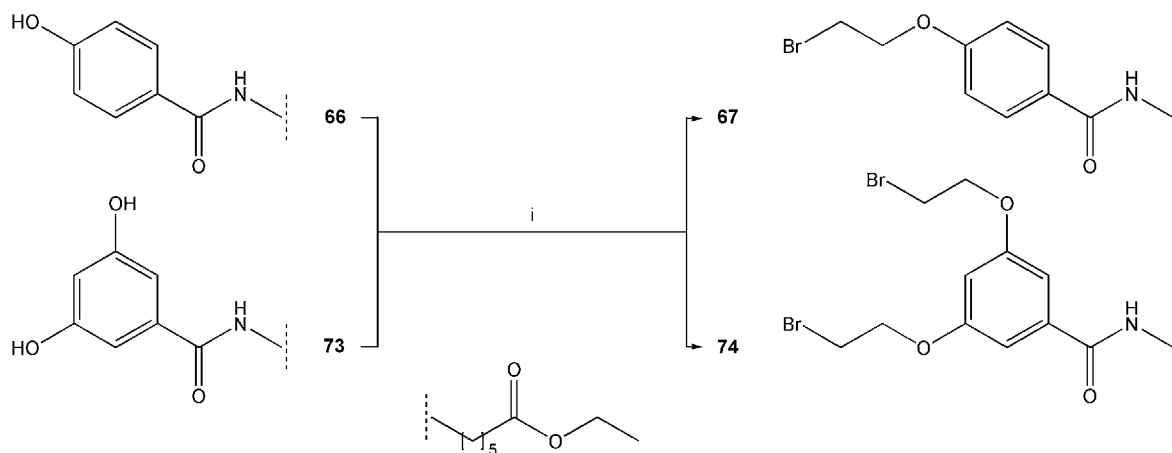
Scheme 14: Introducing the bromoethoxy groups. i) BrCH$_2$CH$_2$Br, K$_2$CO$_3$, 18-crown-6.

acetyl group was chosen for its easy introduction and cleavage. Scheme 13 shows the three starting compounds 4-hydroxy-, 3,5-dihydroxy- and 3,4,5-trihydroxybenzoic acid that were converted into their protected counterparts by the action of acetic anhydride in pyridine.

65 and **72** were subsequently reacted with ethyl 6-aminohexanoate to introduce the linker followed by deprotection as shown in Scheme 12. The resulting hydroxy-benzamides **66** and **73** were then reacted with 1,2-dibromoethane by a procedure of Sarkar *et al.*[78], where the alkylating reagent is used as the solvent and therefore in enormous excess. This alkylation step afforded

the bromoethoxy-functionalized compounds **67** and **74** after column chromatography in excellent and good yields, respectively (Scheme 14).

Following these promising results, attempts were undertaken to apply the same strategy to the 3,4,5-trihydroxbenzamide. However, the adjacent hydroxy groups allow a double attack of the 1,2-dibromoethane resulting in the formation of an anellated benzo[*b*][1,4]dioxine **91** (Scheme 15). To circumvent this dilemma the use of 2-bromoethanol was considered for the introduction of the ethyl ethers. The primary hydroxy groups were intended to be subsequently converted into their bromo-analogues by an Ap-
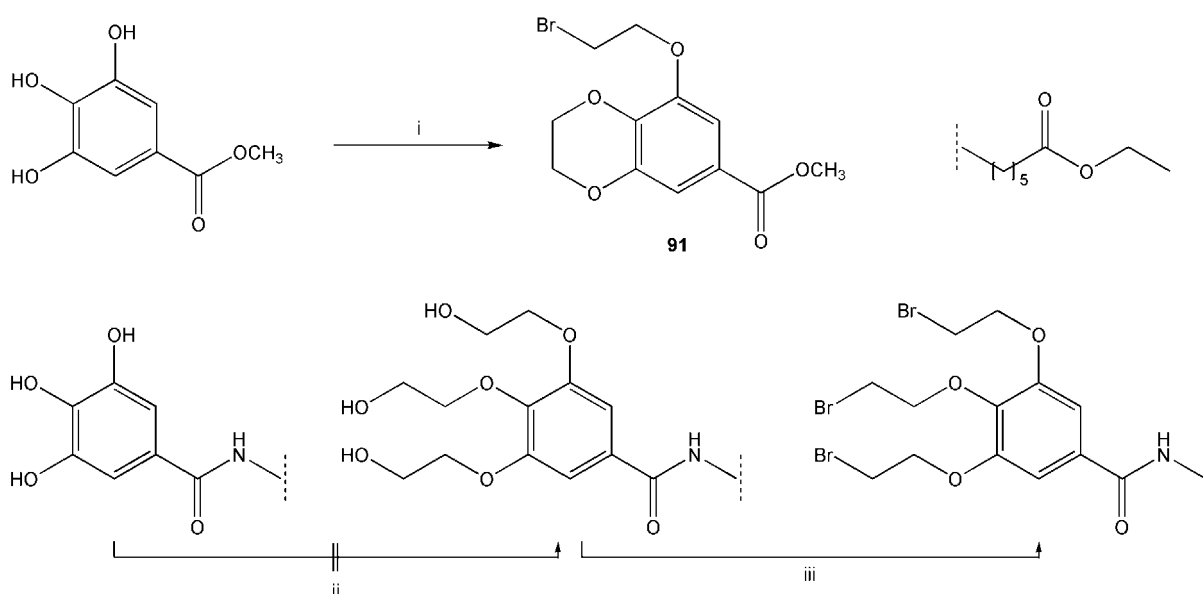
Scheme 15: Alkylating the 3,4,5-trihydroxybenzene derivative I. i) BrCH$_2$CH$_2$Br, K$_2$CO$_3$, 18-crown-6.
ii) BrCH$_2$CH$_2$OH, K$_2$CO$_3$, 18-crown-6. iii) CBr$_4$, PPh$_3$, THF.
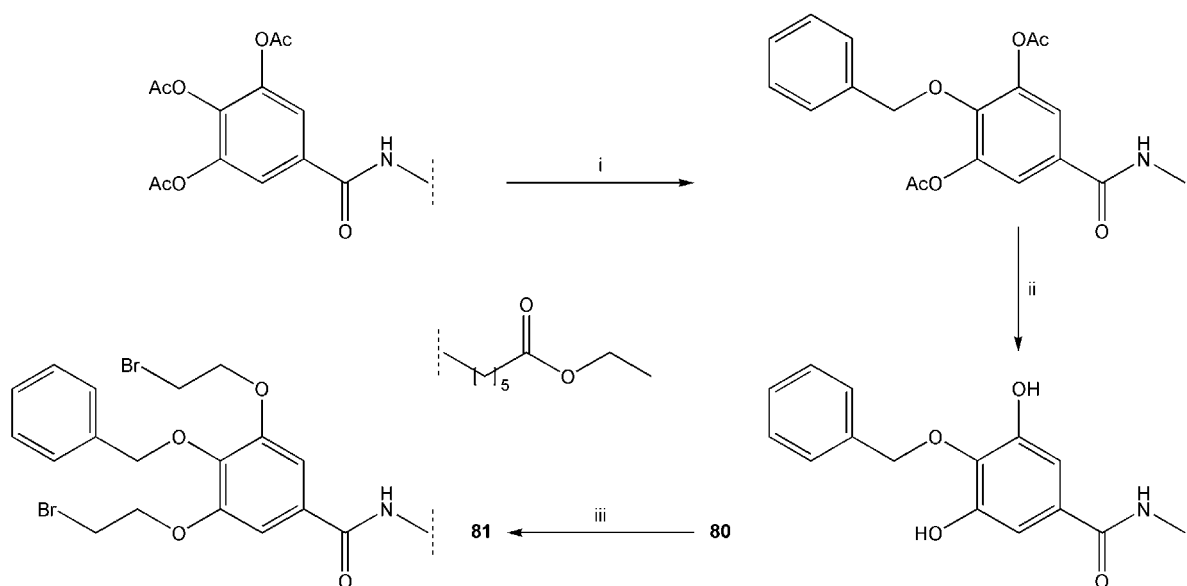
Scheme 16: Alkylating the 3,4,5-trihydroxybenzene derivative II. i) BnCl, K_2CO_3, KI, Me_2CO. ii) K_2CO_3, H_2O, MeOH, EtOAc. iii) $BrCH_2CH_2Br$, K_2CO_3, 18-crown-6.

pel reaction with tetrabromomethane and triphenylphosphine. Alas, already the alkylation using 2-bromoethanol resulted in an unusable product mixture accompanied by high amounts of different crown ethers and the approach was dropped straight away. So, returning to the alkylation procedure used for the mono- and dihydroxybenzamide, another route had to be found avoiding the formation of a benzo[*b*][1,4]dioxine like **91**.

As the *p*-hydroxy group of the 3,4,5-trihydroxoxybenzamide is the crucial point for the successful introduction of the bromoethoxy side chains, search went for a regioselective protection. Pearson *et al.*[79] reported the regioselective benzylation of methyl 3,4,5-

tris(acetyloxy)benzoate using benzyl chloride and K_2CO_3 in acetone. Adapting this procedure, a selective benzyl protection of the *p*-hydroxy group was achieved as depicted in Scheme 16. The subsequent alkylation of **80** gave the 4-benzyloxy-3,5-bis(bromoethoxy)-substituted compound **81** in excellent yield.

The following quaternization of compounds **67** and **74** was achieved using a tenfold excess of triethylamine and nitromethane as the solvent (Scheme 17). The bromide salts **68** and **75** were recovered from solution by precipitation using ethyl acetate. Throughout synthesis the precipitation of the quaternary compounds from ethyl acetate proved to be the most convenient pro-
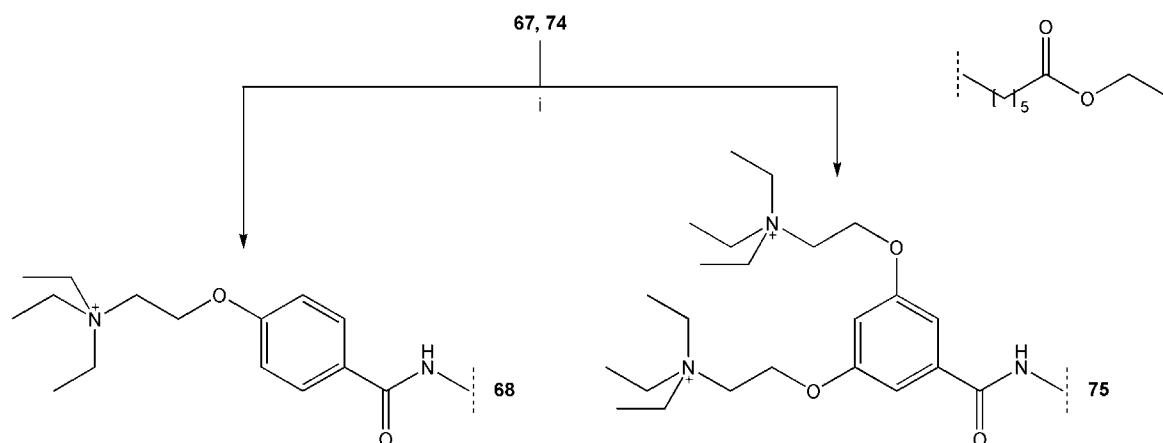
Scheme 17: Quaternization. i) 10 eq. Et_3N, $MeNO_2$.
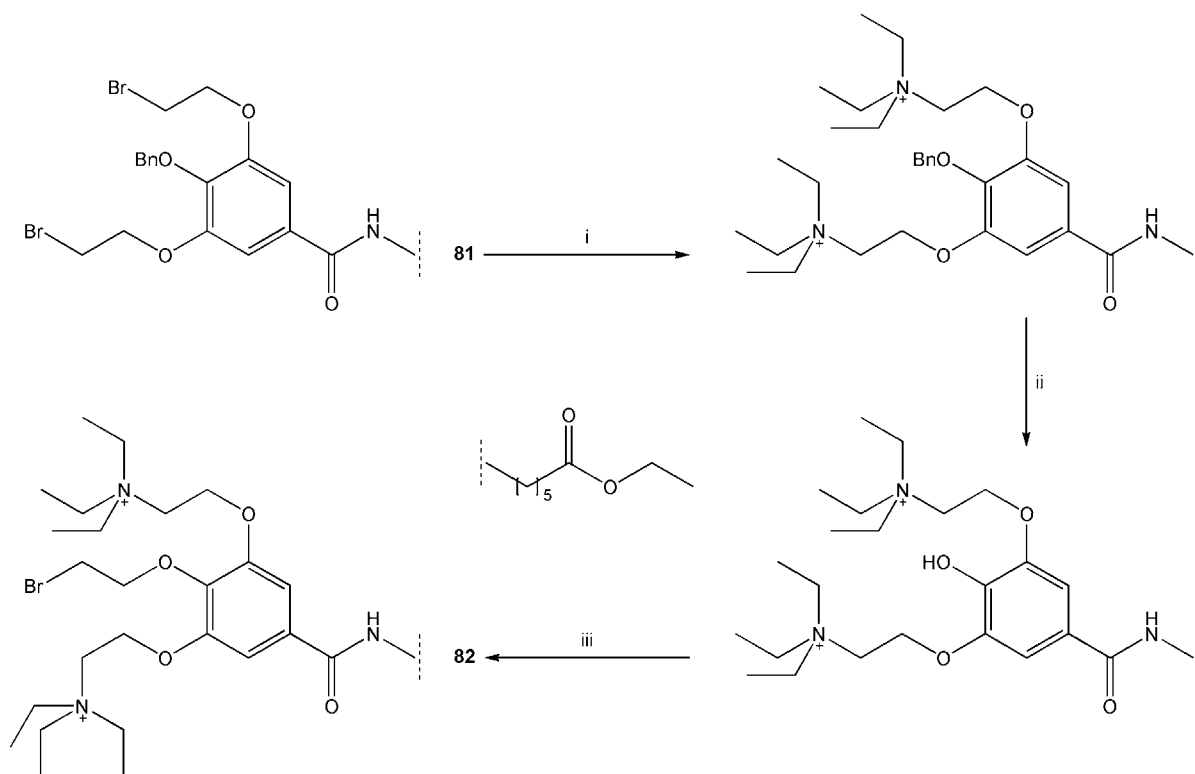
Scheme 18: Alkylation of the bisquaternary intermediate. i) 10 eq. Et$_3$N, MeNO$_2$. ii) H$_2$, Pd/C, MeOH. iii) BrCH$_2$CH$_2$Br, K$_2$CO$_3$, 18-crown-6, MeCN.

cedure to obtain clean and solid compounds, as it also allowed the separation of reagents and side products. In general, the quaternary compounds, especially the hydrazides formed during the next step, were found to be hygroscopic and were therefore stored protected from moisture.

Regarding the anticipated trisquaternary compound, the next step of synthesis was the quaternization of the two *meta*-substituents. Following the procedure presented before, the benzyl-protected 3,5-bis(bromoethoxy)-compound **81** was reacted with triethylamine and subsequently

deprotected by hydrogenolysis (Scheme 18). The following alkylation using 1,2-dibromoethane was carried out as with compounds **66**, **73** and **80** (Scheme 14, Scheme 16). The only change was, that a 1:1 mixture of 1,2-dibromoethane and acetonitrile was used to dissolve the already bisquaternary educt. Simple separation of the inorganic salts, followed by evaporation of the acetonitrile yielded a suspension of **82** that was collected by suction filtration. The final quaternization step to the trisquaternary intermediate **83** required a modification of the established quaternization procedure. The quaternization using
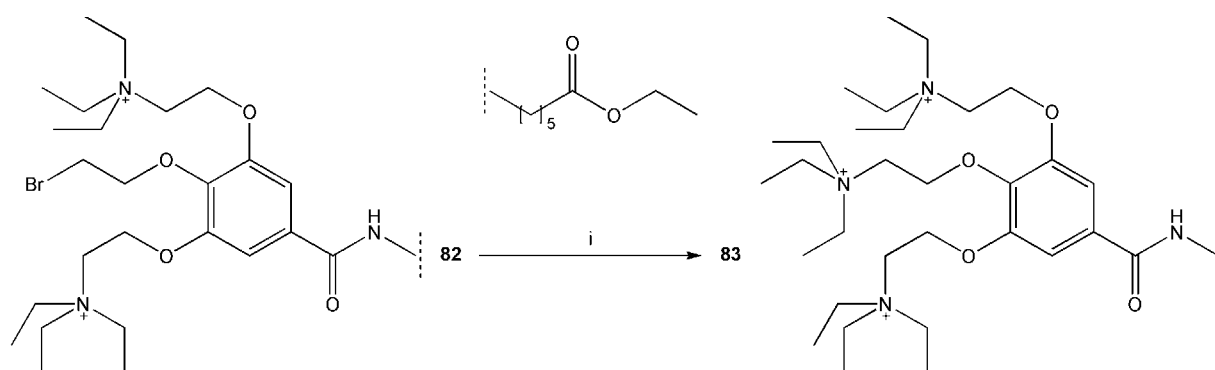
Scheme 19: Quaterniaztion of the bisquaternary intermediate. i) 10 eq. Et$_3$N, MeCN, 100 °C.
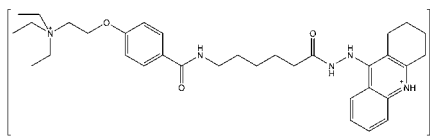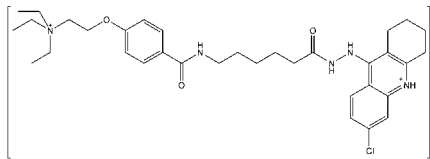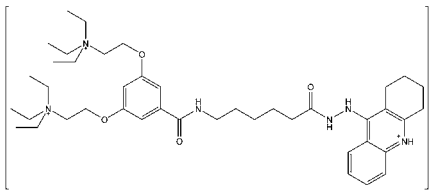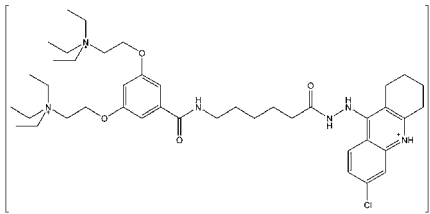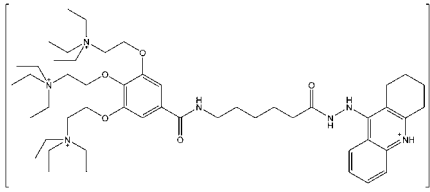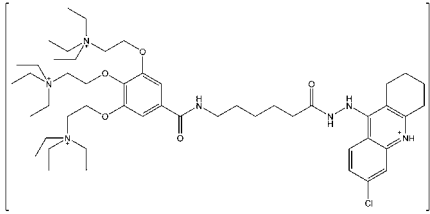
nitromethane as the solvent resulted in a crude and colored product that could not be purified by recrystallization or RP-column chromatography. The CH-acidity of the solvent was held responsible for this problem and nitromethane was therefore replaced by acetonitrile. The reaction conditions still had to be intensified to achieve an acceptable conversion and the reaction was therefore carried out in the already mentioned glass reactors (Scheme 19). Now, that the mono-, bis- and trisquaternary ester interme-

diates **68**, **75** and **83** had been obtained, they were subjected to hydrazide formation as discussed with the trimethoxy-substituted analogues (Scheme 8). Again the reaction time had to be increased to achieve an almost complete conversion that allowed recovery by precipitation from ethyl acetate. The subsequent reaction with 9-chloro- or 6,9-dichloro-1,2,3,4-tetrahydroacridine was carried out unmodified (Scheme 20) yielding the final compounds **70**, **71**, **77**, **78**, **85** and **86** (Table 3).
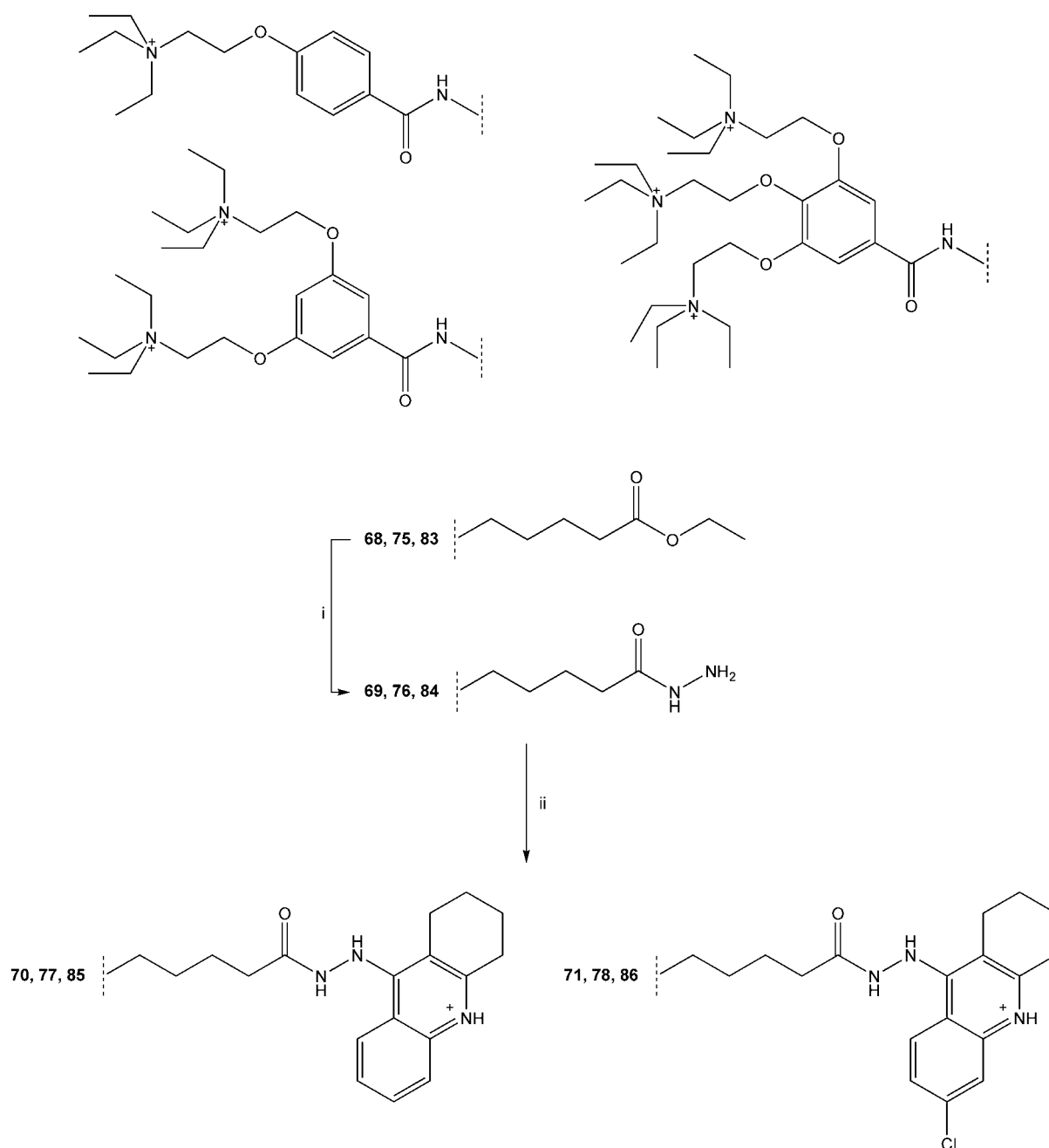
Scheme 20: Hybrid formation. i) 25 eq. N$_2$H$_4$, EtOH, ΔT. ii) 9-chloro- or 6,9-dichloro-1,2,3,4-tetrahydroacridine, EtOH, 140 °C.

Table 3: Quaternary compounds.

Compound	Structure	Formula	MW $[\frac{g}{mol}]$	Yield[a] [%]
70		$C_{34}H_{49}BrClN_5O_3$	691.15	36
71		$C_{34}H_{48}BrCl_2N_5O_3$	725.60	38
77		$C_{42}H_{67}Br_2ClN_6O_4$	915.29	20
78		$C_{42}H_{66}Br_2Cl_2N_6O_4$	949.74	25
85		$C_{50}H_{85}Br_3ClN_7O_5$	1139.43	15
86		$C_{50}H_{84}Br_3Cl_2N_7O_5$	1173.88	15

a Total yield for all steps.

3 Docking studies

To investigate possible binding modes of the final compounds molecular docking studies were carried out. They were intended to reveal hydrogen bonding partners along the active site gorge of acetylcholinesterase and should suggest possible π-π-interactions between the ligands two aromatic moieties and aromatic residues located at the peripheral and or the active binding site. In addition possible π-cation-interactions between aromatic or anionic side chains at the peripheral binding site and the quaternary side chains of the gallamine derived inhibitors might be discovered.

3.1 Structure preparation and docking procedure

Enzyme and ligand structures

Crystal structures of several acetylcholinesterase complexes (1ACJ[81], 1EVE[82], 1ZGB[83], 1N5R[84] and 1N5M[84]) were retrieved from the Protein Data Bank[85]; if not stated otherwise, residue numbering throughout this chapter refers to *Torpedo californica*. Unnecessary information from the PDB files was dropped by keeping only the ATOM entries, missing side chain atoms were generated using the repair feature of the ADT suite[86] and polar hydrogens were added. Using the CORINA[87] web service three-dimensional coordinates were obtained for the ligands. OpenBabel[88] was used to convert these PDB files to MOL2 format that allowes the addition of partial charges which were calculated by MOPAC[89]. As opposed to the GOLD[90] docking software AutoDock[91] has no ring flipping feature, that would allow the annellated tetrahydro-cyclohexene ring to change its conformation. Fortunately it can be observed from the crystal structures above and the one obtained for the precursor 6,9-dichloro-1,2,3,4-tetrahydroacridine (Figure 13) that only one tacrine conformer is energetically favoured. Therefore the right conformer and the protonation at the endocyclic nitrogen has to be considered when generating these coordinates. Due to the energy minimization the
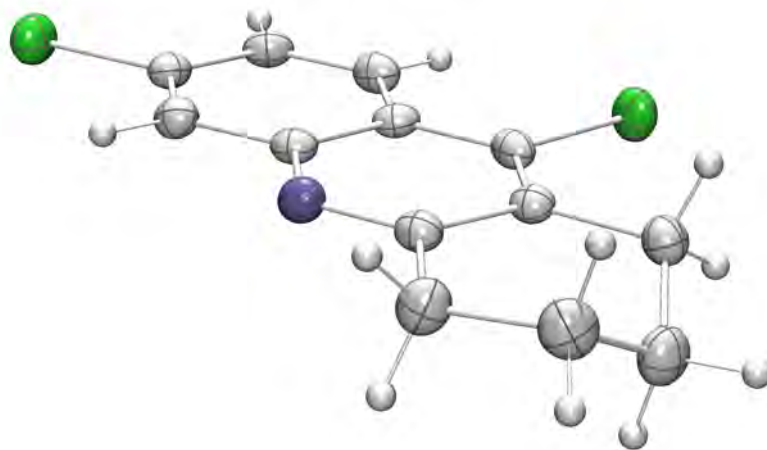
Figure 13: ORTEP[80] plot of 6,9-dichloro-1,2,3,4-tetrahydroacridine showing the energetically favoured conformation of the annellated tetrahydro-cyclohexene ring.
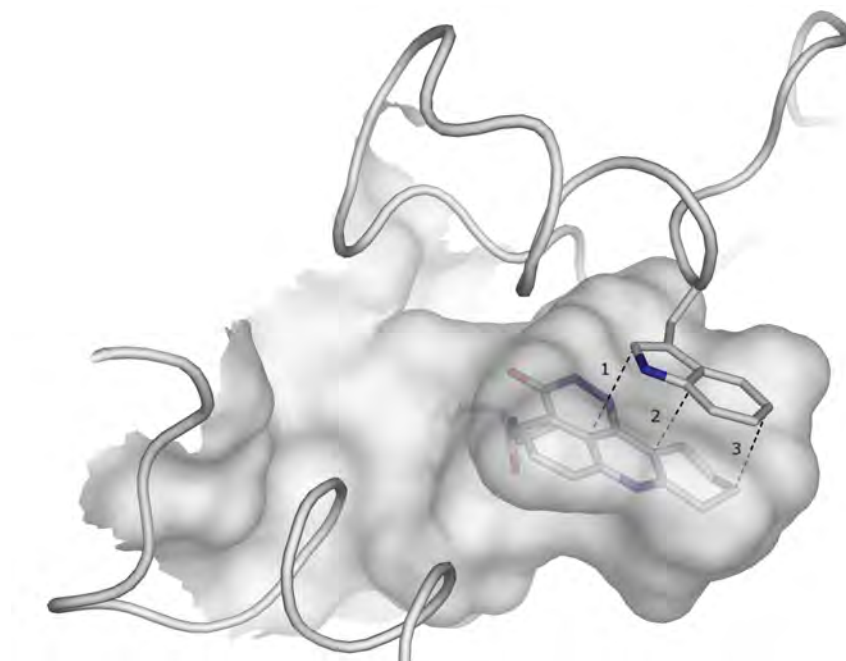
Figure 14: Three distance constraints (Å) fixating the tacrine moiety in a position close to the crystal structure: 1. 3.20-3.50, 2. 3.50-3.70 and 3. 3.60-3.90.

structures from the CORINA algorithm tend to be stretched, which gives a good bias towards the anticipated binding mode.

GOLD

The GOLD docking software was used to dock compounds of the two trimethoxybenzene-substituted series into the active site of acetyl-cholinesterase as it is found in the crystal structures 1EVE[82], 1ACJ[81] and 1ZGB[83]. To allow GOLD to correctly detect the ligand structures, especially the free rotation of bonds and the aromaticity of rings, the ligand PDB structures retrieved from CORINA were converted into the MOL2 format using OpenBabel. The protein file was prepared keeping the PDB format and a 17 Å radius sphere centering on the CD2 hydrogen of His[440] was chosen for cavity detection. GOLD uses the LIGSITE[92] algorithm to automatically locate solvent accessible residues along the given binding site. The genetic parameters were left by their default values with a population of 100 chromosomes on 5 islands. For every ligand 20 docking runs were carried out applying a maximum of 100000 genetic operations. Special weight parameters govern the relative frequencies of the three types of operations that can occur during a genetic optimisation: point mutation of the chro-

mosome, migration of a population member from one island to another, and crossover of two chromosomes. Each time the genetic algorithm selects an operator, it does so at random, and any bias in this choice is determined by the operator weights, that were set at a ratio of 95:95:10 mutation:crossover:migration. As was seen in the crystal structures containing tacrine or a tacrine derived compound, the tacrine moiety always fits in the same position independent from substitution at its primary amino group. Therefore the GOLD option to define special constraints was used to force the docking process to place the tacrine moiety into the desired position. It does so by adding a term to its fitness function that evaluates the satisfaction of the constraints supplied by the user. Three distance constraints were chosen which pinpoint the orientation of the tacrine moiety with respect to Trp[84] as it is observed in a π-π-stacking in the crystal structures 1ACJ[81] and 1ZGB[83] (Figure 14).

AutoDock

AutoDock was used to discover possible binding modes of the gallamine-analogues. As opposed to GOLD, that estimates only inter- and intramolecular hydrogen-bonding and van der Waals energies, AutoDock implements a more meticulous

scoring procedure. In addition to the evaluation of hydrophobic and hydrogen-bonding contacts there are further terms regarding electrostatic interactions, the ligands torsional entropy and desolvation upon binding. This was thought to drive the docking process into the right direction with respect to the quaternary side chains. The docking grid (180000 points, 50x60x60, 0.375 Å) was centered between Tyr[121] and Phe[330] to stretch the complete distance from the active to the peripheral binding site. A population of 100 chromosomes and a set of 100000 generations with the rigid root placed at the center of mass was chosen for 100 runs. This resulted in negative binding energies ΔG_{bind} for all compounds, with a stepwise decrease of freed energy as the substitution pattern increased. This is probably due to the increasing amount of torsional energy, that exceedes the energy estimation for the binding process. The genetic operations used by AutoDock include point mutations and chromosome crossover, while it lacks a migration factor as there are no islands inside its genetic algorithm.

LIGPLOT

LIGPLOT[93] was used as an independent tool to discover hydrogen-bonding interactions from the docked complexes. LIGPLOT transfers the three-dimensional situation around the ligand into a two-dimensional perspective detecting hydrophobic and hydrophilic interactions and depicting them as shown in Figure 15. Hydrogen bonds are shown as dashed lines with their length denoted, while hydrophobic contacts are indicated by little rays pointing from the ligand atoms to the corresponding amino acids and *vice versa*. The use of LIGPLOT eases the detection of hydrogen-bonding residues along the active site gorge. PyMOL[94] offers a comparable feature that looks for polar contacts and was used to verify the LIGPLOT findings.

STC

To compare the docking results retrieved from GOLD and AutoDock with respect to the ligand affinity it seemed reasonable to compare the energy of binding values for all substances. As the fitness score of GOLD does not supply values for ΔG_{bind} that are comparable to those retrieved from AutoDock, the STC[95] program suite was used. The STC program suite consists mainly of two modules, of which the first calculates the difference in polar and non-polar solvent accessible surface area upon ligand binding. From this a second module calculates the thermodynamic parameters, of which ΔG_{bind} was selected for comparison.
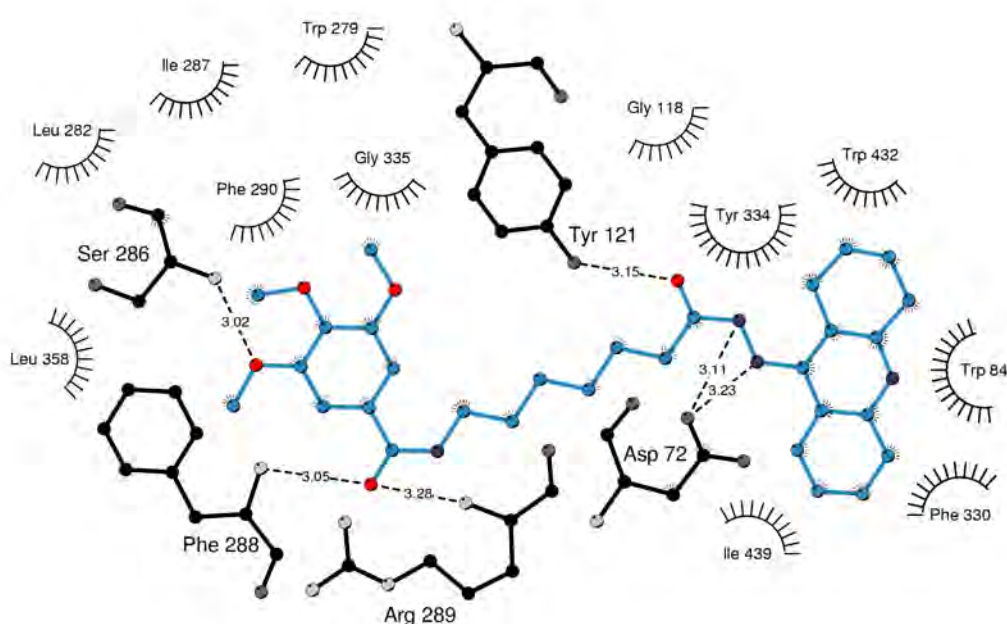
Figure 15: LIGPLOT for compound **31**.

a

b
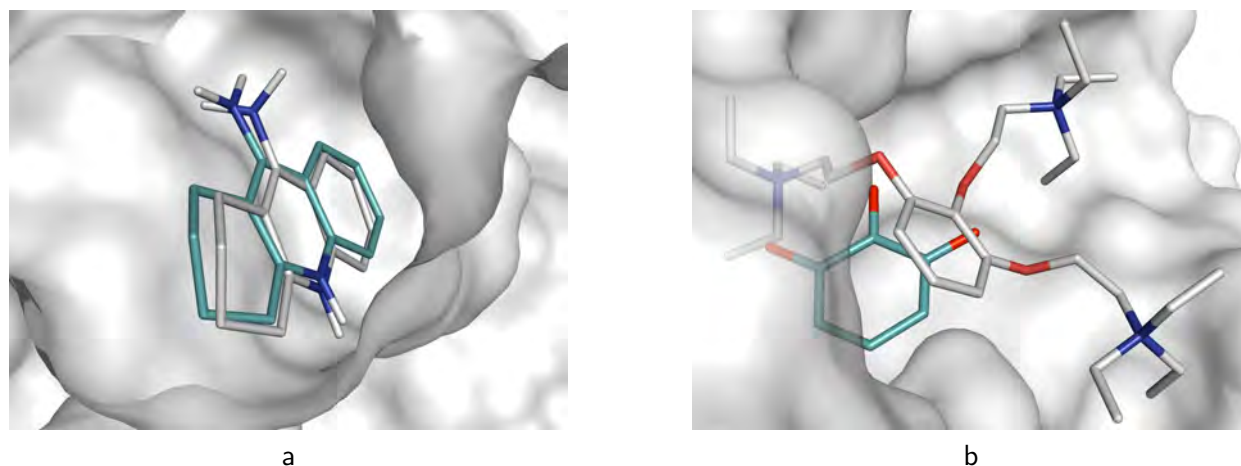
Figure 16: Redocked conformations ▢ of tacrine (a) and gallamine (b) in comparison with their original ▢ orientations.

3.2 Docking validation

To validate the applied docking procedures a classical redocking approach was undertaken. Tacrine and gallamine were removed from their corresponding crystal structures (1ACJ[81], 1N5M[84]) and rebuilt by the same procedure as applied for ligand preparation. They were then docked into the gorge without any bias towards the active or peripheral binding site and the top-scored poses were compared with their original position in the crystal structure.

As can be seen in Figure 16a the predicted positioning of tacrine comes very close to the one observed in 1ACJ[81]. The RMSD calculated by PyMOL[94] adds up to 0.561 Å which is accounted by the literature[96] to be a very good fit. Looking at gallamine in Figure 16b the matching is not as good as with tacrine but still acceptable. The crystal structure of acetylcholinesterase in complex with gallamine (1N5M[84]) does not state the conformation of the quaternary side chains. The RMSD comparison refers therefore only to the tris-substituted benzene moiety and gives a value of 2.498 Å. From a total of 100 runs 87 % located the gallamine ligand at the peripheral binding site, which demonstrates its clear bias to bind peripherally.

A redocking of the gorge stretching inhibitor A1E[83] gives an RMSD of 3.112 Å which is 1 Å away from the accepted limit for good docking results. One has to keep in mind though, that a notable contribution to the total RMSD comes from atoms that belong to the alkyl linker, as it is with A1E and compounds investigated within this work. The docking of alkyl chains rests solely upon van der Waals energies and therefore bears a pool of uncertainty that significantly contributes to the RMSD. By contrast the docking at the active and peripheral binding site is based on a variety of interactions, including hydrophobic contacts, and gives trustworthy results as illustrated in Figure 16.

3.3 Hydrophobic and hydrogen-bonding ligand-protein interactions

The following outlines the results from the GOLD docking studies carried out for the final compounds derived from 3,4,5-trimethoxybenzoic and 3-(3,4,5-trimethoxyphenyl)propionic acid. To avoid confusion the active site gorge of acetyl-cholinesterase was split into three distinct parts – the entrance of the gorge, its middle, and the active site. Each part is discussed separately looking at selected examples to illustrate the different kind of interactions.

a b c
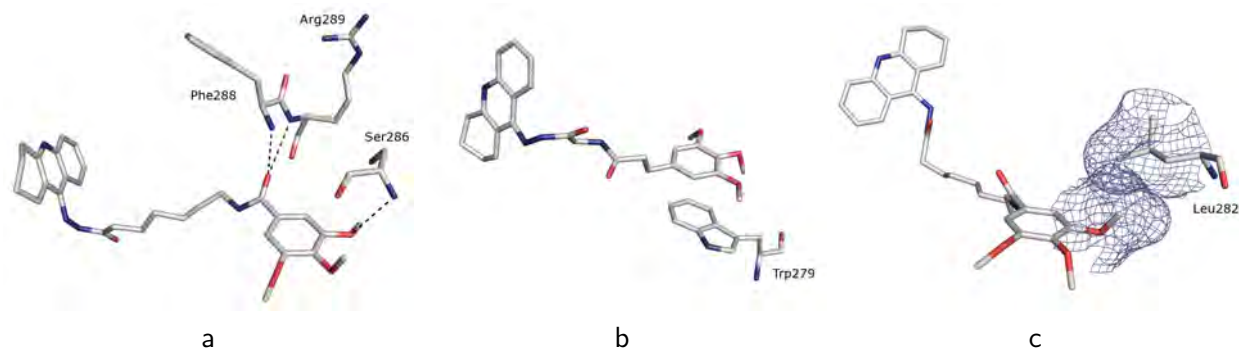
Figure 17: a) Compound **31** forming hydrogen bonds with backbone nitrogens from Ser^{286}, Phe^{288} and Arg^{289}. b) π-π-stacking between compound **48** and Trp^{279}. c) Hydrophobic contacts between compound **39** and Leu^{282} represented by their hydrophobic surfaces.

Gorge entrance

Figure 18 shows those residues located at the lip of the gorge, that were found to interact with compounds from both series. From this it can easily be recognized that the interacting residues are found in a discrete region of the gorge entrance and are not evenly spread around. The reason for this is that hydrogen bond acceptors dominate the outward directed part of the ligands, *i.e.* the three methoxy groups and in the case of the benzamides also the amide carbonyl. These

look for hydrogen bond donors as backbone nitrogens, but the uncovered part of the gorge entrance offers only backbone carbonyls. In Figure 17 some of the interactions found are shown in detail. Figure 17a shows the amide carbonyl of **31** forming two hydrogen bonds with the backbone nitrogens of Phe^{288} and Arg^{289} while the oxygen of one methoxy group is interacting with Ser^{286}. Another driving force towards the observed binding direction is a possible π-π-stacking between the trimethoxy-benzene moiety and Trp^{279}. A coplanar stacking as it is depicted for **48** in Fig-
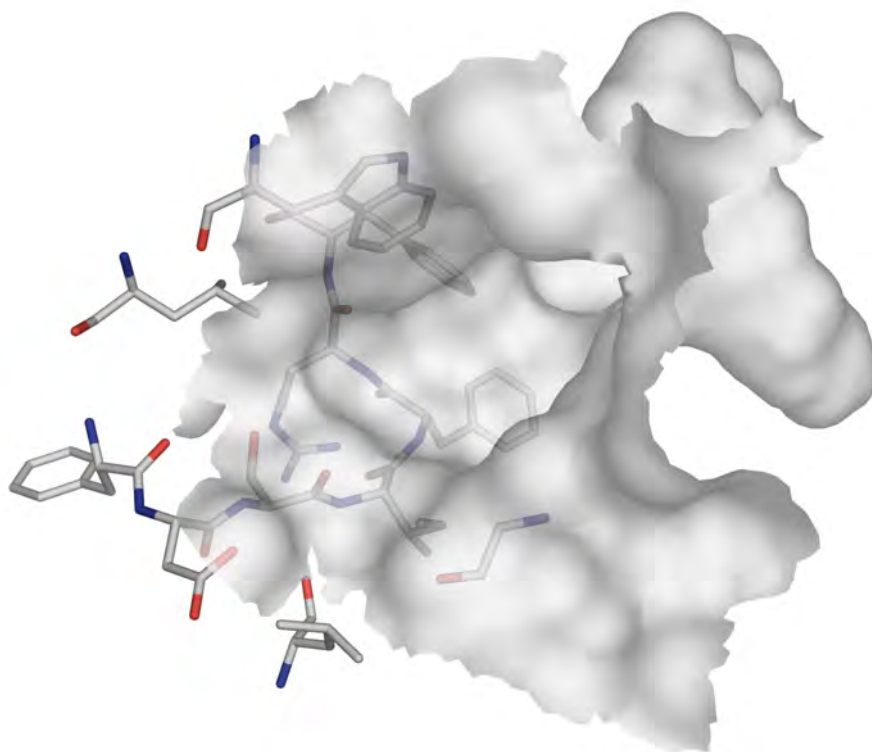
Figure 18: Amino acid residues interacting at the gorge entrance: Trp^{279}, Leu^{282}, Phe^{284}, Asp^{285}, Ser^{286}, Ile^{287}, Phe^{288}, Arg^{289}, Phe^{290}, Gly^{335}, Leu^{358}.
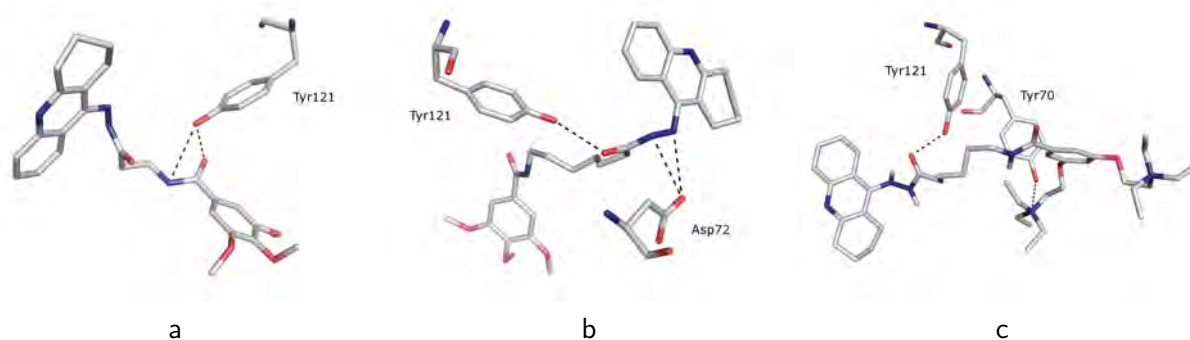
Figure 19: a) The benzamide of compound **16** interacting with Tyr^{121}. b) The hydrazide of compound **31** pinpointed by Asp^{72} and Tyr^{121}. c) Polar contacts between compound **78** and the phenolic groups of Tyr^{70} and Tyr^{121}.

ure 17b was observed in several docking experiments, though π-π-interactions are not explicitly included into the GOLD scoring function. In addition to this also hydrophobic contacts contribute to the binding. In Figure 17c is illustrated how the methoxy groups of **39** may rotate to maximise the area of hydrophobic surface contact.

Mid-gorge

Looking at the amino acids found to interact at the gorge middle, one sees that they are arranged like a ring (Figure 20) and not stacked in a dis-

tinct area as for the gorge entrance. The interactions observed are formed likewise by backbone amides and functional groups from involved amino acids. While Phe^{290}, Phe^{330}, Phe^{331} and Tyr^{70} contribute through their backbone, Asp^{72}, Tyr^{121} and Ser^{122} form hydrogen bonds through their hydroxy groups. Figure 19a and Figure 19b illustrate that the benzamide moiety of compound **16** comes into reach of Tyr^{121} when the linker length shortens to two methylene groups. The anticipated hydrogen bonds between Asp^{72} and Tyr^{121} and the hydrazide linker were found with the docking of compound **31** (Figure 19b) and similar observations were reported[97] during this
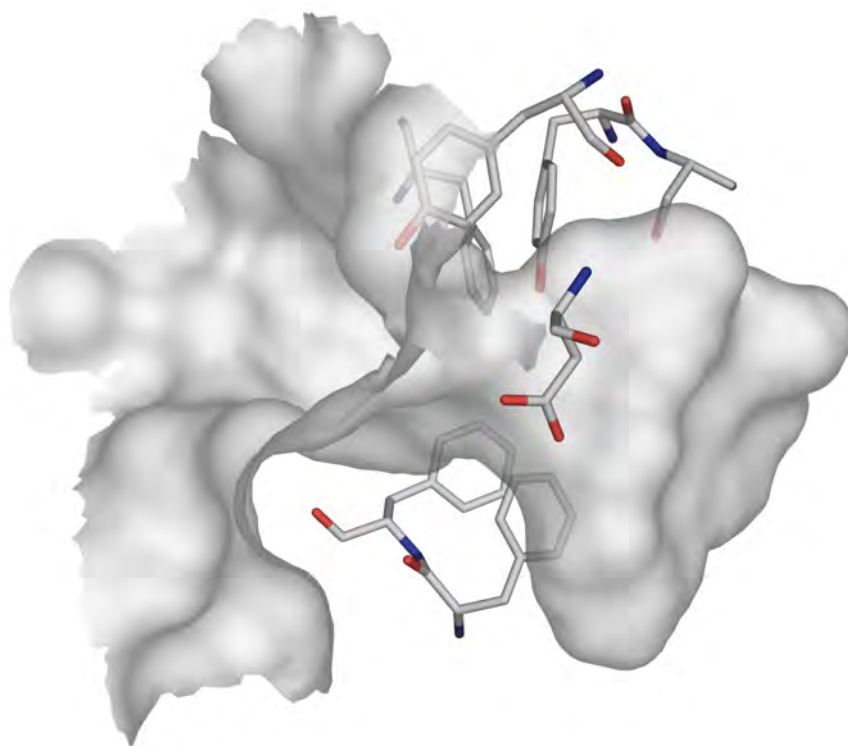
Figure 20: Interactions along the gorge: Tyr^{70}, Asp^{72}, Tyr^{121}, Ser^{122}, Phe^{290}, Phe^{330}, Phe^{331}.
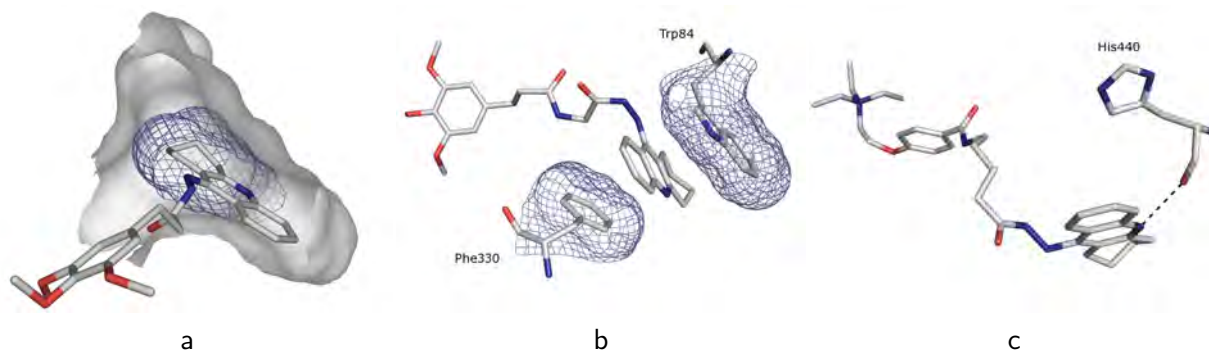
Figure 21: a) The 1,2,3,4-tetrahydroacridine ring system fits perfectly into the active site pocket. b) A π-π-stacking between Trp[84], Phe[330] and the aromatic acridine system forming a so called *sandwich*. c) His[440], one of the three catalytic amino acid residues, forming a backbone hydrogen bond towards the pyridinium nitrogen.

investigation. Figure 19c finally shows how Tyr[70] can interact with a quaternary side chain of compound **78**, as the linker adheres again to Tyr[121].

Active site

According to those amino acids involved, primarily aliphatic and aromatic ones (Figure 22), the active site is dominated by hydrophobic and electrostatic interactions. Figure 21a shows how the tacrine moiety fits precisely into the active site pocket of acetylcholinesterase. No specific inter- actions were found for the annelated cyclohexene ring, but its steric characteristics are tailored to allow a perfect fit. An important energetic contribution comes from the π-π-stacking between Trp[84], Phe[330] and the aromatic acridine system as depicted in Figure 21b. A final locking comes from a hydrogen bond between the pyridinium nitrogen of the tacrine moiety and the backbone carbonyl of His[440], which is in accordance with the crystal structure (Figure 21c). At this point it has to be mentioned that this hydrogen bond was not found for the human enzyme, where a tyrosine replaces Phe[330] (see also Section 3.5).
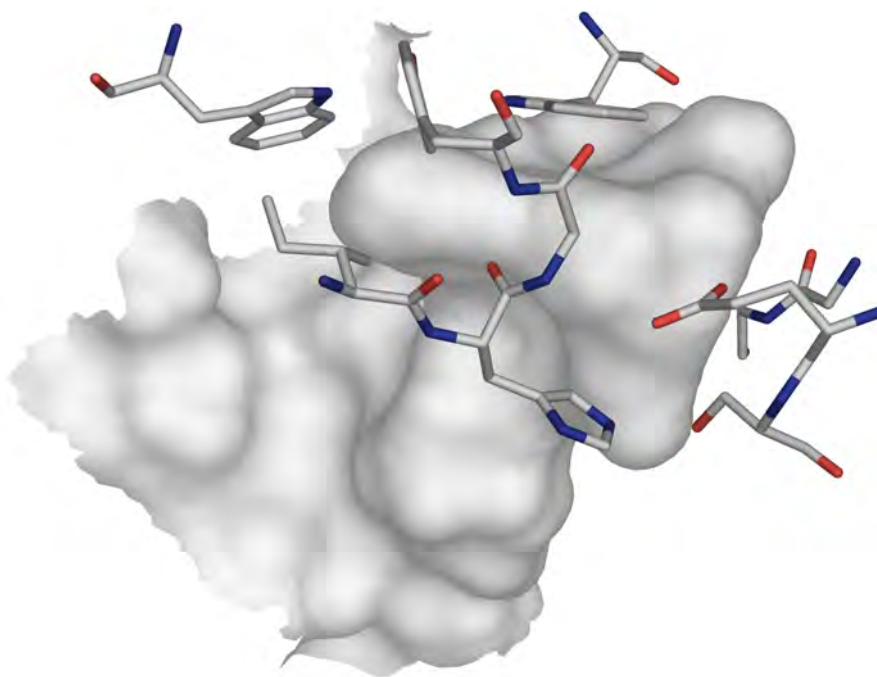
Figure 22: Active site interactions: Trp[84], Gly[117], Gly[118], Gln[199], Ser[200], Phe[330], Trp[432], Ile[439], His[440], Gly[441], Tyr[442].

3.4 Polar contacts of the gallamine analogues

To investigate the binding mode of the gallamine derived compounds **70**, **77** and **85** special attention was payed to the quaternary side chains. Using APBS[98] electrostatic maps of the surface potential of acetylcholinesterase were generated to locate possible binding partners. Typical distances for cation-π-interactions or salt bridges respectivly were obtained by analysis of the acetylcholinesterase complexes with decamethonium (1ACL[81]) and edrophonium (1AX9[99]). Within these complexes the quaternary ammonium group was found at 4.5 Å distance to either Trp[84] or Trp[279]. Looking at compound **70** four possible binding partners were located in the *lower lip* of the gorge, formed by residues 282 through 291 (Figure 23). The backbone carbonyl oxygens of Phe[284] and Ser[286], and the side chain oxygens of Asp[285] and Ser[286] form the base of a pyramid that has the ammonium nitrogen of compound **70** at its top. The average edge length was found to be 4.9 Å and thus within comparable dimensions to the distances observed in the crystal structures. While one ammonium group of compound **77** is located at almost the same position as the one of compound **70**, the other one is not pointing towards the gorge entrance. Instead it is directed to the gorge middle, where it is found on an axis connecting the mid-gorge Tyr[70] with Tyr[334] at the lip of the gorge (Figure 24). The little movement observed for the other quaternary group, brings it out of reach of all four possible binding partners. Figure 24 shows therefore only two interactions, though this is likely an artefact from the docking process. Compound **85**, carrying three quaternary side chains and representing the closest gallamine-tacrine dimer, was the most complex ligand to dock with a high amount of flexibility. This resulted in overall low docking energies that are probably due to a high amount of torsional constraints. Nevertheless does the highest ranked pose again address the lower gorge lip, an important cation bindig site found for all quaternary compounds (Figure 25). As the two remaining side chains are in *meta*-position to each other, a turn of one side chain inevitably implicates a movement of the other. While one of them is pointing into the gorge, the other is also oriented towards the gorge entrance. The mid-gorge does not offer cation interacting groups in suitable position and hydrophobic interactions originating from the three ethyl groups are the driving force for the docking of the one side chain.
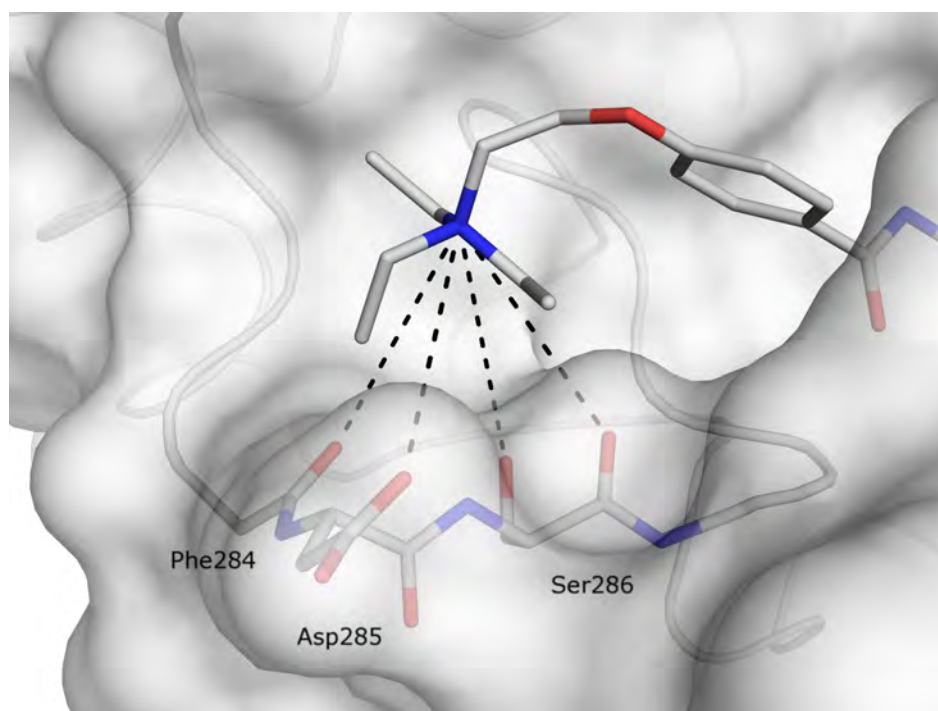
Figure 23: Polar contacts of compound **70** docked into acetylcholinesterase.
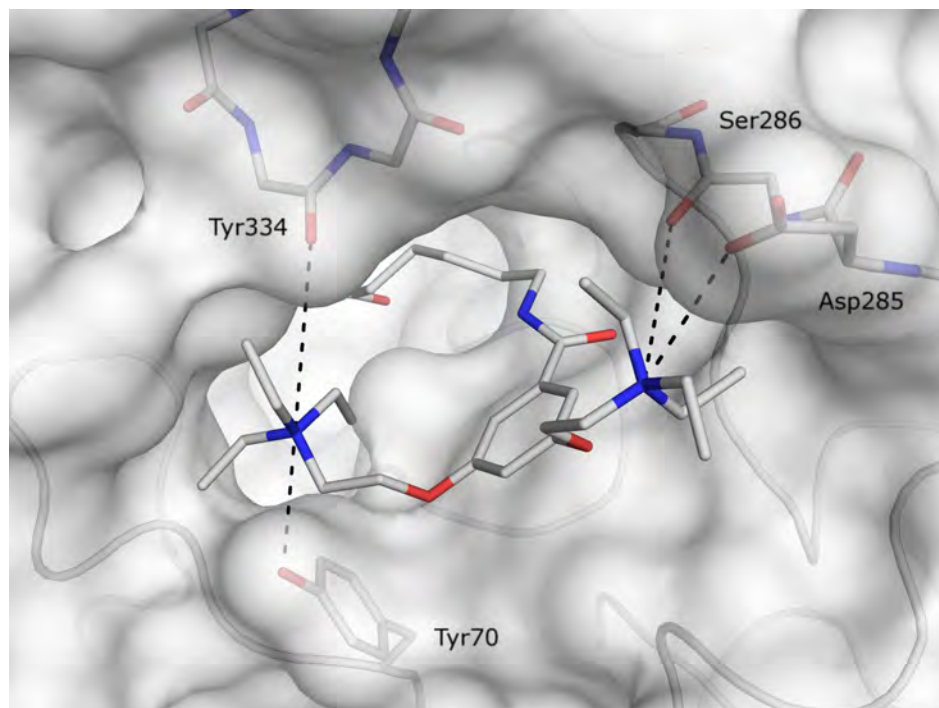
Figure 24: Polar contacts of compound **77** docked into acetylcholinesterase.
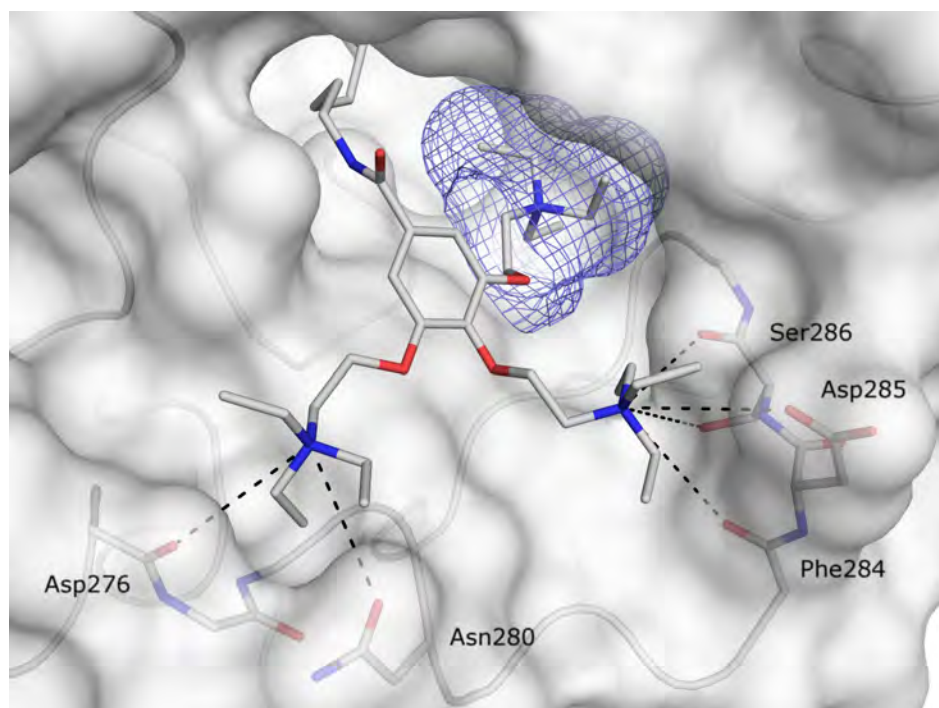
Figure 25: Polar contacts of compound **85** docked into acetylcholinesterase.
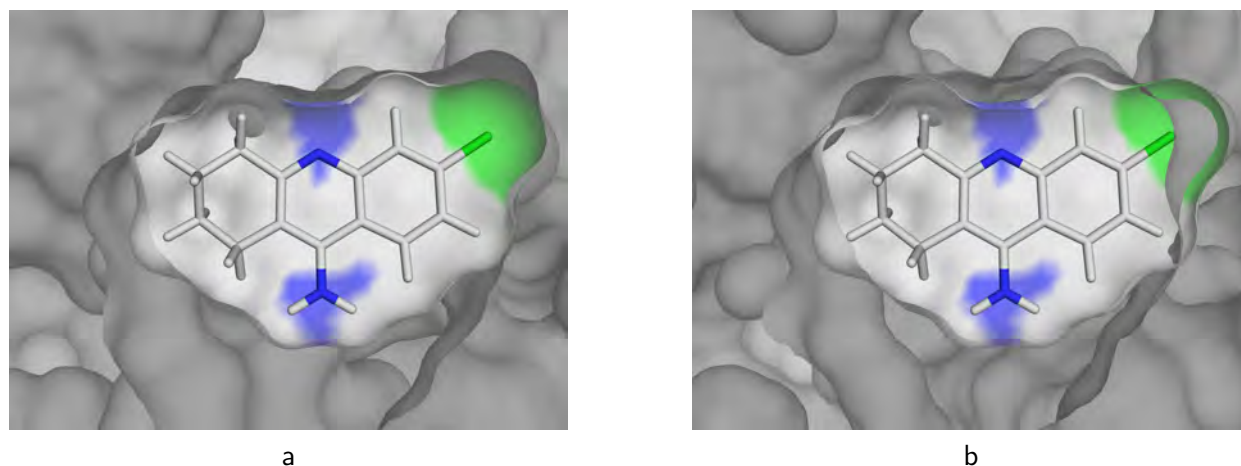
Figure 26: Acetylcholinesterase selectivity: 6-chloro-1,2,3,4-tetrahydroacridine posed into a) HsAChE and b) HsBChE.

3.5 Cholinesterase selectivity

Chapter 4 shows that a chlorine substitution at C6 of the tacrine moiety turns selectivity from butyryl- to acetylcholinesterase by up to a 5-fold. Savini *et al.*[100] suggested that the substitution of Pro[446] in HsAChE by the bulkier Met[437] in HsBChE does not allow the perfect accomodation of the tacrine analogue as in HsAChE. Figure 26 shows a comparison of 6-chloro-1,2,3,4-tetrahydroacridine binding to human acetyl- or butyrylcholinesterase. One can see that the active site pocket of butyrylcholinesterase is too small to accommodate the chlorine, while it perfectly fits into acetylcholinesterase. To avoid this situation the 6-chloro-1,2,3,4-tetrahydroacridine needs to move only little out of the BChE active site pocket. This small impairment is reflected by the small gain in selectivity towards AChE. To see if

also docking investigations would proof the BChE selectivity of compounds **8**, **56** and **60**, compound **60** was docked into human AChE[33] and BChE[34]. Unfortunately no insight was gained on this selectivity. As depicted in Figure 27 **60** binds to AChE and BChE in similar fashion. As expected, the tacrin moiety is oriented towards the active site, while the trimethoxy benzene ring resides at the gorge entrance, where it switches the side between AChE and BChE. From the point of docking though, the binding to AChE frees more energy than to BChE (STC ΔG_{bind}: AChE -14.66 kcal/mol, BChE -11.51 kcal/mol) and thus predicts a selectivity towards AChE. Probably induced folding of the gorge entrance upon binding leads to this selectivity, which cannot be observed by molecular docking.
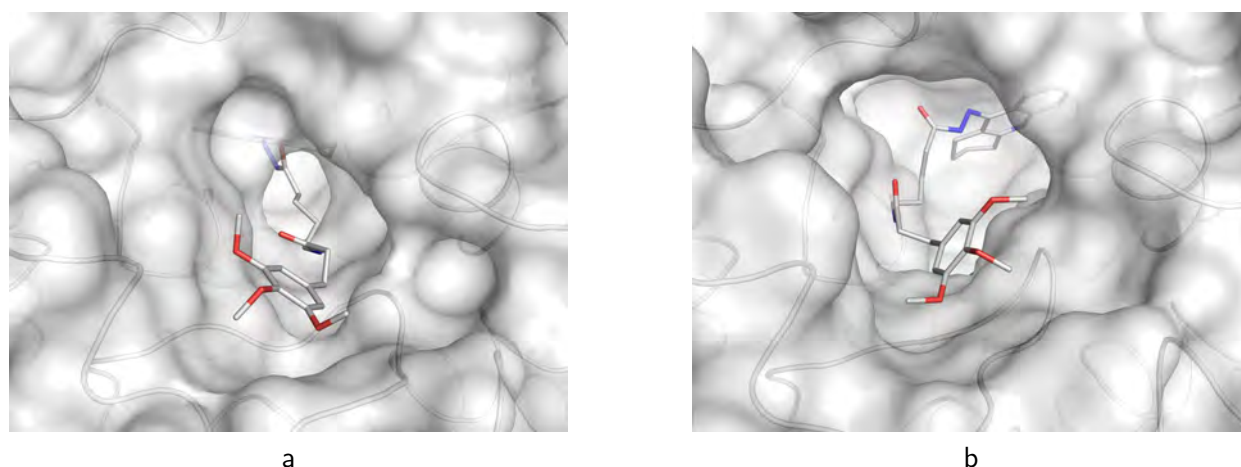
Figure 27: Butyrylcholinesterase selectivity: compound **60** docked into a) HsAChE and b) HsBChE.

4 Enzyme kinetics

4.1 Theoretical background

Reversible enzyme inhibition

Reversible enzyme inhibition refers to the negative action of small molecules on enzyme activity. These small molecules, also called ligands, will bind to either the ortho- or allosteric binding site of the enzyme and thus impair the enzyme in its catalytic function, *e.g.* the hydrolysis of acetylcholine by acetylcholinesterase. A group of individual kinetic processes contributing to the overall observation are summarized in Figure 28.

Either the substrate S or the inhibitor I can bind to the free enzyme E, resulting in two binary complexes ES or EI. The equilibrium constant of the EI complex formation is called K_{ic}, the one for ES complex K_S. Both binary complexes may bind additionaly S or I, which in both cases leads to the ternary enzyme-substrate-inhibitor complex ESI. The equilibrium constants leading to ESI are referred to as K_{Si} and K_{iu}. In cases where the ESI complex retains catalytic activity it may still process the substrate leading to the product P with a corresponding rate constant k_6. Obviously the ES complex will also cleave the substrate with a specific rate constant k_2. The Michaelis constant K_m describes the dissociation of the enzyme-substrate complex and is defined in Eq. 1.

$$K_S = \frac{k_{-1}}{k_1} = \frac{[\text{E}][\text{S}]}{[\text{ES}]} \quad K_{Si} = \frac{k_{-5}}{k_5} = \frac{[\text{EI}][\text{S}]}{[\text{ESI}]}$$

$$K_{ic} = \frac{k_{-3}}{k_3} = \frac{[\text{E}][\text{I}]}{[\text{EI}]} \quad K_{iu} = \frac{k_{-4}}{k_4} = \frac{[\text{ES}][\text{I}]}{[\text{ESI}]}$$

$$K_m = \frac{k_{-1} + k_2}{k_1} \tag{1}$$

Eq. 2 constitutes $[\text{E}]_0$, the overall enzyme concentration, as the sum of free enzyme and all complexes; transformation to Eq. 3 gives the corresponding expression for $[\text{E}]$.

$$[\text{E}]_0 = [\text{E}] + [\text{ES}] + [\text{EI}] + [\text{ESI}] \tag{2}$$

$$= [\text{E}] + [\text{ES}] + \frac{[\text{E}][\text{I}]}{K_{ic}} + \frac{[\text{ES}][\text{I}]}{K_{iu}}$$
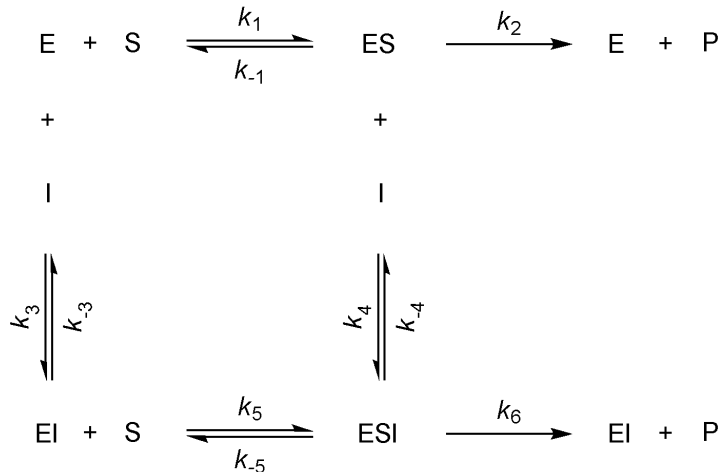
Figure 28: Reversible enzyme inhibition: a schematic representation. E = enzyme, S = substrate, I = inhibitor, P = product

$$[E] = [E]_0 - [ES] - \frac{[E][I]}{K_{ic}} - \frac{[ES][I]}{K_{iu}}$$

$$[E] + \frac{[E][I]}{K_{ic}} = [E]_0 - [ES]\left(1 + \frac{[I]}{K_{iu}}\right)$$

$$[E] = \frac{[E]_0 - [ES]\left(1 + \frac{[I]}{K_{iu}}\right)}{1 + \frac{[I]}{K_{ic}}} \tag{3}$$

The combination of an [EI] equivalent and the differential equation for the concentration of free enzyme (Eq. 4) leads to the steady-state expression shown in Eq. 5.

$$0 = \frac{d[E]}{dt} = (k_{-1} + k_2)[ES] - (k_1[S] + k_3[I])[E]$$
$$+ k_{-3}[EI] \tag{4}$$

$$0 = (k_{-1} + k_2)[ES] - (k_1[S] + k_3[I])[E] + k_{-3}[EI]$$

$$0 = (k_{-1} + k_2)[ES] - (k_1[S] + k_3[I])[E] + k_3[E][I]$$

$$0 = (k_{-1} + k_2)[ES] - k_1[S][E]$$

$$[E] = \frac{(k_{-1} + k_2)[ES]}{k_1[S]} \tag{5}$$

Eq. 3 and 5 lead subsequently to an expression for the concentration of the enzyme-substrate complex [ES] that substitutes the discrete rate constants through their corresponding equilibrium constants (Eq. 6).

$$\frac{(k_{-1} + k_2)[ES]}{k_1[S]} = \frac{[E]_0 - [ES]\left(1 + \frac{[I]}{K_{iu}}\right)}{1 + \frac{[I]}{K_{ic}}}$$

$$\frac{[E]_0}{1 + \frac{[I]}{K_{ic}}} = [ES]\left(\frac{1 + \frac{[I]}{K_{iu}}}{1 + \frac{[I]}{K_{ic}}} + \frac{k_{-1} + k_2}{k_1[S]}\right)$$

$$= [ES]\left(\frac{1 + \frac{[I]}{K_{iu}}}{1 + \frac{[I]}{K_{ic}}} + \frac{K_m}{[S]}\right)$$

$$[ES] = \frac{[E]_0}{\left(1 + \frac{[I]}{K_{ic}}\right)\left(\dfrac{1 + \frac{[I]}{K_{iu}}}{1 + \frac{[I]}{K_{ic}}} + \dfrac{K_m}{[S]}\right)}$$

$$[ES] = \frac{[E]_0}{\dfrac{K_m}{[S]}\left(1 + \frac{[I]}{K_{ic}}\right) + \left(1 + \frac{[I]}{K_{iu}}\right)} \tag{6}$$

Finally, the differential equation for the product formation (Eq. 7) gives a relation between the observed reaction velocity v and the enzyme substrate complex concentration [ES]. In combination with Eq. 6, $V_1 = k_2[E]_0$ and $V_2 = k_6[E]_0$ one gets to the fundamental kinetic expression of reversible enzyme inhibition, Eq. 8.

$$v = \frac{d[P]}{dt} = k_2[ES] + k_6[ESI]$$

$$= \left(k_2 + \frac{k_6[I]}{K_{iu}}\right)[ES] \tag{7}$$

$$= \frac{\left(k_2 + \dfrac{k_6[I]}{K_{iu}}\right)[E]_0}{\dfrac{K_m}{[S]}\left(1 + \frac{[I]}{K_{ic}}\right) + \left(1 + \frac{[I]}{K_{iu}}\right)}$$

$$= \frac{V_1 + V_2 \dfrac{[I]}{K_{iu}}}{\dfrac{K_m}{[S]}\left(1 + \frac{[I]}{K_{ic}}\right) + \left(1 + \frac{[I]}{K_{iu}}\right)}$$

$$= \frac{\left(V_1 + V_2 \dfrac{[I]}{K_{iu}}\right)[S]}{K_m\left(1 + \frac{[I]}{K_{ic}}\right) + [S]\left(1 + \frac{[I]}{K_{iu}}\right)} \tag{8}$$

Mixed-type enzyme inhibition

Now, put the case that the enzyme-substrate-inhibitor complex [ESI] is incapable of substrate processing a so called dead-end complex is formed (Figure 29). With $k_6 = 0$ also V_2 becomes zero and Eq. 8 can be simplified to Eq. 9. Lineweaver and Burk[101] established a graphical representation of this expression taking the reciprocal of both the observed velocity and the used substrate concentration (Figure 31).

$$E \;+\; S \;\underset{k_{-1}}{\overset{k_1}{\rightleftharpoons}}\; ES \;\xrightarrow{\;k_2\;}\; E \;+\; P$$

$$+ \qquad\qquad\qquad +$$

$$I \qquad\qquad\qquad I$$

$$k_3 \Big\Updownarrow k_{-3} \qquad\qquad k_4 \Big\Updownarrow k_{-4}$$

$$EI \;+\; S \;\underset{k_{-5}}{\overset{k_5}{\rightleftharpoons}}\; ESI$$
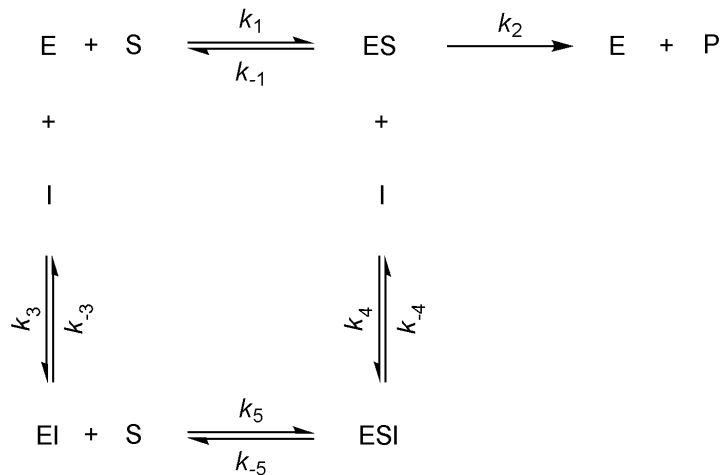
Figure 29: Complete enzyme inhibition: the ESI complex is incapable of substrate processing, $k_6 = 0$.

As can be concluded from Eq. 10, a corresponding diagram will lead to a linearized representation. The intercept with the abscissa results to $1/\text{-}K_\mathrm{m}$ if no inhibitor was present during the measurement[102].

$$v = \frac{V[S]}{K_\mathrm{m}\left(1 + \dfrac{[I]}{K_\mathrm{ic}}\right) + [S]\left(1 + \dfrac{[I]}{K_\mathrm{iu}}\right)} \tag{9}$$

$$\frac{1}{v} = \frac{K_\mathrm{m}\left(1 + \dfrac{[I]}{K_\mathrm{ic}}\right) + [S]\left(1 + \dfrac{[I]}{K_\mathrm{iu}}\right)}{V[S]}$$

$$= \frac{K_\mathrm{m}\left(1 + \dfrac{[I]}{K_\mathrm{ic}}\right)}{V} \cdot \frac{1}{[S]} + \frac{1 + \dfrac{[I]}{K_\mathrm{iu}}}{V} \tag{10}$$

Secondary plots are typically used to determine the equilibrium constants K_ic and K_iu. From the primary Lineweaver-Burk plot either slopes or intercepts are plotted against their corresponding inhibitor concentrations (Figure 32, 33). This produces again a line that crosses the abscissa at $1/\text{-}K_\mathrm{ic}$ or $1/\text{-}K_\mathrm{iu}$, respectively.

To minimize the error, that results from the second linerization process, it is recommended to use the slope or intercept for [I]=0 (Figure 32,

33) when analyzing the graph. Pictorially speaking this means that the trendline is parallelized through the intercept obtained for [I]=0, thus slightly shifting the K_ic and K_iu values.

$$\text{slopes} = \frac{K_\mathrm{m}\left(1 + \dfrac{[I]}{K_\mathrm{ic}}\right)}{V} \qquad \text{intercepts} = \frac{1 + \dfrac{[I]}{K_\mathrm{iu}}}{V}$$

$$0 = \frac{K_\mathrm{m}\left(1 + \dfrac{[I]_{0,\mathrm{s}}}{K_\mathrm{ic}}\right)}{V} \qquad 0 = \frac{1 + \dfrac{[I]_{0,\mathrm{i}}}{K_\mathrm{iu}}}{V}$$

$$K_\mathrm{ic} = [I]_{0,\mathrm{s}} \qquad\qquad K_\mathrm{iu} = [I]_{0,\mathrm{i}}$$

When obtaining the primary data it is of utmost importance to use every single data point for any fitting process. It is common practice to average data points that result from multiple determinations, *e.g.* three observations for one concentration in a concentration dependent assay. From a mathematical point of view this results in the same trendline, but minimizes the trendline error (SEM) as it results from a least square method. One has to carefully separate this from the scatter of measurement, which is reflected by the standard deviation of the data points. Only the use of all data points allows the interpretation of the SEM as a quality criterion.

4.2 Assay
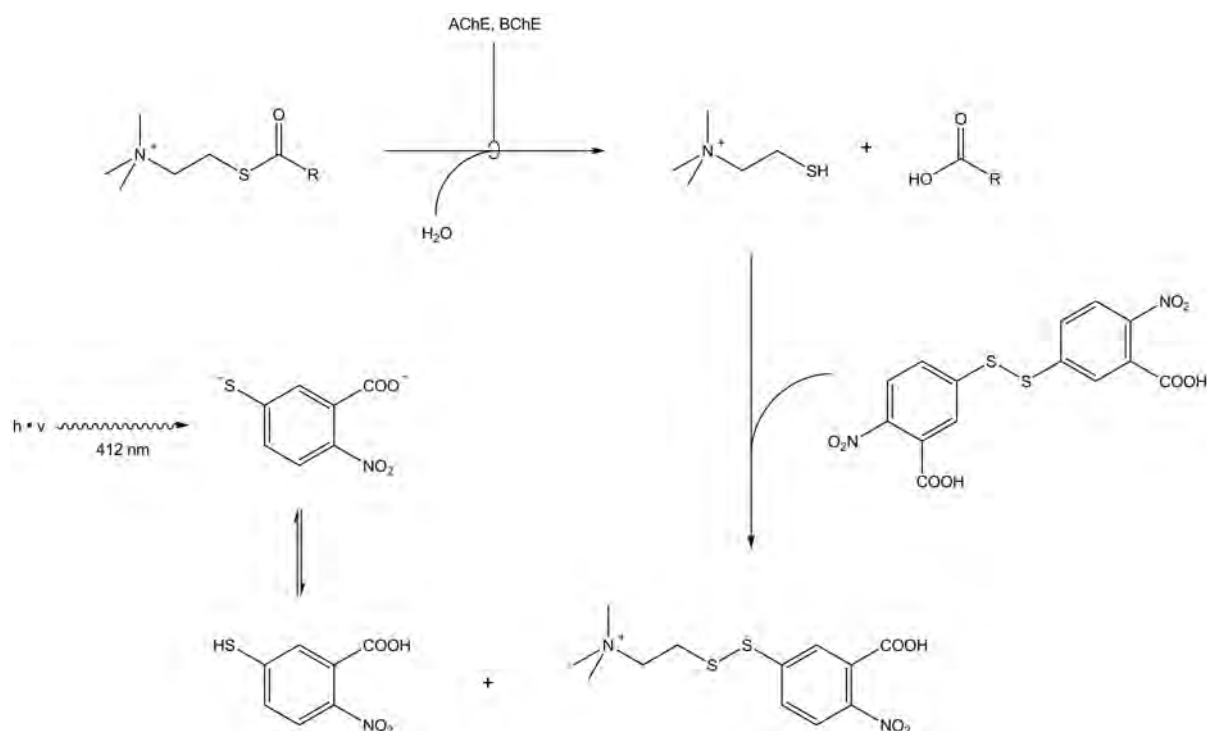
Figure 30: Ellman assay: AChE and BChE liberate SCh (thiocholine), that subsequently cleaves DTNB (5,5'-dithiobis-(2-nitrobenzoic acid)) to release MNB (5-mercapto-2-nitrobenzoic acid), that absorbes at 412 nm, R = methyl or butyl.

Enzyme activity of acetyl- and butyryl-cholinesterase was assayed following the procedure established by Ellman *et al.*[103] (Figure 30). Key reaction of this assay is the cleavage of 5,5'-dithiobis-(2-nitrobenzoic acid) (DTNB) by thiocholine (SCh) that frees equimolar amounts of 5-mercapto-2-nitrobenzoic acid (MNB). MNB has a strong yellow color and its formation can be conveniently followed using a spectrophotometer. This procedure allows the real time measurement of enzyme activity, as thiocholine is released by AChE and BChE from acetyl- (ASCh) or butyrylthiocholine (BSCh), respectively.

The following conditions were applied: assay buffer was 100 mM sodium phosphate, 100 mM sodium chloride at pH 7.3. DTNB (7 mM), ASCh (10 mM) and BSCh (10 mM) were dissolved in assay buffer and kept at 0 °C. Stock solutions of the inhibitors (5 mM) were prepared in a 1:1 mixture of 0.1 M hydrochloric acid and acetonitrile. Subsequent dilutions were prepared using the same solvent.

Acetylcholinesterase was purchased from Fluka (Deisenhofen, Germany) (*Electrophorus electricus*), Sigma (Steinheim, Germany) (*Homo sapiens*) and butyrylcholinesterase from Lee Biosolutions (St. Louis, USA) (*Homo sapiens*). Acetylcholinesterase from *Torpedo californica* was a kind gift from the Institute for Physiological Chemistry, University of Bonn, Germany. Enzyme stock solutions of AChE (~3 U/ml) and BChE (~10 U/ml) in assay buffer were kept at 0 °C. Appropriate dilutions were prepared immediately before starting the measurement.

10 µl of a cholinesterase solution (~3 U/ml) was added to a cuvette containing 825 µl assay buffer, 50 µl DTNB solution, 55 µl acetonitrile and 10 µl inhibitor solution. The solution was thoroughly mixed and incubated for 15 minutes at 25 °C. The reaction was initiated by adding 50 µl of the ASCh- or BSCh-solution and subsequently followed for 5 minutes at 412 nm using a Varian Cary 50 spectrophotometer. Data analysis was performed using the Grace software[104].

4.3 Results

Determination of K_m, K_{ic} and K_{iu}

Compound **35** was chosen as a representative of the donepezil analogues for detailed examination of the binding mode.

As pointed out above, an approach according to Lineweaver and Burk[101] was undertaken. Starting from the IC_{50} value of 3.64 nM, that was obtained for **35** as discussed below, a range of four inhibitor concentrations [0, 2, 4, 6 nM] was selected. For each of these the enzyme activity was assessed at four different substrate concentrations [250, 500, 750, 1000 µM]. Figure 31 shows the corresponding Lineweaver-Burk plot, where the reciprocals of both variables are used. Following Dixon[102] one can use the trendline for [I]=0 to obtain K_m. Producing the line to the left of the vertical axis finally leads to an intercept with the abscissa at $1/\text{-}K_m$. From this, K_m was calculated to be 598 ± 20 µM, which is in accordance with the literature[105]. The overall high K_m value is probably due to the presence of 6 % acetonitrile.

From the Lineweaver-Burk plot, where the trendlines intersect slightly below the abscissa, it can be concluded, that compound **35** binds to both,

the binary complexe ES and the free enzyme E, with slight preference for the enzyme-substrate complex. Inhibitors that show this preference are therefore referred to as mixed-type inhibitors of slightly more uncompetitive character. The degree of preference between ES and E is defined as α with $\alpha = K_{iu}/K_{ic}$. To reinforce this finding from the Lineweaver-Burk, plot K_{ic} and K_{iu} were also obtained from secondary plots. As explained before, either the slopes (Figure 32) or intercepts (Figure 33) are plotted against their corresponding inhibitor concentrations. The abscissa intercept produces $K_{ic} = 3.70 \pm 0.15$ nM and $K_{iu} = 3.25 \pm 0.18$ nM, respectively. The α value results to 0.88 ± 0.06, which is in accordance with the finding, that **35** is slightly more uncompetitive.

The docking studies showed that all compounds bind more or less tightly to the peripheral binding site. This is consistent with the kinetic findings for compound **35** and can be expected to hold true for the other compounds. The trimethoxybenzene moiety allows these substances to bind to the PAS, no matter whether the active site is occupied or not, and results in slightly more uncompetitive inhibitors.
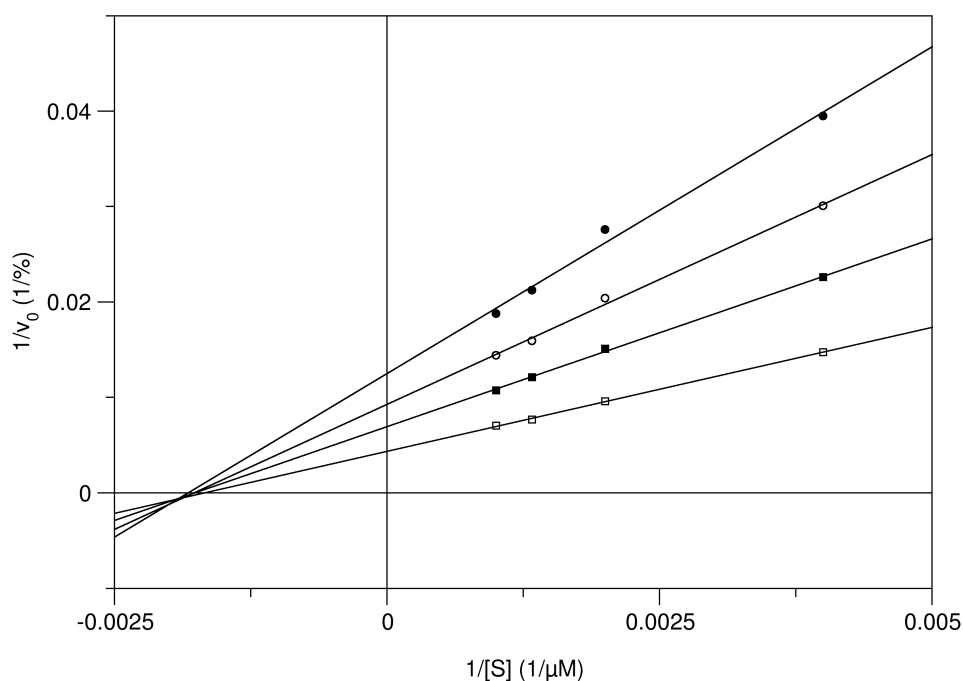
Figure 31: Lineweaver-Burk plot. •: [**35**] = 6 nM, ○: [**35**] = 4 nM, ■: [**35**] = 2 nM, □: no inhibitor.
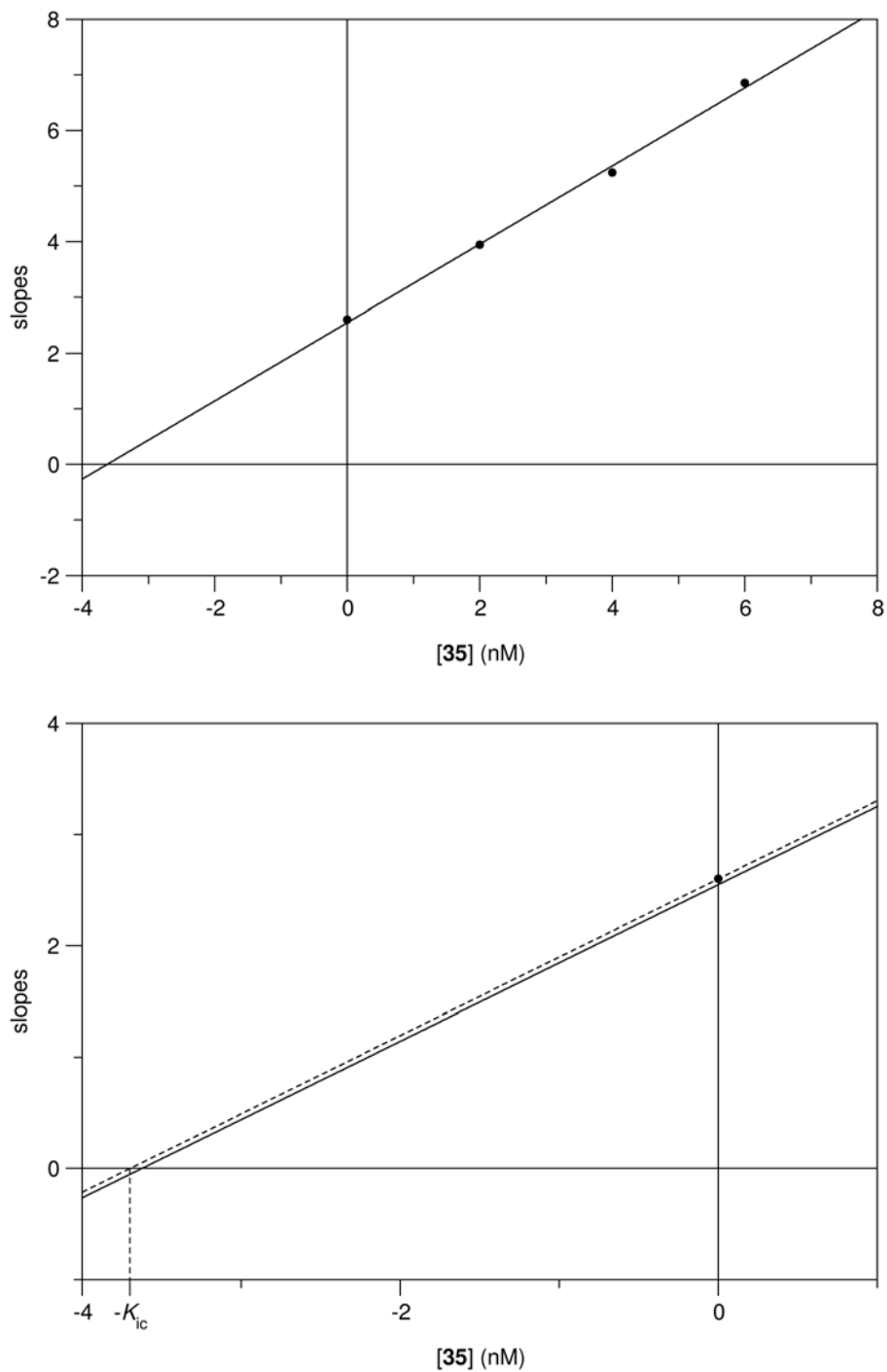
Figure 32: K_{ic} determination: the lower graph shows a closeup of the parallelization process. $K_{ic} = 3.70 \pm 0.15\,\text{nM}$
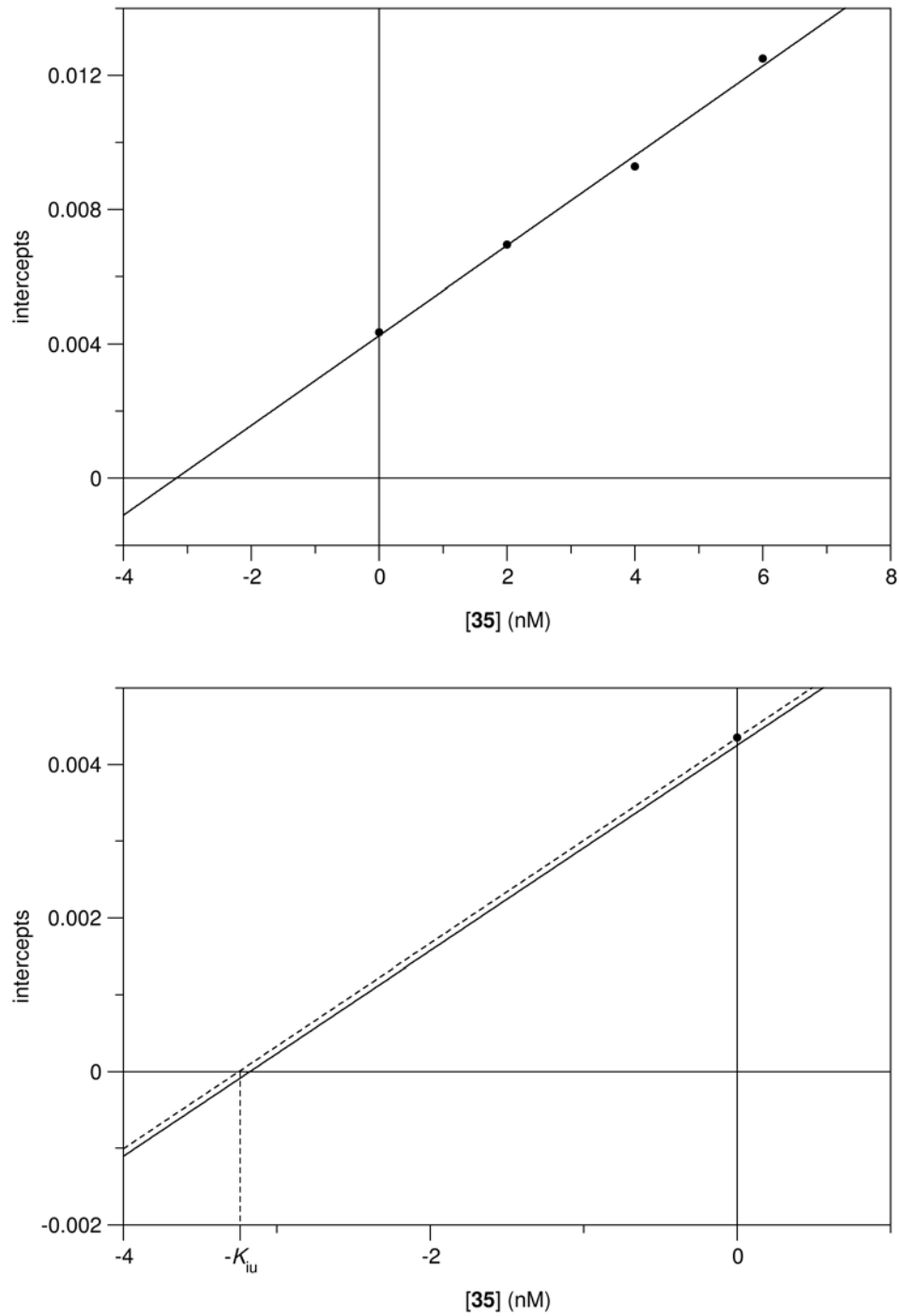
Figure 33: K_{iu} determination: the lower graph shows a closeup of the paralleliza-
tion process. $K_{iu} = 3.25 \pm 0.18\,\text{nM}$

Determination of IC$_{50}$ values

One possibility to compare the inhibitory potency of a series of inhibitors is the use of IC$_{50}$ values, that represent those inhibitor concentrations that reduce the enzyme activity to 50 %. Alternatively, K_{ic} values can be used, which are independent from the applied substrate concentration and may therefore be used for comparison with data from other assays. As the IC$_{50}$ value is located inside the intervall $[K_{ic}, K_{iu}]$ it is obvious, that the closer α gets to 1, the closer K_{ic} gets to IC$_{50}$ (Eq. 11).

$$\lim_{\alpha \to 1} K_{ic} = K_{iu} = \text{IC}_{50} \qquad (11)$$

For mixed-type inhibitors it is much less time-consuming to obtain IC$_{50}$ values, than K_{ic} values, because the substrate concentration needs not to be varied. In cases were α is close to 1, as it was found for **35** and suggested for all other compounds, IC$_{50}$ values are a reasonable tool for comparison.

Their determination typically involves a preliminary screening to obtain an estimate. Stepwise dilutions are prepared and investigated until a concentration is found that results in a 20-80 % inhibition of the target enzyme and an estimate IC$_{50}$ value is calculated using Eq. 12. From this a range of inhibitor concentrations spanning the estimate is chosen and the corresponding enzyme activity is determined. The activity values are then plotted against concentrations as depicted in Figure 34. The hyperbolic trendline is obtained by non-linear regression analysis using Eq. 13.

$$\text{IC}_{50} = \frac{[\text{I}]}{\frac{v_0}{v} - 1} \qquad (12)$$

$$v = \frac{v_0}{1 + \frac{[\text{I}]}{\text{IC}_{50}}} \qquad (13)$$

The following tables list the obtained IC$_{50}$ values for four cholinesterases: acetylcholinesterase from *Electrophorus electricus*, *Torpedo californica*, *Homo sapiens* and butyrylcholinesterase from *Homo sapiens* (part of the kinetic measurements were carried out by C.M. González Tanarro). Additionally, the selectivity between human acetyl- and butyrylcholinesterase (Eq. 14) is given, where values larger than 1 state a selectivity and its degree towards butyrylcholinesterase.

$$selectivity = \frac{\text{HsAChE IC}_{50}}{\text{HsBChE IC}_{50}} \qquad (14)$$
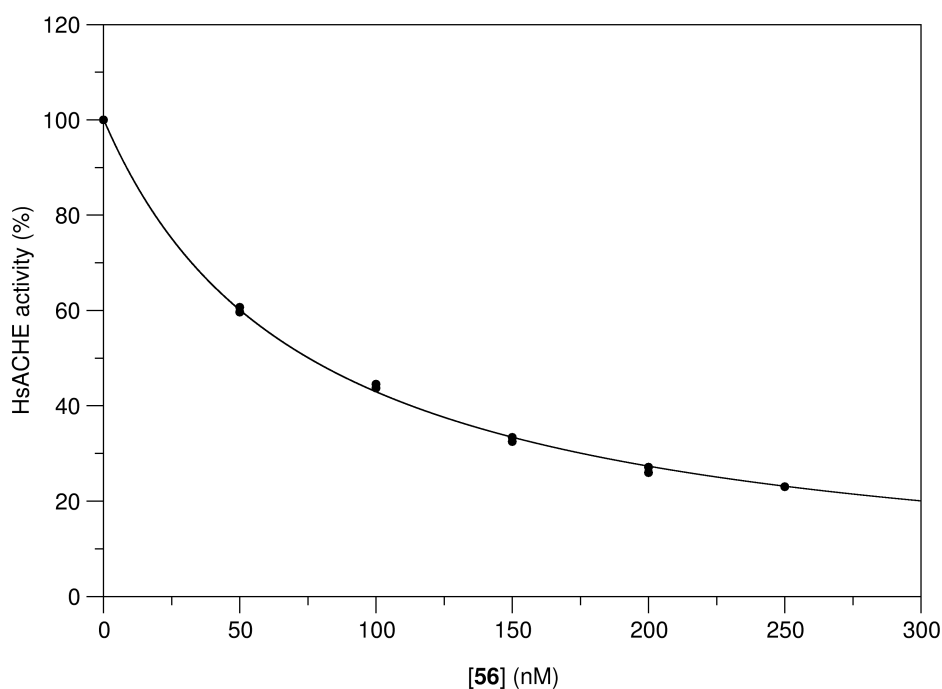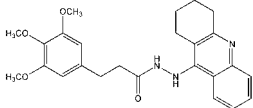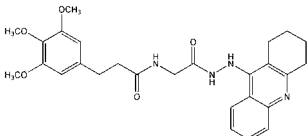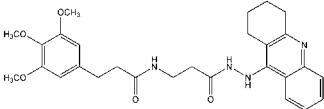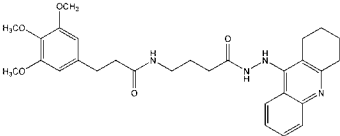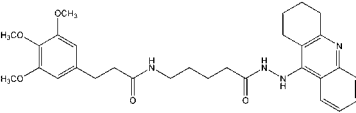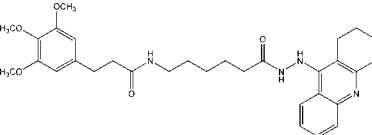
Figure 34: IC$_{50}$ determination.

Table 4: IC$_{50}$ values [nM] $\pm$ SEM of compounds derived from 3,4,5-trimethoxybenzoic acid.

Compound	Structure	EeAChE[106]	TcAChE
8		2260 $\pm$ 142	21.1 $\pm$ 0.9
12		104 $\pm$ 4	163 $\pm$ 13
16		100 $\pm$ 3	49.5 $\pm$ 2.0
20		60.5 $\pm$ 4.8	26.3 $\pm$ 2.0
24		20.2 $\pm$ 1.1	18.1 $\pm$ 2.1
28		20.1 $\pm$ 1.4	55.7 $\pm$ 4.3
31		9.76 $\pm$ 0.44	25.2 $\pm$ 0.8
32		131 $\pm$ 5	1260 $\pm$ 105
35		3.64 $\pm$ 0.38	17.2 $\pm$ 0.3
36		78.9 $\pm$ 5.6	647 $\pm$ 23
39		2.73 $\pm$ 0.25	5.99 $\pm$ 0.44
40		77.2 $\pm$ 2.9	691 $\pm$ 16

Table 5: IC$_{50}$ values [nM] $\pm$ SEM of compounds derived from 3-(3,4,5-trimethoxyphenyl)-propionic acid.

Compound	Structure	EeAChE[106]	TcAChE
44		294 $\pm$ 28	40.1 $\pm$ 2.1
48		122 $\pm$ 8	40.1 $\pm$ 4.3
52		102 $\pm$ 10	68.9 $\pm$ 4.4
56		52.1 $\pm$ 5.4	158 $\pm$ 1
60		54.7 $\pm$ 3.4	102 $\pm$ 4
64		20.2 $\pm$ 2.0	39.8 $\pm$ 1.0

Comparing the compounds, belonging either to the 3,4,5-trimethoxybenzoic or the 3-(3,4,5-trimethoxyphenyl)propionic acid series (Table 4, 5, 7 and 8), two major trends are observed.

With increasing linker length one finds a steady increase in potency towards acetylcholinesterase. This is perfectly seen with AChE from *Electrophorus electricus* and with little exceptions for the human enzyme, but not for AChE from *Torpedo californica*. Table 10 shows an amino acid sequence alignment for the investigated acetylcholinesterases with highlighted residues, that contribute to the gorge. While EeAChE and HsAChE are very close with respect to their gorge forming residues, the enzyme from *Torpedo californica* differs in 17 % from EeAChE and HsAChE. This can explain, why TcAChE does not show the steady increase in potency, but accepts also smaller hybrids as good inhibitors.
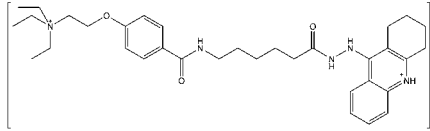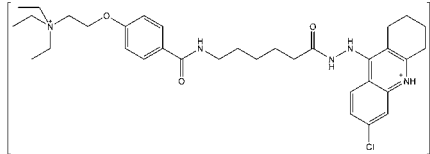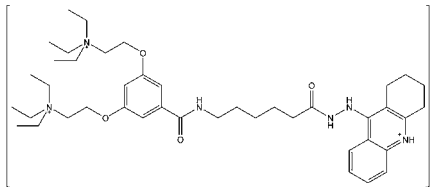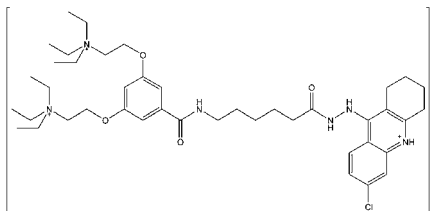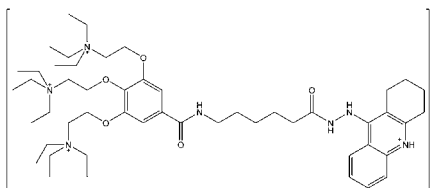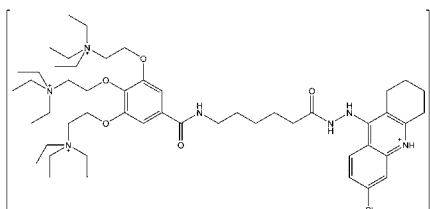
In contrast to other reports[71,107], that found a seven methylene linker to be the optimal distance

for heterobivalent inhibitors of AChE, this work shows that also considerably longer spacers will lead to potent inhibitors of cholinesterases. The most potent AChE inhibitors incorporate a spacer of eleven or twelve atoms inside their chain. Most of the final compounds synthesized show IC$_{50}$ values in the lower nanomolar range.

When comparing donepezil analogues of equal overall linker length, *i.e.* **28** to **56** and **31** to **60**, one finds, that compounds derived from 3,4,5-trimethoxybenzoic acid are superior to those derived from 3-(3,4,5-trimethoxyphenyl)propionic acid. It is probably the benzoic acid moiety, that mimicks the indanone of donepezil more closely and therefore leads to superior inhibitors.

Until now literature reports[100,108,109] state, that a C6-chlorine substitution of tacrine increases potency towards both, HsAChE and EeAChE. But for compounds **32**, **36** and **40** the opposite is observed. The chlorine substitution at C6 of the tacrine moiety results in a notable loss of inhibi-

Table 6: IC$_{50}$ values [nM] $\pm$ SEM of quaternary compounds.

Compound	Structure	EeAChE	TcAChE
70		0.467 $\pm$ 0.032	17.6 $\pm$ 1.6
71		26.0 $\pm$ 1.9	127 $\pm$ 3
77		1.28 $\pm$ 0.05	8.59 $\pm$ 0.27
78		48.0 $\pm$ 3.4	301 $\pm$ 10
85		28.9 $\pm$ 2.4	27.7 $\pm$ 1.6
86		90.0 $\pm$ 3.4	334 $\pm$ 41

tory potency towards the acetylcholinesterase from *Electrophorus electricus* and *Torpedo californica* (Table 4). Only for the human enzyme, some improvement inside the gallamine series was found when chlorine-substituted at C6 (Table 7). Nevertheless, one has to keep in mind that the binding mode of these hydrazine analogues may slightly differ from tacrine and thus be impaired by the chlorine substitution (see also Chapter 3).

With the mono-quaternary gallamine derivate **70** the most potent acetylcholinesterase inhibitor of

the three series was found with an IC$_{50}$ value of about 500 pM (Table 6). All gallamine derivatives (Table 6 and 9) lost stepwise in potency towards AChE, as their degree of substitution increased. They still show significantly improved inhibitory potency compared to tacrine and gallamine (Figure 8), but the real gallamine-tacrine dimer **85** is not the expected most potent inhibitor. The reason for this steady loss in potency is probably not the increase in charge, but rather the bulky alkyl residues, that impair the binding by consuming torsional energy (see also Chapter 3).

Table 7: IC$_{50}$ values [nM] $\pm$ SEM of compounds derived from 3,4,5-trimethoxybenzoic acid.

Compound	Structure	HsAChE	HsBChE[106]	Selectivity
8		386 ± 24	1.70 ± 0.18	227
12		51.6 ± 2.1	27.6 ± 1.0	1.9
16		89.2 ± 6.2	12.8 ± 1.1	7.0
20		241 ± 8	7.13 ± 0.46	34
24		17.0 ± 1.4	1.68 ± 0.15	10.1
28		18.2 ± 0.6	0.969 ± 0.098	18.8
31		5.65 ± 0.31	0.523 ± 0.018	10.80
32		7.76 ± 0.76	17.7 ± 0.8	0.4
35		5.24 ± 0.20	0.293 ± 0.014	17.9
36		5.93 ± 0.41	33.2 ± 1.2	0.2
39		5.08 ± 0.22	1.38 ± 0.04	3.68
40		5.81 ± 0.87	11.9 ± 0.4	0.5

Table 8: IC$_{50}$ values [nM] $\pm$ SEM of compounds derived from 3-(3,4,5-trimethoxyphenyl)propionic acid.

Compound	Structure	HsAChE	HsBChE[106]	Selectivity
44		365 $\pm$ 21	12.1 $\pm$ 0.3	30
48		40.7 $\pm$ 3.5	24.0 $\pm$ 0.6	1.7
52		135 $\pm$ 5	6.03 $\pm$ 0.33	22
56		72.1 $\pm$ 1.6	0.226 $\pm$ 0.018	319.0
60		59.0 $\pm$ 0.52	0.139 $\pm$ 0.011	424.5
64		8.39 $\pm$ 0.14	0.141 $\pm$ 0.004	59.50

As pointed out before also butyrylcholinesterase is considered a valuable target for the treatment of Alzheimer's disease. Therefore, also the inhibitory potential of the final compounds towards HsBChE was investigated. Except for those compounds, that carry a chlorine at C6 of their tacrine moiety, all compounds show a preference for BChE regarding the human cholinesterases (Table 7, 8 and 9). Three compounds, **8**, **56** and **60**, were found as very selective inhibtors, with selectivity ratios between 200 and 400. The chlorine substitution turns this selectivity, as can be clearly seen in Table 7 and 9. The selectivity towards acetylcholinesterase is only of little extend, up to a 5-fold, which has been already reported for 6-chloro-1,2,3,4-tetrahydroacridine[108]. For those compounds with selectivity towards butyrylcholinesterase no trend regarding the linker length is observed, but comparing compounds of equal overall linker length, *i.e.* **28** and **56** or **31** and **60**, shows that the type of linker has significant influence on the selectivity. The introduction of an amide bond inside the linker (**56** and **60**) improves selectivity compared to compounds with the amide bond at linker end (**28** and **31**).

Though the reason for this remains unclear, hydrogen bonds to the AChE mid-gorge, *i.e.* Tyr[124] and Tyr[337], may lead to unfavourable, torsional constraints of the alkyl linker. This negative contribution may actually exceed the gain from remaining hydrophobic contacts and result in a less efficient binding. On the other hand the BChE gorge offers more space and relies mainly on hydrophobic interactions. Here the linker orientation may not be driven by hydrogen bonds and result in a positive energy contribution, a more efficient binding.

Table 9: IC$_{50}$ values [nM] $\pm$ SEM of quaternary compounds.
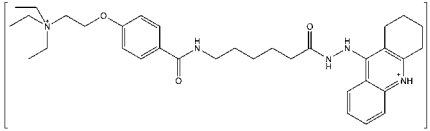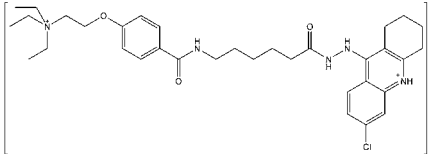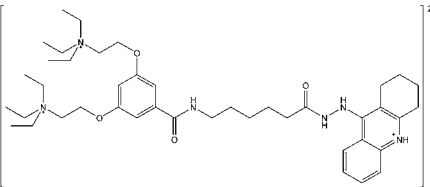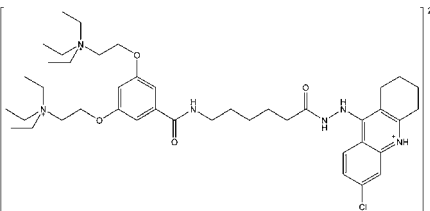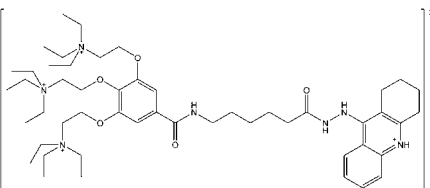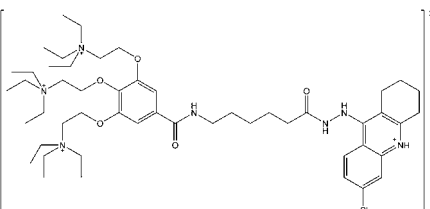
Compound	Structure	HsAChE	HsBChE[106]	Selectivity
70		7.61 $\pm$ 0.41	1.50 $\pm$ 0.08	5.07
71		5.44 $\pm$ 0.48	8.55 $\pm$ 0.42	0.64
77		15.8 $\pm$ 0.8	1.42 $\pm$ 0.07	11.1
78		6.75 $\pm$ 0.36	16.7 $\pm$ 1.9	0.4
85		23.2 $\pm$ 1.2	2.40 $\pm$ 0.14	9.7
86		6.54 $\pm$ 0.44	26.5 $\pm$ 0.9	0.3

Table 10: Sequence alignment of EeAChE (PDB 1C2O), HsAChE (PDB 1B41) and TcAChE (PDB 1EVE). Gorge-forming amino acids are highlighted: ☐ = sequence identical, ☐ = sequence different.

```
EeAChE     5    DPQLLVRVRGGQLRGIRLKAPGGPVSAFLGIPFAEPPVGSRRFMPPEPKR    54
HsAChE     5    DAELLVTVRGGRLRGIRLKTPGGPVSAFLGIPFAEPPMGPRRFLPPEPKQ    54
TcAChE     3    HSELLVNTKSGKVMGTRVPVLSSHISAFLGIPFAEPPVGNMRFRRPEPKK    52

EeAChE    55    PWSGVLDATTFQNVCYQYVDTLYPGFEGTEMWNPNRELSEDCLYLNVWTP   104
HsAChE    55    PWSGVVDATTFQSVCYQYVDTLYPGFEGTEMWNPNRELSEDCLYLNVWTP   104
TcAChE    53    PWSGVWNASTYPNNCQQYVDEQFPGFSGSEMWNPNREMSEDCLYLNIWVP   102

EeAChE   105    YPRPASPTPVLIWIYGGGFYSGAASLDVYDGRFLAQVEGAVLVSMNYRVG   154
HsAChE   105    YPRPTSPTPVLVWIYGGGFYSGASSLDVYDGRFLVQAERTVLVSMNYRVG   154
TcAChE   103    SPRPKS-TTVMVWIYGGGFYSGSSTLDVYNGKYLAYTEEVVLVSLSYRVG   151

EeAChE   155    TFGFLALPGSREAPGNVGLLDQRLALQWVQENIAAFGGDPMSVTLFGESA   204
HsAChE   155    AFGFLALPGSREAPGNVGLLDQRLALQWVQENVAAFGGDPTSVTLFGESA   204
TcAChE   152    AFGFLALHGSQEAPGNVGLLDQRMALQWVHDNIQFFGGDPKTVTIFGESA   201

EeAChE   205    GAASVGMHILSLPSRSLFHRAVLQSGTPNGPWATVSAGEARRRATLLARL   254
HsAChE   205    GAASVGMHLLSPPSRGLFHRAVLQSGAPNGPWATVGMGEARRRATQLAHL   254
TcAChE   202    GGASVGMHILSPGSRDLFRRAILQSGSPNCPWASVSVAEGRRRAVELGRN   251

EeAChE   255    VGCPPGGAGGNDTELIACLRTRPAQDLVDHEWHVLPQESIFRFSFVPVVD   304
HsAChE   255    VGCPPGGTGGNDTELVACLRTRPAQVLVNHEWHVLPQESVFRFSFVPVVD   304
TcAChE   252    LNCNLN----SDEELIHCLREKKPQELIDVEWNVLPFDSIFRFSFVPVID   297

EeAChE   305    GDFLSDTPEALINTGDFQDLQVLVGVVKDEGSYFLVYGVPGFSKDNESLI   354
HsAChE   305    GDFLSDTPEALINAGDFHGLQVLVGVVKDEGSYFLVYGAPGFSKDNESLI   354
TcAChE   298    GEFFPTSLESMLNSGNFKKTQILLGVNKDEGSFFLLYGAPGFSKDSESKI   347

EeAChE   355    SRAQFLAGVRIGVPQASDLAAEAVVLHYTDWLHPEDPTHLRDAMSAVVGD   404
HsAChE   355    SRAEFLAGVRVGVPQVSDLAAEAVVLHYTDWLHPEDPARLREALSDVVGD   404
TcAChE   348    SREDFMSGVKLSVPHANDLGLDAVTLQYTDWMDDNNGIKNRDGLDDIVGD   397

EeAChE   405    HNVVCPVAQLAGRLAAQGARVYAYIFEHRASTLTWPLWMGVPHGYEIEFI   454
HsAChE   405    HNVVCPVAQLAGRLAAQGARVYAYVFEHRASTLSWPLWMGVPHGYEIEFI   454
TcAChE   398    HNVICPLMHFVNKYTKFGNGTYLYFFNHRASNLVWPEWMGVIHGYEIEFV   447

EeAChE   455    FGLPLDPSLNYTTEERIFAQRLMKYWTNFARTGDPNDPRDSKSPQWPPYT   504
HsAChE   455    FGIPLDPSRNYTAEEKIFAQRLMRYWANFARTGDPNEPRDPKAPQWPPYT   504
TcAChE   448    FGLPLVKELNYTAEEEALSRRIMHYWATFAKTGNPNEPHSQES-KWPLFT   496

EeAChE   505    TAAQQYVSLNLKPLEVRRGLRAQTCAFWNRFLPKLLSAT              543
HsAChE   505    AGAQQYVSLDLRPLEVRRGLRAQACAFWNRFLPKLLSAT              543
TcAChE   497    TKEQKFIDLNTEPMKVHQRLRVQMCVFWNQFLPKLLNAT              535
```

Table 11: Sequence alignment of HsAChE (PDB 1B41) and HsBChE (PDB 1P0I). Important amino acids referred to inside the text are highlighted: ▮.

```
HsAChE     5    DAELLVTVRGGRLRGIRLKTPGGPVSAFLGIPFAEPPMGPRRFLPPEPKQ     54
HsBCHE     1    EDDIIIATKNGKVRGMQLTVFGGTVTAFLGIPYAQPPLGRLRFKKPQSLT     50

HsAChE     55   PWSGVVDATTFQSVCYQYVDTLYPGFEGTEMWNPNRELSEDCLYLNVWTP     104
HsBCHE     51   KWSDIWNATKYANSCCQNIDQSFPGFHGSEMWNPNTDLSEDCLYLNVWIP     100

HsAChE     105  YPRPTSPTPVLVWIYGGGFYSGASSLDVYDGRFLVQAERTVLVSMNYRVG     154
HsBCHE     101  APKPKNAT-VLIWIYGGGFQTGTSSLHVYDGKFLARVERVIVVSMNYRVG     149

HsAChE     155  AFGFLALPGSREAPGNVGLLDQRLALQWVQENVAAFGGDPTSVTLFGESA     204
HsBCHE     150  ALGFLALPGNPEAPGNMGLFDQQLALQWVQKNIAAFGGNPKSVTLFGESA     199

HsAChE     205  GAASVGMHLLSPPSRGLFHRAVLQSGAPNGPWATVGMGEARRRATQLAHL     254
HsBCHE     200  GAASVSLHLLSPGSHSLFTRAILQSGSFNAPWAVTSLYEARNRTLNLAKL     249

HsAChE     255  VGCPPGGTGGNDTELVACLRTRPAQVLVNHEWHVLPQESVFRFSFVPVVD     304
HsBCHE     250  TGCS----RENETEIIKCLRNKDPQEILLNEAFVVPYGTPLSVNFGPTVD     295

HsAChE     305  GDFLSDTPEALINAGDFHGLQVLVGVVKDEGSYFLVYGAPGFSKDNESLI     354
HsBCHE     296  GDFLTDMPDILLELGQFKKTQILVGVNKDEGTAFLVYGAPGFSKDNNSII     345

HsAChE     355  SRAEFLAGVRVGVPQVSDLAAEAVVLHYTDWLHPEDPARLREALSDVVGD     404
HsBCHE     346  TRKEFQEGLKIFFPGVSEFGKESILFHYTDWVDDQRPENYREALGDVVGD     395

HsAChE     405  HNVVCPVAQLAGRLAAQGARVYAYVFEHRASTLSWPLWMGVPHGYEIEFI     454
HsBCHE     396  YNFICPALEFTKKFSEWGNNAFFYYFEHRSSKLPWPEWMGVMHGYEIEFV     445

HsAChE     455  FGIPLDPSRNYTAEEKIFAQRLMRYWANFARTGDPNEPRDPKAPQWPPYT     504
HsBCHE     446  FGLPLERRDQYTKAEEILSRSIVKRWANFAKYGNPQETQN-QSTSWPVFK     494

HsAChE     505  AGAQQYVSLDLRPLEVRRGLRAQACAFWNRFLPKLLSAT     543
HsBCHE     495  STEQKYLTLNTESTRIMTKLRAQQCRFWTSFFPKV----     529
```

5 Receptor kinetics

The following section will briefly outline the results from receptor binding studies that were carried out by Cieslik *et al.*[110] (M_2 receptor) and Bogan *et al.*[111] (M_1 receptor). It will only highlight some aspects, that have been discovered, but will be published elsewere. Nevertheless this outline will contribute to an overall perspective of the pharmacological profile of the gallamine-tacrine hybrid inhibitors, especially of compounds **70** and **77**.

5.1 The M_1 receptor

The investigation of interactions between the gallamine and tacrine derived compounds and the M_1 receptor are only preliminary and not statistically secured. Nevertheless they show a promising influence on the [^{3}H]NMS binding. As can be seen in Figure 35, the addition of any compound **70**, **71** or **77** remarkably impairs the total binding of [^{3}H]NMS to M_1 receptors. A closer look on the three dose-response curves (Figure 36) shows that they differ with respect to their inflection points and the control curve. This suggests an allosteric interaction, because a direct competition between the orthosteric ligand, *i.e.* acetylcholine or [^{3}H]NMS, and the additional ligand would not shift the inflection points. These preliminary findings have to be reinforced, before a pharmacological action on the human M_1 receptor can be assumed.
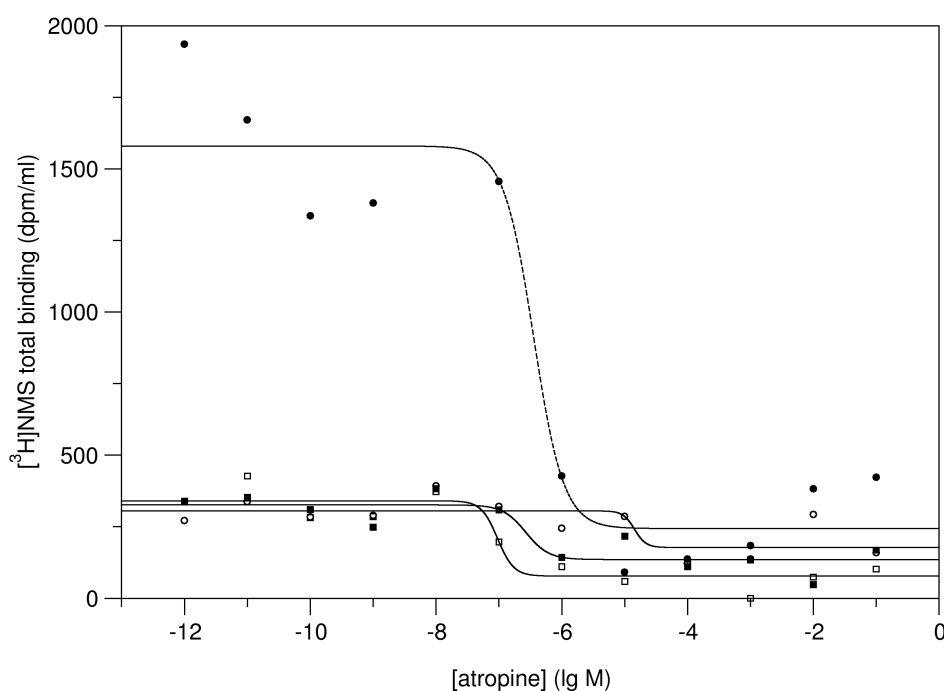
Figure 35: Compounds **70**, **71** and **77** significantly reduce the total binding of [^{3}H]NMS (tritiated *N*-methyl scopolamine) to human M_1 receptors. ● control, □ [PWE70] = ■ [PWE71] = ○ [PWE77] = 100 μM.
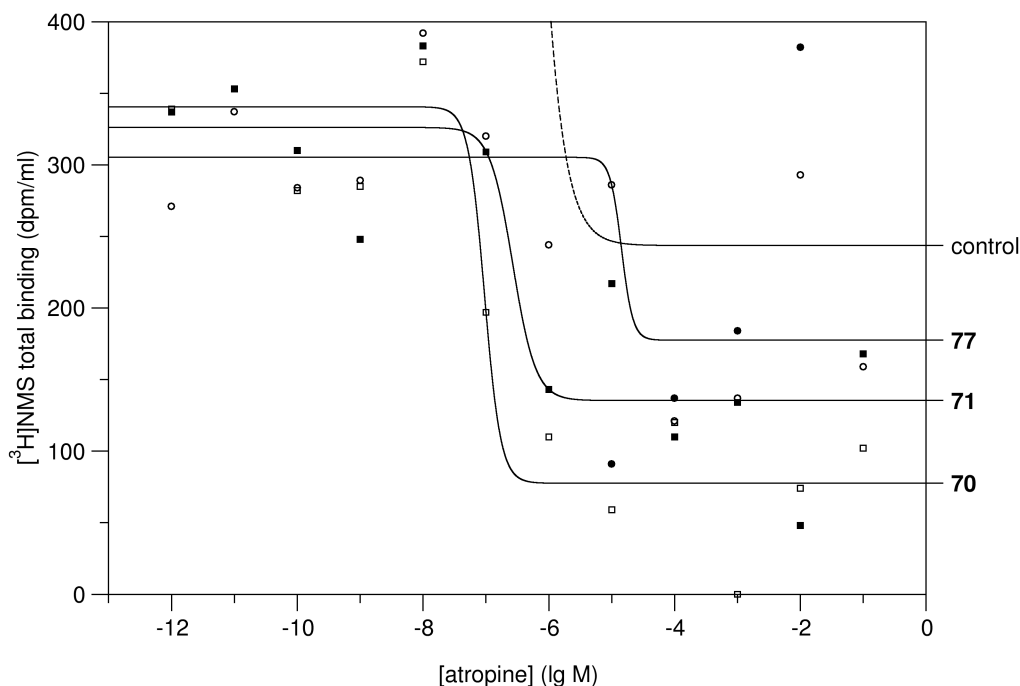
Figure 36: The effect on atropine induced [^{3}H]NMS dissociation differs for all three compounds **70**, **71** and **77**.

5.2 The M$_2$ receptor

Detailed investigations were undertaken to elucidate the interaction of compounds **70** and **77** with M$_2$ receptors. It was found that both compounds retard the [^{3}H]NMS dissociation as depicted in Figure 37. The effect of tacrine and gallamine, the two binding moieties combined in **70** and **77**, was estimated for comparison. They were found to retard [^{3}H]NMS dissociation in lower micromolar range (tacrine: $pEC_{50,diss} = 5.20 \pm 0.03$, gallamine: $pEC_{50,diss} = 6.94 \pm 0.09$), whereas compounds **70** and **77** were equieffective already in lower nanomolar concentrations (**70**: $pEC_{50,diss} = 8.88 \pm 0.06$, **77**: $pEC_{50,diss} = 9.07 \pm 0.09$). This is the 100/135-fold of gallamine and even the 5000/7000-fold compared to tacrine.

Another interesting observation is shown in Figure 38. Compounds **70** and **77** do not only effect the dissociation of [^{3}H]NMS from M$_2$ receptors, but they also interact with its associa-

tion. It was found that compound **77** impairs the binding of [^{3}H]NMS with increasing concentrations, which is referred to as negative cooperativity ($\alpha < 1$). This can be expected, because tacrine and gallamine have already been found to show a negative cooperativity. Suprisingly compound **70** shows the adverse effect. With increasing concentrations it enhances the [^{3}H]NMS binding upto 157 %, and is therefore referred to possess positive cooperativity ($\alpha > 1$).

Until now, none of the chlorine substituted analogues **71**, **78** or **86**, nor the exact gallamine-tacrine hybrid **85** have been investigated with respect to their allosteric action on M$_2$ receptors. It will be a challenge to establish comparable results for M$_1$ and M$_2$ receptors looking for subtype selective characteristics, that may make them valuable tools in pharmacological research.
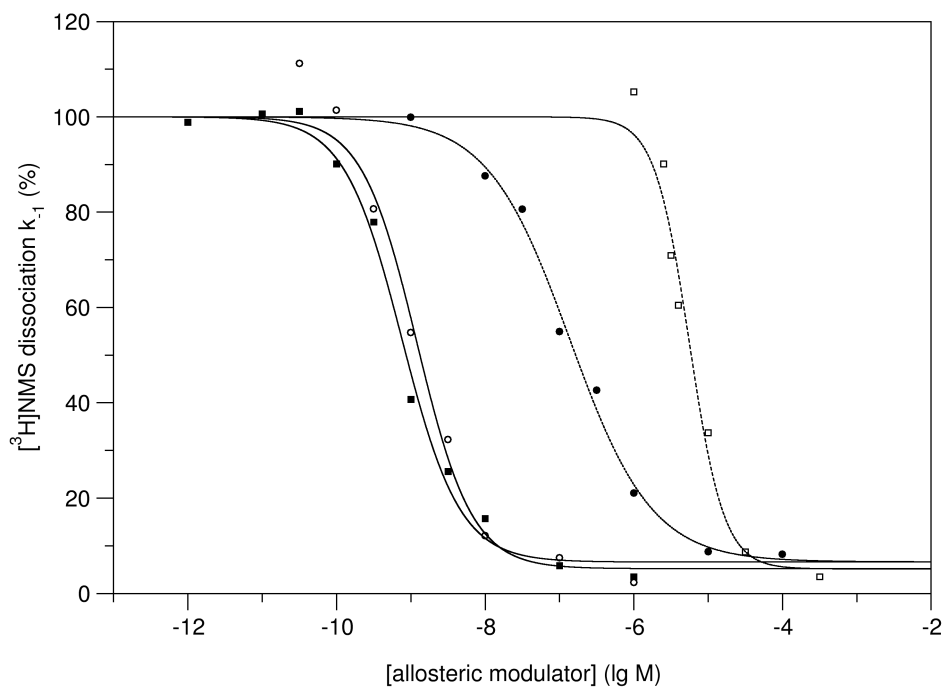
Figure 37: All allosteric modulators, tacrine ($\square$), gallamine ($\bullet$), **70** ($\circ$) and **77** ($\blacksquare$), retard the [^{3}H]NMS dissociation. While gallamine and tacrine effect the M$_2$ receptor in micromolar range, the novel compounds **70** and **77** do so already in nanomolar concentrations. 1 µM Atropine was used to induce dissociation.
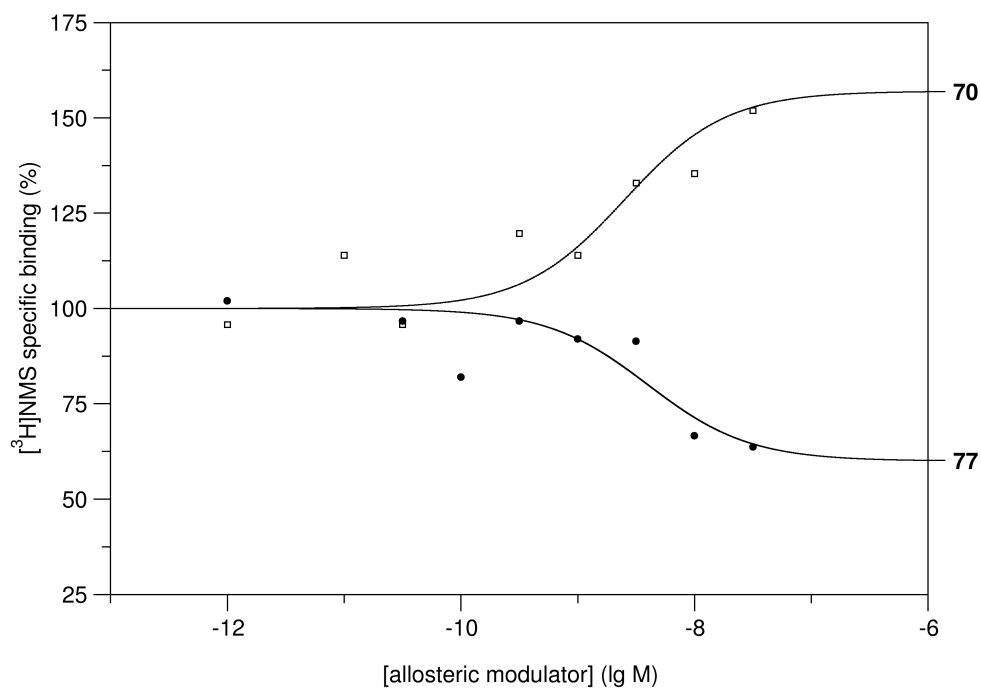
Figure 38: Compound **70** enhances the specific binding of [^{3}H]NMS ($\alpha = 1.904 \pm 0.365$), whereas compound **77** retardes it ($\alpha = 0.525 \pm 0.076$).

6 Summary

The aim of this work was the synthesis of a series of gallamine and tacrine derived heterodimers and their evalution as cholinesterase inhibitors. The design of these compounds predestines them to act as allosteric modulators of muscarinic receptors, which went beyond the scope of this dissertation.

As depicted in Scheme 21, 22 and 23 the anticipated gallamine-tacrine hybrids were based on an ω-aminocarboxylic hydrazide linker. The linker chemistry was established with a 3,4,5-trimethoxybenzene as a gallamine analogue, using reaction conditions, that would also allow the reaction of quaternary structures (Scheme 21). The final coupling of the carboxylic hydrazide and the 9-chloro-1,2,3,4-tetrahydroacridine required harsh reaction conditions and only the use of small glass reactors allowed the reaction to proceede. The synthesis of the first two series, de-
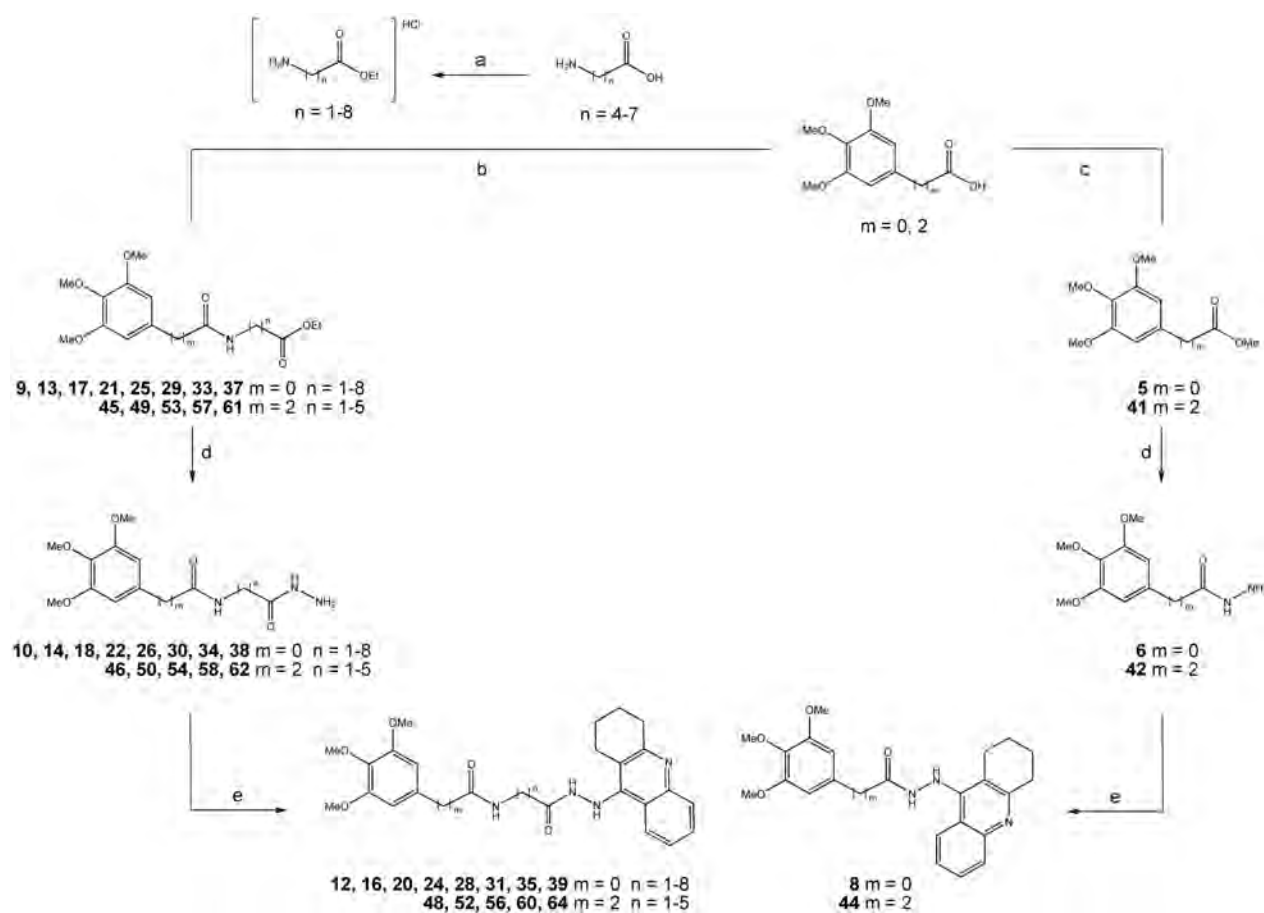
Scheme 21: Synthesis of two 3,4,5-trimethoxybenzene derived series **9-64**: a) SOCl$_2$, EtOH, RT, 12 h; b) 1. (COCl)$_2$, CH$_2$Cl$_2$, RT, 2 h; 2. H$_2$N(CH$_2$)$_n$COOEt • HCl, DIEA, CH$_2$Cl$_2$, RT, 1 h; c) 1. (COCl)$_2$, CH$_2$Cl$_2$, RT, 2 h; 2. MeOH, RT, 1 h; d) N$_2$H$_4$, EtOH, 80 °C, 24 h; e) 1. 9-chloro-1,2,3,4-tetrahydroacridine, EtOH, 140 °C, 24 h; 2. NaOH, H$_2$O.

rived from either 3,4,5-trimethoxybenzoic or 3-(3,4,5-trimethoxyphenyl)propionic acid, and their evaluation as inhibitors of acetylcholinesterase led to an optimal spacer length between the active and peripheral binding site directed groups of eleven to twelve atoms. Some of these compounds showed remarkable selectivity towards butyrylcholinesterase with IC_{50} values below 250 pM.

The synthesis of the gallamine-tacrine hybrids involved a difficult sequence to build up the gallamine moiety. Especially the sensitivity to oxidation was a major obstacle to overcome. Considering the length of the gallamine side chains,

6-aminohexanoic acid was selected to link the gallamine and tacrine moieties. As shown in Scheme 22 the chemical access towards the quaternary side chains was first attempted with 4-hydroxy- and 3,5-dihydroxybenzoic acid that are unsusceptible to oxidation. The main focus during this stage of the synthesis was put on the recovery of the quaternary intermediates and their purification. It was found that precipitation from ethyl acetate was the only way to recover them in solid form. Scheme 23 depicts the efforts undertaken to prevent oxidation of the gallic acid derived intermediates. Unfortunately, the alkylation of methyl 3,4,5-trihydroxybenzoate with 1,2-dibromoethane led to the formation of a
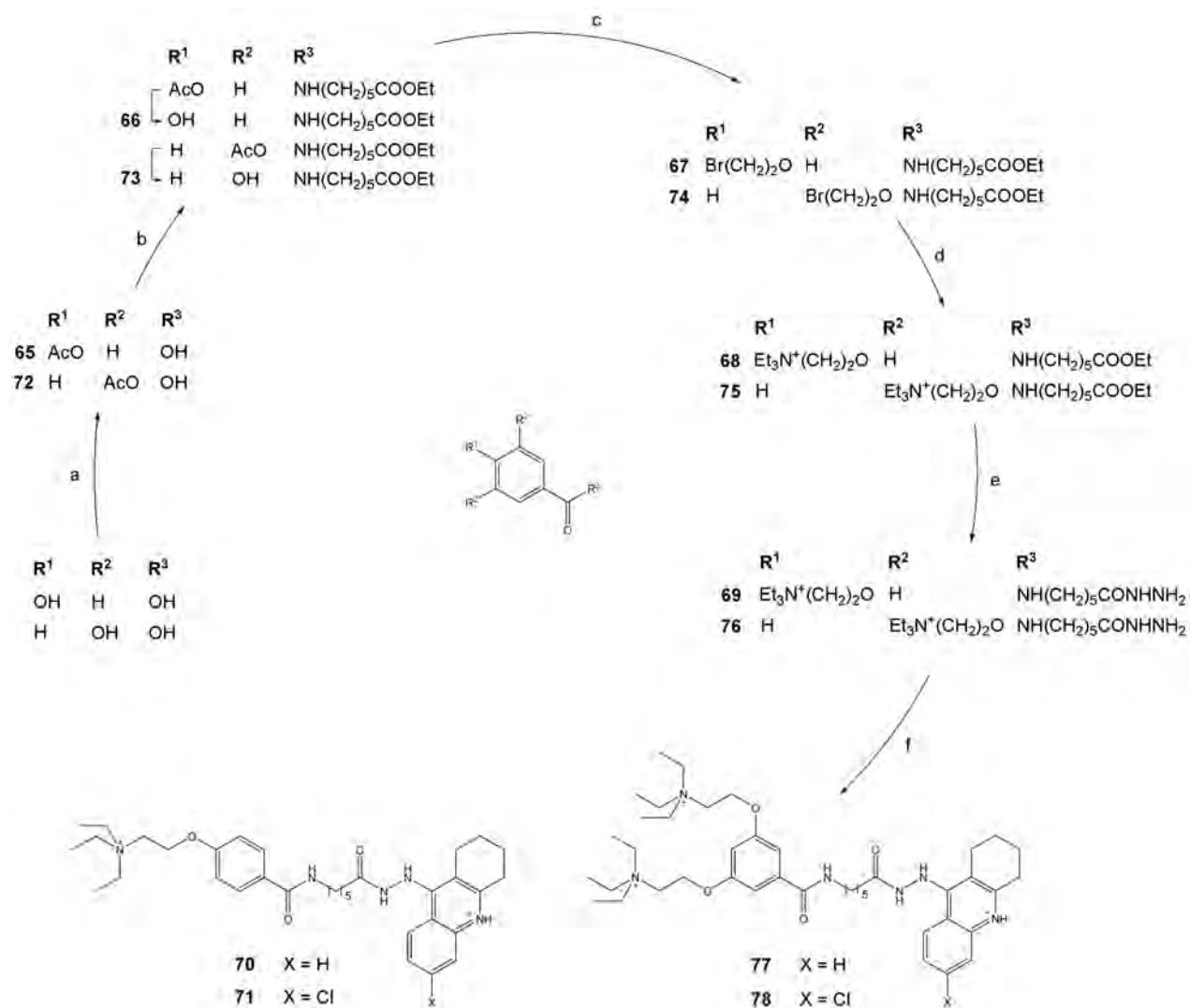
Scheme 22: Synthesis of the mono- and bisquaternary gallamine-tacrine hybrids **70**, **71**, **77** and **78**: a) Ac_2O, Py, RT, 1 h; b) 1. $(COCl)_2$, CH_2Cl_2, RT, 2 h; 2. $H_2N(CH_2)_5COOEt \cdot HCl$, DIEA, CH_2Cl_2, RT, 1 h; 3. K_2CO_3, MeOH, RT, 12 h; c) K_2CO_3, 18-crown-6, $(CH_2Br)_2$, 80 °C, 36 h; d) Et_3N, $MeNO_2$, 60 °C, 24 h; e) N_2H_4, EtOH, 80 °C, 72 h; f) 6,9-dichloro-/9-chloro-1,2,3,4-tetrahydroacridine, EtOH, 140 °C, 24 h.

benzo[b][1,4]dioxine and forced a selective protection of the *p*-hydroxy group. It was further found that the *p*-hydroxy group plays a key role in oxidation processes. Its deprotection has to be carried out very carefully protected from oxygen.

Kinetic investigations revealed, that the trimethoxybenzene substituted compounds had remarkable inhibitory potential towards cholinesterases. These substances showed IC$_{50}$ values in lower nanomolar range towards human AChE and even in picomolar range towards human BChE. Some of the final compounds exhibited surprising selectivity towards BChE with selectivity ratios of 250 to 400. The gallamine-tacrine hybrids and simplified analogues with one
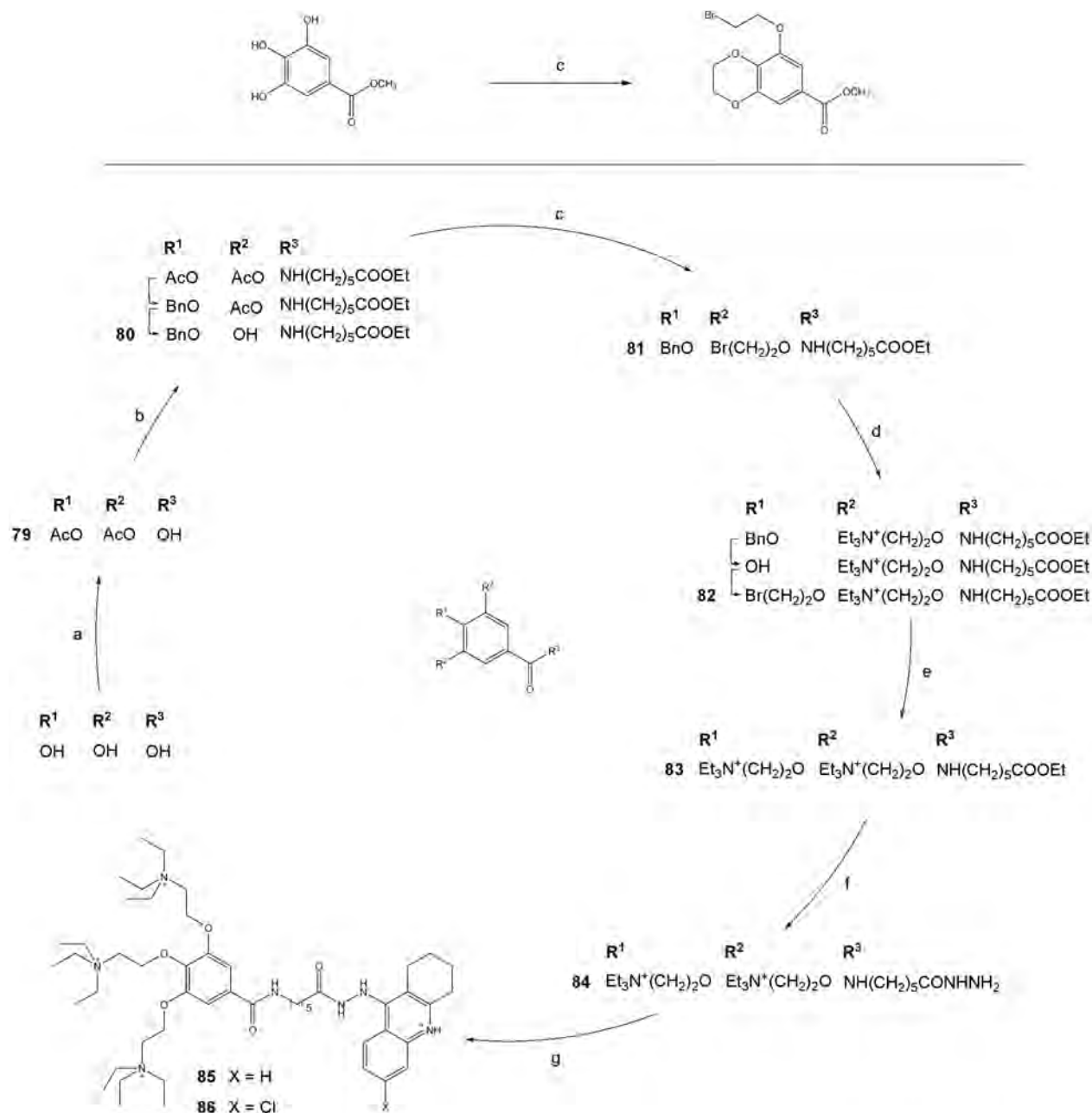
Scheme 23: Synthesis of the trisquaternary gallamine-tacrine hybrids **85** and **86**: a) Ac$_2$O, Py, RT, 1 h; b) 1. (COCl)$_2$, CH$_2$Cl$_2$, RT, 2 h; 2. H$_2$N(CH$_2$)$_5$COOEt • HCl, DIEA, CH$_2$Cl$_2$, RT, 1 h; 3. BnCl, K$_2$CO$_3$, KI, Me$_2$CO, reflux, 18 h; 4. K$_2$CO$_3$, EtOAc, MeOH, H$_2$O, reflux, 1 h; c) K$_2$CO$_3$, 18-crown-6, (CH$_2$Br)$_2$, 80 °C, 36 h; d) 1. Et$_3$N, MeNO$_2$, 60 °C, 24 h; 2. H$_2$, Pd/C, MeOH, 6 h; 3. K$_2$CO$_3$, 18-crown-6, (CH$_2$Br)$_2$, MeCN, 80 °C, 36 h; e) Et$_3$N, MeCN, 100 °C, 48 h; f) N$_2$H$_4$, EtOH, 80 °C, 72 h; g) 6,9-dichloro-/9-chloro-1,2,3,4-tetrahydroacridine, EtOH, 140 °C, 24 h.

or two quaternary side chains lost in potency with increasing substitution of the gallamine moiety, but were still active in lower nanomolar range. The introduction of a chlorine substitution into the tacrine moiety turned selectivity towards AChE.

Detailed molecular docking studies revealed amino acid residues along the AChE gorge, that were addressed by the novel hydrazide linker introduced with this work. In addition, possible interaction partners at the outmost gorge entrance were discovered, that have not been considered so far in the literature. The docking of the gallamine derived compounds led to a concise binding model of the quaternary side chains. The docking poses obtained can explain the loss in potency with increasing substitution pattern. The selectivity characteristics derived from the kinetic investigation were only partly found during the docking process.

Receptor binding studies using the gallamine-tacrine hybrids showed very promising results for the interaction with muscarinic receptors. These novel compounds combining already known allosteric modulators of the muscarinic M_2 receptor were notably more potent than their building blocks. Additionally one of the investigated compounds showed a positive cooperativity with the orthosteric ligand, a characteristic that has not been observed for tacrine nor for gallamine.

In conclusion, this work provides a novel class of highly potent cholinesterase inhibitors, that express remarkable allosteric potency at M_2 receptors. Preliminary findings for the M_1 receptor promise similar effects and their determination may become a challenging project for the future. From a synthetic point of view this work gives a concise entry towards quaternary substituted ligands of cholinesterases and muscarinic receptors. Further investigations may involve the variation of substitution pattern at the gallamine moiety (Figure 39a), the optimization of linker length regarding the muscarinic receptors (Figure 39b) and the distance between the quaternary nitrogen and the gallamine π-system (Figure 39c).
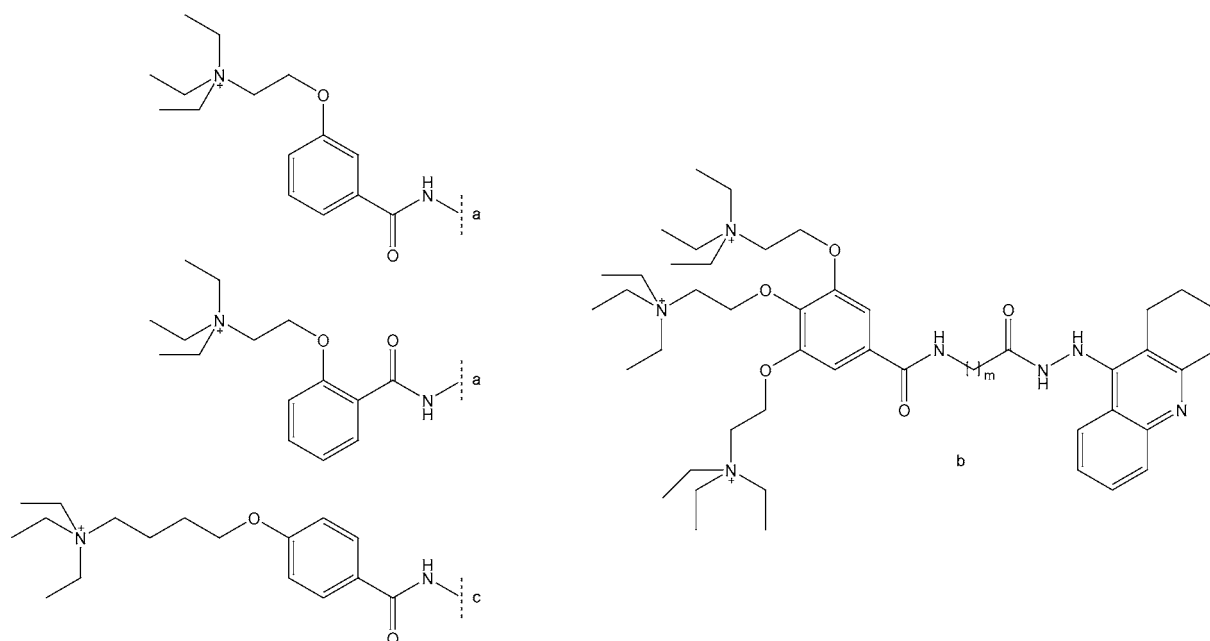
Figure 39: Further investiagtions may include a variation of substitution position (a), alter the distance between the quaternary center and the π-system (b) or reveal the optimal distance between the gallamine and tacrine moieties (c).

7 Compounds

Chemicals

Solvents and chemicals were purchased from Acros (Geel, Belgium), Fluka (Taufkirchen, Germany), Merck (Darmstadt, Germany), Lancaster (Mühlheim a. M., Germany) or Aldrich (Steinheim, Germany) and stated at least a 95 % purity.

In case that anhydrous solvents were used for synthesis the commercial source was dried by the following procedures, destilled and stored over molecular sieve. Methanol was dried using magnesium and iodine, ethanol using sodium and all other solvents like dichloromethane, nitromethane, ethyl acetate, acetonitrile and toluene were dried using phophorus pentoxide.

Instruments

NMR spectra were obtained on a Bruker Avance DRX 500 spectrometer. ^{1}H NMR spectra were recorded at 500 MHz, the ^{13}C NMR spectra at 125 MHz. Chemical shifts δ are given in ppm referring to the signal center using the solvent peaks for reference: CDCl$_3$ 7.26 ppm/77.0 ppm and DMSO-d_6 2.49 ppm/39.7 ppm. To characterize the spin multiplicity the following abbreviations are used: *s* singlet, *bs* broad singlet, *d* doublet, *bd* broad doublet, *dd* doublet of doublets, *ddd* doublet of doublet of doublets, *t* triplet, *q* quartet, *quint* quintet, *sext* sextet, *m* multiplet.

The CHN elemental composition was determined using the VarioEL elemental analizer at the Institute for Pharmaceutical Chemistry Endenich.

Melting points were determined using a Boëtius melting point apparatus from VEB Wägetechnik Rapido PHMK and are uncorrected.

TLC was carried out using aluminium sheets coated with silica 60 F$_{254}$ that allowed for detection with UV light at 254 nm. Unmodified silica (70–230 mesh) was used for CC, the respective eluents are stated within each compounds description.

9-Chloro-1,2,3,4-tetrahydroacridine
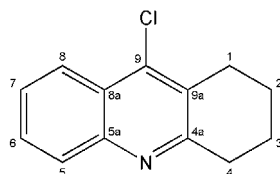
Synthesis: 10.0 mmol (1.99 g) 1,3,4,10-tetrahydro-9(2*H*)-acridinone are added to 107.0 mmol (10.0 ml) of phosphorus(V) oxychloride and the reaction mixture is refluxed (120 °C) for 3 hours. After cooling to room temperature ice is added to the green solution to quench excess phosphorus(V) oxychloride and the volume is extended to 220 ml with water. When adjusting the pH to 10 using a solution of 13 g sodium hydroxide in 30 ml water a yellowish solid precipitates. The reaction mixture is extracted two times with 250 ml ethyl acetate and the combined organic layers are evaporated in vacuo. Flash column chromatography using ethyl acetate and silica gel yields the final product **1** that needs no further purification.

Yield: 1.69 g (78 %), $C_{13}H_{12}ClN$, $M_R = 217.70$ g/mol
Yellow crystals

^{1}H NMR δ:
[DMSO-*d_6*]

1.80-1.89 (m, 4H, H–2,3)	7.72 (ddd, 1H, *J* = 1.3 7.0 8.4 Hz, H–6)
2.90 (app. bs, 2H, H–1)	7.91 (dd, 1H, *J* = 0.7 8.5 Hz, H–5)
2.99 (app. bs, 2H, H–4)	8.07 (dd, 1H, *J* = 1.0 8.5 Hz, H–8)
7.61 (ddd, 1H, *J* = 1.3 7.0 8.4 Hz, H–7)	

^{13}C NMR δ:
[DMSO-*d_6*]

22.10 (C–2)	22.12 (C–3)	27.07 (C–1)	33.66 (C–4)
123.23 (C–8)	124.62 (C–8a)	127.03 (C–7)	128.66 (C–5)
128.75 (C–9a)	129.59 (C–6)	140.02 (C–9)	146.28 (C–5a)
159.48 (C–4a)			

Melting Point: 67 °C, lit.[65] 65-67 °C

EA:

Calculated:	C: 71.72 %	H: 5.56 %	Cl: 16.29 %	N: 6.43 %
Found:	C: 71.83 %	H: 5.68 %		N: 6.47 %

6,9-Dichloro-1,2,3,4-tetrahydroacridine
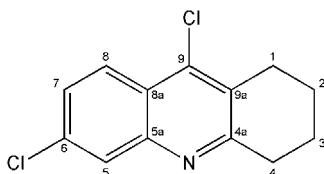
Synthesis: 214.0 mmol (20.0 ml) of phosphorus(V) oxychloride are carefully added to a mixture of 50.0 mmol (8.58 g) 2-amino-4-chlorobenzoic acid and 50.0 mmol (4.91 g) cyclohexanone and the reaction mixture is heated to reflux for 2 hours. After cooling to room temperature ice is added to the brown solution to quench excess phosphorus(V) oxychloride and the pH is neutralized using sodium hydroxide. The yellow suspension is extended to 250 ml with water and extracted three times with ethyl acetate. The combined organic phases are dried using anhydrous sodium sulfate and subsequently evaporated in vacuo. Flash column chromatography using ethyl acetate and petrol ether in a ratio of 1:2, followed by recrystallization from acetone yields the final product **2**.

Yield: 7.22 g (57 %), $C_{13}H_{11}Cl_2N$, $M_R = 252.14$ g/mol
Amber-colored crystals

^{1}H NMR δ:
[DMSO-d_6]

1.80-1.90 (m, 4H, H–2,3)	7.58 (dd, 1H, J = 2.2 9.2 Hz, H–7)
2.86 (app. bs, 2H, H–1)	7.90 (d, 1H, J = 2.2 Hz, H–5)
2.97 (app. bs, 2H, H–4)	8.02 (d, 1H, J = 9.2 Hz, H–8)

^{13}C NMR δ:
[DMSO-d_6]

21.94 (C–2,3)	27.03 (C–1)	33.66 (C–4)	123.27 (C–8a)
125.34 (C–8)	127.18 (C–5)	127.51 (C–7)	129.32 (C–9a)
134.19 (C–6)	140.08 (C–9)	146.44 (C–5a)	161.04 (C–4a)

Melting Point: 92 °C, lit.[67] 77-79 °C

EA:

Calculated:	C: 61.93 %	H: 4.40 %	Cl: 28.12 %	N: 5.56 %
Found:	C: 62.01 %	H: 4.53 %		N: 5.53 %

9-Hydrazino-1,2,3,4-tetrahydroacridine HCl
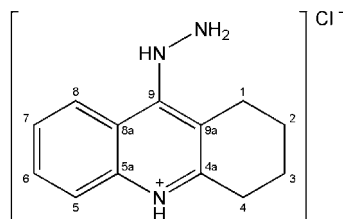
Synthesis: 10.0 mmol (2.18 g) 9-chloro-1,2,3,4-tetrahydroacridine (**1**) are heated in a solution of 20.6 mmol (1.0 ml hydrazine hydrate, 100 %) in 5 ml ethanol to 140 °C for 5 hours by means of a sealed bomb. After cooling to room temperature the reaction mixture is neutralized using concentrated hydrochloric acid and the remaining precipitate is recovered by suction filtration. Washing with diethyl ether and drying over phosphorus(V) oxide yields **3** as a powder that needs no further purification.

Yield: 1.60 g (64 %), $C_{13}H_{16}ClN_3$, $M_R = 249.74$ g/mol
Peach crystals, very hygroscopic

^{1}H NMR δ:
[DMSO-d_6]

1.75-1.84 (m, 4H, H–2,3)	7.77 (app. t, 1H, $J = 7.7$ Hz, H–6)
2.51 (app. s, 2H, H–1)	7.86 (app. d, 1H, $J = 8.2$ Hz, H–8)
2.92 (t, 2H, $J = 5.7$ Hz, H–4)	9.56 (app. s, 1H, H–5)
5.41 (s, 2H, NH$_2$)	9.69 (s, 1H, NHNH$_2$)
7.42 (app. t, 1H, $J = 7.9$ Hz, H–7)	13.52 (s, 1H, N$^+$H)

^{13}C NMR δ:
[DMSO-d_6]

20.53 (C–2)	21.49 (C–3)	23.49 (C–1)	27.76 (C–4)
107.74 (C–8a)	114.45 (C–5)	118.42 (C–8)	123.50 (C–7)
128.48 (C–6)	132.53 (C–9a)	138.45 (C–5a)	148.66 (C–4a)
153.28 (C–9)			

Melting Point: 273-280 °C (decomposition)

EA: Calculated: C: 62.52 % H: 6.46 % Cl: 14.20 % N: 16.83 %
Found:

9-Hydrazino-1,2,3,4-tetrahydroacridine
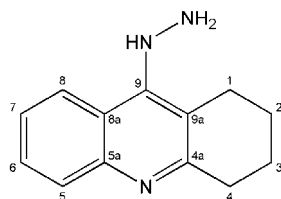
Synthesis: 2.0 mmol (0.50 g) of 9-hydrazino-1,2,3,4-tetrahydroacridine hydrochloride (**3**) are dissolved in 20 ml of water and 10.0 ml 1 M sodium hydroxide solution is added. The aqueous layer is extracted twice with dichloromethane, the combined organic phases are dried using anhydrous sodium sulfate and the solvent is evaporated in vacuo. The remaining foam can be recrystallized from ethyl acetate and n-hexane for analytical purposes to obtain **4**.

Yield: 0.39 g (92 %), $C_{13}H_{15}N_3$, $M_R = 213.28$ g/mol
Orange crystals, very hygroscopic

^{1}H NMR δ:
[CDCl$_3$]

1.85-1.93 (m, 4H, H–2,3)	7.35 (ddd, 1H, $J = 1.6\ 7.0\ 8.4$ Hz, H–7)
2.75 (t, 2H, $J = 6.0$ Hz, H–1)	7.54 (ddd, 1H, $J = 1.6\ 6.9\ 8.4$ Hz, H–6)
3.04 (t, 2H, $J = 6.0$ Hz, H–4)	7.88 (app. d, 1H, $J = 8.5$ Hz, H–8)
3.98 (s, 2H, NH$_2$)	8.39 (dd, 1H, $J = 1.0\ 8.5$ Hz, H–5)
5.75 (bs, 1H, N$\underline{H}$NH$_2$)	

^{13}C NMR δ:
[CDCl$_3$]

22.70 (C–2)	22.91 (C–3)	24.63 (C–1)	33.99 (C–4)
115.59 (C–9a)	119.63 (C–8a)	123.21 (C–8)	123.85 (C–7)
128.38 (C–6)	128.61 (C–5)	147.39 (C–5a)	150.10 (C–9)
158.45 (C–4a)			

Melting Point: 98 °C

EA: Calculated: C: 73.21 %   H: 7.09 %   N: 19.70 %
Found:

Methyl 3,4,5-trimethoxybenzoate

Synthesis: 10.0 mmol sodium are added to 20 ml anhydrous methanol while stirring. Once the formation of sodium methylate is complete 10.0 mmol (2.31 g) 3,4,5-trimethoxybenzoyl chloride are dissolved in the reaction mixture. Stirring at room temperature for 5 hours yields a suspension that is evaporated in vacuo. Extracting the solid residue with dichloromethane from a saturated solution of sodium hydrogen carbonate, drying with anhydrous sodium sulfate and evaporation in vacuo yields the final product **5** which needs no further purification.

Yield: 1.88 g (83 %), $C_{11}H_{14}O_5$, $M_R = 226.23$ g/mol
White crystals

^{1}H NMR δ: 3.88 (s, 12H, H–1,7,8)   7.27 (s, 2H, H–4)
[CDCl$_3$]

^{13}C NMR δ: 52.19 (C–1)   56.21 (C–7)   60.88 (C–8)   106.78 (C–4)
[CDCl$_3$]   125.12 (C–3)   142.16 (C–6)   152.91 (C–5)   166.68 (C–2)

Melting Point: 76 °C, lit.[112] 81-82 °C

EA: Calculated: C: 58.40 %   H: 6.24 %   O: 35.36 %
Found: C: 58.31 %   H: 6.14 %

3,4,5-Trimethoxybenzohydrazide

Synthesis: To a mixture of 51.4 mmol hydrazine (2.5 ml hydrazine hydrate, 100 %) and 20 ml absolute ethanol 5.0 mmol (1.13 g) methyl 3,4,5-trimethoxybenzoate (**5**) are added and the solution is heated to reflux for about 24 hours. The course of the reaction is followed by TLC and once no more ester can be detected the solvent and excess hydrazine are evaporated in vacuo. The crude product is recrystallized from ethanol for further purification to obtain **6**.

Yield: 0.85 g (75 %), $C_{10}H_{14}N_2O_4$, $M_R = 226.23$ g/mol
White needles

^{1}H NMR δ: 3.69 (s, 3H, H–7)   7.15 (s, 2H, H–3)
[DMSO-d_6] 3.80 (s, 6H, H–6)   9.67 (s, 1H, N$\underline{H}$NH$_2$)
4.44 (s, 2H, NH$_2$)

^{13}C NMR δ: 56.11 (C–6)   60.17 (C–7)   104.65 (C–3)   128.57 (C–2)
[DMSO-d_6] 139.95 (C–5)   152.73 (C–4)   165.48 (C–1)

Melting Point: 158 °C, lit.[113] 162 °C

EA: $C_{10}H_{14}N_2O_4 \cdot 0.5\ H_2O$
Calculated: C: 51.06 % H: 6.43 % N: 11.91 % O: 30.61 %
Found: C: 51.03 % H: 6.40 % N: 11.92 %

N′-1,2,3,4-Tetrahydroacridin-9-yl-3,4,5-trimethoxybenzohydrazide HCl

Synthesis: 2.0 mmol (0.44 g) 9-chloro-1,2,3,4-tetrahydroacridine (**1**) and 2.0 mmol (0.65 g) *N*-(3-hydrazino-3-oxopropyl)-3,4,5-trimethoxybenzamide (**6**) dissolved in 20 ml absolute ethanol are heated to 140 °C for 24 hours by means of a sealed bomb. Cooling to room temperature yields **7** as a crude product that needs no further purification.

Yield: 0.84 g (95 %), $C_{23}H_{26}ClN_3O_4$, $M_R = 443.93$ g/mol
Yellow crystals

^{1}H NMR δ: 1.82 (app. bs, 4H, H–9,10)   7.88 (app. t, 1H, $J = 7.7$ Hz, H–18)
[DMSO-d_6] 2.78 (app. bs, 2H, H–11)   8.04 (app. d, 1H, $J = 8.5$ Hz, H–16)
3.11 (app. bs, 2H, H–8)   8.72 (app. d, 1H, $J = 8.8$ Hz, H–19)
3.74 (s, 3H, H–7)   9.86 (s, 1H, CON<u>H</u>NH)
3.85 (s, 6H, H–6)   11.71 (s, 1H, CONHN<u>H</u>)
7.35 (s, 2H, H–3)   14.47 (s, 1H, N$^+$H)
7.60 (app. t, 1H, $J = 7.7$ Hz, H–17)

^{13}C NMR δ: 20.24 (C–10)   21.46 (C–9)   24.26 (C–11)   28.33 (C–8)
[DMSO-d_6] 56.35 (C–6)   60.25 (C–7)   105.48 (C–3)   111.61 (C–12)
115.37 (C–15)   119.56 (C–16)   124.04 (C–19)   126.10 (C–17)
126.43 (C–2)   133.09 (C–18)   137.41 (C–20)   141.08 (C–5)
153.01 (C–4,13)   155.61 (C–14)   165.35 (C–1)

Melting Point: 214 °C

EA: Calculated: C: 62.23 %   H: 5.90 %   Cl: 7.99 %   N: 9.47 %   O: 14.42 %
Found: C: 62.00 %   H: 5.83 %   N: 9.49 %

N′-1,2,3,4-Tetrahydroacridin-9-yl-3,4,5-trimethoxybenzohydrazide

Synthesis: A solution of 0.5 mmol (0.22 g) N′-1,2,3,4-tetrahydroacridin-9-yl-3,4,5-trimethoxy-benzohydrazide hydrochloride (**7**) in 5 ml ethanol and 20 ml water is mixed with 1 ml of 1 M sodium hydroxide solution to liberate the base. The orange precipitate **8** formed is recovered by suction filtration, washed with diethyl ether and dried using phosphorus pentoxide.

Yield: 0.17 g (83 %), $C_{23}H_{25}N_3O_4$, $M_R = 407.48$ g/mol
Yellow crystals

^{1}H NMR δ:
[CDCl$_3$]

1.65-1.77 (m, 4H, H–9,10)	7.47 (app. dd, 1H, $J = 7.7$ 8.2 Hz, H–17)
2.40 (t, 2H, $J = 5.2$ Hz, H–11)	7.42 (s, 2H, H–3)
2.70 (t, 2H, $J = 5.5$ Hz, H–8)	7.51 (ddd, 1H, $J = 1.3$ 7.6 7.7 Hz, H–18)
3.82 (s, 6H, H–6)	7.75 (app. d, 1H, $J = 8.5$ Hz, H–16)
3.85 (s, 3H, H–7)	9.95 (app. d, 1H, $J = 7.3$ Hz, H–19)

^{13}C NMR δ:
[CDCl$_3$]

21.08 (C–10)	21.82 (C–9)	22.54 (C–11)	28.30 (C–8)
56.01 (C–6)	60.88 (C–7)	104.52 (C–3)	107.65 (C–12)
116.08 (C–19)	118.55 (C–17)	123.23 (C–2)	129.60 (C–18)
131.61 (C–16)	131.87 (C–15)	139.63 (C–13)	139.69 (C–5)
145.68 (C–20)	147.03 (C–14)	152.81 (C–4)	166.90 (C–1)

Melting Point: 244 °C

EA: $C_{23}H_{25}N_3O_4$ • 0.5 H_2O
Calculated: C: 66.33 % H: 6.29 % N: 10.09 % O: 17.29 %
Found: C: 66.10 % H: 6.63 % N: 9.91 %

Ethyl ((3,4,5-trimethoxybenzoyl)amino)acetate
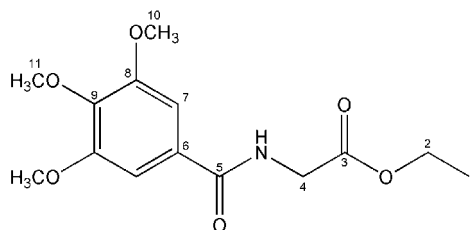
|	
Synthesis:	10.0 mmol (1.40 g) ethyl aminoacetate hydrochloride are suspended in a solution of 10.0 mmol (2.31 g) 3,4,5-trimethoxybenzoyl chloride in 20 ml anhydrous dichloromethane and 20.0 mmol (3.5 ml) of *N*-ethyl-*N,N*-diisopropylamine are added dropwise. Washing with 0.1 M hydrochloric acid, a saturated solution of sodium hydrogen carbonate and water followed by drying with anhydrous sodium sulfate and evaporation in vacuo yields a crude product which is further purified by recrystallization from ethyl acetate to produce **9**.

Yield: 1.83 g (62 %), $C_{14}H_{19}NO_6$, M_R = 297.31 g/mol
White crystals

^{1}H NMR δ:
[DMSO-*d$_6$*]

1.20 (t, 3H, *J* = 6.9 Hz, H–1)	4.12 (q, 2H, *J* = 7.0 Hz, H–2)
3.71 (s, 3H, H–11)	7.20 (s, 2H, H–7)
3.82 (s, 6H, H–10)	8.86 (t, 1H, *J* = 5.8 Hz, NH)
3.98 (d, 2H, *J* = 6.0 Hz, H–4)	

^{13}C NMR δ:
[DMSO-*d$_6$*]

14.23 (C–1)	41.51 (C–4)	56.14 (C–10)	60.21 (C–11)
60.54 (C–2)	105.05 (C–7)	128.93 (C–6)	140.37 (C–9)
152.75 (C–8)	166.13 (C–5)	170.04 (C–3)	

Melting Point: 107 °C, lit.[114] 109 °C

EA:

Calculated:	C: 56.56 %	H: 6.44 %	N: 4.71 %	O: 32.29 %
Found:	C: 56.49 %	H: 6.80 %	N: 4.72 %	

N-(2-Hydrazino-2-oxoethyl)-3,4,5-trimethoxybenzamide
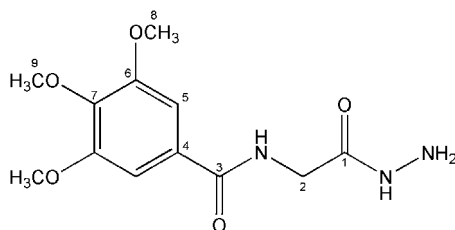
Synthesis: To a mixture of 51.4 mmol hydrazine (2.5 ml hydrazine hydrate, 100 %) and 20 ml absolute ethanol 5.0 mmol (1.49 g) ethyl ((3,4,5-trimethoxybenzoyl)amino)acetate (**9**) are added and the solution is heated to reflux for about 24 hours. The course of the reaction is followed by TLC and once no more ester can be detected the solvent and excess hydrazine are evaporated in vacuo. The crude product is recrystallized from ethanol for further purification to obtain **10**.

**Yield:** 1.02 g (72 %), $C_{12}H_{17}N_3O_5$, $M_R = 283.28$ g/mol
White powder

^{1}H NMR δ:
[DMSO-d_6]

3.70 (s, 3H, H–9)	7.21 (s, 2H, H–5)
3.82 (d, 2H, J = 5.7 Hz, H–2)	8.65 (t, 1H, J = 5.8 Hz, N<u>H</u>CH$_2$)
3.82 (s, 6H, H–8)	9.08 (s, 1H, N<u>H</u>NH$_2$)
4.20 (s, 2H, NH$_2$)	

^{13}C NMR δ:
[DMSO-d_6]

41.58 (C–2)	56.15 (C–8)	60.21 (C–9)	105.17 (C–5)
129.41 (C–4)	140.19 (C–7)	152.65 (C–6)	166.04 (C–3)
168.48 (C–1)			

Melting Point: 164 °C, lit.[115] 167-168 °C

EA:

Calculated:	C: 50.88 %	H: 6.05 %	N: 14.83 %	O: 28.24 %
Found:	C: 50.37 %	H: 5.86 %	N: 14.73 %	

3,4,5-Trimethoxy-*N*-(2-oxo-2-(2-(1,2,3,4-tetrahydroacridin-9-yl)hydrazino)ethyl)benzamide HCl
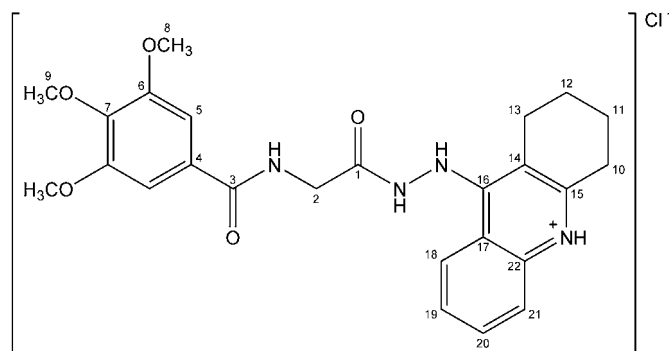
| **Synthesis:** | 2.0 mmol (0.44 g) 9-Chloro-1,2,3,4-tetrahydroacridine (**1**) and 2.0 mmol (0.57 g) *N*-(2-hydrazino-2-oxoethyl)-3,4,5-trimethoxybenzamide (**10**) are dissolved in 20 ml absolute ethanol and heated to 140 °C for 24 hours by means of a sealed bomb. Cooling to -20 °C yields **11** as yellow crystals that neeed no further purification. |

Yield: 0.80 g (80 %), $C_{25}H_{29}ClN_4O_5$, $M_R = 500.98$ g/mol
Yellow crystals

^{1}H NMR δ:
**[DMSO-d_6]**

1.76-1.86 (m, 4H, H–11,12)	7.88 (ddd, 1H, *J* = 1.0 7.1 8.4 Hz, H–20)
2.73 (app. bs, 2H, H–13)	8.02 (app. dd, 1H, *J* = 1.0 8.5 Hz, H–18)
3.08 (t, 2H, *J* = 5.7 Hz, H–10)	8.73 (app. d, 1H, *J* = 8.5 Hz, H–21)
3.70 (s, 3H, H–9)	9.05 (t, 1H, *J* = 6.0 Hz, N$\underline{H}$CH$_2$)
3.83 (s, 6H, H–8)	9.73 (s, 1H, CON$\underline{H}$NH)
4.05 (d, 2H, *J* = 6.0 Hz, H–2)	11.19 (s, 1H, CONHN$\underline{H}$)
7.28 (s, 2H, H–5)	14.46 (s, 1H, N$^+$H)
7.57 (ddd, 1H, *J* = 1.0 7.7 7.9 Hz, H–19)	

^{13}C NMR δ:
[DMSO-d_6]

20.27 (C–11)	21.48 (C–12)	24.22 (C–13)	28.32 (C–10)
41.62 (C–2)	56.24 (C–8)	60.25 (C–9)	105.29 (C–5)
111.34 (C–14)	115.13 (C–17)	119.41 (C–18)	124.44 (C–21)
126.04 (C–19)	129.10 (C–4)	133.04 (C–20)	137.39 (C–22)
140.36 (C–7)	152.70 (C–6,15)	155.06 (C–16)	166.28 (C–3)
169.15 (C–1)			

Melting Point: 188 °C

EA: $C_{25}H_{29}ClN_4O_5 \cdot H_2O$
Calculated: C: 57.86 % H: 6.02 % Cl: 6.83 % N: 10.80 % O: 18.50 %
Found: C: 57.74 % H: 6.04 % N: 10.65 %

3,4,5-Trimethoxy-*N*-(2-oxo-2-(2-(1,2,3,4-tetrahydroacridin-9-yl)hydrazino)ethyl)benzamide
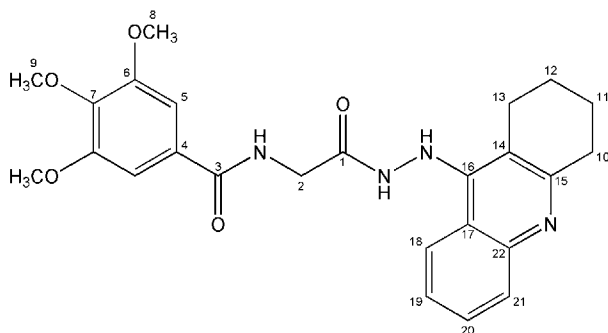
Synthesis:	A solution of 0.5 mmol (0.25 g) 3,4,5-trimethoxy-*N*-(2-oxo-2-(2-(1,2,3,4-tetrahydro-acridin-9-yl)hydrazino)ethyl)benzamide hydrochloride (**11**) in 5 ml ethanol and 20 ml water is mixed with 1 ml of 1 M sodium hydroxide solution to liberate the base. The yellow precipitate **12** formed is recovered by suction filtration, washed with diethyl ether and dried using phosphorus pentoxide.
Yield:	0.23 g (99 %), $C_{25}H_{28}N_4O_5$, M_R = 464.52 g/mol Yellow crystals

^{1}H NMR δ:
[DMSO-*d$_6$*]

1.80 (app. bs, 4H, H–11,12)	7.29 (app. bs, 1H, H–19)
2.82 (app. bs, 2H, H–13)	7.52 (app. t, 1H, J = 7.4 Hz, H–20)
2.89 (app. bs, 2H, H–10)	7.59-7.94 (app. bs, 1H, CONH̲NH))
3.69 (s, 3H, H–9)	7.69 (app. d, 1H, J = 7.9 Hz, H–18)
3.80 (s, 6H, H–8)	8.22-8.55 (app. bs, 1H, H–21)
3.91 (d, 2H, J = 5.7 Hz, H–2)	8.63 (t, 1H, J = 5.5 Hz, NH̲CH$_2$)
7.18 (s, 2H, H–5)	10.14-10.46 (app. bs, 1H, CONHNH̲)

^{13}C NMR δ:
[DMSO-*d$_6$*]

22.41 (C–12)	22.68 (C–11)	24.71 (C–13)	33.54 (C–10)
41.11 (C–2)	56.14 (C–8)	60.22 (C–9)	105.11 (C–5)
119.11 (C–17)	123.56 (C–19,21)	128.13 (C–18,20)	129.40 (C–4)
140.21 (C–7)	152.66 (C–6)	166.04 (C–3)	169.07 (C–1)

Melting Point: 235 °C (decomposition)

EA: $C_{25}H_{28}N_4O_5 \cdot 2 H_2O$
Calculated:	C: 59.99 %	H: 6.44 %	N: 11.19 %	O: 22.37 %
Found:	C: 60.05 %	H: 6.56 %	N: 11.12 %	

Ethyl 3-((3,4,5-trimethoxybenzoyl)amino)propanoate

Synthesis: 10.0 mmol (2.12 g) of 3,4,5-trimethoxybenzoic acid are dissolved in 20 ml anhydrous dichloromethane with catalytic amounts of *N,N*-dimethylformamide. While stirring the subsequent addition of 11.6 mmol (1.0 ml) of oxalyl chloride generates the acyl chloride. Once the gas evolution has ceased remaining hydrogen chloride, excess oxalyl chloride and the solvent are removed by evaporation in vacuo. The residue is again taken up in 10 ml of dichloromethane and 10.0 mmol (1.54 g) of ethyl 3-aminopropanoate hydrochloride are suspended in the solution. Dropwise addition of 20.0 mmol (3.5 ml) *N*-ethyl-*N,N*-diisopropylamine yields a clear solution which sometimes contains some precipitated *N*-ethyl-*N,N*-diisopropylamine hydrochloride. Washing with water and a saturated solution of sodium hydrogen carbonate, drying with anhydrous sodium sulfate and evaporation in vacuo yields a crude product which is further purified by recrystallization from ethyl acetate and n-hexane to produce **13**.

Yield: 2.76 g (89 %), $C_{15}H_{21}NO_6$, $M_R = 311.33$ g/mol
White crystals

^{1}H NMR δ:
[DMSO-*d_6*]

1.17 (t, 3H, $J = 7.1$ Hz, H–1)	3.81 (s, 6H, H–11)
2.56 (t, 2H, $J = 6.9$ Hz, H–4)	4.06 (q, 2H, $J = 7.1$ Hz, H–2)
3.47 (app. q, 2H, $J = 7.0$ Hz, H–5)	7.15 (s, 2H, H–8)
3.69 (s, 3H, H–12)	8.48 (t, 1H, NH)

^{13}C NMR δ:
[DMSO-*d_6*]

14.20 (C–1)	34.00 (C–4)	35.74 (C–5)	56.15 (C–11)
60.05 (C–2)	60.19 (C–12)	104.96 (C–8)	129.66 (C–7)
140.14 (C–10)	152.68 (C–9)	165.85 (C–6)	171.44 (C–3)

Melting Point: 68 °C

EA:

Calculated:	C: 57.87 %	H: 6.80 %	N: 4.50 %	O: 30.83 %
Found:	C: 57.79 %	H: 6.96 %	N: 4.59 %	

N-(3-Hydrazino-3-oxopropyl)-3,4,5-trimethoxybenzamide
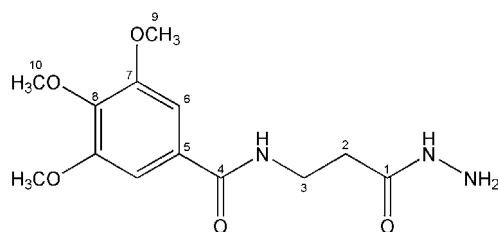
Synthesis: To a mixture of 51.4 mmol hydrazine (2.5 ml hydrazine hydrate, 100 %) and 20 ml absolute ethanol 5.0 mmol (1.56 g) ethyl 3-((3,4,5-trimethoxybenzoyl)amino)propanoate (**13**) are added and the solution is heated to reflux for about 24 hours. The course of the reaction is followed by TLC and once no more ester can be detected the solvent and excess hydrazine are evaporated in vacuo. The crude product is recrystallized from ethanol for further purification to obtain **14**.

Yield: 1.00 g (67 %), $C_{13}H_{19}N_3O_5$, $M_R = 297.31$ g/mol
White crystals

^{1}H NMR δ:
[DMSO-d_6]

2.13 (t, 2H, J = 7.3 Hz, H–2)	3.88 (4.16 (s, 2H, NH$_2$)
3.44 (app. q, 2H, J = 5.7 Hz, H–3)	7.16 (s, 2H, H–6)
3.68 (s, 3H, H–10)	8.45 (t, 1H, J = 5.7 Hz, N$\underline{H}$CH$_2$)
3.81 (s, 6H, H–9)	9.01 (s, 1H, N$\underline{H}$NH$_2$)

^{13}C NMR δ:
[DMSO-d_6]

33.81 (C–2)	36.26 (C–3)	56.14 (C–9)	60.20 (C–10)
104.95 (C–6)	129.80 (C–5)	140.06 (C–8)	152.67 (C–7)
165.72 (C–4)	169.89 (C–1)		

Melting Point: 171 °C

EA:

Calculated:	C: 52.52 %	H: 6.44 %	N: 14.13 %	O: 26.91 %
Found:	C: 52.51 %	H: 6.45 %	N: 14.14 %	

3,4,5-Trimethoxy-*N*-(3-oxo-3-(2-(1,2,3,4-tetrahydroacridin-9-yl)hydrazino)propyl)benzamide HCl
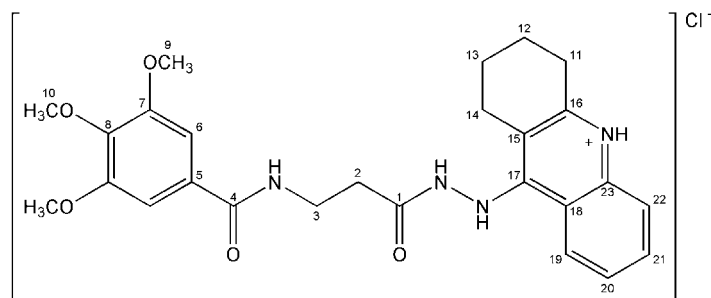
Synthesis: 2.0 mmol (0.44 g) 9-chloro-1,2,3,4-tetrahydroacridine (**1**) and 2.0 mmol (0.59 g) *N*-(3-hydrazino-3-oxopropyl)-3,4,5-trimethoxybenzamide (**14**) dissolved in 20 ml absolute ethanol are heated to 140 °C for 24 hours by means of a sealed bomb. Cooling to room temperature yields **15** as a crude product that needs no further purification.

Yield: 0.98 g (95 %), $C_{26}H_{31}ClN_4O_5$, $M_R = 515.01$ g/mol
Yellow crystals

^{1}H NMR δ:
[DMSO-*d_6*]

1.67 (app. bd, 2H, $J = 4.8$ Hz, H–13)	7.48 (app. t, 1H, $J = 7.7$ Hz, H–20)
1.72 (app. bd, 2H, $J = 5.1$ Hz, H–12)	7.83 (app. t, 1H, $J = 7.6$ Hz, H–21)
2.62 (t, 2H, $J = 6.8$ Hz, H–2)	8.00 (app. d, 1H, $J = 7.9$ Hz, H–19)
2.66 (t, 2H, $J = 6.0$ Hz, H–14)	8.63 (app. d, 1H, $J = 8.5$ Hz, H–22)
3.06 (t, 2H, $J = 6.3$ Hz, H–11)	8.67 (t, 1H, $J = 5.5$ Hz, NHCH$_2$)
3.49 (app. q, 2H, $J = 6.4$ Hz, H–3)	9.72 (s, 1H, CONHNH)
3.70 (s, 3H, H–10)	11.05 (s, 1H, CONHNH)
3.81 (s, 6H, H–9)	14.43 (s, 1H, N$^+$H)
7.22 (s, 2H, H–6)	

^{13}C NMR δ:
[DMSO-*d_6*]

20.13 (C–13)	21.41 (C–12)	24.35 (C–14)	28.27 (C–11)
33.26 (C–2)	35.80 (C–3)	56.22 (C–9)	60.22 (C–10)
105.09 (C–6)	111.38 (C–15)	115.19 (C–18)	119.44 (C–19)
123.92 (C–22)	125.99 (C–20)	129.55 (C–5)	132.99 (C–21)
137.28 (C–23)	140.17 (C–8)	152.69 (C–7)	152.90 (C–16)
155.25 (C–17)	165.81 (C–4)	170.44 (C–1)	

Melting Point: 214 °C

EA: $C_{26}H_{31}ClN_4O_5$ • 0.5 H$_2$O

Calculated:	C: 59.59 %	H: 6.16 %	Cl: 6.77 %	N: 10.69 %	O: 16.79 %
Found:	C: 59.83 %	H: 6.47 %		N: 10.68 %	

3,4,5-Trimethoxy-*N*-(3-oxo-3-(2-(1,2,3,4-tetrahydroacridin-9-yl)hydrazino)propyl)benzamide
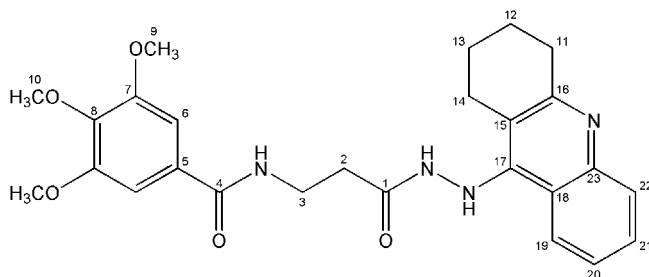
Synthesis: A solution of 0.5 mmol (0.26 g) 3,4,5-trimethoxy-*N*-(3-oxo-3-(2-(1,2,3,4-tetrahydro-acridin-9-yl)hydrazino)propyl)benzamide hydrochloride (**15**) in 5 ml ethanol and 20 ml water is mixed with 1 ml of 1 M sodium hydroxide solution to liberate the base. The reaction mixture is extracted 4 times with 25 ml ethyl acetate, dried using anhydrous sodium sulfate and evaporated in vacuo to yield the final product **16** which needs no further purification.

Yield: 0.23 g (96 %), $C_{26}H_{30}N_4O_5$, $M_R = 479.32$ g/mol
Yellow crystals

^{1}H NMR δ: 1.62-1.72 (m, 4H, H–12,13)
[DMSO-d_6] 2.45 (t, 2H, $J = 7.0$ Hz, H–2)
2.75 (app. bs, 2H, H–14)
2.86 (app. bs, 2H, H–11)
3.41 (app. q, 2H, $J = 6.4$ Hz, H–3)
3.70 (s, 3H, H–10)
3.79 (s, 6H, H–9)
7.16 (s, 2H, H–6)

7.23 (ddd, 1H, $J = 1.0$ 7.6 7.7 Hz, H–20)
7.47 (ddd, 1H, $J = 1.0$ 7.4 7.6 Hz, H–21)
7.69 (app. d, 1H, $J = 8.2$ Hz, H–19)
7.75 (s, 1H, CON<u>H</u>NH)
8.31 (app. s, 1H, H–22)
8.49 (t, 1H, $J = 5.5$ Hz, N<u>H</u>CH$_2$)
10.16 (s, 1H, CONHN<u>H</u>)

^{13}C NMR δ:
[DMSO-d_6]

22.36 (C–13)	22.70 (C–12)	25.02 (C–14)	33.22 (C–2)
33.68 (C–11)	36.02 (C–3)	56.14 (C–9)	60.20 (C–10)
104.98 (C–6)	115.66 (C–15)	119.04 (C–18)	123.00 (C–22)
123.51 (C–20)	127.98 (C–21)	128.29 (C–19)	129.69 (C–5)
140.12 (C–8)	146.66 (C–23)	148.59 (C–17)	152.69 (C–7)
158.21 (C–16)	165.77 (C–4)	170.48 (C–1)	

Melting Point: 217 °C

EA: $C_{26}H_{30}N_4O_5 \cdot 1\ H_2O$
Calculated: C: 62.89 % H: 6.50 % N: 11.28 % O: 19.33 %
Found: C: 62.93 % H: 6.75 % N: 10.88 %

Ethyl 4-((3,4,5-trimethoxybenzoyl)amino)butanoate

Synthesis: 10.0 mmol (2.12 g) of 3,4,5-trimethoxybenzoic acid are dissolved in 20 ml anhydrous dichloromethane with catalytic amounts of *N,N*-dimethylformamide. While stirring the subsequent addition of 11.6 mmol (1.0 ml) of oxalyl chloride generates the acyl chloride. Once the gas evolution has ceased remaining hydrogen chloride, excess oxalyl chloride and the solvent are removed by evaporation in vacuo. The residue is again taken up in 10 ml of dichloromethane and 10.0 mmol (1.68 g) of ethyl 4-aminobutanoate hydrochloride are suspended in the solution. Dropwise addition of 20.0 mmol (3.5 ml) *N*-ethyl-*N,N*-diisopropylamine yields a clear solution which sometimes contains some precipitated *N*-ethyl-*N,N*-diisopropylamine hydrochloride. Washing with water and a saturated solution of sodium hydrogen carbonate, drying with anhydrous sodium sulfate and evaporation in vacuo yields a crude product which is further purified by recrystallization from ethyl acetate and n-hexane to obtain **17**.

Yield: 2.47 g (76 %), $C_{16}H_{23}NO_6$, $M_R = 325.36$ g/mol
White crystals

^{1}H NMR δ:
[CDCl$_3$]

1.22 (t, 3H, $J = 7.1$ Hz, H–1)	3.88 (s, 6H, H–12)
1.94 (app. quint, 2H, $J = 6.7$ Hz, H–5)	4.10 (q, 2H, $J = 7.2$ Hz, H–2)
2.43 (t, 2H, $J = 6.8$ Hz, H–4)	6.76 (bs, 1H, NH)
3.47 (app. q, 2H, $J = 6.3$ Hz, H–6)	7.02 (s, 2H, H–9)
3.85 (s, 3H, H–13)	

^{13}C NMR δ:
[CDCl$_3$]

14.14 (C–1)	24.08 (C–5)	32.26 (C–4)	40.08 (C–6)
56.22 (C–12)	60.69 (C–13)	60.86 (C–2)	104.25 (C–9)
129.82 (C–8)	140.73 (C–11)	153.11 (C–10)	167.01 (C–7)
174.23 (C–3)			

Melting Point: 76 °C, lit.[116] 74-75 °C

EA:

Calculated:	C: 59.07 %	H: 7.13 %	N: 4.30 %	O: 29.50 %
Found:	C: 58.76 %	H: 7.58 %	N: 4.40 %	

N-(4-Hydrazino-4-oxobutyl)-3,4,5-trimethoxybenzamide
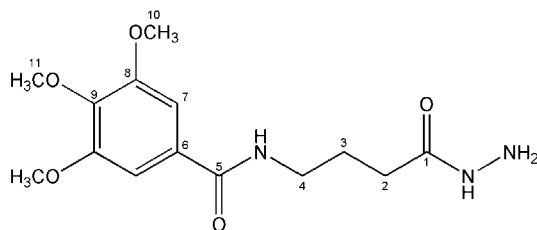
Synthesis: To a mixture of 51.4 mmol hydrazine (2.5 ml hydrazine hydrate, 100 %) and 20 ml absolute ethanol 5.0 mmol (1.63 g) ethyl 4-((3,4,5-trimethoxybenzoyl)amino)butanoate (**17**) are added and the solution is heated to reflux for about 24 hours. The course of the reaction is followed by TLC and once no more ester can be detected the solvent and excess hydrazine are evaporated in vacuo. The crude product is recrystallized from ethanol for further purification to yield **18**.

Yield: 1.06 g (68 %), $C_{14}H_{21}N_3O_5$, $M_R = 311.34$ g/mol
White crystals

^{1}H NMR δ:
[DMSO-d_6]

1.74 (app. quint, 2H, $J = 7.3$ Hz, H–3)	4.20 (s, 2H, NH$_2$)
2.07 (t, 2H, $J = 7.4$ Hz, H–2)	7.16 (s, 2H, H–7)
3.23 (app. q, 2H, $J = 6.5$ Hz, H–4)	8.40 (t, 1H, $J = 5.5$ Hz, N<u>H</u>CH$_2$)
3.69 (s, 3H, H–11)	8.94 (s, 1H, N<u>H</u>NH$_2$)
3.81 (s, 6H, H–10)	

^{13}C NMR δ:
[DMSO-d_6]

25.49 (C–3)	31.23 (C–2)	39.20 (C–4)	56.15 (C–10)
60.19 (C–11)	104.93 (C–7)	129.93 (C–6)	140.02 (C–9)
152.67 (C–8)	165.66 (C–5)	171.45 (C–1)	

Melting Point: 107 °C

EA:

Calculated:	C: 54.01 %	H: 6.80 %	N: 13.50 %	O: 25.69 %
Found:	C: 53.77 %	H: 6.97 %	N: 12.68 %	

3,4,5-Trimethoxy-*N*-(4-oxo-4-(2-(1,2,3,4-tetrahydroacridin-9-yl)hydrazino)butyl)benzamide HCl

Synthesis: 2.0 mmol (0.44 g) 9-Chloro-1,2,3,4-tetrahydroacridine (**1**) and 2.0 mmol (0.62 g) *N*-(4-hydrazino-4-oxobutyl)-3,4,5-trimethoxybenzamide (**18**) dissolved in 20 ml absolute ethanol are heated to 140 °C for 24 hours by means of a sealed bomb. Cooling to room temperature and evaporation in vacuo yields a crude product that is recrystallized from nitromethane for further purification to produce **19**.

Yield: 0.76 g (72 %), $C_{27}H_{33}ClN_4O_5$, $M_R = 529.04$ g/mol
Yellow crystals

^{1}H NMR δ:
[DMSO-*d_6*]

1.76-1.87 (m, 6H, H–3,13,14)	7.60 (app. t, 1H, $J = 7.4$ Hz, H–21)
2.36 (t, 2H, $J = 7.4$ Hz, H–2)	7.88 (app. t, 1H, $J = 7.7$ Hz, H–22)
2.70 (t, 2H, $J = 6.0$ Hz, H–15)	7.99 (app. d, 1H, $J = 8.2$ Hz, H–20)
3.07 (t, 2H, $J = 6.0$ Hz, H–12)	8.55 (t, 1H, $J = 5.5$ Hz, NH̲CH$_2$)
3.29 (app. bs, 7H, H–4)	8.67 (app. d, 1H, $J = 8.8$ Hz, H–23)
3.69 (s, 3H, H–11)	9.64 (s, 1H, CONH̲NH)
3.81 (s, 6H, H–10)	11.06 (s, 1H, CONHNH̲)
7.21 (s, 2H, H–7)	14.35 (s, 1H, N$^+$H)

^{13}C NMR δ:
[DMSO-*d_6*]

20.27 (C–14)	21.43 (C–13)	24.19 (C–15)	24.95 (C–12)
28.34 (C–3)	30.80 (C–2)	38.97 (C–4)	56.19 (C–10)
60.20 (C–11)	105.03 (C–7)	111.27 (C–16)	115.15 (C–19)
119.60 (C–20)	124.12 (C–23)	125.94 (C–21)	129.81 (C–6)
133.02 (C–22)	137.51 (C–24)	140.05 (C–9)	152.66 (C–8)
152.79 (C–17)	155.15 (C–18)	165.71 (C–5)	171.83 (C–1)

Melting Point: 150 °C

EA:
$C_{27}H_{33}ClN_4O_5 \cdot H_2O$

Calculated:	C: 59.28 %	H: 6.45 %	Cl: 6.48 %	N: 10.24 %	O: 17.55 %
Found:	C: 59.09 %	H: 6.43 %		N: 10.27 %	

3,4,5-Trimethoxy-*N*-(4-oxo-4-(2-(1,2,3,4-tetrahydroacridin-9-yl)hydrazino)butyl)benzamide

Synthesis: A solution of 0.5 mmol (0.26 g) 3,4,5-trimethoxy-*N*-(4-oxo-4-(2-(1,2,3,4-tetrahydro-acridin-9-yl)hydrazino)butyl)benzamide hydrochloride (**19**) in 5 ml ethanol and 20 ml water is mixed with 1 ml of 1 M sodium hydroxide solution to liberate the base. The reaction mixture is extracted 4 times with 25 ml ethyl acetate, dried using anhydrous sodium sulfate and evaporated in vacuo to yield the final product **20** which needs no further purification.

Yield: 0.21 g (85 %), $C_{27}H_{32}N_4O_5$, $M_R = 493.34$ g/mol
Yellow crystals

^{1}H NMR δ:
[DMSO-*d$_6$*]

1.71 (app. quint, 2H, *J* = 7.3 Hz, H–3)	7.15 (s, 2H, H–7)
1.75-1.85 (m, 4H, H–13,14)	7.31 (ddd, 1H, *J* = 1.0 7.6 7.7 Hz, H–21)
2.17 (t, 2H, *J* = 7.4 Hz, H–2)	7.51 (ddd, 1H, *J* = 1.3 7.0 8.3 Hz, H–22)
2.81 (app. bs, 2H, H–15)	7.67 (s, 1H, CON<u>H</u>NH)
2.90 (app. bs, 2H, H–12)	7.70 (app. d, 1H, *J* = 8.5 Hz, H–20)
3.22 (app. q, 2H, *J* = 6.5 Hz, H–4)	8.31 (app. d, 1H, *J* = 7.3 Hz, H–23)
3.69 (s, 3H, H–11)	8.38 (app. bs, 1H, N<u>H</u>CH$_2$)
3.79 (s, 6H, H–10)	10.09 (s, 1H, CONHN<u>H</u>)

^{13}C NMR δ:
[DMSO-*d$_6$*]

22.49 (C–14)	22.70 (C–13)	24.89 (C–15)	25.19 (C–3)
30.81 (C–2)	33.73 (C–12)	39.14 (C–4)	56.13 (C–10)
60.19 (C–11)	104.92 (C–7)	115.59 (C–16)	119.10 (C–19)
123.09 (C–23)	123.54 (C–21)	127.99 (C–22)	128.43 (C–20)
129.86 (C–6)	140.04 (C–9)	146.75 (C–24)	148.71 (C–18)
152.67 (C–8)	158.18 (C–17)	165.64 (C–5)	171.86 (C–1)

Melting Point: 145 °C

EA:
$C_{27}H_{32}N_4O_5$ • 1 H_2O
Calculated: C: 63.51 % H: 6.71 % N: 10.97 % O: 18.80 %
Found: C: 63.73 % H: 7.01 % N: 10.63 %

Ethyl 5-((3,4,5-trimethoxybenzoyl)amino)pentanoate
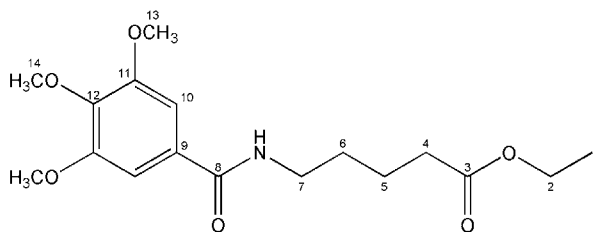
Synthesis: 20.0 mmol (2.34 g) 5-aminopentanoic acid are dissolved in 20 ml absolute ethanol and 30.0 mmol (2.2 ml) thionyl chloride is added dropwise while stirring. The reaction mixture is stirred for 12 hours at room temperature and subsequently evaporated in vacuo. The resulting foam is recrystallized from ethyl acetate to obtain ethyl 5-aminopentanoate hydrochloride. 10.0 mmol (2.12 g) of 3,4,5-trimethoxybenzoic acid are dissolved in 20 ml anhydrous dichloromethane with catalytic amounts of *N,N*-dimethylformamide. While stirring the subsequent addition of 11.6 mmol (1.0 ml) of oxalyl chloride generates the acyl chloride. Once the gas evolution has ceased remaining hydrogen chloride, excess oxalyl chloride and the solvent are removed by evaporation in vacuo. The residue is again taken up in 10 ml of dichloromethane and 10.0 mmol (1.82 g) of ethyl 5-aminopentanoate hydrochloride are suspended in the solution. Dropwise addition of 20.0 mmol (3.5 ml) *N*-ethyl-*N,N*-diisopropylamine yields a clear solution which sometimes contains some precipitated *N*-ethyl-*N,N*-diisopropylamine hydrochloride. Washing with water and a saturated solution of sodium hydrogen carbonate, drying with anhydrous sodium sulfate and evaporation in vacuo yields a crude product which is further purified by recrystallization from ethyl acetate and n-hexane to produce **21**.

Yield: 3.02 g (89 %), $C_{17}H_{25}NO_6$, $M_R = 339.39$ g/mol
White crystals

^{1}H NMR δ:
[DMSO-d_6]

1.16 (t, 3H, $J = 7.1$ Hz, H–1)	3.81 (s, 6H, H–13)
1.48-1.60 (m, 4H, H–5,6)	4.04 (q, 2H, $J = 7.0$ Hz, H–2)
2.32 (t, 2H, $J = 7.1$ Hz, H–4)	7.16 (s, 2H, H–10)
3.24 (app. q, 2H, $J = 5.8$ Hz, H–7)	8.37 (t, 1H, $J = 5.7$ Hz, NH)
3.69 (s, 3H, H–14)	

^{13}C NMR δ:
[DMSO-d_6]

14.24 (C–1)	22.15 (C–5)	28.78 (C–6)	33.33 (C–4)
38.98 (C–7)	56.14 (C–13)	59.79 (C–2)	60.18 (C–14)
104.92 (C–10)	129.96 (C–9)	140.01 (C–12)	152.67 (C–11)
165.59 (C–8)	172.92 (C–3)		

Melting Point: 100 °C

EA:

Calculated:	C: 60.16 %	H: 7.42 %	N: 4.13 %	O: 28.29 %
Found:	C: 59.86 %	H: 7.60 %	N: 4.15 %	

N-(5-Hydrazino-5-oxopentyl)-3,4,5-trimethoxybenzamide
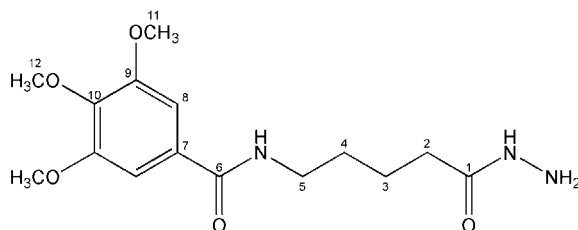
Synthesis: To a mixture of 51.4 mmol hydrazine (2.5 ml hydrazine hydrate, 100 %) and 20 ml absolute ethanol 5.0 mmol (1.70 g) ethyl 5-((3,4,5-trimethoxybenzoyl)amino)pentanoate (**21**) are added and the solution is heated to reflux for about 24 hours. The course of the reaction is followed by TLC and once no more ester can be detected the solvent and excess hydrazine are evaporated in vacuo. The crude product is recrystallized from ethanol for further purification to obtain **22**.

Yield: 1.16 g (71 %), $C_{15}H_{23}N_3O_5$, $M_R = 325.36$ g/mol
White crystals

^{1}H NMR δ:
[DMSO-*d$_6$*]

1.43-1.57 (m, 4H, H–3,4)	4.12 (s, 2H, NH$_2$)
2.04 (t, 2H, $J = 7.1$ Hz, H–2)	7.16 (s, 2H, H–8)
3.23 (app. q, 2H, $J = 6.4$ Hz, H–5)	8.36 (t, 1H, $J = 5.7$ Hz, N<u>H</u>CH$_2$)
3.69 (s, 3H, H–12)	8.90 (s, 1H, N<u>H</u>NH$_2$)
3.81 (s, 6H, H–11)	

^{13}C NMR δ:
[DMSO-*d$_6$*]

22.99 (C–3)	29.05 (C–4)	33.30 (C–2)	39.19 (C–5)
56.15 (C–11)	60.19 (C–12)	104.92 (C–8)	129.98 (C–7)
140.00 (C–10)	152.67 (C–9)	165.56 (C–6)	171.60 (C–1)

Melting Point: 154 °C

EA: $C_{15}H_{23}N_3O_5$ • 0.5 H$_2$O
Calculated: C: 53.88 %   H: 7.23 %   N: 12.57 %   O: 26.32 %
Found: C: 53.49 %   H: 7.63 %   N: 12.18 %

3,4,5-Trimethoxy-*N*-(5-oxo-5-(2-(1,2,3,4-tetrahydroacridin-9-yl)hydrazino)pentyl)benzamide HCl
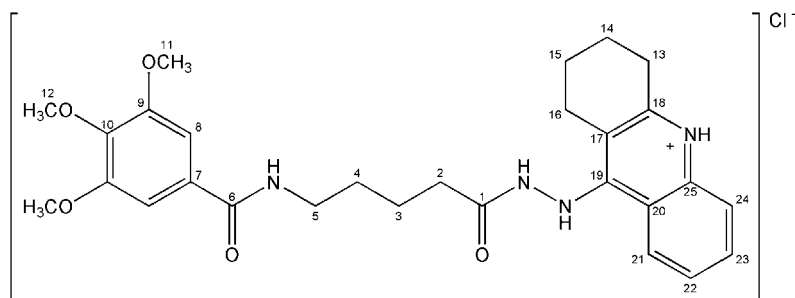
Synthesis:	2.0 mmol (0.44 g) 9-Chloro-1,2,3,4-tetrahydroacridine (**1**) and 2.0 mmol (0.65 g) *N*-(5-hydrazino-5-oxopentyl)-3,4,5-trimethoxybenzamide (**22**) dissolved in 20 ml absolute ethanol are heated to 140 °C for 24 hours by means of a sealed bomb. Evaporation in vacuo yields a crude product that is dissolved in a mixture of 5 ml ethanol and 5 ml diethyl ether. Cooling to -20 °C results in an oily layer that is separated by decantation. Removal of remaining solvent in vacuo yields the final product **23**.

Yield: 0.42 g (39 %), $C_{28}H_{35}ClN_4O_5$, $M_R = 543.06$ g/mol
Brown crystals

^{1}H NMR δ:
[DMSO-*d_6*]

1.50-1.63 (m, 4H, H–3,4)	7.56 (ddd, 1H, *J* = 0.6 7.9 7.9 Hz, H–22)
1.80 (app. bs, 4H, H–14,15)	7.84 (ddd, 1H, *J* = 1.0 7.7 7.7 Hz, H–23)
2.32 (t, 2H, *J* = 7.1 Hz, H–2)	7.99 (app. dd, 1H, *J* = 0.7 8.5 Hz, H–21)
2.69 (app. bs, 2H, H–16)	8.51 (t, 1H, *J* = 5.7 Hz, N$\underline{H}$CH$_2$)
3.07 (app. bs, 2H, H–13)	8.66 (app. d, 1H, *J* = 8.8 Hz, H–24)
3.26 (app. q, 2H, *J* = 6.1 Hz, H–5)	9.62 (s, 1H, CON$\underline{H}$NH)
3.69 (s, 3H, H–12)	11.02 (s, 1H, CONHN$\underline{H}$)
3.81 (s, 6H, H–11)	14.37 (s, 1H, N$^+$H)
7.21 (s, 2H, H–8)	

^{13}C NMR δ:
[DMSO-*d_6*]

20.24 (C–15)	21.39 (C–14)	22.32 (C–3)	24.18 (C–16)
28.26 (C–13)	28.95 (C–4)	32.82 (C–2)	38.86 (C–5)
56.20 (C–11)	60.19 (C–12)	104.98 (C–8)	111.23 (C–17)
115.10 (C–20)	119.47 (C–21)	124.15 (C–24)	125.88 (C–22)
129.91 (C–7)	133.02 (C–23)	137.40 (C–25)	140.01 (C–10)
152.67 (C–9)	155.30 (C–19)	165.56 (C–6)	171.87 (C–1)

Melting Point: 160 °C

EA: $C_{28}H_{35}ClN_4O_5$ • 1 H_2O
Calculated: C: 59.94 %   H: 6.65 %   Cl: 6.32 %   N: 9.99 %   O: 17.11 %
Found: C: 60.01 %   H: 7.19 %   N: 9.86 %

3,4,5-Trimethoxy-*N*-(5-oxo-5-(2-(1,2,3,4-tetrahydroacridin-9-yl)hydrazino)pentyl)benzamide
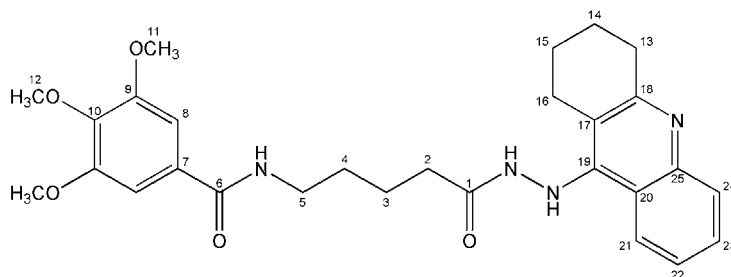
Synthesis: A solution of 0.5 mmol (0.27 g) 3,4,5-trimethoxy-*N*-(5-oxo-5-(2-(1,2,3,4-tetrahydro-acridin-9-yl)hydrazino)pentyl)benzamide hydrochloride (**23**) in 5 ml ethanol and 20 ml water is mixed with 1 ml of 1 M sodium hydroxide solution to liberate the base. The reaction mixture is extracted 4 times with 25 ml ethyl acetate, dried using anhydrous sodium sulfate and evaporated in vacuo to yield the final product **24** which needs no further purification.

Yield: 0.23 g (91 %), $C_{28}H_{34}N_4O_5$, $M_R = 506.60$ g/mol
Yellow crystals

^{1}H NMR δ:
[DMSO-*d$_6$*]

1.42-1.55 (m, 4H, H–3,4)	7.15 (s, 2H, H–8)
1.72-1.83 (m, 4H, H–14,15)	7.29 (ddd, 1H, $J = 1.0$ 7.7 7.7 Hz, H–22)
2.13 (t, 2H, $J = 6.9$ Hz, H–2)	7.48 (ddd, 1H, $J = 1.3$ 7.6 7.6 Hz, H–23)
2.81 (app. bs, 2H, H–16)	7.67 (s, 1H, CONH<u>N</u>H)
2.89 (app. bs, 2H, H–13)	7.70 (app. d, 1H, $J = 8.5$ Hz, H–21)
3.21 (app. q, 2H, $J = 6.1$ Hz, H–5)	8.31 (app. d, 1H, $J = 9.8$ Hz, H–24)
3.69 (s, 3H, H–12)	8.33 (t, 1H, $J = 5.8$ Hz, N<u>H</u>CH$_2$)
3.80 (s, 6H, H–11)	10.04 (s, 1H, CONHN<u>H</u>)

^{13}C NMR δ:
[DMSO-*d$_6$*]

22.51 (C–15)	22.63 (C–14)	22.71 (C–3)	24.91 (C–16)
29.00 (C–4)	32.85 (C–2)	33.77 (C–13)	39.06 (C–5)
56.16 (C–11)	60.21 (C–12)	104.92 (C–8)	115.58 (C–17)
119.10 (C–20)	123.14 (C–24)	123.49 (C–22)	127.95 (C–23)
128.40 (C–21)	129.96 (C–7)	140.03 (C–10)	146.78 (C–25)
148.79 (C–19)	152.68 (C–9)	158.17 (C–18)	165.54 (C–6)
171.98 (C–1)			

Melting Point: 194 °C

EA:

Calculated:	C: 66.39 %	H: 6.76 %	N: 11.06 %	O: 15.79 %
Found:	C: 66.01 %	H: 6.94 %	N: 10.81 %	

Ethyl 6-((3,4,5-trimethoxybenzoyl)amino)hexanoate
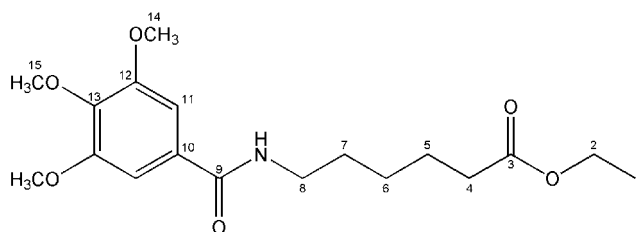
Synthesis: 20.0 mmol (2.62 g) 6-aminohexanoic acid are dissolved in 20 ml absolute ethanol and 30.0 mmol (2.2 ml) thionyl chloride is added dropwise while stirring. The reaction mixture is stirred for 12 hours at room temperature and subsequently evaporated in vacuo. The resulting foam is recrystallized from ethyl acetate to obtain ethyl 6-aminohexanoate hydrochloride. 10.0 mmol (1.96 g) ethyl 6-aminohexanoate hydrochloride and equimolar amounts (2.31 g) of 3,4,5-trimethoxybenzoyl chloride are dissolved in 20 ml anhydrous dichloromethane and 20.0 mmol (3.5 ml) of *N*-ethyl-*N,N*-diisopropylamine are added dropwise. Washing with 0.1 M hydrochloric acid, a saturated solution of sodium hydrogen carbonate and water followed by drying with anhydrous sodium sulfate and evaporation in vacuo yields a crude product which is further purified by recrystallization from ethyl acetate to yield **25**.

Yield: 2.20 g (62 %), $C_{18}H_{27}NO_6$, $M_R = 353.42$ g/mol
White lints

^{1}H NMR δ:
[DMSO-d_6]

1.15 (t, 3H, $J = 7.1$ Hz, H–1)	3.69 (s, 3H, H–15)
1.30 (app. quint, 2H, $J = 7.3$ Hz, H–6)	3.81 (s, 6H, H–14)
1.51 (app. quint, 2H, $J = 7.6$ Hz, H–7)	4.03 (q, 2H, $J = 7.2$ Hz, H–2)
1.55 (app. quint, 2H, $J = 7.9$ Hz, H–5)	7.15 (s, 2H, H–11)
2.28 (t, 2H, $J = 7.6$ Hz, H–4)	8.34 (t, 1H, $J = 5.7$ Hz, NH)
3.23 (app. q, 2H, $J = 6.6$ Hz, H–8)	

^{13}C NMR δ:
[DMSO-d_6]

14.24 (C–1)	24.37 (C–5)	26.07 (C–6)	29.00 (C–7)
33.59 (C–4)	39.21 (C–8)	56.14 (C–14)	59.75 (C–2)
60.18 (C–15)	104.92 (C–11)	130.02 (C–10)	139.99 (C–13)
152.66 (C–12)	165.56 (C–9)	172.95 (C–3)	

Melting Point: 79 °C, lit.[117] 83-84.5 °C

EA:

Calculated:	C: 61.17 %	H: 7.70 %	N: 3.96 %	O: 27.16 %
Found:	C: 60.81 %	H: 7.72 %	N: 4.04 %	

N-(6-Hydrazino-6-oxohexyl)-3,4,5-trimethoxybenzamide
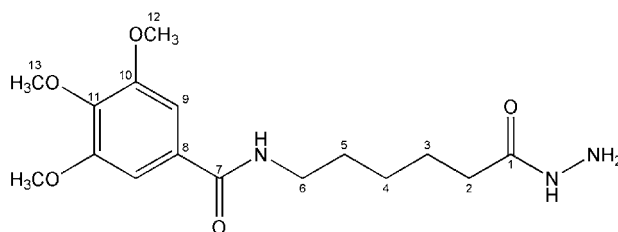
Synthesis: To a mixture of 51.4 mmol hydrazine (2.5 ml hydrazine hydrate, 100 %) and 20 ml absolute ethanol 5.0 mmol (1.77 g) ethyl 6-((3,4,5-trimethoxybenzoyl)amino)hexanoate (**25**) are added and the solution is heated to reflux for about 24 hours. The course of the reaction is followed by TLC and once no more ester can be detected the solvent and excess hydrazine are evaporated in vacuo. The crude product is recrystallized from ethanol for further purification to obtain **26**.

Yield: 1.36 g (80 %), $C_{16}H_{25}N_3O_5$, $M_R = 339.39$ g/mol
White crystals

^{1}H NMR δ: 1.26 (app. quint, 2H, $J = 7.6$ Hz, H–4) 3.81 (s, 6H, H–12)
[DMSO-d_6] 1.51 (app. sext, 4H, $J = 7.1$ Hz, H–3,5) 4.11 (s, 2H, NH$_2$)
2.01 (t, 2H, $J = 7.4$ Hz, H–2) 7.16 (s, 2H, H–9)
3.22 (app. q, 2H, $J = 6.6$ Hz, H–6) 8.43 (t, 1H, $J = 5.7$ Hz, N<u>H</u>CH$_2$)
3.69 (s, 3H, H–13) 8.88 (s, 1H, N<u>H</u>NH$_2$)

^{13}C NMR δ: 25.15 (C–3) 26.35 (C–4) 29.13 (C–5) 33.52 (C–2)
[DMSO-d_6] 39.34 (C–6) 56.15 (C–12) 60.18 (C–13) 104.92 (C–9)
130.02 (C–8) 139.98 (C–11) 152.66 (C–10) 165.55 (C–7)
171.67 (C–1)

Melting Point: 105 °C

EA: Calculated: C: 56.62 % H: 7.42 % N: 12.38 % O: 23.57 %
Found: C: 56.65 % H: 7.47 % N: 12.37 %

3,4,5-Trimethoxy-*N*-(6-oxo-6-(2-(1,2,3,4-tetrahydroacridin-9-yl)hydrazino)hexyl)benzamide HCl
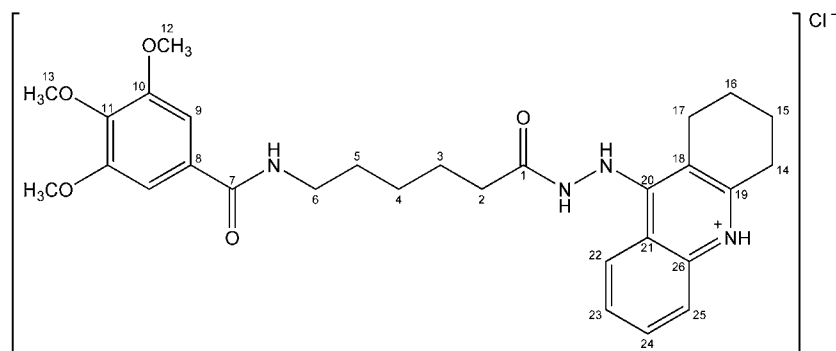
Synthesis:	2.0 mmol (0.44 g) 9-Chloro-1,2,3,4-tetrahydroacridine (**1**) and 2.0 mmol (0.68 g) *N*-(6-hydrazino-6-oxohexyl)-3,4,5-trimethoxybenzamide (**26**) dissolved in 20 ml absolute ethanol are heated to 140 °C for 24 hours by means of a sealed bomb. Cooling to room temperature and evaporation in vacuo yields a crude product that is recrystallized from nitromethane for further purification to produce **27**.

Yield: 0.58 g (52 %), $C_{29}H_{37}ClN_4O_5$, $M_R = 557.09$ g/mol
Yellow crystals

^{1}H NMR δ:
[DMSO-*d$_6$*]

1.31 (app. quint, 2H, $J = 7.6$ Hz, H–4)	7.18 (s, 2H, H–9)
1.53 (app. quint, 2H, $J = 7.4$ Hz, H–5)	7.59 (ddd, 1H, $J = 0.7$ 7.8 7.9 Hz, H–23)
1.57 (app. quint, 2H, $J = 7.5$ Hz, H–3)	7.87 (app. t, 1H, $J = 7.4$ Hz, H–24)
1.82 (app. bs, 4H, H–15,16)	7.99 (app. d, 1H, $J = 8.5$ Hz, H–22)
2.28 (t, $J = 7.3$ Hz, H–2)	8.45 (t, 1H, $J = 5.5$ Hz, N<u>H</u>CH$_2$)
2.69 (app. bs, 2H, H–17)	8.66 (app. d, 1H, $J = 8.5$ Hz, H–25)
3.08 (app. bs, 2H, H–14)	9.61 (s, 1H, CON<u>H</u>NH)
3.23 (app. q, 2H, $J = 6.6$ Hz, H–6)	10.96 (s, 1H, CONHN<u>H</u>)
3.69 (s, 3H, H–13)	14.34 (s, 1H, N$^+$H)
3.81 (s, 6H, H–12)	

^{13}C NMR δ:
[DMSO-*d$_6$*]

20.27 (C–16)	21.39 (C–15)	24.15 (C–17)	24.51 (C–3)
26.29 (C–4)	28.29 (C–14)	29.05 (C–5)	33.05 (C–2)
39.24 (C–6)	56.18 (C–12)	60.19 (C–13)	104.97 (C–9)
111.24 (C–18)	115.11 (C–21)	119.53 (C–22)	124.16 (C–25)
125.88 (C–23)	129.99 (C–8)	133.04 (C–24)	137.46 (C–26)
139.98 (C–11)	152.65 (C–10)	152.71 (C–19)	155.28 (C–20)
165.56 (C–7)	171.89 (C–1)		

Melting Point: 210 °C

EA: $C_{29}H_{37}ClN_4O_5$ • 0.5 H_2O
Calculated: C: 61.53 % H: 6.77 % Cl: 6.26 % N: 9.90 % O: 15.54 %
Found: C: 61.68 % H: 7.15 % N: 9.64 %

3,4,5-Trimethoxy-*N*-(6-oxo-6-(2-(1,2,3,4-tetrahydroacridin-9-yl)hydrazino)hexyl)benzamide
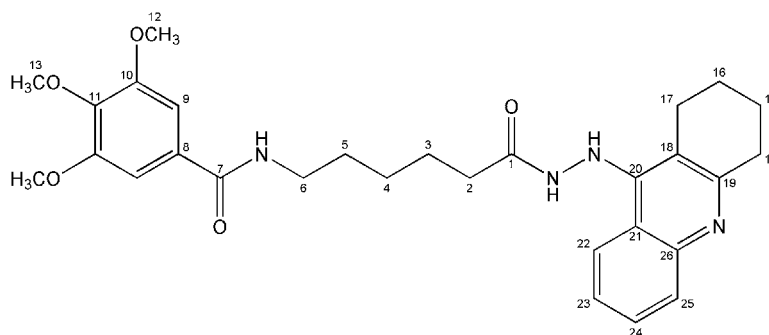
Synthesis: A solution of 0.5 mmol (0.28 g) 3,4,5-trimethoxy-*N*-(6-oxo-6-(2-(1,2,3,4-tetrahydro-acridin-9-yl)hydrazino)hexyl)benzamide hydrochloride (**27**) in 5 ml ethanol and 20 ml water is mixed with 1 ml of 1 M sodium hydroxide solution to liberate the base. The reaction mixture is extracted 4 times with 25 ml ethyl acetate, dried using anhydrous sodium sulfate and evaporated in vacuo to yield the final product **28** which needs no further purification.

Yield: 0.25 g (96 %), $C_{29}H_{36}N_4O_5$, $M_R = 520.63$ g/mol
Yellow crystals

¹H NMR δ: 1.23 (app. quint, 2H, $J = 7.6$ Hz, H–4)   7.15 (s, 2H, H–9)
[DMSO-*d₆*]   1.48 (app. sext, 4H, $J = 7.5$ Hz, H–3,5)   7.31 (ddd, 1H, $J = 1.3$ 7.1 8.4 Hz, H–23)
1.74-1.84 (m, 4H, H–15,16)   7.51 (ddd, 1H, $J = 1.3$ 6.6 8.3 Hz, H–24)
2.10 (t, $J = 7.3$ Hz, H–2)   7.66 (s, 1H, CON<u>H</u>NH)
2.81 (app. bs, 2H, H–17)   7.70 (app. d, 1H, $J = 8.2$ Hz, H–22)
2.90 (t, $J = 5.8$ Hz, H–14)   8.31 (app. d, 1H, $J = 5.7$ Hz, H–25)
3.18 (app. q, 2H, $J = 6.6$ Hz, H–6)   8.32 (t, 1H, $J = 5.5$ Hz, N<u>H</u>CH₂)
3.69 (s, 3H, H–13)   10.03 (s, 1H, CONHN<u>H</u>)
3.80 (s, 6H, H–12)

¹³C NMR δ:
[DMSO-*d₆*]

22.50 (C–16)	22.69 (C–15)	24.83 (C–3,17)	26.28 (C–4)
29.09 (C–5)	33.08 (C–2)	33.72 (C–14)	39.30 (C–6)
56.14 (C–12)	60.18 (C–13)	104.91 (C–9)	115.51 (C–18)
119.06 (C–21)	123.20 (C–25)	123.46 (C–23)	127.98 (C–24)
128.36 (C–22)	130.00 (C–8)	139.99 (C–11)	146.75 (C–26)
148.81 (C–20)	152.66 (C–10)	158.08 (C–19)	165.54 (C–7)
171.99 (C–1)			

Melting Point: 175 °C

EA: Calculated: C: 66.90 %   H: 6.97 %   N: 10.76 %   O: 15.37 %
Found: C: 66.58 %   H: 7.12 %   N: 10.47 %

Ethyl 7-((3,4,5-trimethoxybenzoyl)amino)heptanoate
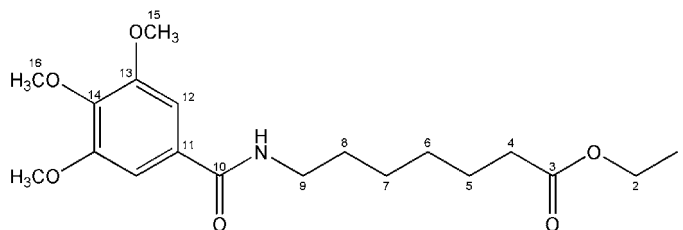
Synthesis: 20.0 mmol (2.90 g) 7-aminoheptanoic acid are dissolved in 20 ml absolute ethanol and 30.0 mmol (2.2 ml) thionyl chloride is added dropwise while stirring. The reaction mixture is stirred for 12 hours at room temperature and subsequently evaporated in vacuo. The resulting foam is recrystallized from ethyl acetate to obtain ethyl 7-aminoheptanoate hydrochloride. 10.0 mmol (2.12 g) of 3,4,5-trimethoxybenzoic acid are dissolved in 20 ml anhydrous dichloromethane with catalytic amounts of *N,N*-dimethylformamide. While stirring the subsequent addition of 11.6 mmol (1.0 ml) of oxalyl chloride generates the acyl chloride. Once the gas evolution has ceased remaining hydrogen chloride, excess oxalyl chloride and the solvent are removed by evaporation in vacuo. The residue is again taken up in 10 ml of dichloromethane and 10.0 mmol (2.10 g) of ethyl 7-aminoheptanoate hydrochloride are suspended in the solution. Dropwise addition of 20.0 mmol (3.5 ml) *N*-ethyl-*N,N*-diisopropylamine yields a clear solution which sometimes contains some precipitated *N*-ethyl-*N,N*-diisopropylamine hydrochloride. Washing with water and a saturated solution of sodium hydrogen carbonate, drying with anhydrous sodium sulfate and evaporation in vacuo yields a crude product which is further purified by recrystallization from ethyl acetate and n-hexane to produce **29**.

Yield: 2.91 g (79 %), $C_{19}H_{29}NO_6$, $M_R = 367.44$ g/mol
White lints

^{1}H NMR δ:
[DMSO-d_6]

1.16 (t, 3H, *J* = 7.1 Hz, H–1)	3.68 (s, 3H, H–16)
1.29 (app. quint, 4H, *J* = 7.3 Hz, H–6,7)	3.81 (s, 6H, H–15)
1.46-1.56 (m, 4H, H–5,8)	4.03 (q, 2H, *J* = 7.1 Hz, H–2)
2.26 (t, 2H, *J* = 7.4 Hz, H–4)	7.15 (s, 2H, H–12)
3.23 (app. q, 2H, *J* = 6.6 Hz, H–9)	8.33 (t, 1H, *J* = 5.5 Hz, NH)

^{13}C NMR δ:
[DMSO-d_6]

14.25 (C–1)	24.52 (C–5)	26.28 (C–7)	28.32 (C–6)
29.15 (C–8)	33.60 (C–4)	39.37 (C–9)	56.14 (C–15)
59.74 (C–2)	60.18 (C–16)	104.91 (C–12)	130.04 (C–11)
139.98 (C–14)	152.66 (C–13)	165.56 (C–10)	172.98 (C–3)

Melting Point: 86 °C

EA:

Calculated:	C: 62.11 %	H: 7.96 %	N: 3.81 %	O: 26.13 %
Found:	C: 61.93 %	H: 8.11 %	N: 3.87 %	

N-(7-Hydrazino-7-oxoheptyl)-3,4,5-trimethoxybenzamide
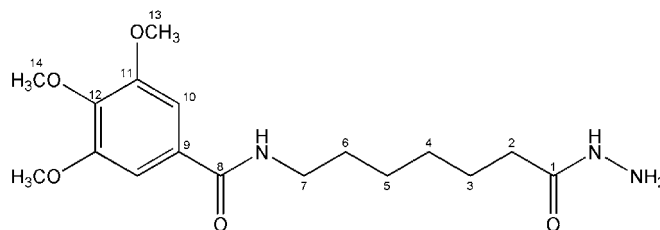
Synthesis: To a mixture of 51.4 mmol hydrazine (2.5 ml hydrazine hydrate, 100 %) and 20 ml absolute ethanol 5.0 mmol (1.84 g) ethyl 7-((3,4,5-trimethoxybenzoyl)amino)heptanoate (**29**) are added and the solution is heated to reflux for about 24 hours. The course of the reaction is followed by TLC and once no more ester can be detected the solvent and excess hydrazine are evaporated in vacuo. The crude product is recrystallized from ethanol for further purification to obtain **30**.

Yield: 1.16 g (66 %), $C_{17}H_{27}N_3O_5$, $M_R = 353.42$ g/mol
White crystals

^{1}H NMR δ: 1.21-1.33 (m, 4H, H–4,5) 3.81 (s, 6H, H–13)
[DMSO-d_6] 1.49 (app. sext, 4H, $J = 6.8$ Hz, H–3,6) 4.12 (s, 2H, NH$_2$)
1.99 (t, 2H, $J = 7.4$ Hz, H–2) 7.15 (s, 2H, H–10)
3.22 (app. q, 2H, $J = 6.6$ Hz, H–7) 8.43 (t, 1H, $J = 5.5$ Hz, N$\underline{H}$CH$_2$)
3.69 (s, 3H, H–14) 8.87 (s, 1H, N$\underline{H}$NH$_2$)

^{13}C NMR δ: 25.30 (C–3) 26.39 (C–5) 28.55 (C–4) 29.24 (C–6)
[DMSO-d_6] 33.52 (C–2) 39.37 (C–7) 56.15 (C–13) 60.18 (C–14)
104.91 (C–10) 130.04 (C–9) 139.97 (C–12) 152.66 (C-11)
165.55 (C–8) 171.71 (C–1)

Melting Point: 133 °C

EA: Calculated: C: 57.77 % H: 7.70 % N: 11.89 % O: 22.64 %
Found: C: 57.58 % H: 7.64 % N: 11.53 %

3,4,5-Trimethoxy-*N*-(7-oxo-7-(2-(1,2,3,4-tetrahydroacridin-9-yl)hydrazino)heptyl)benzamide
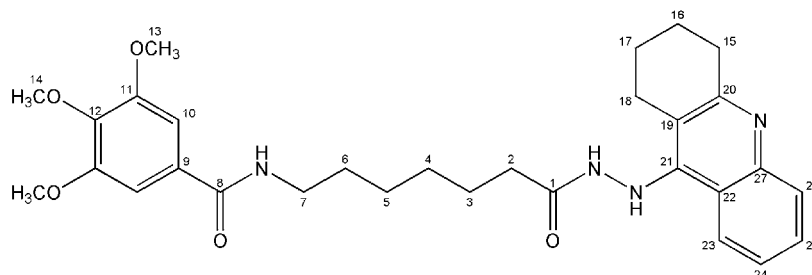
Synthesis: 2.0 mmol (0.44 g) 9-Chloro-1,2,3,4-tetrahydroacridine (**1**) and 2.0 mmol (0.71 g) *N*-(7-hydrazino-7-oxoheptyl)-3,4,5-trimethoxybenzamide (**30**) dissolved in 20 ml absolute ethanol are heated to 140 °C for 24 hours by means of a sealed bomb. Cooling to room temperature and evaporation in vacuo yields a crude product that is taken up in 5 ml ethanol and diluted with 20 ml water. Addition of 2.5 ml 1N sodium hydroxide solution liberates the base as an oily layer. After decantating the remaining water the oily residue is suspended in 25 ml ethyl acetate and heated to reflux. The final product **31** precipitates and is recovered by suction filtration without the need for further purification.

Yield: 0.67 g (63 %), $C_{30}H_{38}N_4O_5$, $M_R = 534.66$ g/mol
Yellow powder

^{1}H NMR δ:
[DMSO-d_6]

1.16-1.29 (m, 4H, H–4,5)	7.15 (s, 2H, H–10)
1.45 (app. sext, 4H, $J = 6.7$ Hz, H–3,6)	7.31 (ddd, 1H, $J = 1.3\ 6.8\ 8.3$ Hz, H–24)
1.73-1.85 (m, 4H, H–16,17)	7.51 (ddd, 1H, $J = 1.3\ 6.8\ 8.3$ Hz, H–25)
2.09 (t, 2H, $J = 7.3$ Hz, H–2)	7.69 (s, 1H, CONH̲NH)
2.81 (app. bs, 2H, H–18)	7.70 (app. d, 1H, $J = 7.6$ Hz, H–23)
2.90 (t, 2H, $J = 6.0$ Hz, H–15)	8.32 (app. d, 1H, $J = 5.7$ Hz, H–26)
3.20 (app. q, 2H, $J = 6.6$ Hz, H–7)	8.33 (t, 1H, $J = 5.7$ Hz, NH̲CH$_2$)
3.69 (s, 3H, H–14)	10.04 (s, 1H, CONHNH̲)
3.81 (s, 6H, H–13)	

^{13}C NMR δ:
[DMSO-d_6]

22.47 (C–17)	22.67 (C–16)	24.81 (C–18)	25.01 (C–3)
26.39 (C–5)	28.49 (C–4)	29.23 (C–6)	33.09 (C–2)
33.60 (C–18)	39.36 (C–7)	56.14 (C–13)	60.18 (C–14)
104.91 (C–10)	115.44 (C–19)	118.99 (C–22)	123.25 (C–26)
123.49 (C–24)	128.08 (C–25)	128.16 (C–23)	130.04 (C–9)
139.98 (C–12)	146.56 (C–27)	148.94 (C–21)	152.66 (C–11)
158.03 (C–20)	165.56 (C–8)	172.03 (C–1)	

Melting Point: 193 °C

EA: $C_{30}H_{38}N_4O_5 \cdot 0.5\ H_2O$
Calculated: C: 66.28 % H: 7.23 % N: 10.31 % O: 16.19 %
Found: C: 66.67 % H: 7.44 % N: 10.08 %

3,4,5-Trimethoxy-*N*-(7-oxo-7-(2-(6-chloro-1,2,3,4-tetrahydroacridin-9-yl)hydrazino)heptyl)-benzamide HCl
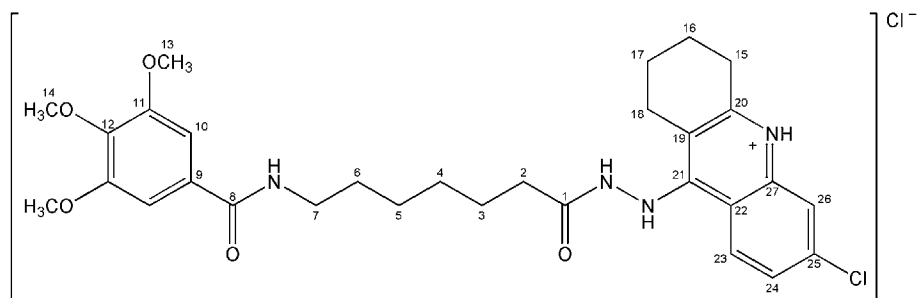
Synthesis: 1.0 mmol (0.25 g) 6,9-Dichloro-1,2,3,4-tetrahydroacridine (**2**) and 1.0 mmol (0.35 g) *N*-(7-hydrazino-7-oxoheptyl)-3,4,5-trimethoxybenzamide (**30**) dissolved in 10 ml absolute ethanol are heated to 140 °C for 24 hours by means of a sealed bomb. The solution is filtered and evaporated in vacuo. The remaining foam is recrystallized from nitromethane to yield the final product **32**.

Yield: 0.53 g (87 %), $C_{30}H_{38}Cl_2N_4O_5$, $M_R = 605.56$ g/mol
Yellow powder

^{1}H NMR δ:
[DMSO-*d$_6$*]

1.26-1.33 (m, 4H, H–4,5)	7.18 (s, 2H, H–10)
1.46-1.58 (m, 4H, H–3,6)	7.64 (dd, 1H, J = 2.2 9.2 Hz, H–24)
1.81 (app. bs, 4H, H–16,17)	8.11 (d, 1H, J = 2.3 Hz, H–26)
2.28 (t, 2H, J = 7.3 Hz, H–2)	8.45 (t, 1H, J = 5.7 Hz, NHCH$_2$)
2.66 (app. bs, 2H, H–18)	8.70 (d, 1H, J = 9.5 Hz, H–23)
3.07 (app. bs, 2H, H–15)	9.73 (s, 1H, CONHNH)
3.23 (app. q, 2H, J = 6.6 Hz, H–7)	11.07 (s, 1H, CONHNH)
3.68 (s, 3H, H–14)	14.69 (s, 1H, N$^+$H)
3.81 (s, 6H, H–13)	

^{13}C NMR δ:
[DMSO-*d$_6$*]

20.16 (C–17)	21.25 (C–16)	24.01 (C–18)	24.67 (C–3)
26.36 (C–5)	28.27 (C–15)	28.53 (C–4)	29.22 (C–6)
33.06 (C–2)	39.37 (C–7)	56.18 (C–13)	60.18 (C–14)
104.97 (C–10)	111.57 (C–19)	113.64 (C–22)	118.33 (C–26)
126.22 (C–24)	126.60 (C–23)	130.02 (C–9)	137.52 (C–27)
138.21 (C–25)	139.96 (C–12)	152.65 (C–11)	153.29 (C–20)
155.18 (C–21)	165.56 (C–8)	171.97 (C–1)	

Melting Point: 191 °C

EA: $C_{30}H_{38}Cl_2N_4O_5 \cdot H_2O$

Calculated:	C: 57.78 %	H: 6.47 %	Cl: 11.37 %	N: 8.98 %	O: 15.39 %
Found:	C: 57.96 %	H: 6.58 %		N: 9.13 %	

Ethyl 8-((3,4,5-trimethoxybenzoyl)amino)octanoate

Synthesis: 20.0 mmol (3.18 g) 8-aminooctanoic acid are dissolved in 20 ml absolute ethanol and 30.0 mmol (2.2 ml) thionyl chloride is added dropwise while stirring. The reaction mixture is stirred for 12 hours at room temperature and subsequently evaporated in vacuo. The resulting foam is recrystallized from ethyl acetate to obtain ethyl 8-aminooctanoate hydrochloride. 10.0 mmol (2.12 g) of 3,4,5-trimethoxybenzoic acid are dissolved in 20 ml anhydrous dichloromethane with catalytic amounts of *N,N*-dimethylformamide. While stirring the subsequent addition of 11.6 mmol (1.0 ml) of oxalyl chloride generates the acyl chloride. Once the gas evolution has ceased remaining hydrogen chloride, excess oxalyl chloride and the solvent are removed by evaporation in vacuo. The residue is again taken up in 10 ml of dichloromethane and 10.0 mmol (2.24 g) of ethyl 8-aminooctanoate hydrochloride are suspended in the solution. Dropwise addition of 20.0 mmol (3.5 ml) *N*-ethyl-*N,N*-diisopropylamine yields a clear solution which sometimes contains some precipitated *N*-ethyl-*N,N*-diisopropylamine hydrochloride. Washing with water and a saturated solution of sodium hydrogen carbonate, drying with anhydrous sodium sulfate and evaporation in vacuo yields a crude product which is further purified by recrystallization from ethyl acetate and n-hexane to obtain **33**.

Yield: 3.05 g (80 %), $C_{20}H_{31}NO_6$, $M_R = 381.47$ g/mol
White lints

^{1}H NMR δ:
[DMSO-d_6]

1.16 (t, 3H, $J = 7.1$ Hz, H–1)	3.69 (s, 3H, H–17)
1.28 (bs, 6H, H–6,7,8)	3.81 (s, 6H, H–16)
1.46-1.55 (m, 4H, H–5,9)	4.03 (q, 2H, $J = 7.1$ Hz, H–2)
2.25 (t, 2H, $J = 7.4$ Hz, H–4)	7.15 (s, 2H, H–13)
3.23 (app. q, 2H, $J = 6.6$ Hz, H–10)	8.33 (t, 1H, $J = 5.5$ Hz, NH)

^{13}C NMR δ:
[DMSO-d_6]

14.25 (C–1)	24.54 (C–4)	26.48 (C–8)	28.52 (C–6)
28.54 (C–7)	29.27 (C–9)	33.63 (C–3)	39.37 (C–10)
56.14 (C–16)	59.73 (C–2)	60.18 (C–17)	104.91 (C–13)
130.04 (C–12)	139.98 (C–15)	152.66 (C–14)	165.54 (C–11)
172.99 (C–3)			

Melting Point: 85 °C

EA:

Calculated:	C: 62.97 %	H: 8.19 %	N: 3.67 %	O: 25.16 %
Found:	C: 63.14 %	H: 8.69 %	N: 3.62 %	

N-(8-Hydrazino-8-oxooctyl)-3,4,5-trimethoxybenzamide

Synthesis: To a mixture of 51.4 mmol hydrazine (2.5 ml hydrazine hydrate, 100 %) and 20 ml absolute ethanol 5.0 mmol (1.91 g) ethyl 8-((3,4,5-trimethoxybenzoyl)amino)octanoate (**33**) are added and the solution is heated to reflux for about 24 hours. The course of the reaction is followed by TLC and once no more ester can be detected the solvent and excess hydrazine are evaporated in vacuo. The crude product is recrystallized from ethanol for further purification to produce **34**.

Yield: 1.19 g (65 %), $C_{18}H_{29}N_3O_5$, $M_R = 367.45$ g/mol
White crystals

^{1}H NMR δ: 1.18-1.32 (m, 6H, H–4,5,6) 3.81 (s, 6H, H–14)
[DMSO-d_6] 1.43-1.54 (m, 4H, H–3,7) 4.11 (s, 2H, NH$_2$)
1.99 (t, 2H, $J = 7.4$ Hz, H–2) 7.15 (s, 2H, H–11)
3.23 (app. q, 2H, $J = 6.6$ Hz, H–8) 8.34 (t, 1H, $J = 5.7$ Hz, NHCH$_2$)
3.69 (s, 3H, H–15) 8.86 (s, 1H, NHNH$_2$)

^{13}C NMR δ: 25.30 (C–3) 26.54 (C–6) 28.64 (C–4) 28.73 (C–5)
[DMSO-d_6] 29.32 (C–7) 33.54 (C–2) 39.40 (C–8) 56.14 (C–14)
60.18 (C–15) 104.91 (C–11) 130.04 (C–10) 139.97 (C–13)
152.66 (C–12) 165.54 (C–9) 171.72 (C–1)

Melting Point: 135 °C

EA: Calculated: C: 58.84 % H: 7.95 % N: 11.44 % O: 21.77 %
Found:

3,4,5-Trimethoxy-*N*-(8-oxo-8-(2-(1,2,3,4-tetrahydroacridin-9-yl)hydrazino)octyl)benzamide
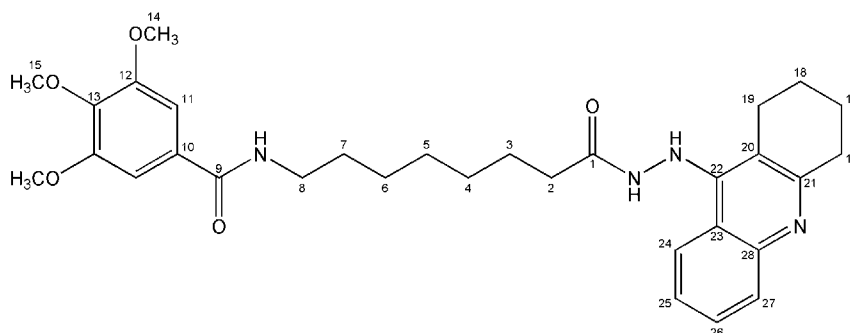
Synthesis: 2.0 mmol (0.44 g) 9-Chloro-1,2,3,4-tetrahydroacridine (**1**) and 2.0 mmol (0.73 g) *N*-(8-hydrazino-8-oxooctyl)-3,4,5-trimethoxybenzamide (**34**) dissolved in 20 ml absolute ethanol are heated to 140 °C for 24 hours by means of a sealed bomb. Cooling to room temperature and evaporation in vacuo yields a crude product that is taken up in 5 ml ethanol and diluted with 20 ml water. Addition of 2.5 ml 1N sodium hydroxide solution liberates the base as an oily layer. After decantating the remaining water the oily residue is suspended in 25 ml ethyl acetate and heated to reflux. The final product **35** precipitates and is recovered by suction filtration without the need for further purification.

Yield: 0.83 g (76 %), $C_{31}H_{40}N_4O_5$, M_R = 548.68 g/mol
Yellow powder

^{1}H NMR δ:
[DMSO-*d_6*]

1.12-1.27 (m, 6H, H–4,5,6)	7.16 (s, 2H, H–11)
1.45 (app. sext, 4H, *J* = 7.8 Hz, H–3,7)	7.30 (ddd, 1H, *J* = 1.3 6.8 8.4 Hz, H–25)
1.74-1.84 (m, 4H, H–17,18)	7.50 (ddd, 1H, *J* = 1.0 6.8 8.4 Hz, H–26)
2.08 (t, 2H, *J* = 7.3 Hz, H–2)	7.68 (s, 1H, CON<u>H</u>NH)
2.81 (app. bs, 2H, H–19)	7.69 (app. d, 1H, *J* = 7.9 Hz, H–24)
2.90 (t, 2H, *J* = 6.0 Hz, H–16)	8.31 (app. d, 1H, *J* = 9.2 Hz, H–27)
3.21 (app. q, 2H, *J* = 6.7 Hz, H–8)	8.33 (t, 1H, *J* = 5.7 Hz, N<u>H</u>CH₂)
3.69 (s, 3H, H–15)	10.03 (s, 1H, CONHN<u>H</u>)
3.81 (s, 6H, H–14)	

^{13}C NMR δ:
[DMSO-*d_6*]

22.49 (C–18)	22.68 (C–17)	24.81 (C–19)	25.00 (C–3)
26.52 (C–6)	28.64 (C–4,5)	29.30 (C–7)	33.09 (C–2)
33.65 (C–16)	39.37 (C–8)	56.14 (C–14)	60.18 (C–15)
104.91 (C–11)	115.47 (C–20)	119.03 (C–23)	123.24 (C–27)
123.45 (C–25)	128.01 (C–26)	128.23 (C–24)	130.03 (C–10)
139.98 (C–13)	146.64 (C–28)	148.89 (C–22)	152.66 (C–12)
157.98 (C–21)	165.53 (C–9)	172.04 (C–1)	

Melting Point: 187 °C

EA:

Calculated:	C: 67.86 %	H: 7.35 %	N: 10.21 %	O: 14.58 %
Found:	C: 67.53 %	H: 7.35 %	N: 10.25 %	

3,4,5-Trimethoxy-*N*-(8-oxo-8-(2-(6-chloro-1,2,3,4-tetrahydroacridin-9-yl)hydrazino)octyl)-benzamide HCl
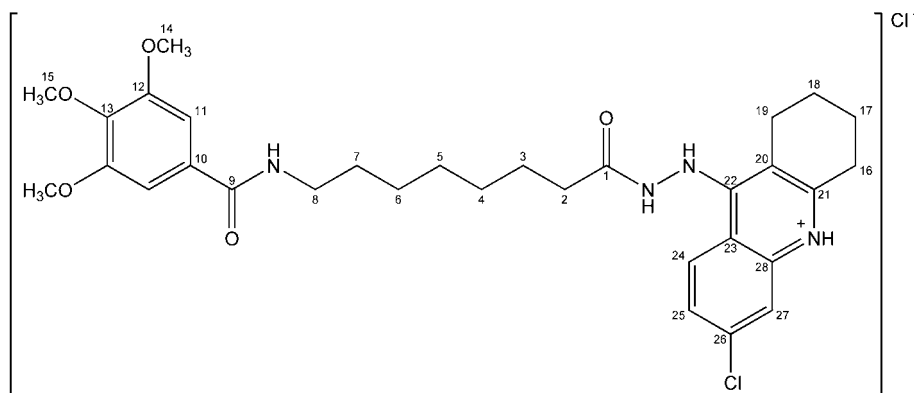
Synthesis: 1.0 mmol (0.25 g) 6,9-Dichloro-1,2,3,4-tetrahydroacridine (**2**) and 1.0 mmol (0.37 g) *N*-(8-hydrazino-8-oxooctyl)-3,4,5-trimethoxybenzamide (**34**) dissolved in 10 ml absolute ethanol are heated to 140 °C for 24 hours by means of a sealed bomb. The solution is filtered and evaporated in vacuo. The remaining foam is recrystallized from nitromethane to yield the final product **36**.

Yield: 0.56 g (91 %), $C_{31}H_{40}Cl_2N_4O_5$, $M_R = 619.59$ g/mol
Yellow powder

¹H NMR δ: 1.28 (app. bs, 6H, H–4,5,6)   7.18 (s, 2H, H–11)
[DMSO-*d₆*] 1.46-1.57 (m, 4H, H–3,7)   7.63 (dd, 1H, *J* = 1.9 9.3 Hz, H–25)
1.81 (app. bs, 4H, H–17,18)   8.09 (d, 1H, *J* = 2.2 Hz, H–27)
2.27 (t, 2H, *J* = 7.3 Hz, H–2)   8.44 (t, 1H, *J* = 5.7 Hz, NH<u>C</u>H₂)
2.66 (app. bs, 2H, H–19)   8.69 (d, 1H, *J* = 9.5 Hz, H–24)
3.06 (app. bs, 2H, H–16)   9.72 (s, 1H, CON<u>H</u>NH)
3.23 (app. q, 2H, *J* = 6.6 Hz, H–8)   11.05 (s, 1H, CONHN<u>H</u>)
3.68 (s, 3H, H–15)   14.64 (s, 1H, N⁺H)
3.81 (s, 6H, H–14)

¹³C NMR δ:

20.16 (C–18)	21.25 (C–17)	24.01 (C–19)	24.65 (C–3)
26.51 (C–6)	28.29 (C–16)	28.58 (C–5)	28.72 (C–4)
29.29 (C–7)	33.05 (C–2)	39.36 (C–8)	56.17 (C–14)
60.18 (C–15)	104.94 (C–11)	111.60 (C–20)	113.65 (C–23)
118.34 (C–27)	126.21 (C–25)	126.59 (C–24)	130.01 (C–10)
137.51 (C–28)	138.21 (C–26)	139.96 (C–13)	152.64 (C–12)
153.32 (C–21)	155.19 (C–22)	165.54 (C–9)	171.97 (C–1)

[DMSO-*d₆*]

Melting Point: 183 °C

EA: $C_{31}H_{40}Cl_2N_4O_5 \bullet H_2O$
Calculated: C: 58.40 %   H: 6.64 %   Cl: 11.12 %   N: 8.79 %   O: 15.06 %
Found: C: 58.66 %   H: 6.77 %   N: 8.72 %

Ethyl 9-((3,4,5-trimethoxybenzoyl)amino)nonanoate
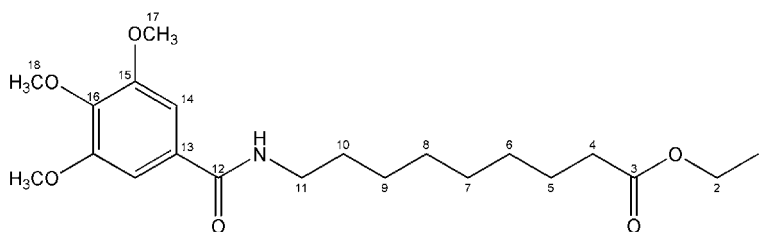
Synthesis: 24.0 mmol (5.54 g) Ethyl hydrogen sebacate are dissolved in 30 ml toluene and 26.0 mmol (5.6 ml) diphenyl phosphoryl azide and 26.0 mmol (3.6 ml) triethyl amine are added. The solution is heated to 80 °C for 2 hours to allow isocyanate formation. Subsequently, 20 ml anhydrous *tert*-butanol are added and the reaction mixture is re-fluxed for 12 hours. After cooling to room temperature the solvent is evaporated in vacuo, and the remaining residue is taken up in 100 ml diethyl ether. Filtering through silica gel, washing with 100 ml diethyl ether and evaporation in vacuo yields the Boc-protected ethyl 9-amino-nonanoate as a colorless oil. This oil is dissolved in 20 ml ethyl acetate and 20 ml 4 M hydrochloric acid in ethyl acetate are added to precipitate ethyl 9-aminononanoate hydrochloride. 10.0 mmol (2.12 g) of 3,4,5-trimethoxybenzoic acid are dissolved in 20 ml anhydrous dichloromethane with catalytic amounts of *N,N*-dimethylformamide. While stirring the subsequent addition of 11.6 mmol (1.0 ml) of oxalyl chloride generates the acyl chloride. Once the gas evolution has ceased remaining hydrogen chloride, excess oxalyl chloride and the solvent are removed by evaporation in vacuo. The residue is again taken up in 10 ml of dichloromethane and 10.0 mmol (2.38 g) of ethyl 9-aminononanoate hydrochloride are suspended in the solution. Drop-wise addition of 20.0 mmol (3.5 ml) *N*-ethyl-*N,N*-diisopropylamine yields a clear so-lution which sometimes contains some precipitated *N*-ethyl-*N,N*-diisopropylamine hy-drochloride. Washing with water and a saturated solution of sodium hydrogen car-bonate, drying with anhydrous sodium sulfate and evaporation in vacuo yields a crude product which is further purified by recrystallization from ethyl acetate and n-hexane to yield **37**.

Yield: 3.24 g (82 %), $C_{21}H_{33}NO_6$, M_R = 395.50 g/mol
White crystals

^{1}H NMR δ: 1.15 (t, 3H, J = 7.3 Hz, H–1)   3.69 (s, 3H, H–18)
[DMSO-d_6]   1.22-1.32 (m, 8H, H–6,7,8,9)   3.81 (s, 6H, H–17)
          1.46-1.55 (m, 4H, H–5,10)   4.03 (q, 2H, J = 7.1 Hz, H–2)
          2.25 (t, 2H, J = 7.4 Hz, H–4)   7.15 (s, 2H, H–14)
          3.23 (app. q, 2H, J = 6.6 Hz, H–11)   8.33 (t, 1H, J = 5.7 Hz, NH)

^{13}C NMR δ: 14.24 (C–1)   24.57 (C–5)   26.56 (C–9)   28.51 (C–8)
[DMSO-d_6]   28.73 (C–7)   28.74 (C–6)   29.29 (C–10)   33.64 (C–4)
          39.40 (C–11)   56.13 (C–17)   59.72 (C–2)   60.17 (C–18)
          104.90 (C–14)   130.04 (C–13)   139.97 (C–16)   152.65 (C–15)
          165.52 (C–12)   172.99 (C–3)

Melting Point: 83 °C

EA: Calculated: C: 63.78 %   H: 8.41 %   N: 3.54 %   O: 24.27 %
          Found: C: 63.50 %   H: 8.46 %   N: 3.69 %

N-(9-Hydrazino-9-oxononyl)-3,4,5-trimethoxybenzamide

Synthesis:	To a mixture of 51.4 mmol hydrazine (2.5 ml hydrazine hydrate, 100 %) and 20 ml absolute ethanol 5.0 mmol (1.98 g) ethyl 9-((3,4,5-trimethoxybenzoyl)amino)nonanoate (**37**) are added and the solution is heated to reflux for about 24 hours. The course of the reaction is followed by TLC and once no more ester can be detected the solvent and excess hydrazine are evaporated in vacuo. The crude product is recrystallized from ethanol for further purification to obtain **38**.

Yield: 1.46 g (77 %), $C_{19}H_{31}N_3O_5$, $M_R = 381.47$ g/mol
White crystals

¹H NMR δ:
[DMSO-*d₆*]

1.17-1.33 (m, 8H, H–4,5,6,7)	3.81 (s, 6H, H–15)
1.42-1.54 (m, 4H, H–3,8)	4.12 (bs, 2H, NH₂)
1.98 (t, 2H, $J = 7.4$ Hz, H–2)	7.15 (s, 2H, H–12)
3.22 (app. q, 2H, $J = 6.6$ Hz, H–9)	8.36 (t, 1H, $J = 5.5$ Hz, NHCH₂)
3.68 (s, 3H, H–16)	8.88 (s, 1H, NHNH₂)

¹³C NMR δ:
[DMSO-*d₆*]

25.38 (C–3)	26.67 (C–7)	28.80 (C–6)	28.87 (C–5)
28.88 (C–4)	29.38 (C–8)	33.58 (C–2)	39.46 (C–9)
56.15 (C–15)	60.22 (C–16)	104.86 (C–12)	130.06 (C–11)
139.93 (C–14)	152.69 (C–13)	165.56 (C–10)	171.76 (C–1)

Melting Point: 136 °C

EA:

Calculated:	C: 59.82 %	H: 8.19 %	N: 11.02 %	O: 20.97 %
Found:	C: 59.92 %	H: 8.48 %	N: 10.39 %	

3,4,5-Trimethoxy-*N*-(9-oxo-9-(2-(1,2,3,4-tetrahydroacridin-9-yl)hydrazino)nonyl)benzamide

Synthesis: 2.0 mmol (0.44 g) 9-Chloro-1,2,3,4-tetrahydroacridine (**1**) and 2.0 mmol (0.76 g) *N*-(9-hydrazino-9-oxononyl)-3,4,5-trimethoxybenzamide (**38**) dissolved in 20 ml absolute ethanol are heated to 140 °C for 24 hours by means of a sealed bomb. Cooling to room temperature and evaporation in vacuo yields a crude product that is taken up in 5 ml ethanol and diluted with 20 ml water. Addition of 2.5 ml 1N sodium hydroxide solution liberates the base as an oily layer. After decanting the remaining water the oily residue is suspended in 25 ml ethyl acetate and heated to reflux. The final product **39** precipitates and is recovered by suction filtration without the need for further purification.

Yield: 0.61 g (54 %), $C_{32}H_{42}N_4O_5$, M_R = 562.71 g/mol
Yellow powder

^{1}H NMR δ:
[DMSO-*d₆*]

1.09-1.33 (m, 8H, H–4,5,6,7)	7.16 (s, 2H, H–12)
1.38-1.56 (m, 4H, H–3,8)	7.30 (app. t, 1H, J = 7.3 Hz, H–26)
1.73-1.88 (m, 4H, H–18,19)	7.51 (app. t, 1H, J = 7.4 Hz, H–27)
2.07 (t, 2H, J = 7.1 Hz, H–2)	7.64 (s, 1H, CON<u>H</u>NH)
2.82 (app. bs, 2H, H–20)	7.70 (app. d, 1H, J = 8.2 Hz, H–25)
2.90 (app. bs, 2H, H–17)	8.31 (app. d, 1H, J = 8.5 Hz, H–28)
3.22 (app. q, 2H, J = 6.2 Hz, H–9)	8.34 (t, 1H, J = 4.7 Hz, N<u>H</u>CH₂)
3.69 (s, 3H, H–16)	10.02 (s, 1H, CONHN<u>H</u>)
3.81 (s, 6H, H–15)	

^{13}C NMR δ:
[DMSO-*d₆*]

22.54 (C–19)	22.71 (C–18)	24.84 (C–20)	25.02 (C–3)
26.61 (C–7)	28.65 (C–6)	28.82 (C–4,5)	29.34 (C–8)
33.06 (C–2)	33.78 (C–17)	39.42 (C–9)	56.15 (C–15)
60.18 (C–16)	104.91 (C–12)	115.60 (C–21)	119.12 (C–24)
123.21 (C–28)	123.44 (C–26)	127.93 (C–27)	128.41 (C–25)
130.04 (C–11)	139.98 (C–14)	146.82 (C–29)	148.83 (C–23)
152.66 (C–13)	158.13 (C–22)	165.54 (C–10)	172.06 (C–1)

Melting Point: 165 °C

EA: $C_{32}H_{42}N_4O_5$ • 0.5 H_2O
Calculated: C: 67.23 %   H: 7.58 %   N: 9.80 %   O: 15.39 %
Found: C: 67.83 %   H: 7.68 %   N: 9.87 %

3,4,5-Trimethoxy-*N*-(9-oxo-9-(2-(6-chloro-1,2,3,4-tetrahydroacridin-9-yl)hydrazino)nonyl)-benzamide HCl

Synthesis: 1.0 mmol (0.25 g) 6,9-Dichloro-1,2,3,4-tetrahydroacridine (**2**) and 1.0 mmol (0.38 g) *N*-(9-hydrazino-9-oxononyl)-3,4,5-trimethoxybenzamide (**38**) dissolved in 10 ml absolute ethanol are heated to 140 °C for 24 hours by means of a sealed bomb. The solution is filtered and evaporated in vacuo. The remaining foam is recrystallized from nitromethane to yield the final product **40**.

Yield: 0.55 g (86 %), $C_{32}H_{42}Cl_2N_4O_5$, $M_R = 633.61$ g/mol
Yellow powder

^{1}H NMR δ: 1.26 (app. bs, 8H, H–4,5,6,7)

[DMSO-*d₆*]   1.46-1.56 (m, 4H, H–3,8)
1.81 (app. bs, 4H, H–18,19)
2.27 (t, 2H, $J = 7.3$ Hz, H–2)
2.66 (app. bs, 2H, H–20)
3.07 (app. bs, 2H, H–17)
3.23 (app. q, 2H, $J = 6.7$ Hz, H–9)
3.68 (s, 3H, H–16)
3.81 (s, 6H, H–15)

7.17 (s, 2H, H–12)
7.63 (dd, 1H, $J = 2.2$ 9.2 Hz, H–26)
8.10 (d, 1H, $J = 2.2$ Hz, H–28)
8.43 (t, 1H, $J = 5.7$ Hz, N<u>H</u>CH$_2$)
8.69 (d, 1H, $J = 9.5$ Hz, H–25)
9.71 (s, 1H, CON<u>H</u>NH)
11.04 (s, 1H, CONHN<u>H</u>)
14.66 (s, 1H, N$^+$H)

^{13}C NMR δ:

[DMSO-*d₆*]

20.17 (C–19)	21.25 (C–18)	24.00 (C–20)	24.71 (C–3)
26.62 (C–7)	28.29 (C–17)	28.75 (C–5,6)	28.82 (C–4)
29.34 (C–8)	33.07 (C–2)	39.37 (C–9)	56.17 (C–15)
60.18 (C–16)	104.95 (C–12)	111.62 (C–21)	113.66 (C–24)
118.34 (C–28)	126.21 (C–26)	126.62 (C–25)	130.02 (C–11)
137.52 (C–29)	138.22 (C–27)	139.96 (C–14)	152.65 (C–13)
153.31 (C–22)	155.23 (C–23)	165.53 (C–10)	171.96 (C–1)

Melting Point: 187 °C

EA: $C_{32}H_{42}Cl_2N_4O_5 \cdot H_2O$

Calculated:	C: 58.98 %	H: 6.81 %	Cl: 10.88 %	N: 8.60 %	O: 14.73 %
Found:	C: 59.30 %	H: 6.65 %		N: 8.74 %	

Methyl 3-(3,4,5-trimethoxyphenyl)propanoate
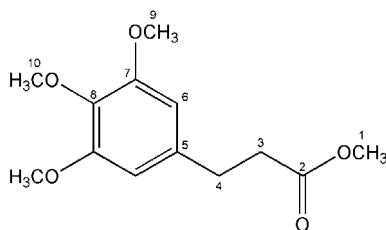
Synthesis:	10.0 mmol (2.40 g) of 3-(3,4,5-trimethoxyphenyl)propanoic acid are dissolved in 20 ml anhydrous dichloromethane with catalytic amounts of *N,N*-dimethyl-formamide. While stirring the subsequent addition of 11.6 mmol (1.0 ml) of oxalyl chloride generates the acyl chloride. Once the gas evolution has ceased remaining hydrogen chloride, excess oxalyl chloride and the solvent are removed by evaporation in vacuo. In a separate flask 10.0 mmol sodium are added to 20 ml anhydrous methanol while stirring. Once the formation of sodium methylate is complete the reaction mixture is added to the acyl chloride obtained in the first reaction. Stirring at room temperature for 5 hours yields a suspension that is evaporated in vacuo. Extracting the solid residue with dichloromethane from a saturated solution of sodium hydrogen carbonate, drying with anhydrous sodium sulfate and evaporation in vacuo yields the final product **41** which is purified by flash column chromatography using ethyl acetate. The oily residue crystallizes after several days at room temperature.

Yield: 2.10 g (83 %), $C_{13}H_{18}O_5$, $M_R = 254.28$ g/mol
White crystals

^{1}H NMR δ:
[DMSO-d_6]

2.62 (t, 2H, $J = 7.7$ Hz, H–3)	3.61 (s, 3H, H–10)
2.77 (t, 2H, $J = 7.7$ Hz, H–4)	3.73 (s, 6H, H–9)
3.59 (s, 3H, H–1)	6.51 (s, 2H, H–5)

^{13}C NMR δ:
[DMSO-d_6]

30.77 (C–3)	35.14 (C–4)	51.41 (C–1)	55.94 (C–9)
60.06 (C–10)	105.68 (C–5)	136.00 (C–6)	136.32 (C–8)
152.88 (C–7)	172.85 (C–2)		

Melting Point: 45 °C

EA:

Calculated:	C: 61.41 %	H: 7.13 %	O: 31.46 %
Found:	C: 61.08 %	H: 7.12 %	

3-(3,4,5-Trimethoxyphenyl)propanohydrazide
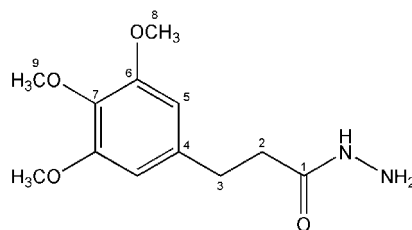
Synthesis: To a mixture of 51.4 mmol hydrazine (2.5 ml hydrazine hydrate, 100 %) and 20 ml absolute ethanol 5.0 mmol (1.27 g) methyl 3-(3,4,5-trimethoxyphenyl)propanoate (**41**) are added and the solution is heated to reflux for about 24 hours. The course of the reaction is followed by TLC and once no more ester can be detected the solvent and excess hydrazine are evaporated in vacuo. The crude product is recrystallized from methanol for further purification to obtain **42**.

Yield: 0.99 g (78 %), $C_{12}H_{18}N_2O_4$, $M_R = 254.29$ g/mol
White crystals

^{1}H NMR δ:
[DMSO-d_6]

2.31 (t, 2H, $J = 7.9$ Hz, H–2)	4.15 (s, 2H, NH$_2$)
2.74 (t, 2H, $J = 7.9$ Hz, H–3)	6.48 (s, 2H, H–5)
3.60 (s, 3H, H–9)	8.93 (s, 1H, N$\underline{H}$NH$_2$)
3.73 (s, 6H, H–8)	

^{13}C NMR δ:
[DMSO-d_6]

31.48 (C–3)	35.26 (C–2)	55.93 (C–8)	60.06 (C–9)
105.60 (C–5)	135.88 (C–4)	137.04 (C–7)	152.83 (C–6)
170.93 (C–1)			

Melting Point: 125 °C, lit.[118] 127-128 °C

EA:

Calculated:	C: 56.68 %	H: 7.13 %	N: 11.02 %	O: 25.17 %
Found:	C: 56.67 %	H: 7.30 %	N: 10.96 %	

N'-1,2,3,4-Tetrahydroacridin-9-yl-3-(3,4,5-trimethoxyphenyl)propanohydrazide HCl
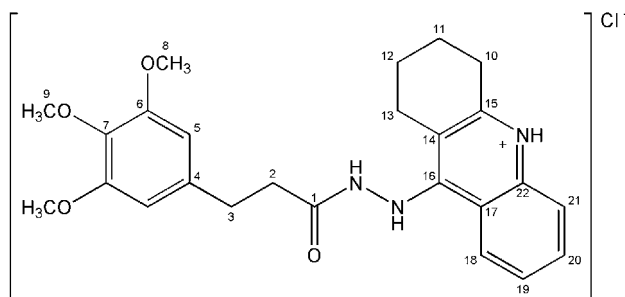
Synthesis:	2.0 mmol (0.44 g) 9-chloro-1,2,3,4-tetrahydroacridine (**1**) and 2.0 mmol (0.51 g) 3-(3,4,5-trimethoxyphenyl)propanohydrazide (**42**) dissolved in 20 ml absolute ethanol are heated to 140 °C for 24 hours by means of a sealed bomb. Cooling to room temperature and evaporation in vacuo yields a crude product that is recrystallized from nitromethane for further purification to obtain **43**.

Yield: 0.71 g (75 %), $C_{25}H_{30}ClN_3O_4$, M_R = 471.98 g/mol
White powder

^{1}H NMR δ:
[DMSO-d_6]

1.70-1.84 (m, 4H, H–11,12)	7.52 (app. t, 1H, J = 7.6 Hz, H–19)
2.61 (m, 4H, H–2,13)	7.87 (ddd, 1H, J = 1.0 7.1 8.4 Hz, H–20)
2.80 (t, 2H, J = 7.6 Hz, H–3)	8.00 (app. dd, 1H, J = 0.6 8.5 Hz, H–18)
3.07 (t, 2H, J = 6.2 Hz, H–10)	8.60 (app. d, 1H, J = 8.5 Hz, H–21)
3.62 (s, 3H, H–9)	9.66 (app. bs, 1H, CONH<u>N</u>H)
3.71 (s, 6H, H–8)	11.05 (s, 1H, CONHN<u>H</u>)
6.52 (s, 2H, H–5)	14.38 (app. bs, 1H, N$^+$H)

^{13}C NMR δ:
[DMSO-d_6]

20.20 (C–12)	21.40 (C–11)	24.21 (C–13)	28.28 (C–10)
30.69 (C–3)	34.67 (C–2)	55.95 (C–8)	60.04 (C–9)
105.77 (C–5)	111.26 (C–14)	115.11 (C–17)	119.49 (C–18)
124.02 (C–21)	125.88 (C–19)	133.00 (C–20)	136.00 (C–4)
136.50 (C–7)	137.39 (C–22)	152.78 (C–15)	152.87 (C–6)
155.12 (C–16)	171.24 (C–1)		

Melting Point: 236 °C

EA: $C_{25}H_{30}ClN_3O_4$ • 0.5 H_2O

Calculated:	C: 62.43 %	H: 6.50 %	Cl: 7.37 %	N: 8.74 %	O: 14.97 %
Found:	C: 62.29 %	H: 6.73 %		N: 8.96 %	

N'-1,2,3,4-Tetrahydroacridin-9-yl-3-(3,4,5-trimethoxyphenyl)propanohydrazide
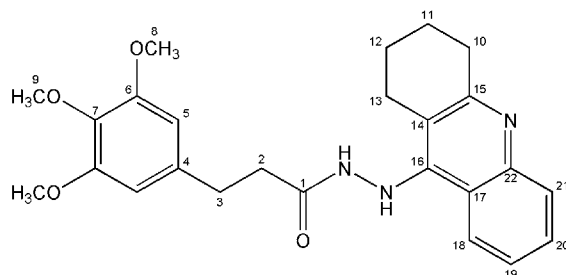
Synthesis:	A solution of 0.5 mmol (0.24 g) N'-1,2,3,4-tetrahydroacridin-9-yl-3-(3,4,5-trimethoxyphenyl)propanohydrazide hydrochloride (**43**) in 5 ml ethanol and 20 ml water is mixed with 1 ml of 1 M sodium hydroxide solution to liberate the base. The reaction mixture is extracted 4 times with 25 ml ethyl acetate, dried using anhydrous sodium sulfate and evaporated in vacuo to yield the final product **44** which needs no further purification.

Yield: 0.19 g (87 %), $C_{25}H_{29}N_3O_4$, $M_R = 435.52$ g/mol
Yellow crystals

^{1}H NMR δ:
[DMSO-d_6]

1.69-1.82 (m, 4H, H–11,12)	6.43 (s, 2H, H–5)
2.42 (t, 2H, $J = 7.6$ Hz, H–2)	7.30 (app. t, 1H, $J = 7.3$ Hz, H–19)
2.69-2.73 (m, 4H, H–3,13)	7.51 (ddd, 1H, $J = 1.3\ 6.8\ 8.3$ Hz, H–20)
2.90 (t, 2H, $J = 6.0$ Hz, H–10)	7.71 (app. d, 2H, $J = 6.6$ Hz, H–18,CON<u>H</u>NH)
3.60 (s, 3H, H–9)	8.30 (app. d, 1H, $J = 8.5$ Hz, H–21)
3.66 (s, 6H, H–8)	10.04 (s, 1H, CONHN<u>H</u>)

^{13}C NMR δ:
[DMSO-d_6]

22.44 (C–12)	22.68 (C–11)	24.93 (C–13)	31.01 (C–3)
33.73 (C–10)	34.73 (C–2)	55.85 (C–8)	60.02 (C–9)
105.58 (C–5)	115.78 (C–14)	119.13 (C–17)	123.03 (C–21)
123.54 (C–19)	127.97 (C–20)	128.40 (C–18)	135.90 (C–4)
136.76 (C–7)	146.74 (C–22)	148.61 (C–16)	152.81 (C–6)
158.24 (C–15)	171.33 (C–1)		

Melting Point: 196 °C

EA:

Calculated:	C: 68.95 %	H: 6.71 %	N: 9.65 %	O: 14.69 %
Found:	C: 68.62 %	H: 7.15 %	N: 9.49 %	

Ethyl ((3-(3,4,5-trimethoxyphenyl)propanoyl)amino)acetate

Synthesis: 10.0 mmol (2.40 g) of 3-(3,4,5-trimethoxyphenyl)propanoic acid are dissolved in 20 ml anhydrous dichloromethane with catalytic amounts of *N,N*-dimethyl-formamide. While stirring the subsequent addition of 11.6 mmol (1.0 ml) of oxalyl chloride generates the acyl chloride. Once the gas evolution has ceased remaining hydrogen chloride, excess oxalyl chloride and the solvent are removed by evaporation in vacuo. The residue is again taken up in 10 ml of dichloromethane and 10.0 mmol (1.40 g) ethyl aminoacetate hydrochloride are suspended in the solution. Dropwise addition of 20.0 mmol (3.5 ml) *N*-ethyl-*N,N*-diisopropylamine yields a clear solution which sometimes contains some precipitated *N*-ethyl-*N,N*-diisopropylamine hydrochloride. Washing with water and a saturated solution of sodium hydrogen carbonate, drying with anhydrous sodium sulfate and evaporation in vacuo yields a crude product which is further purified by flash column chromato-graphy using ethyl acetate to produce **45**.

Yield: 2.29 g (70 %), $C_{16}H_{23}NO_6$, $M_R = 325.36$ g/mol
White crystals

^{1}H NMR δ:
[CDCl$_3$]

1.26 (t, 3H, $J = 7.1$ Hz, H–1)	4.00 (d, 2H, $J = 5.1$ Hz, H–4)
2.52 (t, 2H, $J = 7.7$ Hz, H–6)	4.19 (q, 2H, $J = 7.1$ Hz, H–2)
2.90 (t, 2H, $J = 7.7$ Hz, H–7)	5.92 (bs, 1H, NH)
3.79 (s, 3H, H–13)	6.40 (s, 2H, H–9)
3.82 (s, 6H, H–12)	

^{13}C NMR δ:
[CDCl$_3$]

14.10 (C–1)	31.86 (C–7)	38.20 (C–6)	41.37 (C–4)
56.05 (C–12)	60.80 (C–13)	61.56 (C–2)	105.21 (C–9)
136.38 (C–8)	136.47 (C–11)	153.21 (C–10)	169.94 (C–3)
172.05 (C–5)			

Melting Point: 69 °C

EA:

Calculated:	C: 59.07 %	H: 7.13 %	N: 4.30 %	O: 29.50 %
Found:	C: 59.30 %	H: 7.45 %	N: 4.40 %	

N-(2-Hydrazino-2-oxoethyl)-3-(3,4,5-trimethoxyphenyl)propanamide

Synthesis:	To a mixture of 51.4 mmol hydrazine (2.5 ml hydrazine hydrate, 100 %) and 20 ml absolute ethanol 5.0 mmol (1.63 g) ethyl ((3-(3,4,5-trimethoxyphenyl)propanoyl)amino)acetate (**45**) are added and the solution is heated to reflux for about 3 hours. The course of the reaction is followed by TLC and once no more ester can be detected the solvent and excess hydrazine are evaporated in vacuo. The crude product is recrystallized from ethanol for further purification to produce **46**.

Yield:	1.16 g (75 %), $C_{14}H_{21}N_3O_5$, M_R = 311.34 g/mol White lints

^{1}H NMR δ:
[DMSO-d_6]

2.42 (t, 2H, *J* = 7.9 Hz, H–4)	4.17 (s, 2H, NH$_2$)
2.74 (t, 2H, *J* = 7.9 Hz, H–5)	6.50 (s, 2H, H–7)
3.61 (s, 3H, H–11)	8.03 (t, 1H, *J* = 5.8 Hz, N<u>H</u>CH$_2$)
3.64 (d, 2H, *J* = 5.7 Hz, H–2)	8.97 (s, 1H, N<u>H</u>NH$_2$)
3.74 (s, 6H, H–10)	

^{13}C NMR δ:
[DMSO-d_6]

31.40 (C–5)	36.98 (C–4)	40.88 (C–2)	55.91 (C–10)
60.07 (C–11)	105.59 (C–7)	135.84 (C–6)	137.21 (C–9)
152.84 (C–8)	168.43 (C–3)	171.88 (C–1)	

Melting Point: 170 °C

EA:

Calculated:	C: 54.01 %	H: 6.80 %	N: 13.50 %	O: 25.69 %
Found:	C: 54.01 %	H: 6.99 %	N: 13.35 %	

3-(3,4,5-Trimethoxyphenyl)-*N*-(2-oxo-2-(2-(1,2,3,4-tetrahydroacridin-9-yl)hydrazino)ethyl)-propanamide HCl
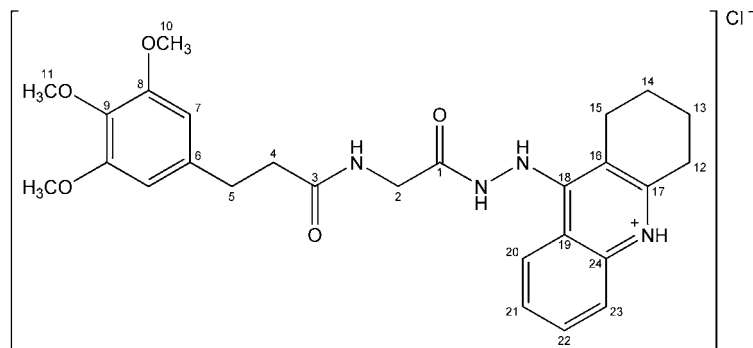
Synthesis:	2.0 mmol (0.44 g) 9-Chloro-1,2,3,4-tetrahydroacridine (**1**) and 2.0 mmol (0.62 g) *N*-(2-hydrazino-2-oxoethyl)-3-(3,4,5-trimethoxyphenyl)propanamide (**46**) are dissolved in 20 ml absolute ethanol and heated to 140 °C for 24 hours by means of a sealed bomb. Cooling to room temperature yields a crude product that is recrystallized from nitromethane for further purification to obtain **47**.

Yield: 0.67 g (63 %), $C_{27}H_{33}ClN_4O_5$, $M_R = 529.04$ g/mol
Yellow crystals

¹H NMR δ:
[DMSO-*d₆*]

1.82 (app. bs, 4H, H–13,14)	7.59 (app. t, 1H, $J = 7.9$ Hz, H–21)
2.46 (t, 2H, $J = 8.1$ Hz, H–4)	7.89 (app. t, 1H, $J = 7.7$ Hz, H–22)
2.71 (app. bs, 2H, H–15)	8.01 (app. d, 1H, $J = 8.5$ Hz, H–20)
2.77 (t, 2H, $J = 7.7$ Hz, H–5)	8.35 (t, 1H, $J = 6.0$ Hz, NHCH₂)
3.09 (app. bs, 2H, H–12)	8.69 (app. d, 1H, $J = 8.5$ Hz, H–23)
3.59 (s, 3H, H–10)	9.69 (s, 1H, CONHNH)
3.70 (s, 6H, H–11)	11.02 (s, 1H, CONHNH)
3.87 (d, 2H, $J = 6.0$ Hz, H–2)	14.39 (s, 1H, N⁺H)
6.49 (s, 2H, H–7)	

¹³C NMR δ:
[DMSO-*d₆*]

20.27 (C–14)	21.47 (C–13)	24.18 (C–15)	28.33 (C–12)
31.37 (C–5)	36.93 (C–4)	40.73 (C–2)	55.87 (C–10)
60.05 (C–11)	105.60 (C–7)	111.34 (C–16)	115.12 (C–19)
119.45 (C–20)	124.34 (C–23)	126.08 (C–21)	133.05 (C–22)
135.86 (C–6)	137.12 (C–9)	137.40 (C–24)	152.78 (C–17)
152.83 (C–8)	155.05 (C–18)	169.14 (C–3)	172.27 (C–1)

Melting Point: 215 °C

EA:

Calculated:	C: 61.30 %	H: 6.29 %	Cl: 6.70 %	N: 10.59 %	O: 15.12 %
Found:	C: 61.31 %	H: 6.37 %		N: 10.60 %	

3-(3,4,5-Trimethoxyphenyl)-*N*-(2-oxo-2-(2-(1,2,3,4-tetrahydroacridin-9-yl)hydrazino)ethyl)-propanamide
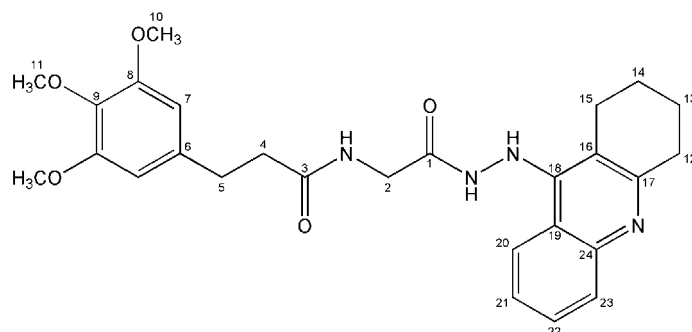
Synthesis: A solution of 0.5 mmol (0.26 g) 3-(3,4,5-trimethoxyphenyl)-*N*-(2-oxo-2-(2-(1,2,3,4-tetrahydroacridin-9-yl)hydrazino)ethyl)propanamide hydrochloride (**47**) in 5 ml ethanol and 20 ml water is mixed with 1 ml of 1 M sodium hydroxide solution to liberate the base. The reaction mixture is extracted 4 times with 25 ml ethyl acetate and while drying with anhydrous sodium sulfate a yellow precipitate is formed. Therefore the mixture is heated to reflux and absolute ethanol is used to redissolve the precipitate. Filtration and cooling to room temperature yields the final product **48** which is recovered by suction filtration.

Yield: 0.12 g (49 %), $C_{27}H_{32}N_4O_5$, M_R = 492.57 g/mol
Yellow crystals

^{1}H NMR δ:
[DMSO-*d$_6$*]

1.71-1.87 (m, 4H, H–13,14)	6.47 (s, 2H, H–7)
2.40 (t, J = 7.6 Hz, H–4)	7.32 (app. t, 1H, J = 7.3 Hz, H–21)
2.73 (t, J = 7.6 Hz, H–5)	7.52 (app. t, 1H, J = 7.3 Hz, H–22)
2.83 (app. bs, 2H, H–15)	7.71 (app. d, 1H, J = 11.1 Hz, H–20)
2.91 (app. bs, 2H, H–12)	7.73 (s, 1H, CONH̲NH)
3.59 (s, 3H, H–11)	8.04 (bs, 1H, NH̲CH$_2$)
3.70 (s, 6H, H–10)	8.30 (app. d, 1H, J = 7.9 Hz, H–23)
3.73 (d, J = 5.7 Hz, H–2)	10.13 (s, 1H, CONHNH̲)

^{13}C NMR δ:
[DMSO-*d$_6$*]

22.51 (C–14)	22.75 (C–13)	24.90 (C–15)	31.42 (C–5)
33.77 (C–12)	36.96 (C–4)	40.20 (C–2)	55.87 (C–10)
60.04 (C–11)	105.57 (C–7)	116.05 (C–16)	119.24 (C–19)
123.05 (C–23)	123.69 (C–21)	127.98 (C–22)	128.37 (C–20)
135.82 (C–6)	137.16 (C–9)	146.72 (C–24)	148.55 (C–18)
152.82 (C–8)	158.24 (C–17)	169.02 (C–3)	171.91 (C–1)

Melting Point: 228 °C

EA: $C_{27}H_{32}N_4O_5$ • 0.5 H_2O
Calculated: C: 64.65 % H: 6.63 % N: 11.17 % O: 17.54 %
Found: C: 65.02 % H: 6.91 % N: 11.01 %

Ethyl 3-((3-(3,4,5-trimethoxyphenyl)propanoyl)amino)propanoate

Synthesis:	10.0 mmol (2.40 g) of 3-(3,4,5-trimethoxyphenyl)propanoic acid are dissolved in 20 ml anhydrous dichloromethane with catalytic amounts of N,N-dimethyl-formamide. While stirring the subsequent addition of 11.6 mmol (1.0 ml) of oxalyl chloride generates the acyl chloride. Once the gas evolution has ceased remaining hydrogen chloride, excess oxalyl chloride and the solvent are removed by evaporation in vacuo. The residue is again taken up in 10 ml of dichloromethane and 10.0 mmol (1.54 g) of ethyl 3-aminopropanoate hydrochloride are suspended in the solution. Dropwise addition of 20.0 mmol (3.5 ml) N-ethyl-N,N-diisopropylamine yields a clear solution which sometimes contains some precipitated N-ethyl-N,N-diisopropylamine hydrochloride. Washing with water and a saturated solution of sodium hydrogen carbonate, drying with anhydrous sodium sulfate and evaporation in vacuo yields a crude product that is further purified by column chromatography using silical gel 60 and eluating with ethyl acetate and methanol in a ratio of 2:1 to yield **49**.

Yield: 3.22 g (95 %), $C_{17}H_{25}NO_6$, $M_R = 339.39$ g/mol
Yellow oil

^{1}H NMR δ:
[DMSO-d_6]

1.17 (t, 3H, $J = 7.1$ Hz, H–1)	3.60 (s, 3H, H–14)
2.34 (t, 2H, $J = 7.7$ Hz, H–4)	3.73 (s, 6H, H–13)
2.40 (t, 2H, $J = 7.0$ Hz, H–7)	4.04 (q, 2H, $J = 7.1$ Hz, H–2)
2.72 (t, 2H, $J = 7.9$ Hz, H–8)	6.48 (s, 2H, H–10)
3.25 (app. q, 2H, $J = 6.5$ Hz, H–5)	7.88 (t, 1H, $J = 5.5$ Hz, NH)

^{13}C NMR δ:
[DMSO-d_6]

14.18 (C–1)	31.52 (C–8)	34.04 (C–4)	34.80 (C–7)
37.08 (C–5)	55.88 (C–13)	60.00 (C–2)	60.05 (C–14)
105.59 (C–10)	135.85 (C–9)	137.11 (C–12)	152.81 (C–11)
171.39 (C–3)	171.61 (C–6)		

Refraction: n_D^{20} 1.58

EA: Calculated: C: 60.16 % H: 7.42 % N: 4.13 % O: 28.29 %
Found:

N-(3-Hydrazino-3-oxopropyl)-3-(3,4,5-trimethoxyphenyl)propanamide

Synthesis: To a mixture of 51.4 mmol hydrazine (2.5 ml hydrazine hydrate, 100 %) and 20 ml absolute ethanol 5.0 mmol (1.70 g) ethyl 3-((3-(3,4,5-trimethoxyphenyl)propanoyl)amino)propanoate (**49**) are added and the solution is heated to reflux for about 3 hours. The course of the reaction is followed by TLC and once no more ester can be detected the solvent and excess hydrazine are evaporated in vacuo. The crude product is recrystallized from ethanol for further purification to obtain **50**.

Yield: 1.32 g (81 %), $C_{15}H_{23}N_3O_5$, $M_R = 325.36$ g/mol
White crystals

^{1}H NMR δ:
[DMSO-d_6]

2.16 (t, 2H, $J = 7.3$ Hz, H–2)
2.33 (t, 2H, $J = 7.9$ Hz, H–5)
2.72 (t, 2H, $J = 6.7$ Hz, H–6)
3.23 (app. q, 2H, $J = 6.3$ Hz, H–3)
3.60 (s, 3H, H–12)

3.73 (s, 6H, H–11)
4.12 (bs, 2H, NH$_2$)
6.48 (s, 2H, H–8)
7.83 (t, 1H, $J = 5.5$ Hz, N<u>H</u>CH$_2$)
8.96 (s, 1H, N<u>H</u>NH$_2$)

^{13}C NMR δ:
[DMSO-d_6]

31.55 (C–6)	33.81 (C–5)	35.41 (C–2)	37.18 (C–3)
55.91 (C–11)	60.07 (C–12)	105.58 (C–8)	135.85 (C–7)
137.19 (C–10)	152.83 (C–9)	169.84 (C–4)	171.50 (C–1)

Melting Point: 150 °C

EA:

Calculated:	C: 55.37 %	H: 7.13 %	N: 12.91 %	O: 24.59 %
Found:	C: 55.31 %	H: 7.38 %	N: 12.75 %	

3-(3,4,5-Trimethoxyphenyl)-*N*-(3-oxo-3-(2-(1,2,3,4-tetrahydroacridin-9-yl)hydrazino)-propyl)propanamide HCl
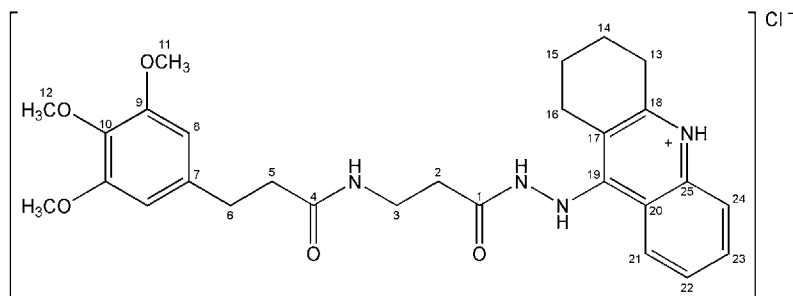
Synthesis:	2.0 mmol (0.44 g) 9-Chloro-1,2,3,4-tetrahydroacridine (**1**) and 2.0 mmol (0.65 g) *N*-(3-hydrazino-3-oxopropyl)-3-(3,4,5-trimethoxyphenyl)propanamide (**50**) are dissolved in 20 ml absolute ethanol and heated to 140 °C for 24 hours by means of a sealed bomb. Cooling to room temperature yields a crude product that is recrystallized from nitromethane for further purification to produce **51**.

Yield: 0.85 g (84 %), $C_{28}H_{35}ClN_4O_5$, $M_R = 543.06$ g/mol
Yellow crystals

^{1}H NMR δ:
[DMSO-*d$_6$*]

1.82 (app. bs, 4H, H–14,15)	6.49 (s, 2H, H–8)
2.36 (t, 2H, $J = 7.7$ Hz, H–2)	7.59 (app. t, 1H, $J = 7.7$ Hz, H–22)
2.45 (t, 2H, $J = 7.1$ Hz, H–5)	7.88 (app. t, 1H, $J = 7.6$ Hz, H–23)
2.70 (app. bs, 2H, H–16)	8.03 (app. d, 1H, $J = 7.9$ Hz, H–22,N<u>H</u>CH$_2$)
2.73 (t, 2H, $J = 7.9$ Hz, H–6)	8.66 (app. d, 1H, $J = 8.8$ Hz, H–24)
3.09 (app. bs, 2H, H–13)	9.70 (s, 1H, CON<u>H</u>NH)
3.27 (app. q, 2H, $J = 6.5$ Hz, H–3)	11.06 (s, 1H, CONHN<u>H</u>)
3.60 (s, 3H, H–12)	14.49 (s, 1H, N$^+$H)
3.73 (s, 6H, H–11)	

^{13}C NMR δ:
[DMSO-*d$_6$*]

20.21 (C–15)	21.47 (C–14)	24.27 (C–16)	28.28 (C–13)
31.55 (C–6)	33.39 (C–5)	34.87 (C–2)	37.17 (C–3)
55.93 (C–11)	60.08 (C–12)	105.60 (C–8)	111.30 (C–17)
115.16 (C–20)	119.48 (C–21)	124.05 (C–24)	126.00 (C–22)
133.04 (C–23)	135.85 (C–7)	137.15 (C–10)	137.35 (C–25)
152.82 (C–18)	155.20 (C–19)	170.32 (C–4)	171.68 (C–1)

Melting Point: 215 °C

EA: $C_{28}H_{35}ClN_4O_5$ • 0.5 H_2O

Calculated:	C: 60.92 %	H: 6.57 %	Cl: 6.42 %	N: 10.15 %	O: 15.94 %
Found:	C: 61.12 %	H: 6.91 %		N: 10.14 %	

3-(3,4,5-Trimethoxyphenyl)-*N*-(3-oxo-3-(2-(1,2,3,4-tetrahydroacridin-9-yl)hydrazino)-propyl)propanamide
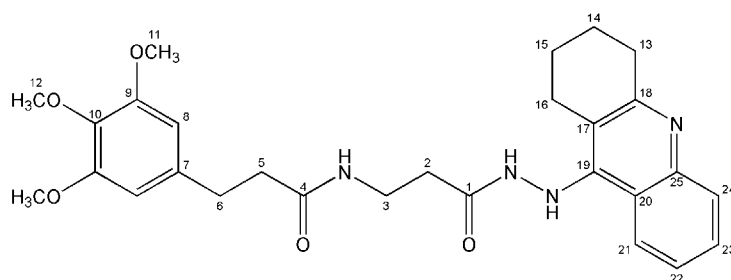
Synthesis: A solution of 0.5 mmol (0.27 g) 3-(3,4,5-trimethoxyphenyl)-*N*-(3-oxo-3-(2-(1,2,3,4-tetrahydroacridin-9-yl)hydrazino)propyl)propanamide hydrochloride (**51**) in 5 ml ethanol and 20 ml water is mixed with 1 ml of 1 M sodium hydroxide solution to liberate the base. The reaction mixture is extracted 4 times with 25 ml ethyl acetate, dried using anhydrous sodium sulfate and evaporated in vacuo to yield the final product **52** which needs no further purification.

Yield: 0.22 g (87 %), $C_{28}H_{34}N_4O_5$, $M_R = 506.60$ g/mol
Yellow crystals

^{1}H NMR δ:
[DMSO-*d$_6$*]

1.73-1.85 (m, 4H, H–14,15)	6.46 (s, 2H, H–8)
2.25-2.31 (m, 4H, H–2,5)	7.32 (app. t, 1H, $J = 7.4$ Hz, H–22)
2.69 (t, 2H, $J = 7.7$ Hz, H–6)	7.50 (app. t, 1H, $J = 7.4$ Hz, H–23)
2.81 (app. bs, 2H, H–16)	7.67 (s, 1H, CON<u>H</u>NH)
2.91 (app. bs, 2H, H–13)	7.72 (app. d, 1H, $J = 8.2$ Hz, H–21)
3.18 (q, 2H, $J = 6.4$ Hz, H–3)	7.83 (t, 1H, $J = 5.5$ Hz, N<u>H</u>CH$_2$)
3.60 (s, 3H, H–12)	8.29 (app. d, 1H, $J = 8.6$ Hz, H–24)
3.73 (s, 6H, H–11)	10.09 (s, 1H, CONHN<u>H</u>)

^{13}C NMR δ:
[DMSO-*d$_6$*]

22.49 (C–15)	22.74 (C–14)	24.94 (C–16)	31.53 (C–6)
33.26 (C–5)	33.77 (C–13)	35.02 (C–2)	37.15 (C–3)
55.90 (C–11)	60.07 (C–12)	105.57 (C–8)	115.70 (C–17)
119.11 (C–20)	123.00 (C–24)	123.58 (C–22)	127.96 (C–23)
128.43 (C–21)	135.85 (C–7)	137.15 (C–10)	146.77 (C–25)
148.62 (C–19)	152.81 (C–9)	158.21 (C–18)	170.39 (C–4)
171.54 (C–1)			

Melting Point: 211 °C

EA: $C_{28}H_{34}N_4O_5$ • 1.5 H$_2$O
Calculated: C: 63.02 % H: 6.99 % N: 10.50 % O: 19.49 %
Found: C: 63.38 % H: 7.05 % N: 10.40 %

Ethyl 4-((3-(3,4,5-trimethoxyphenyl)propanoyl)amino)butanoate

Synthesis: 10.0 mmol (2.40 g) of 3-(3,4,5-trimethoxyphenyl)propanoic acid are dissolved in 20 ml anhydrous dichloromethane with catalytic amounts of *N,N*-dimethyl-formamide. While stirring the subsequent addition of 11.6 mmol (1.0 ml) of oxalyl chloride generates the acyl chloride. Once the gas evolution has ceased remaining hydrogen chloride, excess oxalyl chloride and the solvent are removed by evaporation in vacuo. The residue is again taken up in 10 ml of dichloromethane and 10.0 mmol (1.68 g) of ethyl 4-aminobutanoate hydrochloride are suspended in the solution. Dropwise addition of 20.0 mmol (3.5 ml) *N*-ethyl-*N,N*-diisopropylamine yields a clear solution which sometimes contains some precipitated *N*-ethyl-*N,N*-diisopropylamine hydrochloride. Washing with water and a saturated solution of sodium hydrogen carbonate, drying with anhydrous sodium sulfate and evaporation in vacuo yields a crude product which is further purified by recrystallization from ethyl acetate and n-hexane to obtain **53**.

Yield: 3.23 g (91 %), $C_{18}H_{27}NO_6$, $M_R = 353.42$ g/mol
White crystals

^{1}H NMR δ: 1.17 (t, 3H, $J = 7.3$ Hz, H–1) 3.60 (s, 3H, H–15)
[DMSO-d_6] 1.61 (app. quint, 2H, $J = 7.3$ Hz, H–5) 3.73 (s, 6H, H–14)
2.23 (t, 2H, $J = 7.6$ Hz, H–4) 4.03 (q, 2H, $J = 7.2$ Hz, H–2)
2.34 (t, 2H, $J = 7.7$ Hz, H–8) 6.48 (s, 2H, H–11)
2.73 (t, 2H, $J = 7.7$ Hz, H–9) 7.79 (t, 1H, $J = 5.5$ Hz, NH)
3.04 (app. q, 2H, $J = 6.5$ Hz, H–6)

^{13}C NMR δ: 14.21 (C–1) 24.74 (C–5) 31.05 (C–4) 31.57 (C–9)
[DMSO-d_6] 37.19 (C–8) 37.88 (C–6) 55.89 (C–14) 59.85 (C–2)
60.05 (C–15) 105.60 (C–11) 135.86 (C–10) 137.16 (C–13)
152.81 (C–12) 171.45 (C–3) 172.71 (C–7)

Melting Point: 44 °C

EA: Calculated: C: 61.17 % H: 7.70 % N: 3.96 % O: 27.16 %
Found: C: 61.40 % H: 7.76 % N: 4.13 %

N-(4-Hydrazino-4-oxobutyl)-3-(3,4,5-trimethoxyphenyl)propanamide
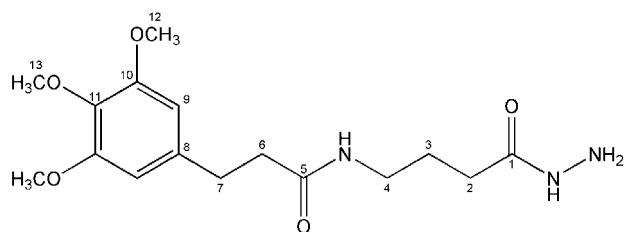
Synthesis: To a mixture of 51.4 mmol hydrazine (2.5 ml hydrazine hydrate, 100 %) and 20 ml absolute ethanol 5.0 mmol (1.77 g) ethyl 4-((3-(3,4,5-trimethoxyphenyl)propanoyl)amino)butanoate (**53**) are added and the solution is heated to reflux for about 3 hours. The course of the reaction is followed by TLC and once no more ester can be detected the solvent and excess hydrazine are evaporated in vacuo. The crude product is recrystallized from ethanol for further purification to produce **54**.

Yield: 0.87 g (51 %), $C_{16}H_{25}N_3O_5$, $M_R = 339.39$ g/mol
White crystals

^{1}H NMR δ:
[DMSO-d_6]

1.58 (app. quint, 2H, $J = 7.3$ Hz, H–3)
1.98 (t, 2H, $J = 7.6$ Hz, H–2)
2.34 (app. dd, 2H, $J = 7.9$ 8.8 Hz, H–6)
2.73 (t, 2H, $J = 7.9$ Hz, H–7)
3.01 (app. q, 2H, $J = 6.6$ Hz, H–4)
3.60 (s, 3H, H–13)

3.73 (s, 6H, H–12)
4.13 (s, 2H, NH$_2$)
6.48 (s, 2H, H–9)
7.79 (t, 1H, $J = 5.5$ Hz, NHCH$_2$)
8.88 (s, 1H, NHNH$_2$)

^{13}C NMR δ:
[DMSO-d_6]

25.61 (C–3)	31.12 (C–2)	31.62 (C–7)	37.26 (C–6)
38.31 (C–4)	55.90 (C–12)	60.07 (C–13)	105.59 (C–9)
135.85 (C–8)	137.21 (C–11)	152.82 (C–10)	171.36 (C–5)
171.41 (C–1)			

Melting Point: 140 °C

EA:

Calculated:	C: 56.62 %	H: 7.42 %	N: 12.38 %	O: 23.57 %
Found:	C: 56.37 %	H: 7.42 %	N: 12.02 %	

3-(3,4,5-Trimethoxyphenyl)-*N*-(4-oxo-4-(2-(1,2,3,4-tetrahydroacridin-9-yl)hydrazino)-butyl)propanamide HCl
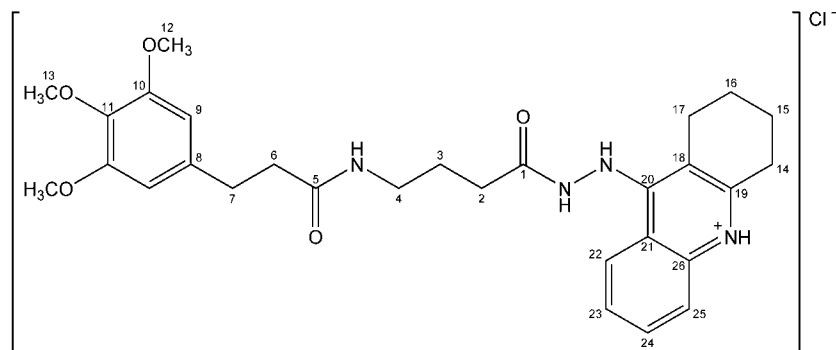
Synthesis: 2.0 mmol (0.44 g) 9-Chloro-1,2,3,4-tetrahydroacridine (**1**) and 2.0 mmol (0.68 g) *N*-(4-hydrazino-4-oxobutyl)-3-(3,4,5-trimethoxyphenyl)propanamide (**54**) are dissolved in 20 ml absolute ethanol and heated to 140 °C for 24 hours by means of a sealed bomb. Cooling to room temperature yields a crude product that is recrystallized from nitromethane for further purification to yield **55**.

Yield: 0.79 g (71 %), $C_{29}H_{37}ClN_4O_5$, $M_R = 557.09$ g/mol
Slightly yellow crystals

^{1}H NMR δ: 1.64 (app. quint, 2H, $J = 7.3$ Hz, H–3)
[DMSO-d_6]   1.83 (app. bs, 4H, H–15,16)
2.27 (t, 2H, $J = 7.4$ Hz, H–2)
2.37 (t, 2H, $J = 7.9$ Hz, H–6)
2.69 (app. bs, 2H, H–17)
2.75 (t, 2H, $J = 7.7$ Hz, H–7)
3.06 (m, 4H, H–4,14)
3.60 (s, 3H, H–13)
3.73 (s, 6H, H–12)

6.50 (s, 2H, H–9)
7.59 (ddd, 1H, $J = 1.3$ 7.1 8.6 Hz, H–23)
7.88 (ddd, 1H, $J = 1.3$ 7.0 8.4 Hz, H–24)
7.94 (t, 1H, $J = 5.7$ Hz, NHCH$_2$)
8.00 (app. dd, 1H, $J = 1.0$ 8.6 Hz, H–22)
8.66 (app. d, 1H, $J = 8.9$ Hz, H–25)
9.63 (s, 1H, CONHNH)
11.02 (s, 1H, CONHNH)
14.33 (s, 1H, N$^+$H)

^{13}C NMR δ: 20.24 (C–16)   21.40 (C–15)   24.14 (C–17)   25.04 (C–3)
[DMSO-d_6]   28.26 (C–14)   30.70 (C–2)   31.63 (C–7)   37.22 (C–6)
38.17 (C–4)   55.92 (C–12)   60.07 (C–13)   105.61 (C–9)
111.21 (C–18)   115.08 (C–21)   119.47 (C–22)   124.15 (C–25)
125.95 (C–23)   133.09 (C–24)   135.84 (C–8)   137.18 (C–11)
137.39 (C–26)   152.69 (C–19)   152.81 (C–10)   155.26 (C–20)
171.53 (C–5)   171.67 (C–1)

Melting Point: 130 °C

EA: $C_{29}H_{37}ClN_4O_5 \cdot H_2O$
Calculated: C: 60.57 %   H: 6.84 %   Cl: 6.16 %   N: 9.74 %   O: 16.69 %
Found: C: 60.85 %   H: 7.05 %   N: 9.86 %

3-(3,4,5-Trimethoxyphenyl)-*N*-(4-oxo-4-(2-(1,2,3,4-tetrahydroacridin-9-yl)hydrazino)-butyl)propanamide
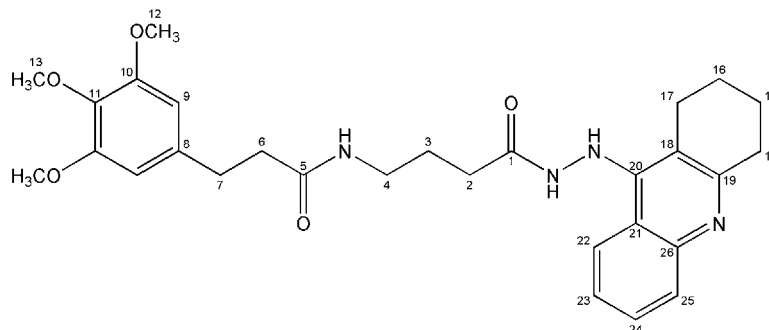
Synthesis:	A solution of 0.5 mmol (0.28 g) 3-(3,4,5-trimethoxyphenyl)-*N*-(4-oxo-4-(2-(1,2,3,4-tetrahydroacridin-9-yl)hydrazino)butyl)propanamide hydrochloride (**55**) in 5 ml ethanol and 20 ml water is mixed with 1 ml of 1 M sodium hydroxide solution to liberate the base. The reaction mixture is extracted 4 times with 25 ml ethyl acetate, dried using anhydrous sodium sulfate and evaporated in vacuo to yield the final product **56** which needs no further purification.

Yield: 0.22 g (85 %), $C_{29}H_{36}N_4O_5$, $M_R = 520.63$ g/mol
Yellow crystals

^{1}H NMR δ:
[DMSO-*d$_6$*]

1.56 (app. quint, 2H, $J = 7.3$ Hz, H–3)	3.71 (s, 6H, H–12)
1.75-1.85 (m, 4H, H–15,16)	6.47 (s, 2H, H–9)
2.08 (t, 2H, $J = 7.6$ Hz, H–2)	7.31 (ddd, 1H, $J = 1.0$ 7.7 7.7 Hz, H–23)
2.33 (app. dd, 2H, $J = 8.2$ 9.1 Hz, H–6)	7.51 (ddd, 1H, $J = 1.3$ 6.9 8.3 Hz, H–24)
2.73 (t, 2H, $J = 7.9$ Hz, H–7)	7.66 (s, 1H, CONHNH)
2.81 (app. bs, 2H, H–17)	7.71 (app. d, 1H, $J = 8.6$ Hz, H–22)
2.90 (app. bs, 2H, H–14)	7.77 (t, 1H, $J = 5.5$ Hz, NHCH$_2$)
3.00 (app. q, 2H, $J = 7.9$ Hz, H–4)	8.30 (app. d, 1H, $J = 8.2$ Hz, H–25)
3.59 (s, 3H, H–13)	10.04 (s, 1H, CONHNH)

^{13}C NMR δ:
[DMSO-*d$_6$*]

22.50 (C–16)	22.70 (C–15)	24.87 (C–17)	25.28 (C–3)
30.73 (C–2)	31.61 (C–7)	33.76 (C–14)	37.23 (C–6)
38.29 (C–4)	55.89 (C–12)	60.06 (C–13)	105.58 (C–9)
115.61 (C–18)	119.11 (C–21)	123.10 (C–25)	123.53 (C–23)
127.97 (C–24)	128.43 (C–22)	135.85 (C–8)	137.18 (C–11)
146.79 (C–26)	148.72 (C–20)	152.81 (C–10)	158.18 (C–19)
171.42 (C–5)	171.74 (C–1)		

Melting Point: 141 °C

EA: $C_{29}H_{36}N_4O_5$ • 0.5 H_2O
Calculated: C: 65.77 % H: 7.04 % N: 10.58 % O: 16.61 %
Found: C: 65.98 % H: 7.31 % N: 10.35 %

Ethyl 5-((3-(3,4,5-trimethoxyphenyl)propanoyl)amino)pentanoate

Synthesis: 10.0 mmol (2.40 g) of 3-(3,4,5-trimethoxyphenyl)propanoic acid are dissolved in 20 ml anhydrous dichloromethane with catalytic amounts of *N,N*-dimethyl-formamide. While stirring the subsequent addition of 11.6 mmol (1.0 ml) of oxalyl chloride generates the acyl chloride. Once the gas evolution has ceased remaining hydrogen chloride, excess oxalyl chloride and the solvent are removed by evaporation in vacuo. The residue is again taken up in 10 ml of dichloromethane and 10.0 mmol (1.82 g) of ethyl 5-aminopentanoate hydrochloride are suspended in the solution. Dropwise addition of 20.0 mmol (3.5 ml) *N*-ethyl-*N,N*-diisopropylamine yields a clear solution which some-times contains some precipitated *N*-ethyl-*N,N*-diisopropylamine hydrochloride. Wash-ing with water and a saturated solution of sodium hydrogen carbonate, drying with anhydrous sodium sulfate and evaporation in vacuo yields a crude product which is further purified by recrystallization from ethyl acetate and n-hexane to produce **57**.

Yield: 3.53 g (96 %), $C_{19}H_{29}NO_6$, $M_R = 367.44$ g/mol
Yellow oil

^{1}H NMR δ:
[DMSO-*d$_6$*]

1.16 (t, 3H, $J = 7.1$ Hz, H–1)	3.02 (app. q, 2H, $J = 6.5$ Hz, H–7)
1.36 (app. quint, 2H, $J = 7.3$ Hz, H–6)	3.60 (s, 3H, H–16)
1.47 (app. quint, 2H, $J = 7.5$ Hz, H–5)	3.73 (s, 6H, H–15)
2.25 (t, 2H, $J = 7.4$ Hz, H–4)	4.03 (q, 2H, $J = 7.0$ Hz, H–2)
2.34 (t, 2H, $J = 7.9$ Hz, H–9)	6.48 (s, 2H, H–12)
2.73 (t, 2H, $J = 7.7$ Hz, H–10)	7.76 (t, 1H, $J = 5.5$ Hz, NH)

^{13}C NMR δ:
[DMSO-*d$_6$*]

14.99 (C–1)	22.75 (C–5)	29.45 (C–6)	32.36 (C–10)
34.00 (C–4)	37.96 (C–9)	38.86 (C–7)	56.63 (C–15)
60.52 (C–16)	60.79 (C–2)	106.34 (C–12)	136.59 (C–11)
137.93 (C–14)	153.55 (C–13)	172.05 (C–3)	173.61 (C–8)

Refraction: n_D^{20} 1.52

EA: Calculated: C: 62.11 % H: 7.96 % N: 3.81 % O: 26.13 %
Found:

N-(5-Hydrazino-5-oxopentyl)-3-(3,4,5-trimethoxyphenyl)propanamide
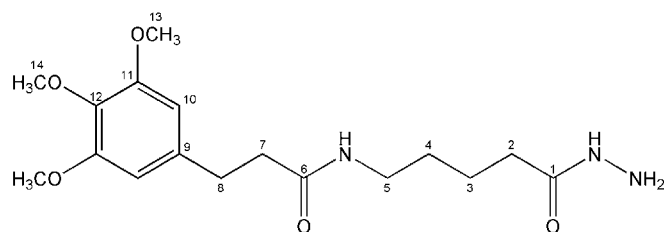
Synthesis: To a mixture of 51.4 mmol hydrazine (2.5 ml hydrazine hydrate, 100 %) and 20 ml absolute ethanol 5.0 mmol (1.84 g) ethyl 5-((3-(3,4,5-trimethoxyphenyl)propanoyl)amino)pentanoate (**57**) are added and the solution is heated to reflux for about 3 hours. The course of the reaction is followed by TLC and once no more ester can be detected the solvent and excess hydrazine are evaporated in vacuo. The crude product is recrystallized from ethanol and diethyl ether for further purification to obtain **58**.

Yield: 1.09 g (62 %), $C_{17}H_{27}N_3O_5$, $M_R = 353.42$ g/mol
White crystals

^{1}H NMR δ: 1.33 (app. quint, 2H, $J = 7.3$ Hz, H–4)   3.60 (s, 3H, H–14)
[DMSO-d_6]   1.45 (app. quint, 2H, $J = 7.5$ Hz, H–3)   3.73 (s, 6H, H–13)
1.98 (t, 2H, $J = 7.3$ Hz, H–2)   4.11 (s, 2H, NH$_2$)
2.33 (t, 2H, $J = 7.7$ Hz, H–7)   6.48 (s, 2H, H–11)
2.73 (t, 2H, $J = 7.9$ Hz, H–8)   7.75 (t, 1H, $J = 5.5$ Hz, NHCH$_2$)
3.01 (app. q, 2H, $J = 6.5$ Hz, H–5)   8.87 (s, 1H, NHNH$_2$)

^{13}C NMR δ: 22.82 (C–3)   28.96 (C–4)   31.63 (C-8)   33.19 (C–2)
[DMSO-d_6]   37.25 (C–7)   38.33 (C–5)   55.90 (C–13)   60.07 (C–14)
105.95 (C–10)   135.84 (C–9)   137.23 (C–12)   152.81 (C–11)
171.28 (C–6)   171.54 (C–1)

Melting Point: 126 °C

EA: Calculated: C: 57.77 %   H: 7.70 %   N: 11.89 %   O: 22.64 %
Found: C: 57.44 %   H: 7.75 %   N: 11.77 %

3-(3,4,5-Trimethoxyphenyl)-*N*-(5-oxo-5-(2-(1,2,3,4-tetrahydroacridin-9-yl)hydrazino)-pentyl)propanamide HCl
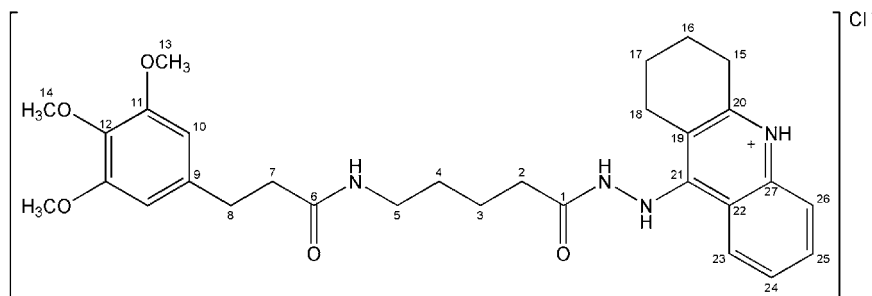
Synthesis:	2.0 mmol (0.44 g) 9-Chloro-1,2,3,4-tetrahydroacridine (**1**) and 2.0 mmol (0.71 g) *N*-(5-hydrazino-5-oxobutyl)-3-(3,4,5-trimethoxyphenyl)propanamide (**58**) are dissolved in 20 ml absolute ethanol and heated to 140 °C for 24 hours by means of a sealed bomb. Evaporation in vacuo yields a crude product that is dissolved in a mixture of 5 ml ethanol and 5 ml diethyl ether. Cooling to -20 °C results in an oily layer that is separated by decantation. Removal of remaining solvent in vacuo yields the final product **59**.

Yield: 0.64 g (56 %), $C_{30}H_{39}ClN_4O_5$, M_R = 571.12 g/mol
Yellow crystals

^{1}H NMR δ:
[DMSO-*d₆*]

1.38 (app. quint, 2H, *J* = 7.2 Hz, H–4)	3.72 (s, 6H, H–13)
1.50 (app. quint, 2H, *J* = 7.4 Hz, H–3)	6.49 (s, 2H, H–10)
1.82 (app. bs, 4H, H–16,17)	7.58 (ddd, 1H, *J* = 1.0 7.1 8.5 Hz, H–24)
2.27 (t, 2H, *J* = 7.4 Hz, H–2)	7.87 (ddd, 1H, *J* = 1.0 7.1 8.4 Hz, H–25)
2.36 (t, 2H, *J* = 7.9 Hz, H–7)	7.89 (t, 1H, *J* = 5.7 Hz, NH̲CH$_2$)
2.69 (app. bs, 2H, H–18)	8.04 (app. dd, 1H, *J* = 1.0 8.5 Hz, H–23)
2.73 (t, 2H, *J* = 7.9 Hz, H–8)	8.67 (app. d, 1H, *J* = 8.5 Hz, H–26)
3.03 (app. q, 2H, *J* = 6.3 Hz, H–5)	9.63 (s, 1H, CONH̲NH)
3.09 (app. bs, 2H, H–15)	11.06 (s, 1H, CONHNH̲)
3.60 (s, 3H, H–14)	14.53 (s, 1H, N$^+$H)

^{13}C NMR δ:
[DMSO-*d₆*]

20.26 (C–17)	21.41 (C–16)	22.17 (C–3)	24.16 (C–18)
28.25 (C–15)	28.89 (C–4)	31.69 (C–8)	32.70 (C–2)
37.26 (C–7)	38.12 (C–5)	55.93 (C–13)	60.08 (C–14)
105.62 (C–10)	111.19 (C–19)	115.11 (C–22)	119.47 (C–23)
124.19 (C–26)	125.88 (C–24)	133.02 (C–25)	135.84 (C–9)
137.22 (C–12)	137.43 (C–27)	152.68 (C–20)	152.82 (C–11)
155.29 (C–21)	171.40 (C–6)	171.81 (C–1)	

Melting Point: 90 °C

EA: Calculated: C: 63.09 % H: 6.88 % Cl: 6.21 % N: 9.81 % O: 14.01 %
Found:

3-(3,4,5-Trimethoxyphenyl)-*N*-(5-oxo-5-(2-(1,2,3,4-tetrahydroacridin-9-yl)hydrazino)-pentyl)propanamide
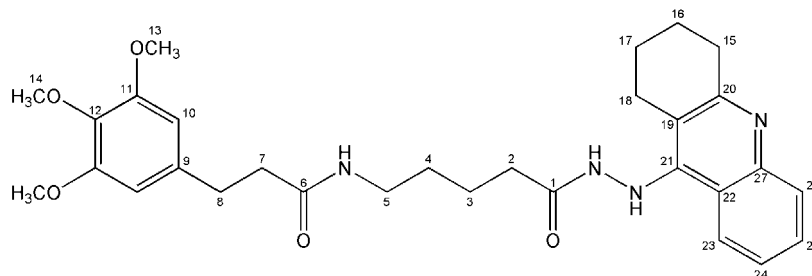
Synthesis:	A solution of 0.5 mmol (0.29 g) 3-(3,4,5-trimethoxyphenyl)-*N*-(5-oxo-5-(2-(1,2,3,4-tetrahydroacridin-9-yl)hydrazino)pentyl)propanamide hydrochloride (**59**) in 5 ml ethanol and 20 ml water is mixed with 1 ml of 1 M sodium hydroxide solution to liberate the base. The reaction mixture is extracted 4 times with 25 ml ethyl acetate, dried using anhydrous sodium sulfate and evaporated in vacuo to yield the final product **60** which needs no further purification.

Yield: 0.25 g (94 %), $C_{30}H_{38}N_4O_5$, M_R = 534.66 g/mol
Yellow crystals

^{1}H NMR δ:
[DMSO-d_6]

1.29 (app. quint, 2H, J = 7.1 Hz, H–4)
1.42 (app. quint, 2H, J = 7.6 Hz, H–3)
1.75-1.84 (m, 4H, H–16,17)
2.08 (t, 2H, J = 7.3 Hz, H–2)
2.32 (t, 2H, J = 7.9 Hz, H–7)
2.72 (t, 2H, J = 7.9 Hz, H–8)
2.81 (app. bs, 2H, H–18)
2.90 (app. bs, 2H, H–15)
2.98 (app. q, 2H, J = 6.4 Hz, H–5)
3.60 (s, 3H, H–14)

3.72 (s, 6H, H–13)
6.47 (s, 2H, H–10)
7.31 (ddd, 1H, J = 1.0 6.9 8.4 Hz, H–24)
7.50 (ddd, 1H, J = 1.3 7.0 8.2 Hz, H–25)
7.65 (s, 1H, CONHNH)
7.70 (app. d, 1H, J = 8.5 Hz, H–23)
7.73 (t, 1H, J = 5.9 Hz, NHCH$_2$)
8.31 (app. d, 1H, J = 8.6 Hz, H–26)
10.03 (s, 1H, CONHNH)

^{13}C NMR δ:
[DMSO-d_6]

22.40 (C–17)	22.52 (C–16)	22.71 (C–3)	24.86 (C–18)
28.84 (C–4)	31.65 (C–8)	32.67 (C–2)	33.77 (C–15)
37.25 (C–7)	38.18 (C–5)	55.90 (C–13)	60.06 (C–14)
105.59 (C–10)	115.59 (C–19)	119.11 (C–22)	123.15 (C–26)
123.48 (C–24)	127.94 (C–25)	128.41 (C–23)	135.84 (C–9)
137.21 (C–12)	146.80 (C–27)	148.76 (C–21)	152.81 (C–11)
158.16 (C–20)	171.28 (C–6)	171.92 (C–1)	

Melting Point: 88 °C

EA:
$C_{30}H_{38}N_4O_5$ • 2 H_2O
Calculated: C: 63.14 % H: 7.42 % N: 9.82 % O: 19.62 %
Found: C: 63.20 % H: 7.66 % N: 9.48 %

Ethyl 6-((3-(3,4,5-trimethoxyphenyl)propanoyl)amino)hexanoate
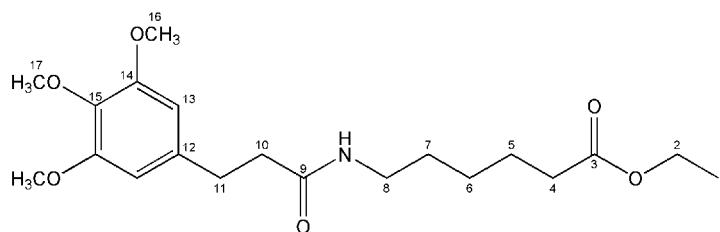
Synthesis: 10.0 mmol (2.40 g) of 3-(3,4,5-trimethoxyphenyl)propanoic acid are dissolved in 20 ml anhydrous dichloromethane with catalytic amounts of *N,N*-dimethyl-formamide. While stirring the subsequent addition of 11.6 mmol (1.0 ml) of oxalyl chloride generates the acyl chloride. Once the gas evolution has ceased remaining hydrogen chloride, excess oxalyl chloride and the solvent are removed by evaporation in vacuo. The residue is again taken up in 10 ml of dichloromethane and 10.0 mmol (1.96 g) ethyl 6-aminohexanoate hydrochloride are suspended in the solution. Dropwise addition of 20.0 mmol (3.5 ml) *N*-ethyl-*N,N*-diisopropylamine yields a clear solution which some-times contains some precipitated *N*-ethyl-*N,N*-diisopropylamine hydrochloride. Wash-ing with water and a saturated solution of sodium hydrogen carbonate, drying with anhydrous sodium sulfate and evaporation in vacuo yields a crude product which is further purified by flash column chromatography using ethyl acetate to yield **61**.

Yield: 3.37 g (88 %), $C_{20}H_{31}NO_6$, $M_R = 381.47$ g/mol
White crystals

^{1}H NMR δ:
[CDCl$_3$]

1.22 (t, 3H, J = 7.3 Hz, H–1)	3.20 (app. q, 2H, J = 6.6 Hz, H–8)
1.28 (app. quint, 2H, J = 7.7 Hz, H–6)	3.79 (s, 3H, H–17)
1.44 (app. quint, 2H, J = 7.3 Hz, H–7)	3.81 (s, 6H, H–16)
1.58 (app. quint, 2H, J = 7.6 Hz, H–5)	4.09 (q, 2H, J = 7.2 Hz, H–2)
2.26 (t, 2H, J = 7.4 Hz, H–4)	5.53 (bs, 1H, NH)
2.43 (t, 2H, J = 7.6 Hz, H–10)	6.40 (s, 2H, H–13)
2.88 (t, 2H, J = 7.6 Hz, H–11)	

^{13}C NMR δ:
[CDCl$_3$]

14.21 (C–1)	24.34 (C–5)	26.23 (C–6)	29.14 (C–7)
32.20 (C–11)	34.02 (C–4)	38.66 (C–10)	39.29 (C–8)
56.06 (C–16)	60.26 (C–17)	60.81 (C–2)	105.26 (C–13)
136.35 (C–12)	136.67 (C–15)	153.18 (C–14)	172.09 (C–3)
173.60 (C–9)			

Melting Point: 64 °C

EA:

Calculated:	C: 62.97 %	H: 8.19 %	N: 3.67 %	O: 25.16 %
Found:	C: 63.13 %	H: 8.35 %	N: 3.72 %	

N-(6-Hydrazino-6-oxohexyl)-3-(3,4,5-trimethoxyphenyl)propanamide
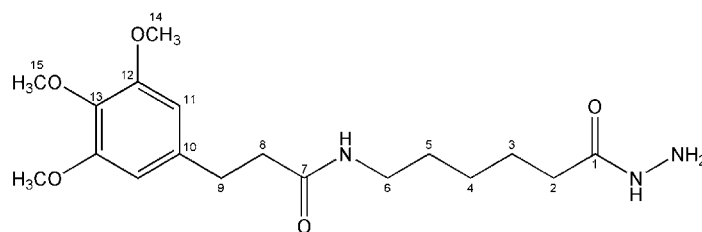
Synthesis:	To a mixture of 51.4 mmol hydrazine (2.5 ml hydrazine hydrate, 100 %) and 20 ml absolute ethanol 5.0 mmol (1.91 g) ethyl 6-((3-(3,4,5-trimethoxyphenyl)propanoyl)amino)hexanoate (**61**) are added and the solution is heated to reflux for 24 hours. The course of the reaction is followed by TLC and once no more ester can be detected the solvent and excess hydrazine are evaporated in vacuo. The crude product is recrystallized from 5 ml ethanol for further purification to produce **62**.

Yield: 1.48 g (81 %), $C_{18}H_{29}N_3O_5$, M_R = 367.45 g/mol
White crystals

^{1}H NMR δ:
[DMSO-d_6]

1.18 (app. quint, 2H, J = 7.8 Hz, H–4)
1.34 (app. quint, 2H, J = 7.3 Hz, H–5)
1.45 (app. quint, 2H, J = 7.6 Hz, H–3)
1.97 (t, 2H, J = 7.4 Hz, H–2)
2.33 (t, 2H, J = 7.7 Hz, H–8)
2.73 (t, 2H, J = 7.7 Hz, H–9)
3.00 (app. q, 2H, J = 6.6 Hz, H–6)

3.60 (s, 3H, H–15)
3.73 (s, 6H, H–14)
4.11 (s, 2H, NH$_2$)
6.48 (s, 2H, H–11)
7.73 (t, 1H, J = 5.5 Hz, N<u>H</u>CH$_2$)
8.86 (s, 1H, N<u>H</u>NH$_2$)

^{13}C NMR δ:
[DMSO-d_6]

25.07 (C–3)	26.22 (C–4)	29.08 (C–5)	31.63 (C–9)
33.48 (C–2)	37.24 (C–8)	38.45 (C–6)	55.90 (C–14)
60.07 (C–15)	105.60 (C–11)	135.83 (C–10)	137.22 (C–13)
152.80 (C–12)	171.26 (C–7)	171.65 (C–1)	

Melting Point: 102 °C

EA:

Calculated:	C: 58.84 %	H: 7.95 %	N: 11.44 %	O: 21.77 %
Found:	C: 58.74 %	H: 8.03 %	N: 11.29 %	

3-(3,4,5-Trimethoxyphenyl)-*N*-(6-oxo-6-(2-(1,2,3,4-tetrahydroacridin-9-yl)hydrazino)-hexyl)propanamide HCl
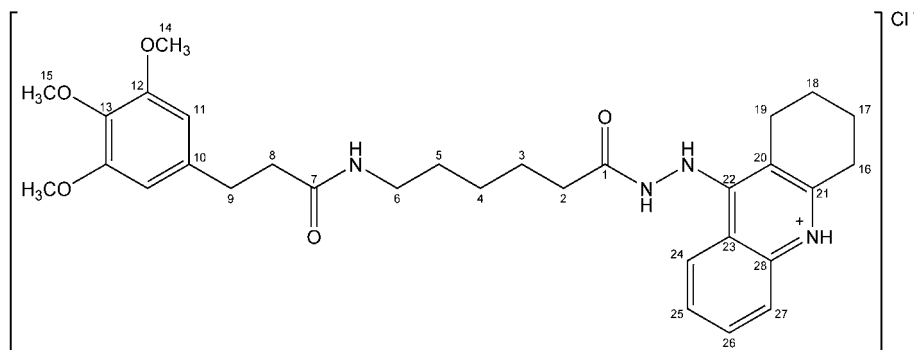
Synthesis:	2.0 mmol (0.44 g) 9-Chloro-1,2,3,4-tetrahydroacridine (**1**) and 2.0 mmol (0.73 g) *N*-(6-hydrazino-6-oxohexyl)-3-(3,4,5-trimethoxyphenyl)propanamide (**62**) are dissolved in 20 ml absolute ethanol and heated to 140 °C for 24 hours by means of a sealed bomb. Cooling to room temperature yields a crude product that is recrystallized from nitromethane for further purification to obtain **63**.

Yield: 0.70 g (60 %), $C_{31}H_{41}ClN_4O_5$, M_R = 585.14 g/mol
Yellow crystals

^{1}H NMR δ:
[DMSO-*d$_6$*]

1.22 (app. quint, 2H, *J* = 7.5 Hz, H–4)	3.73 (s, 6H, H–14)
1.36 (app. quint, 2H, *J* = 7.3 Hz, H–5)	6.48 (s, 2H, H–11)
1.51 (app. quint, 2H, *J* = 7.5 Hz, H–3)	7.59 (ddd, 1H, *J* = 1.3 7.1 8.7 Hz, H–25)
1.82 (app. bs, 4H, H–17,18)	7.82 (t, 1H, *J* = 5.5 Hz, NH̲CH$_2$)
2.25 (t, 2H, *J* = 7.4 Hz, H–2)	7.88 (ddd, 1H, *J* = 1.0 7.1 8.4 Hz, H–26)
2.35 (t, 2H, *J* = 7.7 Hz, H–8)	8.01 (app. dd, 1H, *J* = 1.0 8.5 Hz, H–24)
2.69 (app. bs, 2H, H–19)	8.66 (app. d, 1H, *J* = 8.8 Hz, H–27)
2.73 (t, 2H, *J* = 7.9 Hz, H–9)	9.60 (s, 1H, CONH̲NH)
3.00 (app. q, 2H, *J* = 6.5 Hz, H–6)	10.97 (s, 1H, CONHNH̲)
3.08 (app. bs, 2H, H–16)	14.39 (s, 1H, N$^+$H)
3.60 (s, 3H, H–15)	

^{13}C NMR δ:
[DMSO-*d$_6$*]

20.29 (C–18)	21.41 (C–17)	24.15 (C–19)	24.47 (C–3)
26.16 (C–4)	28.31 (C–16)	29.03 (C–5)	31.65 (C–9)
33.01 (C–2)	37.23 (C–8)	38.43 (C–6)	55.92 (C–14)
60.08 (C–15)	105.62 (C–11)	111.26 (C–20)	115.14 (C–23)
119.55 (C–24)	124.17 (C–27)	125.87 (C–25)	133.03 (C–26)
135.84 (C–10)	137.22 (C–13)	137.50 (C–28)	152.71 (C–21)
152.80 (C–12)	155.28 (C–22)	171.33 (C–7)	171.87 (C–1)

Melting Point: 125 °C

EA: $C_{31}H_{41}ClN_4O_5$ • 0.5 H_2O

Calculated:	C: 62.67 %	H: 7.13 %	Cl: 5.97 %	N: 9.43 %	O: 14.81 %
Found:	C: 62.39 %	H: 7.25 %		N: 9.42 %	

3-(3,4,5-Trimethoxyphenyl)-*N*-(6-oxo-6-(2-(1,2,3,4-tetrahydroacridin-9-yl)hydrazino)-hexyl)propanamide
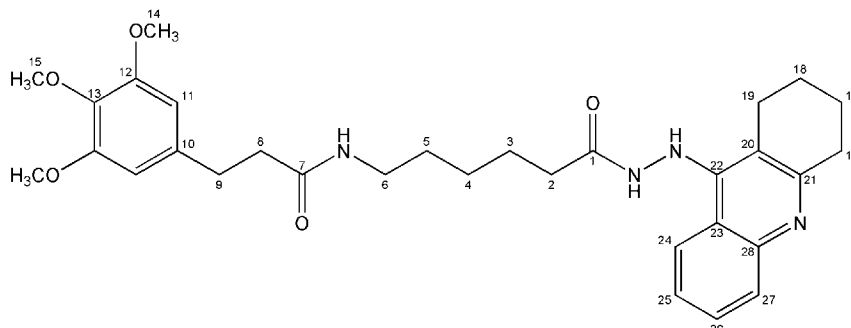
Synthesis:	A solution of 0.5 mmol (0.29 g) 3-(3,4,5-trimethoxyphenyl)-*N*-(6-oxo-6-(2-(1,2,3,4-tetrahydroacridin-9-yl)hydrazino)hexyl)propanamide hydrochloride (**63**) in 5 ml ethanol and 20 ml water is mixed with 1 ml of 1 M sodium hydroxide solution to liberate the base. The reaction mixture is extracted 4 times with 25 ml ethyl acetate, dried using anhydrous sodium sulfate and evaporated in vacuo to yield the final product **64** which needs no further purification.

Yield: 0.27 g (98 %), $C_{31}H_{40}N_4O_5$, M_R = 548.68 g/mol
Yellow crystals

^{1}H NMR δ:
[DMSO-d_6]

1.14 (app. sext, 2H, *J* = 7.3 Hz, H–4)	3.60 (s, 3H, H–15)
1.30 (app. quint, 2H, *J* = 7.3 Hz, H–5)	3.72 (s, 6H, H–14)
1.43 (app. quint, 2H, *J* = 7.5 Hz, H–3)	6.48 (s, 2H, H–11)
1.74-1.84 (m, 4H, H–17,18)	7.31 (ddd, 1H, *J* = 1.0 6.9 8.4 Hz, H–25)
2.06 (t, 2H, *J* = 7.4 Hz, H–2)	7.51 (ddd, 1H, *J* = 1.3 6.9 8.3 Hz, H–26)
2.32 (t, 2H, *J* = 7.7 Hz, H–8)	7.65 (s, 1H, CON<u>H</u>NH)
2.73 (t, 2H, *J* = 7.7 Hz, H–9)	7.70 (app. d, 1H, *J* = 5.7 Hz, H–24)
2.81 (app. bs, 2H, H–19)	7.71 (bs, 1H, N<u>H</u>CH₂)
2.90 (t, 2H, *J* = 5.8 Hz, H–16)	8.31 (app. d, 1H, *J* = 8.2 Hz, H–27)
2.95 (app. q, 2H, *J* = 6.6 Hz, H–6)	10.02 (s, 1H, CONHN<u>H</u>)

^{13}C NMR δ:
[DMSO-d_6]

22.53 (C–18)	22.72 (C–17)	24.76 (C–3)	24.86 (C–19)
26.14 (C–4)	29.06 (C–5)	31.63 (C–9)	33.04 (C–2)
33.78 (C–16)	37.24 (C–8)	38.46 (C–6)	55.91 (C–14)
60.08 (C–15)	105.62 (C–11)	115.58 (C–20)	119.10 (C–23)
123.20 (C–27)	123.48 (C–25)	127.97 (C–26)	128.42 (C–24)
135.85 (C–10)	137.23 (C–13)	146.81 (C–28)	148.81 (C–22)
152.82 (C–12)	158.16 (C–21)	171.26 (C–7)	172.00 (C–1)

Melting Point: 110 °C

EA:

$C_{31}H_{40}N_4O_5$ • 0.5 H_2O
Calculated: C: 66.76 % H: 7.41 % N: 10.05 % O: 15.78 %
Found: C: 66.36 % H: 7.32 % N: 10.10 %

4-Acetyloxybenzoic acid
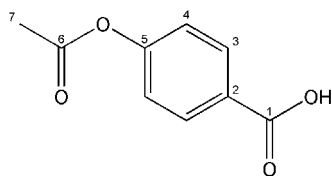
Synthesis: 0.15 mol (20.7 g) 4-Hydroxybenzoic acid are dissolved in a mixture of 50 ml pyridine and 50 ml acetic anhydride. After stirring at room temperature for one hour the reaction mixture is poured into 500 ml water and the pH is adjusted to about 2 using concentrated hydrochloric acid. The solution is extracted three times with 500 ml ethyl acetate, dried using anhydrous sodium sulfate and the solvent is evaporated in vacuo. The remaining crude product is washed with petrol ether and recrystallized from ethyl acetate to yield **65**.

Yield: 19.5 g (72 %), $C_9H_8O_4$, $M_R = 180.16$ g/mol
White needles

^{1}H NMR δ: 2.28 (s, 3H, H–7) 7.98 (ddd, 2H, $J = 2.2$ 2.5 8.9 Hz, H–3)
[DMSO-d_6] 7.25 (ddd, 2H, $J = 2.4$ 2.5 8.9 Hz, H–4) 12.96 (bs, 1H, COOH)

^{13}C NMR δ: 21.01 (C–7) 122.18 (C–4) 128.47 (C–2) 130.99 (C–3)
[DMSO-d_6] 154.09 (C–5) 166.74 (C–6) 168.97 (C–1)

Melting Point: 195 °C, lit. [119] 187-192 °C

EA: Calculated: C: 60.00 % H: 4.48 % O: 35.52 %
  Found: C: 59.70 % H: 4.31 %

Ethyl 6-((4-hydroxybenzoyl)amino)hexanoate
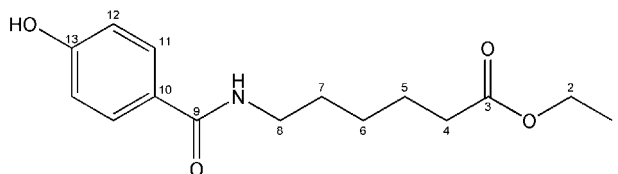
Synthesis: 30.0 mmol (5.40 g) 4-Acetyloxybenzoic acid (**65**) are dissolved in 50 ml anhydrous dichloromethane with catalytic amounts of *N,N*-dimethylformamide. While stirring the subsequent addition of 34.4 mmol (3.0 ml) of oxalyl chloride generates the acyl chloride. Once the gas evolution has ceased remaining hydrogen chloride, excess oxalyl chloride and the solvent are removed by evaporation in vacuo. The residue is again taken up in 20 ml of dichloromethane and 30.0 mmol (5.88 g) ethyl 6-aminohexanoate hydrochloride are suspended in the solution. Dropwise addition of 60.0 mmol (10.5 ml) *N*-ethyl-*N,N*-diisopropylamine yields a clear solution which sometimes contains some precipitated *N*-ethyl-*N,N*-diisopropylamine hydrochloride. Washing with water and a saturated solution of sodium hydrogen carbonate, drying with anhydrous sodium sulfate and evaporation in vacuo yields a white solid that is dissolved in 60 ml anhydrous methanol. After adding 3.2 mmol (0.44 g) potassium carbonate and stirring for 12 hours the solution is poured into 200 ml water and 4 ml 2 M hydrochloric acid. The resulting suspension is extrated three times using ethyl acetate and the combined organic phases are dried using anhydrous sodium sulfate. Evaporation in vacuo yields **66** as a white solid that needs no further purification.

Yield: 7.71 g (92 %), $C_{15}H_{21}NO_4$, $M_R = 279.34$ g/mol
White powder

^{1}H NMR δ: 1.15 (t, 3H, $J = 7.1$ Hz, H–1)   4.03 (q, 2H, $J = 7.1$ Hz, H–2)
[DMSO-d_6] 1.28 (app. quint, 2H, $J = 7.6$ Hz, H–6)   6.76 (ddd, 2H, $J = 2.4$ 2.9 9.5 Hz, H–12)
1.48 (app. quint, 2H, $J = 7.4$ Hz, H–7)   7.68 (ddd, 2H, $J = 2.4$ 2.9 9.5 Hz, H–11)
1.53 (app. quint, 2H, $J = 7.5$ Hz, H–5)   8.12 (t, 1H, $J = 5.7$ Hz, NH)
2.26 (t, 2H, $J = 7.4$ Hz, H–4)   9.86 (s, 1H, OH)
3.19 (app. q, 2H, $J = 6.5$ Hz, H–8)

^{13}C NMR δ: 14.24 (C–1)   24.37 (C–5)   26.07 (C–6)   29.04 (C–7)
[DMSO-d_6] 33.62 (C–4)   38.98 (C–8)   59.75 (C–2)   114.81 (C–12)
125.60 (C–10)   129.11 (C–11)   160.04 (C–13)   165.92 (C–9)
172.97 (C–3)

Melting Point: 75 °C

EA: Calculated: C: 64.50 %   H: 7.58 %   N: 5.01 %   O: 22.91 %
Found: C: 64.45 %   H: 7.70 %   N: 5.04 %

Ethyl 6-((4-(2-bromoethoxy)benzoyl)amino)hexanoate
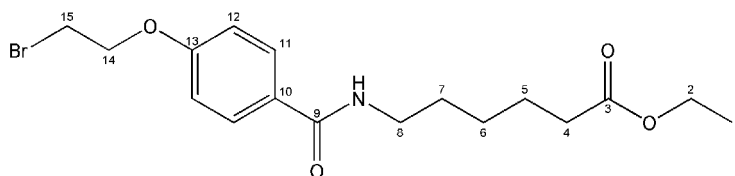
Synthesis: 25.0 mmol (6.98 g) Ethyl 6-((4-hydroxybenzoyl)amino)hexanoate (**66**), 150.0 mmol (20.73 g) potassium carbonate and 3.8 mmol (1.00 g) 18-crown-6 are suspended in 120 ml 1,2-dibromoethane and heated to 80 °C for 36 hours while stirring. Subsequent removal of the inorganic salts by suction filtration, washing with dichloromethane and evaporation in vacuo yields a crude product that is subjected to column chromatography using petrol ether and ethyl acetate in a ratio of 1:2. The final product **67** is recovered from the first fractions as a white solid.

Yield: 8.74 g (91 %), $C_{17}H_{24}BrNO_4$, $M_R = 386.29$ g/mol
White powder

^{1}H NMR δ:
[DMSO-d_6]

1.15 (t, 3H, $J = 7.1$ Hz, H–1)	3.80 (t, 2H, $J = 5.5$ Hz, H–15)
1.29 (app. quint, 2H, $J = 7.6$ Hz, H–6)	4.03 (q, 2H, $J = 7.1$ Hz, H–2)
1.50 (app. quint, 2H, $J = 7.3$ Hz, H–7)	4.37 (t, 2H, $J = 5.4$ Hz, H–14)
1.54 (app. quint, 2H, $J = 7.6$ Hz, H–5)	7.00 (ddd, 2H, $J = 2.5$ 2.8 9.8 Hz, H–12)
2.27 (t, 2H, $J = 7.4$ Hz, H–4)	7.80 (ddd, 2H, $J = 2.5$ 2.8 9.8 Hz, H–11)
3.21 (app. q, 2H, $J = 6.6$ Hz, H–8)	8.26 (t, 1H, $J = 5.7$ Hz, NH)

^{13}C NMR δ:
[DMSO-d_6]

14.24 (C–1)	24.36 (C–5)	26.05 (C–6)	28.97 (C–7)
31.37 (C–15)	33.60 (C–4)	39.05 (C–8)	59.75 (C–2)
67.99 (C–14)	114.19 (C–12)	127.58 (C–10)	129.09 (C–11)
160.16 (C–13)	165.58 (C–9)	172.95 (C–3)	

Melting Point: 82 °C

EA:

Calculated:	C: 52.86 %	H: 6.26 %	Br: 20.69 %	N: 3.63 %	O: 16.57 %
Found:	C: 52.85 %	H: 6.24 %		N: 3.72 %	

2-(4-(((6-Ethoxy-6-oxohexyl)amino)carbonyl)phenoxy)-*N,N,N*-triethylethanaminium bromide
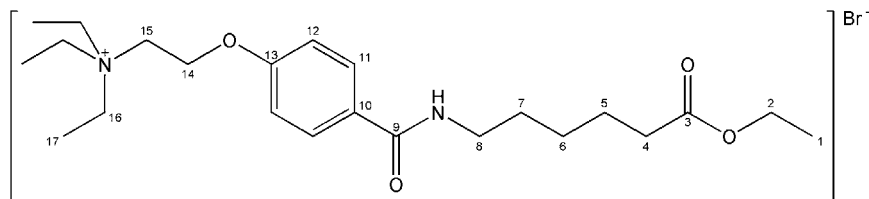
Synthesis: 20.0 mmol (7.73 g) Ethyl 6-((4-(2-bromoethoxy)benzoyl)amino)hexanoate (**67**) are heated to 60 °C for 24 hours in a solution of 200.0 mmol (27.9 ml) triethyl amine and 100 ml anhydrous nitromethane. After cooling to room temperature the solvent and excess amine are evaporated in vacuo and the oily residue is taken up in 10 ml absolute ethanol. Pouring the alcoholic solution into 1000 ml of ethyl acetate yields the final product **68** as a white precipitate.

Yield: 7.54 g (77 %), $C_{23}H_{39}BrN_2O_4$, M_R = 487.48 g/mol
White powder, hygroscopic

¹H NMR δ:
[DMSO-*d₆*]

1.15 (t, 3H, J = 7.1 Hz, H–1)	3.38 (q, 6H, J = 7.2 Hz, H–16)
1.23 (t, 9H, J = 7.3 Hz, H–17)	3.69 (t, 2H, J = 4.9 Hz, H–15)
1.29 (app. quint, 2H, J = 7.6 Hz, H–6)	4.03 (q, 2H, J = 7.2 Hz, H–2)
1.50 (app. quint, 2H, J = 7.3 Hz, H–7)	4.45 (t, 2H, J = 4.7 Hz, H–14)
1.54 (app. quint, 2H, J = 7.5 Hz, H–5)	7.03 (ddd, 2H, J = 2.4 2.8 9.8 Hz, H–12)
2.27 (t, 2H, J = 7.4 Hz, H–4)	7.85 (ddd, 2H, J = 2.5 2.9 9.6 Hz, H–11)
3.21 (app. q, 2H, J = 6.6 Hz, H–8)	8.30 (t, 1H, J = 5.7 Hz, NH)

¹³C NMR δ:
[DMSO-*d₆*]

7.45 (C–17)	14.25 (C–1)	24.35 (C–5)	26.05 (C–6)
28.98 (C–7)	33.60 (C–4)	39.06 (C–8)	53.09 (C–16)
55.29 (C–15)	59.75 (C–2)	61.34 (C–14)	114.22 (C–12)
127.85 (C–10)	129.06 (C–11)	159.61 (C–13)	165.46 (C–9)
172.96 (C–3)			

EA: $C_{23}H_{39}BrN_2O_4$ • 0.5 H_2O

Calculated:	C: 55.64 %	H: 8.12 %	Br: 16.09 %	N: 5.64 %	O: 14.50 %
Found:	C: 55.17 %	H: 8.39 %		N: 5.42 %	

N,N,N-Triethyl-2-(4-(((6-hydrazino-6-oxohexyl)amino)carbonyl)phenoxy)ethanaminium bromide
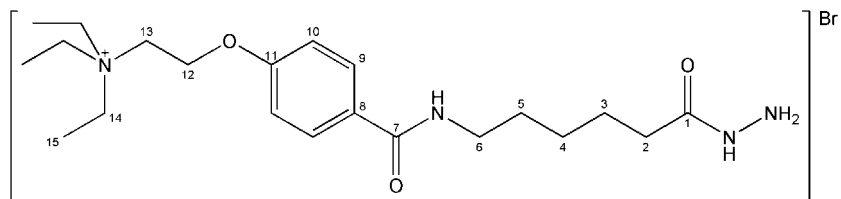
Synthesis: 2.0 mmol   (0.97 g)   2-(4-(((6-Ethoxy-6-oxohexyl)amino)carbonyl)phenoxy)-*N,N,N*-triethylethanaminium bromide (**68**) are dissolved in a mixture of 51.4 mmol hydrazine (2.5 ml hydrazine hydrate, 100 %) and 20 ml absolute ethanol and the solution is heated to 80 °C for 72 hours in a sealed bomb. After cooling to room temperature 80 ml absolute ethanol are added and the solution is evaporated in vacuo. The remaining residue is taken up in 10 ml absolute ethanol and poured into 300 ml ethyl acetate at -20 °C while stirring to yield the final product **69** that is recovered by suction filtration. For analytical purposes the precipitate is lyophilized from 20 ml of water to remove traces of ethyl acetate.

Yield: 0.81 g (86 %), $C_{21}H_{37}BrN_4O_3$, $M_R = 473.45$ g/mol
White powder, very hygroscopic

^{1}H NMR δ: 1.23 (t, 9H, $J = 7.3$ Hz, H–15)   4.12 (s, 2H, NH_2)
[DMSO-d_6]   1.26 (app. quint, 2H, $J = 7.6$ Hz, H–4)   4.44 (t, 2H, $J = 4.7$ Hz, H–12)
1.50 (app. sext, 4H, $J = 7.2$ Hz, H–3,5)   7.03 (ddd, 2H, $J = 2.4$ 2.9 9.8 Hz, H–10)
2.00 (t, 2H, $J = 7.4$ Hz, H–2)   7.85 (ddd, 2H, $J = 2.5$ 2.9 9.8 Hz, H–9)
3.21 (app. q, 2H, $J = 6.6$ Hz, H–6)   8.30 (t, 1H, $J = 5.7$ Hz, N$\underline{H}$CH$_2$)
3.38 (q, 6H, $J = 7.3$ Hz, H–14)   8.88 (s, 1H, N$\underline{H}$NH$_2$)
3.69 (t, 2H, $J = 4.9$ Hz, H–13)

^{13}C NMR δ: 7.45 (C–15)   25.13 (C–3)   26.33 (C–4)   29.12 (C–5)
[DMSO-d_6]   33.52 (C–2)   39.19 (C–6)   53.09 (C–14)   55.29 (C–13)
61.33 (C–12)   114.22 (C–10)   127.86 (C–8)   129.07 (C–9)
159.60 (C–11)   165.44 (C–7)   171.66 (C–1)

EA: Calculated: C: 53.27 %   H: 7.88 %   Br: 16.88 %   N: 11.83 %   O: 10.14 %
Found:

N,N,N-Triethyl-2-(4-(((6-(2-(1,2,3,4-tetrahydroacridin-9-yl)hydrazino)-6-oxohexyl)amino)-carbonyl)phenoxy)ethanaminium bromide HCl
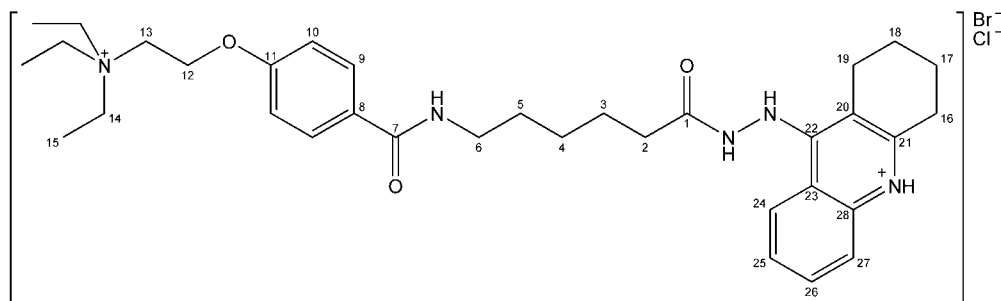
Synthesis: 1.0 mmol (0.47 g) N,N,N-Triethyl-2-(4-(((6-hydrazino-6-oxohexyl)amino)carbonyl)-phenoxy)ethanaminium bromide (**69**) and 1.0 mmol (0.22 g) 9-chloro-1,2,3,4-tetrahydroacridine (**1**) are dissolved in 20 ml absolute ethanol and heated to 140 °C for 24 hours by means of a sealed bomb. After cooling to room temperature and evaporating the solvent in vacuo the remaining residue is taken up in 10 ml absolute ethanol and poured into 300 ml ethyl acetate while stirring to yield the final product **70** that is recovered by suction filtration. For analytical purposes the precipitate is lyophilized from 20 ml of 0.1 M hydrochloric acid to remove traces of ethyl acetate.

Yield: 0.62 g (90 %), $C_{34}H_{49}BrClN_5O_3$, $M_R = 691.15$ g/mol
Yellow powder, hygroscopic

^{1}H NMR δ:
[DMSO-d_6]

1.22 (t, 9H, $J = 7.1$ Hz, H–15)	4.45 (t, 2H, $J = 4.7$ Hz, H–12)
1.29 (app. quint, 2H, $J = 7.6$ Hz, H–4)	7.03 (app. d, 2H, $J = 8.9$ Hz, H–10)
1.51 (app. quint, 2H, $J = 7.3$ Hz, H–5)	7.57 (ddd, 1H, $J = 1.0\ 7.3\ 8.6$ Hz, H–25)
1.56 (app. quint, 2H, $J = 7.6$ Hz, H–3)	7.85 (ddd, 1H, $J = 1.0\ 7.1\ 8.6$ Hz, H–26)
1.80 (app. bs, 4H, H–17,18)	7.88 (app. d, 2H, $J = 8.9$ Hz, H–9)
2.29 (t, 2H, $J = 7.2$ Hz, H–2)	8.09 (app. dd, 1H, $J = 0.7\ 8.7$ Hz, H–24)
2.69 (app. bs, 2H, H–19)	8.42 (t, 1H, $J = 5.2$ Hz, N<u>H</u>CH$_2$)
3.09 (app. bs, 2H, H–16)	8.69 (app. d, 1H, $J = 8.8$ Hz, H–27)
3.20 (app. q, 2H, $J = 6.2$ Hz, H–6)	9.65 (s, 1H, CON<u>H</u>NH)
3.39 (q, 6H, $J = 7.3$ Hz, H–14)	11.15 (s, 1H, CONHN<u>H</u>)
3.70 (t, 2H, $J = 4.9$ Hz, H–13)	14.68 (s, 1H, N$^+$H)

^{13}C NMR δ:
[DMSO-d_6]

7.51 (C–15)	20.26 (C–18)	21.43 (C–17)	24.18 (C–19)
24.55 (C–3)	26.32 (C–4)	28.24 (C–16)	29.08 (C–5)
33.09 (C–2)	39.13 (C–6)	53.14 (C–14)	55.35 (C–13)
61.41 (C–12)	111.13 (C–20)	114.24 (C–10)	115.10 (C–23)
119.42 (C–24)	124.27 (C–27)	125.82 (C–25)	127.83 (C–8)
129.16 (C–9)	132.96 (C–26)	137.44 (C–28)	152.61 (C–21)
155.29 (C–22)	159.64 (C–11)	165.50 (C–7)	171.90 (C–1)

EA: $C_{34}H_{49}BrClN_5O_3$ • 2 H_2O

Calculated:	C: 56.16 %	H: 7.35 %	Br: 10.99 % Cl: 4.88 %	N: 9.63 %	O: 11.00 %
Found:	C: 55.73 %	H: 7.40 %		N: 9.66 %	

2-(4-(((6-(2-(6-Chloro-1,2,3,4-tetrahydroacridin-9-yl)hydrazino)-6-oxohexyl)amino)-carbonyl)phenoxy)-*N,N,N*-triethylethanaminium bromide HCl
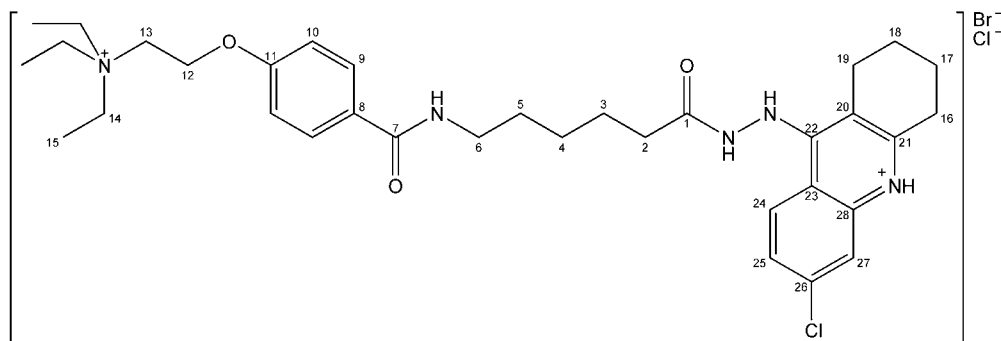
Synthesis: 1.0 mmol (0.47 g) *N,N,N*-Triethyl-2-(4-(((6-hydrazino-6-oxohexyl)amino)carbonyl)-phenoxy)ethanaminium bromide (**69**) and 1.0 mmol (0.25 g) 6,9-dichloro-1,2,3,4-tetrahydroacridine (**2**) are dissolved in 10 ml absolute ethanol and heated to 140 °C for 24 hours by means of a sealed bomb. After cooling to room temperature the reaction mixture is poured into 300 ml ethyl acetate while stirring to yield the final product **71** that is recovered by suction filtration. For analytical purposes the precipitate is lyophilized from 20 ml of 0.1 M hydrochloric acid to remove traces of ethyl acetate.

Yield: 0.68 g (94 %), $C_{34}H_{48}BrCl_2N_5O_3$, $M_R = 725.60$ g/mol
Yellow powder, hygroscopic

^{1}H NMR δ:
[DMSO-d_6]

1.22 (t, 9H, $J = 7.3$ Hz, H–15)	4.45 (t, 2H, $J = 4.6$ Hz, H–12)
1.29 (app. quint, 2H, $J = 7.6$ Hz, H–4)	7.02 (app. d, 2H, $J = 8.9$ Hz, H–10)
1.52 (app. quint, 2H, $J = 7.3$ Hz, H–5)	7.64 (dd, 1H, $J = 2.2\ 9.5$ Hz, H–25)
1.56 (app. quint, 2H, $J = 7.3$ Hz, H–3)	7.87 (app. d, 2H, $J = 8.8$ Hz, H–9)
1.80 (app. bs, 4H, H–17,18)	8.19 (d, 1H, $J = 2.2$ Hz, H–27)
2.30 (t, 2H, $J = 7.3$ Hz, H–2)	8.41 (t, 1H, $J = 5.4$ Hz, N$\underline{H}$CH$_2$)
2.66 (app. bs, 2H, H–19)	8.73 (d, 1H, $J = 9.5$ Hz, H–24)
3.07 (app. bs, 2H, H–16)	9.77 (s, 1H, CON$\underline{H}$NH)
3.25 (app. q, 2H, $J = 6.3$ Hz, H–6)	11.18 (s, 1H, CONHN$\underline{H}$)
3.39 (q, 6H, $J = 7.3$ Hz, H–14)	14.88 (s, 1H, N$^+$H)
3.70 (t, 2H, $J = 4.7$ Hz, H–13)	

^{13}C NMR δ:
[DMSO-d_6]

7.49 (C–15)	20.16 (C–18)	21.28 (C–17)	24.05 (C–19)
24.49 (C–3)	26.29 (C–4)	28.25 (C–16)	29.06 (C–5)
33.10 (C–2)	39.11 (C–6)	53.14 (C–14)	55.34 (C–13)
61.40 (C–12)	111.49 (C–20)	113.64 (C–23)	114.22 (C–10)
118.27 (C–27)	126.19 (C–25)	126.68 (C–24)	127.82 (C–8)
129.13 (C–9)	137.46 (C–28)	138.23 (C–26)	153.22 (C–21)
155.11 (C–22)	159.63 (C–11)	165.50 (C–7)	171.96 (C–1)

EA: $C_{34}H_{48}BrCl_2N_5O_3$ • 2 H_2O

Calculated:	C: 53.62 %	H: 6.88 %	Br: 10.49 % Cl: 9.31 %	N: 9.20 %	O: 10.50 %
Found:	C: 53.46 %	H: 6.91 %		N: 9.33 %	

3,5-Bis(acetyloxy)benzoic acid
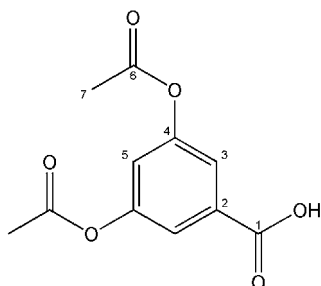
Synthesis:	0.15 mol (23.1 g) 3,5-Dihydroxybenzoic acid are dissolved in a mixture of 50 ml pyridine and 50 ml acetic anhydride. After stirring at room temperature for one hour the reaction mixture is poured into 500 ml water and the pH is adjusted to about 2 using concentrated hydrochloric acid. The solution is extracted three times with 500 ml ethyl acetate, dried using anhydrous sodium sulfate and the solvent is evaporated in vacuo. The remaining crude product is washed with diethyl ether to yield the final product **72**.
Yield:	30.0 g (84 %), $C_{11}H_{10}O_6$, $M_R = 238.20$ g/mol White powder

^{1}H NMR δ: **[DMSO-d_6]**

2.28 (s, 6H, H–7) 7.57 (d, 2H, $J = 2.2$ Hz, H–3)
7.26 (t, 1H, $J = 2.2$ Hz, H–5) 13.34 (s, 1H, COOH)

^{13}C NMR δ: **[DMSO-d_6]**

20.92 (C–7)	120.29 (C–3)	120.50 (C–5)	133.05 (C–2)
151.06 (C–4)	165.89 (C–1)	169.05 (C–6)	

Melting Point: 164 °C, lit.[120] 161 °C

EA:

Calculated: C: 55.47 % H: 4.23 % O: 40.30 %
Found: C: 55.52 % H: 4.29 %

Ethyl 6-((3,5-dihydroxybenzoyl)amino)hexanoate
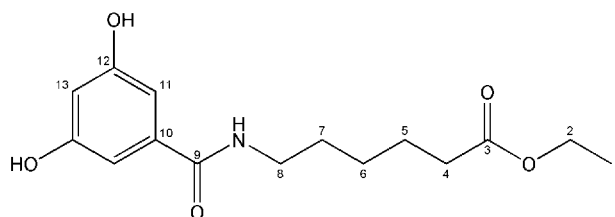
Synthesis: 20.0 mmol (4.76 g) 3,5-Bis(acetyloxy)benzoic acid (**72**) are dissolved in 20 ml anhydrous dichloromethane with catalytic amounts of *N,N*-dimethylformamide. While stirring the subsequent addition of 22.9 mmol (2.0 ml) of oxalyl chloride generates the acyl chloride. Once the gas evolution has ceased remaining hydrogen chloride, excess oxalyl chloride and the solvent are removed by evaporation in vacuo. The residue is again taken up in 10 ml of dichloromethane and 20.0 mmol (3.92 g) ethyl 6-aminohexanoate hydrochloride are suspended in the solution. Dropwise addition of 40.0 mmol (7.0 ml) *N*-ethyl-*N,N*-diisopropylamine yields a clear solution which sometimes contains some precipitated *N*-ethyl-*N,N*-diisopropylamine hydrochloride. Washing with water and a saturated solution of sodium hydrogen carbonate, drying with anhydrous sodium sulfate and evaporation in vacuo yields a crude oil that is dissolved in 60 ml anhydrous methanol. After adding 3.2 mmol (0.44 g) potassium carbonate and stirring for 12 hours the solution is poured into 200 ml water and 4 ml 2 M hydrochloric acid. The resulting precipitate **73** is recovered by suction filtration and needs no further purification.

Yield: 4.76 g (81 %), $C_{15}H_{21}NO_5$, $M_R = 295.34$ g/mol
White powder

^{1}H NMR δ:
[DMSO-d_6]

1.16 (t, 3H, $J = 7.1$ Hz, H–1)
1.27 (app. quint, 2H, $J = 7.7$ Hz, H–6)
1.47 (app. quint, 2H, $J = 7.5$ Hz, H–7)
1.53 (app. quint, 2H, $J = 7.6$ Hz, H–5)
2.26 (t, 2H, $J = 7.3$ Hz, H–4)
3.16 (app. q, 2H, $J = 6.6$ Hz, H–8)

4.03 (q, 2H, $J = 7.2$ Hz, H–2)
6.32 (t, 1H, $J = 2.2$ Hz, H–13)
6.63 (d, 2H, $J = 2.2$ Hz, H–11)
8.15 (t, 1H, $J = 5.7$ Hz, NH)
9.35 (s, 2H, OH)

^{13}C NMR δ:
[DMSO-d_6]

14.26 (C–1)	24.35 (C–5)	26.03 (C–6)	28.87 (C–7)
33.63 (C–4)	39.00 (C–8)	59.77 (C–2)	105.00 (C–13)
105.53 (C–11)	137.19 (C–10)	158.31 (C–12)	166.49 (C–9)
172.98 (C–3)			

Melting Point: 78 °C

EA: $C_{15}H_{21}NO_5 \cdot H_2O$
Calculated: C: 57.50 % H: 7.40 % N: 4.47 % O: 30.64 %
Found: C: 57.03 % H: 7.36 % N: 4.50 %

Ethyl 6-((3,5-bis(2-bromoethoxy)benzoyl)amino)hexanoate
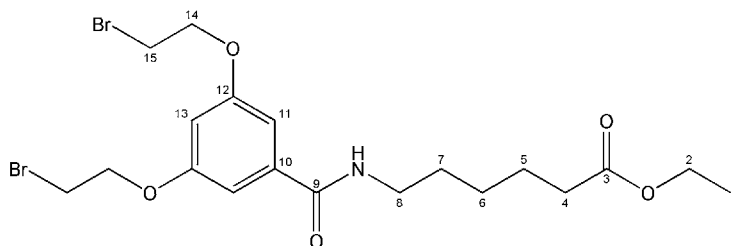
Synthesis: 40.0 mmol (11.81 g) Ethyl 6-((3,5-dihydroxybenzoyl)amino)hexanoate (**73**), 150.0 mmol (20.73 g) potassium carbonate and 3.8 mmol (1.00 g) 18-crown-6 are suspended in 120 ml 1,2-dibromoethane and heated to 80 °C for 36 hours while stirring. Subsequent removal of the inorganic salts by suction filtration, washing with dichloromethane and evaporation in vacuo yields a crude product that is subjected to column chromatography using petrol ether and ethyl acetate in a ratio of 1:2. The final product **74** is recovered from the first fractions as a white solid.

Yield: 13.10 g (64 %), $C_{19}H_{27}Br_2NO_5$, $M_R = 509.24$ g/mol
White powder

^{1}H NMR δ: 1.15 (t, 3H, $J = 7.3$ Hz, H–1)   3.79 (t, 4H, $J = 5.4$ Hz, H–15)
[DMSO-d_6] 1.29 (app. quint, 2H, $J = 7.6$ Hz, H–6)   4.03 (q, 2H, $J = 7.2$ Hz, H–2)
1.50 (app. quint, 2H, $J = 7.6$ Hz, H–7)   4.35 (t, 4H, $J = 5.4$ Hz, H–14)
1.54 (app. quint, 2H, $J = 7.6$ Hz, H–5)   6.69 (t, 1H, $J = 2.2$ Hz, H–13)
2.27 (t, 2H, $J = 7.3$ Hz, H–4)   7.03 (d, 2H, $J = 2.2$ Hz, H–11)
3.21 (app. q, 2H, $J = 6.5$ Hz, H–8)   8.39 (t, 1H, $J = 5.5$ Hz, NH)

^{13}C NMR δ: 14.24 (C–1)   24.34 (C–5)   26.03 (C–6)   28.82 (C–7)
[DMSO-d_6] 31.44 (C–15)   33.59 (C–14)   39.17 (C–8)   59.75 (C–2)
68.19 (C–14)   104.15 (C–13)   106.52 (C–11)   137.05 (C–10)
159.08 (C–12)   165.39 (C–9)   172.95 (C–3)

Melting Point: 98 °C

EA: Calculated: C: 44.81 % H: 5.34 % Br: 31.38 % N: 2.75 % O: 15.71 %
Found: C: 44.75 % H: 5.23 %   N: 2.98 %

2-(3-(((6-Ethoxy-6-oxohexyl)amino)carbonyl)-5-((2-triethylammonio)ethoxy)phenoxy)-*N,N,N*-triethylethanaminium dibromide
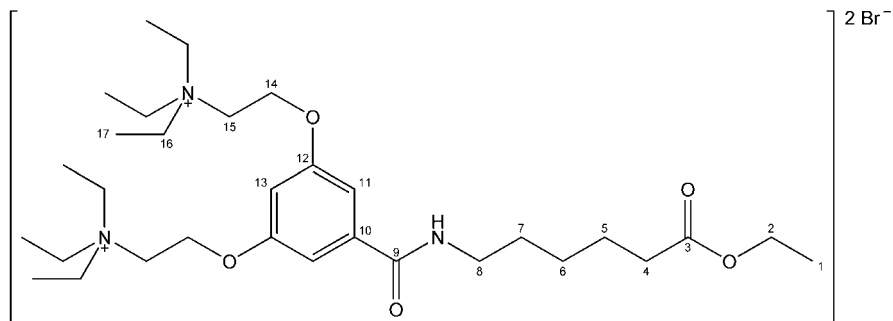
Synthesis: 20.0 mmol (10.18 g) Ethyl 6-((3,5-bis(2-bromoethoxy)benzoyl)amino)hexanoate (**74**) are heated to 60 °C for 24 hours in a solution of 200.0 mmol (27.9 ml) triethyl amine and 100 ml anhydrous nitromethane. After cooling to room temperature the solvent and excess amine are evaporated in vacuo and the oily residue is taken up in 50 ml absolute ethanol. Pouring the alcoholic solution into 900 ml of ethyl acetate yields the final product **75** as a white precipitate.

Yield: 11.5 g (81 %), $C_{31}H_{57}Br_2N_3O_5$, $M_R = 711.62$ g/mol
White powder, hygroscopic

^{1}H NMR δ:
[DMSO-*d$_6$*]

1.16 (t, 3H, $J = 7.1$ Hz, H–1)	3.39 (q, 12H, $J = 7.2$ Hz, H–16)
1.24 (t, 18H, $J = 7.1$ Hz, H–17)	3.69 (t, 4H, $J = 4.7$ Hz, H–15)
1.29 (app. quint, 2H, $J = 7.8$ Hz, H–6)	4.03 (q, 2H, $J = 7.2$ Hz, H–2)
1.52 (app. quint, 2H, $J = 7.3$ Hz, H–7)	4.46 (t, 4H, $J = 4.7$ Hz, H–14)
1.54 (app. quint, 2H, $J = 7.4$ Hz, H–5)	6.75 (t, 1H, $J = 2.2$ Hz, H–13)
2.27 (t, 2H, $J = 7.4$ Hz, H–4)	7.15 (d, 2H, $J = 2.2$ Hz, H–11)
3.23 (app. q, 2H, $J = 6.6$ Hz, H–8)	8.52 (t, 1H, $J = 5.7$ Hz, NH)

^{13}C NMR δ:
[DMSO-*d$_6$*]

7.50 (C–17)	14.26 (C–1)	24.33 (C–5)	26.04 (C–6)
28.94 (C–7)	33.59 (C–4)	39.15 (C–8)	53.11 (C–16)
55.32 (C–15)	59.77 (C–2)	61.72 (C–14)	104.48 (C–13)
106.79 (C–11)	137.08 (C–10)	158.50 (C–12)	165.30 (C–9)
172.96 (C–3)			

EA: $C_{31}H_{57}Br_2N_3O_5 \cdot H_2O$

Calculated:	C: 51.03 %	H: 8.15 %	Br: 21.90 %	N: 5.76 %	O: 13.16 %
Found:	C: 50.76 %	H: 8.20 %		N: 5.84 %	

N,N,N-Triethyl-2-(3-(((6-hydrazino-6-oxohexyl)amino)carbonyl)-5-((2-triethylammonio)-ethoxy)phenoxy)ethanaminium dibromide
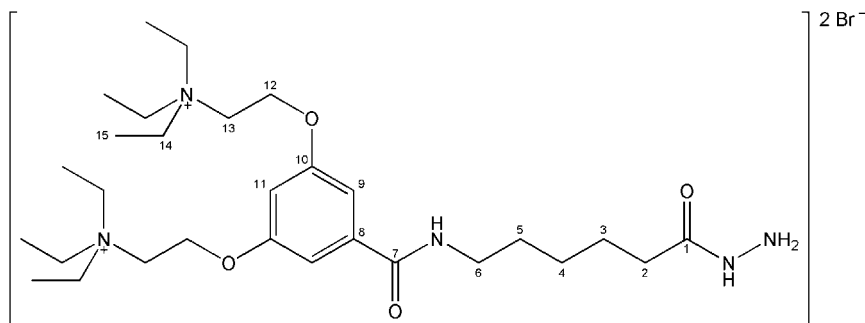
Synthesis: 2.0 mmol (1.42 g) 2-(3-(((6-Ethoxy-6-oxohexyl)amino)carbonyl)-5-((2-triethyl-ammonio)ethoxy)phenoxy)-N,N,N-triethylethanaminium dibromide (**75**) are dissolved in a mixture of 51.4 mmol hydrazine (2.5 ml hydrazine hydrate, 100 %) and 20 ml absolute ethanol and the solution is heated to 80 °C for 72 hours in a sealed bomb. After cooling to room temperature 80 ml absolute ethanol are added and the solution is evaporated in vacuo. The remaining residue is taken up in 10 ml absolute ethanol and poured into 300 ml ethyl acetate while stirring to yield the final product **76** that is recovered by suction filtration. For analytical purposes the precipitate is lyophilized from 20 ml of water to remove traces of ethyl acetate.

Yield: 1.07 g (77 %), $C_{29}H_{55}Br_2N_5O_4$, $M_R = 697.59$ g/mol
White powder, very hygroscopic

^{1}H NMR δ:
[DMSO-d_6]

1.24 (t, 18H, $J = 7.1$ Hz, H–15)
1.27 (m, 2H, H–4)
1.51 (m, 4H, H–3,5)
2.01 (t, 2H, $J = 7.4$ Hz, H–2)
3.22 (app. q, 2H, $J = 6.6$ Hz, H–6)
3.40 (q, 12H, $J = 7.3$ Hz, H–14)
3.69 (t, 4H, $J = 4.9$ Hz, H–13)

4.42 (bs, 2H, NH$_2$)
4.47 (t, 4H, $J = 4.6$ Hz, H–12)
6.76 (t, 1H, $J = 2.4$ Hz, H–11)
7.16 (d, 2H, $J = 2.2$ Hz, H–9)
8.53 (t, 1H, $J = 5.7$ Hz, N$\underline{H}$CH$_2$)
8.95 (s, 1H, N$\underline{H}$NH$_2$)

^{13}C NMR δ:
[DMSO-d_6]

7.50 (C–15)	25.10 (C–3)	26.30 (C–4)	29.04 (C–5)
33.49 (C–2)	39.25 (C–6)	53.11 (C–14)	55.32 (C–13)
61.74 (C–12)	104.52 (C–11)	106.80 (C–9)	137.09 (C–8)
158.50 (C–10)	165.30 (C–7)	171.65 (C–1)	

EA: $C_{29}H_{55}Br_2N_5O_4 \cdot H_2O$
Calculated: C: 48.67 %   H: 8.03 %   Br: 22.33 %   N: 9.79 %   O: 11.18 %
Found: C: 48.55 %   H: 8.16 %   N: 9.50 %

N,N,N-Triethyl-2-(3-(((6-(2-(1,2,3,4-tetrahydroacridin-9-yl)hydrazino)-6-oxohexyl)amino)-carbonyl)-5-((2-triethylammonio)ethoxy)phenoxy)ethanaminium dibromide HCl
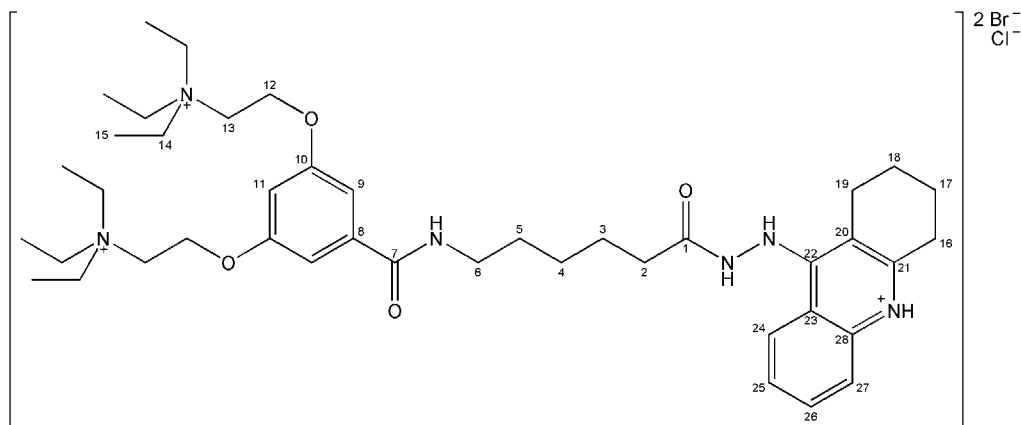
Synthesis: 0.5 mmol (0.35 g) N,N,N-Triethyl-2-(3-(((6-hydrazino-6-oxohexyl)amino)carbonyl)-5-((2-triethylammonio)ethoxy)phenoxy)ethanaminium dibromide (**76**) and 0.5 mmol (0.11 g) 9-chloro-1,2,3,4-tetrahydroacridine (**1**) are dissolved in 20 ml absolute ethanol and heated to 140 °C for 24 hours by means of a sealed bomb. After cooling to room temperature and evaporating the solvent in vacuo the remaining residue is taken up in 10 ml absolute ethanol and poured into 300 ml ethyl acetate while stirring to yield the final product **77** that is recovered by suction filtration. For analytical purposes the precipitate is lyophilized from 20 ml of 0.1 M hydrochloric acid to remove traces of ethyl acetate.

Yield: 0.33 g (72 %), $C_{42}H_{67}Br_2ClN_6O_4$, $M_R = 915.29$ g/mol
Yellow powder, hygroscopic

^{1}H NMR δ:
[DMSO-d_6]

1.23 (t, 18H, $J = 7.1$ Hz, H–15)	4.49 (t, 4H, $J = 4.6$ Hz, H–12)
1.29 (app. quint, 2H, $J = 7.8$ Hz, H–4)	6.77 (t, 1H, $J = 2.2$ Hz, H–11)
1.54 (app. quint, 2H, $J = 7.6$ Hz, H–5)	7.24 (d, 2H, $J = 2.3$ Hz, H–9)
1.56 (app. quint, 2H, $J = 7.6$ Hz, H–3)	7.59 (ddd, 1H, $J = 1.0\ 7.1\ 8.5$ Hz, H–25)
1.81 (app. bs, 4H, H–17,18)	7.87 (ddd, 1H, $J = 1.0\ 7.7\ 8.4$ Hz, H–26)
2.29 (t, 2H, $J = 7.4$ Hz, H–2)	8.06 (app. dd, 1H, $J = 1.0\ 8.5$ Hz, H–24)
2.69 (app. bs, 2H, H–19)	8.69 (app. d, 1H, $J = 8.5$ Hz, H–27)
3.09 (app. bs, 2H, H–16)	8.77 (t, 1H, $J = 5.7$ Hz, NH̲CH$_2$)
3.22 (app. q, 2H, $J = 6.6$ Hz, H–6)	9.65 (s, 1H, CONH̲NH)
3.40 (q, 12H, $J = 7.2$ Hz, H–14)	11.11 (s, 1H, CONHNH̲)
3.69 (t, 4H, $J = 4.9$ Hz, H–13)	14.51 (s, 1H, N$^+$H)

^{13}C NMR δ:
[DMSO-d_6]

7.53 (C–15)	20.27 (C–18)	21.40 (C–17)	24.18 (C–19)
24.53 (C–3)	26.30 (C–4)	28.27 (C–16)	28.99 (C–5)
33.07 (C–2)	39.20 (C–6)	53.14 (C–14)	55.33 (C–13)
61.81 (C–12)	104.60 (C–11)	106.91 (C–9)	111.22 (C–20)
115.10 (C–23)	119.45 (C–24)	124.22 (C–27)	125.88 (C–25)
133.04 (C–26)	137.02 (C–8)	137.42 (C–28)	152.67 (C–21)
155.31 (C–22)	158.51 (C–10)	165.28 (C–7)	171.89 (C–1)

EA: $C_{42}H_{67}Br_2ClN_6O_4 \cdot 3\ H_2O$

Calculated:	C: 52.04 %	H: 7.59 %	Br: 16.49 % Cl: 3.66 %	N: 8.67 %	O: 11.55 %
Found:	C: 51.70 %	H: 7.58 %		N: 8.87 %	

2-(3-(((6-(2-(6-Chloro-1,2,3,4-tetrahydroacridin-9-yl)hydrazino)-6-oxohexyl)amino)carbonyl)-5-((2-triethylammonio)ethoxy)phenoxy)-*N,N,N*-triethylethanaminium dibromide HCl
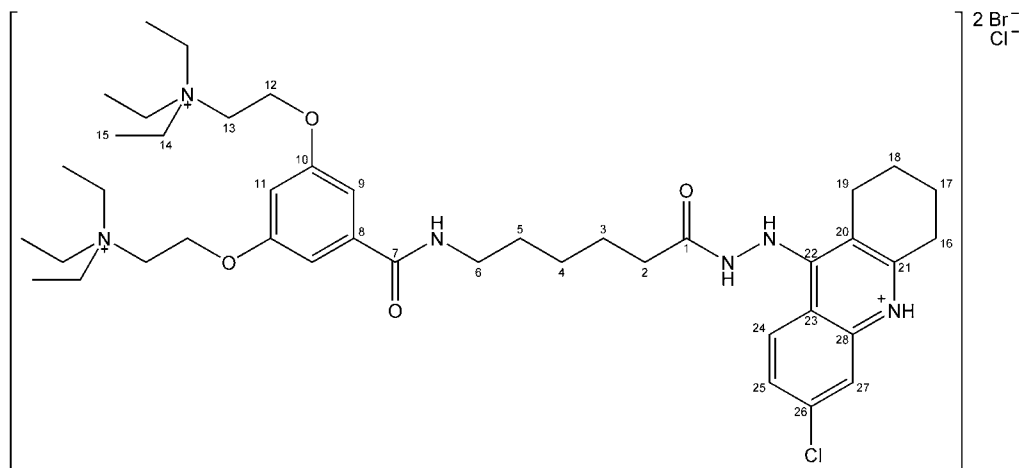
Synthesis:	1.0 mmol (0.70 g) *N,N,N*-Triethyl-2-(3-(((6-hydrazino-6-oxohexyl)amino)carbonyl)-5-((2-triethylammonio)ethoxy)phenoxy)ethanaminium dibromide (**76**) and 1.0 mmol (0.25 g) 6,9-dichloro-1,2,3,4-tetrahydroacridine (**1**) are dissolved in 20 ml absolute ethanol and heated to 140 °C for 24 hours by means of a sealed bomb. After cooling to room temperature the reaction mixture is poured into 300 ml ethyl acetate while stirring to yield the final product **78** that is recovered by suction filtration. For analytical purposes the precipitate is lyophilized from 20 ml of 0.1 M hydrochloric acid to remove traces of ethyl acetate.

Yield: 0.88 g (93 %), $C_{42}H_{66}Br_2Cl_2N_6O_4$, M_R = 949.74 g/mol
Yellow powder, hygroscopic

^{1}H NMR δ:
[DMSO-d_6]

1.23 (t, 18H, *J* = 7.3 Hz, H–15)	4.49 (t, 4H, *J* = 4.3 Hz, H–12)
1.30 (app. quint, 2H, *J* = 7.9 Hz, H–4)	6.76 (t, 1H, *J* = 2.1 Hz, H–11)
1.54 (app. quint, 2H, *J* = 7.6 Hz, H–5)	7.23 (d, 2H, *J* = 2.2 Hz, H–9)
1.56 (app. quint, 2H, *J* = 7.6 Hz, H–3)	7.65 (dd, 1H, *J* = 2.2 9.2 Hz, H–25)
1.80 (app. bs, 4H, H–17,18)	8.18 (d, 1H, *J* = 2.2 Hz, H–27)
2.30 (t, 2H, *J* = 7.3 Hz, H–2)	8.74 (d, 1H, *J* = 9.2 Hz, H–24)
2.66 (app. bs, 2H, H–19)	8.76 (t, 1H, *J* = 5.5 Hz, NH̲CH₂)
3.07 (app. bs, 2H, H–16)	9.77 (s, 1H, CONH̲NH)
3.22 (app. q, 2H, *J* = 6.5 Hz, H–6)	11.18 (s, 1H, CONHNH̲)
3.40 (q, 12H, *J* = 7.2 Hz, H–14)	14.79 (s, 1H, N⁺H)
3.69 (t, 4H, *J* = 4.6 Hz, H–13)	

^{13}C NMR δ:
[DMSO-d_6]

7.55 (C–15)	20.17 (C–18)	21.28 (C–17)	24.08 (C–19)
24.49 (C–3)	26.29 (C–4)	28.25 (C–16)	28.96 (C–5)
33.10 (C–2)	39.20 (C–6)	53.16 (C–14)	55.36 (C–13)
61.82 (C–12)	104.63 (C–11)	106.93 (C–9)	111.53 (C–20)
113.65 (C–23)	118.26 (C–27)	126.23 (C–25)	126.70 (C–24)
137.03 (C–8)	137.48 (C–28)	138.22 (C–26)	153.25 (C–21)
155.16 (C–22)	158.51 (C–10)	165.29 (C–7)	171.96 (C–1)

EA: $C_{42}H_{66}Br_2Cl_2N_6O_4$ • 4 H_2O
Calculated: C: 49.37 % H: 7.30 % Br: 15.64 % Cl: 6.94 % N: 8.22 % O: 12.53 %
Found: C: 49.28 % H: 7.30 % N: 8.41 %

3,4,5-Tris(acetyloxy)benzoic acid
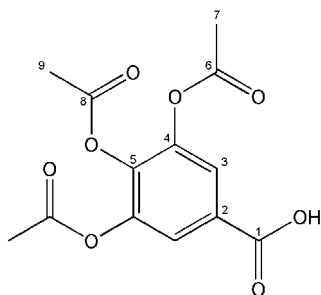
| **Synthesis:** | 0.15 mol (25.5 g) 3,4,5-Trihydroxybenzoic acid are dissolved in a mixture of 60 ml pyridine and 60 ml acetic anhydride. After stirring at room temperature for one hour the reaction mixture is poured into 500 ml water and the pH is acidified using 80 ml concentrated hydrochloric acid. The solution is extracted three times with 500 ml ethyl acetate, dried using anhydrous sodium sulfate and the solvent is evaporated in vacuo. The remaining crude product is washed with petrol ether to yield the final product (**79**). |

Yield: 38.8 g (87 %), $C_{13}H_{12}O_8$, $M_R = 296.23$ g/mol
White powder

^{1}H NMR δ:
[DMSO-d$_6$]

2.29 (s, 6H, H–7)   7.74 (s, 2H, H–3)
2.32 (s, 3H, H–9)   13.39 (s, 1H, COOH)

^{13}C NMR δ:
[DMSO-d$_6$]

19.97 (C–9)	20.50 (C–7)	122.06 (C–3)	129.07 (C–2)
138.42 (C–5)	143.36 (C–4)	165.51 (C–1)	167.04 (C–8)
168.12 (C–6)			

Melting Point: 172 °C, lit.[121] 163 °C

EA:

| Calculated: | C: 52.71 % | H: 4.08 % | O: 43.21 % |
| Found: | C: 52.34 % | H: 4.37 % | |

Ethyl 6-((4-benzyloxy-3,5-dihydroxybenzoyl)amino)hexanoate
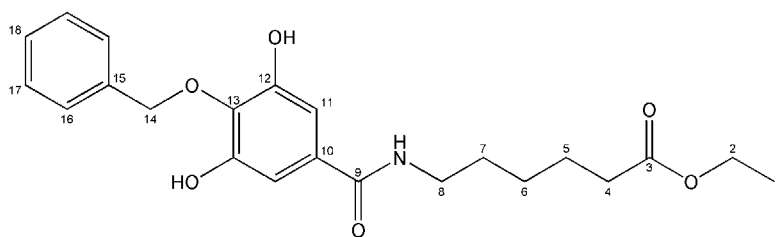
Synthesis: 30.0 mmol (8.89 g) 3,4,5-Tris(acetyloxy)benzoic acid (**79**) and 30.0 mmol (5.88 g) ethyl 6-aminohexanoate hydrochloride are reacted following the standard procedure as described before. The resulting solution is extended to 100 ml with dichloromethane, washed with water, followed by a saturated solution of sodium hydrogen carbonate and dried using anhydrous sodium sulfate. Evaporation in vacuo yields a crude oil that is dissolved in 100 ml anydrous acetone. 60.0 mmol (6.9 ml) Benzyl chloride, 90.0 mmol (12.4 g) potassium carbonate and 9.0 mmol (1.5 g) potassium iodide are added and the reaction mixture is heated to reflux for 18 hours. Subsequent removal of the inorganic salts by suction filtration and evaporation in vacuo yields an oily residue that is washed with n-hexane to remove excess benzyl chloride. 30.0 mmol (4.1 g) Potassium carbonate in 40 ml of water are added to a solution of the residue in a mixture of 200 ml ethyl acetate and 50 ml methanol. After refluxing for one hour and washing with 150 ml water containing 5 ml concentrated hydrochloric acid the reaction mixture is subjected to flash column chromatography using ethyl acetate. Solvent removal in vacuo yields a crude product that is recrystallized from chloroform and n-pentane to yield the final product **80** as a white solid.

Yield: 7.47 g (62 %), $C_{22}H_{27}NO_6$, $M_R = 401.46$ g/mol
White powder

¹H NMR δ: 1.15 (t, 3H, $J = 7.1$ Hz, H–1) 5.00 (s, 2H, H–14)
[DMSO-d_6] 1.27 (app. quint, 2H, $J = 7.7$ Hz, H–6) 6.78 (s, 2H, H–11)
1.46 (app. quint, 2H, $J = 7.3$ Hz, H–7) 7.28 (tt, 1H, $J = 1.4\ 7.4$ Hz, H–18)
1.53 (app. quint, 2H, $J = 7.5$ Hz, H–5) 7.33 (tt, 2H, $J = 1.4\ 6.6$ Hz, H–17)
2.26 (t, 2H, $J = 7.4$ Hz, H–4) 7.50 (app. d, 2H, $J = 6.9$ Hz, H–16)
3.15 (app. q, 2H, $J = 6.5$ Hz, H–8) 8.09 (t, 1H, $J = 5.5$ Hz, NH)
4.03 (q, 2H, $J = 7.0$ Hz, H–2) 9.24 (s, 2H, OH)

¹³C NMR δ: 14.25 (C–1) 24.36 (C–5) 26.03 (C–6) 28.91 (C–7)
[DMSO-d_6] 33.63 (C–4) 39.01 (C–8) 59.77 (C–2) 73.21 (C–14)
106.95 (C–11) 127.79 (C–18) 128.11 (C–17) 128.31 (C–16)
130.38 (C–10) 136.57 (C–13) 138.04 (C–15) 150.54 (C–12)
166.26 (C–9) 172.97 (C–3)

Melting Point: 119 °C

EA: Calculated: C: 65.82 % H: 6.78 % N: 3.49 % O: 23.91 %
Found:

Ethyl 6-((4-benzyloxy-3,5-bis-(2-bromoethoxy)benzoyl)amino)hexanoate

Synthesis: 15.0 mmol (6.02 g) Ethyl 6-((4-benzyloxy-3,5-dihydroxybenzoyl)amino)hexanoate (**80**), 150.0 mmol (20.73 g) potassium carbonate and 3.8 mmol (1.00 g) 18-crown-6 are suspended in 120 ml 1,2-dibromoethane and heated to 80 °C for 36 hours while stirring. Subsequent removal of the inorganic salts by suction filtration, washing with dichloromethane and evaporation in vacuo yields a crude product that is subjected to column chromatography using petrol ether and ethyl acetate in a ratio of 1:2. The final product **81** is recovered from the first fractions as a white solid.

Yield: 8.33 g (90 %), $C_{26}H_{33}Br_2NO_6$, $M_R = 615.36$ g/mol
White powder

^{1}H NMR δ:
[DMSO-d_6]

1.15 (t, 3H, $J = 7.3$ Hz, H–1)
1.30 (app. quint, 2H, $J = 7.7$ Hz, H–6)
1.51 (app. quint, 2H, $J = 7.6$ Hz, H–7)
1.55 (app. quint, 2H, $J = 7.6$ Hz, H–5)
2.27 (t, 2H, $J = 7.4$ Hz, H–4)
3.23 (app. q, 2H, $J = 6.6$ Hz, H–8)
3.84 (t, 4H, $J = 5.4$ Hz, H–20)
4.03 (q, 2H, $J = 7.2$ Hz, H–2)

4.37 (t, 4H, $J = 5.4$ Hz, H–19)
5.07 (s, 2H, H–14)
7.18 (s, 2H, H–11)
7.30 (tt, 1H, $J = 1.6\ 7.3$ Hz, H–18)
7.36 (tt, 2H, $J = 1.3\ 7.0$ Hz, H–17)
7.53 (m, 2H, H–16)
8.35 (t, 1H, $J = 5.7$ Hz, NH)

^{13}C NMR δ:
[DMSO-d_6]

14.24 (C–1)	24.36 (C–5)	26.07 (C–6)	28.99 (C–7)
31.64 (C–20)	33.58 (C–4)	39.21 (C–8)	59.76 (C–2)
68.97 (C–19)	74.35 (C–14)	106.59 (C–11)	128.00 (C–18)
128.23 (C–17)	128.51 (C–16)	130.19 (C–10)	137.67 (C–13)
139.27 (C–15)	151.68 (C–12)	165.32 (C–9)	172.94 (C–3)

Melting Point: 89 °C

EA:

Calculated:	C: 50.75 %	H: 5.41 %	Br: 25.97 %	N: 2.28 %	O: 15.60 %
Found:	C: 50.69 %	H: 5.20 %		N: 2.37 %	

2-(5-(((6-Ethoxy-6-oxohexyl)amino)carbonyl)-2-(2-bromoethoxy)-3-((2-triethylammonio)-ethoxy)phenoxy)-*N,N,N*-triethylethanaminium dibromide

Synthesis: 10.0 mmol (6.15 g) Ethyl 6-((4-benzyloxy-3,5-bis-(2-bromoethoxy)benzoyl)amino)-hexanoate (**81**) are heated to 60 °C for 24 hours in a solution of 100.0 mmol (14.0 ml) triethyl amine and 100 ml anhydrous nitromethane. After cooling to room temperature the solvent and excess amine are thoroughly evaporated in vacuo to allow the deprotection of the intermediate. Hydrogenolysis is carried out using Pd/C (0.8 g) and hydrogen at balloon pressure in anhydrous methanol for 6 hours. Subsequently the catalyst is filtered off and the reaction mixture is evaporated in vacuo. 150.0 mmol (20.73 g) potassium carbonate and 3.8 mmol (1.00 g) 18-crown-6 are added to the remaining oil and the reaction apparatus is protected by argon, followed by the addition of 60 ml 1,2-dibromoethane and 60 ml anhydrous acetonitrile. The suspension is heated to 80 °C for 36 hours and the inorganic salts are removed afterwards. Evaporation of the acetonitrile yields a suspension that is diluted by 50 ml ethyl acetate and the precipitate is recovered by suction filtration. Washing with ethyl acetate and drying in vacuo yields **82** as a white solid that is lyophilized from water for analytical purposes.

Yield: 4.20 g (50 %), $C_{33}H_{60}Br_3N_3O_6$, $M_R = 834.56$ g/mol
White powder, hygroscopic

^{1}H NMR δ:
[DMSO-*d$_6$*]

1.16 (t, 3H, *J* = 7.1 Hz, H–1)
1.24 (t, 18H, *J* = 7.1 Hz, H–17)
1.30 (app. quint, 2H, *J* = 7.6 Hz, H–6)
1.54 (app. quint, 2H, *J* = 7.3 Hz, H–7)
1.54 (app. quint, 2H, *J* = 7.6 Hz, H–5)
2.27 (t, 2H, *J* = 7.4 Hz, H–4)
3.25 (app. q, 2H, *J* = 6.6 Hz, H–8)
3.42 (q, 12H, *J* = 7.2 Hz, H–16)

3.71 (t, 2H, *J* = 6.2 Hz, H–19)
3.74 (t, 4H, *J* = 4.9 Hz, H–15)
4.03 (q, 2H, *J* = 7.2 Hz, H–2)
4.23 (t, 2H, *J* = 6.0 Hz, H–18)
4.50 (t, 4H, *J* = 4.7 Hz, H–14)
7.42 (s, 2H, H–11)
8.62 (t, 1H, *J* = 5.8 Hz, NH)

^{13}C NMR δ:
[DMSO-*d$_6$*]

7.55 (C–17)	14.26 (C–1)	24.35 (C–5)	26.05 (C–6)
29.03 (C–7)	31.93 (C–19)	33.60 (C–4)	39.13 (C–8)
53.18 (C–16)	55.53 (C–15)	59.77 (C–2)	62.57 (C–14)
72.70 (C–18)	107.02 (C–11)	130.49 (C–10)	138.42 (C–13)
150.98 (C–12)	165.17 (C–9)	172.97 (C–3)	

EA:
$C_{33}H_{60}Br_3N_3O_6 \cdot H_2O$
Calculated: C: 46.49 % H: 7.33 % Br: 28.12 % N: 4.93 % O: 13.14 %
Found: C: 46.37 % H: 7.40 % N: 4.91 %

2-(5-(((6-Ethoxy-6-oxohexyl)amino)carbonyl)-2,3-bis((2-triethylammonio)ethoxy)phenoxy)-N,N,N-triethylethanaminium tribromide

Synthesis:	2.0 mmol (1.67 g) 2-(5-(((6-Ethoxy-6-oxohexyl)amino)carbonyl)-2-(2-bromoethoxy)-3-((2-triethylammonio)ethoxy)phenoxy)-N,N,N-triethylethanaminium dibromide (**82**) are suspended in a mixture of 36.0 mmol (5.0 ml) triethyl amine and 20 ml anhydrous acetonitrile. The reaction mixture is heated to 100 °C for 48 hours by means of a sealed bomb. At first the educt dissolves as the temperature raises, but soon the final product **83** precipitates. After cooling to room temperature the white precipitate is collected by suction filtration, washed once with cooled acetonitrile and dried in vacuo.

Yield: 1.30 g (69 %), $C_{39}H_{75}Br_3N_4O_6$, $M_R = 935.76$ g/mol
White powder, hygroscopic

^{1}H NMR δ:
[DMSO-d_6]

1.16 (t, 3H, J = 7.1 Hz, H–1)	3.47 (q, 6H, J = 7.3 Hz, H–20)
1.23 (t, 9H, J = 7.3 Hz, H–21)	3.61 (t, 2H, J = 4.9 Hz, H–19)
1.25 (t, 18H, J = 7.3 Hz, H–17)	3.73 (t, 4H, J = 5.5 Hz, H–15)
1.30 (app. quint, 2H, J = 7.9 Hz, H–6)	4.03 (q, 2H, J = 7.2 Hz, H–2)
1.51-1.59 (m, 4H, H–5,7)	4.26 (t, 2H, J = 4.7 Hz, H–18)
2.27 (t, 2H, J = 7.4 Hz, H–4)	4.55 (t, 4H, J = 5.4 Hz, H–14)
3.25 (app. q, 2H, J = 6.7 Hz, H–8)	7.48 (s, 2H, H–11)
3.45 (q, 12H, J = 7.3 Hz, H–16)	8.71 (t, 1H, J = 5.7 Hz, NH)

^{13}C NMR δ:
[DMSO-d_6]

7.57 (C–17)	7.59 (C–21)	14.26 (C–1)	24.34 (C–5)
26.05 (C–6)	28.99 (C–7)	33.59 (C–4)	39.13 (C–8)
53.20 (C–16,20)	55.06 (C–15)	55.83 (C–19)	59.76 (C–2)
62.19 (C–14)	65.94 (C–18)	106.72 (C–11)	131.10 (C–10)
137.45 (C–13)	150.97 (C–12)	165.05 (C–9)	172.96 (C–3)

EA: $C_{39}H_{75}Br_3N_4O_6$ • H_2O
Calculated: C: 49.11 % H: 8.14 % Br: 25.13 % N: 5.87 % O: 11.74 %
Found: C: 48.90 % H: 8.16 % N: 5.93 %

N,N,N-Triethyl-2-(5-(((6-hydrazino-6-oxohexyl)amino)carbonyl)-2,3-bis((2-triethylammonio)-ethoxy)phenoxy)ethanaminium tribromide
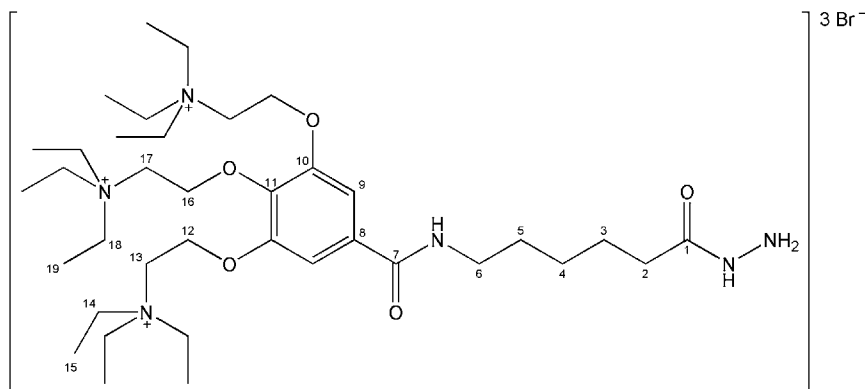
Synthesis: 1.0 mmol   (0.94 g)   2-(5-(((6-Ethoxy-6-oxohexyl)amino)carbonyl)-2,3-bis((2-triethyl-ammonio)ethoxy)phenoxy)-N,N,N-triethylethanaminium tribromide (**83**) are dissolved in a mixture of 51.4 mmol hydrazine (2.5 ml hydrazine hydrate, 100 %) and 20 ml absolute ethanol and the solution is heated to 80 °C for 72 hours in a sealed bomb. After cooling to room temperature 80 ml absolute ethanol are added and the solution is evaporated in vacuo. The remaining residue is taken up in 10 ml absolute ethanol and poured into 300 ml ethyl acetate while stirring to yield the final product **84** that is recovered by suction filtration. For analytical purposes the precipitate is lyophilized from 20 ml of water to remove traces of ethyl acetate.

Yield: 0.84 g (91 %), $C_{37}H_{73}Br_3N_6O_5$, $M_R = 921.74$ g/mol
White powder, very hygroscopic

^{1}H NMR δ:
[DMSO-d_6]

1.23 (t, 9H, $J = 7.2$ Hz, H–19)	3.61 (t, 2H, $J = 4.9$ Hz, H–17)
1.25 (app. t, 20H, $J = 6.9$ Hz, H–4,15)	3.72 (t, 4H, $J = 5.5$ Hz, H–13)
1.51 (app. quint, 2H, $J = 7.6$ Hz, H–5)	4.11 (bs, 2H, NH$_2$)
1.54 (app. quint, 2H, $J = 7.6$ Hz, H–3)	4.26 (t, 2H, $J = 4.9$ Hz, H–16)
2.01 (t, 2H, $J = 7.4$ Hz, H–2)	4.55 (t, 4H, $J = 5.4$ Hz, H–12)
3.25 (app. q, 2H, $J = 6.7$ Hz, H–6)	7.47 (s, 2H, H–9)
3.45 (q, 12H, $J = 7.0$ Hz, H–14)	8.68 (t, 1H, $J = 5.8$ Hz, NHCH$_2$)
3.47 (q, 6H, $J = 7.3$ Hz, H–18)	8.90 (s, 1H, NHNH$_2$)

^{13}C NMR δ:
[DMSO-d_6]

7.57 (C–15)	7.59 (C–19)	25.14 (C–3)	26.32 (C–4)
29.10 (C–5)	33.52 (C–2)	39.26 (C–6)	53.20 (C–14,18)
55.07 (C–13)	55.83 (C–17)	62.18 (C–12)	65.94 (C–16)
106.70 (C–9)	131.14 (C–8)	137.43 (C–11)	150.98 (C–10)
165.07 (C–7)	171.66 (C–1)		

EA: Calculated: C: 48.21 %   H: 7.98 %   Br: 26.01 %   N: 9.12 %   O: 8.68 %
Found:

N,N,N-Triethyl-2-(5-(((6-(2-(1,2,3,4-tetrahydroacridin-9-yl)hydrazino)-6-oxohexyl)amino)-carbonyl)-2,3-bis((2-triethylammonio)ethoxy)phenoxy)ethanaminium tribromide HCl
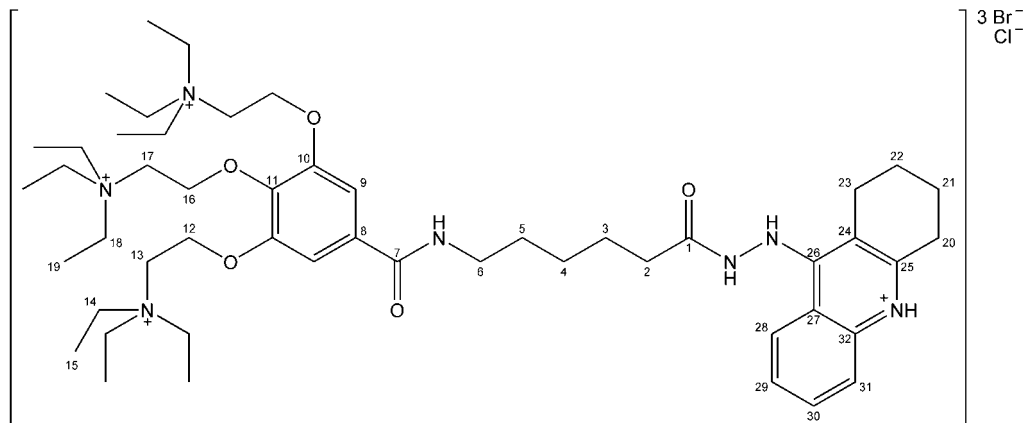
Synthesis:	0.4 mmol (0.37 g) *N,N,N*-Triethyl-2-(5-(((6-hydrazino-6-oxohexyl)amino)carbonyl)-2,3-bis((2-triethylammonio)ethoxy)phenoxy)ethanaminium tribromide (**84**) and 0.4 mmol (0.09 g) 9-chloro-1,2,3,4-tetrahydroacridine (**1**) are dissolved in 10 ml absolute ethanol and heated to 140 °C for 24 hours by means of a sealed bomb. After cooling to room temperature the reaction mixture is poured into 300 ml ethyl acetate while stirring to yield the final product **85** that is recovered by suction filtration. For analytical purposes the precipitate is lyophilized from 10 ml of 0.1 M hydrochloric acid to remove traces of ethyl acetate.

Yield: 0.45 g (98 %), $C_{50}H_{85}Br_3ClN_7O_5$, $M_R = 1139.43$ g/mol
Yellow powder, hygroscopic

^{1}H NMR δ:
[DMSO-d_6]

1.23 (t, 9H, $J = 7.0$ Hz, H–19)	3.75 (t, 4H, $J = 5.5$ Hz, H–13)
1.24 (t, 18H, $J = 7.3$ Hz, H–15)	4.27 (t, 2H, $J = 4.7$ Hz, H–16)
1.30 (app. quint, 2H, $J = 7.4$ Hz, H–4)	4.58 (t, 4H, $J = 5.4$ Hz, H–12)
1.52-1.61 (m, 4H, H–3,5)	7.60 (s, 2H, H–9)
1.81 (app. bs, 4H, H–21,22)	7.60 (ddd, 1H, $J = 1.0\ 5.4\ 7.6$ Hz, H–29)
2.29 (t, 2H, $J = 7.3$ Hz, H–2)	7.87 (ddd, 1H, $J = 0.7\ 7.1\ 8.4$ Hz, H–30)
2.70 (app. bs, 2H, H–23)	8.05 (app. dd, 1H, $J = 0.7\ 8.5$ Hz, H–28)
3.09 (app. bs, 2H, H–20)	8.70 (app. d, 1H, $J = 8.8$ Hz, H–31)
3.24 (app. q, 2H, $J = 6.6$ Hz, H–6)	9.06 (t, 1H, $J = 5.7$ Hz, NHCH$_2$)
3.46 (q, 12H, $J = 7.2$ Hz, H–14)	9.65 (s, 1H, CONHNH)
3.48 (q, 6H, $J = 7.1$ Hz, H–18)	11.09 (s, 1H, CONHNH)
3.63 (t, 2H, $J = 4.7$ Hz, H–17)	14.46 (s, 1H, N$^+$H)

^{13}C NMR δ:
[DMSO-d_6]

7.60 (C–15)	7.62 (C–19)	20.26 (C–22)	21.40 (C–21)
24.18 (C–23)	24.55 (C–3)	26.31 (C–4)	28.23 (C–20)
28.98 (C–5)	33.08 (C–2)	39.20 (C–6)	53.22 (C–14,18)
55.10 (C–13)	55.89 (C–17)	62.31 (C–12)	66.01 (C–16)
106.92 (C–9)	111.20 (C–24)	115.09 (C–27)	119.39 (C–28)
124.26 (C–31)	125.89 (C–29)	131.02 (C–8)	133.04 (C–30)
137.39 (C–32)	137.47 (C–11)	150.99 (C–10)	152.64 (C–25)
155.35 (C–26)	164.98 (C–7)	171.89 (C–1)	

EA: Calculated: C: 52.71 % H: 7.52 % Br: 21.04 % Cl: 3.11 % N: 8.60 % O: 7.02 %
Found:

2-(5-(((6-(2-(6-Chloro-1,2,3,4-tetrahydroacridin-9-yl)hydrazino)-6-oxohexyl)amino)carbonyl)-2,3-bis((2-triethylammonio)ethoxy)phenoxy)-*N,N,N*-triethylethanaminium tribromide HCl
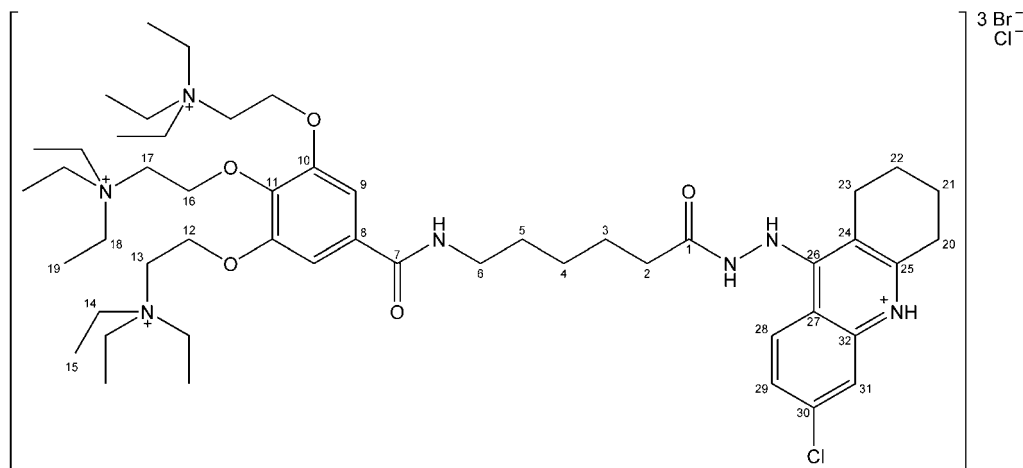
Synthesis:	0.4 mmol (0.37 g) *N,N,N*-Triethyl-2-(5-(((6-hydrazino-6-oxohexyl)amino)carbonyl)-2,3-bis((2-triethylammonio)ethoxy)phenoxy)ethanaminium tribromide (**84**) and 0.4 mmol (0.10 g) 6,9-dichloro-1,2,3,4-tetrahydroacridine (**2**) are dissolved in 10 ml absolute ethanol and heated to 140 °C for 24 hours by means of a sealed bomb. After cooling to room temperature the reaction mixture is poured into 300 ml ethyl acetate while stirring to yield the final product **86** that is recovered by suction filtration. For analytical purposes the precipitate is lyophilized from 10 ml of 0.1 M hydrochloric acid to remove traces of ethyl acetate.

Yield: 0.46 g (98 %), $C_{50}H_{84}Br_3Cl_2N_7O_5$, $M_R = 1173.88$ g/mol
Yellow powder, hygroscopic

^{1}H NMR δ:
[DMSO-d_6]

1.23 (t, 9H, $J = 7.3$ Hz, H–19)	3.74 (t, 4H, $J = 5.5$ Hz, H–13)
1.24 (t, 18H, $J = 7.1$ Hz, H–15)	4.27 (t, 2H, $J = 4.6$ Hz, H–16)
1.30 (app. quint, 2H, $J = 7.9$ Hz, H–4)	4.57 (t, 4H, $J = 5.2$ Hz, H–12)
1.52-1.62 (m, 4H, H–3,5)	7.59 (s, 2H, H–9)
1.81 (app. bs, 4H, H–21,22)	7.67 (dd, 1H, $J = 2.2$ 9.1 Hz, H–29)
2.30 (t, 2H, $J = 7.4$ Hz, H–2)	8.14 (d, 1H, $J = 2.2$ Hz, H–31)
2.66 (app. bs, 2H, H–23)	8.74 (d, 1H, $J = 9.5$ Hz, H–28)
3.07 (app. bs, 2H, H–20)	9.03 (t, 1H, $J = 5.7$ Hz, N<u>H</u>CH$_2$)
3.24 (app. q, 2H, $J = 6.5$ Hz, H–6)	9.77 (s, 1H, CON<u>H</u>NH)
3.46 (q, 12H, $J = 7.0$ Hz, H–14)	11.13 (s, 1H, CONHN<u>H</u>)
3.48 (q, 6H, $J = 7.1$ Hz, H–18)	14.64 (s, 1H, N$^+$H)
3.63 (t, 2H, $J = 4.8$ Hz, H–17)	

^{13}C NMR δ:
[DMSO-d_6]

7.59 (C–15)	7.61 (C–19)	20.16 (C–22)	21.26 (C–21)
24.06 (C–23)	24.47 (C–3)	26.29 (C–4)	28.26 (C–20)
28.97 (C–5)	33.08 (C–2)	39.20 (C–6)	53.21 (C–14,18)
55.09 (C–13)	55.88 (C–17)	62.29 (C–12)	65.99 (C–16)
106.90 (C–9)	111.57 (C–24)	113.65 (C–27)	118.27 (C–31)
126.27 (C–29)	126.67 (C–28)	131.02 (C–8)	137.46 (C–11)
137.51 (C–32)	138.19 (C–30)	150.98 (C–10)	153.27 (C–25)
155.20 (C–26)	164.98 (C–7)	171.95 (C–1)	

EA: Calculated: C: 5.16 % H: 7.21 % Br: 20.42 % Cl: 6.04 % N: 8.35 % O: 6.81 %
Found:

4-((3,4,5-Trimethoxybenzoyl)amino)butanoic acid
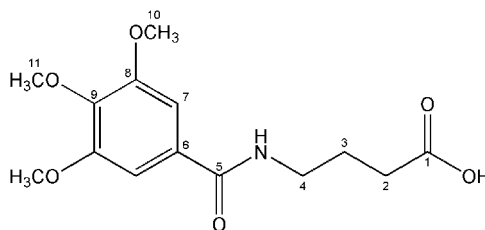
Synthesis: 10 ml 0.1 M sulfuric acid is added to a solution of 10.0 mmol (3.25 g) ethyl 4-((3,4,5-trimethoxybenzoyl)amino)butanoate in 10 ml of acetone and the reaction mixture is heated to reflux. The progress of hydrolysis is followed by TLC and after completion the solvent is evaporated in vacuo. The residue is then taken up in 20 ml ethyl acetate to be dried over anhydrous sodium sulfate. Final evaporation yields a crude product that is recrystallized from ethyl acetate for further purification.

Yield: 2.08 g (64 %), $C_{14}H_{19}NO_6$, $M_R = 297.31$ g/mol
White crystals

^{1}H NMR δ: **[DMSO-d_6]**

1.75 (app. quint, 2H, $J = 7.3$ Hz, H–3)	3.81 (s, 6H, H–10)
2.26 (t, 2H, $J = 7.4$ Hz, H–2)	7.16 (s, 2H, H–7)
3.26 (app. q, 2H, $J = 6.5$ Hz, H–4)	8.39 (t, 1H, $J = 5.5$ Hz, NH)
3.69 (s, 3H, H–11)	12.02 (bs, 1H, COOH)

^{13}C NMR δ: **[DMSO-d_6]**

25.50 (C–3)	32.04 (C–2)	39.60 (C–4)	56.88 (C–10)
60.92 (C–11)	105.67 (C–7)	130.63 (C–6)	140.77 (C–9)
153.41 (C–8)	166.45 (C–5)	175.10 (C–1)	

Melting Point: 137 °C

4-((3-(3,4,5-Trimethoxyphenyl)propanoyl)amino)butanoic acid
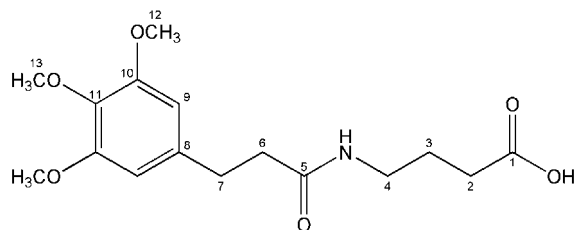
Synthesis: 10 ml 0.1 M sulfuric acid is added to a solution of 10.0 mmol (3.53 g) ethyl 4-((3-(3,4,5-trimethoxyphenyl)propanoyl)amino)butanoate in 10 ml of acetone and the reaction mixture is heated to reflux. The progress of hydrolysis is followed by TLC and after completion the solvent is evaporated in vacuo. The residue is then taken up in 20 ml ethyl acetate to be dried over anhydrous sodium sulfate. Final evaporation yields a crude product that is recrystallized from ethyl acetate for further purification.

Yield: 2.76 g (85 %), $C_{16}H_{23}NO_6$, $M_R = 325.36$ g/mol
White crystals

^{1}H NMR δ: 1.58 (app. quint, 2H, $J = 7.2$ Hz, H–3)   3.60 (s, 3H, H–13)
[DMSO-d_6]   2.17 (t, 2H, $J = 7.4$ Hz, H–2)   3.73 (s, 6H, H–12)
2.34 (t, 2H, $J = 7.7$ Hz, H–6)   6.48 (s, 2H, H–9)
2.74 (t, 2H, $J = 7.7$ Hz, H–7)   7.79 (t, 1H, $J = 5.5$ Hz, NH)
3.04 (app. q, 2H, $J = 6.5$ Hz, H–4)   11.98 (bs, 1H, COOH)

^{13}C NMR δ: 24.80 (C–3)   31.18 (C–2)   31.60 (C–7)   37.22 (C–6)
[DMSO-d_6]   38.01 (C–4)   55.89 (C–12)   60.06 (C–13)   105.60 (C–9)
135.85 (C–8)   137.19 (C–11)   152.82 (C–10)   171.44 (C–5)
174.30 (C–1)

Melting Point: 93 °C

1-(3,4,5-Trimethoxybenzoyl)pyrrolidin-2-one
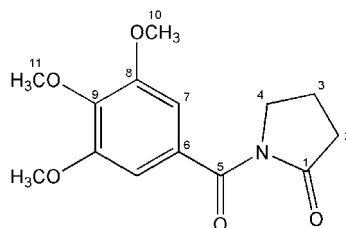
Synthesis: 2.0 mmol (0.59 g) 4-((3,4,5-Trimethoxybenzoyl)amino)butanoic acid and 2.0 mmol (0.2 ml) oxalyl chloride are dissolved in 20 ml anhydrous toluene and heated to reflux for 7 hours. Subsequently, 20 ml water and 25 ml ethyl acetate are added and the mixture is washed twice with 25 ml of a saturated solution of sodium hydrogen carbonate. The organic layer is then dried using anhydrous sodium sulfate and evaporated in vacuo yielding a crude product that is recrystallized from ethyl acetate and n-hexane.

Yield: 0.30 g (53 %), $C_{14}H_{17}NO_5$, $M_R = 279.29$ g/mol
Brown crystals

^{1}H NMR δ: 2.03 (app. quint, 2H, $J = 7.5$ Hz, H–3)   3.77 (s, 6H, H–10)
[DMSO-d_6] 2.53 (t, 2H, $J = 7.9$ Hz, H–2)   3.79 (t, 2H, $J = 7.1$ Hz, H–4)
3.72 (s, 3H, H–11)   6.87 (s, 2H, H–7)

^{13}C NMR δ: 17.27 (C–3)   32.90 (C–2)   46.50 (C–4)   56.27 (C–10)
[DMSO-d_6] 60.23 (C–11)   106.83 (C–7)   130.12 (C–6)   140.52 (C–9)
152.27 (C–8)   169.47 (C–5)   174.69 (C–1)

Melting Point: 103 °C

1-(3-(3,4,5-Trimethoxyphenyl)propanoyl)pyrrolidin-2-one
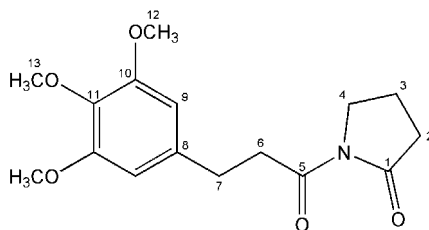
Synthesis: 2.0 mmol (0.65 g) 4-((3-(3,4,5-Trimethoxyphenyl)propanoyl)amino)butanoic acid and 2.0 mmol (0.2 ml) oxalyl chloride are dissolved in 20 ml anhydrous toluene and heated to reflux for 7 hours. Subsequently, 20 ml water and 25 ml ethyl acetate are added and the mixture is washed twice with 25 ml of a saturated solution of sodium hydrogen carbonate. The organic layer is then dried using anhydrous sodium sulfate and evaporated in vacuo yielding a crude product that is recrystallized from ethyl acetate and n-hexane.

Yield: 0.31 g (50 %), $C_{16}H_{21}NO_5$, $M_R = 307.35$ g/mol
Brown crystals

^{1}H NMR δ:
[DMSO-d_6]

1.92 (app. quint, 2H, $J = 7.6$ Hz, H–3)	3.61 (s, 3H, H–13)
2.53 (t, 2H, $J = 8.1$ Hz, H–2)	3.66 (t, 2H, $J = 7.3$ Hz, H–4)
2.77 (t, 2H, $J = 7.7$ Hz, H–6)	3.73 (s, 6H, H–12)
3.08 (t, 2H, $J = 7.9$ Hz, H–7)	6.53 (s, 2H, H–9)

^{13}C NMR δ:
[DMSO-d_6]

16.86 (C–3)	30.33 (C–2)	33.27 (C–7)	38.33 (C–6)
45.33 (C–4)	55.93 (C–12)	60.07 (C–13)	105.82 (C–9)
135.95 (C–8)	136.91 (C–11)	152.87 (C–10)	172.65 (C–5)
175.71 (C–1)			

Melting Point: 117 °C

Methyl 8-(2-bromoethoxy)-2,3-dihydrobenzo[*b*][1,4]dioxine-6-carboxylate
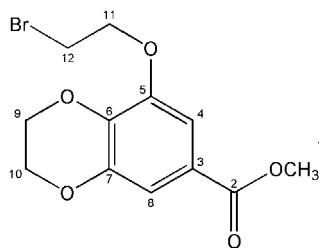
Synthesis: 50.0 mmol (11.3 g) Methyl 3,4,5-trihydroxybenzoate, 150.0 mmol (20.73 g) potassium carbonate and 3.8 mmol (1.00 g) 18-crown-6 are suspended in 120 ml 1,2-dibromoethane and heated to 80 °C for 36 hours while stirring. Removal of the inorganic salts by suction filtration from the hot reaction mixture and subsequent cooling to room temperature precipitates **91** that is recovered again by suction filtration.

Yield: 12.7 g (80 %), $C_{12}H_{13}BrO_5$, $M_R = 317.14$ g/mol
White powder

^{1}H NMR δ: 3.78 (ddd, 2H, $J = 1.0\ 4.9\ 5.4$ Hz, H–12)   4.32 (ddd, 2H, $J = 1.0\ 2.4\ 6.1$ Hz, H–9)
[DMSO-d_6] 3.79 (s, 3H, H–1)   4.34 (ddd, 2H, $J = 1.3\ 4.9\ 5.5$ Hz, H–11)
4.27 (ddd, 2H, $J = 1.3\ 3.0\ 5.7$ Hz, H–10)   7.11 (app. s, 2H, H–4,8)

^{13}C NMR δ: 31.25 (C–12)   52.17 (C–1)   63.94 (C–10)   64.35 (C–9)
[DMSO-d_6] 69.16 (C–11)   107.12 (C–8)   111.88 (C–4)   121.32 (C–3)
138.15 (C–6)   143.85 (C–7)   147.25 (C–5)   165.76 (C–2)

Melting Point: 149 °C

List of Figures

List of Schemes

List of Tables

8 Bibliography

1. Selkoe, D. J. Alzheimer's disease: genes, proteins, and therapy. *Physiol. Rev.* **2001**, *81*, 741–766.

2. Jarrett, J. T.; Berger, E. P.; Lansbury, P. T. The carboxy terminus of the β amyloid protein is critical for the seeding of amyloid formation: implications for the pathogenesis of Alzheimer's disease. *Biochemistry* **1993**, *32*, 4693–4697.

3. Iwatsubo, T.; Odaka, A.; Suzuki, N.; Mizusawa, H.; Nukina, N.; Ihara, Y. Visualization of Aβ42(43) and Aβ40 in senile plaques with end-specific Aβ monoclonals: evidence that an initially deposited species is Aβ42(43). *Neuron* **1994**, *13*, 45–53.

4. Lemere, C. A.; Blusztajn, J. K.; Yamaguchi, H.; Wisniewski, T.; Saido, T. C.; Selkoe, D. J. Sequence of deposition of heterogeneous amyloid β-peptides and APO E in Down syndrome: implications for initial events in amyloid plaque formation. *Neurobiol. Dis.* **1996**, *3*, 16–32.

5. Kosik, K. S.; Joachim, C. L.; Selkoe, D. J. Microtubule-associated protein tau (τ) is a major antigenic component of paired helical filaments in Alzheimer disease. *Proc. Natl. Acad. Sci. USA* **1986**, *83*, 4044–4048.

6. Alonso, A. D.; Zaidi, T.; Novak, M.; Barra, H. S.; Grundke-Iqbal, I.; Iqbal, K. Interaction of tau isoforms with Alzheimer's disease abnormally hyperphosphorylated tau and in vitro phosphorylation into the disease-like protein. *J. Biol. Chem.* **2001**, *276*, 37967–37973.

7. Avila, J.; Lucas, J. J.; Perez, M.; Hernandez, F. Role of tau protein in both physiological and pathological conditions. *Physiol. Rev.* **2004**, *84*, 361–384.

8. Barcikowska, M. New therapeutic approaches in Alzheimer's disease. *Folia Neuropathol.* **2004**, *42*, 251–255.

9. Laskowski, M.; Kato, I. Protein inhibitors of proteinases. *Annu. Rev. Biochem.* **1980**, *49*, 593–626.

10. Bhisetti, G. R.; Saunders, J. O.; Murcko, M. A.; Lepre, C. A.; Britt, J. H., S. D.and Come; Deninger, D. D.; Wang, T. Preparation of β-carbolines and other inhibitors of BACE-1 aspartic proteinase useful against Alzheimer's and other BACE-mediated diseases. Patent WO2002088101 *Chem. Abstr.* **2002**, *137*, 353007.

11. Ghosh, A. K.; Bilcer, G.; Harwood, C.; Kawahama, R.; Shin, D.; Hussain, K. A.; Hong, L.; Loy, J. A.; Nguyen, C.; Koelsch, G.; Ermolieff, J.; Tang, J. Structure-based design: potent inhibitors of human brain memapsin 2 (beta-secretase). *J. Med. Chem.* **2001**, *44*, 2865–2868.

12. Miyamoto, M.; Matsui, J.; Fukumoto, H.; Tarui, N. Preparation of 2-[2-amino- or 2-(N-heterocyclyl)ethyl]-6-(4-biphenylylmethoxy)tetralin derivatives as β-secretase inhibitors. Patent WO2001087293 *Chem. Abstr.* **2001**, *135*, 371744.

13. Citron, M. β-secretase as a target for the treatment of Alzheimer's disease. *J. Neurosci. Res.* **2002**, *70*, 373–379.

14. John, V.; Beck, J. P.; Bienkowski, M. J.; Sinha, S.; Heinrikson, R. L. Human β-secretase (BACE) and BACE inhibitors. *J. Med. Chem.* **2003**, *46*, 4625–4630.

15. Steiner, H. Uncovering γ-secretase. *Curr. Alzheimer Res.* **2004**, *1*, 175–181.

16. Kimberly, W. T.; LaVoie, M. J.; Ostaszewski, B. L.; Ye, W.; Wolfe, M. S.; Selkoe, D. J. γ-secretase is a membrane protein complex comprised of presenilin, nicastrin, Aph-1, and Pen-2. *Proc. Natl. Acad. Sci. USA* **2003**, *100*, 6382–6387.

17. Fortini, M. E. γ-secretase-mediated proteolysis in cell-surface-receptor signalling. *Nat. Rev. Mol. Cell Biol.* **2002**, *3*, 673–684.

18. Massoulié, J.; Anselmet, A.; Bon, S.; Krejci, E.; Legay, C.; Morel, N.; Simon, S. The polymorphism of acetylcholinesterase: post-translational processing, quaternary associations and localization. *Chem Biol Interact* **1999**, *119-120*, 29–42.

19. Soreq, H.; Seidman, S. Acetylcholinesterase–new roles for an old actor. *Nat. Rev. Neurosci.* **2001**, *2*, 294–302.

20. Brenner, T.; Hamra-Amitay, Y.; Evron, T.; Boneva, N.; Seidman, S.; Soreq, H. The role of readthrough acetylcholinesterase in the pathophysiology of myasthenia gravis. *FASEB J.* **2003**, *17*, 214–222.

21. Massoulié, J. The origin of the molecular diversity and functional anchoring of cholinesterases. *Neurosignals* **2002**, *11*, 130–143.

22. Silman, I.; Sussman, J. L. Acetylcholinesterase: 'classical' and 'non-classical' functions and pharmacology. *Curr. Opin. Pharmacol.* **2005**, *5*, 293–302.

23. Genever, P. G.; Birch, M. A.; Brown, E.; Skerry, T. M. Osteoblast-derived acetylcholinesterase: a novel mediator of cell-matrix interactions in bone? *Bone* **1999**, *24*, 297–303.

24. Deutsch, V. R.; Pick, M.; Perry, C.; Grisaru, D.; Hemo, Y.; Golan-Hadari, D.; Grant, A.; Eldor, A.; Soreq, H. The stress-associated acetylcholinesterase variant AChE-R is expressed in human CD34(+) hematopoietic progenitors and its C-terminal peptide ARP promotes their proliferation. *Exp. Hematol.* **2002**, *30*, 1153–1161.

25. Inestrosa, N. C.; Alvarez, A.; Pérez, C. A.; Moreno, R. D.; Vicente, M.; Linker, C.; Casanueva, O. I.; Soto, C.; Garrido, J. Acetylcholinesterase accelerates assembly of amyloid β-peptides into Alzheimer's fibrils: possible role of the peripheral site of the enzyme. *Neuron* **1996**, *16*, 881–891.

26. Alvarez, A.; Alarcón, R.; Opazo, C.; Campos, E. O.; Muñoz, F. J.; Calderón, F. H.; Dajas, F.; Gentry, M. K.; Doctor, B. P.; Mello, F. G. D.; Inestrosa, N. C. Stable complexes involving acetylcholinesterase and amyloid-beta peptide change the biochemical properties of the enzyme and increase the neurotoxicity of Alzheimer's fibrils. *J. Neurosci.* **1998**, *18*, 3213–3223.

27. Darvesh, S.; Hopkins, D. A.; Geula, C. Neurobiology of butyrylcholinesterase. *Nat. Rev. Neurosci.* **2003**, *4*, 131–138.

28. Velan, B.; Kronman, C.; Ordentlich, A.; Flashner, Y.; Leitner, M.; Cohen, S.; Shafferman, A. N-glycosylation of human acetylcholinesterase: effects on activity, stability and biosynthesis. *Biochem. J.* **1993**, *296*, 649–656.

29. Lockridge, O.; Adkins, S.; Du, B. N. L. Location of disulfide bonds within the sequence of human serum cholinesterase. *J. Biol. Chem.* **1987**, *262*, 12945–12952.

30. Chatonnet, A.; Lockridge, O. Comparison of butyrylcholinesterase and acetylcholinesterase. *Biochem. J.* **1989**, *260*, 625–634.

31. Nachon, F.; Nicolet, Y.; Viguié, N.; Masson, P.; Fontecilla-Camps, J. C.; Lockridge, O. Engineering of a monomeric and low-glycosylated form of human butyrylcholinesterase: expression, purification, characterization and crystallization. *Eur. J. Biochem.* **2002**, *269*, 630–637.

32. Sussman, J. L.; Harel, M.; Frolow, F.; Oefner, C.; Goldman, A.; Toker, L.; Silman, I. Atomic structure of acetylcholinesterase from *Torpedo californica*: a prototypic acetylcholine-binding protein. *Science* **1991**, *253*, 872–879.

33. PDB ID: 1B41. Kryger, G.; Harel, M.; Giles, K.; Toker, L.; Velan, B.; Lazar, A.; Kronman, C.; Barak, D.; Ariel, N.; Shafferman, A.; Silman, I.; Sussman, J. L. Structures of recombinant native and E202Q mutant human acetylcholinesterase complexed with the snake-venom toxin fasciculin-II. *Acta Crystallogr. D Biol. Crystallogr.* **2000**, *56*, 1385–1394.

34. PDB ID: 1P0I. Nicolet, Y.; Lockridge, O.; Masson, P.; Fontecilla-Camps, J. C.; Nachon, F. Crystal structure of human butyrylcholinesterase and of its complexes with substrate and products. *J. Biol. Chem.* **2003**, *278*, 41141–41147.

35. Tsim, K. W.; Randall, W. R.; Barnard, E. A. An asymmetric form of muscle acetylcholinesterase contains three subunit types and two enzymic activities in one molecule. *Proc. Natl. Acad. Sci. USA* **1988**, *85*, 1262–1266.

36. Holmquist, M. α/β-hydrolase fold enzymes: structures, functions and mechanisms. *Curr. Protein. Pept. Sci.* **2000**, *1*, 209–235.

37. Rosenberry, T. L. Catalysis by acetylcholinesterase: evidence that the rate-limiting step for acylation with certain substrates precedes general acid-base catalysis. *Proc. Natl. Acad. Sci. USA* **1975**, *72*, 3834–3838.

38. Çokuğraş, A. N. Butyrylcholinesterase: Structure and Physiological Importance *Turk. J. Biochem.* **2003**, *28*, 54–61.

39. Ordentlich, A.; Barak, D.; Kronman, C.; Ariel, N.; Segall, Y.; Velan, B.; Shafferman, A. Functional characteristics of the oxyanion hole in human acetylcholinesterase. *J. Biol. Chem.* **1998**, *273*, 19509–19517.

40. Vellom, D. C.; Radić, Z.; Li, Y.; Pickering, N. A.; Camp, S.; Taylor, P. Amino acid residues controlling acetylcholinesterase and butyrylcholinesterase specificity. *Biochemistry* **1993**, *32*, 12–17.

41. Yu, Q.; Holloway, H. W.; Utsuki, T.; Brossi, A.; Greig, N. H. Synthesis of novel phenserine-based-selective inhibitors of butyrylcholinesterase for Alzheimer's disease. *J. Med. Chem.* **1999**, *42*, 1855–1861.

42. Yu, Q.-S.; Zhu, X.; Holloway, H. W.; Whittaker, N. F.; Brossi, A.; Greig, N. H. Anticholinesterase activity of compounds related to geneserine tautomers. N-Oxides and 1,2-oxazines. *J. Med. Chem.* **2002**, *45*, 3684–3691.

43. Erhard, M. H.; Jüngling, A.; Schöneberg, T.; Szinicz, L.; Lösch, U. A homogeneous immunological detection system for soman using the in vitro protection of acetylcholinesterase by a monoclonal antibody. *Arch. Toxicol.* **1993**, *67*, 220–223.

44. Gilson, M. K.; Straatsma, T. P.; McCammon, J. A.; Ripoll, D. R.; Faerman, C. H.; Axelsen, P. H.; Silman, I.; Sussman, J. L. Open "back door" in a molecular dynamics simulation of acetylcholinesterase. *Science* **1994**, *263*, 1276–1278.

45. Alisaraie, L.; Fels, G. Molecular docking study on the "back door" hypothesis for product clearance in acetylcholinesterase. *J. Mol. Model.* **2006**, *12*, 348–354.

46. Bolognesi, M. L.; Andrisano, V.; Bartolini, M.; Banzi, R.; Melchiorre, C. Propidium-based polyamine ligands as potent inhibitors of acetylcholinesterase and acetylcholinesterase-induced amyloid-β aggregation. *J. Med. Chem.* **2005**, *48*, 24–27.

47. Al-Jafari, A. A. The inhibitory effect of the neuromuscular blocking agent, gallamine triethiodide, on camel retina acetylcholinesterase activity. *Toxicol Lett* **1997**, *90*, 45–51.

48. Giacobini, E. Cholinesterase inhibitors: new roles and therapeutic alternatives. *Pharmacol. Res.* **2004**, *50*, 433–440.

49. Muñoz-Torrero, D.; Camps, P. Dimeric and hybrid anti-Alzheimer drug candidates. *Curr. Med. Chem.* **2006**, *13*, 399–422.

50. Camps, P.; Formosa, X.; Muñoz-Torrero, D.; Petrignet, J.; Badia, A.; Clos, M. V. Synthesis and pharmacological evaluation of huprine-tacrine heterodimers: subnanomolar dual binding site acetylcholinesterase inhibitors. *J. Med. Chem.* **2005**, *48*, 1701–1704.

51. Martinez, A.; Dorronsoro, I.; Rubio, L.; Alonso, D.; Fuertes, A.; Morales-Alcelay, S.; Del Monte, M.; Garcia, E.; Usan, P. Dual binding site acetylcholinesterase inhibitors for the treatment of Alzheimer's disease. Patent WO2004032929. *Chem. Abstr.* **2004**, *140*, 357219.

52. Jordis, U.; Fröhlich, J.; Treu, M.; Hirnschall, M.; Czollner, L.; Kälz, B.; Welzig, S. Preparation of galanthamine analogs for pharmaceutical use as acetyl- and butyrylcholinesterase inhibitors. *Chem. Abstr.* **2001**, *135*, 304054.

53. Campiani, G.; Fattorusso, C.; Butini, S.; Gaeta, A.; Agnusdei, M.; Gemma, S.; Persico, M.; Catalanotti, B.; Savini, L.; Nacci, V.; Novellino, E.; Holloway, H. W.; Greig, N. H.; Belinskaya, T.; Fedorko, J. M.; Saxena, A. Development of molecular probes for the identification of extra interaction sites in the mid-gorge and peripheral sites of butyrylcholinesterase (BuChE). Rational design of novel, selective, and highly potent BuChE inhibitors. *J. Med. Chem.* **2005**, *48*, 1919–1929.

54. Potter, A.; Corwin, J.; Lang, J.; Piasecki, M.; Lenox, R.; Newhouse, P. A. Acute effects of the selective cholinergic channel activator (nicotinic agonist) ABT-418 in Alzheimer's disease. *Psychopharmacology* **1999**, *142*, 334–342.

55. Vernier, J. M.; El-Abdellaoui, H.; Holsenback, H.; Cosford, N. D.; Bleicher, L.; Barker, G.; Bontempi, B.; Chavez-Noriega, L.; Menzaghi, F.; Rao, T. S.; Reid, R.; Sacaan, A. I.; Suto, C.; Washburn, M.; Lloyd, G. K.; McDonald, I. A. 4-[[2-(1-Methyl-2-pyrrolidinyl)ethyl]thio]phenol hydrochloride (SIB-1553A): a novel cognitive enhancer with selectivity for neuronal nicotinic acetylcholine receptors. *J. Med. Chem.* **1999**, *42*, 1684–1686.

56. Kem, W. R. The brain α7 nicotinic receptor may be an important therapeutic target for the treatment of Alzheimer's disease: studies with DMXBA (GTS-21). *Behav. Brain Res.* **2000**, *113*, 169–181.

57. Sauerberg, P.; Olesen, P. H.; Nielsen, S.; Treppendahl, S.; Sheardown, M. J.; Honore, T.; Mitch, C. H.; Ward, J. S.; Pike, A. J.; Bymaster, F. P.; Sawyer, B.; Shannon, H. Novel functional M1 selective muscarinic agonists. Synthesis and structure-activity relationships of 3-(1,2,5-thiadiazolyl)-1,2,5,6- tetrahydro-1-methylpyridines. *J. Med. Chem.* **1992**, *35*, 2274–2283.

58. Bymaster, F. P.; Carter, P. A.; Peters, S. C.; Zhang, W.; Ward, J. S.; Mitch, C. H.; Calligaro, D. O.; Whitesitt, C. A.; DeLapp, N.; Shannon, H. E.; Rimvall, K.; Jeppesen, L.; Sheardown, M. J.; Fink-Jensen, A.; Sauerberg, P. Xanomeline compared to other muscarinic agents on stimulation of phosphoinositide hydrolysis in vivo and other cholinomimetic effects. *Brain Res.* **1998**, *795*, 179–190.

59. Messer, W. S.; Rajeswaran, W. G.; Cao, Y.; Zhang, H. J.; El-Assadi, A. A.; Dockery, C.; Liske, J.; O'Brien, J.; Williams, F. E.; Huang, X. P.; Wroblewski, M. E.; Nagy, P. I.; Peseckis, S. M. Design and development of selective muscarinic agonists for the treatment of Alzheimer's disease: characterization of tetrahydropyrimidine derivatives and development of new approaches for improved affinity and selectivity for M_1 receptors. *Pharm. Acta. Helv.* **2000**, *74*, 135–140.

60. Messer, W. S. Cholinergic agonists and the treatment of Alzheimers disease. *Curr. Top. Med. Chem.* **2002**, *2*, 353–358.

61. Wang, H. Y.; Lee, D. H.; D'Andrea, M. R.; Peterson, P. A.; Shank, R. P.; Reitz, A. B. Aβ1-42 binds to α7 nicotinic acetylcholine receptor with high affinity. Implications for Alzheimer's disease pathology. *J. Biol. Chem.* **2000**, *275*, 5626–5632.

62. Liu, Q.; Kawai, H.; Berg, D. K. β-Amyloid peptide blocks the response of α7-containing nicotinic receptors on hippocampal neurons. *Proc. Natl. Acad. Sci. USA* **2001**, *98*, 4734–4739.

63. Tränkle, C.; Dittmann, A.; Schulz, U.; Weyand, O.; Buller, S.; Jöhren, K.; Heller, E.; Birdsall, N. J. M.; Holzgrabe, U.; Ellis, J.; Höltje, H. D.; Mohr, K. Atypical muscarinic allosteric modulation: cooperativity between modulators and their atypical binding topology in muscarinic M2 and M2/M5 chimeric receptors. *Mol. Pharmacol.* **2005**, *68*, 1597–1610.

64. Jöhren, K.; Höltje, H.-D. A model of the human M2 muscarinic acetylcholine receptor. *J. Comput. Aided. Mol. Des.* **2002**, *16*, 795–801.

65. Michalson, E. T.; D'Andrea, S.; Freeman, J. P.; Szmuszkovicz, J. The synthesis of 9-(1-azetidinyl)-1,2,3,4-tetrahydroacridine. *Heterocycles* **1990**, *30*, 415–425.

66. Bielavsky, J. Analogs of 9-amino-1,2,3,4-tetrahydroacridine. *Collect. Czech. Chem. Commun.* **1977**, *42*, 2802–2808.

67. Recanatini, M.; Cavalli, A.; Belluti, F.; Piazzi, L.; Rampa, A.; Bisi, A.; Gobbi, S.; Valenti, P.; Andrisano, V.; Bartolini, M.; Cavrini, V. SAR of 9-amino-1,2,3,4-tetrahydroacridine-based acetylcholinesterase inhibitors: synthesis, enzyme inhibitory activity, QSAR, and structure-based CoMFA of tacrine analogues. *J. Med. Chem.* **2000**, *43*, 2007–2018.

68. Temple, C.; Elliott, R. D.; Montgomery, J. A. Potential anticancer agents: 5-(N-substituted-aminocarbonyl)- and 5-(N-substituted-aminothiocarbonyl)-5,6,7,8-tetrahydrofolic acids. *J. Med. Chem.* **1988**, *31*, 697–700.

69. Leone-Bay, A.; Paton, D. R.; Freeman, J.; Lercara, C.; O'Toole, D.; Gschneidner, D.; Wang, E.; Harris, E.; Rosado, C.; Rivera, T.; DeVincent, A.; Tai, M.; Mercogliano, F.; Agarwal, R.; Leipold, H.; Baughman, R. A. Synthesis and evaluation of compounds that facilitate the gastrointestinal absorption of heparin. *J. Med. Chem.* **1998**, *41*, 1163–1171.

70. Elsinghorst, P. W.; Gütschow, M. *N*-Acylpyrrolidin-2-ones: Potential inhibitors of serine proteases and esterases. *Poster Contribution DPHG Joint Meeting* **2004**.

71. Carlier, P. R.; Chow, E. S.; Han, Y.; Liu, J.; Yazal, J. E.; Pang, Y. P. Heterodimeric tacrine-based acetylcholinesterase inhibitors: investigating ligand-peripheral site interactions. *J. Med. Chem.* **1999**, *42*, 4225–4231.

72. Carlier, P. R.; Han, Y. F.; Chow, E. S.; Li, C. P.; Wang, H.; Lieu, T. X.; Wong, H. S.; Pang, Y. P. Evaluation of short-tether bis-THA AChE inhibitors. A further test of the dual binding site hypothesis. *Bioorg. Med. Chem.* **1999**, *7*, 351–357.

73. Carlier, P. R.; Du, D. M.; Han, Y.; Liu, J.; Pang, Y. P. Potent, easily synthesized huperzine A-tacrine hybrid acetylcholinesterase inhibitors. *Bioorg. Med. Chem. Lett.* **1999**, *9*, 2335–2338.

74. Boon, J. A.; Levisky, J. A.; Pflug, J. L.; Wilkes, J. S. Friedel-Crafts reactions in ambient-temperature molten salts. *J. Org. Chem.* **1986**, *51*, 480–483.

75. Koel, M. Physical and chemical properties of ionic liquids based on the dialkylimidazolium cation. *Proc. Estonian Acad. Sci. Chem.* **2000**, *49*, 145–155.

76. Fourneau, E. Quaternary ammonium salts of di- and tri-(dialkylaminoalkoxy)-benzenes. Patent US2544076 *Chem. Abstr.* **1951**, *45*, 7146be.

77. Bovet, D.; Depierre, F.; de Lestrange, Y. Curarizing properties of phenolic ethers with quarternary ammonium groups. *Compt. rend.* **1947**, *225*, 74–76.

78. Sarkar, A.; Ilankumaran, P.; Kisanga, P.; Verkade, J. G. First synthesis of a highly basic dendrimer and its catalytic application in organic methodology. *Adv. Synth. Catal.* **2004**, *346*, 1093–1096.

79. Pearson, A. J.; Bruhn, P. R. Studies on the synthesis of aryl ethers using arene-manganese chemistry. *J. Org. Chem.* **1991**, *56*, 7092–7097.

80. ORTEP-III Ver.1.0.3, http://www.ornl.gov/sci/ortep/ortep.html.

81. PDB ID: 1ACJ, 1ACL. Harel, M.; Schalk, I.; Ehret-Sabatier, L.; Bouet, F.; Goeldner, M.; Hirth, C.; Axelsen, P. H.; Silman, I.; Sussman, J. L. Quaternary ligand binding to aromatic residues in the active-site gorge of acetylcholinesterase. *Proc. Natl. Acad. Sci. USA* **1993**, *90*, 9031–9035.

82. PDB ID: 1EVE. Kryger, G.; Silman, I.; Sussman, J. L. Structure of acetylcholinesterase complexed with E2020 (Aricept): implications for the design of new anti-Alzheimer drugs. *Structure Fold. Des.* **1999**, *7*, 297–307.

83. PDB ID: 1ZGB. Haviv, H.; Wong, D. M.; Greenblatt, H. M.; Carlier, P. R.; Pang, Y.-P.; Silman, I.; Sussman, J. L. Crystal packing mediates enantioselective ligand recognition at the peripheral site of acetylcholinesterase. *J. Am. Chem. Soc.* **2005**, *127*, 11029–11036.

84. PDB ID: 1N5M, 1N5R. Bourne, Y.; Taylor, P.; Radić, Z.; Marchot, P. Structural insights into ligand interactions at the acetylcholinesterase peripheral anionic site. *EMBO J.* **2003**, *22*, 1–12.

85. Berman, H. M.; Westbrook, J.; Feng, Z.; Gilliland, G.; Bhat, T. N.; Weissig, H.; Shindyalov, I. N.; Bourne, P. E. The Protein Data Bank. *Nucleic. Acids. Res.* **2000**, *28*, 235–242.

86. AutoDockTools Ver. 1.3, http://www.scripps.edu/~Esanner/python/adt/autotoolsoverview.html.

87. CORINA Ver. 3.2, http://www.molecular-networks.com/online_demos/corina_demo.html.

88. OpenBabel Ver. 2.0.0, http://openbabel.sourceforge.net.

89. MOPAC 2002 Ver. 1.01, http://www.cachesoftware.com/mopac/index.shtml.

90. Jones, G.; Willett, P.; Glen, R. C. Molecular recognition of receptor sites using a genetic algorithm with a description of desolvation. *J. Mol. Biol.* **1995**, *245*, 43–53.

91. Morris, G. M.; Goodsell, D. S.; Halliday, R.; Huey, R.; Hart, W. E.; Belew, R. K.; Olson, A. J. Automated docking using a Lamarckian genetic algorithm and a empirical binding free energy function. *J. Comp. Chem.* **1998**, *19*, 1639–1662.

92. Hendlich, M.; Rippmann, F.; Barnickel, G. LIGSITE: automatic and efficient detection of potential small molecule-binding sites in proteins. *J. Mol. Graph. Model.* **1997**, *15*, 359–363.

93. Wallace, A. C.; Laskowski, R. A.; Thornton, J. M. LIGPLOT: a program to generate schematic diagrams of protein-ligand interactions. *Protein. Eng.* **1995**, *8*, 127–134.

94. PyMOL Molecular Graphics System Ver. 0.99, http://www.pymol.org.

95. Lavigne, P.; Bagu, J. R.; Boyko, R.; Willard, L.; Holmes, C. F.; Sykes, B. D. Structure-based thermodynamic analysis of the dissociation of protein phosphatase-1 catalytic subunit and microcystin-LR docked complexes. *Protein Sci.* **2000**, *9*, 252–264.

96. Nissink, J. W. M.; Murray, C.; Hartshorn, M.; Verdonk, M. L.; Cole, J. C.; Taylor, R. A new test set for validating predictions of protein-ligand interaction. *Proteins* **2002**, *49*, 457–471.

97. Gemma, S.; Gabellieri, E.; Huleatt, P.; Fattorusso, C.; Borriello, M.; Catalanotti, B.; Butini, S.; Angelis, M. D.; Novellino, E.; Nacci, V.; Belinskaya, T.; Saxena, A.; Campiani, G. Discovery

of Huperzine A-Tacrine Hybrids as Potent Inhibitors of Human Cholinesterases Targeting Their Midgorge Recognition Sites. *J. Med. Chem.* **2006**, *49*, 3421–3425.

98. Baker, N. A.; Sept, D.; Joseph, S.; Holst, M. J.; McCammon, J. A. Electrostatics of nanosystems: application to microtubules and the ribosome. *Proc. Natl. Acad. Sci. USA* **2001**, *98*, 10037–10041.

99. PDB ID: 1AX9. Ravelli, R. B.; Raves, M. L.; Ren, Z.; Bourgeois, D.; Roth, M.; Kroon, J.; Silman, I.; Sussman, J. L. Static Laue diffraction studies on acetylcholinesterase. *Acta Crystallogr. D Biol. Crystallogr.* **1998**, *54*, 1359–1366.

100. Savini, L.; Gaeta, A.; Fattorusso, C.; Catalanotti, B.; Campiani, G.; Chiasserini, L.; Pellerano, C.; Novellino, E.; McKissic, D.; Saxena, A. Specific targeting of acetylcholinesterase and butyrylcholinesterase recognition sites. Rational design of novel, selective, and highly potent cholinesterase inhibitors. *J. Med. Chem.* **2003**, *46*, 1–4.

101. Lineweaver, H.; Burk, D. The determination of enzyme dissociation constants. *J. Am. Chem. Soc.* **1934**, *56*, 658–666.

102. Dixon, M. The determination of enzyme inhibitor constants. *Biochem. J.* **1953**, *55*, 179–171.

103. Ellman, G. L.; Courtney, K. D.; Andres, V.; Feather-Stone, R. M. A new and rapid colorimetric determination of acetylcholinesterase activity. *Biochem. Pharmacol.* **1961**, *7*, 88–95.

104. Grace Ver. 5.1.20, http://plasma-gate.weizmann.ac.il/Grace.

105. Pietsch, M.; Gütschow, M. Synthesis of tricyclic 1,3-oxazin-4-ones and kinetic analysis of cholesterol esterase and acetylcholinesterase inhibition. *J. Med. Chem.* **2005**, *48*, 8270–8288.

106. Kinetic measurements were carried out by C. M. Gonzáles Tanarro.

107. Pang, Y. P.; Quiram, P.; Jelacic, T.; Hong, F.; Brimijoin, S. Highly potent, selective, and low cost bis-tetrahydroaminacrine inhibitors of acetylcholinesterase. Steps toward novel drugs for treating Alzheimer's disease. *J. Biol. Chem.* **1996**, *271*, 23646–23649.

108. Gregor, V. E.; Emmerling, M. R.; Lee, C.; Moore, C. J. The synthesis and in vitro acetylcholinesterase and butyrylcholinesterase inhibitory activity of tacrine (Cognex) derivatives. *Bioorg. Med. Chem. Lett.* **1992**, *2*, 861–864.

109. Savini, L.; Campiani, G.; Gaeta, A.; Pellerano, C.; Fattorusso, C.; Chiasserini, L.; Fedorko, J. M.; Saxena, A. Novel and potent tacrine-related hetero- and homobivalent ligands for acetylcholinesterase and butyrylcholinesterase. *Bioorg. Med. Chem. Lett.* **2001**, *11*, 1779–1782.

110. Cieslik, J. Allosterische Modulation der Ligandbindung durch neue Hybridmodulatoren aus Strukturelementen von Tacrin und Gallamin am muskarinischen M$_2$-Acetylcholin-Rezeptor. *Diploma Thesis University of Bonn* **2006**.

111. Bogan, R. Potential interactions at the M$_1$ receptor. *Personal communication* **2006**.

112. Saijo, R.; Nonaka, G.; Nishioka, I. Tannins and related compounds. LXXXIV. Isolation and characterization of five new hydrolyzable tannins from the bark of Mallotus japonicus. *Chem. Pharm. Bull. (Tokyo)* **1989**, *37*, 2063–2070.

113. Clemence, F.; Joliveau-Maushart, C.; Meier, J.; Cerede, J.; Delevallee, F.; Benzoni, J.; Deraedt, R. Synthesis and analgesic activity in the 1,2,4-triazole series. *Eur. J. Med. Chem.* **1985**, *20*, 257–266.

114. Acheson, R. M.; Booth, D. A.; Brettle, R.; Harris, A. M. Synthesis of some acylglycines and related oxazolones. *J. Chem. Soc.* **1960**, 3457–3461.

115. Röhnert, H. Glycylhydrazine compounds. I. Hydrazine compounds of substituted amino acids. *Arch. Pharm.* **1962**, *295*, 697–706.

116. Fominova, O. S.; Skachilova, S. Y.; Ermakov, A. I.; Pleshakov, M. G. Synthesis of esters of γ-aminobutyric acid and its N-substituted derivatives. *Zh. Org. Khim.* **1977**, *13*, 1922–1926.

117. Novak, P.; Jary, J. Synthesis and reactions of N-(3,4,5-trimethoxybenzoyl)-ϵ-caprolactam. *Collect. Czech. Chem. Commun.* **1973**, *38*, 2621–2626.

118. Prata, J. V.; Clemente, D.-T. S.; Prabhakar, S.; Lobo, A. M.; Mourato, I.; Branco, P. S. Intramolecular addition of acyldiazenecarboxylates onto double bonds in the synthesis of heterocycles. *J. Chem. Soc. Perkin Trans. 1* **2002**, *4*, 513–528.

119. Yerlikaya, Z.; Aksoy, S.; Bayramli, E. Structure and properties of fully aromatic thermotropic liquid-crystalline copolyesters containing m-hydroxybenzoic acid units. *J. Appl. Polym. Sci.* **2003**, *90*, 3260–3269.

120. Andrus, M. B.; Liu, J.; Meredith, E. L.; Nartey, E. Synthesis of resveratrol using a direct decarbonylative Heck approach from resorcylic acid. *Tetrahedron Lett.* **2003**, *44*, 4819–4822.

121. Gazit, A.; Yaish, P.; Gilon, C.; Levitzki, A. Tyrphostins I: synthesis and biological activity of protein tyrosine kinase inhibitors. *J. Med. Chem.* **1989**, *32*, 2344–2352.

9 NMR Spectra

Detailed structure elucidation

9-Chloro-1,2,3,4-tetrahydroacridine
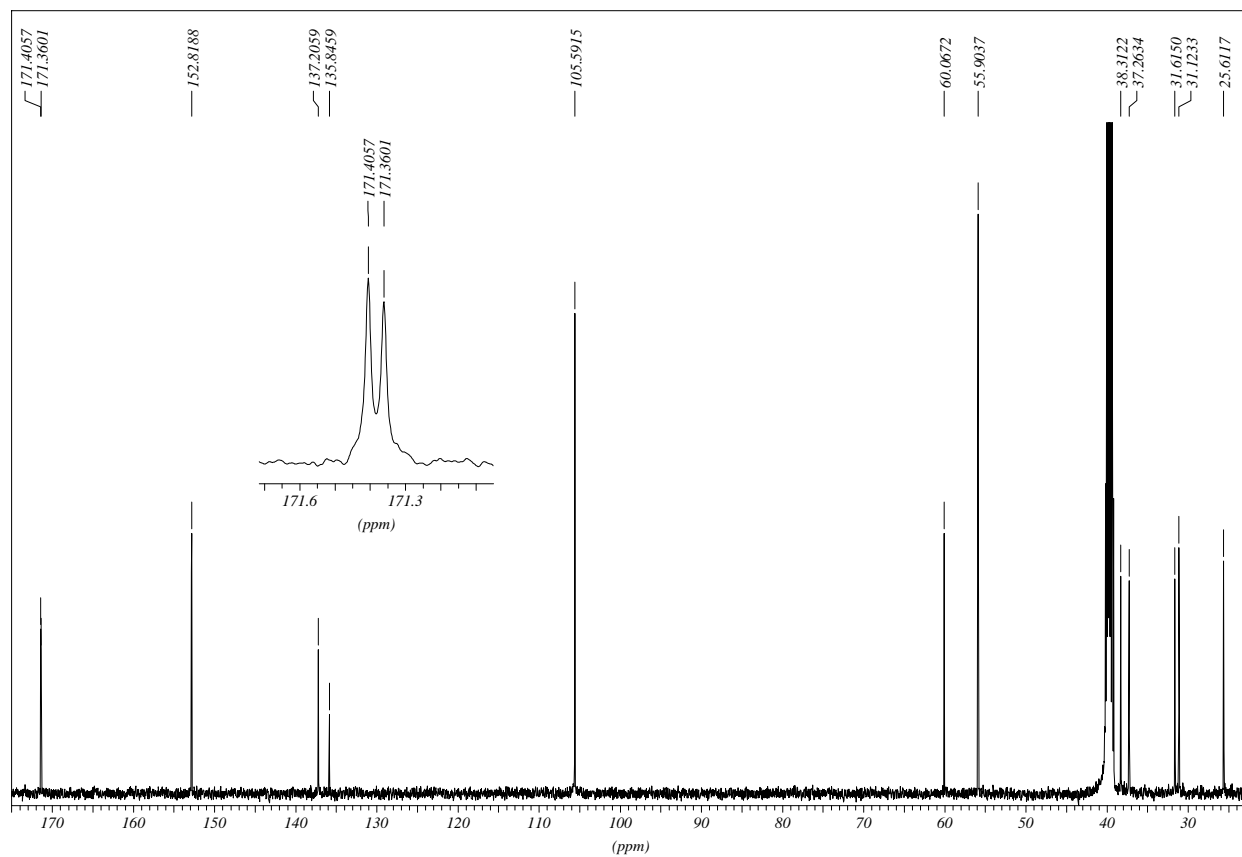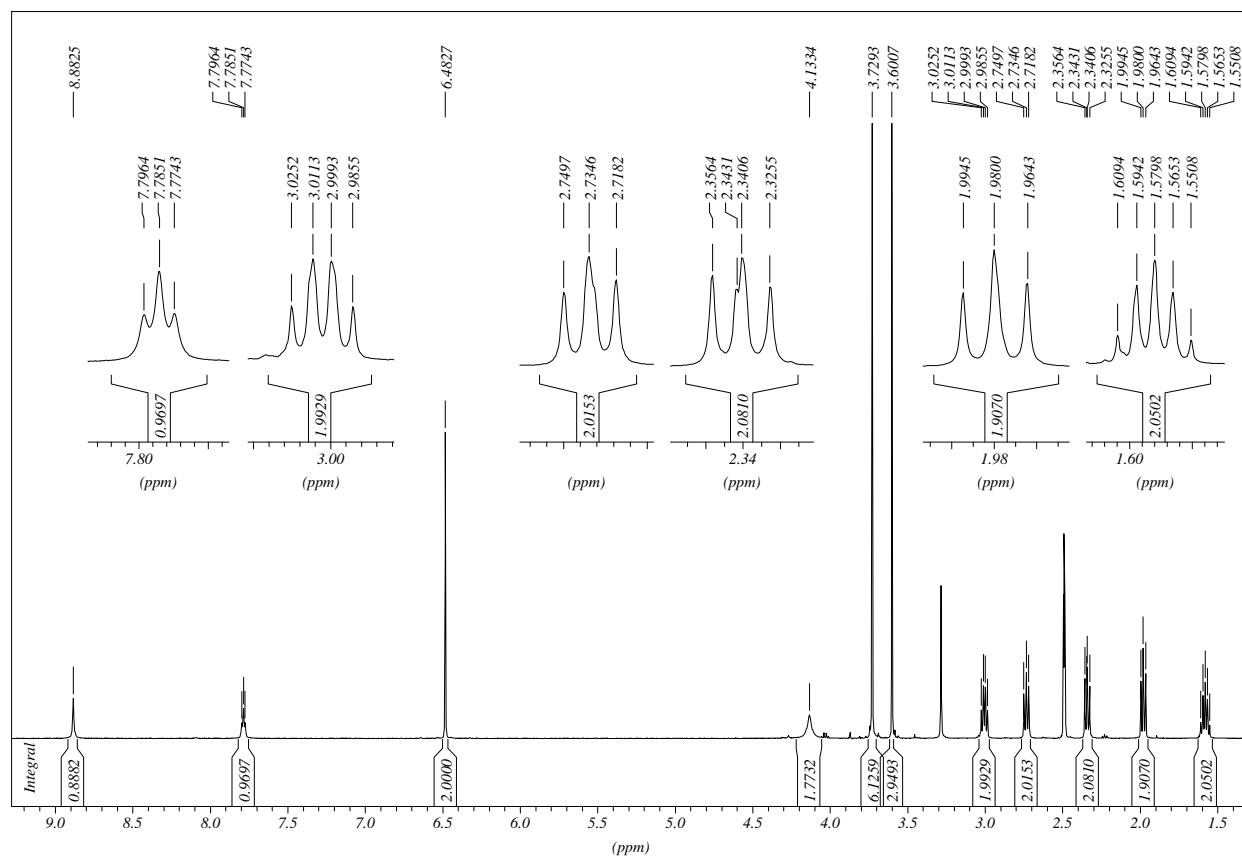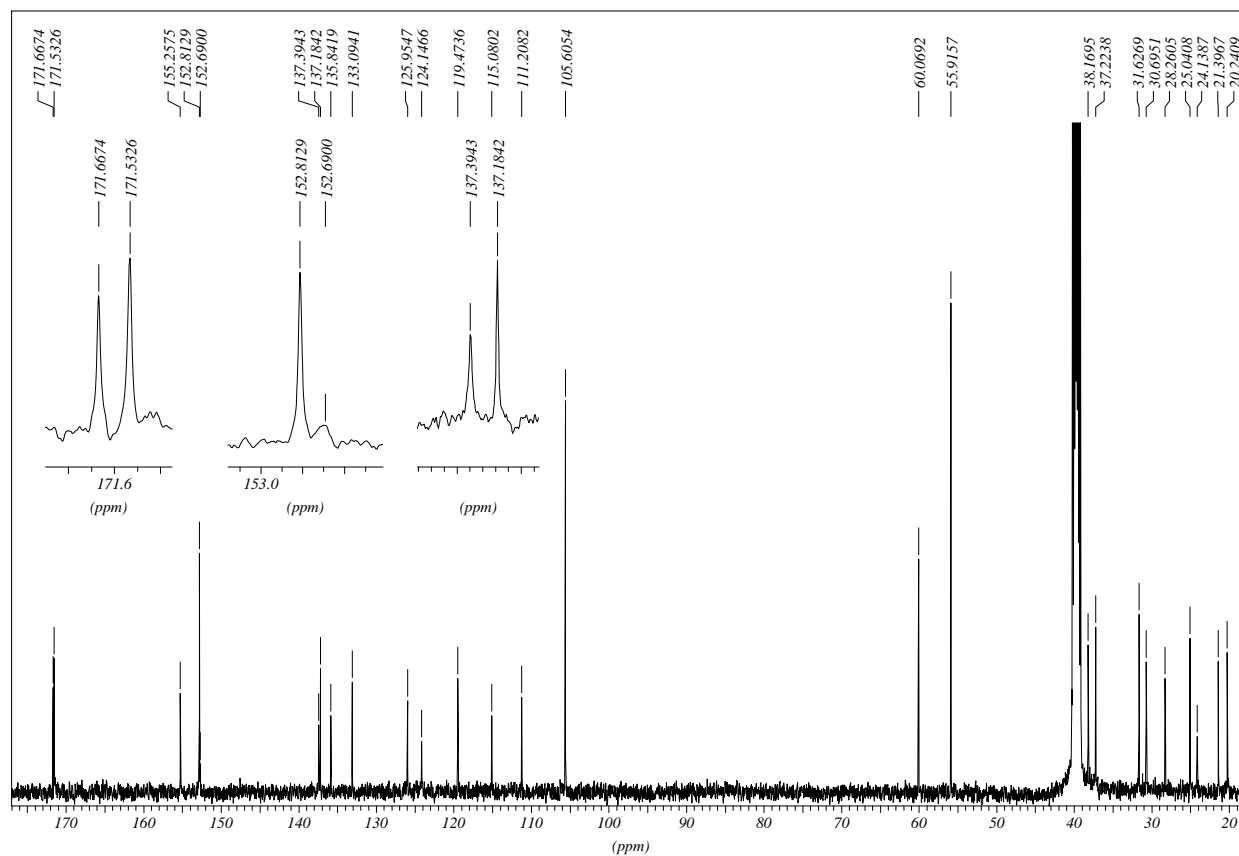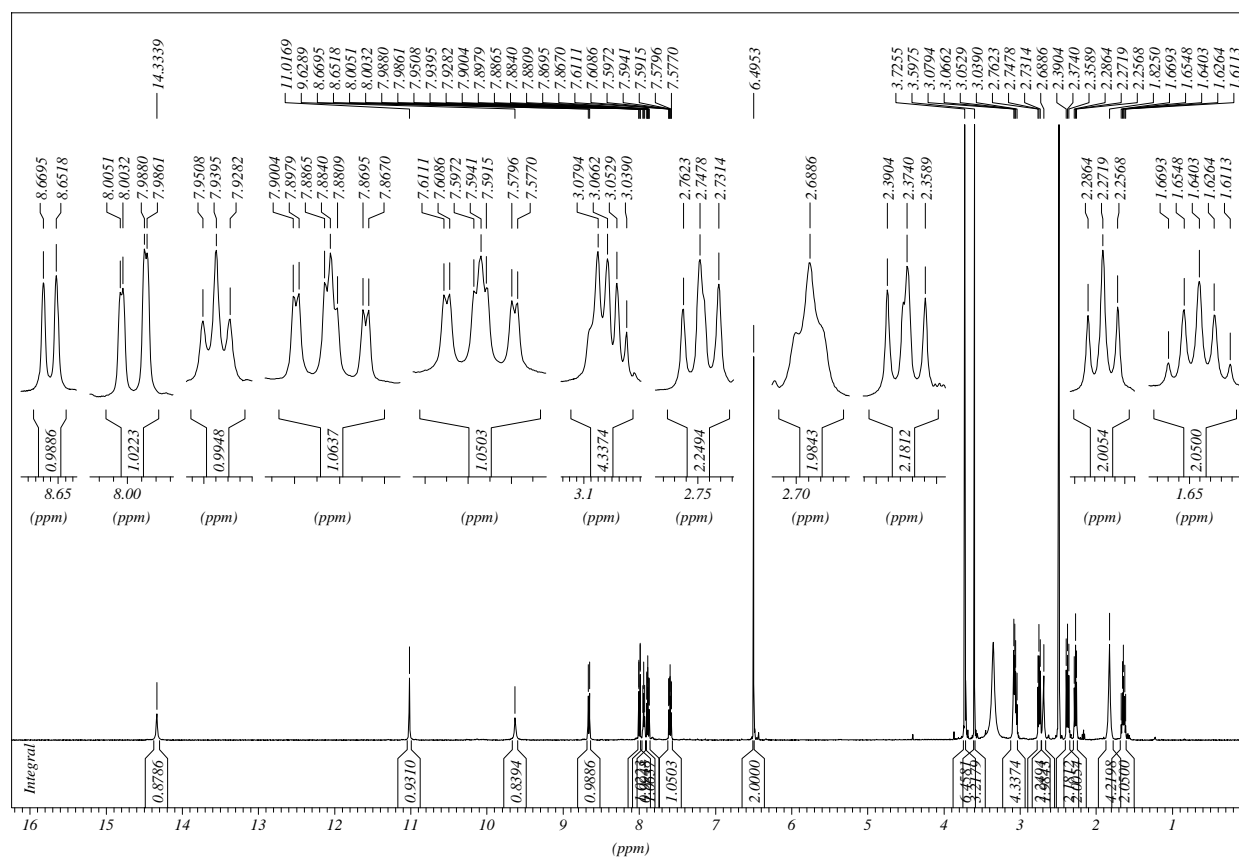
6,9-Dichloro-1,2,3,4-tetrahydroacridine

3-(3,4,5-Trimethoxyphenyl)-*N*-(4-oxo-4-(2-(1,2,3,4-tetrahydroacridin-9-yl)hydrazino)butyl)-propanamide hydrochloride

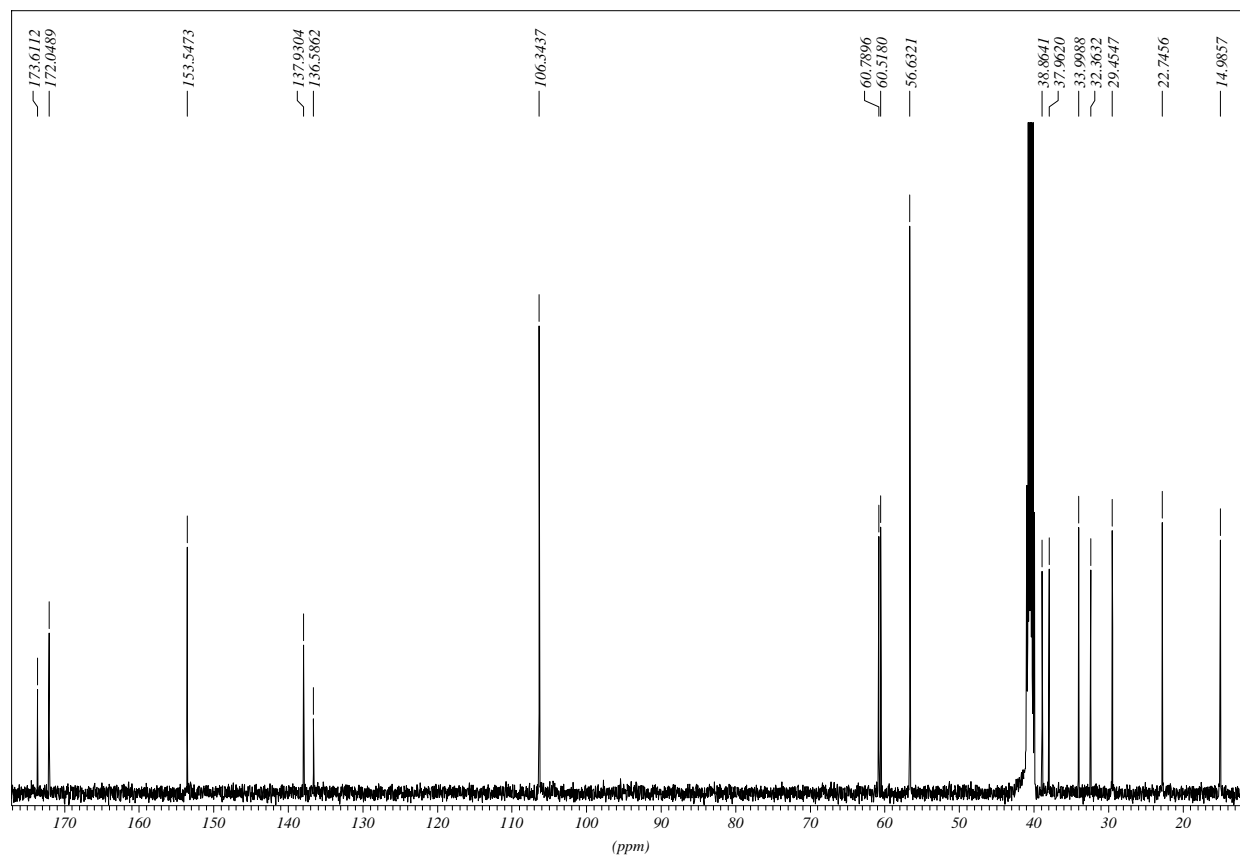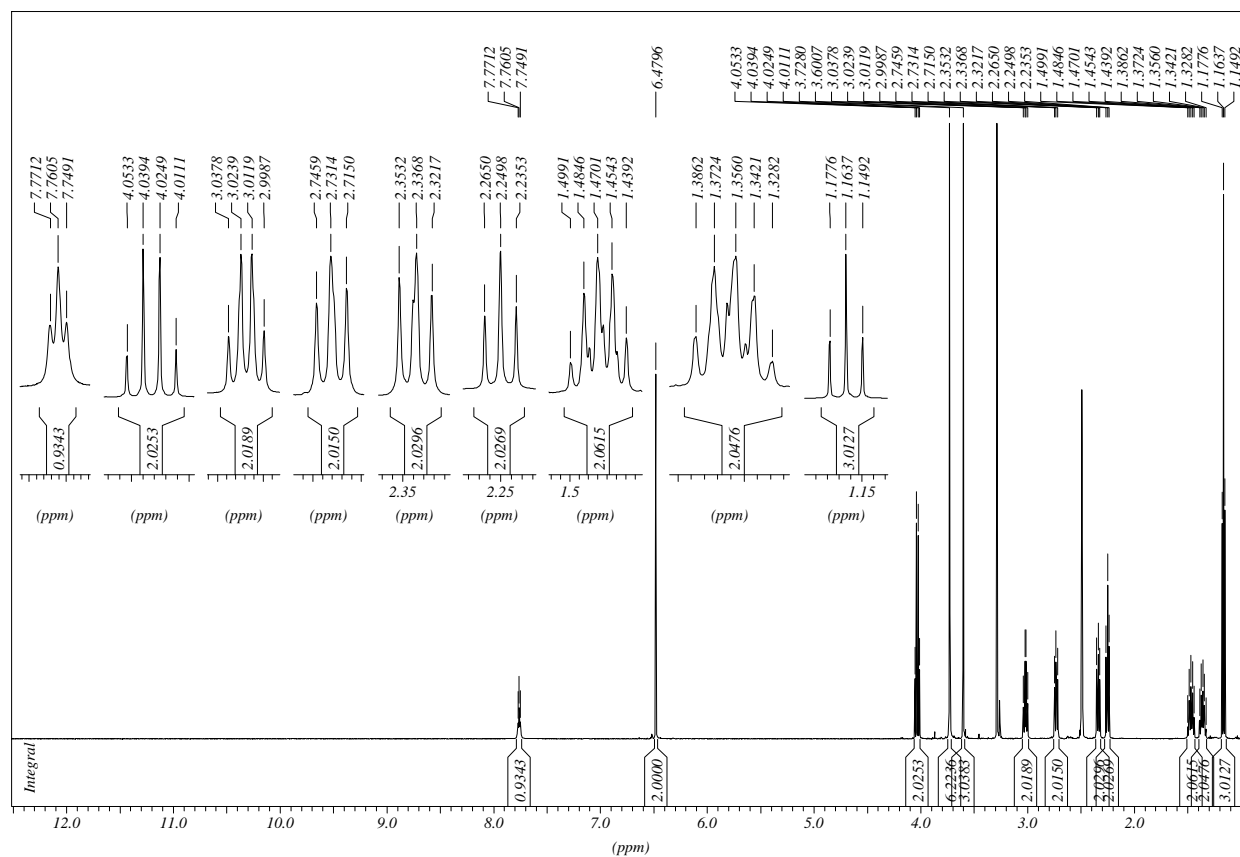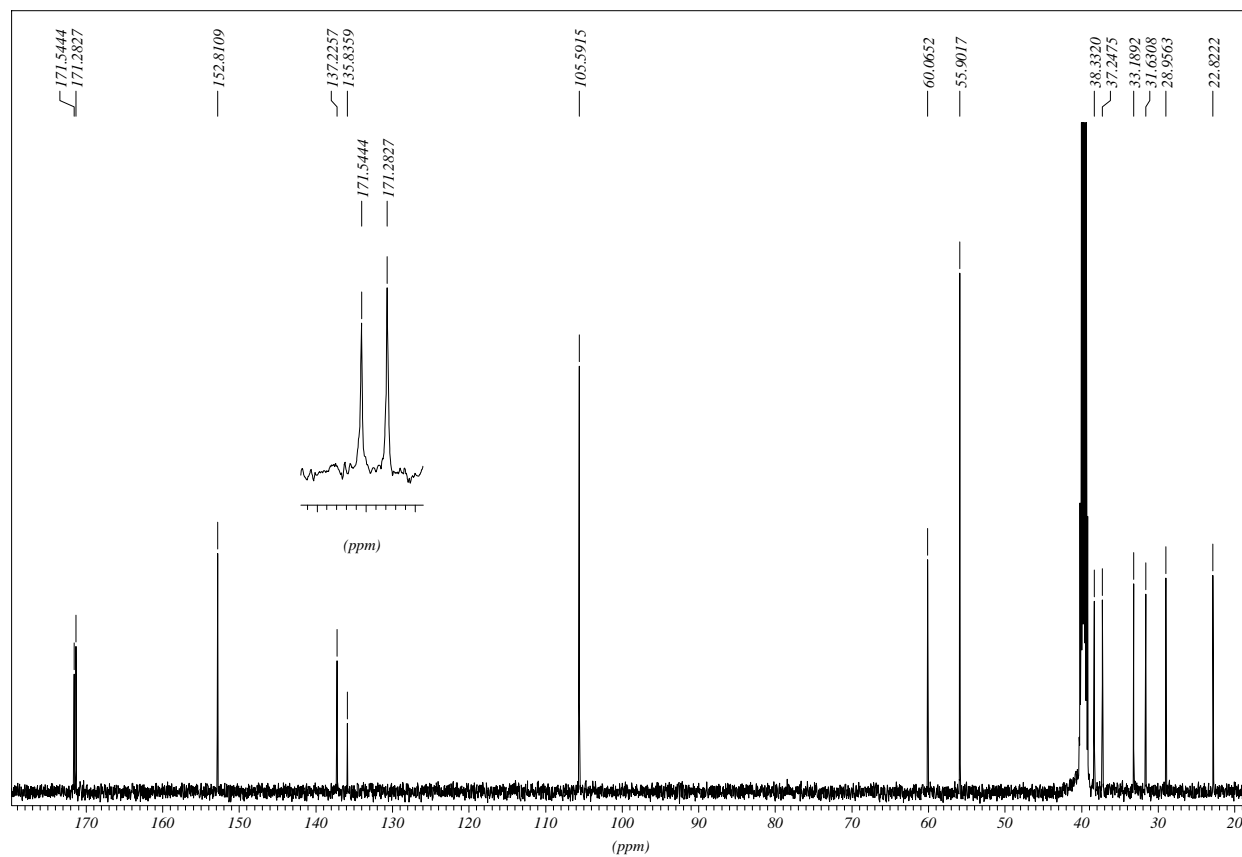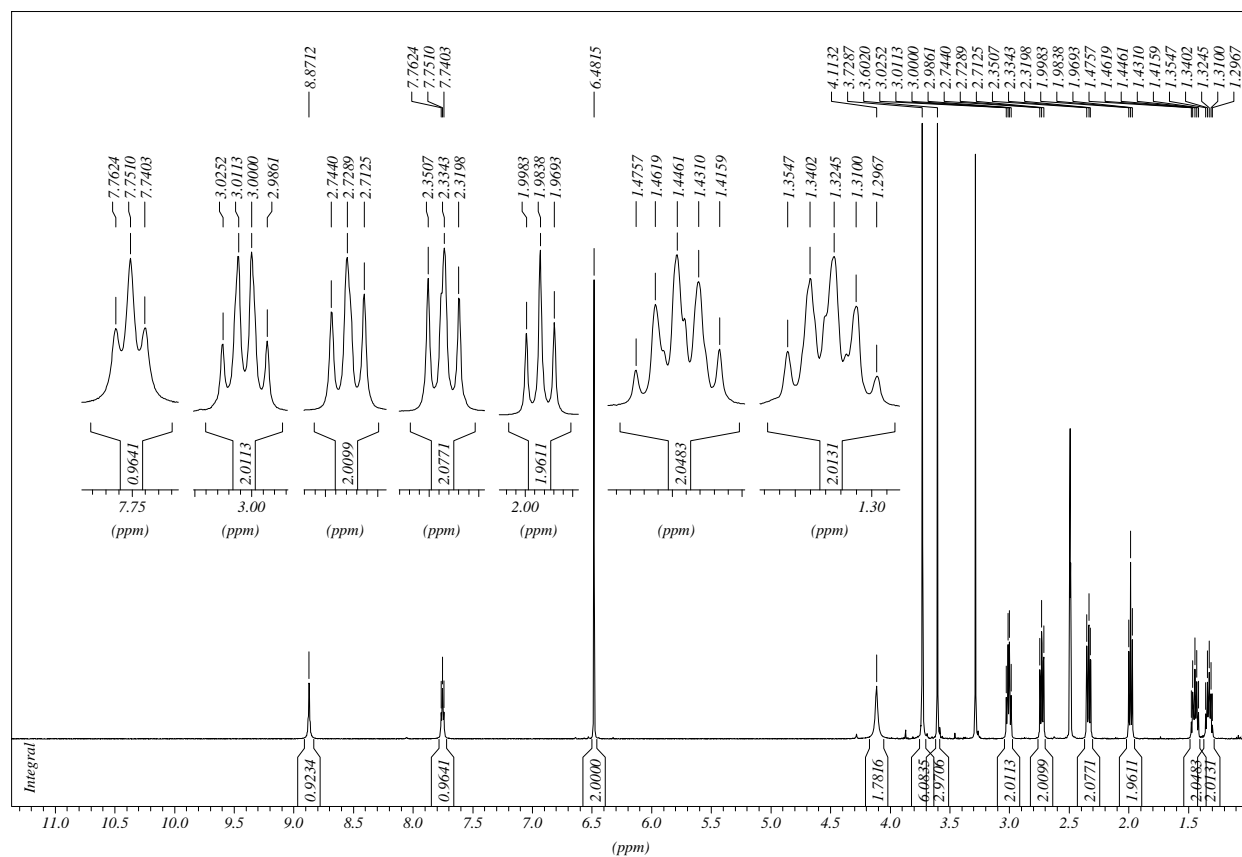3-(3,4,5-Trimethoxyphenyl)-*N*-(4-oxo-4-(2-(1,2,3,4-tetrahydroacridin-9-yl)hydrazino)butyl)-propanamide

2-(4-(((6-(2-(6-Chloro-1,2,3,4-tetrahydroacridin-9-yl)hydrazino)-6-oxohexyl)amino)carbonyl)-phenoxy)-*N,N,N*-triethyl-ethanaminium bromide hydrochloride

The tacrine moiety

Donepezil-Analogs – Derivatives of benzoic acid

(CH$_2$)$_0$-Spacer

(CH$_2$)$_1$-Spacer

(CH$_2$)$_2$-Spacer

(CH$_2$)$_3$-Spacer

(CH$_2$)$_4$-Spacer

(CH$_2$)$_5$-Spacer

(CH$_2$)$_6$-Spacer

(CH$_2$)$_7$-Spacer

(CH$_2$)$_8$-Spacer

Donepezil-Analogs – Derivatives of phenylpropionic acid

(CH$_2$)$_0$-Spacer

(CH$_2$)$_1$-Spacer

(CH$_2$)$_2$-Spacer

(CH$_2$)$_3$-Spacer

(CH$_2$)$_4$-Spacer

(CH$_2$)$_5$-Spacer

Gallamine-Analogs − Monofunctionalized derivatives of benzoic acid

Gallamine-Analogs − Bisfunctionalized derivatives of benzoic acid

Gallamine-Analogs − Trisfunctionalized derivatives of benzoic acid

Further compounds

9-Chloro-1,2,3,4-tetrahydroacridine

HSQC I

9-Chloro-1,2,3,4-tetrahydroacridine
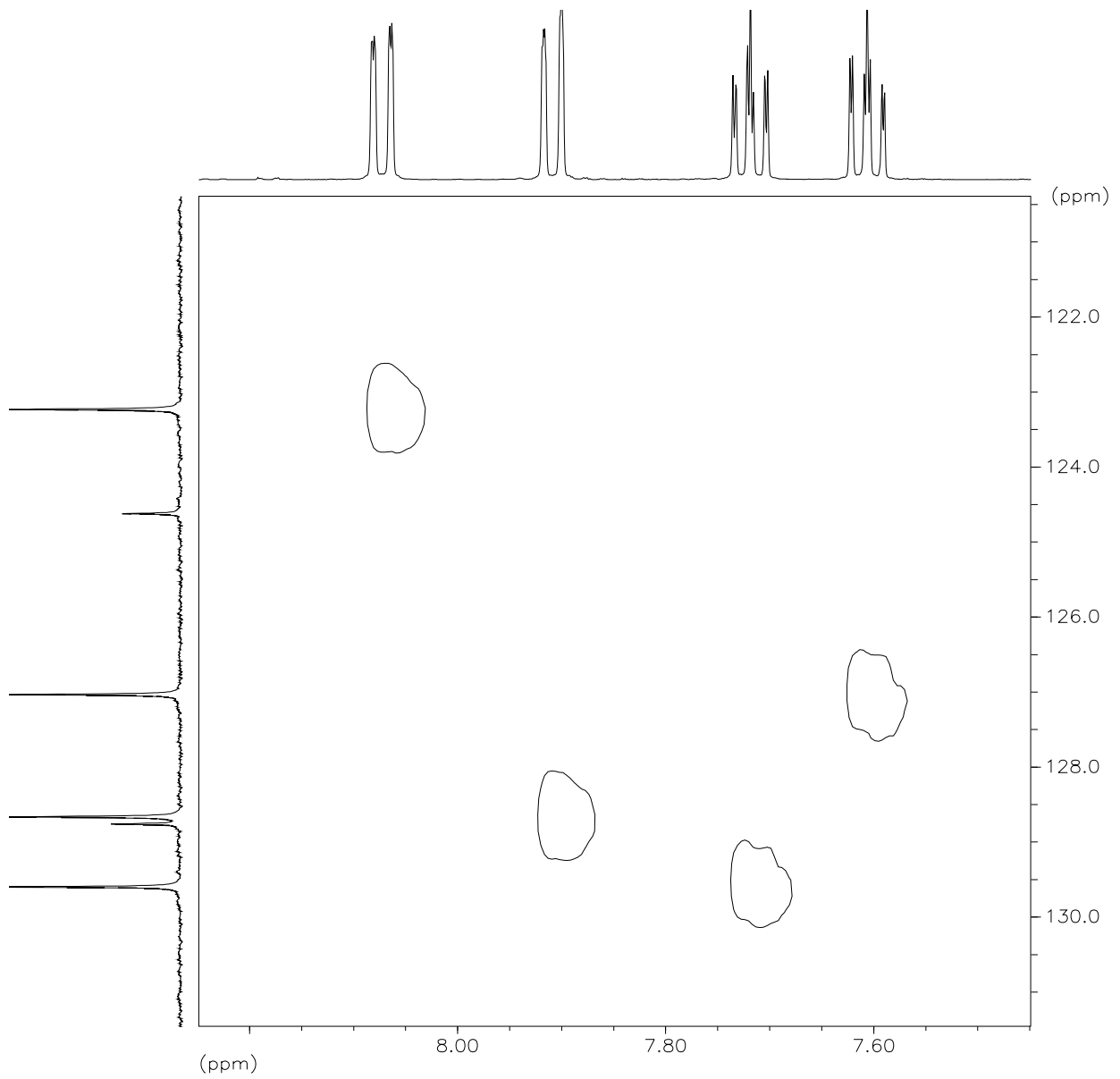
HSQC II

9-Chloro-1,2,3,4-tetrahydroacridine
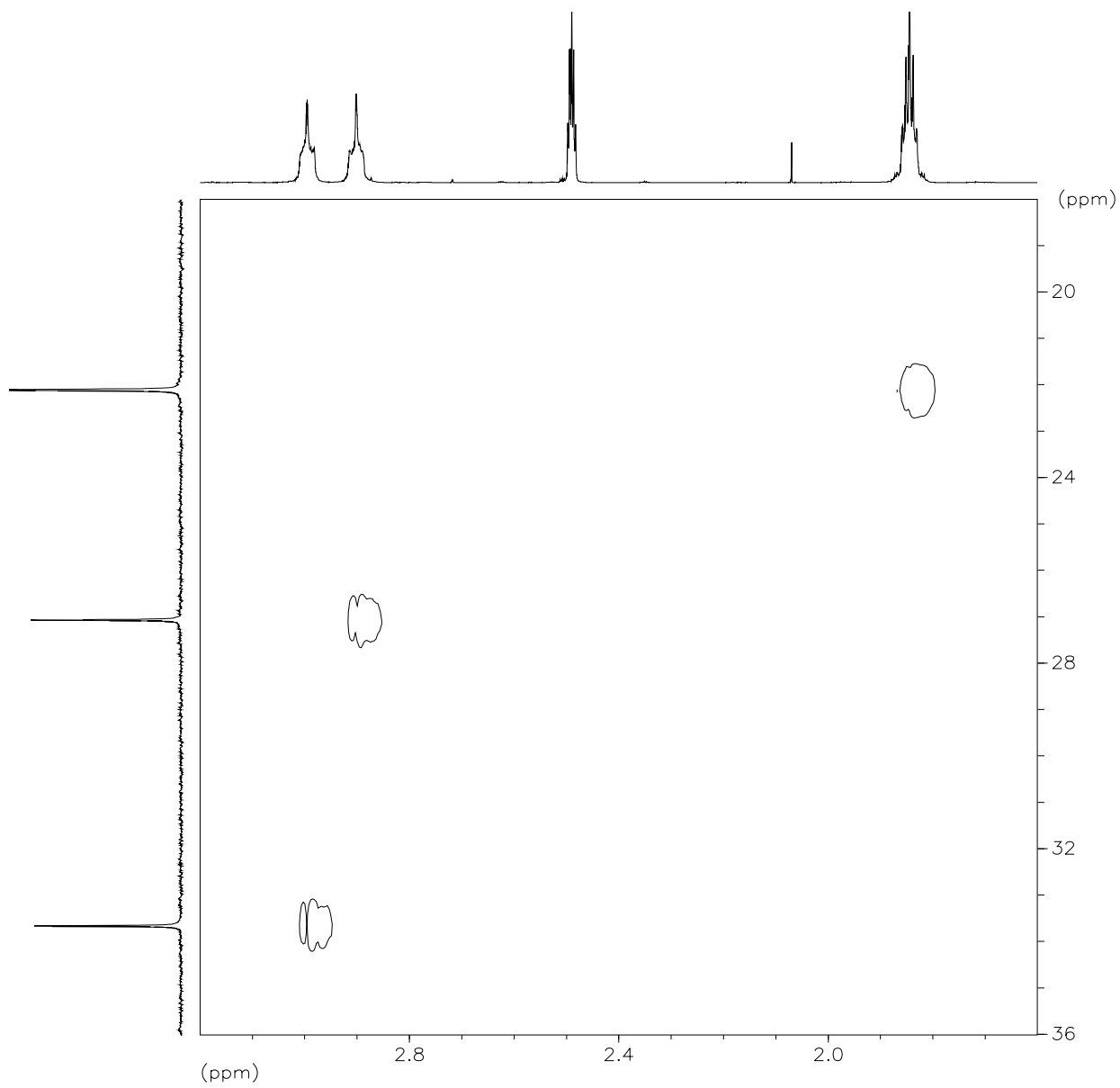
HSQC III

9-Chloro-1,2,3,4-tetrahydroacridine
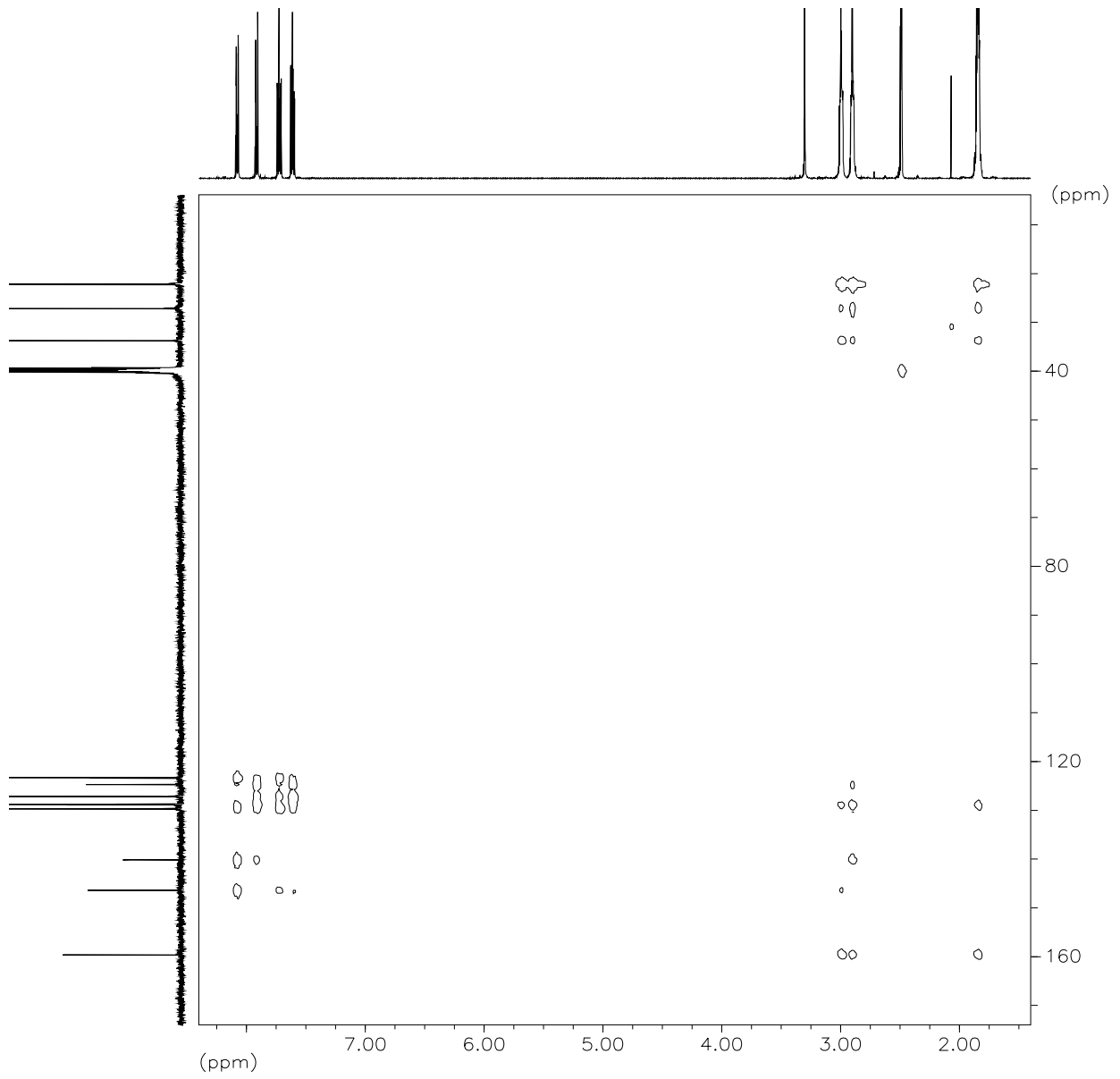
HMBC I

9-Chloro-1,2,3,4-tetrahydroacridine
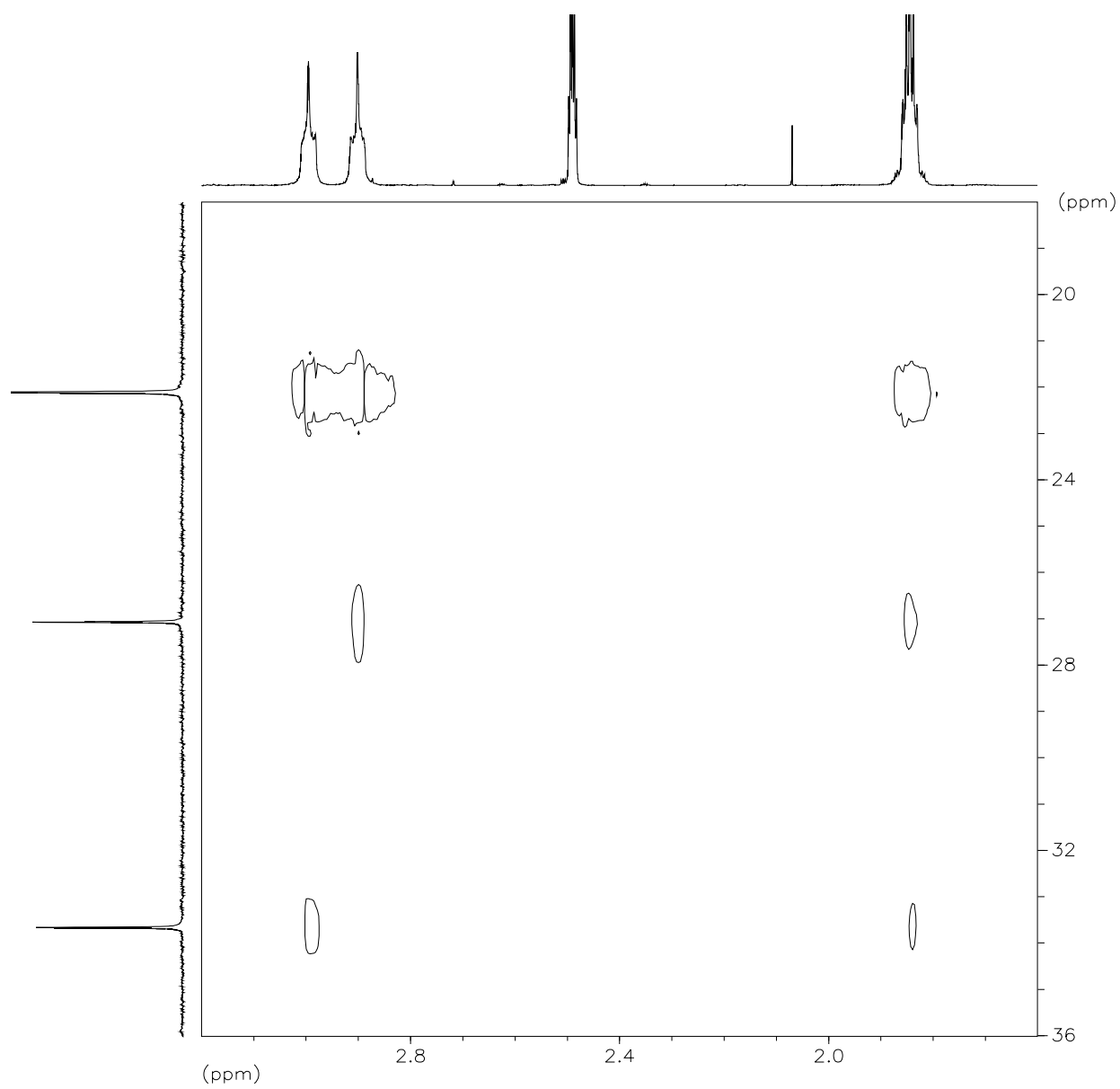
HMBC II

9-Chloro-1,2,3,4-tetrahydroacridine
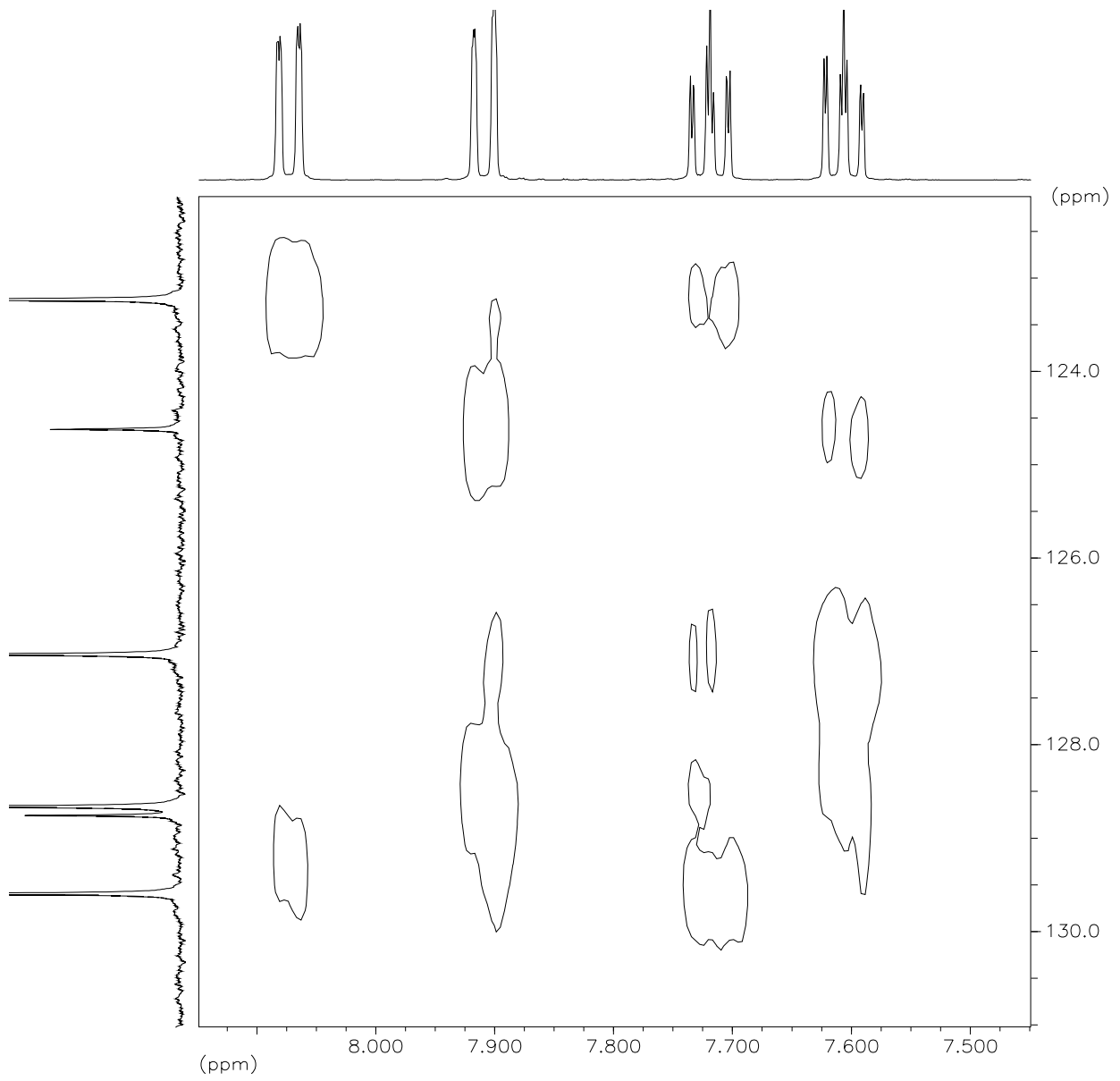
HMBC III

9-Chloro-1,2,3,4-tetrahydroacridine
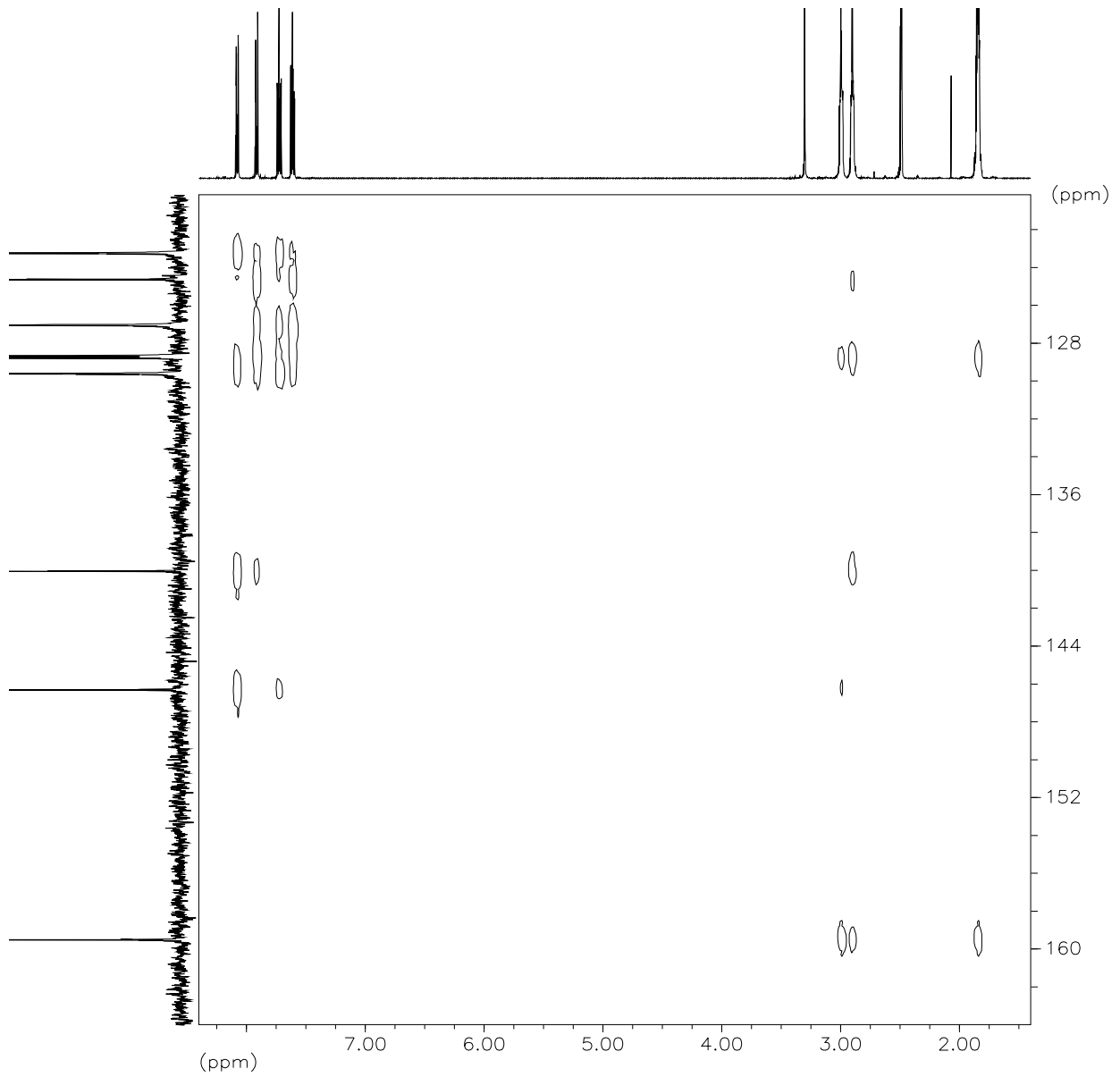
HMBC IV

6,9-Dichloro-1,2,3,4-tetrahydroacridine
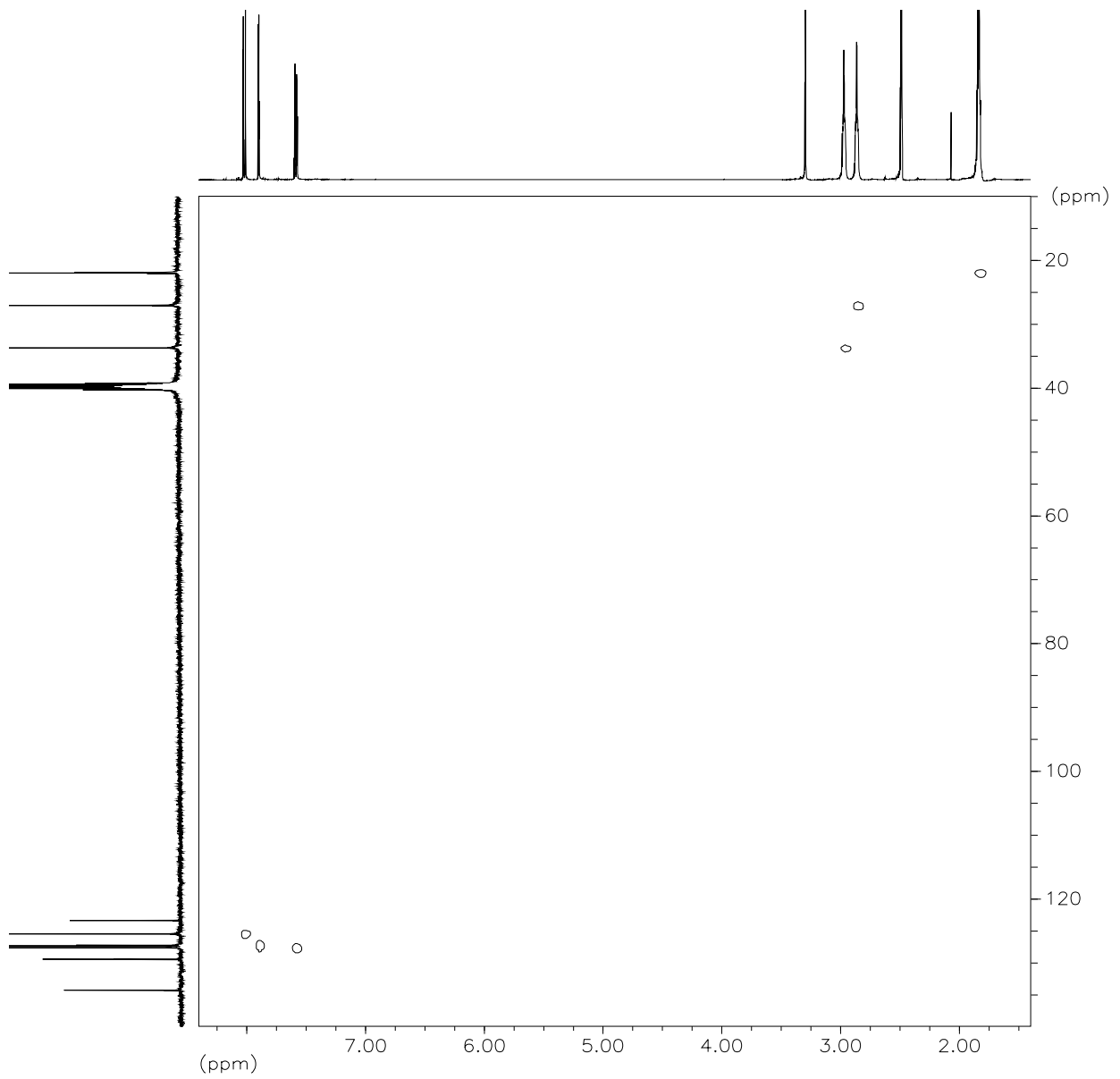
HSQC I

6,9-Dichloro-1,2,3,4-tetrahydroacridine
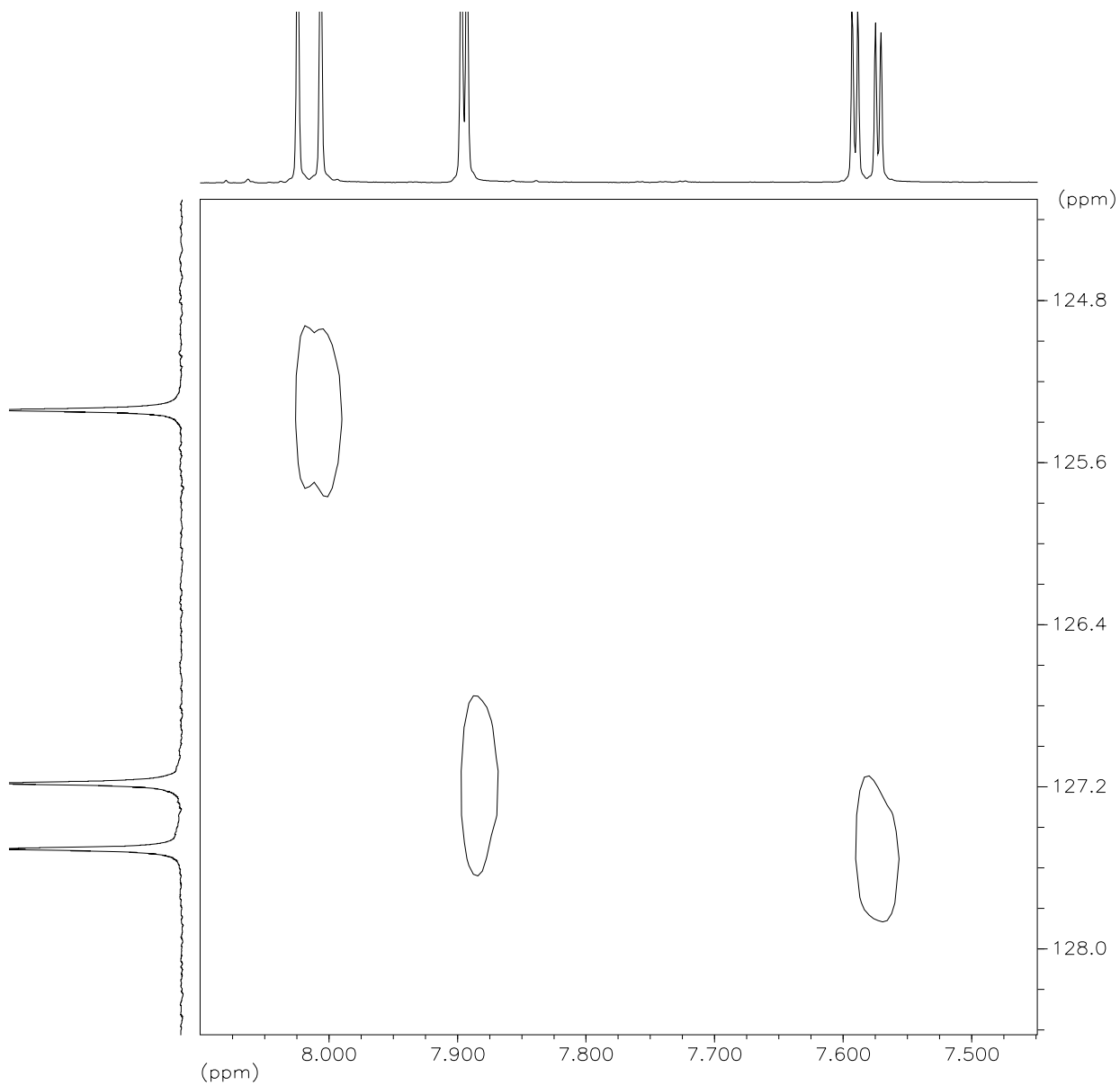
HSQC II

6,9-Dichloro-1,2,3,4-tetrahydroacridine

HSQC III
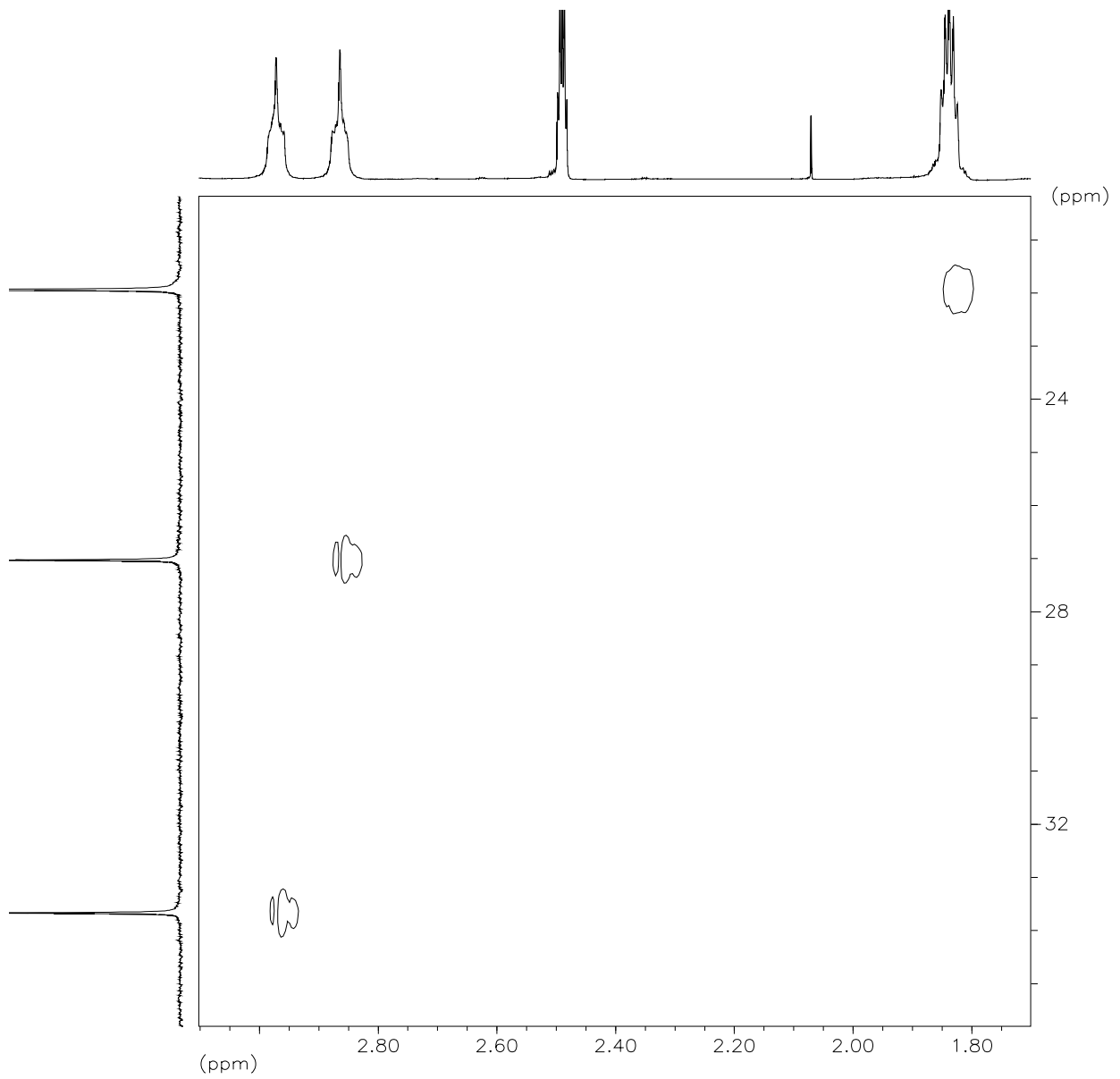
6,9-Dichloro-1,2,3,4-tetrahydroacridine
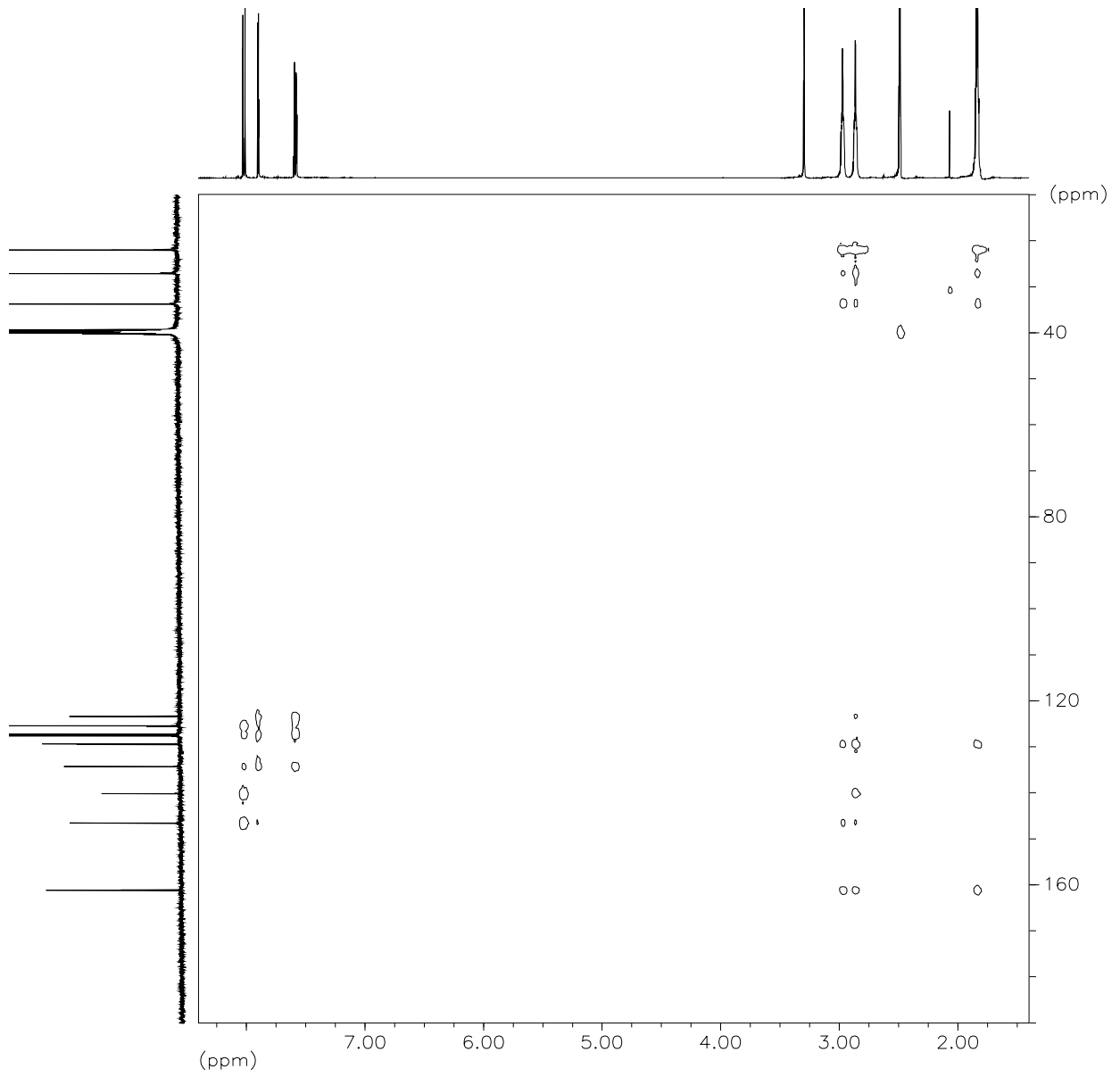
HMBC I

6,9-Dichloro-1,2,3,4-tetrahydroacridine
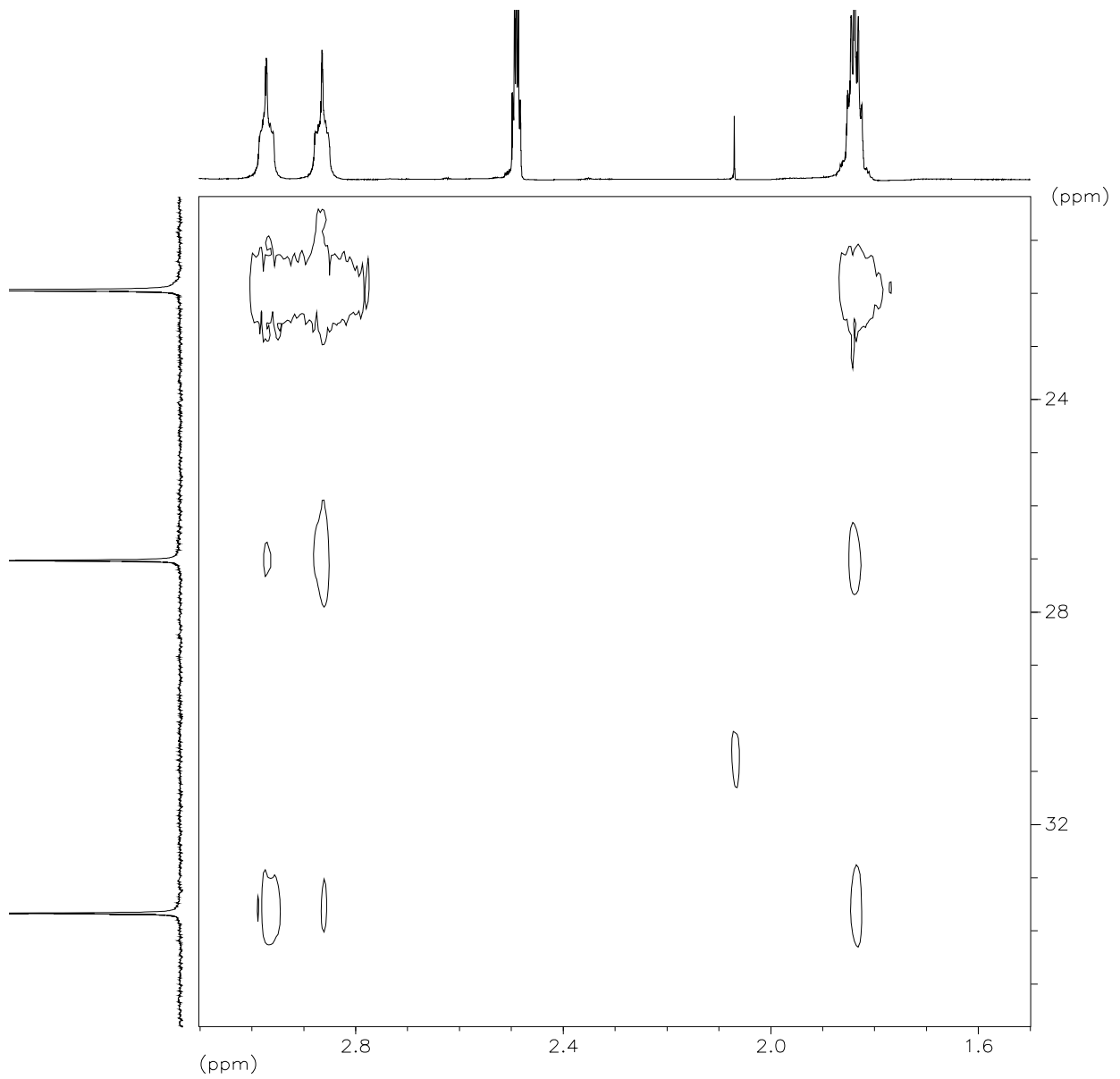
HMBC II

6,9-Dichloro-1,2,3,4-tetrahydroacridine

HMBC III
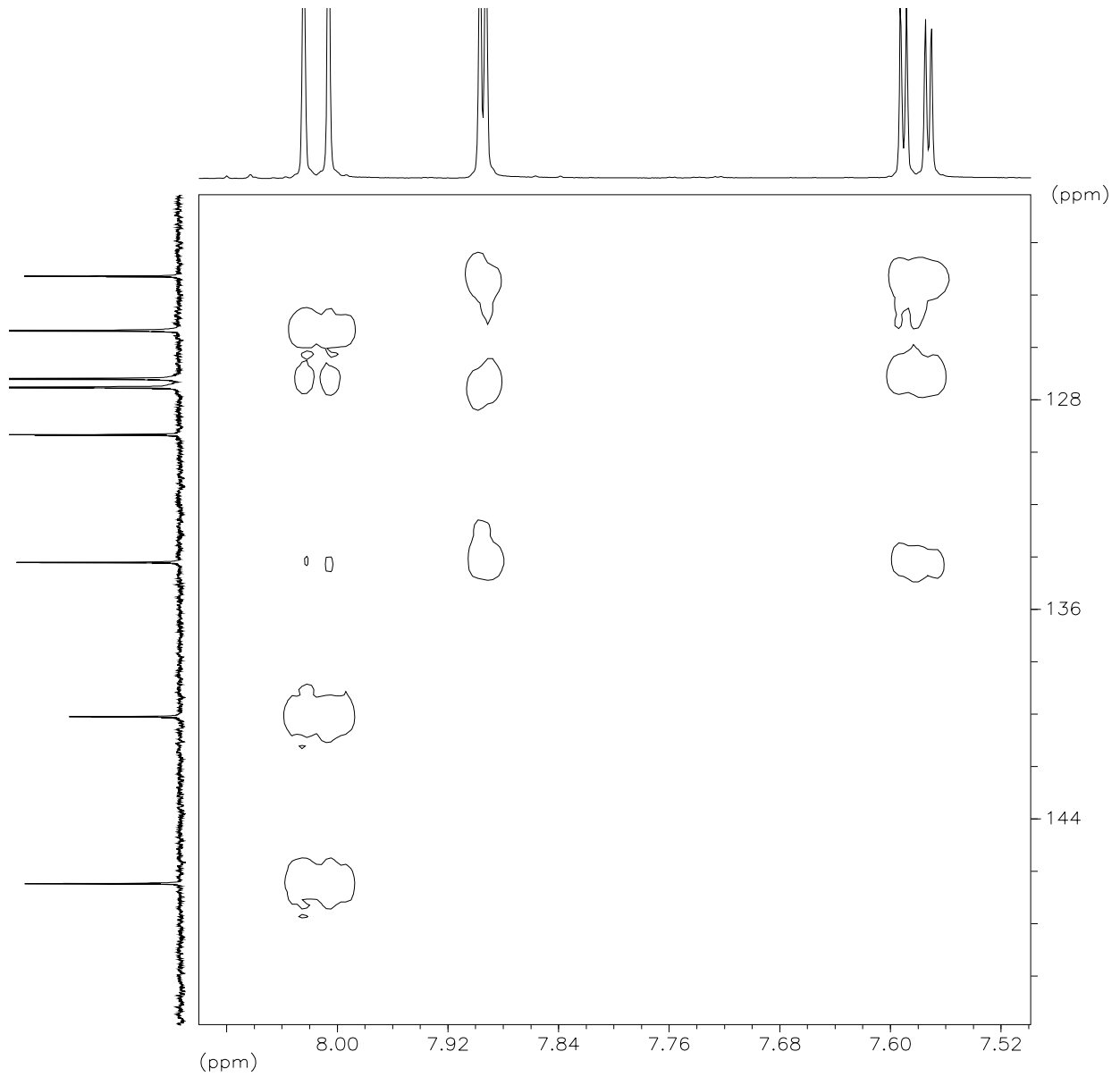
6,9-Dichloro-1,2,3,4-tetrahydroacridine
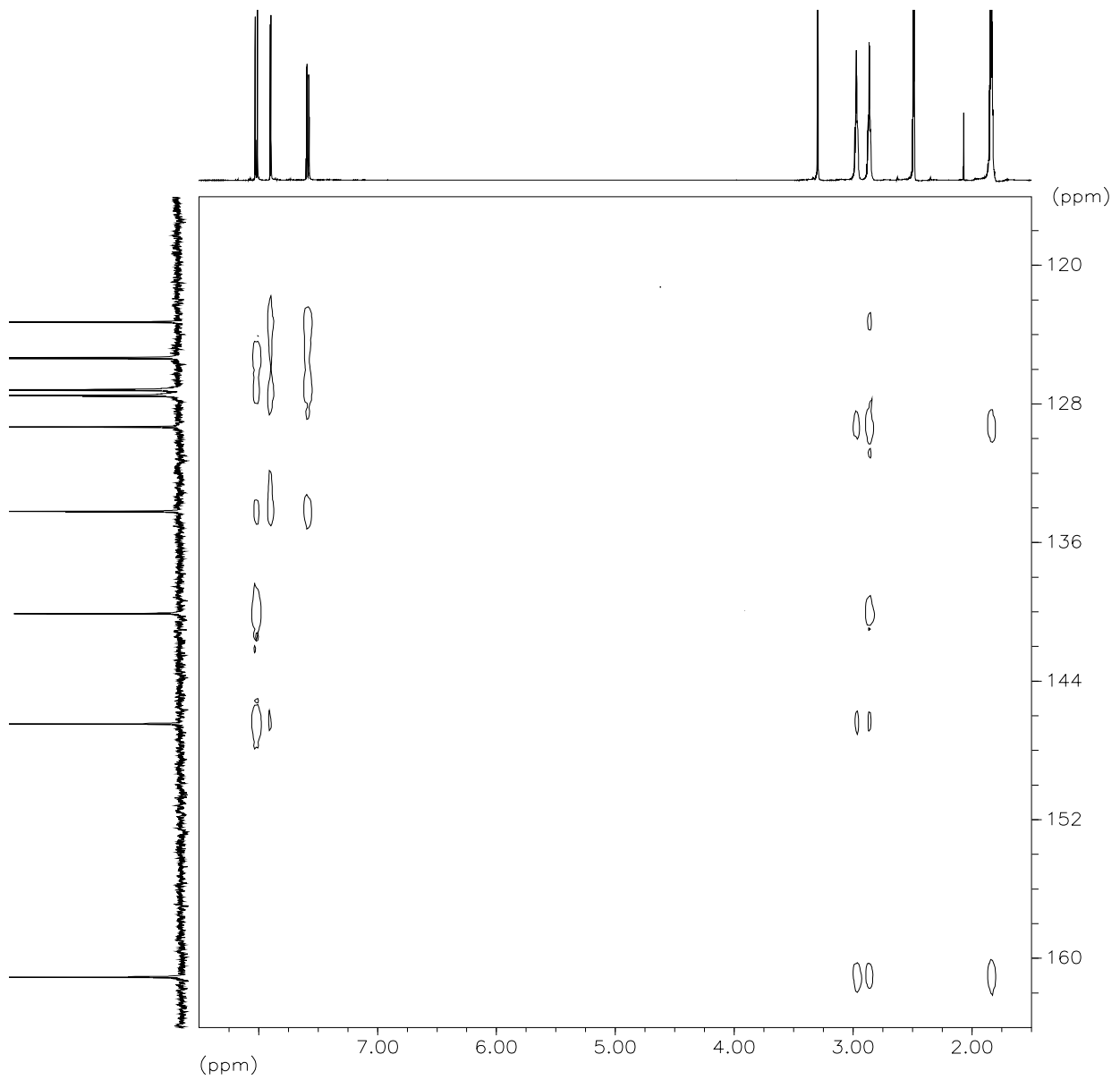
HMBC IV

3-(3,4,5-Trimethoxyphenyl)-*N*-(4-oxo-4-(2-(1,2,3,4-tetrahydroacridin-9-yl)hydrazino)butyl)-propanamide HCl
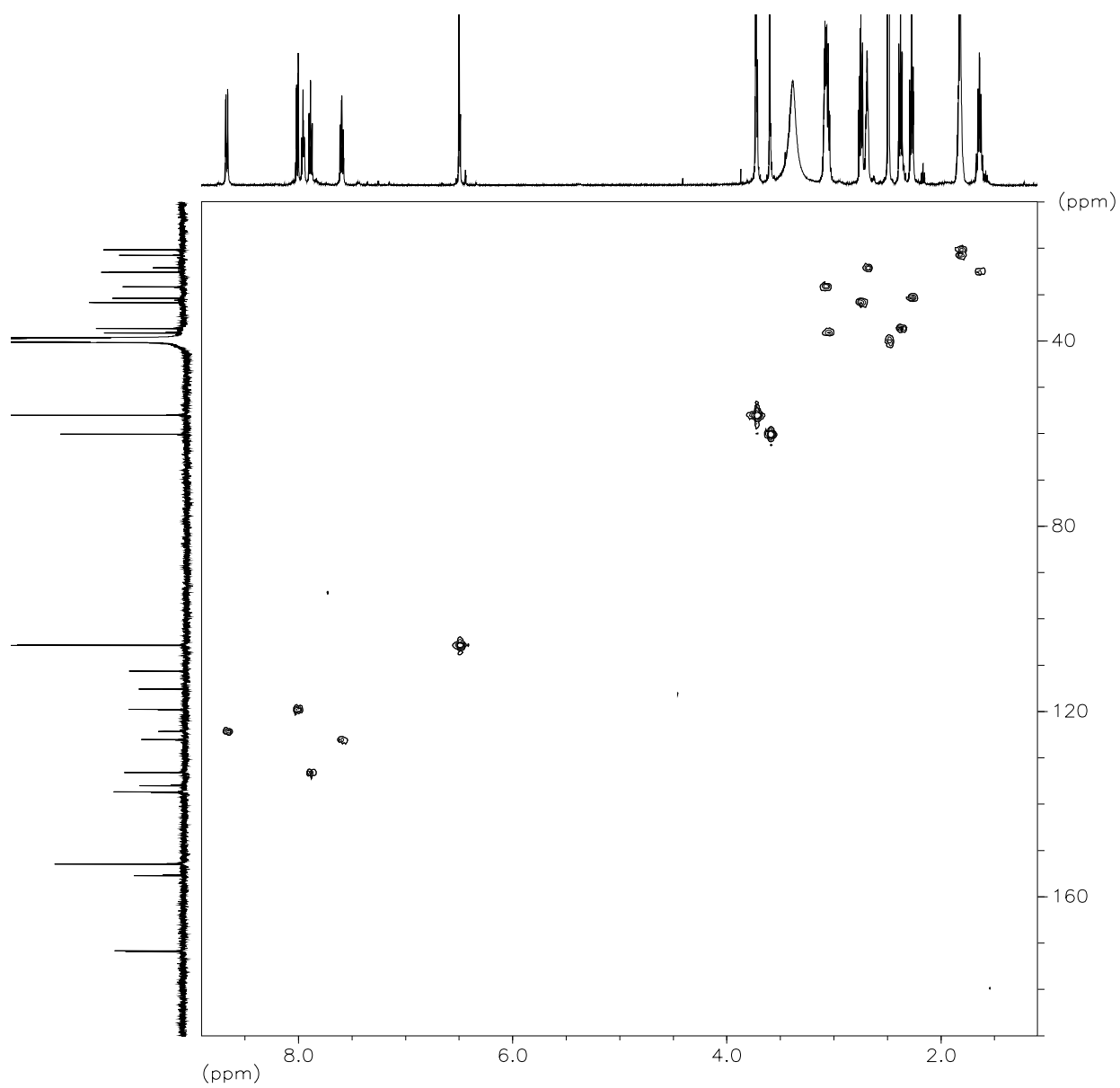
HSQC I

3-(3,4,5-Trimethoxyphenyl)-*N*-(4-oxo-4-(2-(1,2,3,4-tetrahydroacridin-9-yl)hydrazino)butyl)-propanamide HCl
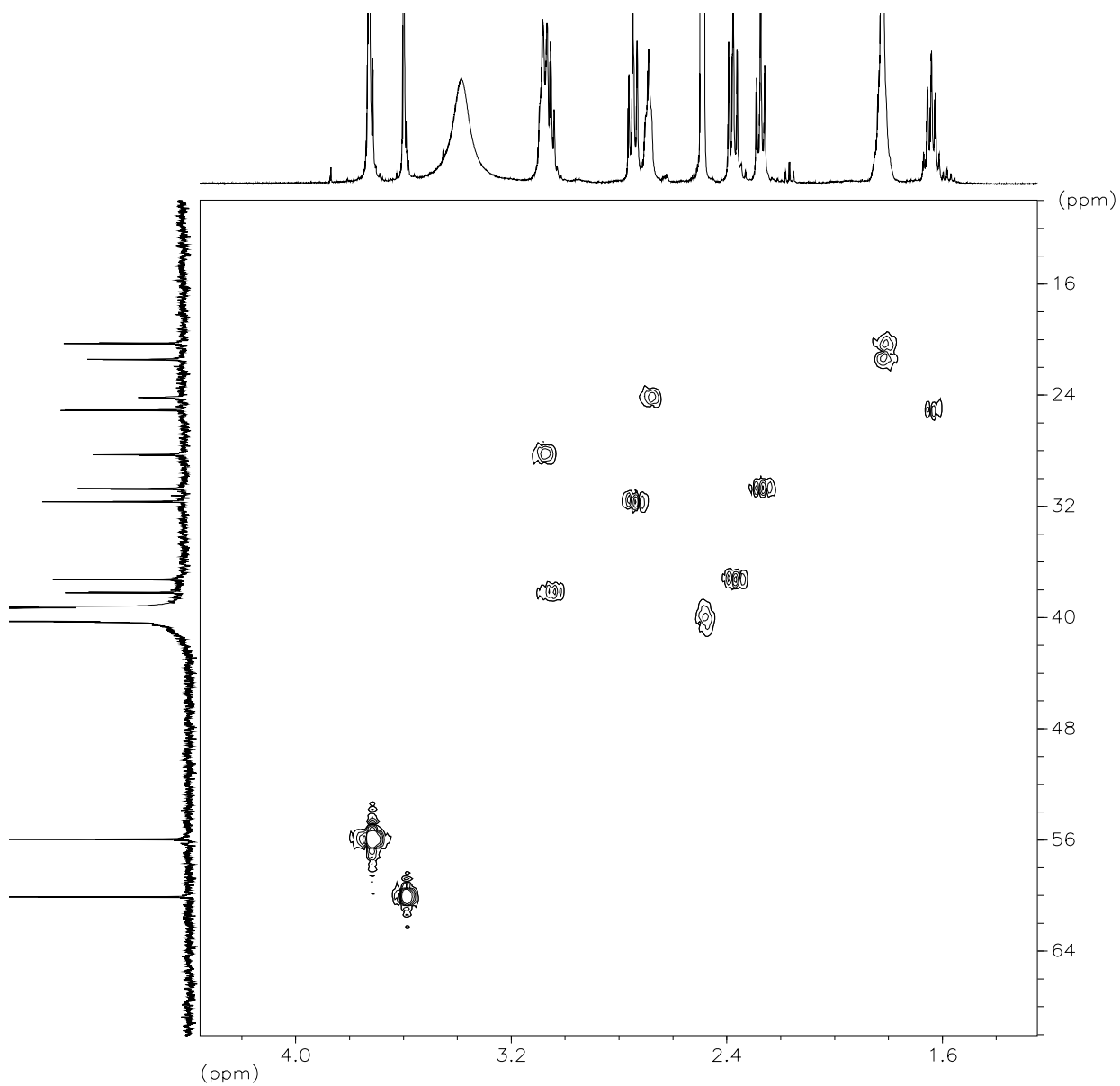
HSQC II

3-(3,4,5-Trimethoxyphenyl)-*N*-(4-oxo-4-(2-(1,2,3,4-tetrahydroacridin-9-yl)hydrazino)butyl)-propanamide HCl

HSQC III
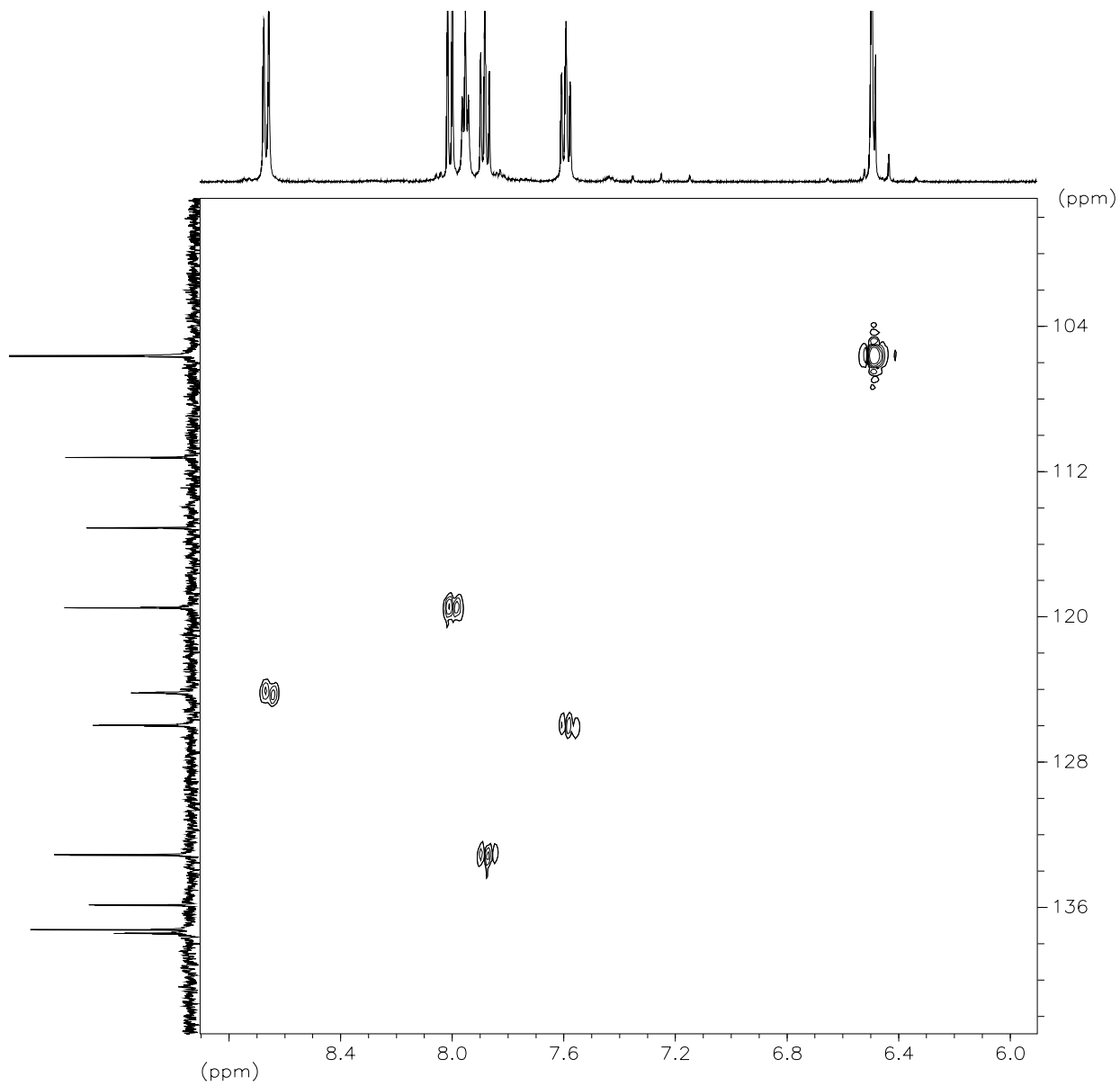
3-(3,4,5-Trimethoxyphenyl)-*N*-(4-oxo-4-(2-(1,2,3,4-tetrahydroacridin-9-yl)hydrazino)butyl)-propanamide HCl
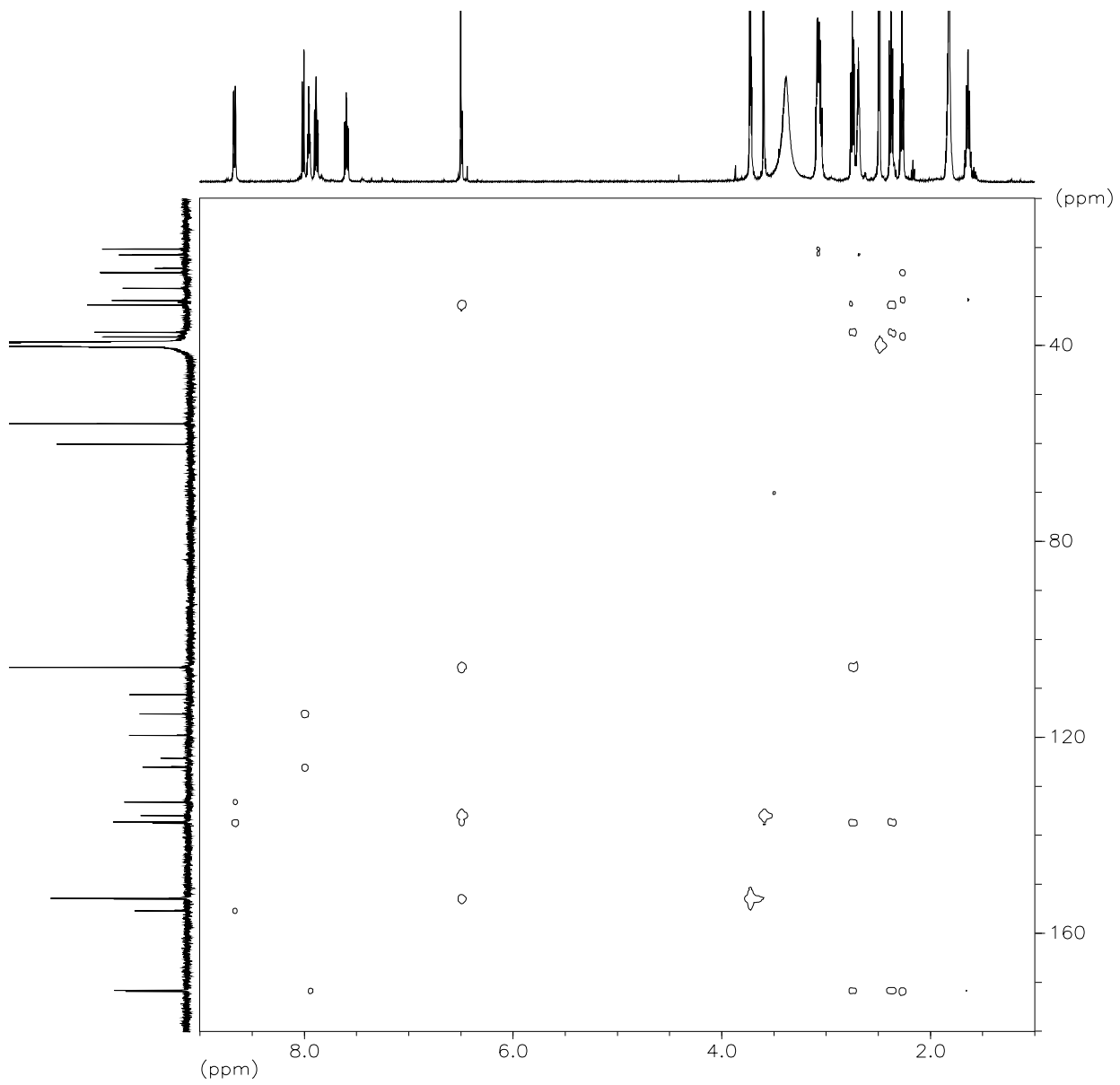
HMBC I

3-(3,4,5-Trimethoxyphenyl)-*N*-(4-oxo-4-(2-(1,2,3,4-tetrahydroacridin-9-yl)hydrazino)butyl)-propanamide HCl
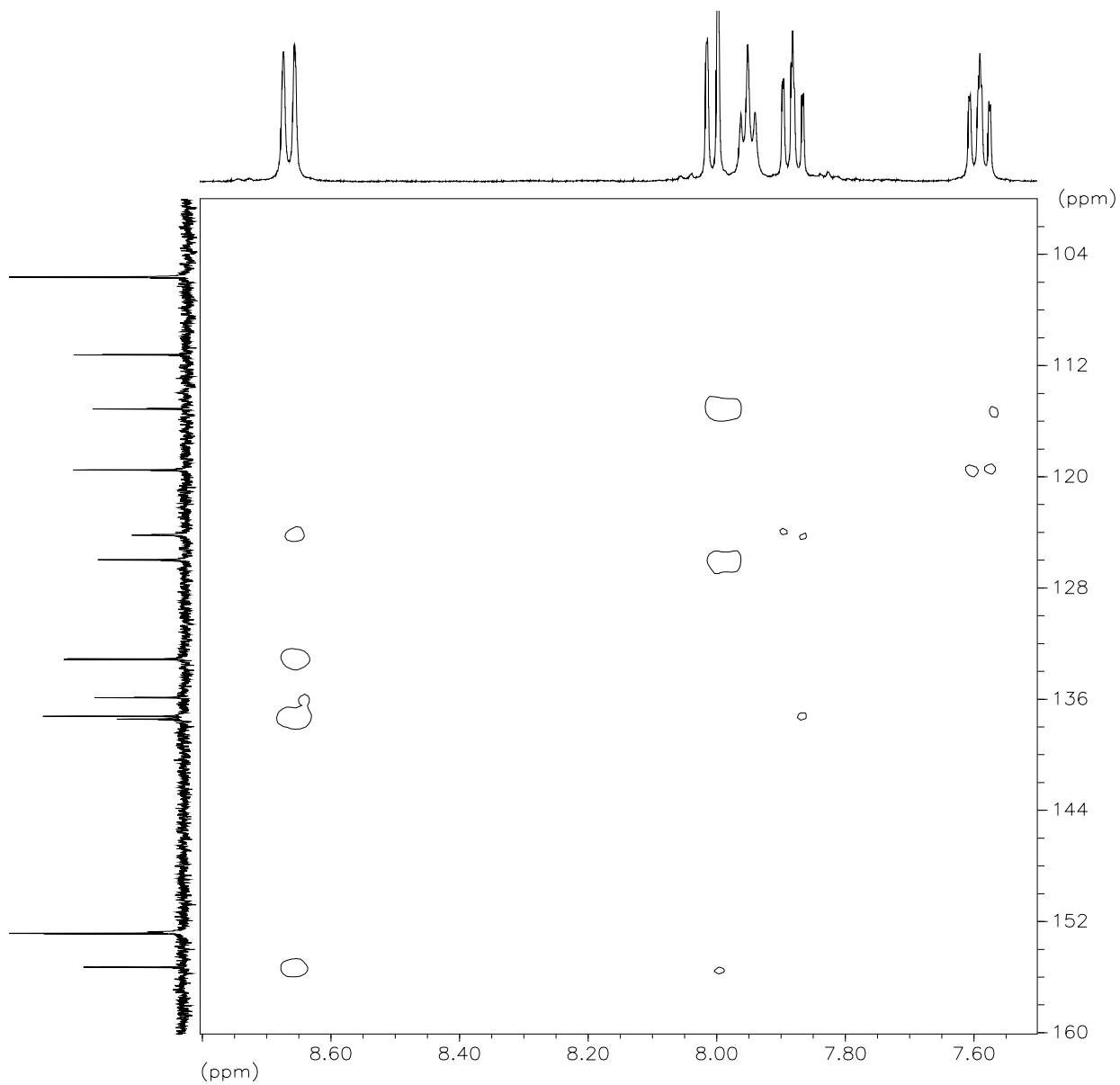
HMBC II

3-(3,4,5-Trimethoxyphenyl)-*N*-(4-oxo-4-(2-(1,2,3,4-tetrahydroacridin-9-yl)hydrazino)butyl)-propanamide HCl

HMBC III
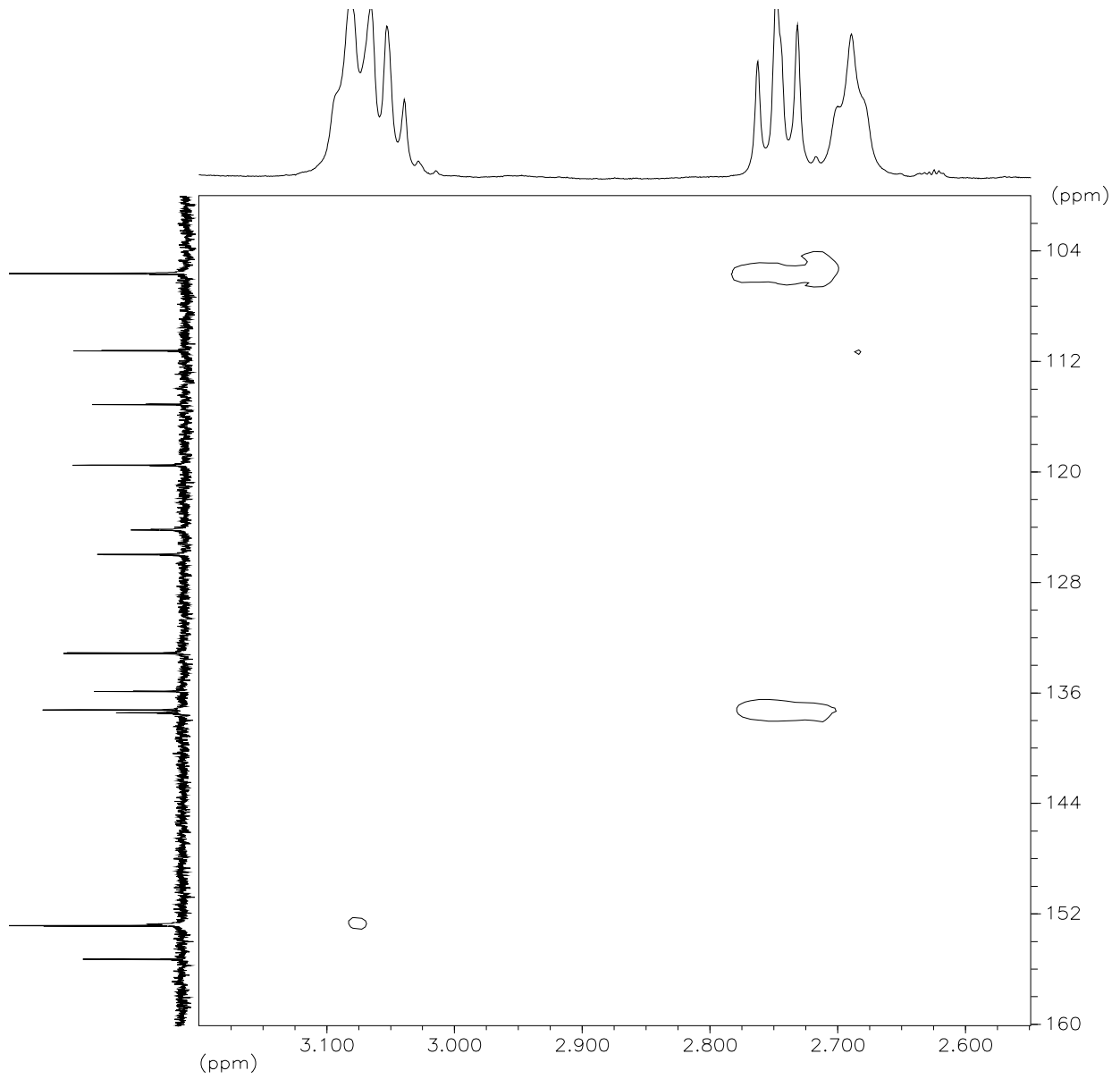
3-(3,4,5-Trimethoxyphenyl)-*N*-(4-oxo-4-(2-(1,2,3,4-tetrahydroacridin-9-yl)hydrazino)butyl)-propanamide
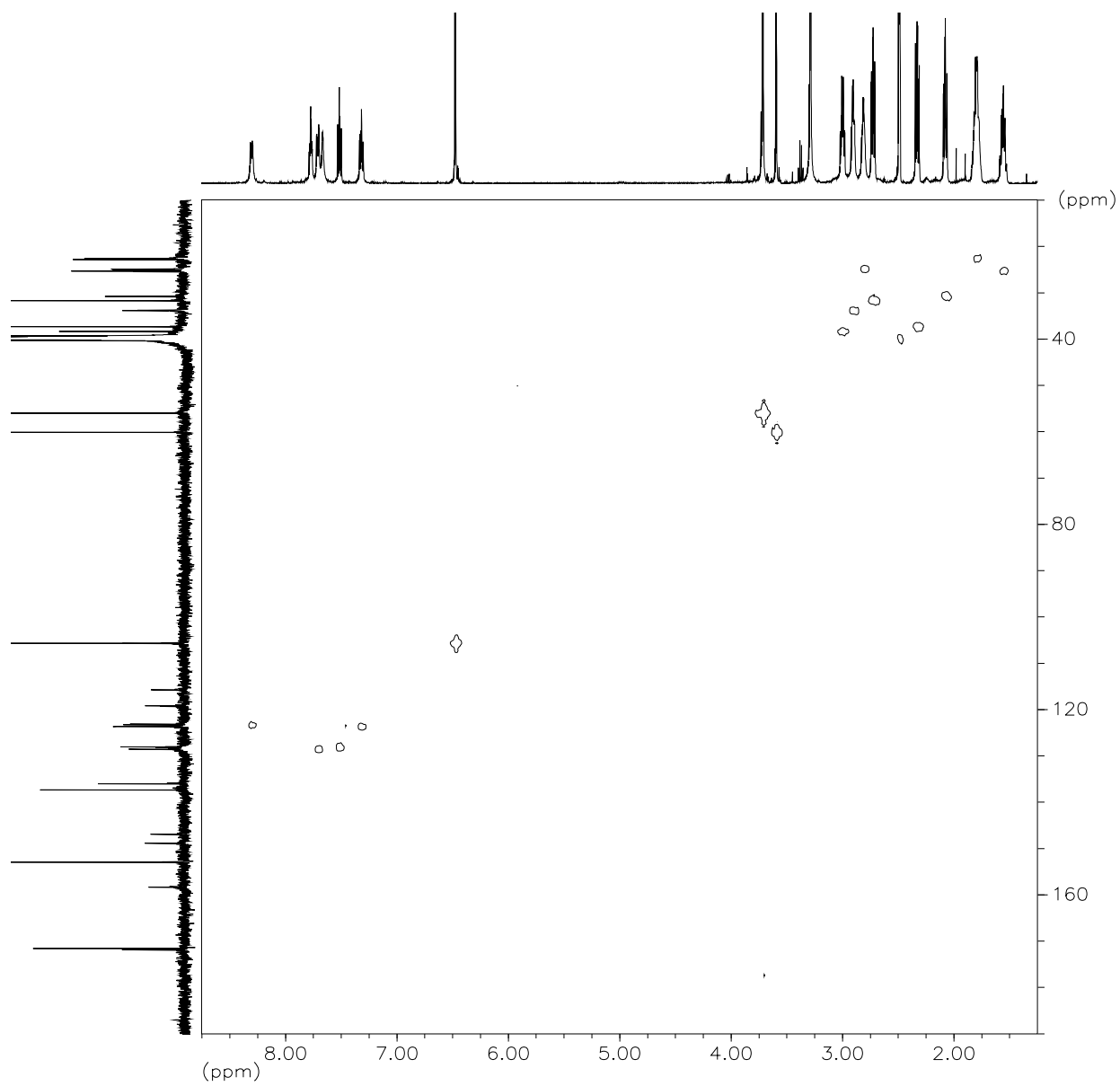
HSQC I

3-(3,4,5-Trimethoxyphenyl)-*N*-(4-oxo-4-(2-(1,2,3,4-tetrahydroacridin-9-yl)hydrazino)butyl)-propanamide
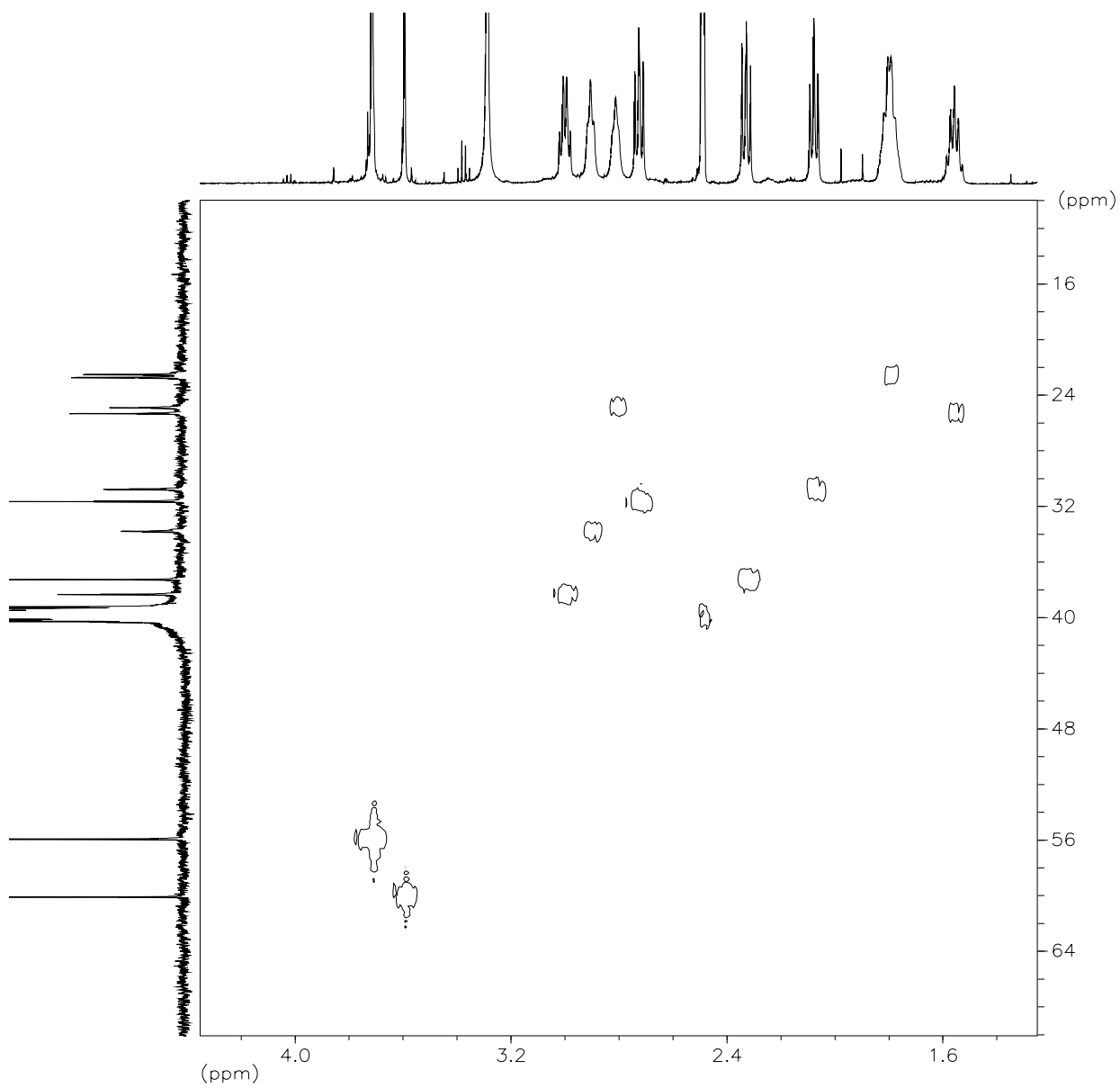
HSQC II

**3-(3,4,5-Trimethoxyphenyl)-*N*-(4-oxo-4-(2-(1,2,3,4-tetrahydroacridin-9-yl)hydrazino)butyl)-propanamide**

HSQC III
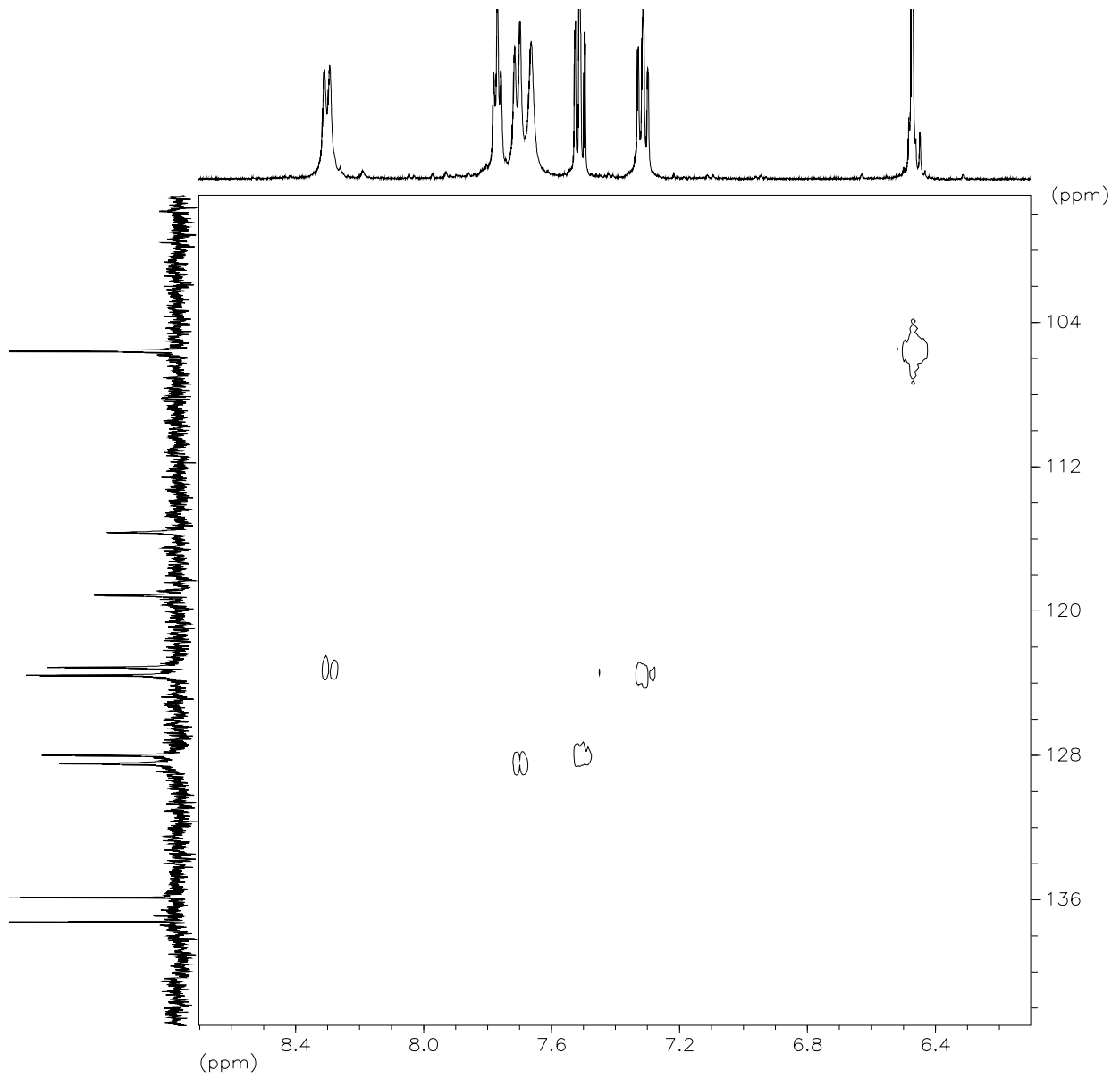
3-(3,4,5-Trimethoxyphenyl)-*N*-(4-oxo-4-(2-(1,2,3,4-tetrahydroacridin-9-yl)hydrazino)butyl)-propanamide
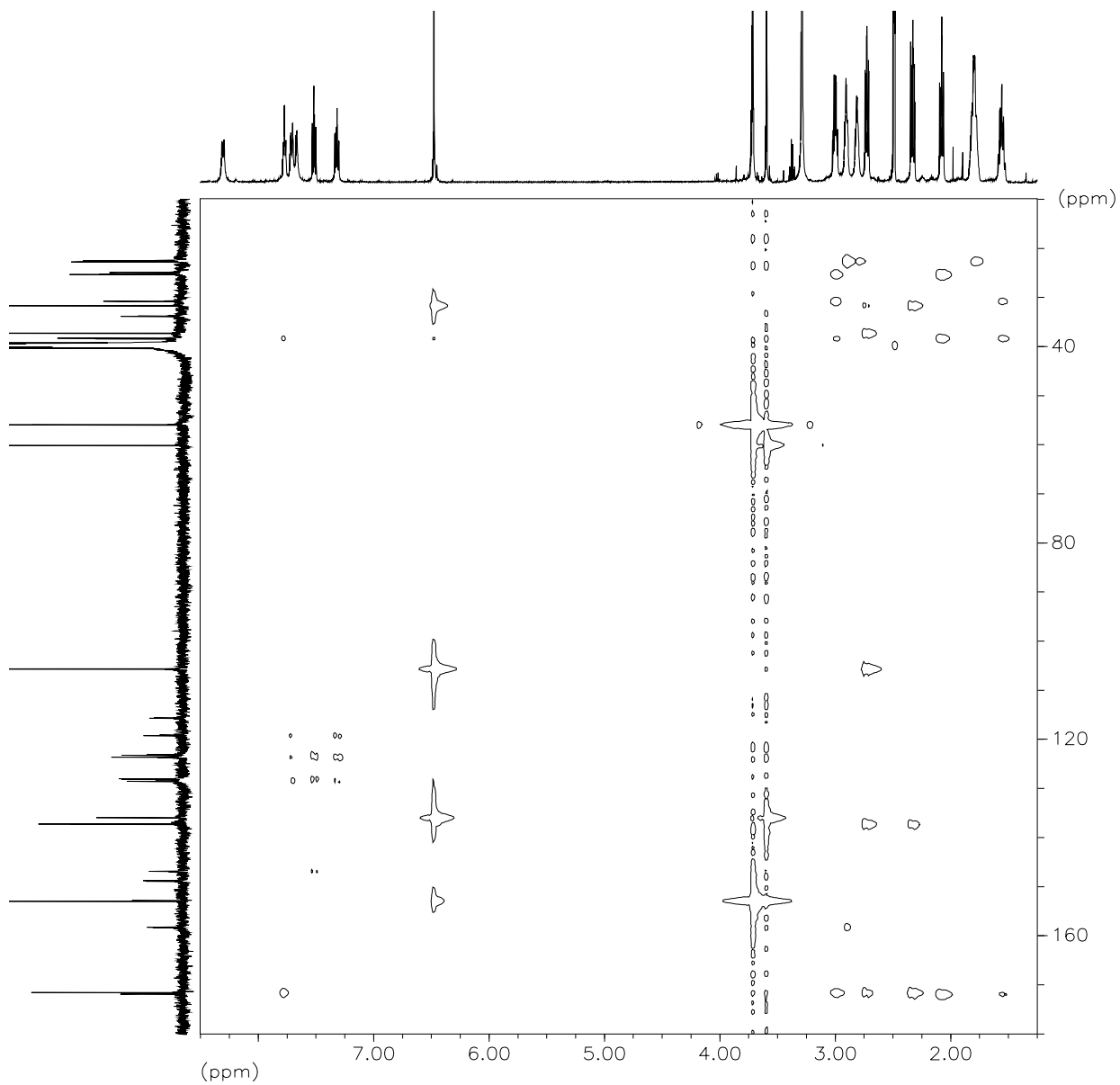
HMBC I

**3-(3,4,5-Trimethoxyphenyl)-*N*-(4-oxo-4-(2-(1,2,3,4-tetrahydroacridin-9-yl)hydrazino)butyl)-propanamide**
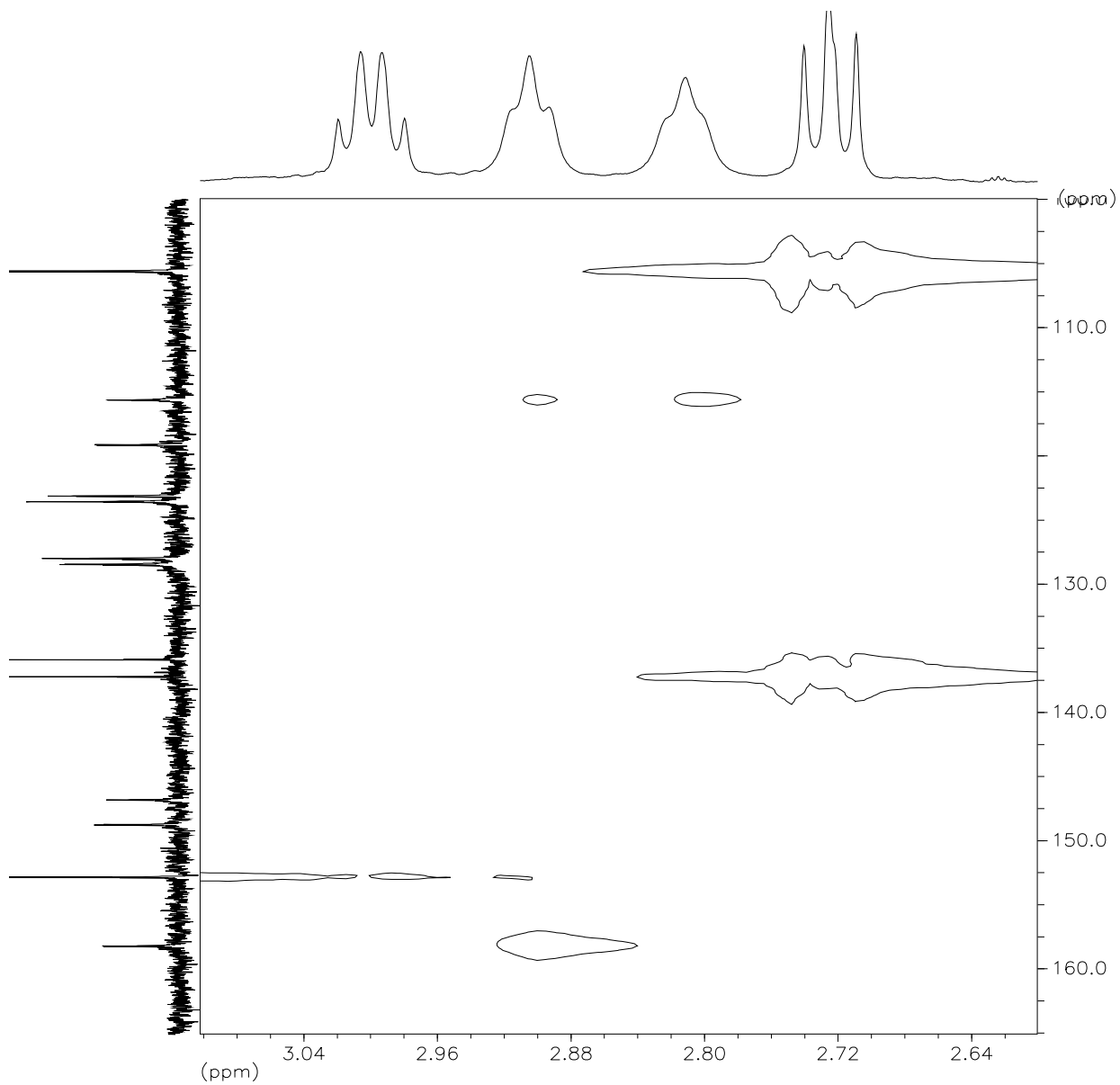
HMBC II

3-(3,4,5-Trimethoxyphenyl)-*N*-(4-oxo-4-(2-(1,2,3,4-tetrahydroacridin-9-yl)hydrazino)butyl)-propanamide

HMBC III
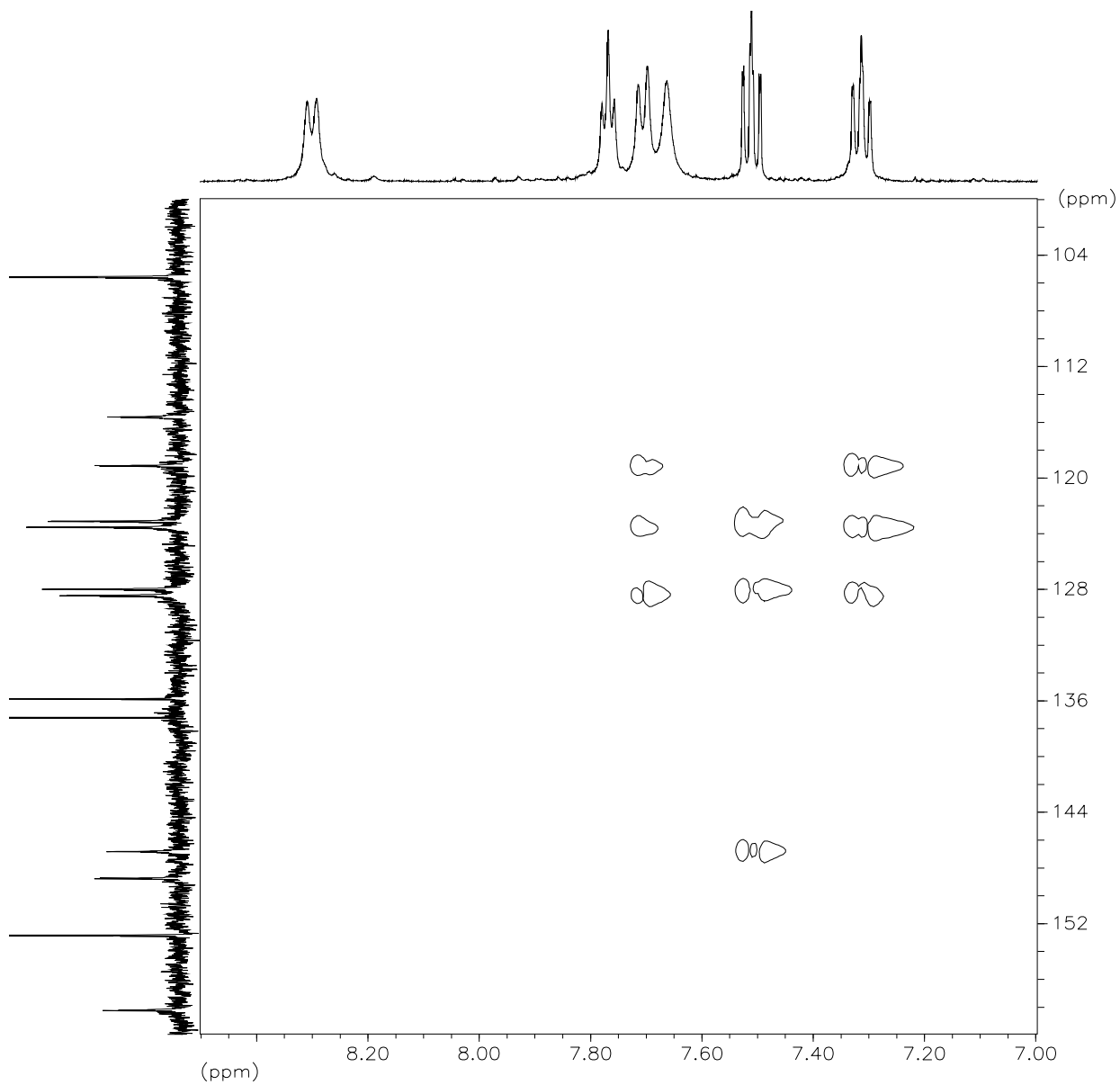
2-(4-(((6-(2-(6-Chloro-1,2,3,4-tetrahydroacridin-9-yl)hydrazino)-6-oxohexyl)amino)carbonyl)-phenoxy)-*N,N,N*-triethyl-ethanaminium bromide HCl
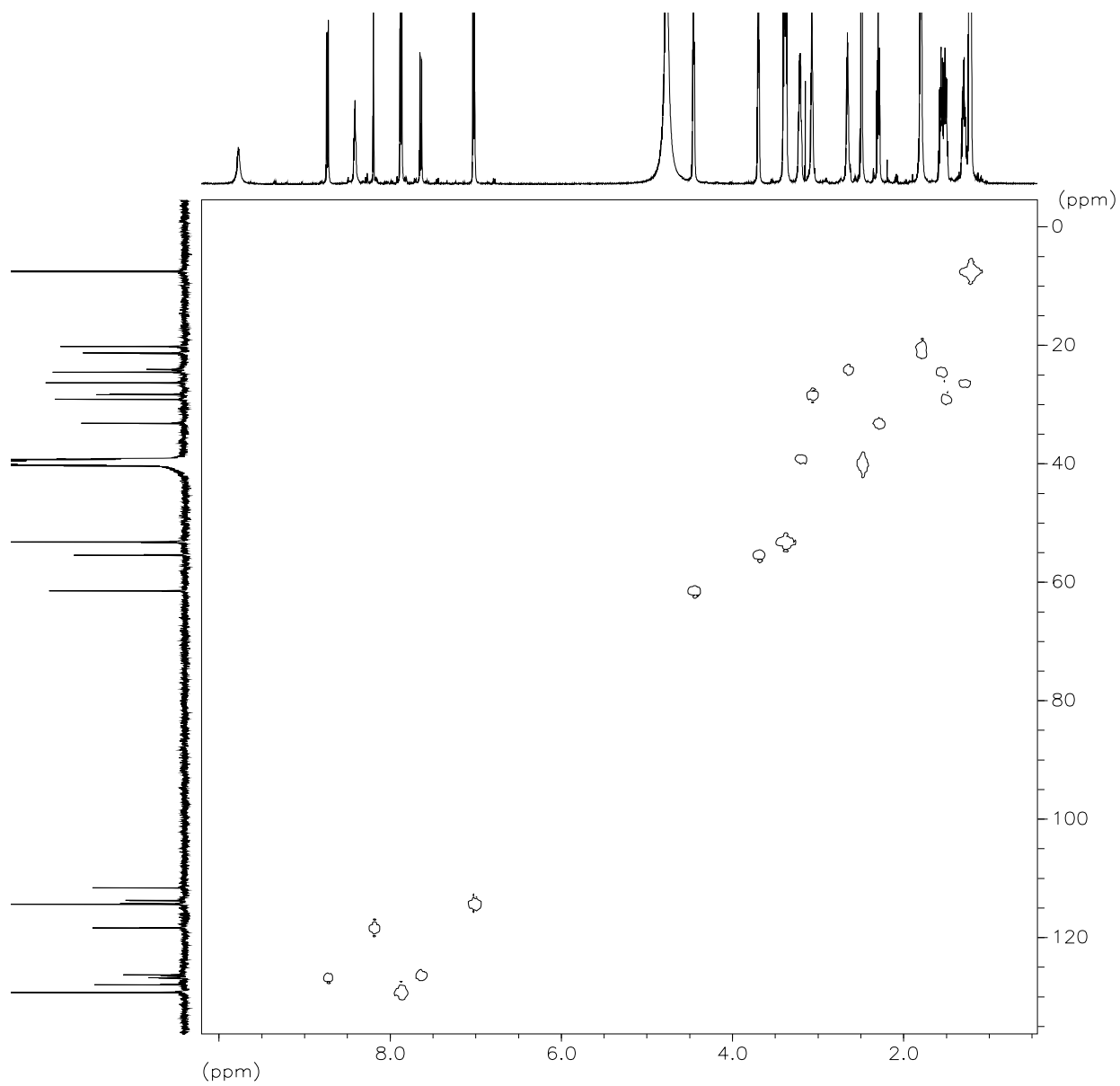
HSQC I

2-(4-(((6-(2-(6-Chloro-1,2,3,4-tetrahydroacridin-9-yl)hydrazino)-6-oxohexyl)amino)carbonyl)-phenoxy)-*N,N,N*-triethyl-ethanaminium bromide HCl
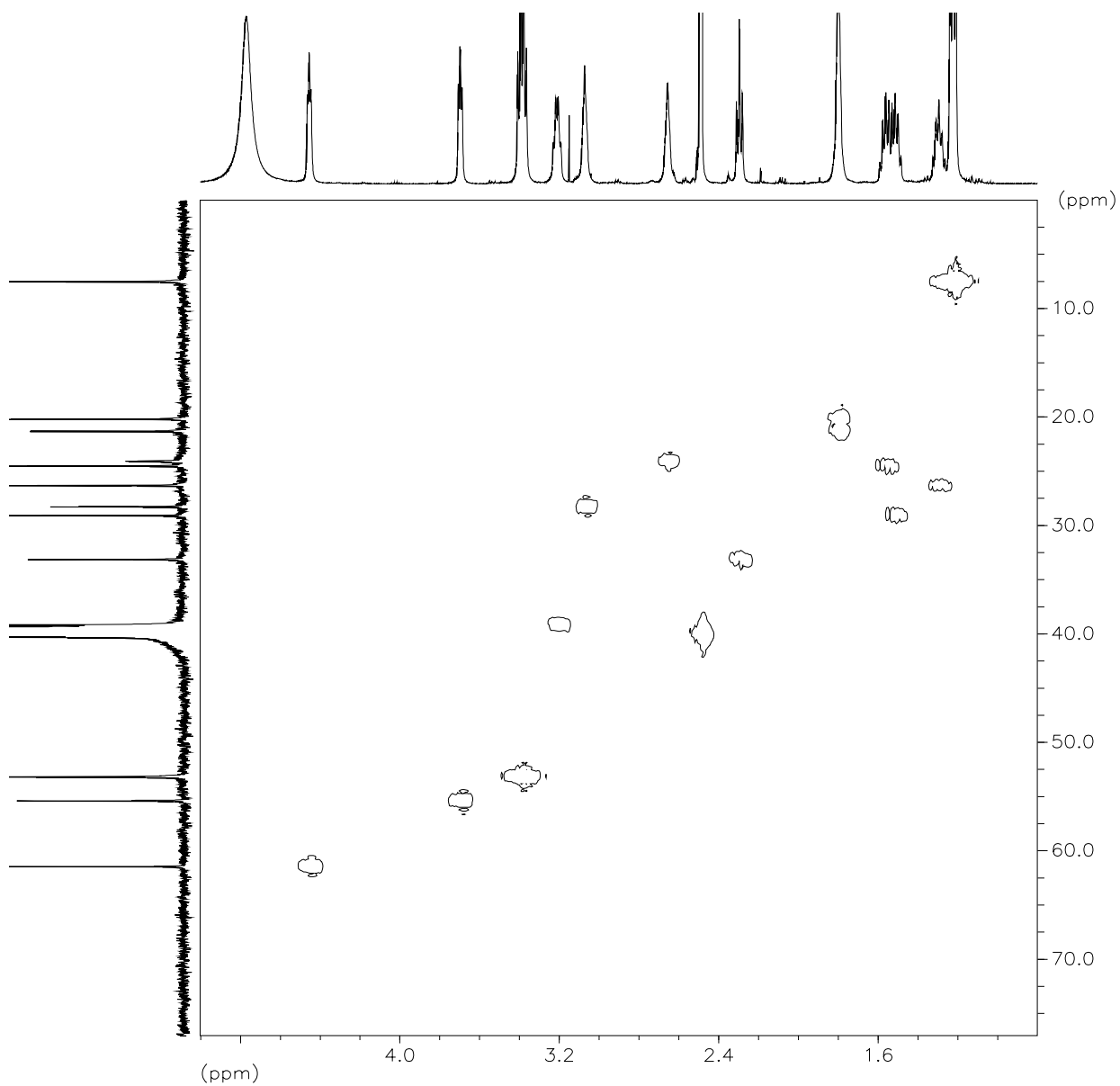
HSQC II

2-(4-(((6-(2-(6-Chloro-1,2,3,4-tetrahydroacridin-9-yl)hydrazino)-6-oxohexyl)amino)carbonyl)-phenoxy)-*N,N,N*-triethyl-ethanaminium bromide HCl

HSQC III
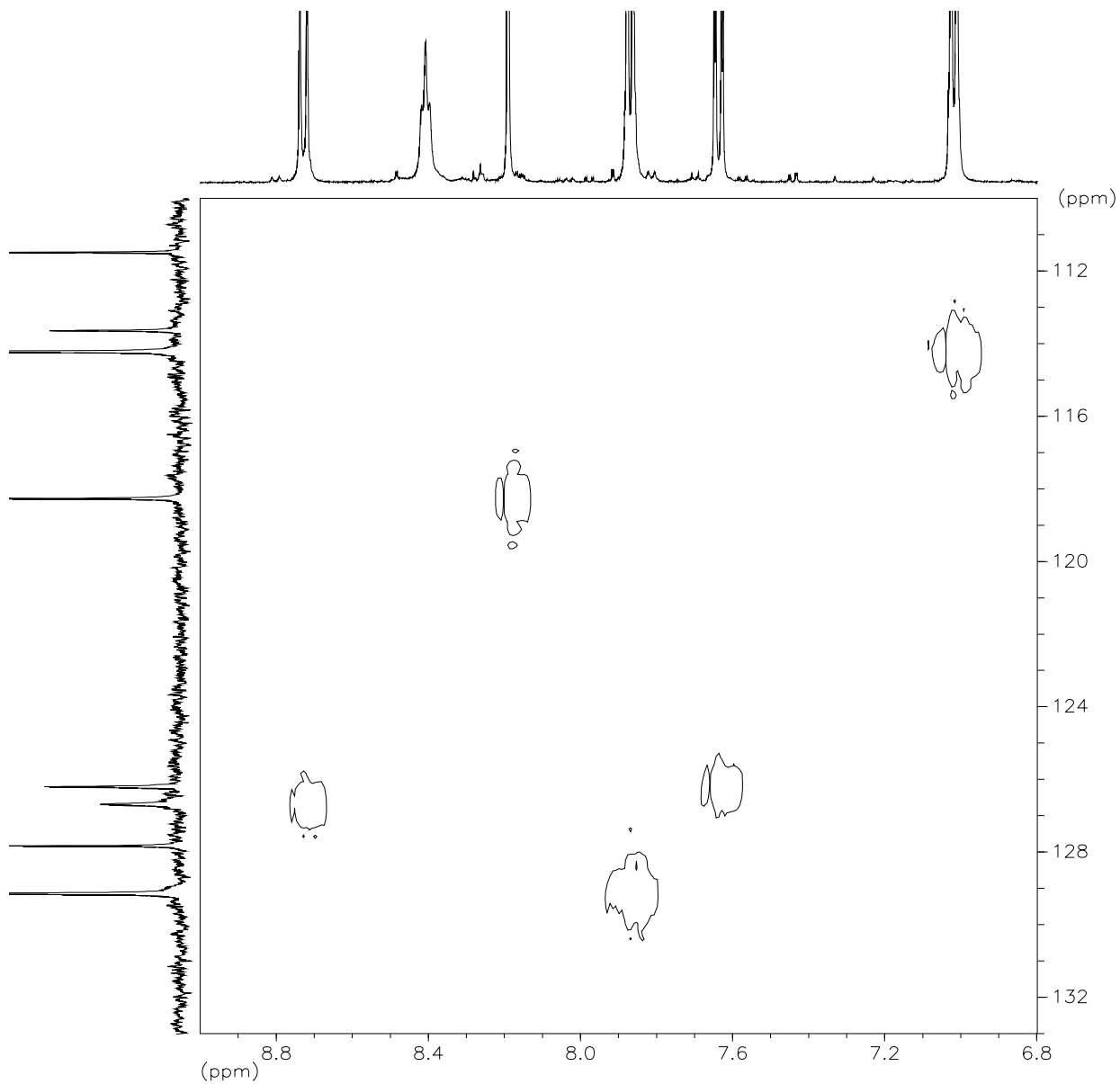
2-(4-(((6-(2-(6-Chloro-1,2,3,4-tetrahydroacridin-9-yl)hydrazino)-6-oxohexyl)amino)carbonyl)-phenoxy)-*N*,*N*,*N*-triethyl-ethanaminium bromide HCl
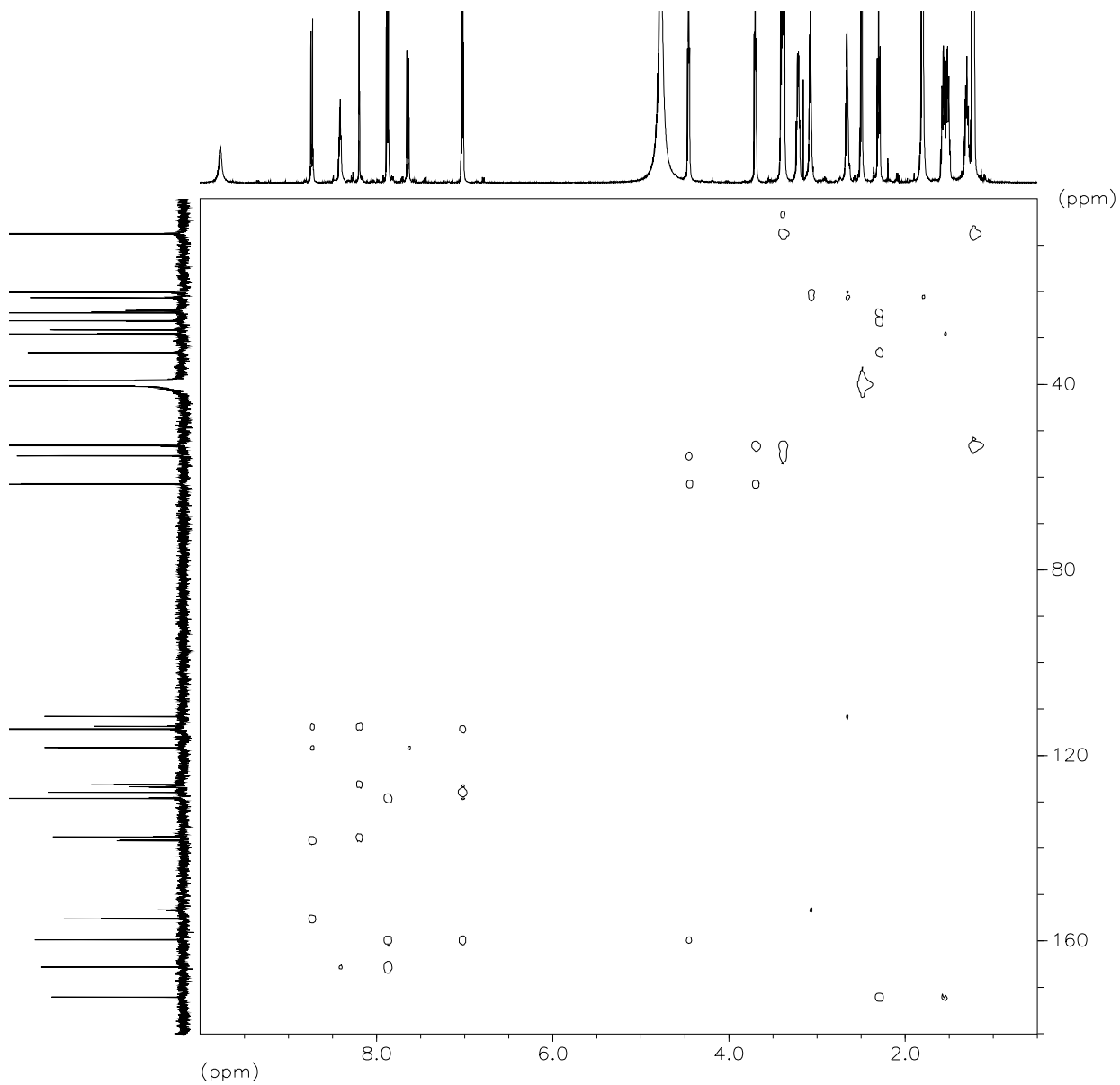
HMBC I

2-(4-(((6-(2-(6-Chloro-1,2,3,4-tetrahydroacridin-9-yl)hydrazino)-6-oxohexyl)amino)carbonyl)-phenoxy)-*N,N,N*-triethyl-ethanaminium bromide HCl
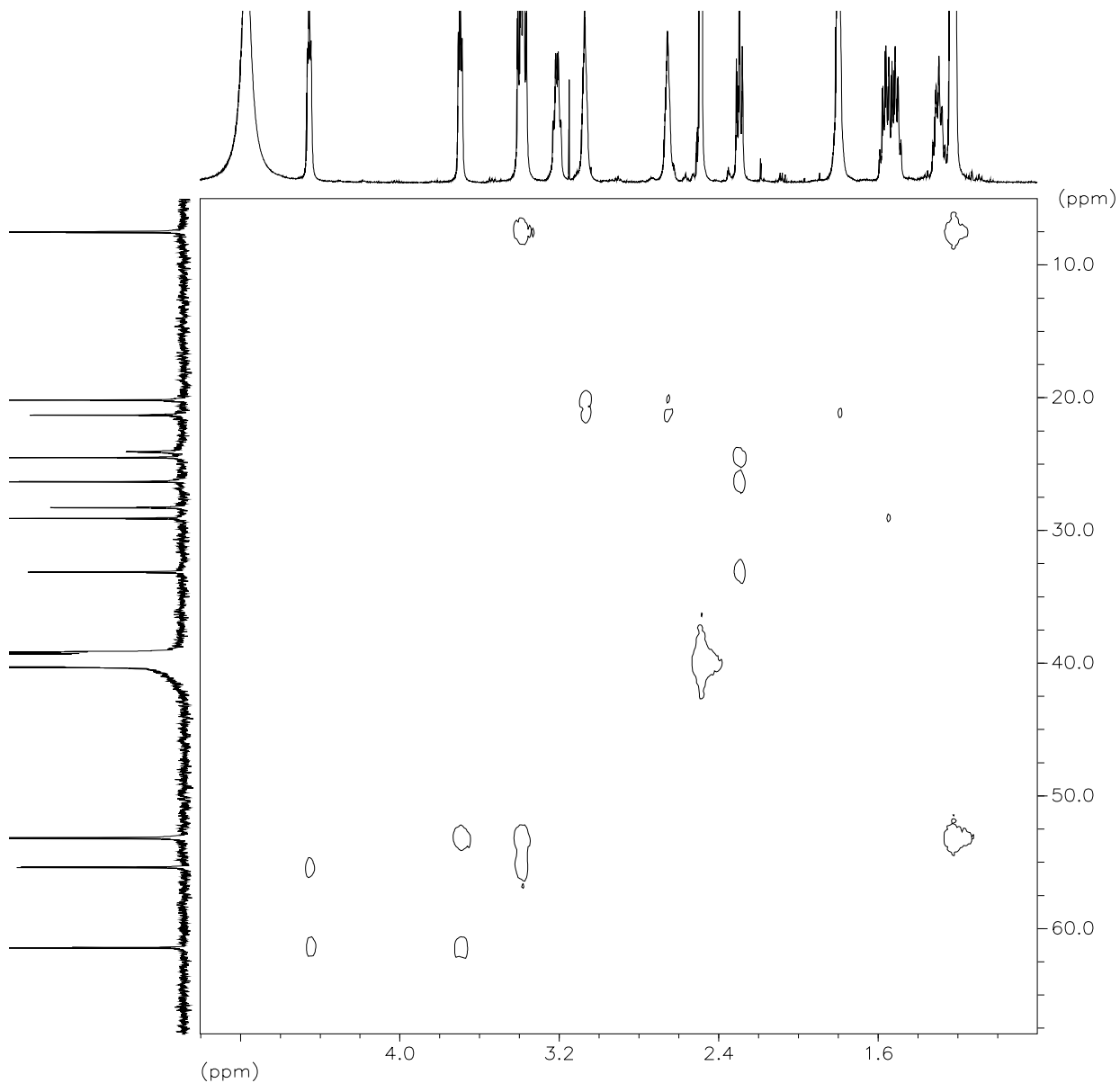
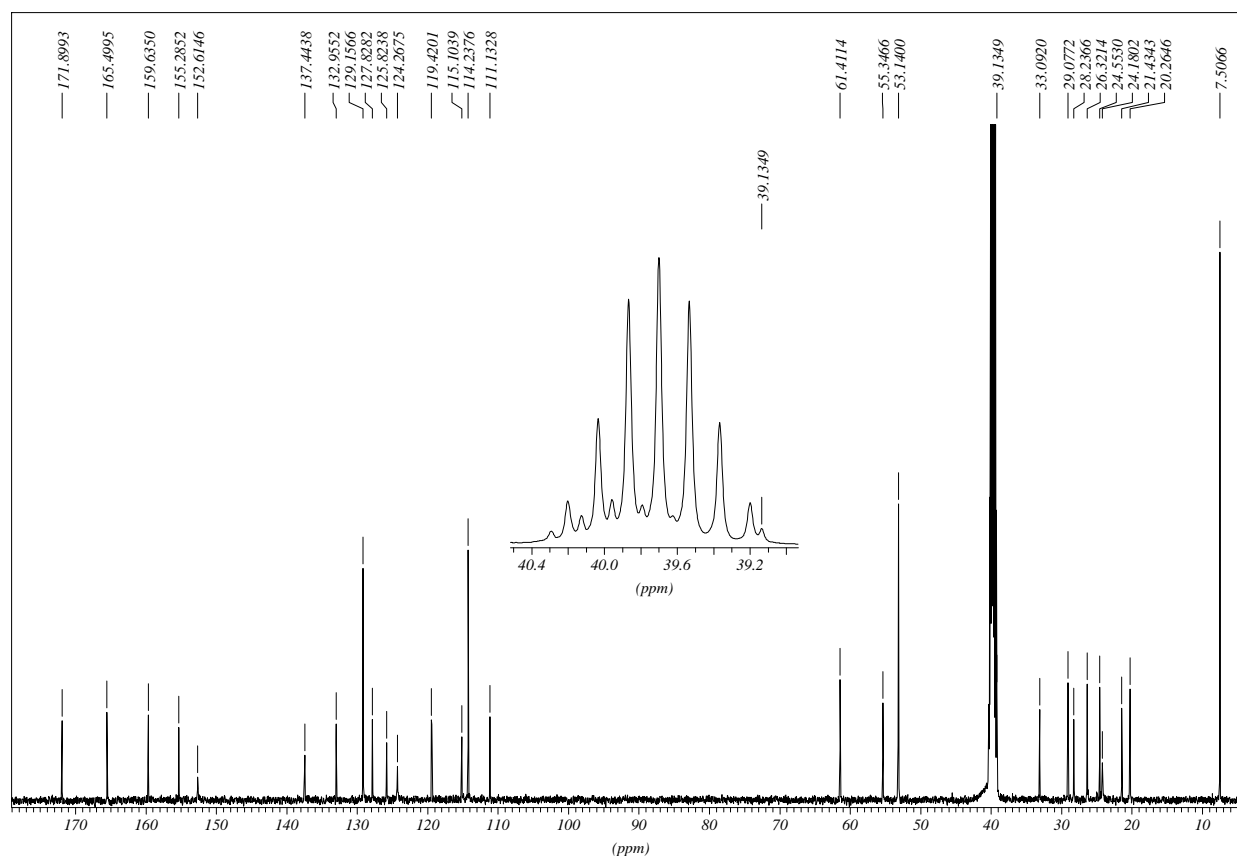HMBC II

2-(4-(((6-(2-(6-Chloro-1,2,3,4-tetrahydroacridin-9-yl)hydrazino)-6-oxohexyl)amino)carbonyl)-phenoxy)-*N,N,N*-triethyl-ethanaminium bromide HCl

HMBC III
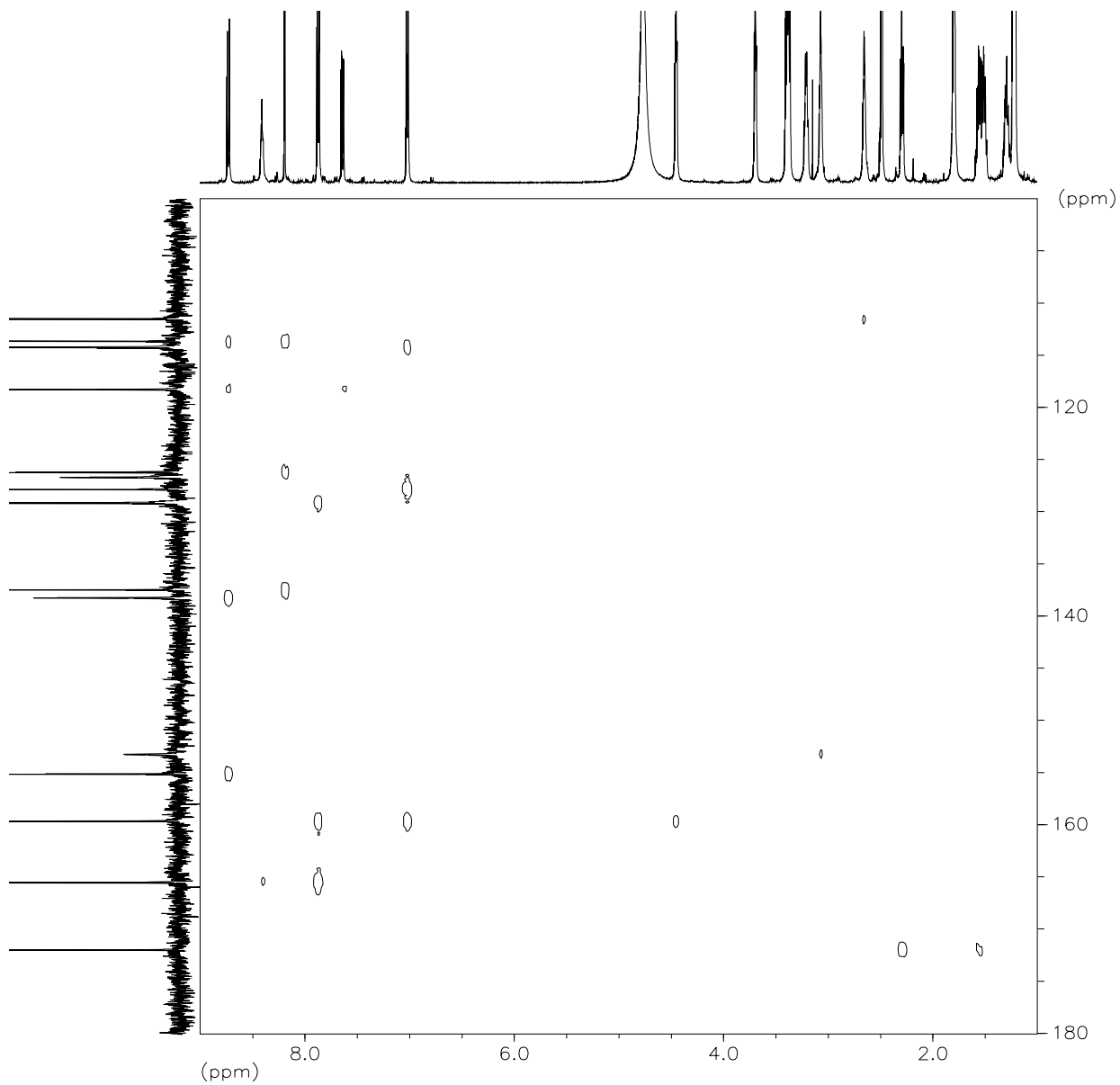
9-Chloro-1,2,3,4-tetrahydroacridine
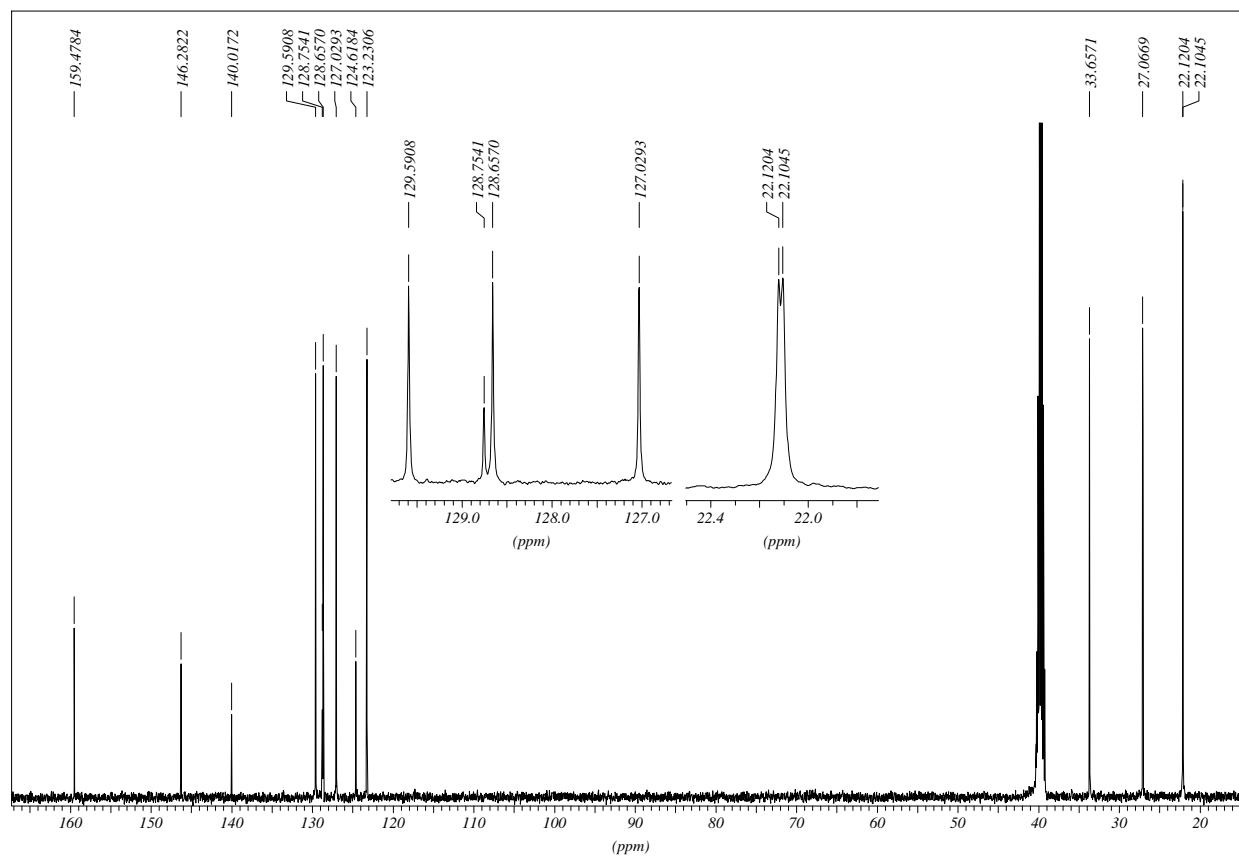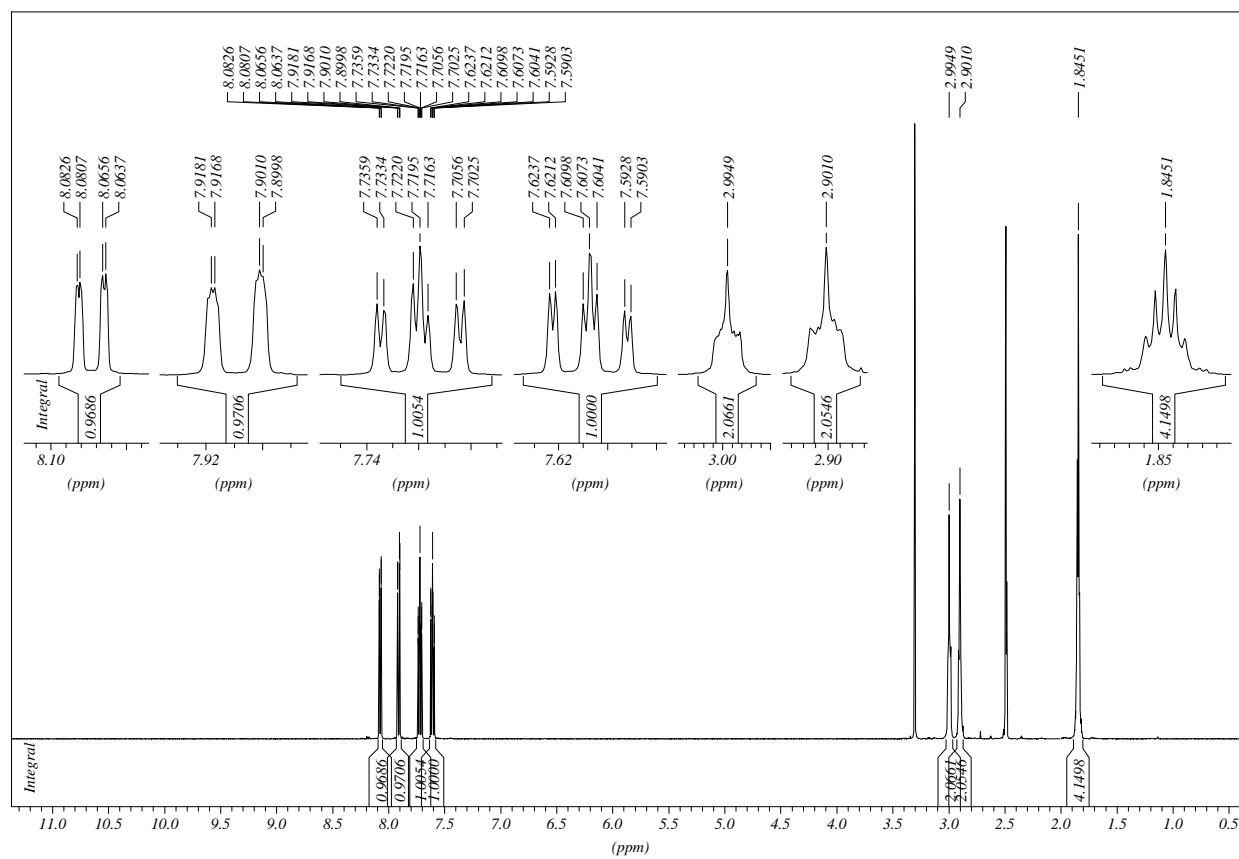
6,9-Dichloro-1,2,3,4-tetrahydroacridine
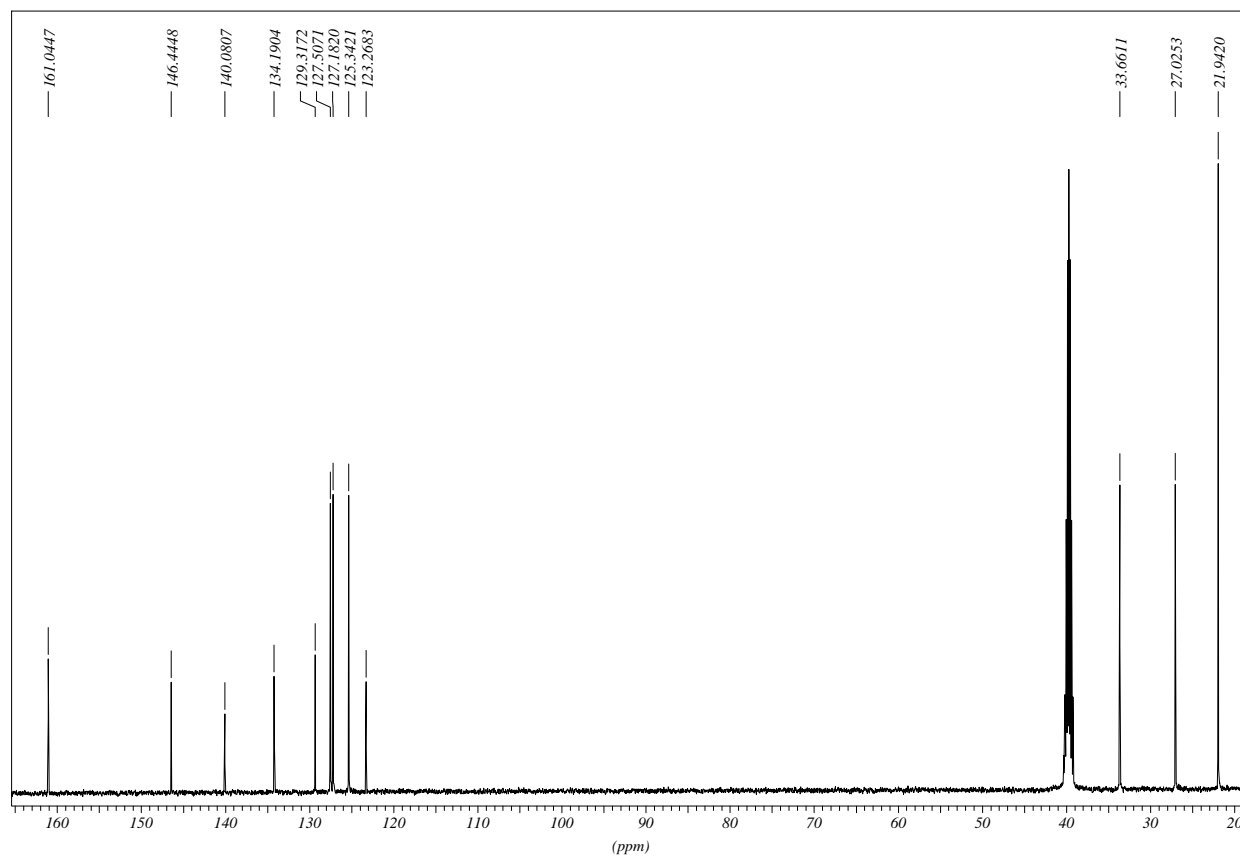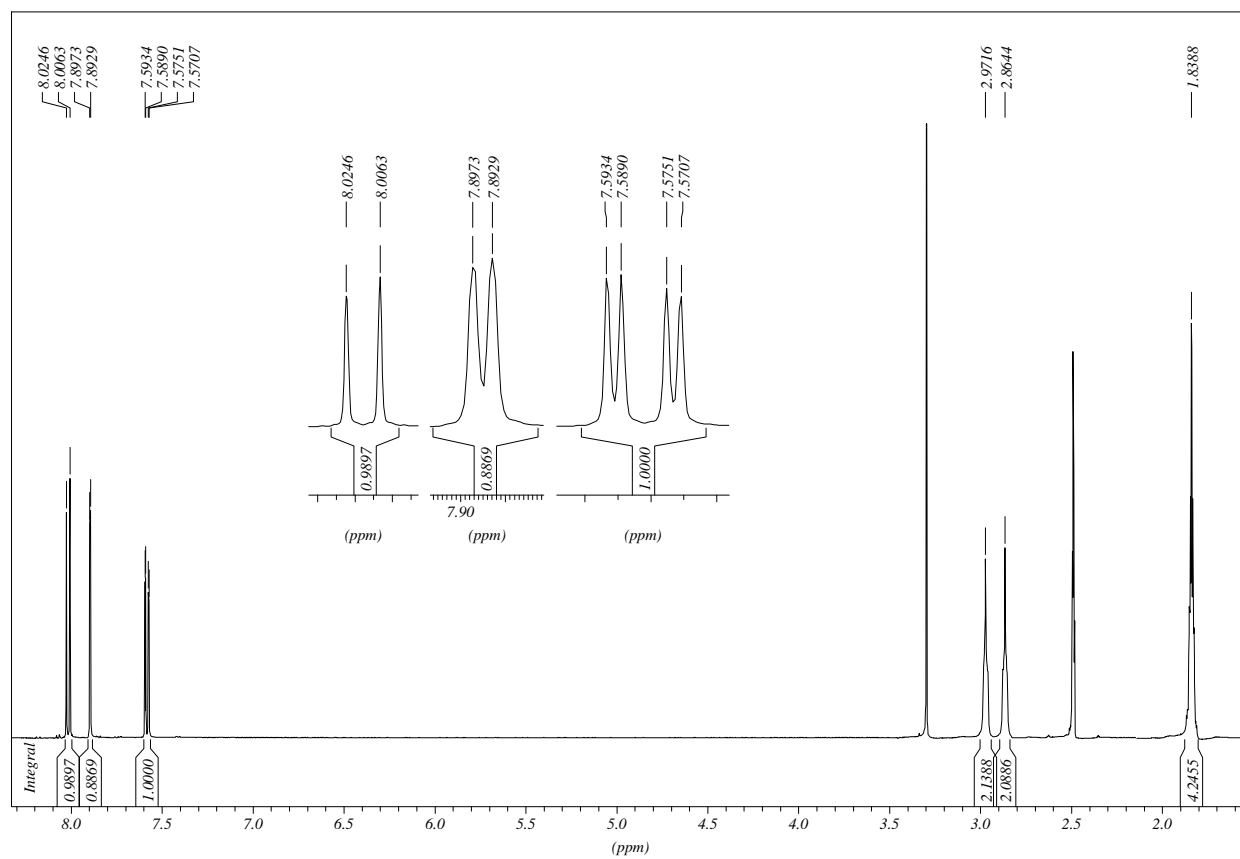
9-Hydrazino-1,2,3,4-tetrahydroacridine HCl
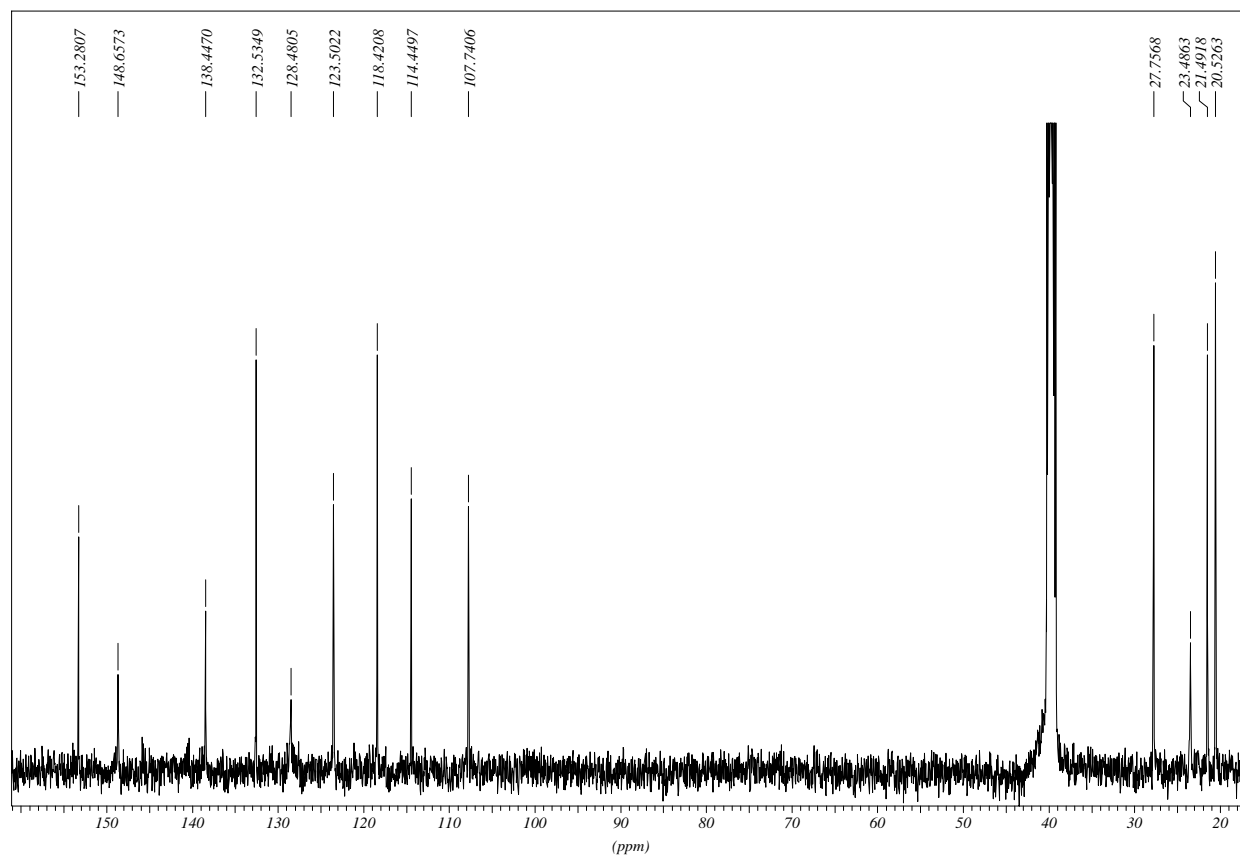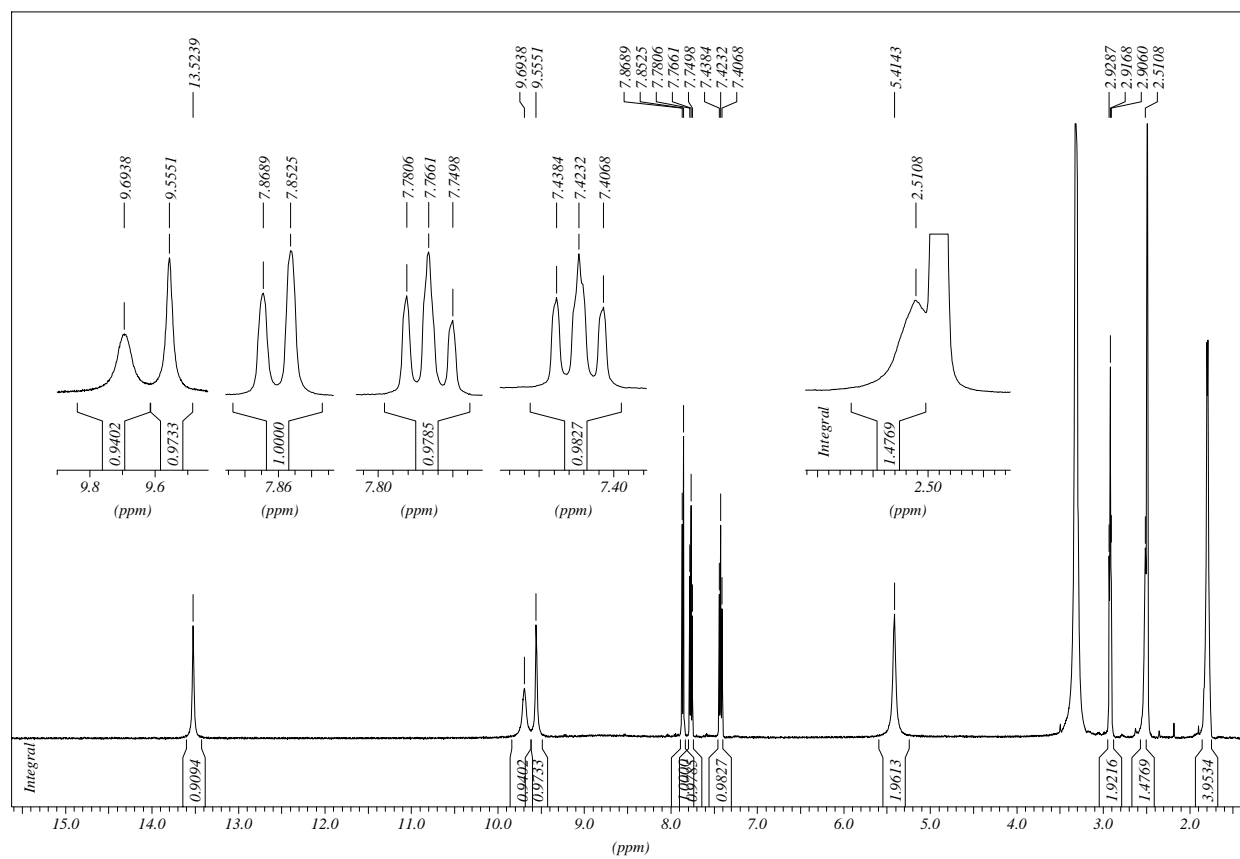
9-Hydrazino-1,2,3,4-tetrahydroacridine
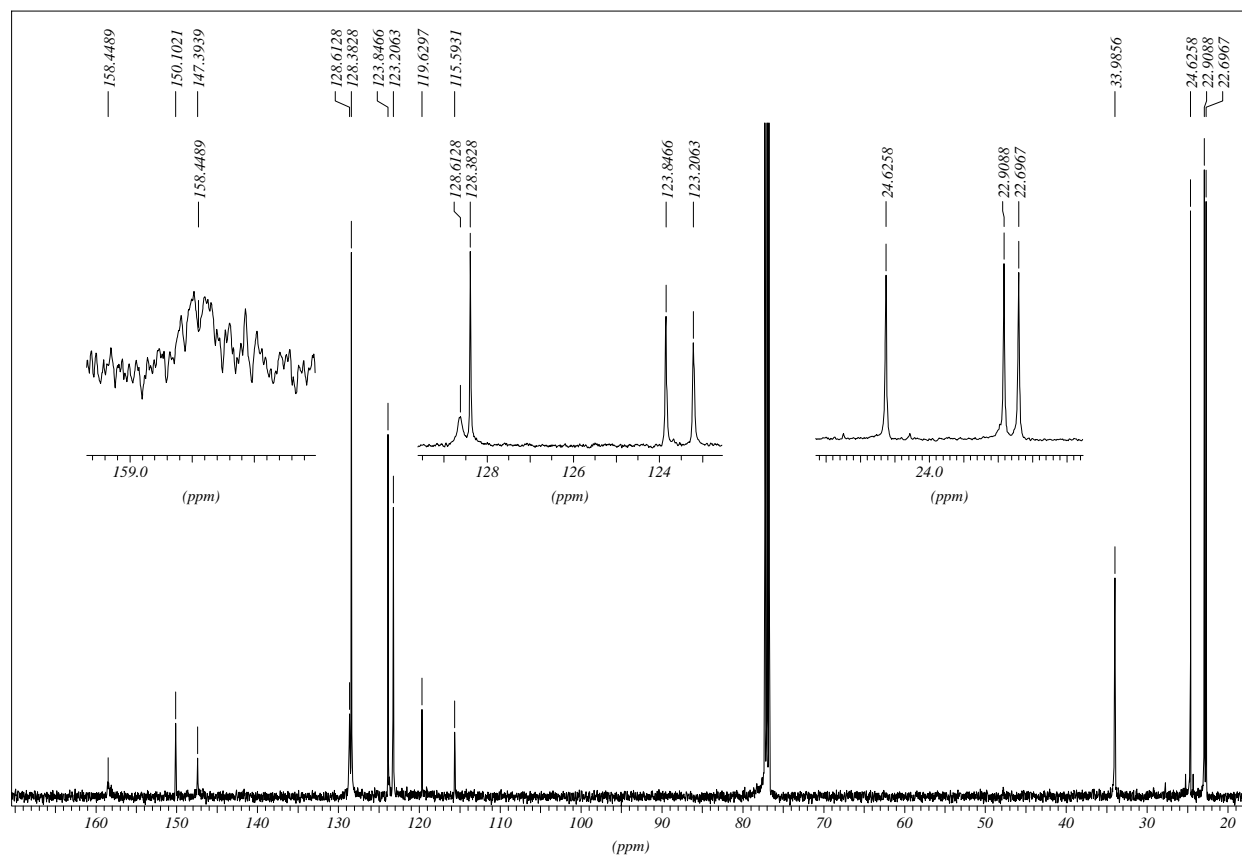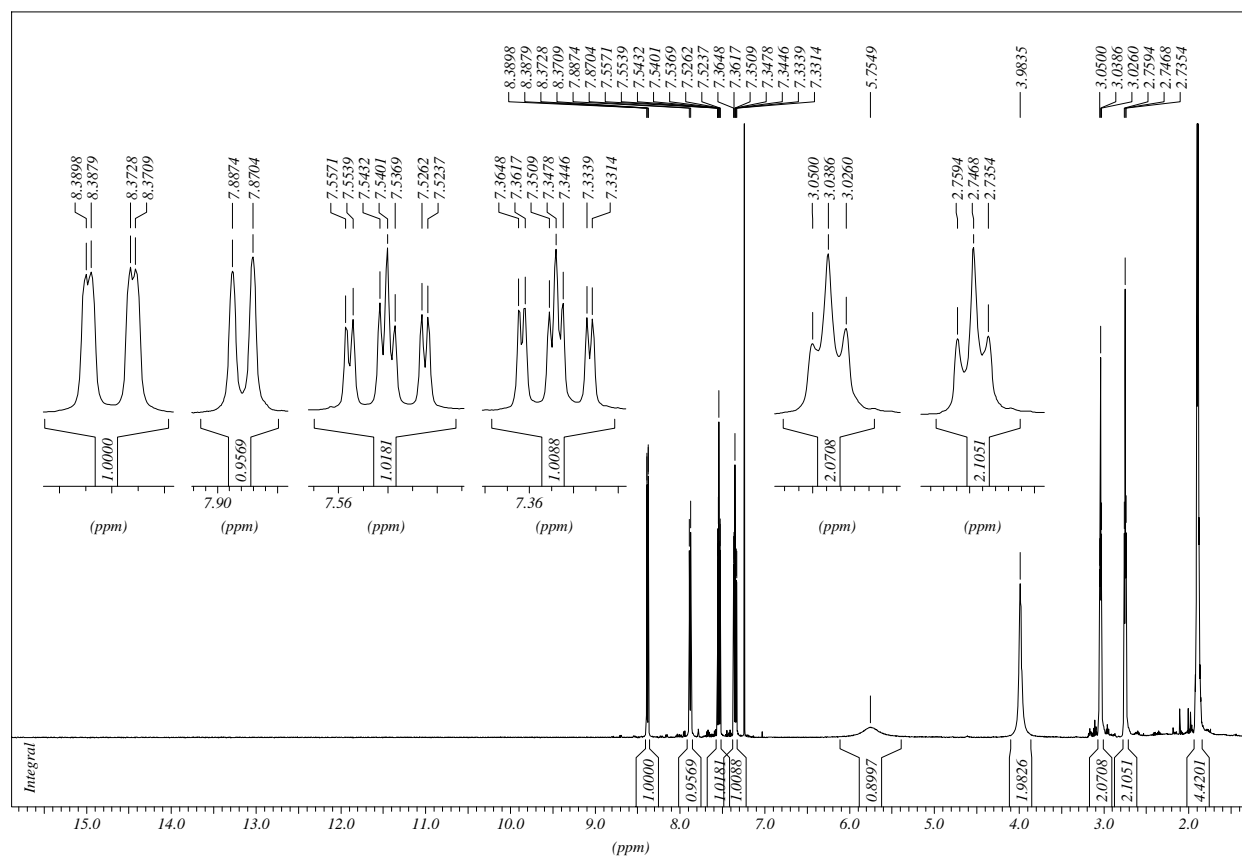
Methyl 3,4,5-trimethoxybenzoate
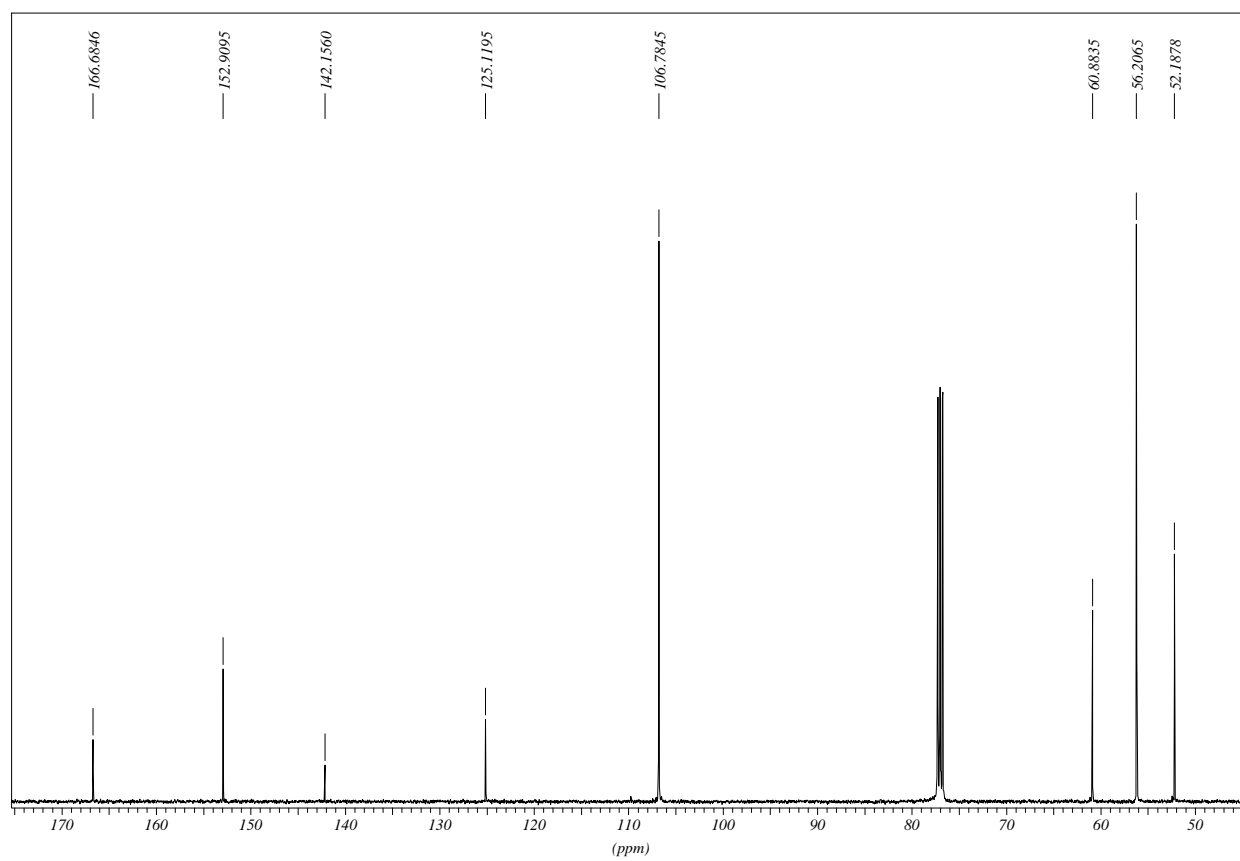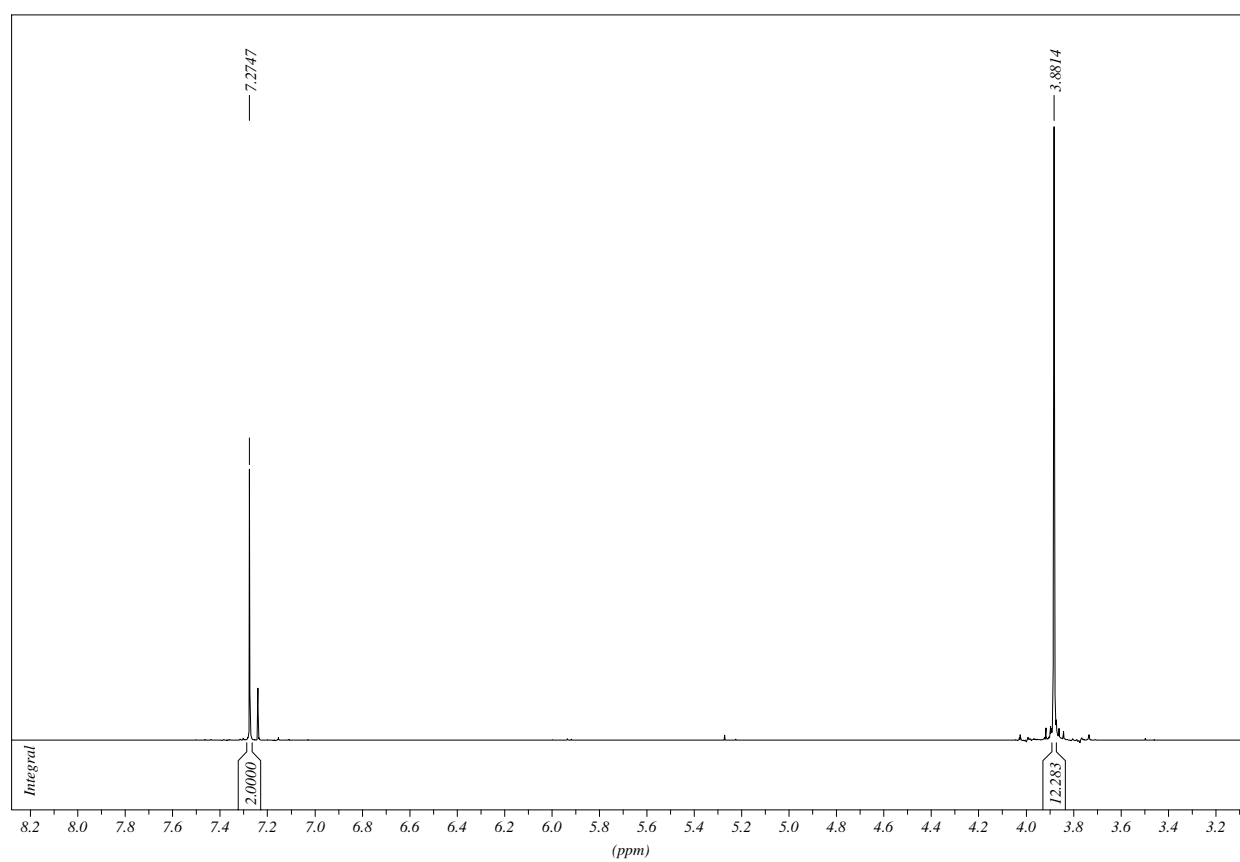
3,4,5-Trimethoxybenzohydrazide
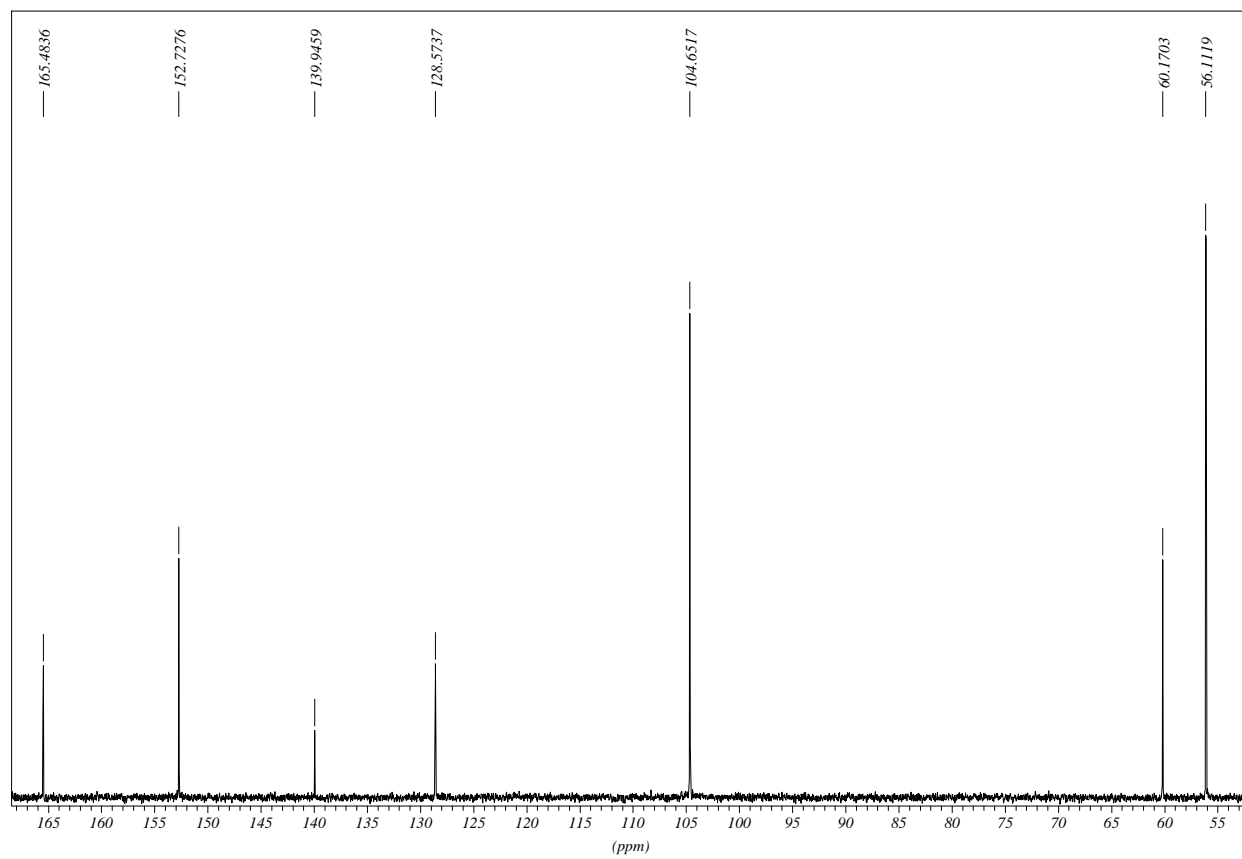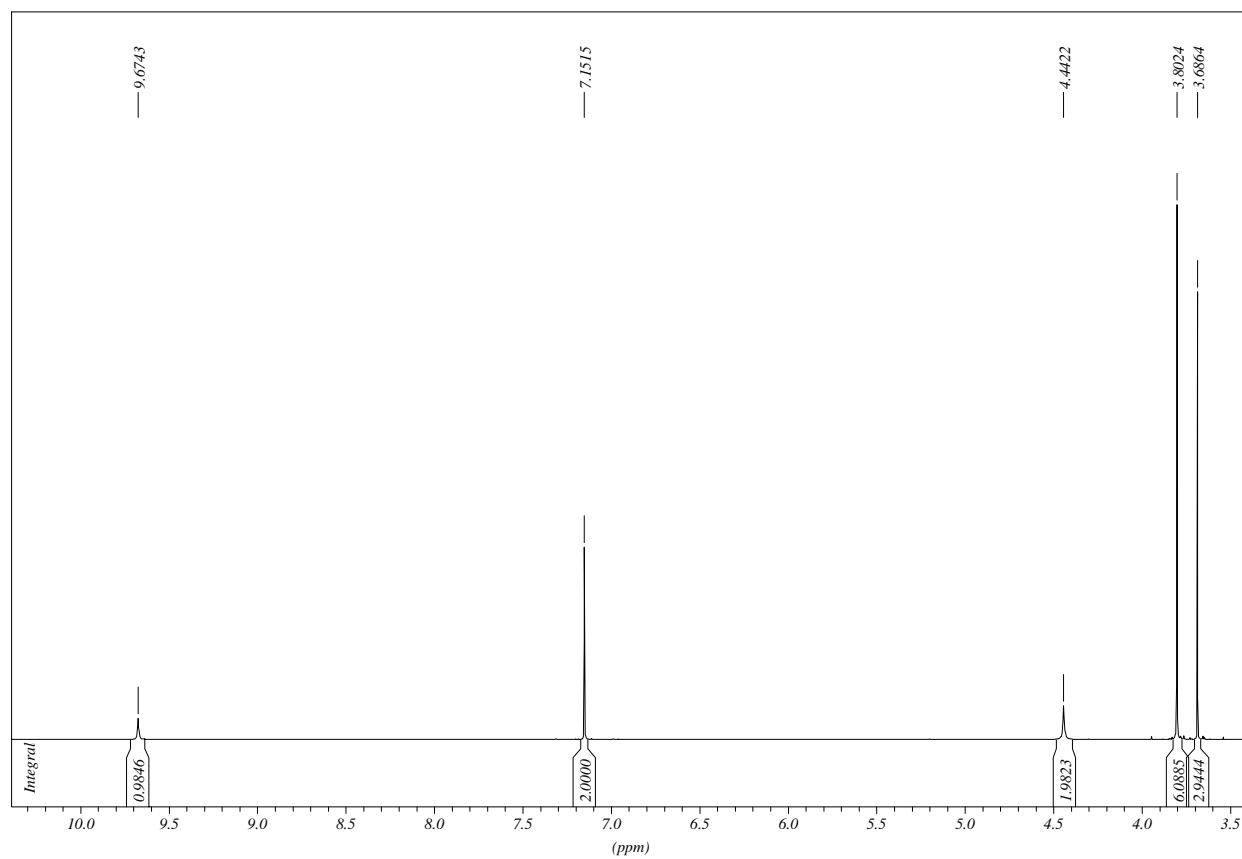
N′-1,2,3,4-Tetrahydroacridin-9-yl-3,4,5-trimethoxybenzohydrazide HCl
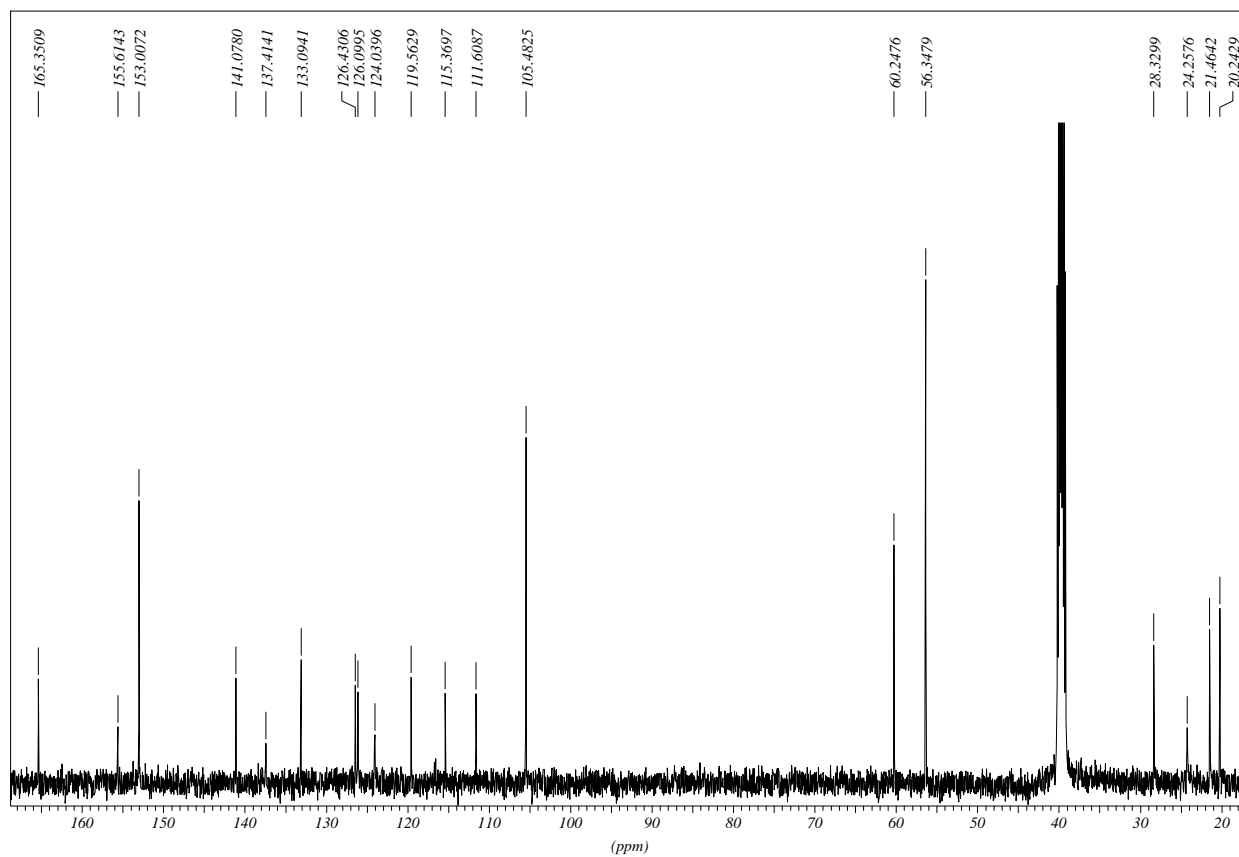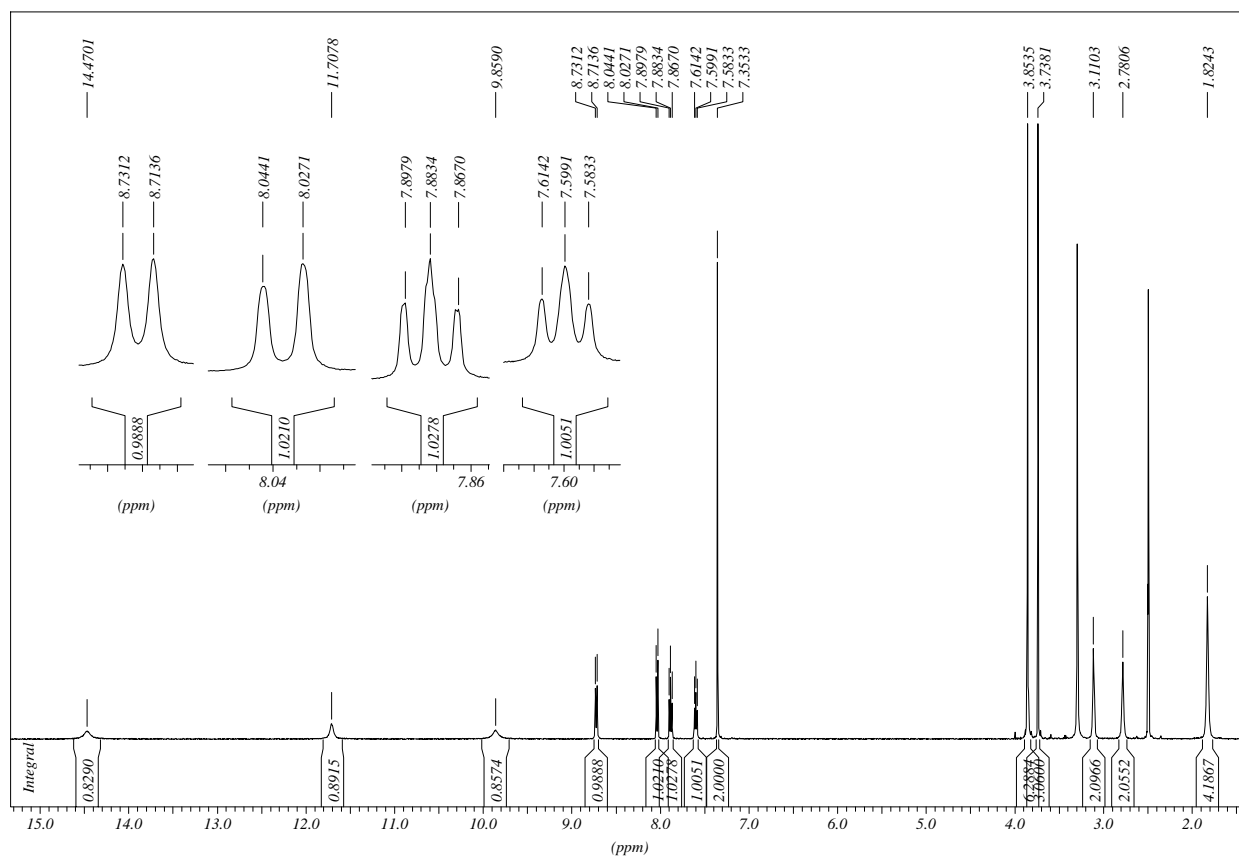
N'-1,2,3,4-Tetrahydroacridin-9-yl-3,4,5-trimethoxybenzohydrazide
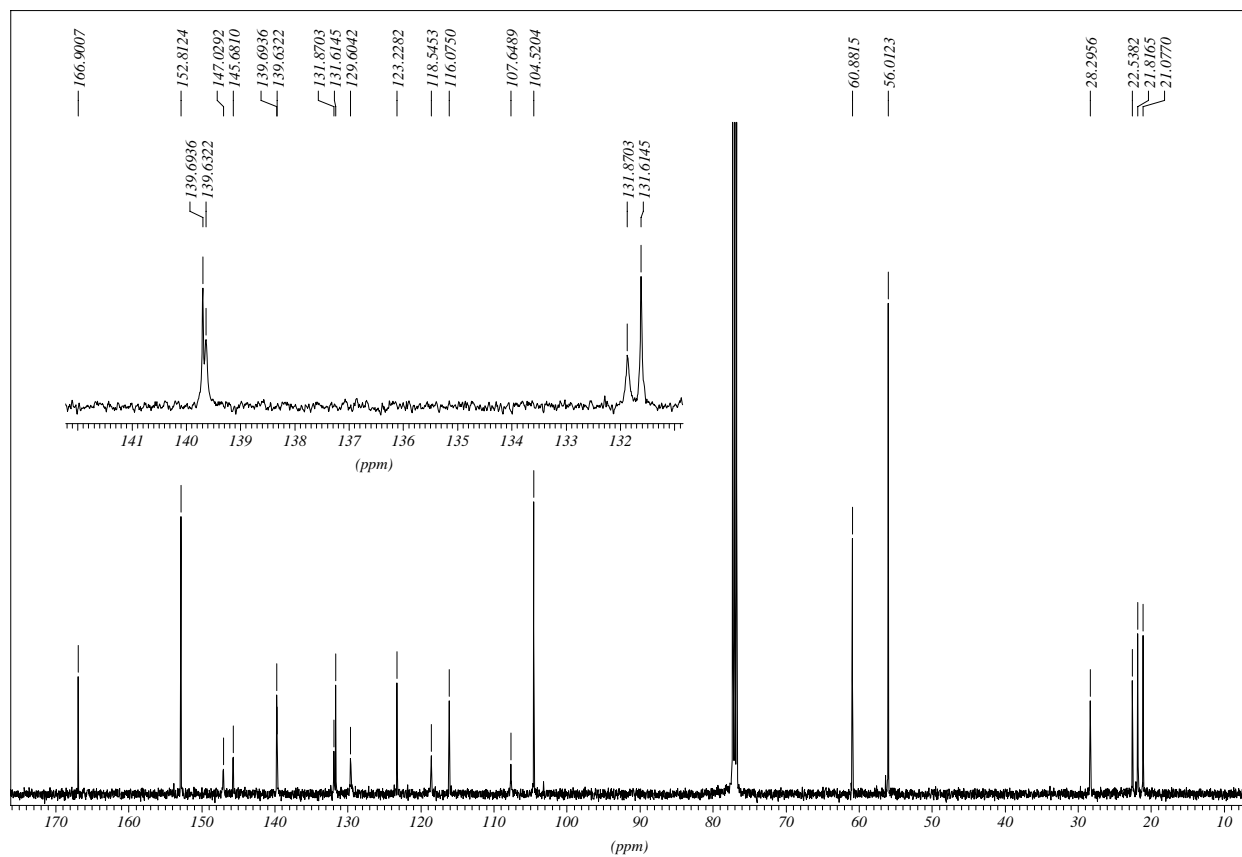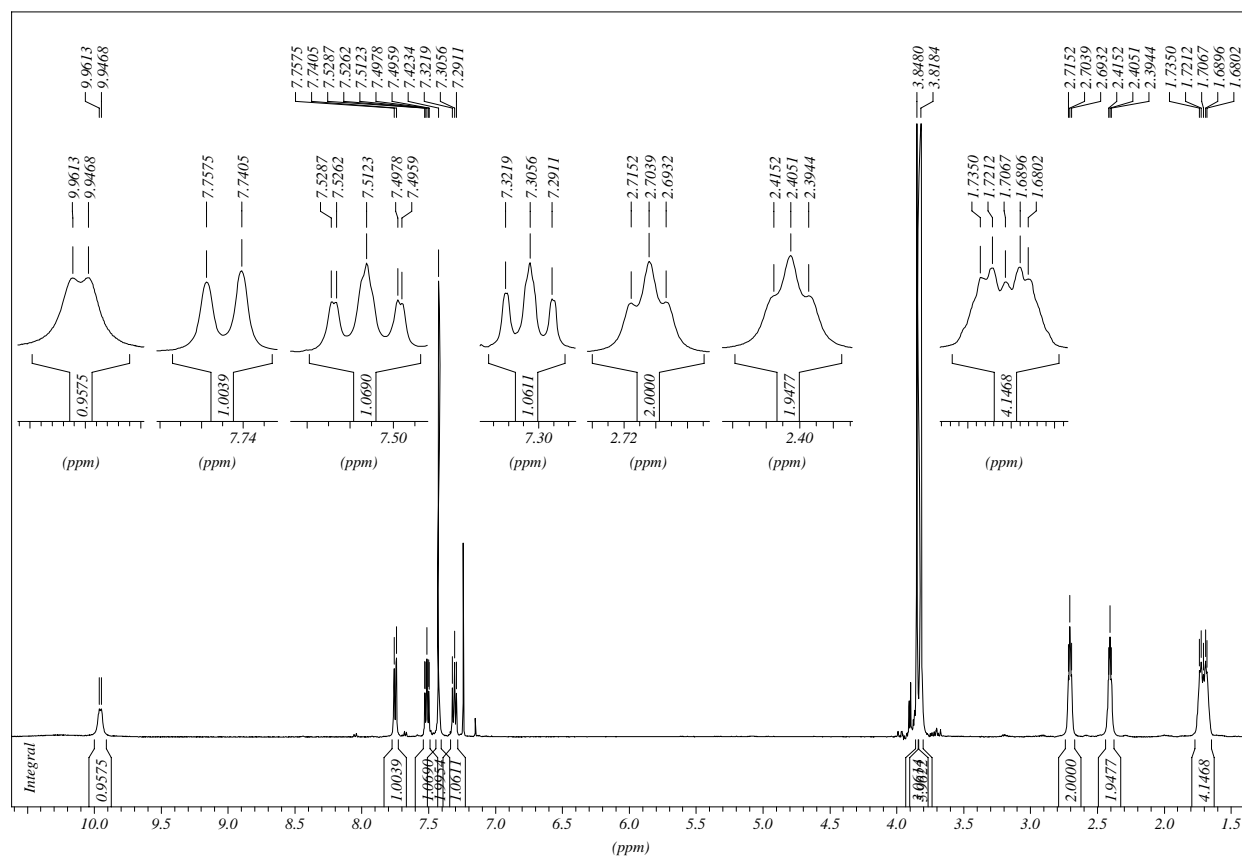
Ethyl ((3,4,5-trimethoxybenzoyl)amino)acetate
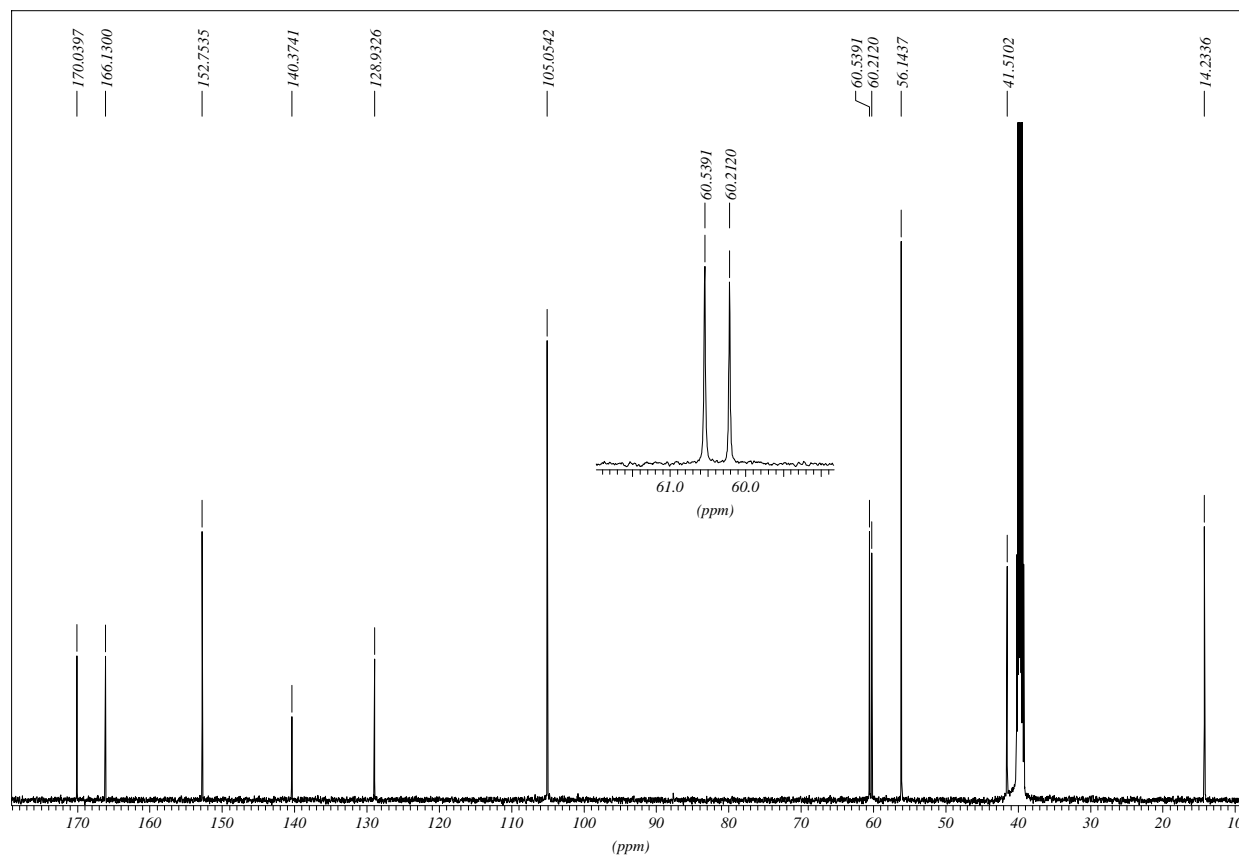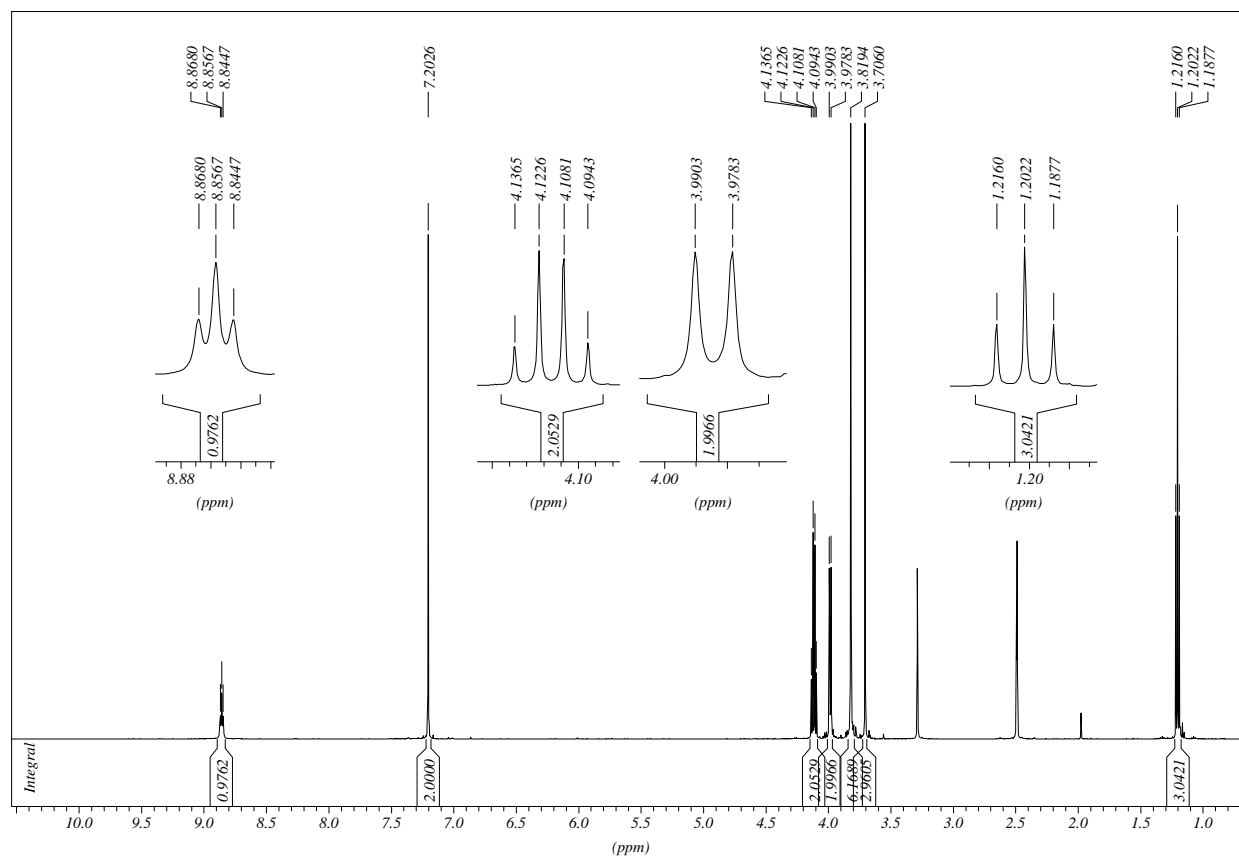
N-(2-Hydrazino-2-oxoethyl)-3,4,5-trimethoxybenzamide
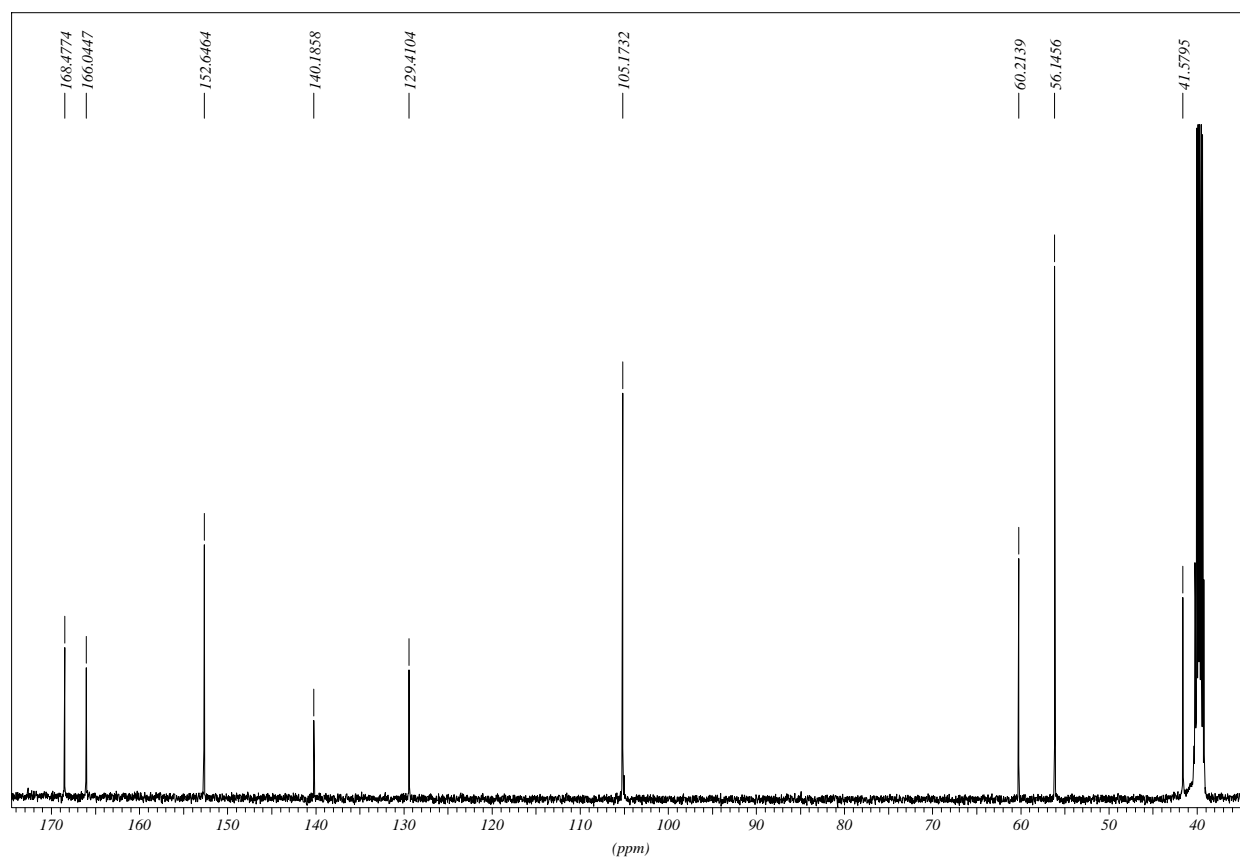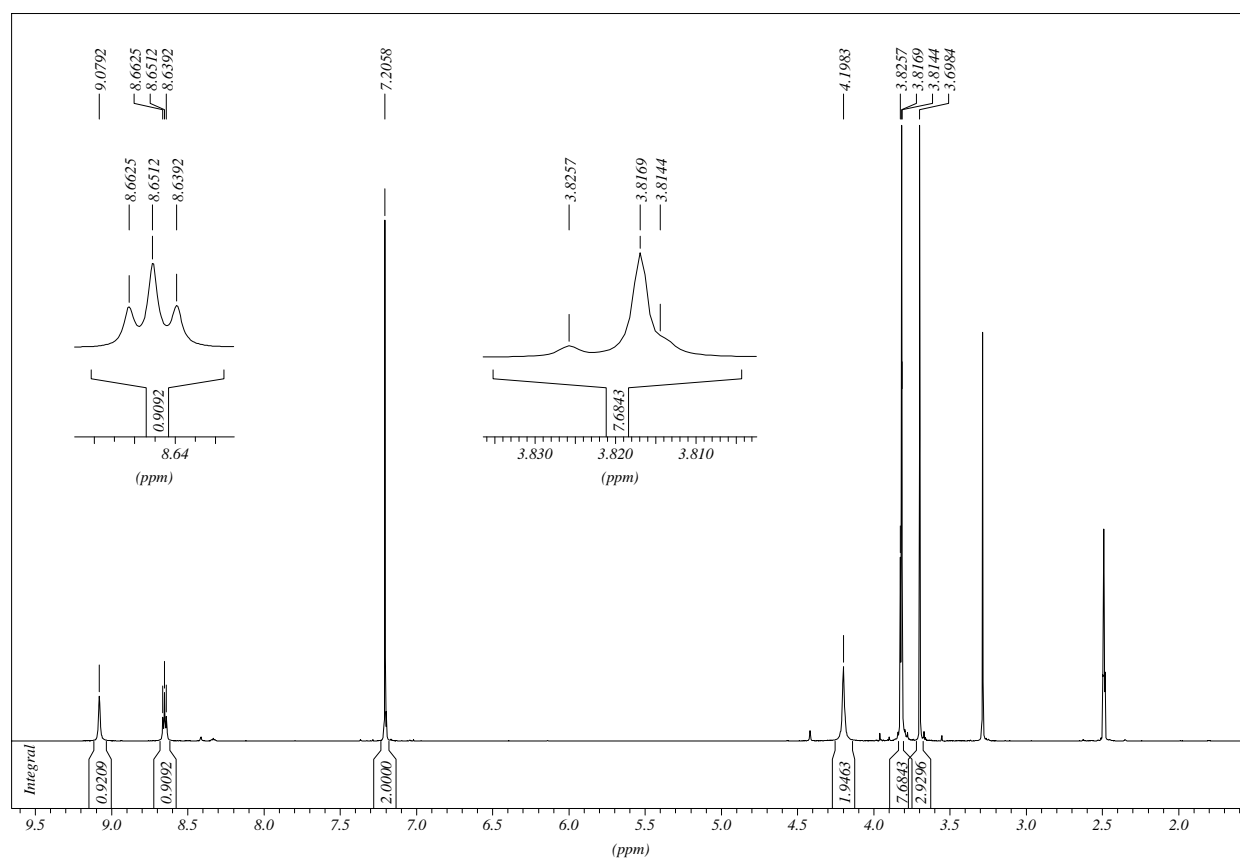
3,4,5-Trimethoxy-*N*-(2-oxo-2-(2-(1,2,3,4-tetrahydroacridin-9-yl)hydrazino)ethyl)benzamide HCl
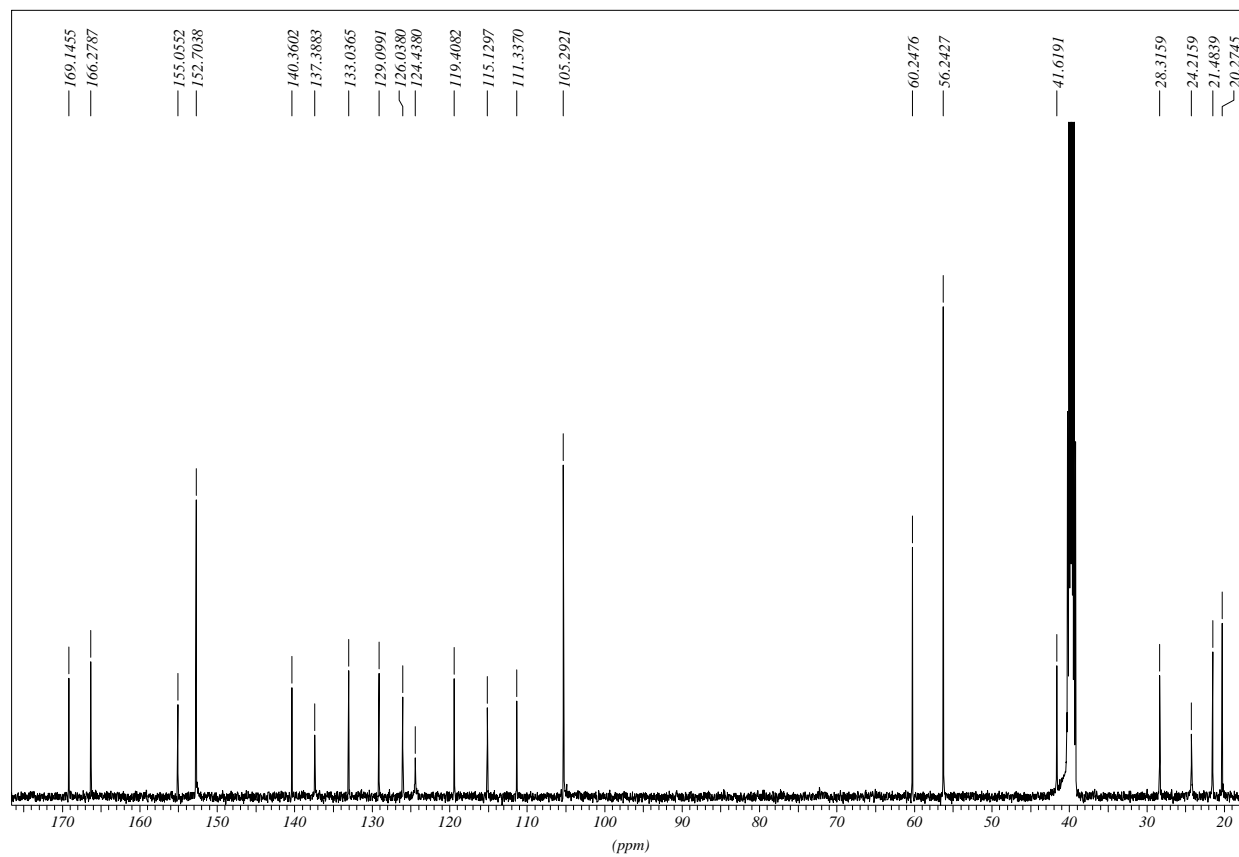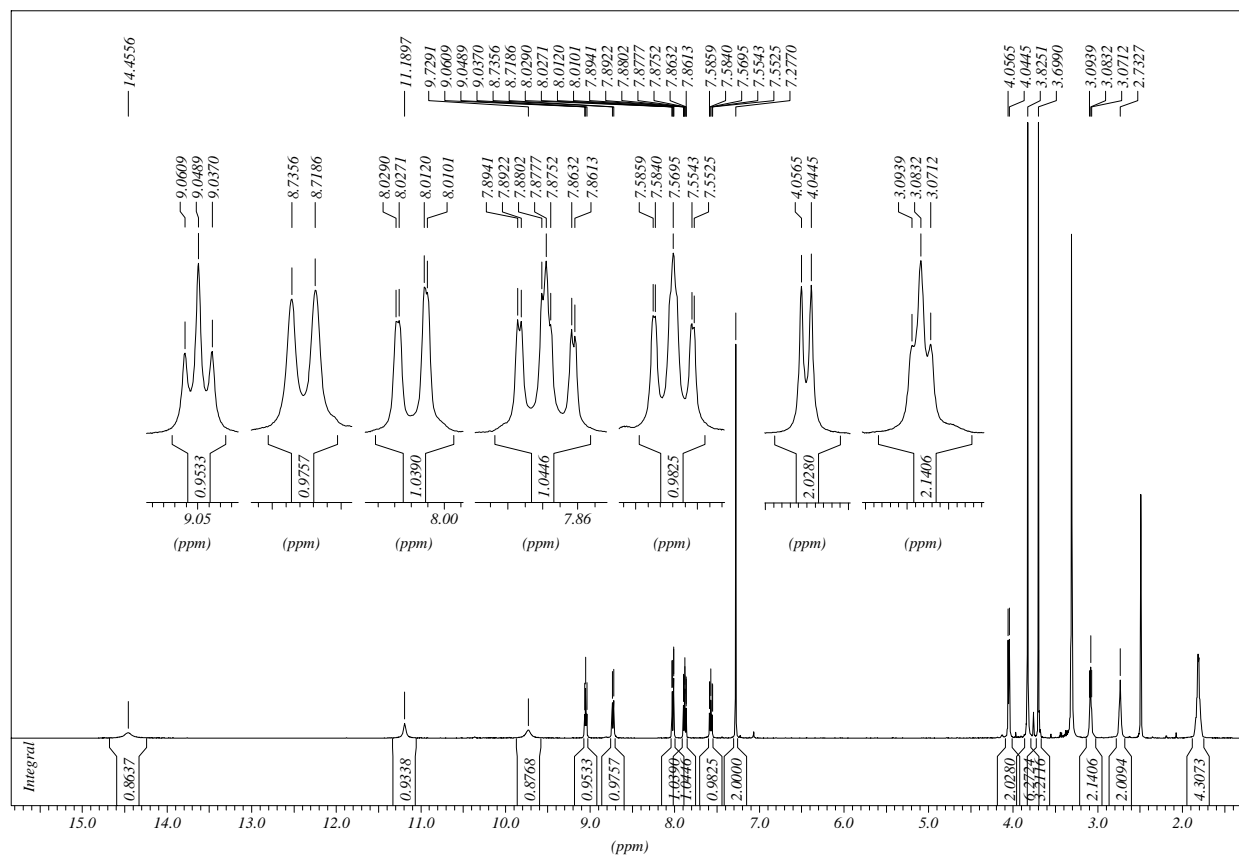
3,4,5-Trimethoxy-*N*-(2-oxo-2-(2-(1,2,3,4-tetrahydroacridin-9-yl)hydrazino)ethyl)benzamide
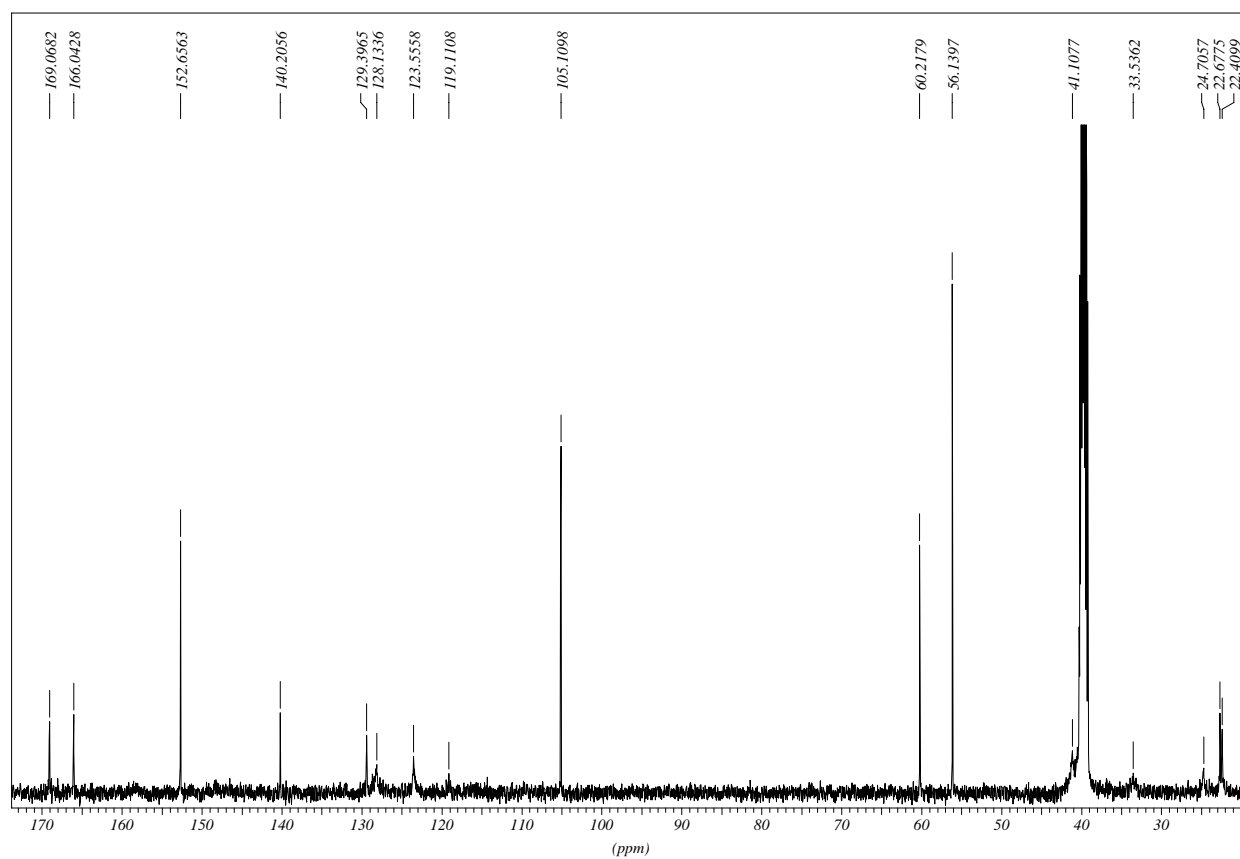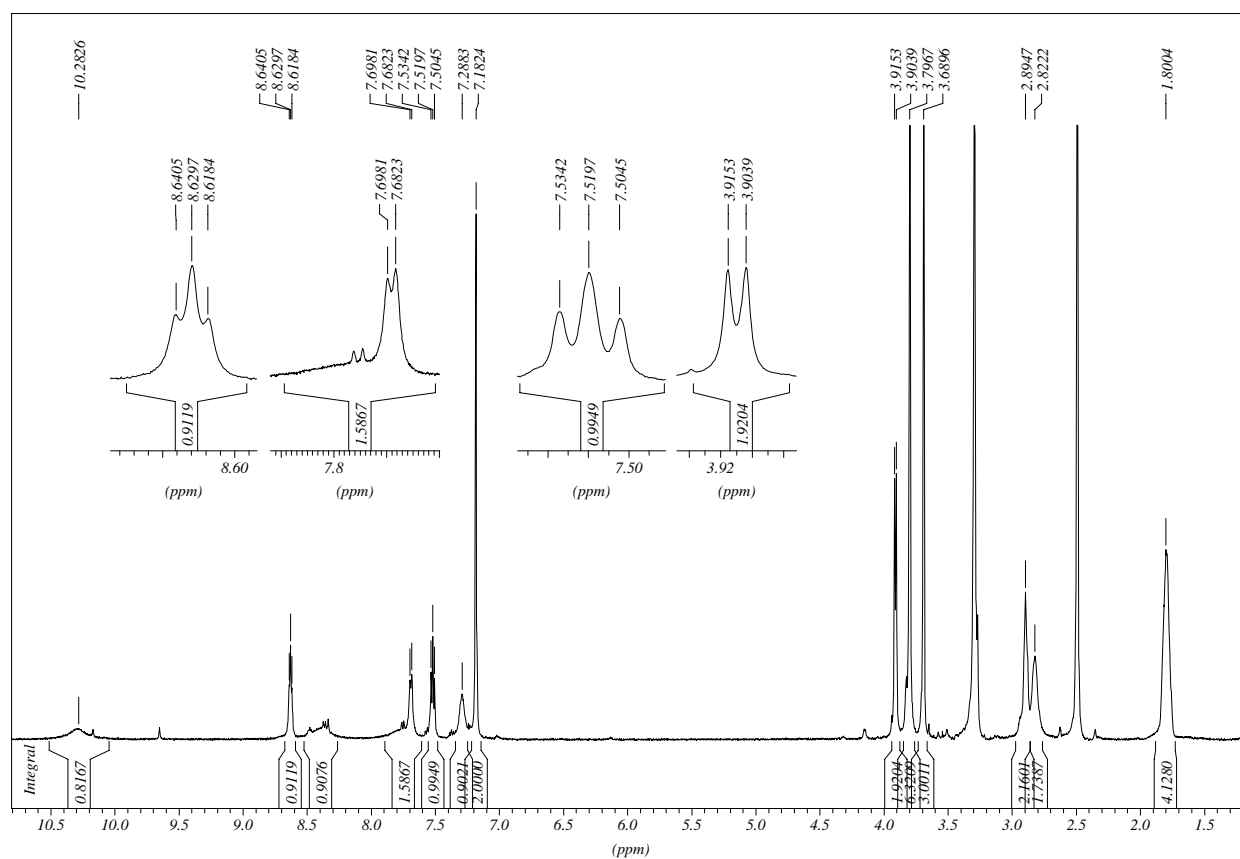
Ethyl 3-((3,4,5-trimethoxybenzoyl)amino)propanoate
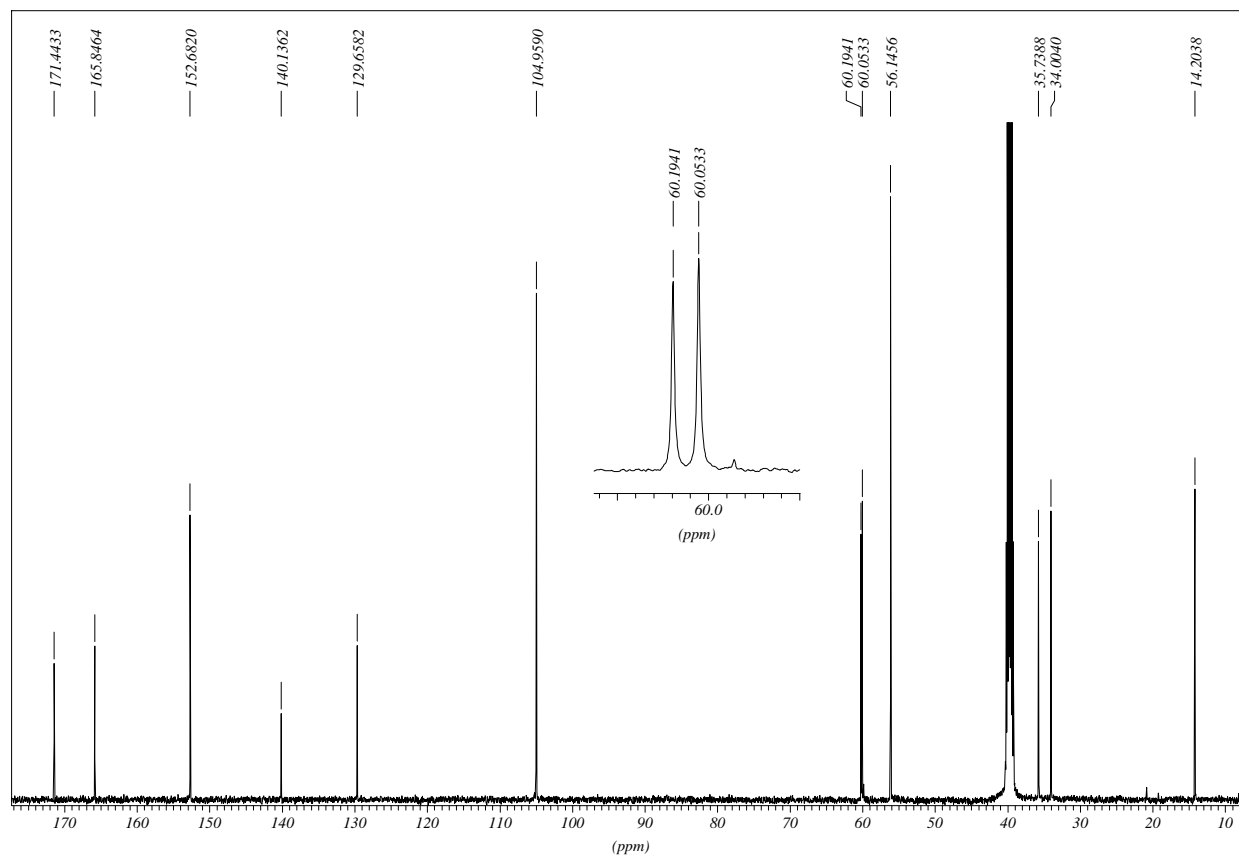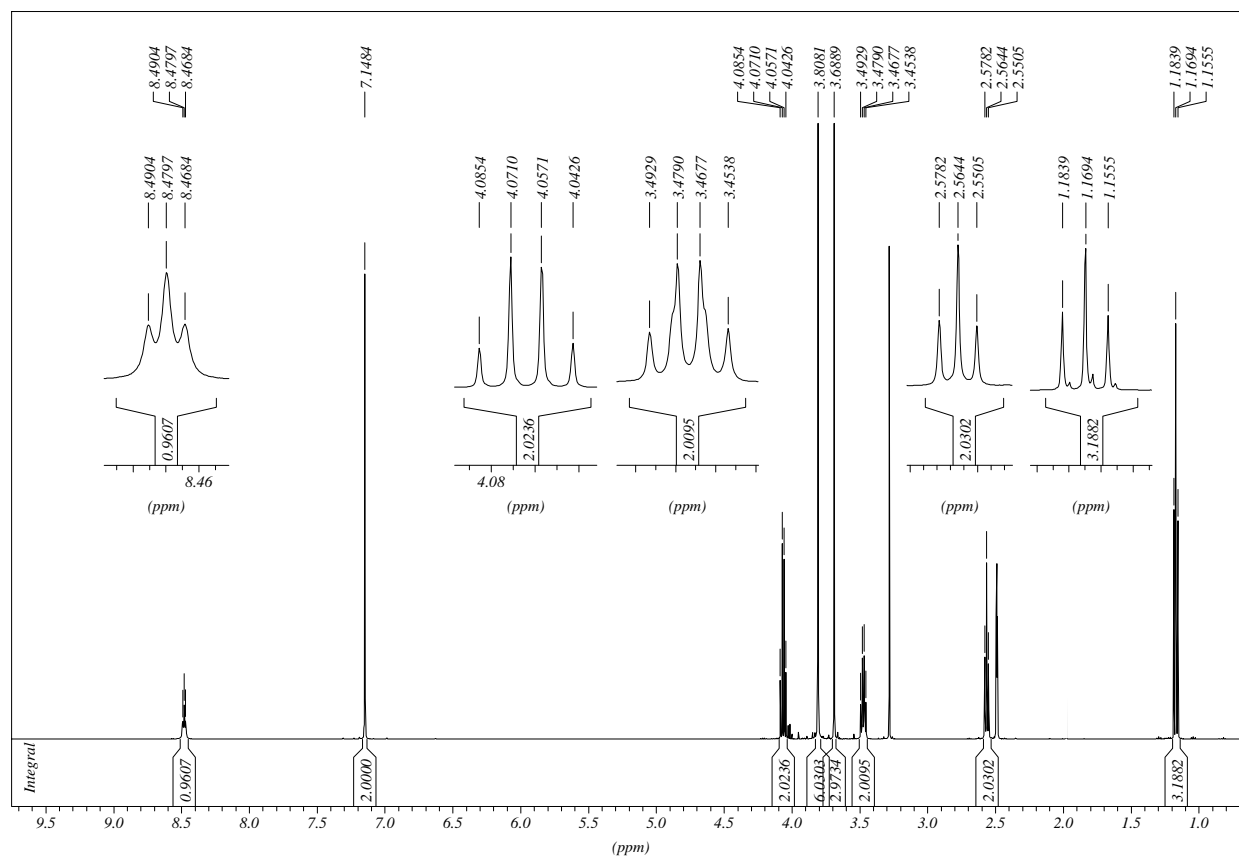
N-(3-Hydrazino-3-oxopropyl)-3,4,5-trimethoxybenzamide
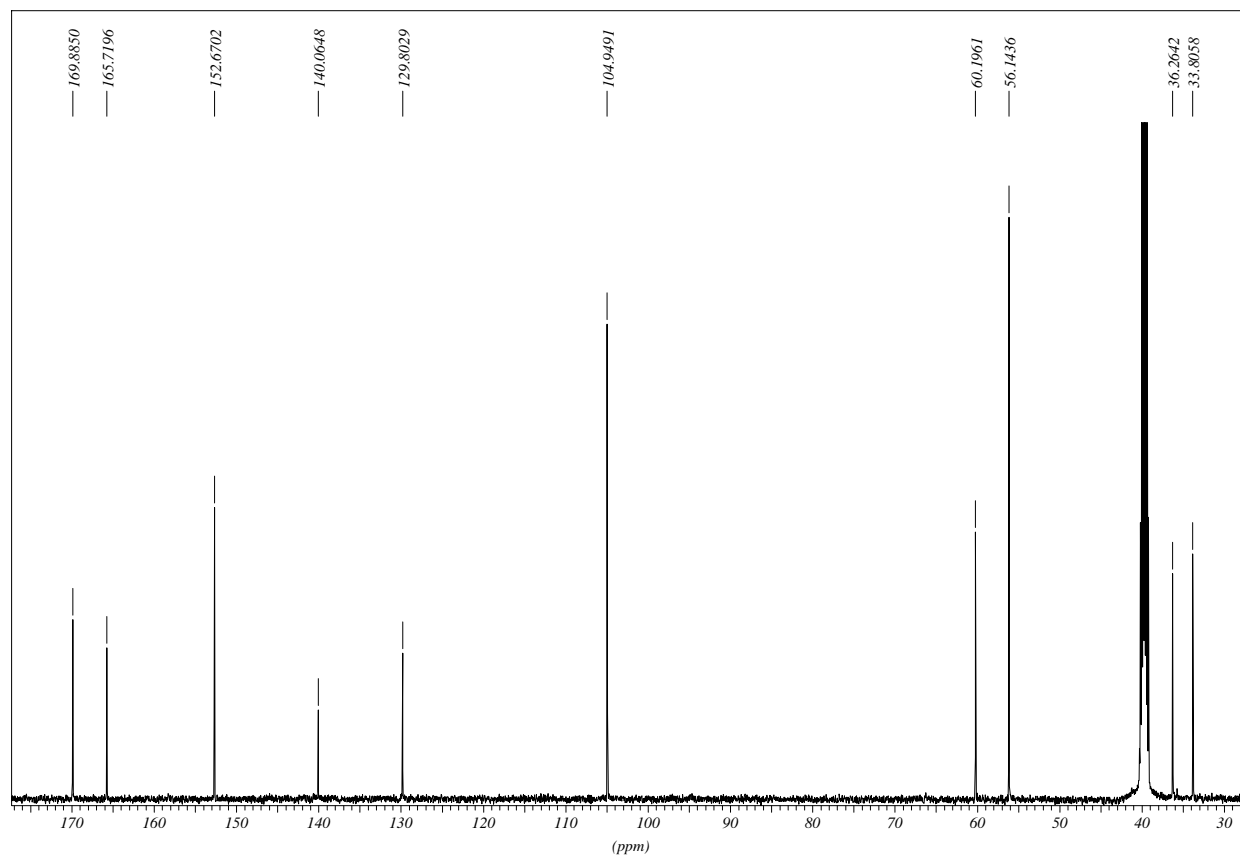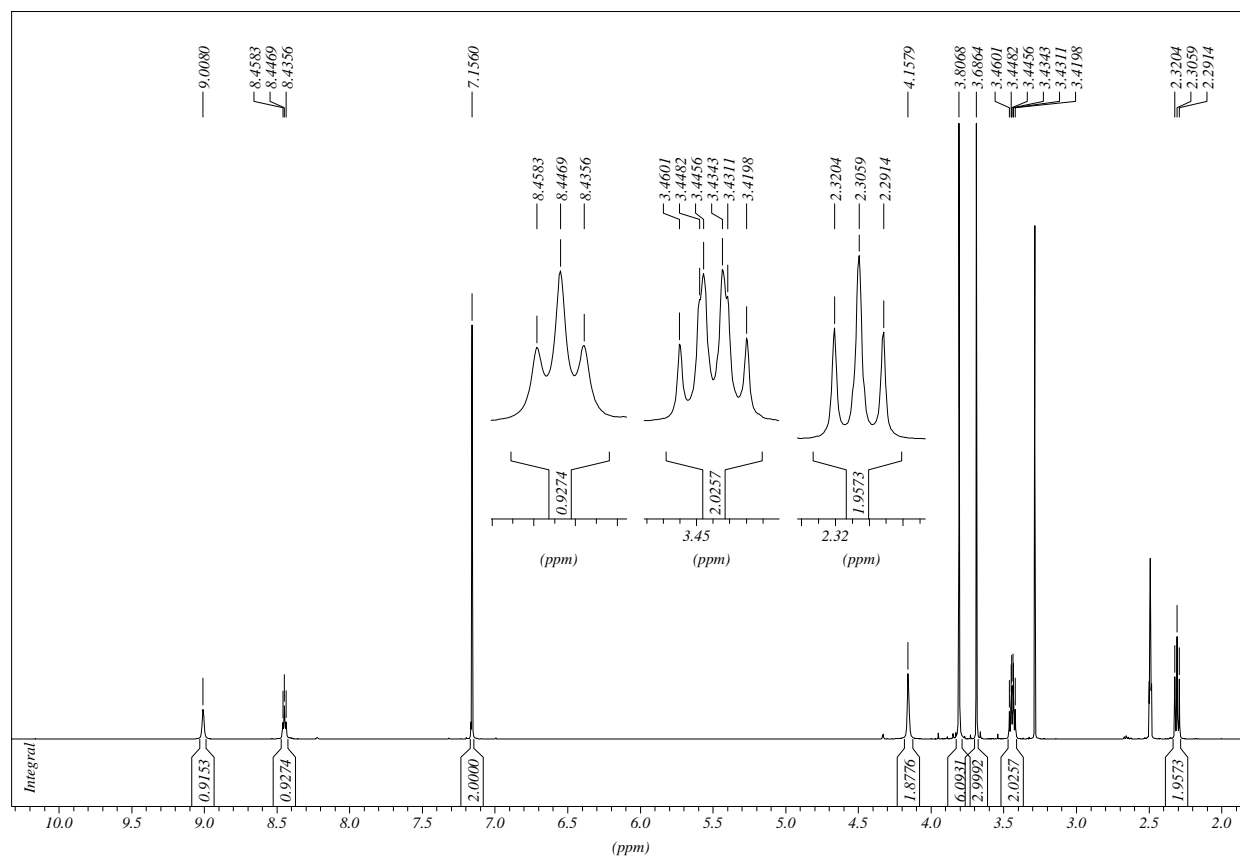
3,4,5-Trimethoxy-*N*-(3-oxo-3-(2-(1,2,3,4-tetrahydroacridin-9-yl)hydrazino)propyl)benzamide HCl
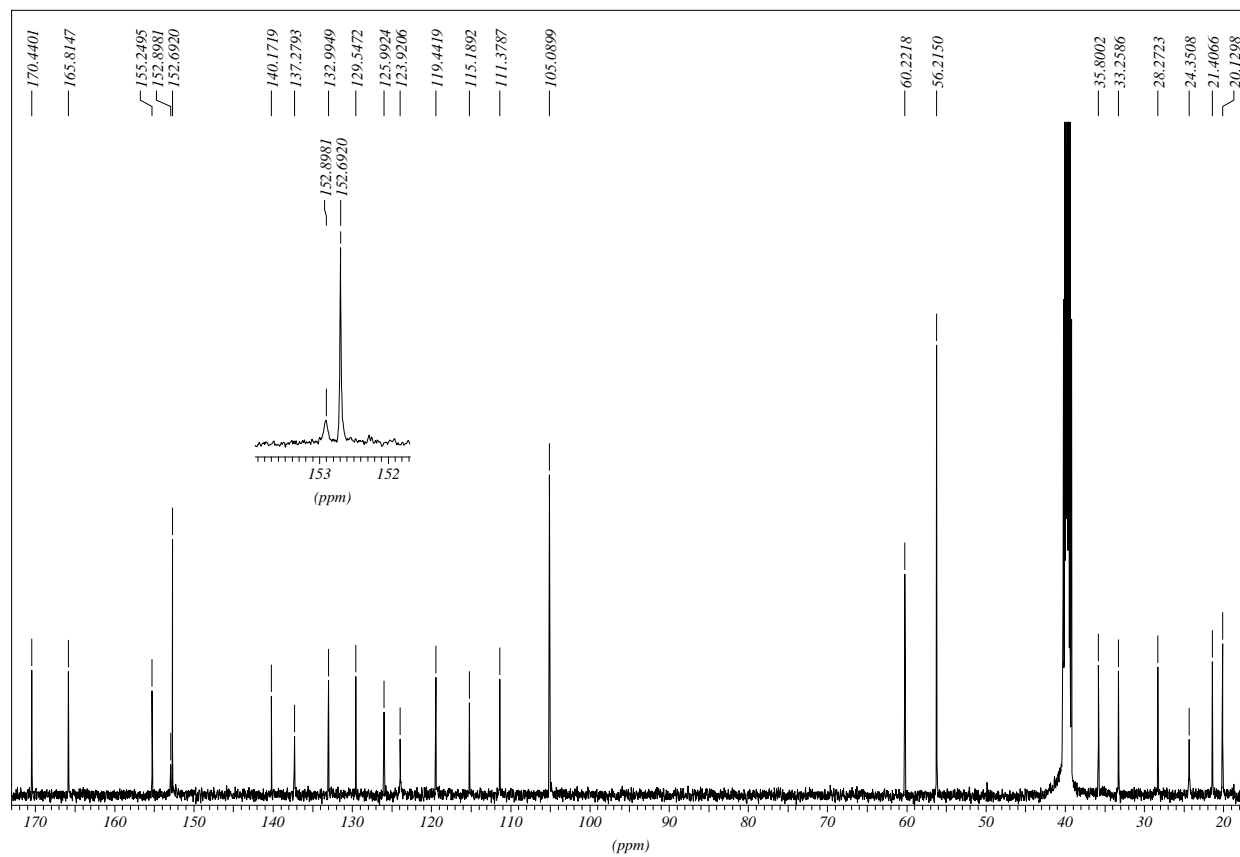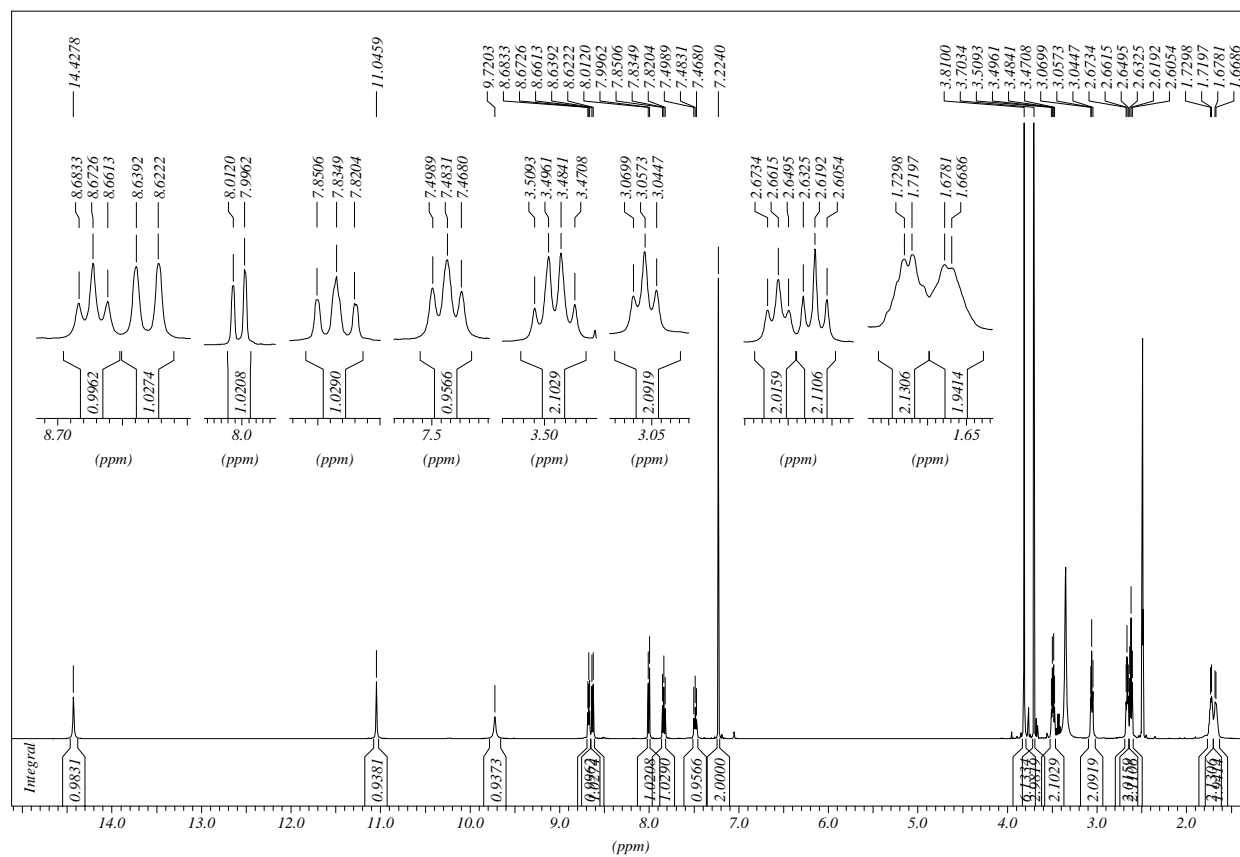
3,4,5-Trimethoxy-*N*-(3-oxo-3-(2-(1,2,3,4-tetrahydroacridin-9-yl)hydrazino)propyl)benzamide
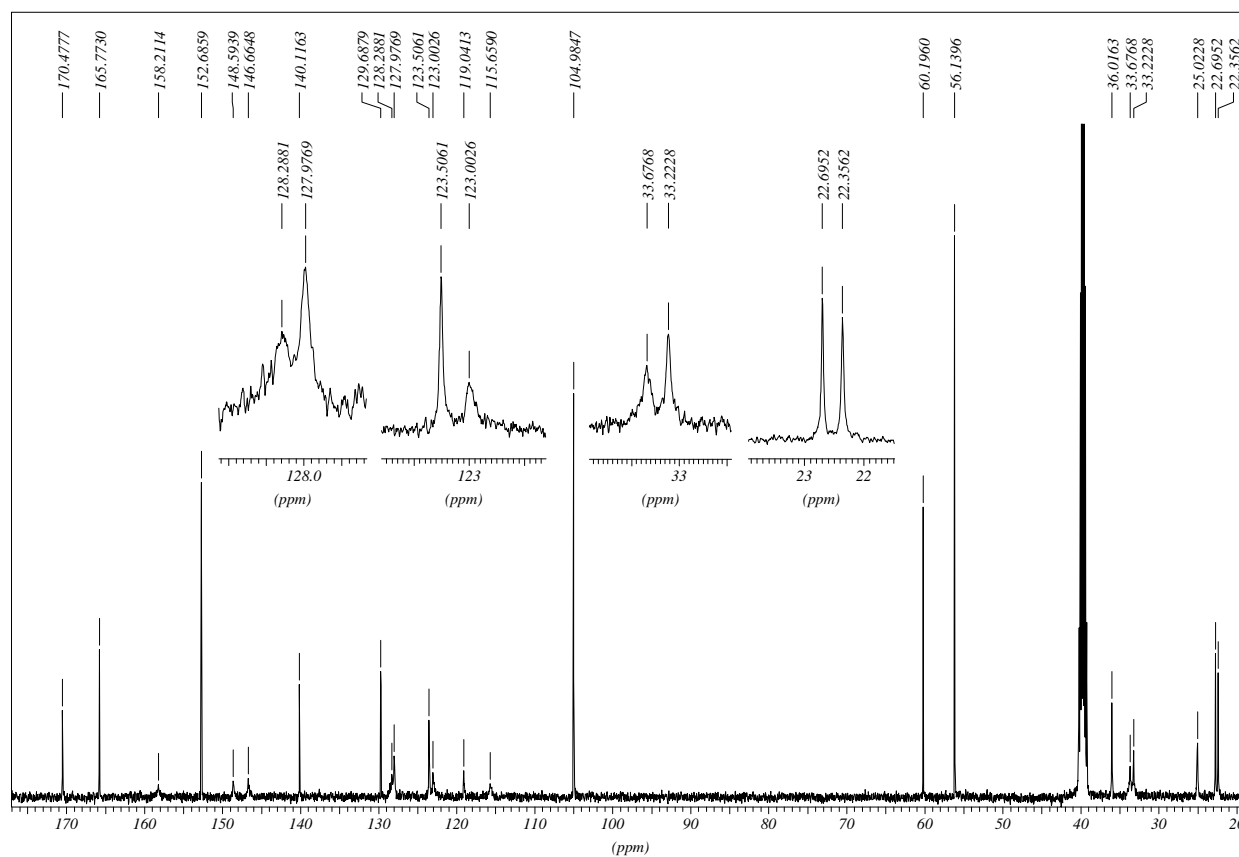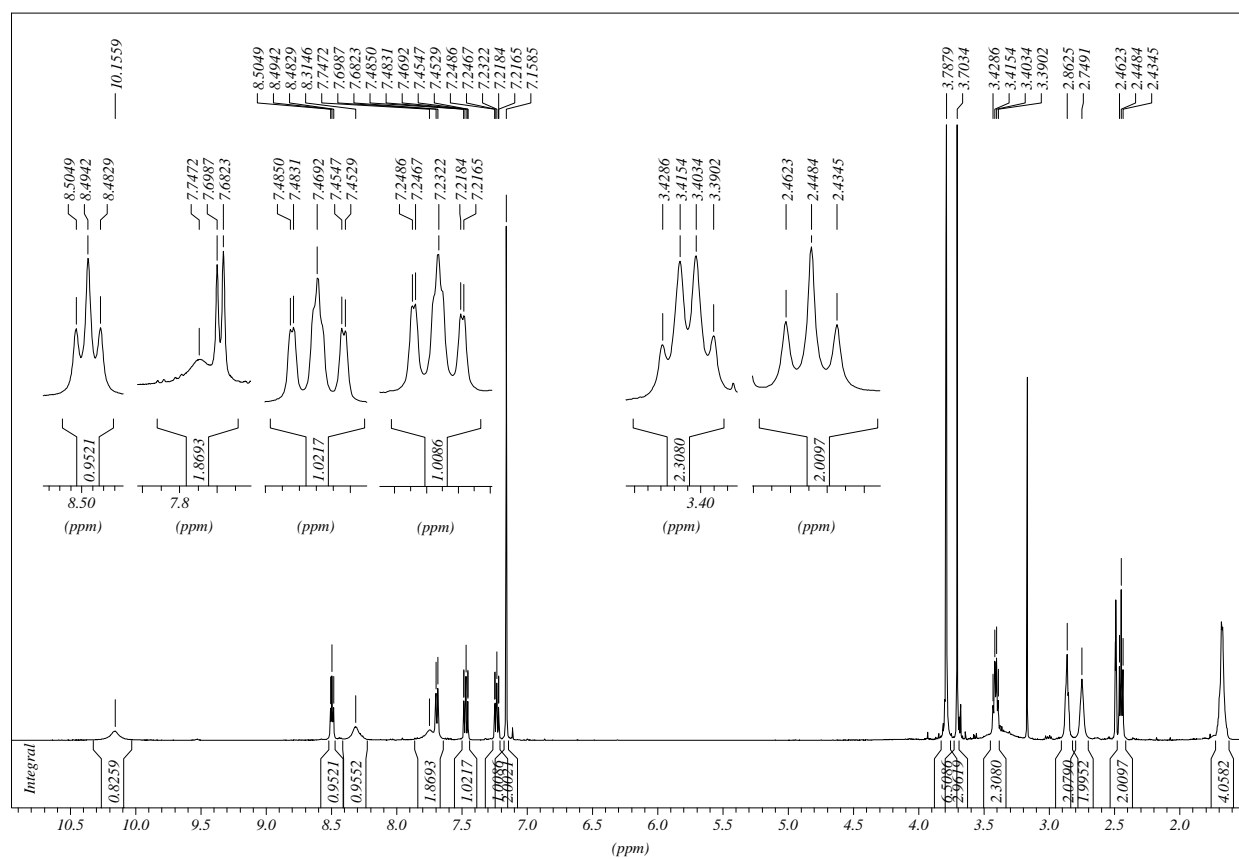
Ethyl 4-((3,4,5-trimethoxybenzoyl)amino)butanoate
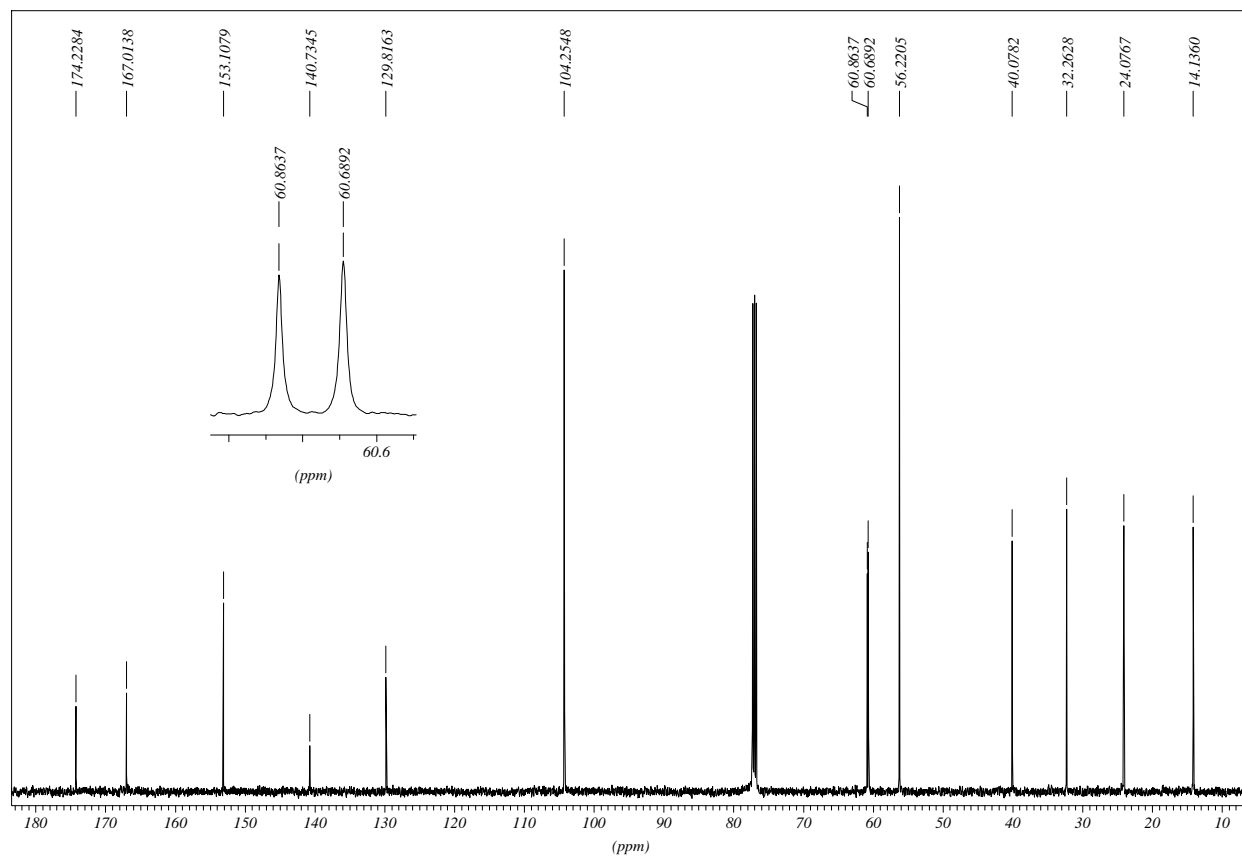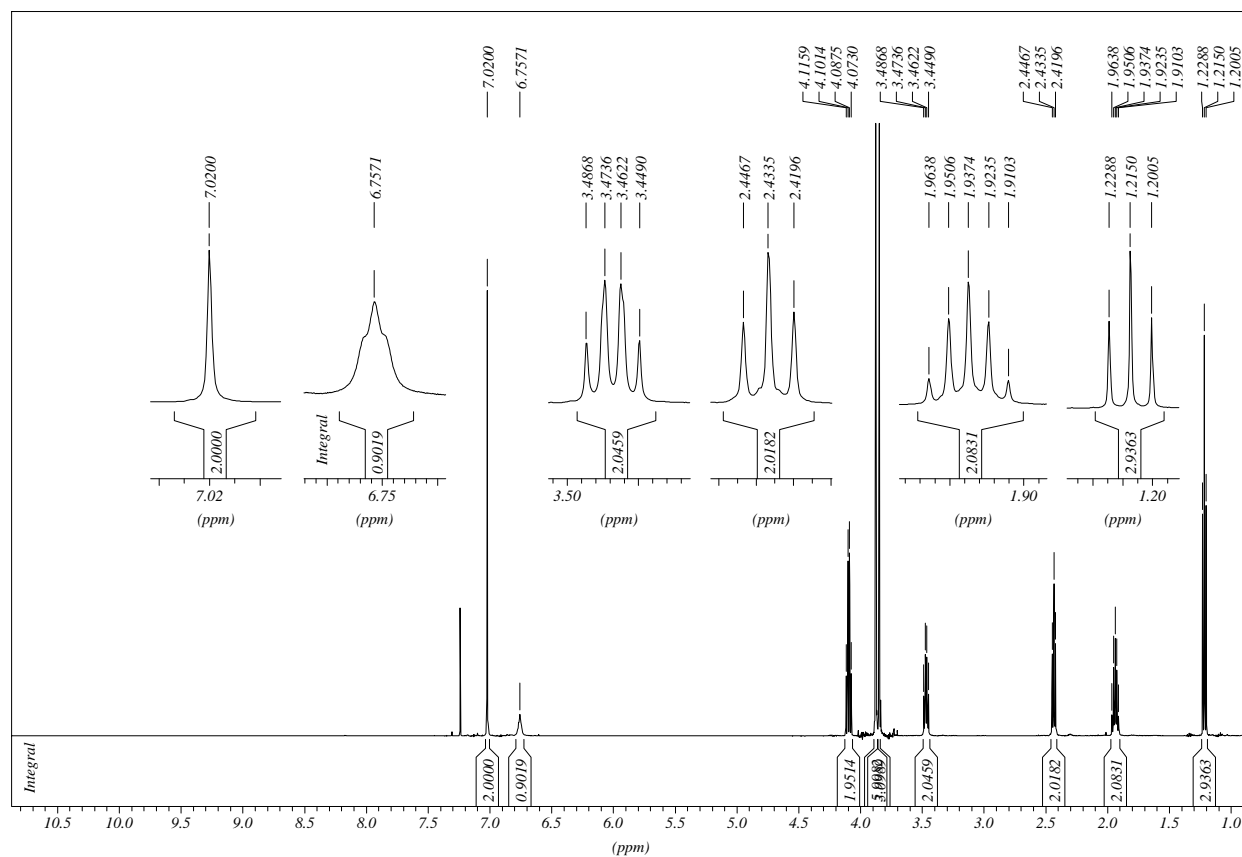
N-(4-Hydrazino-4-oxobutyl)-3,4,5-trimethoxybenzamide
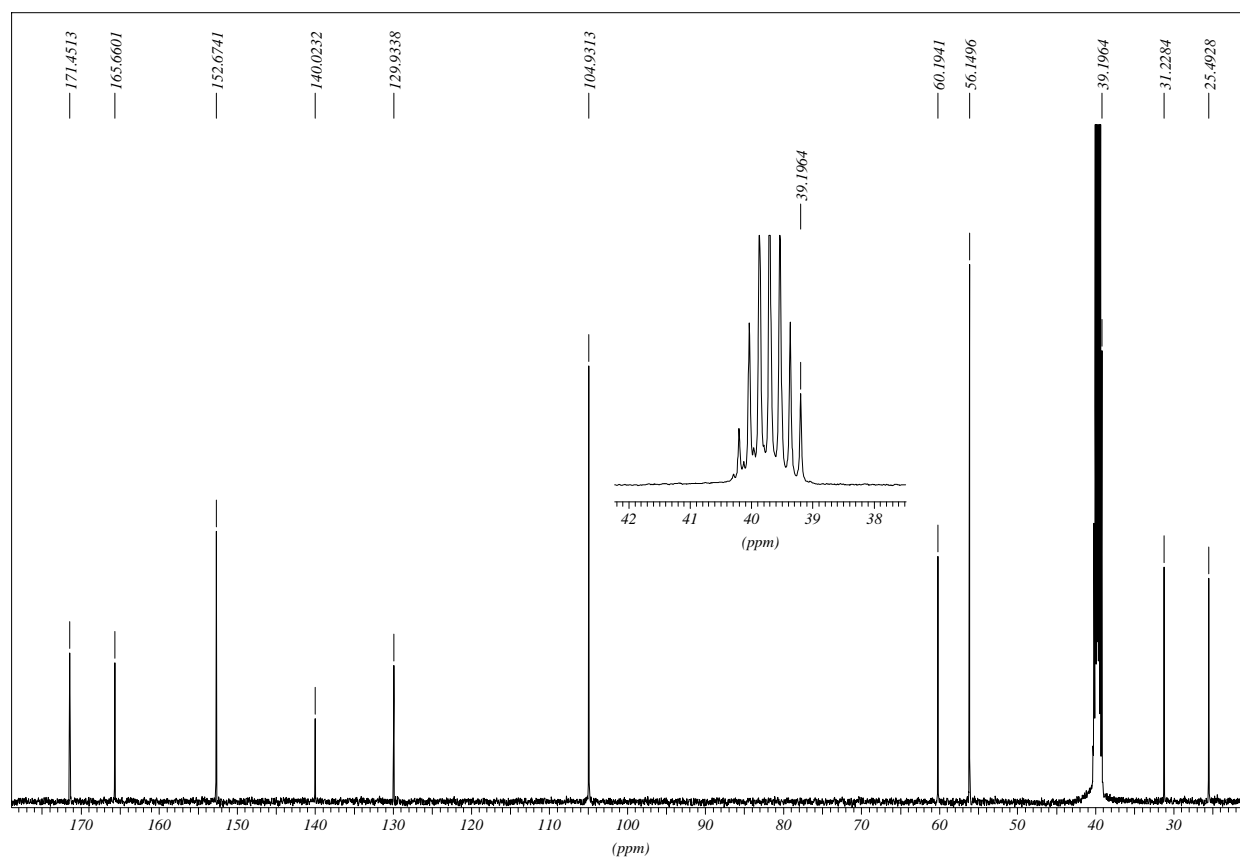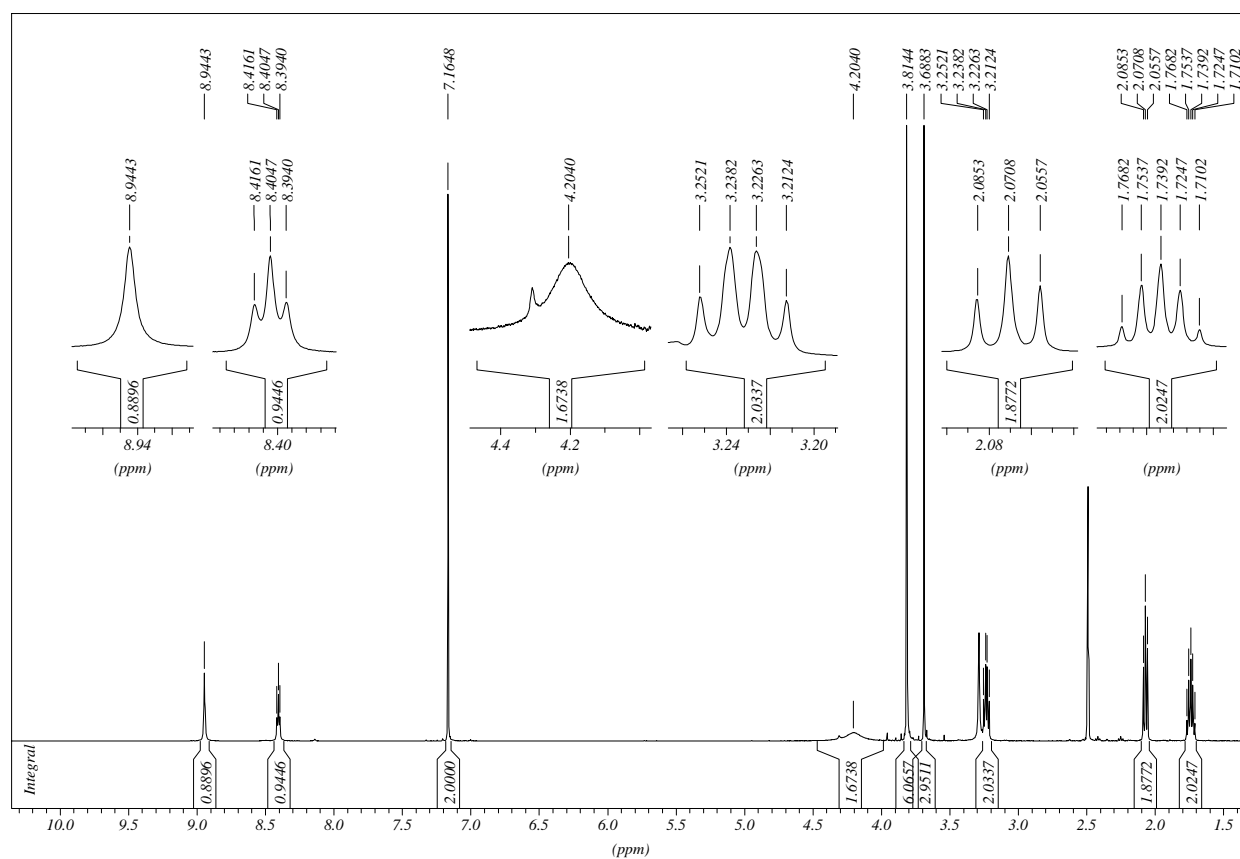
3,4,5-Trimethoxy-*N*-(4-oxo-4-(2-(1,2,3,4-tetrahydroacridin-9-yl)hydrazino)butyl)benzamide HCl
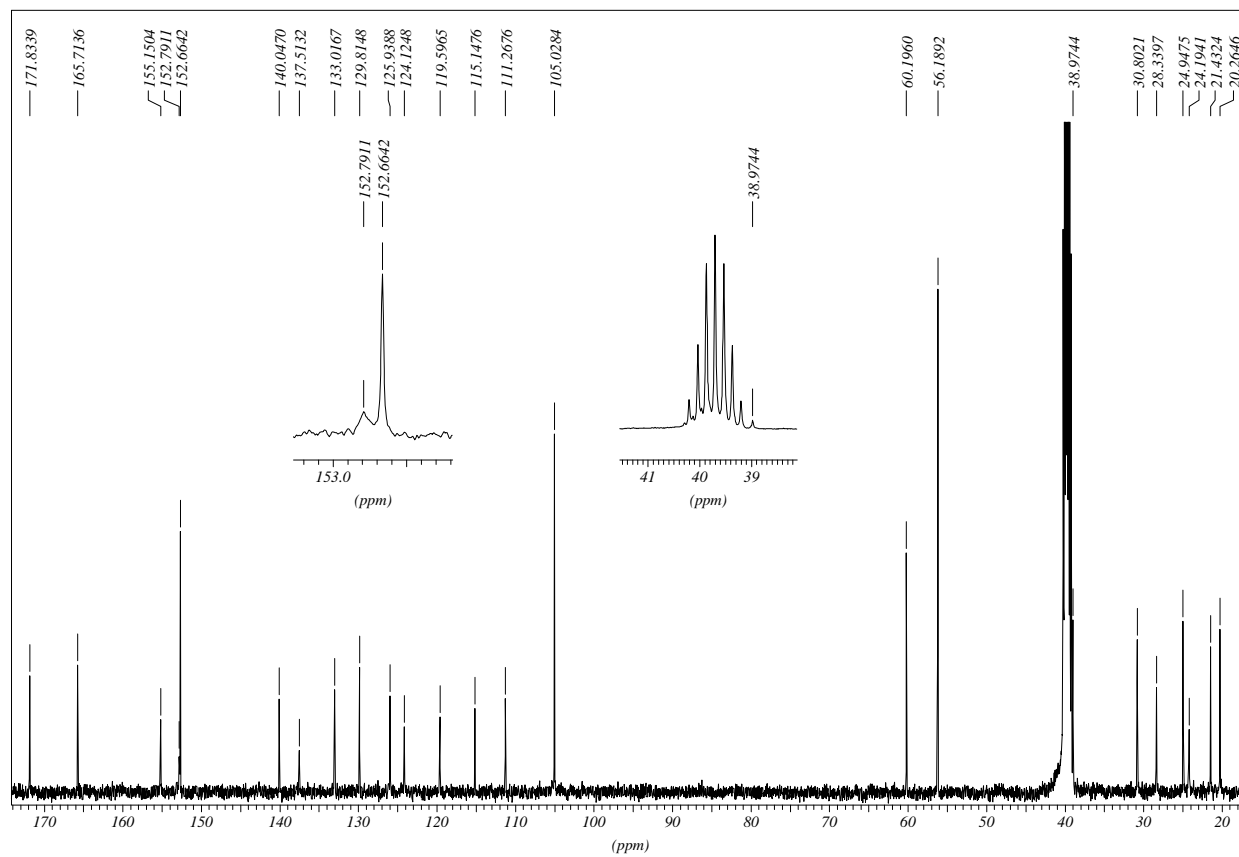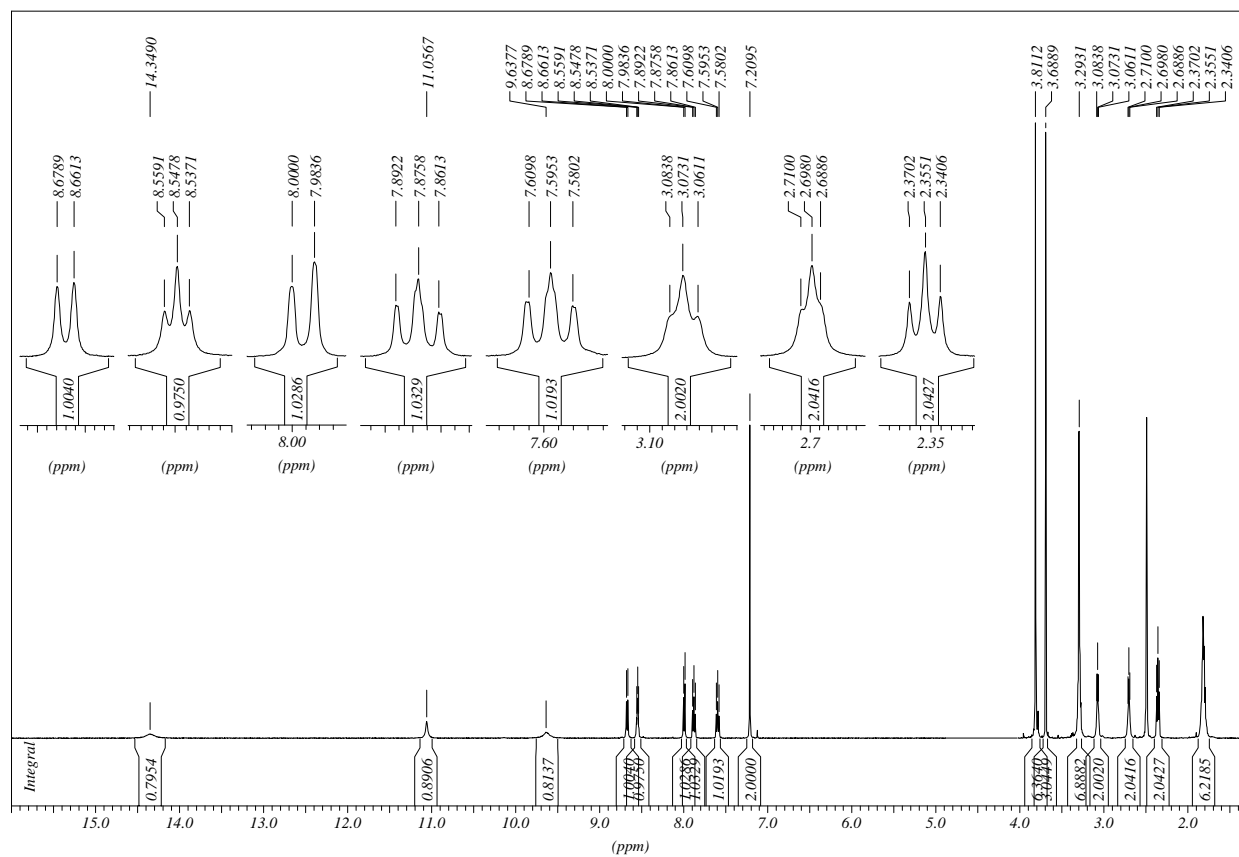
3,4,5-Trimethoxy-*N*-(4-oxo-4-(2-(1,2,3,4-tetrahydroacridin-9-yl)hydrazino)butyl)benzamide
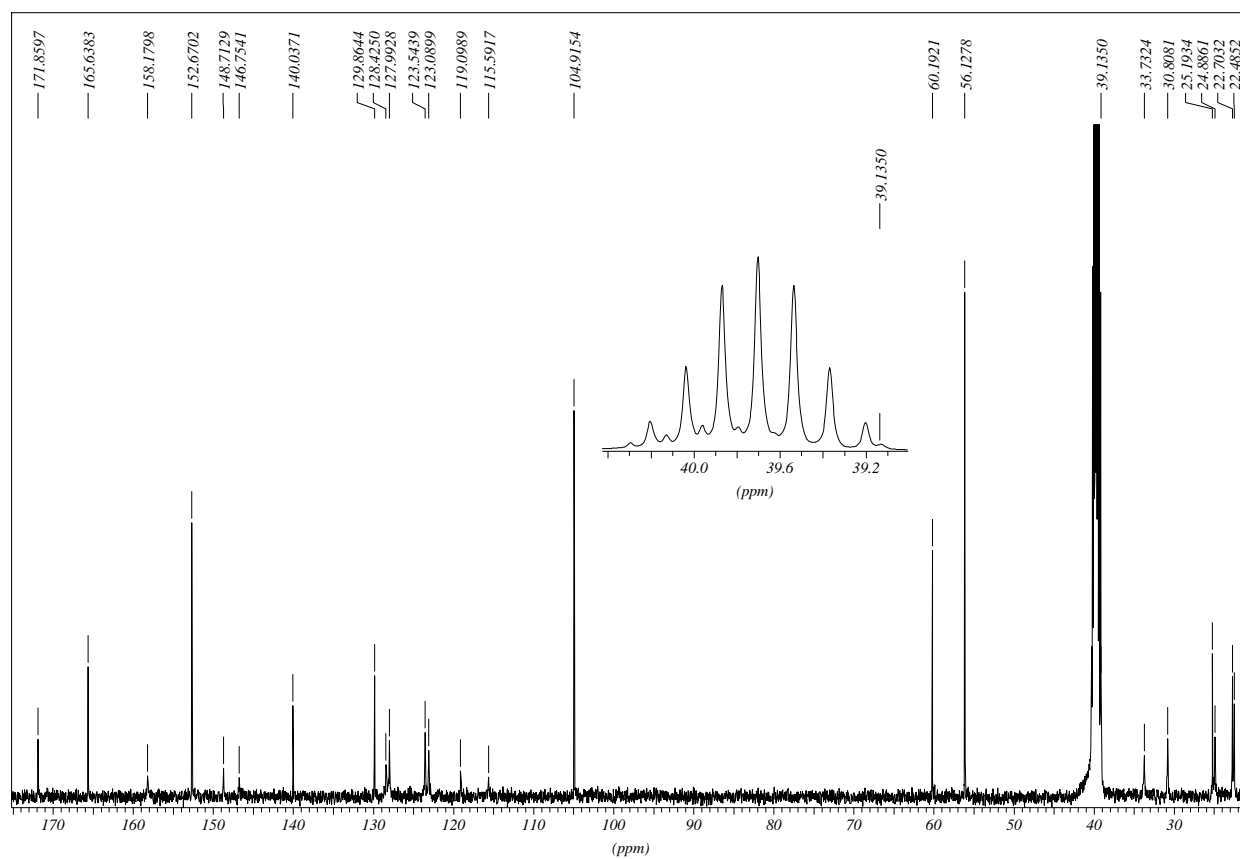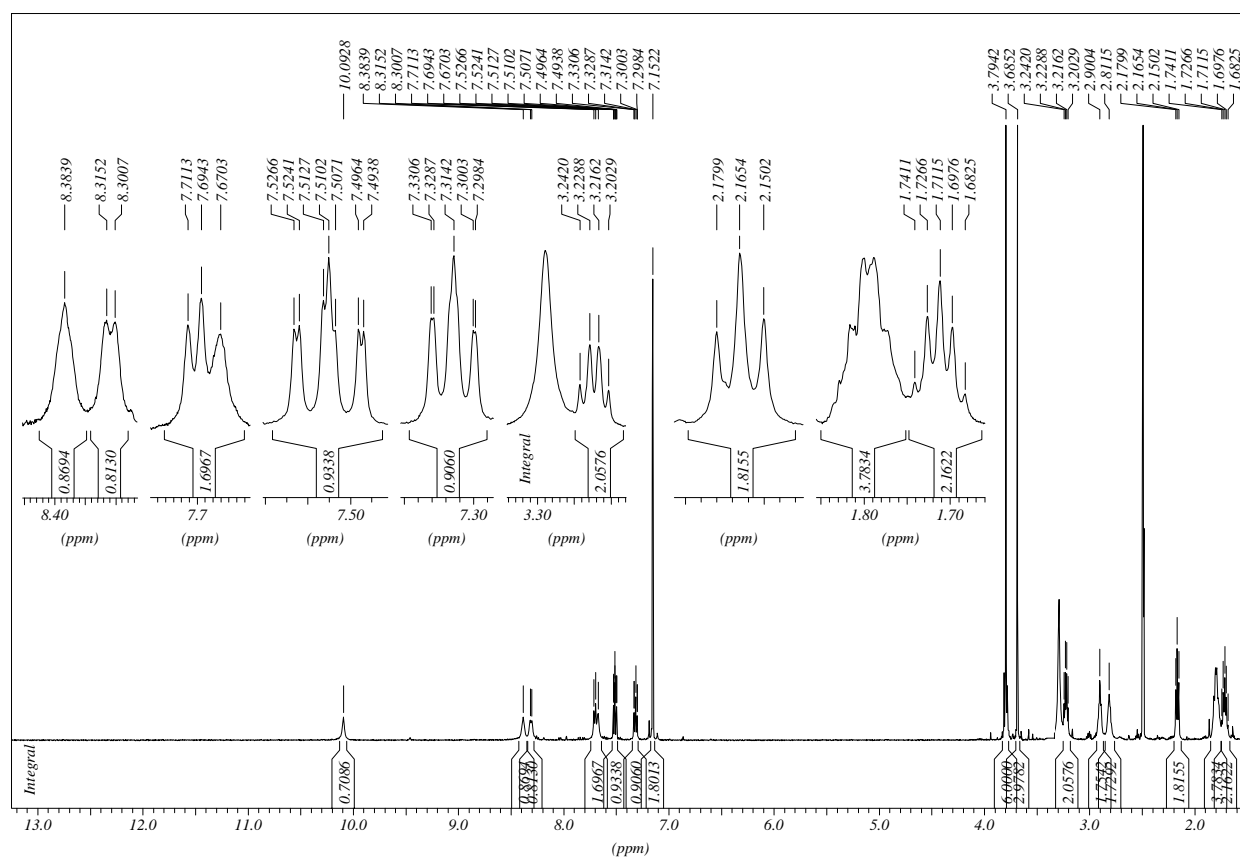
Ethyl 5-((3,4,5-trimethoxybenzoyl)amino)pentanoate
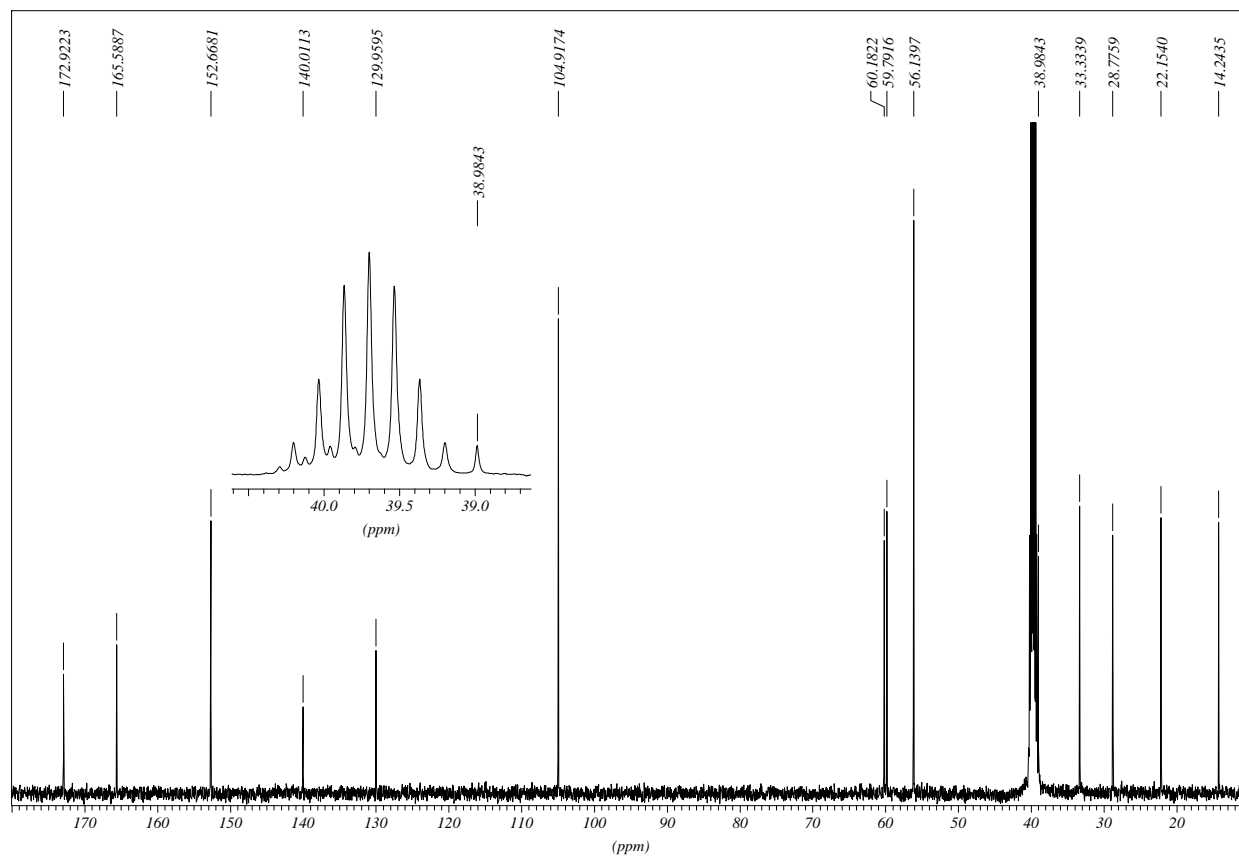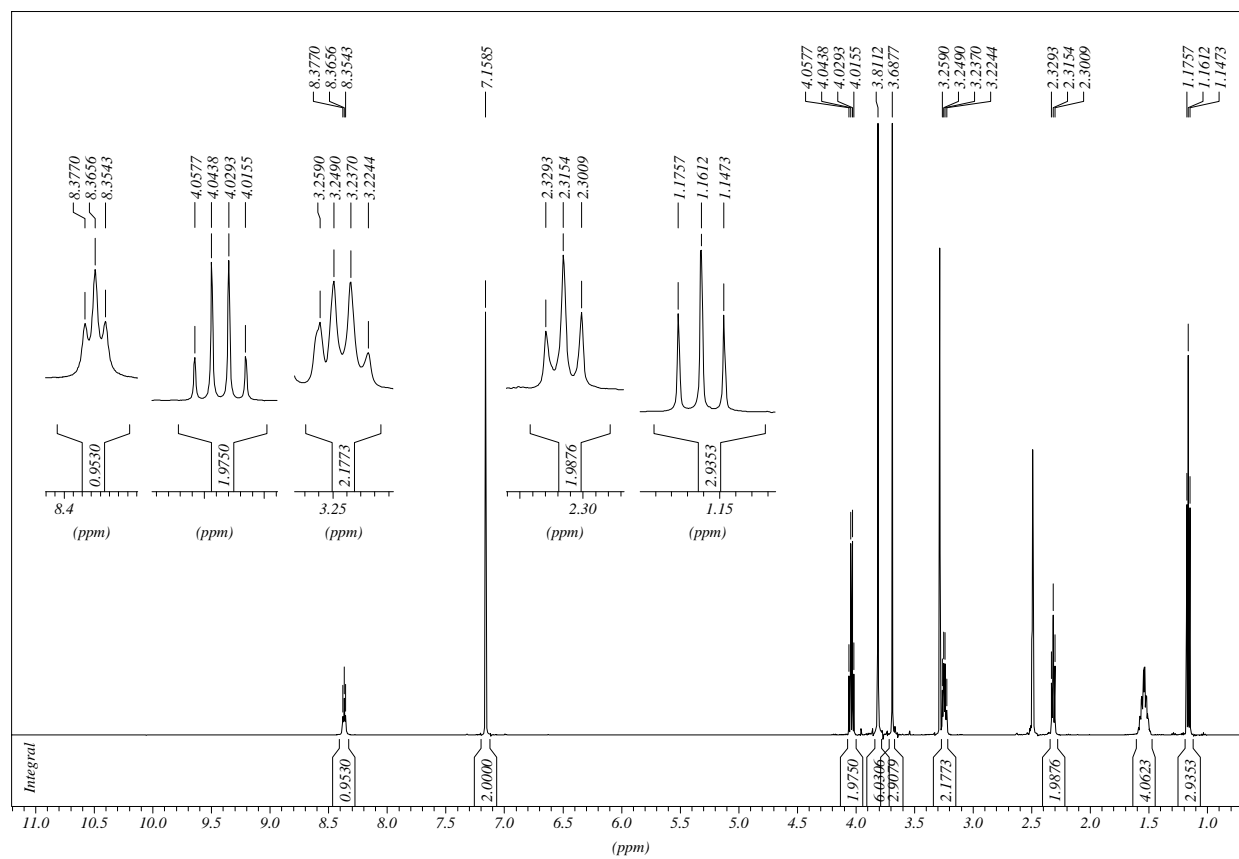
N-(5-Hydrazino-5-oxopentyl)-3,4,5-trimethoxybenzamide
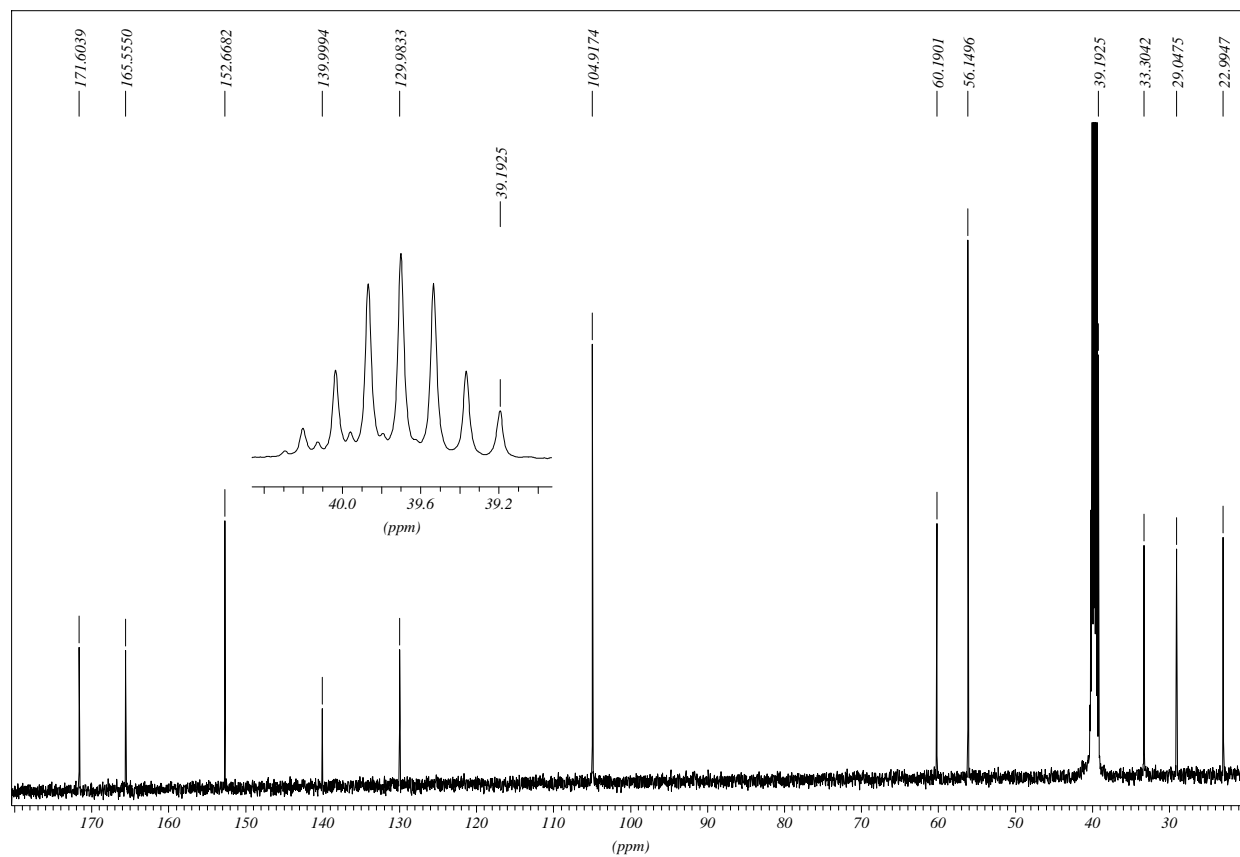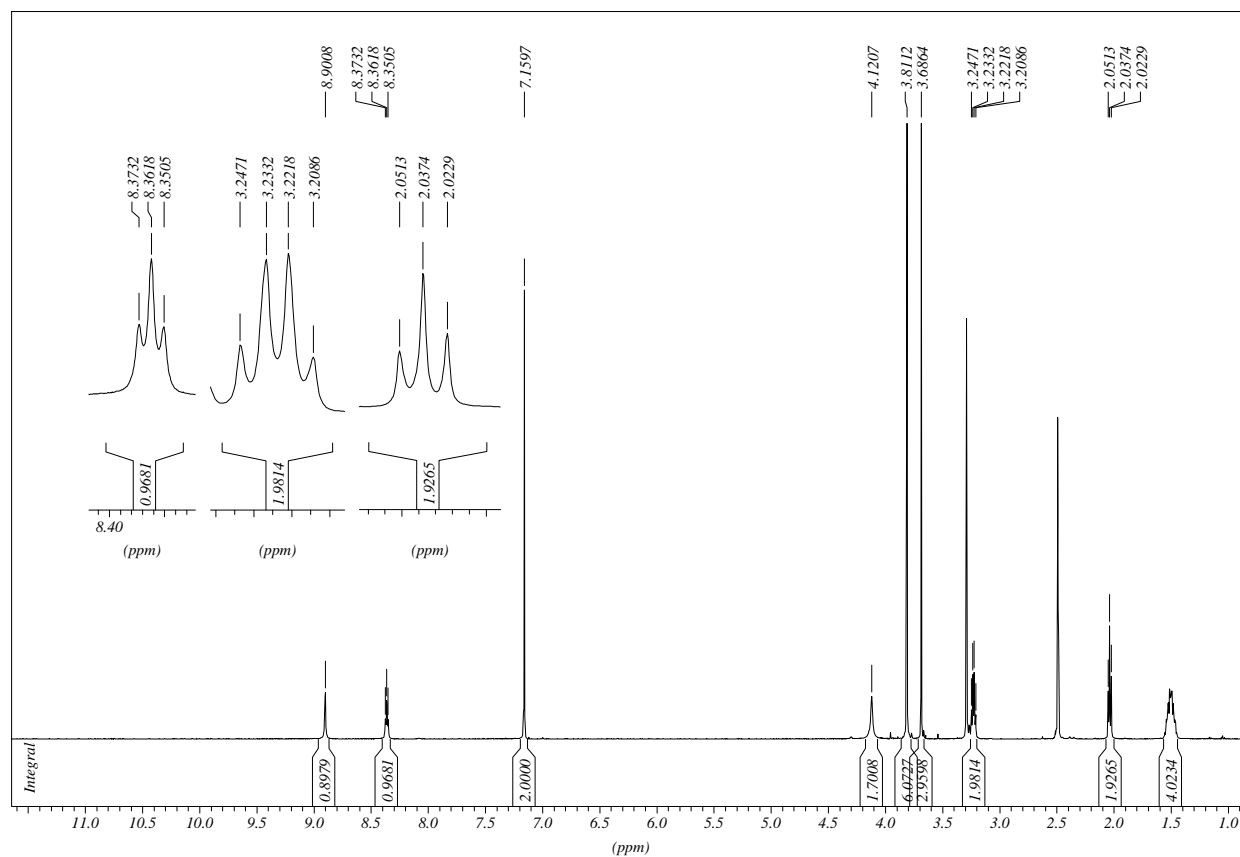
3,4,5-Trimethoxy-*N*-(5-oxo-5-(2-(1,2,3,4-tetrahydroacridin-9-yl)hydrazino)pentyl)benzamide HCl
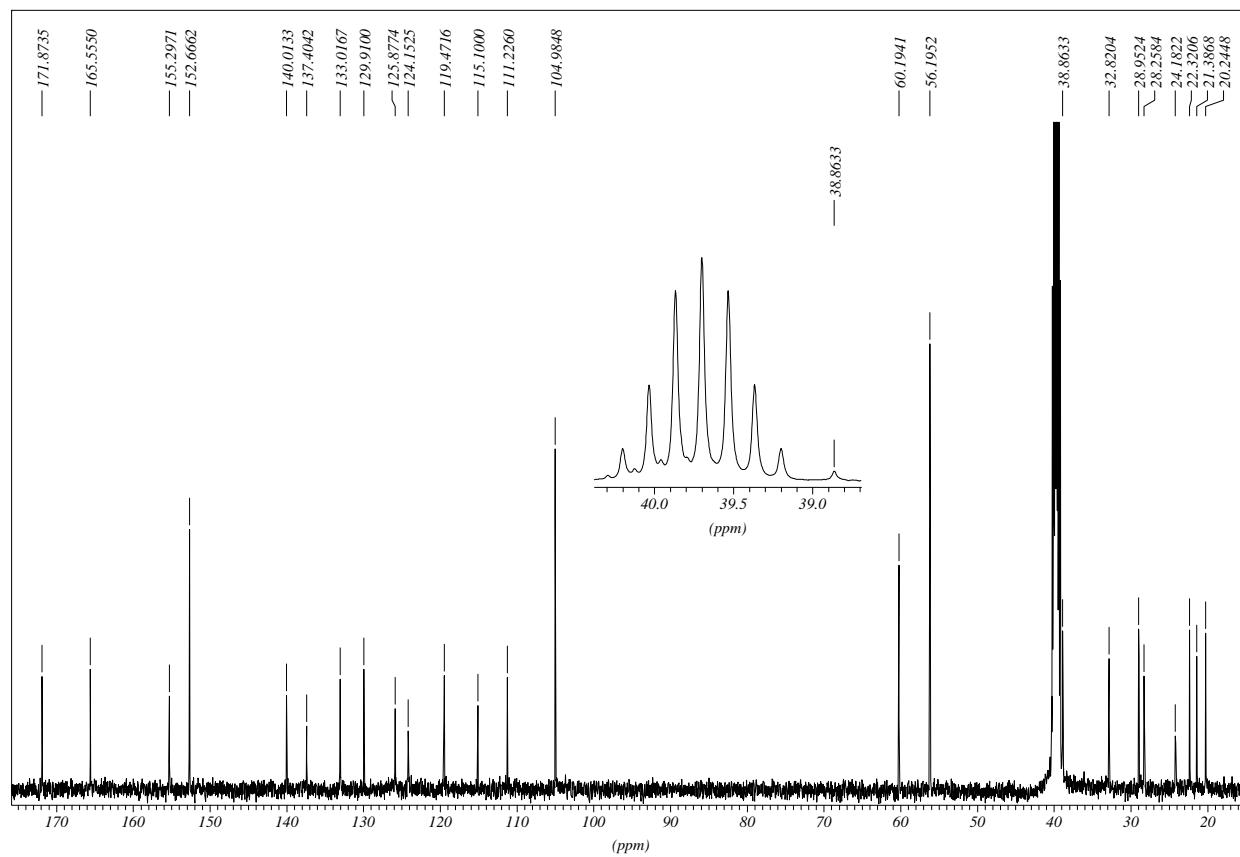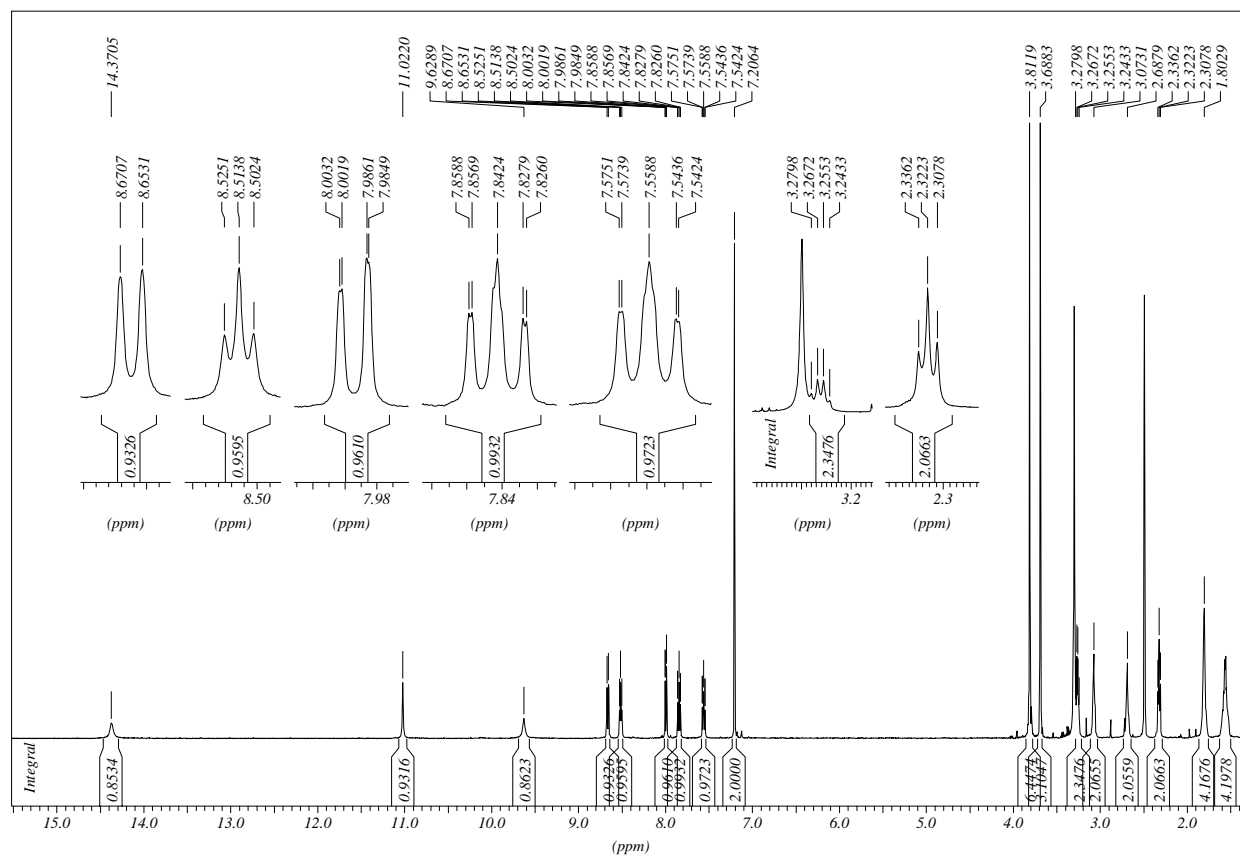
3,4,5-Trimethoxy-*N*-(5-oxo-5-(2-(1,2,3,4-tetrahydroacridin-9-yl)hydrazino)pentyl)benzamide
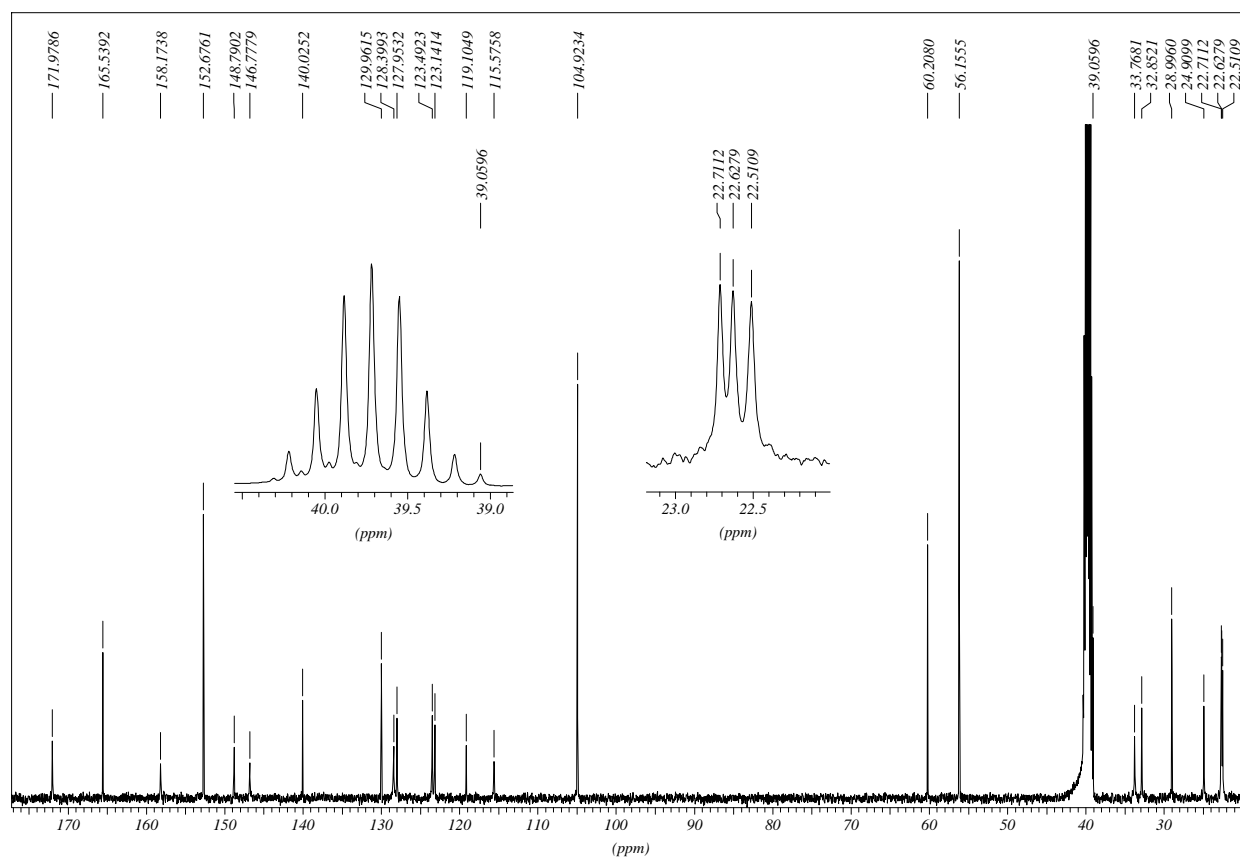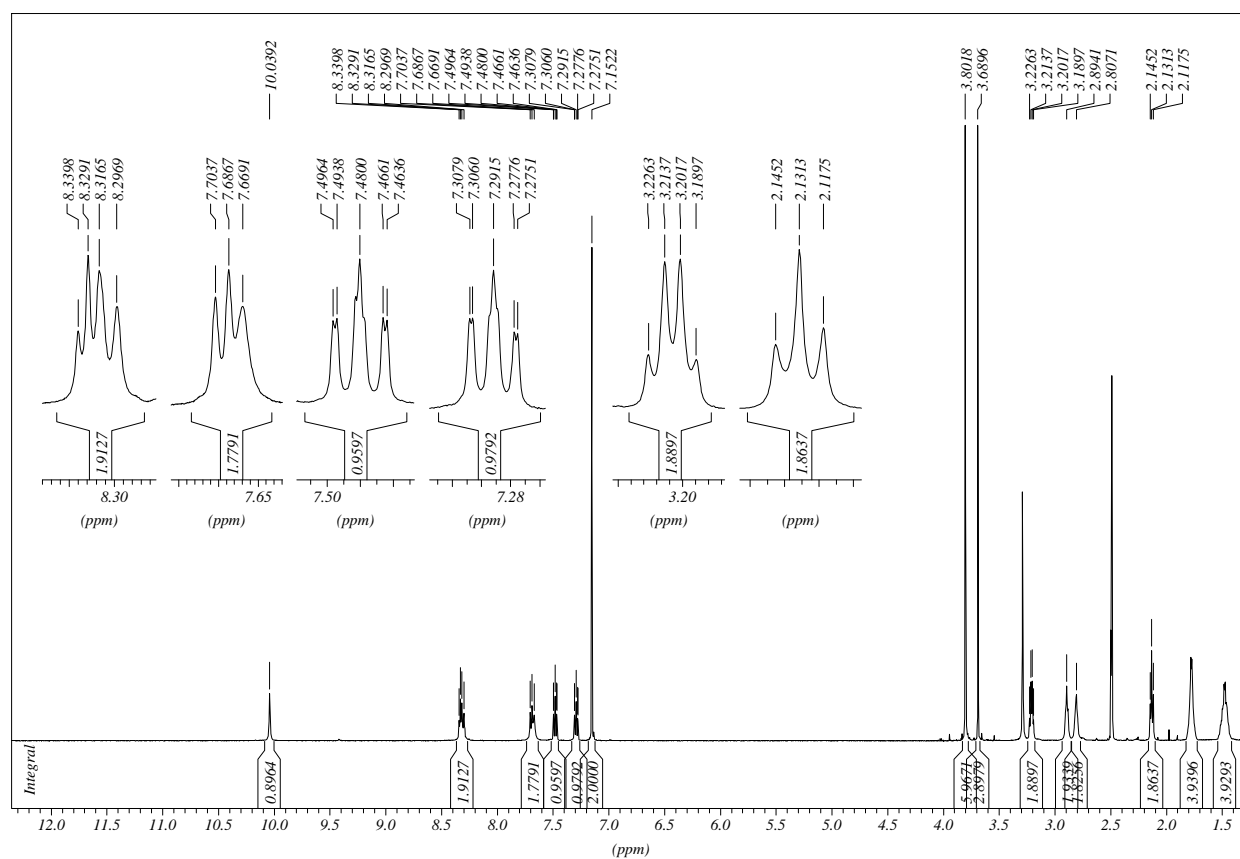
Ethyl 6-((3,4,5-trimethoxybenzoyl)amino)hexanoate
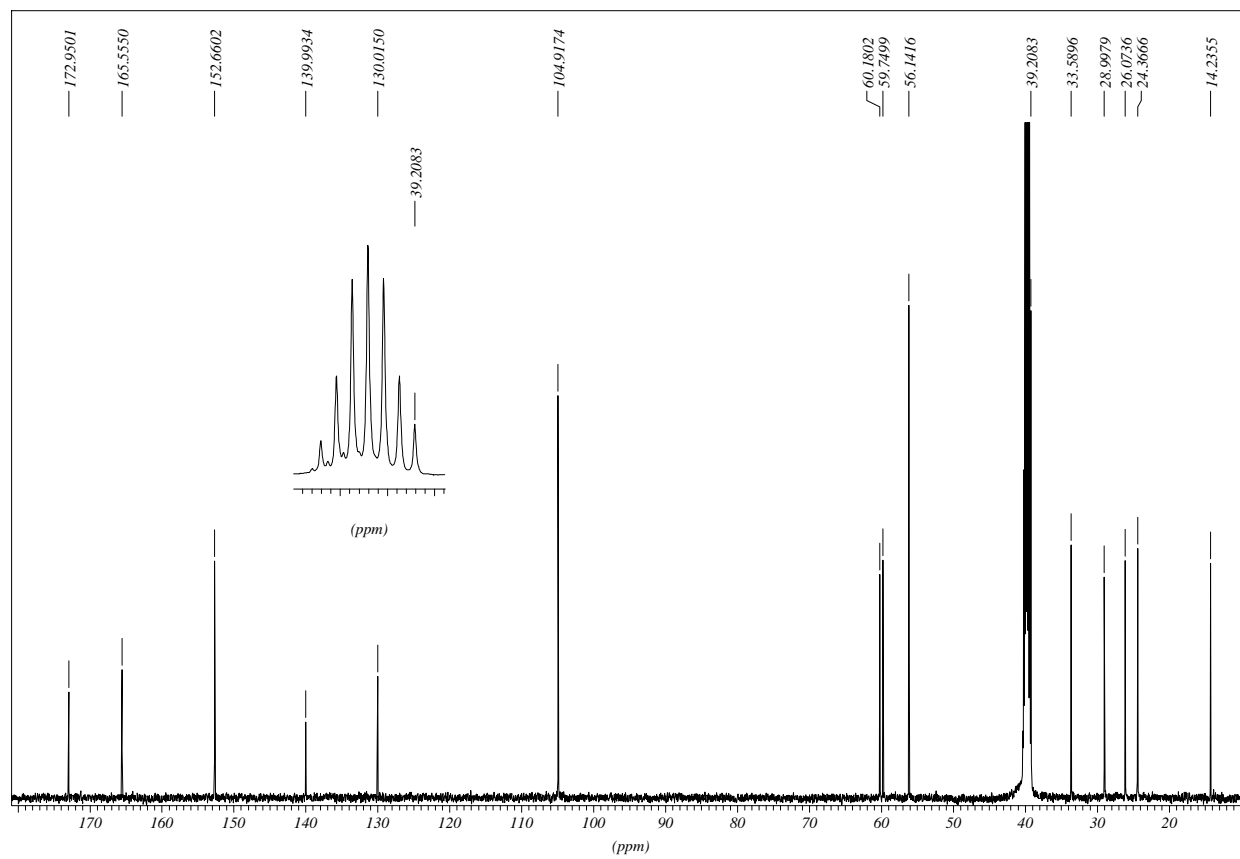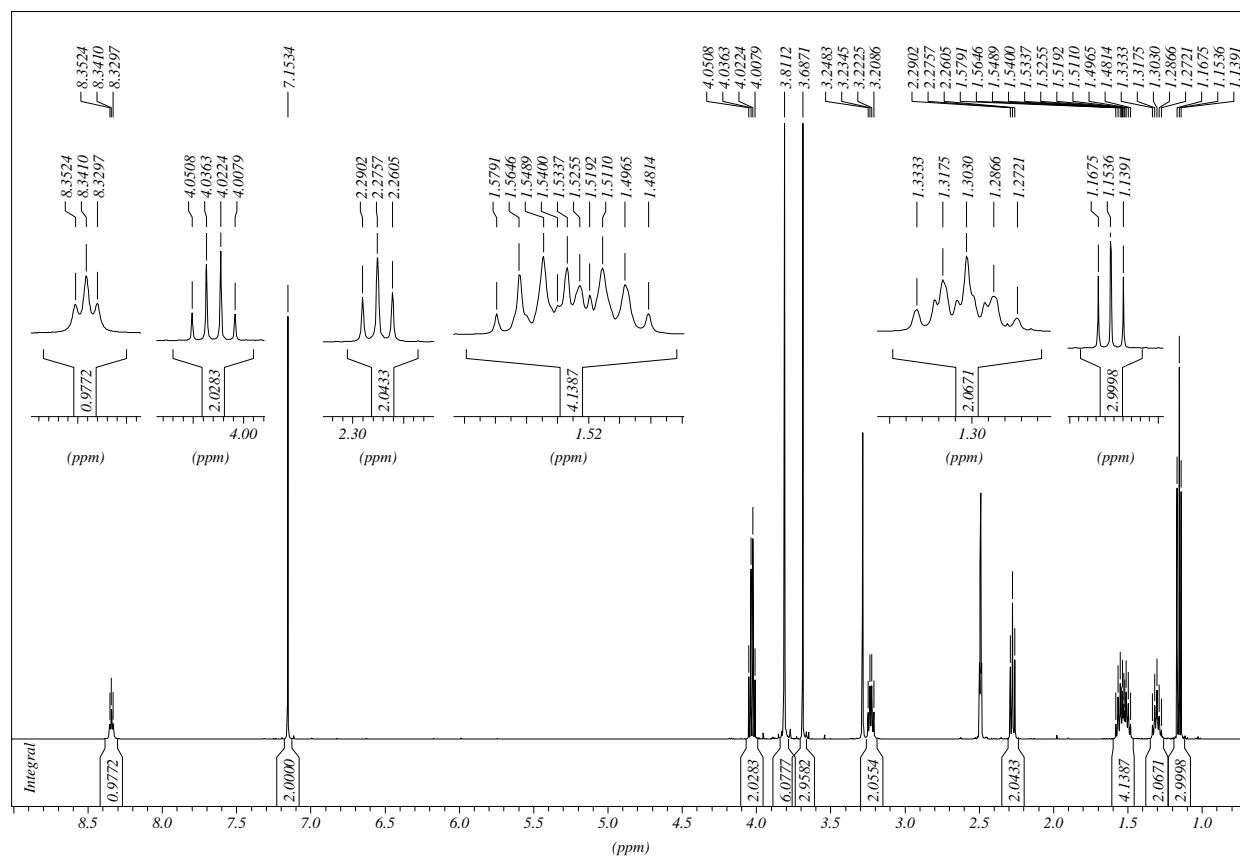
N-(6-Hydrazino-6-oxohexyl)-3,4,5-trimethoxybenzamide
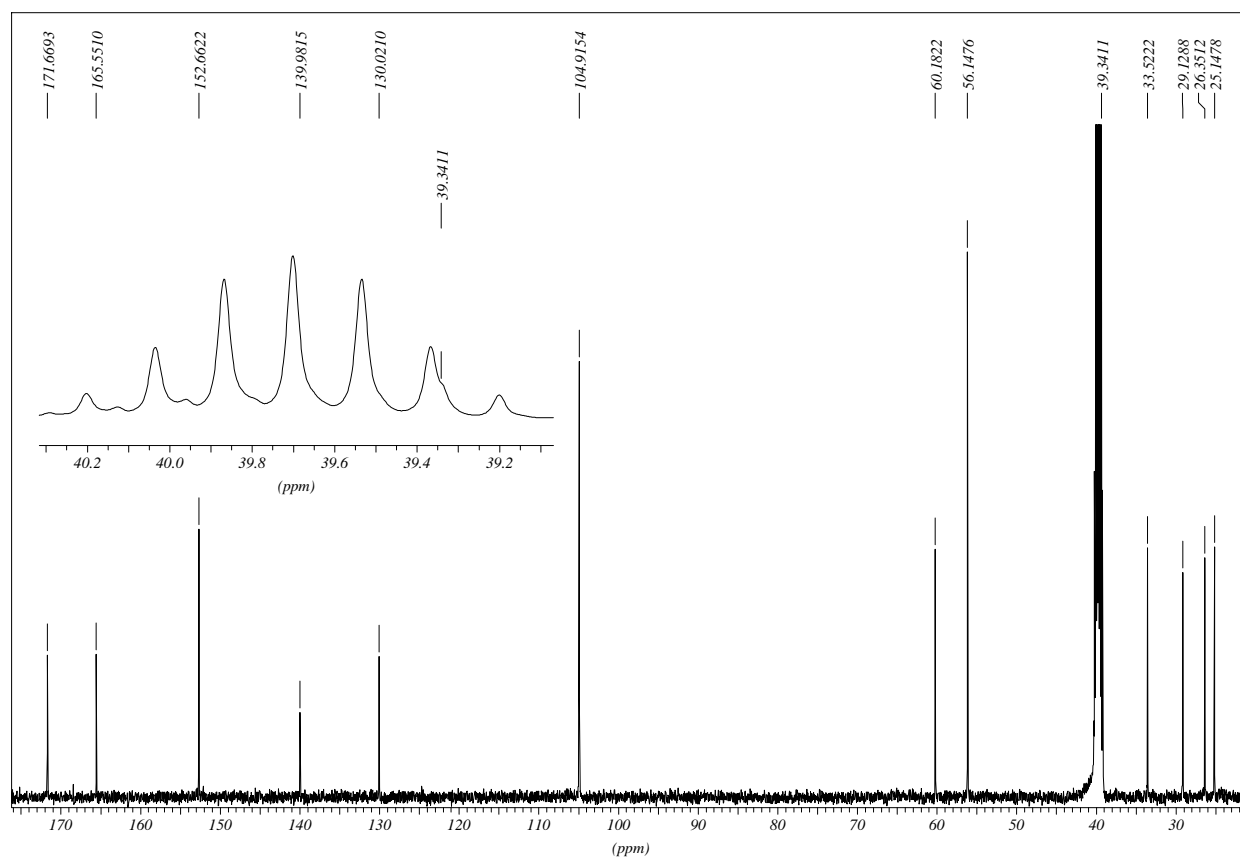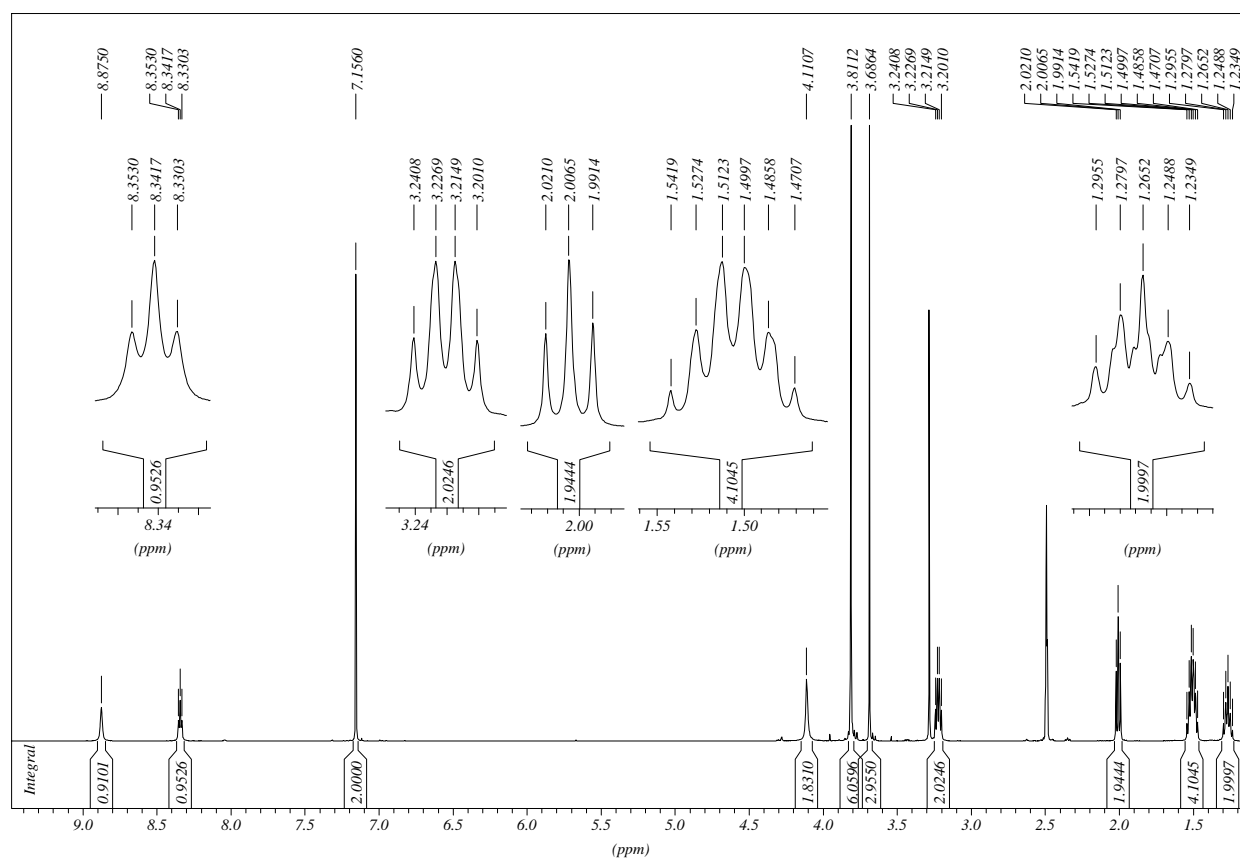
3,4,5-Trimethoxy-*N*-(6-oxo-6-(2-(1,2,3,4-tetrahydroacridin-9-yl)hydrazino)hexyl)benzamide HCl
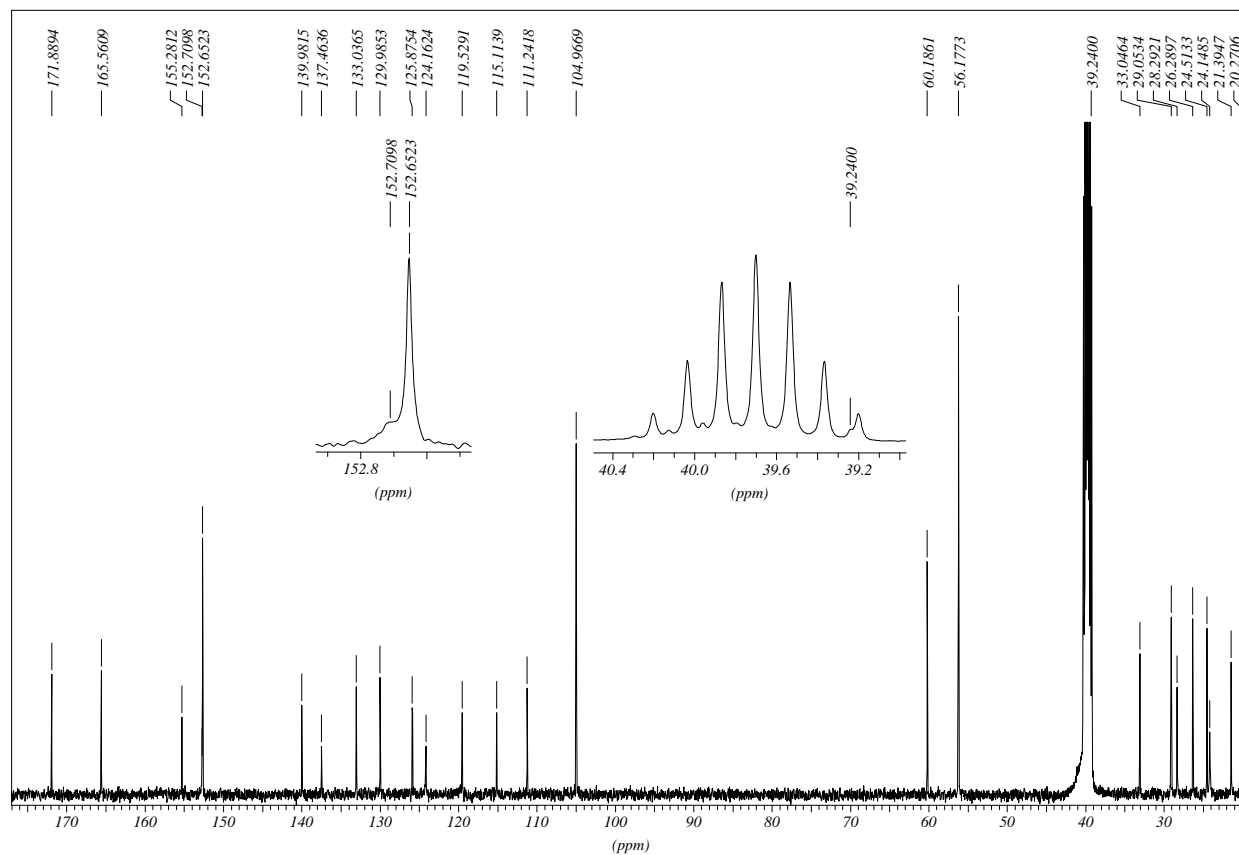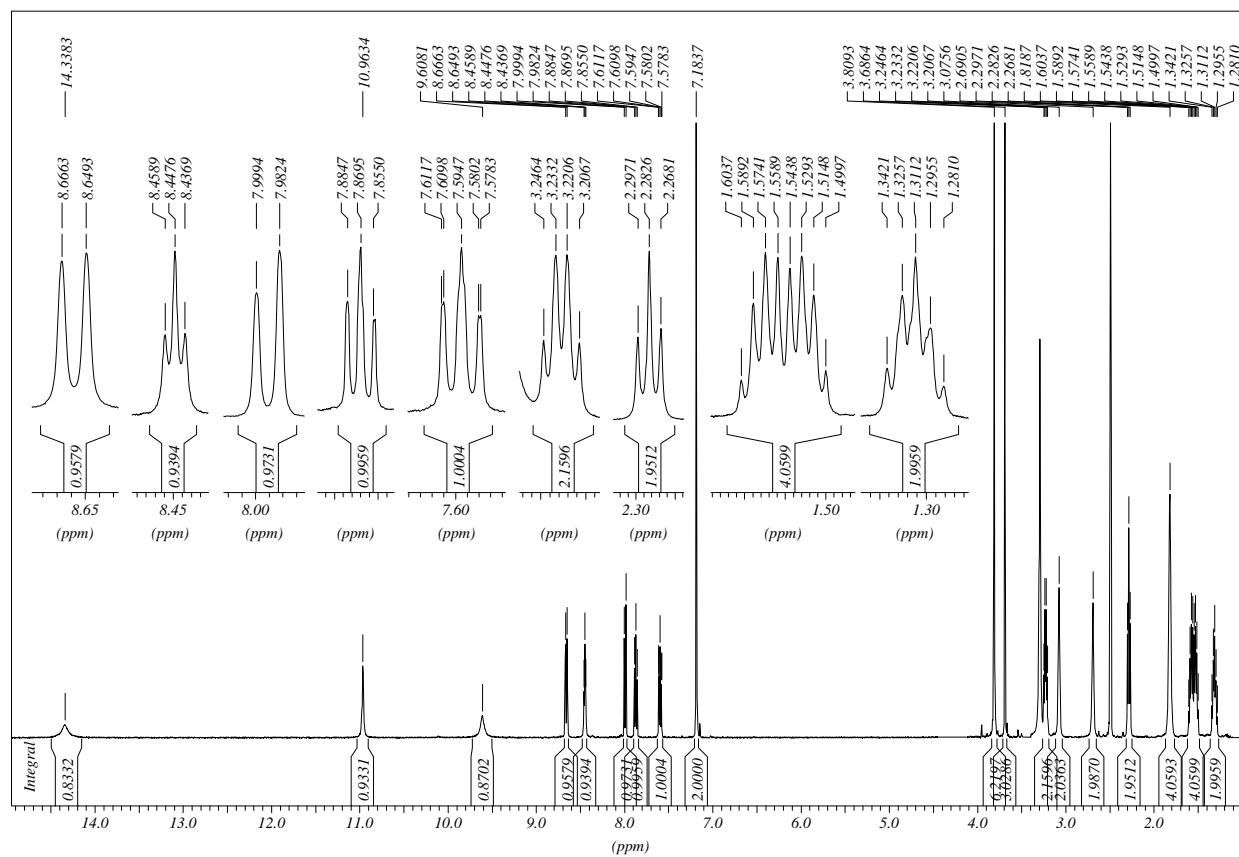
3,4,5-Trimethoxy-*N*-(6-oxo-6-(2-(1,2,3,4-tetrahydroacridin-9-yl)hydrazino)hexyl)benzamide
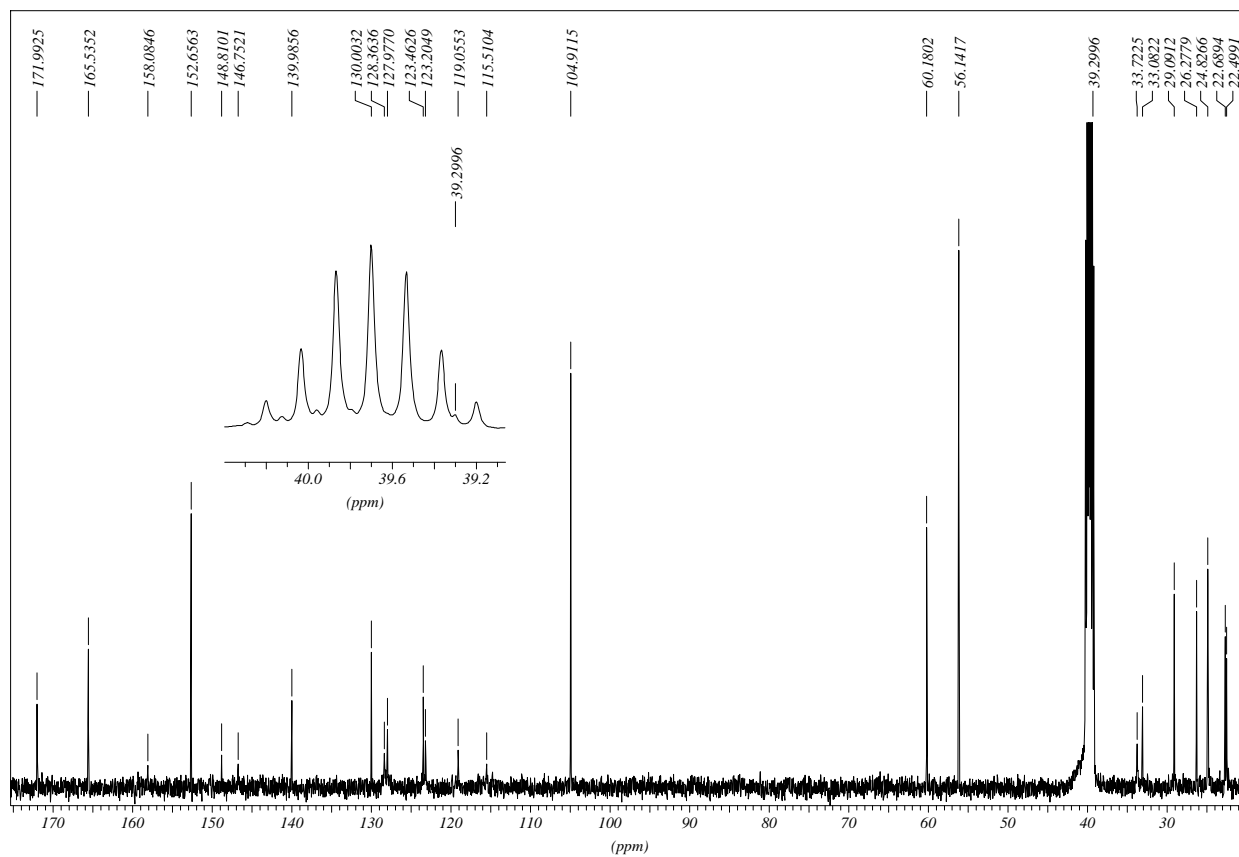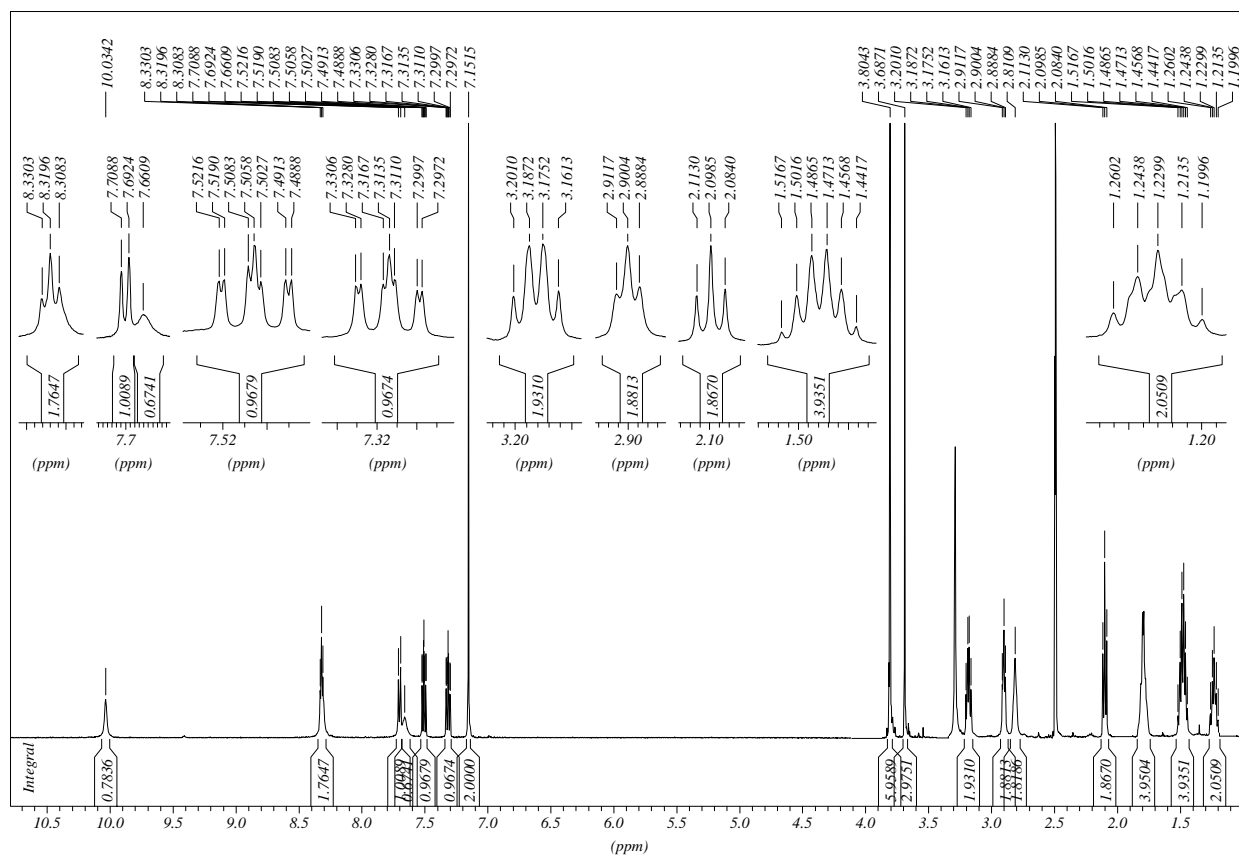
Ethyl 7-((3,4,5-trimethoxybenzoyl)amino)heptanoate
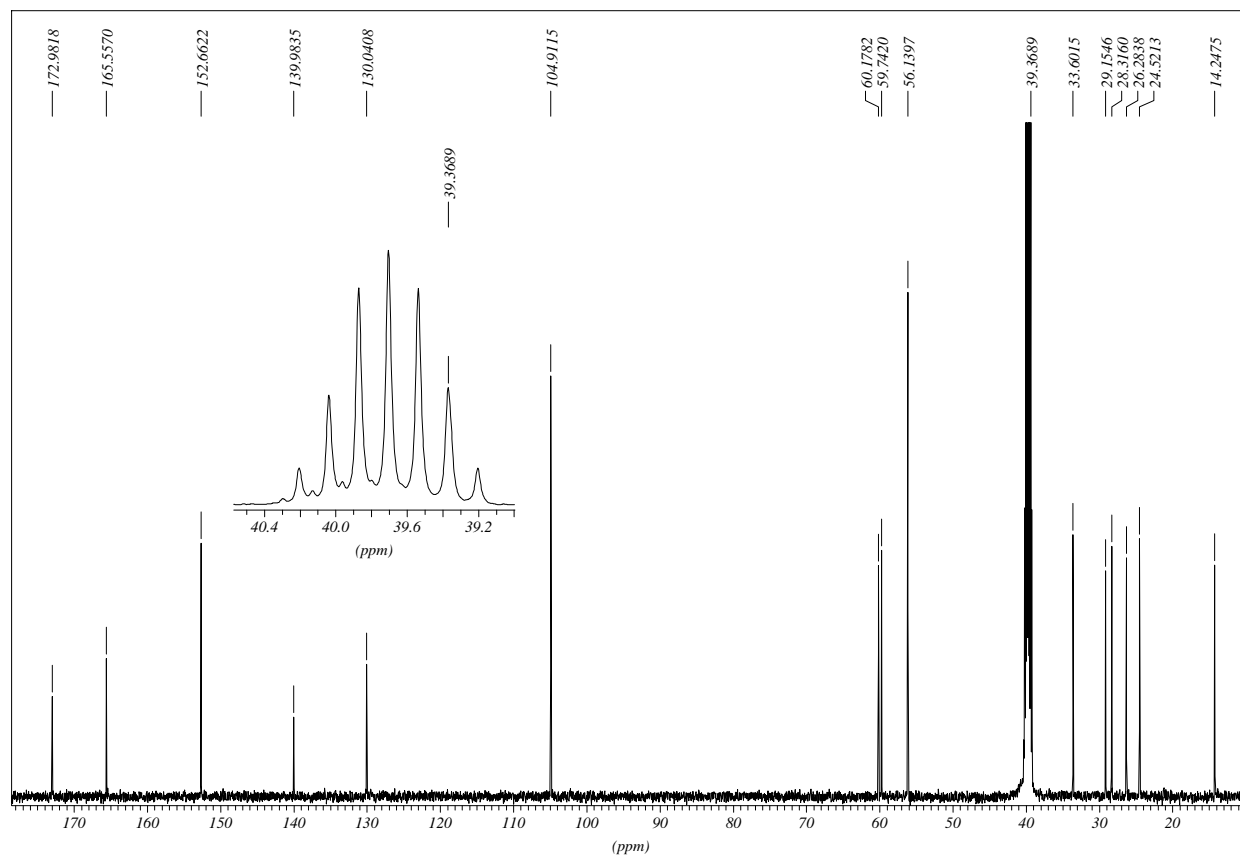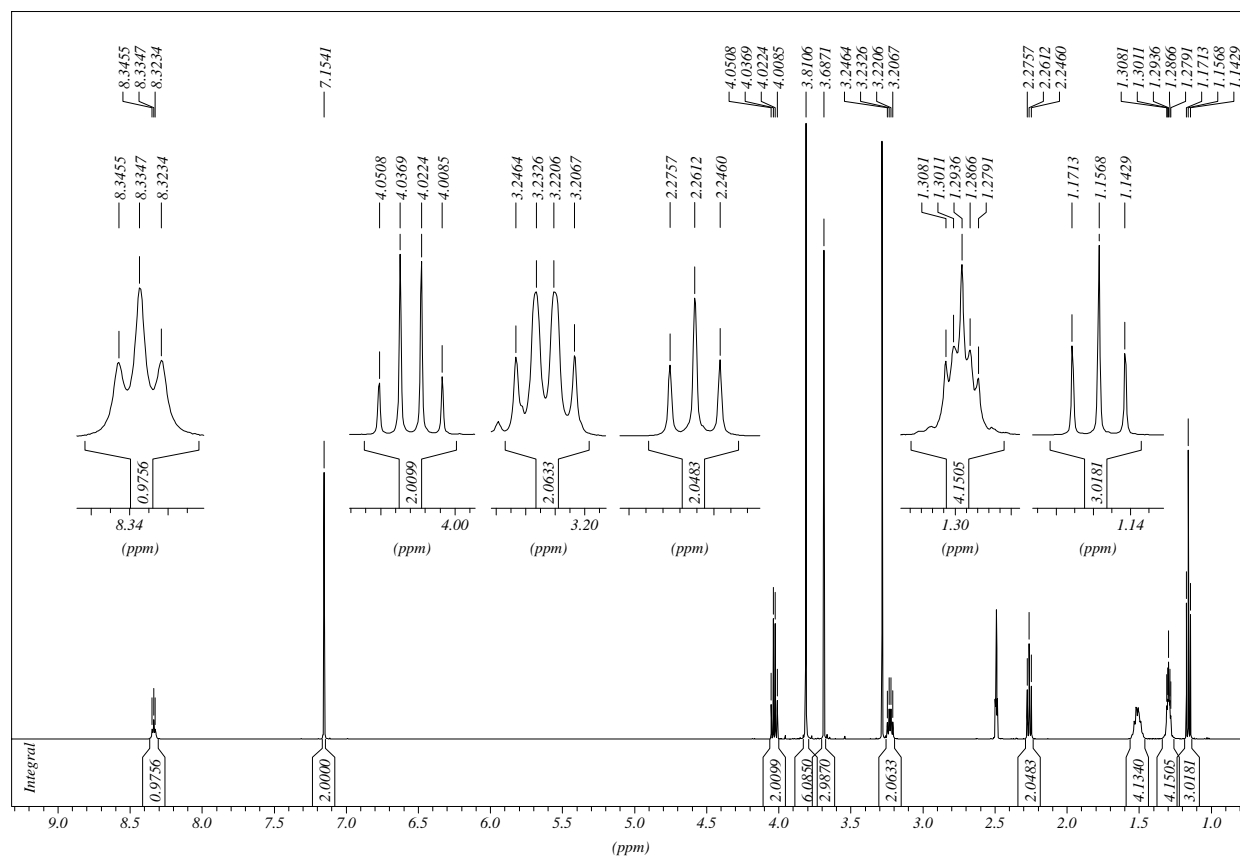
N-(7-Hydrazino-7-oxoheptyl)-3,4,5-trimethoxybenzamide

3,4,5-Trimethoxy-*N*-(7-oxo-7-(2-(1,2,3,4-tetrahydroacridin-9-yl)hydrazino)heptyl)benzamide

3,4,5-Trimethoxy-*N*-(7-oxo-7-(2-(6-chloro-1,2,3,4-tetrahydroacridin-9-yl)hydrazino)heptyl)-benzamide HCl
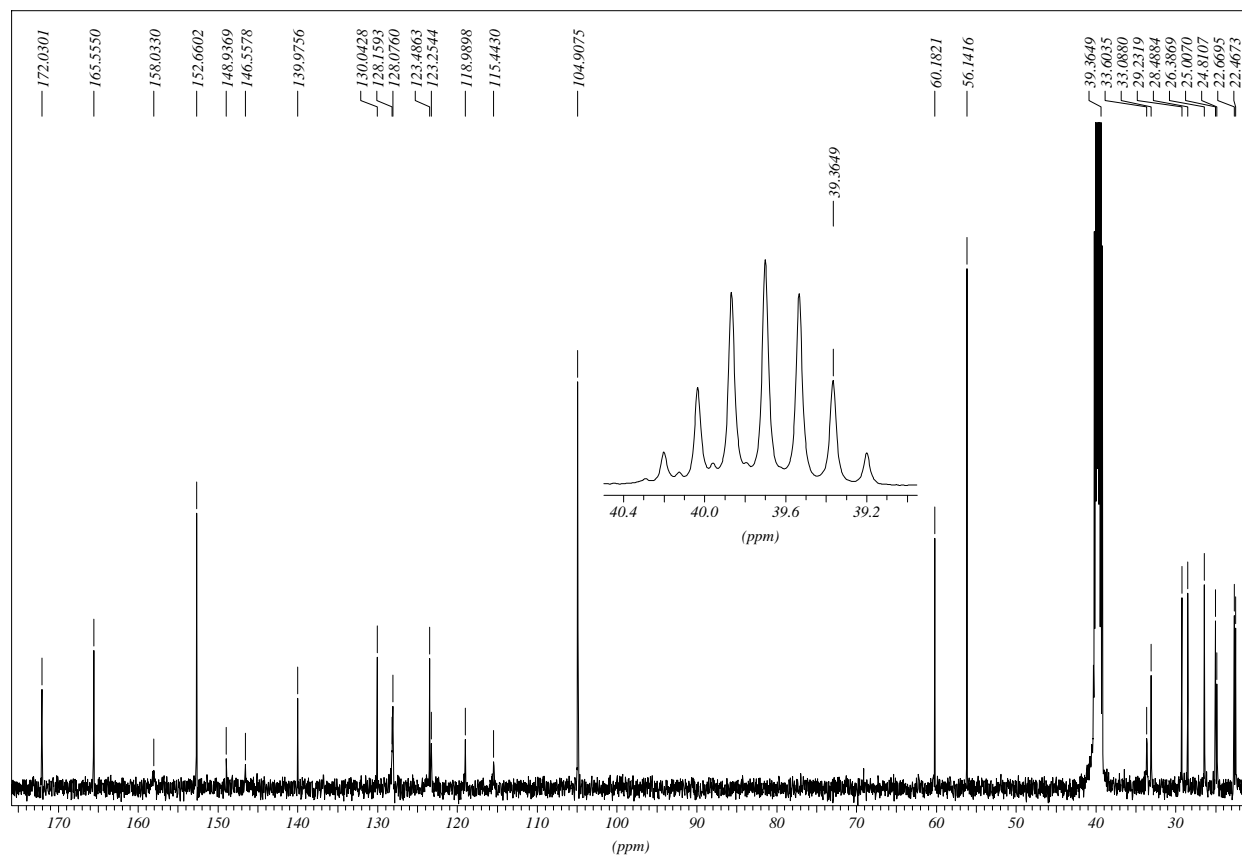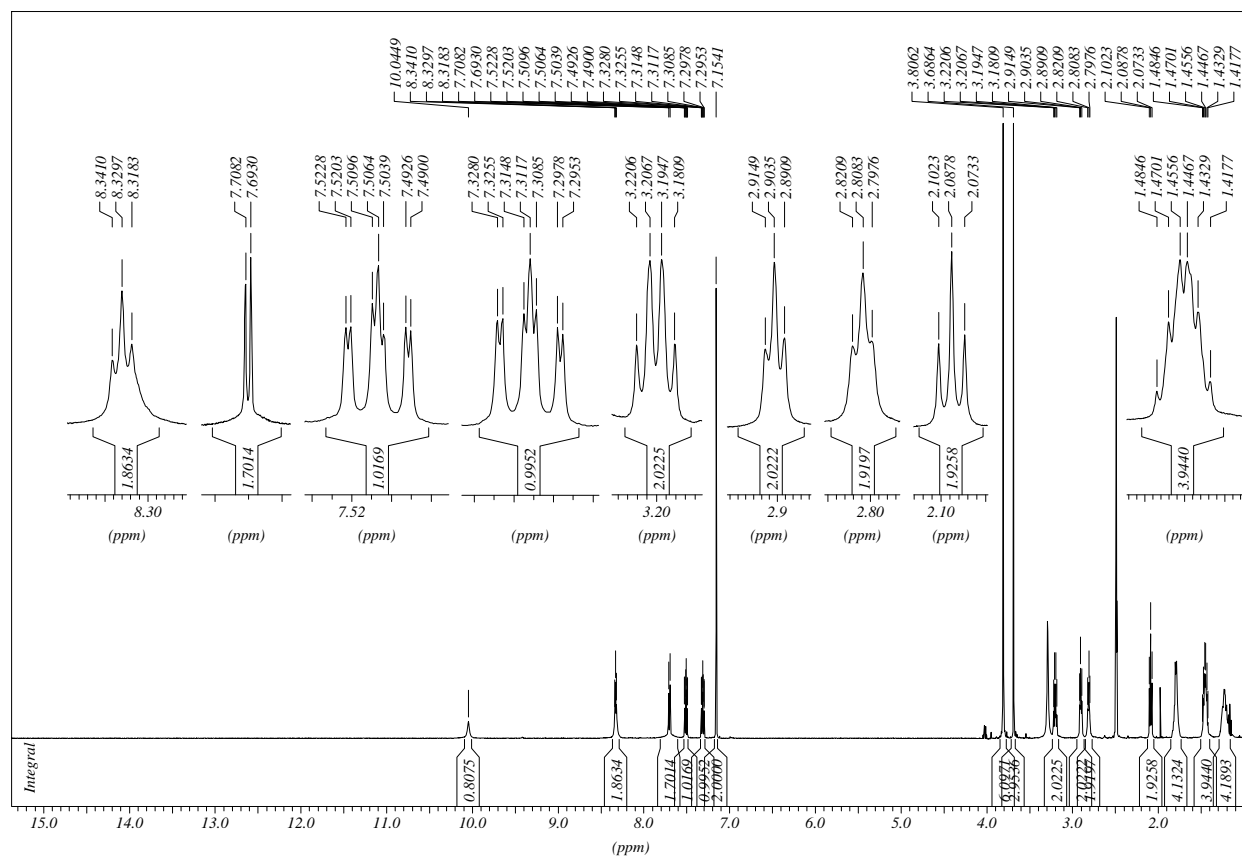
Ethyl 8-((3,4,5-trimethoxybenzoyl)amino)octanoate
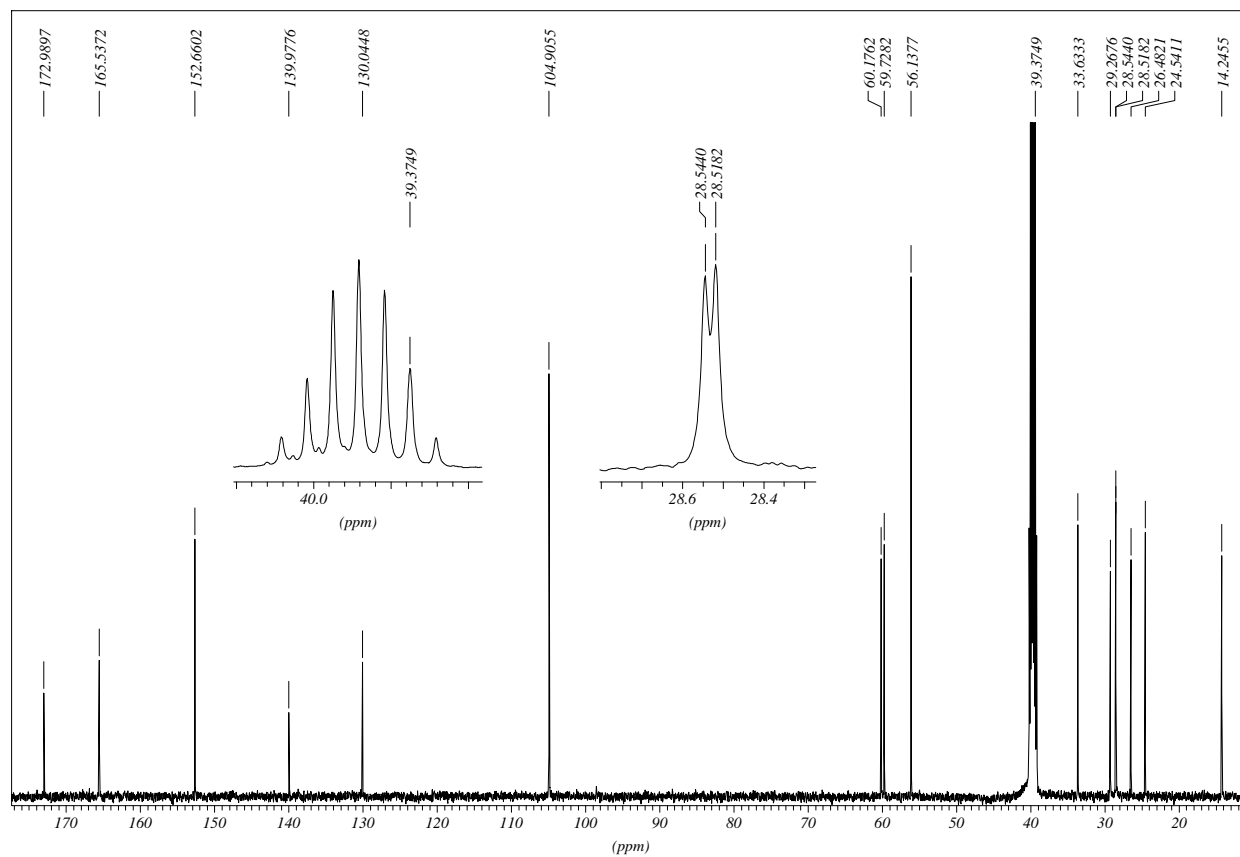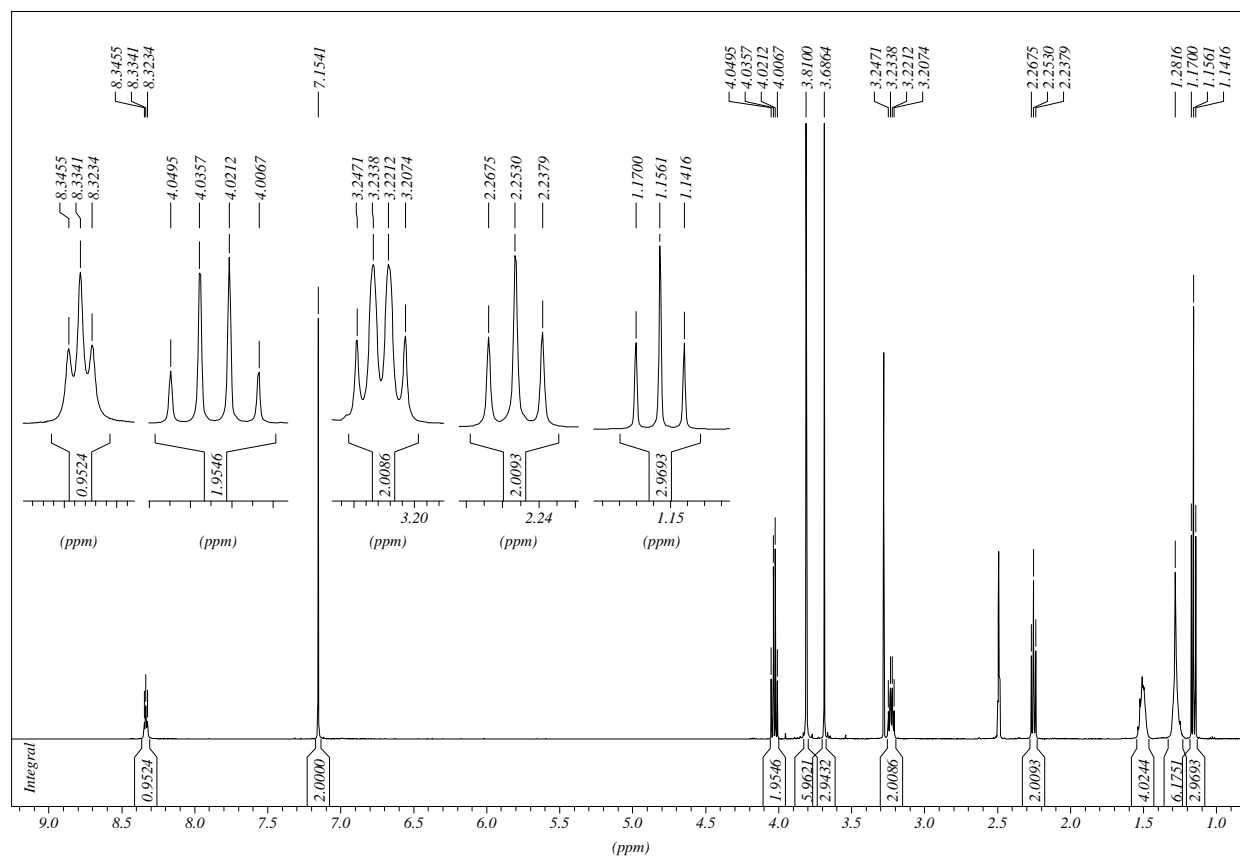
N-(8-Hydrazino-8-oxooctyl)-3,4,5-trimethoxybenzamide
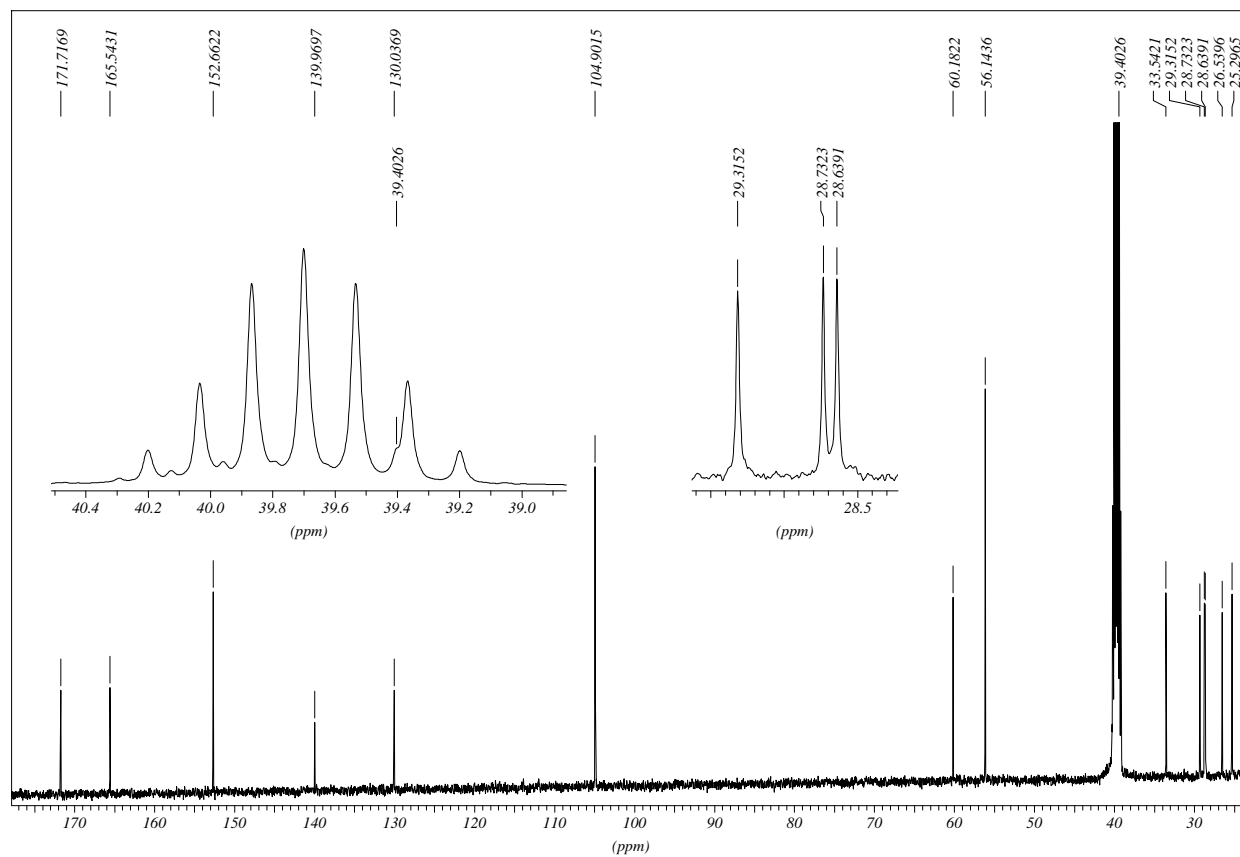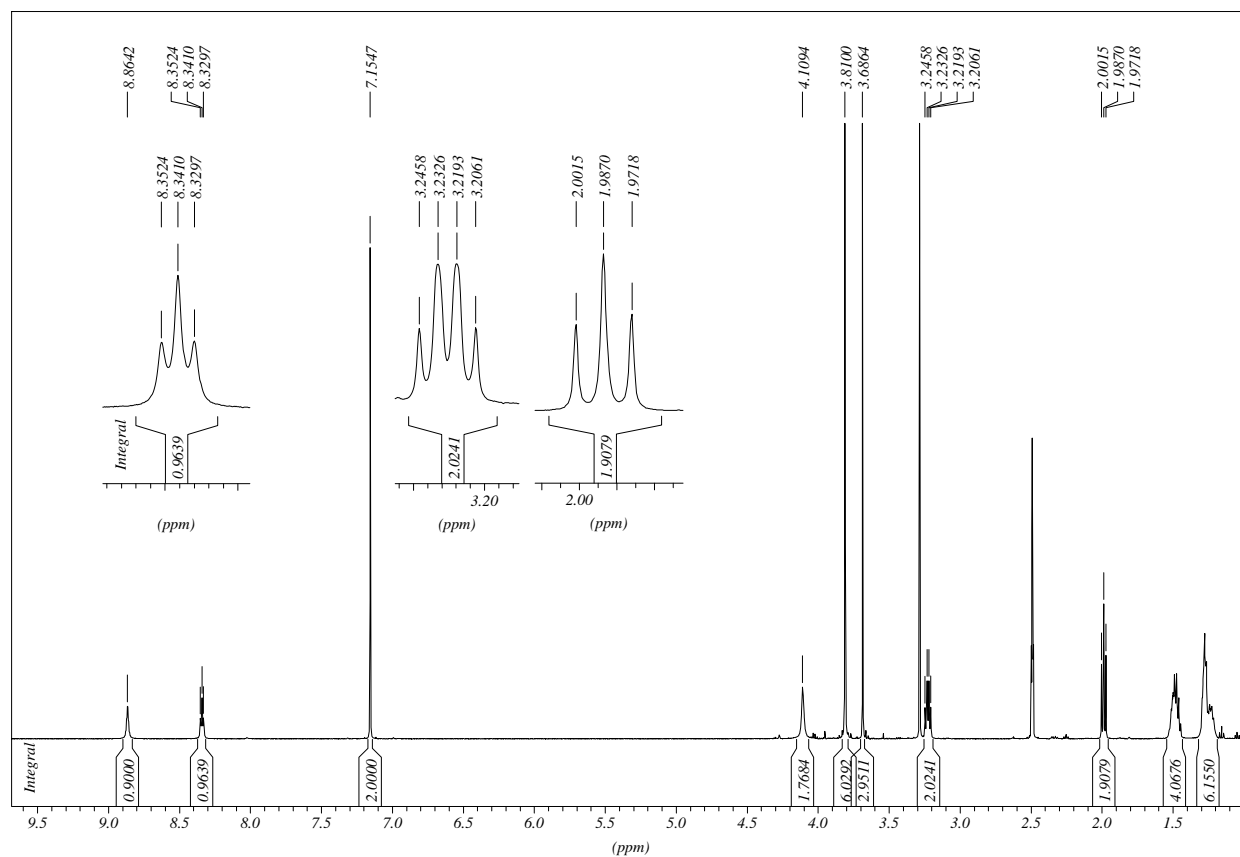
3,4,5-Trimethoxy-*N*-(8-oxo-8-(2-(1,2,3,4-tetrahydroacridin-9-yl)hydrazino)octyl)benzamide
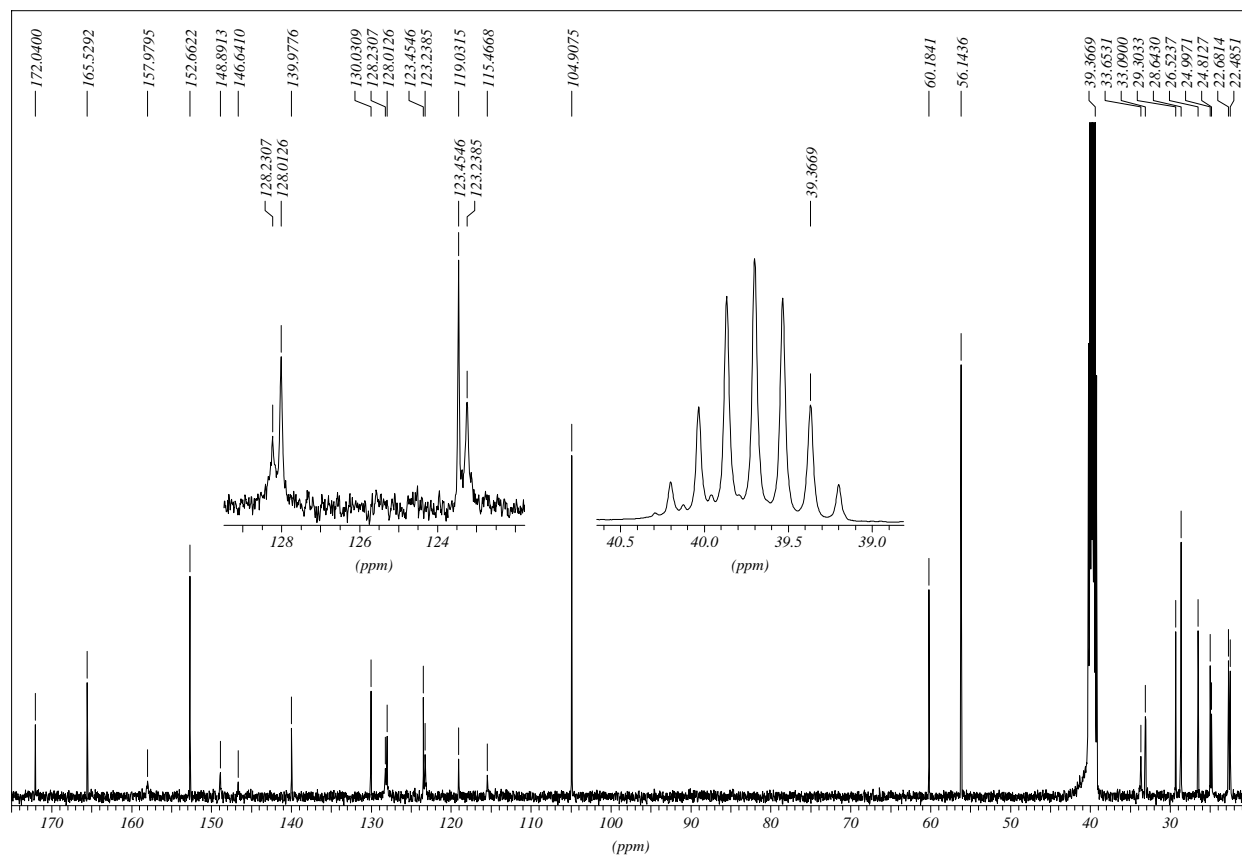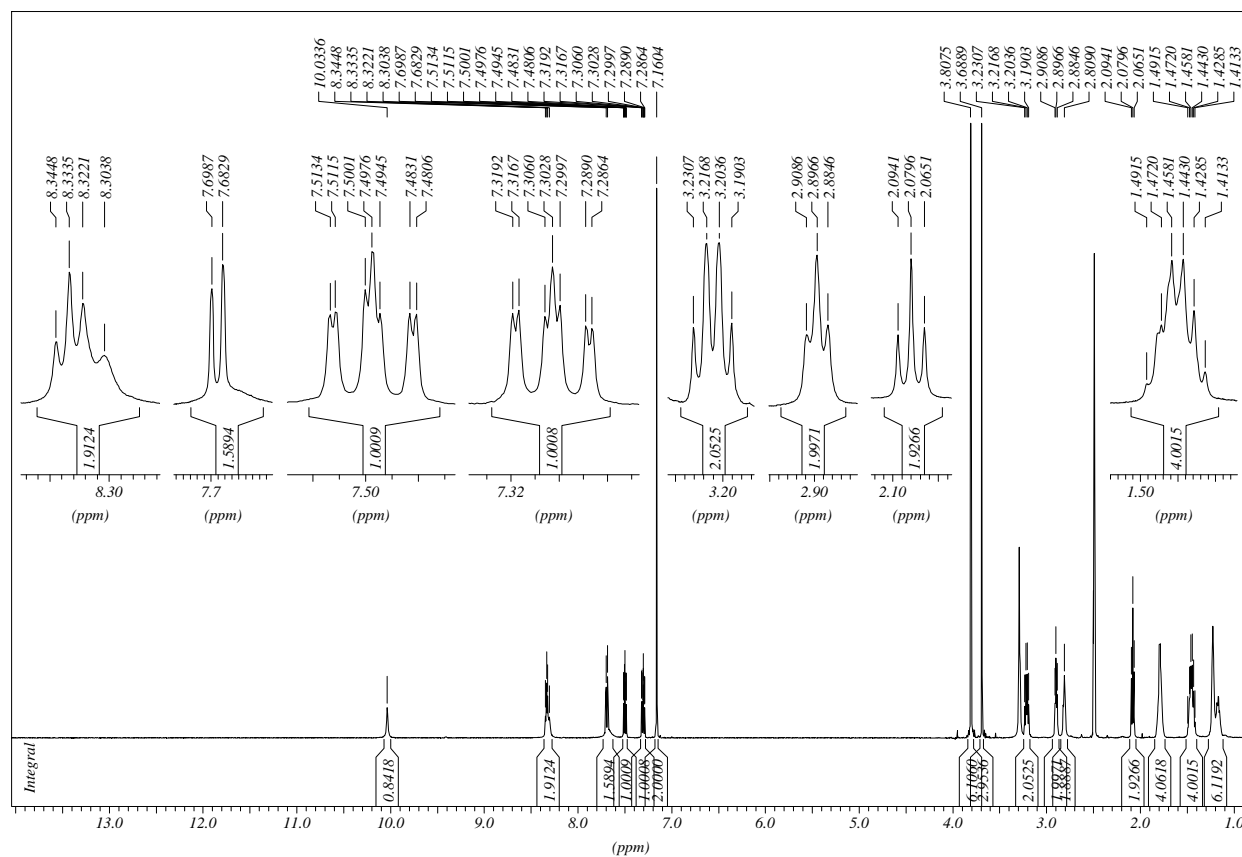
3,4,5-Trimethoxy-*N*-(8-oxo-8-(2-(6-chloro-1,2,3,4-tetrahydroacridin-9-yl)hydrazino)octyl)-benzamide HCl

Ethyl 9-((3,4,5-trimethoxybenzoyl)amino)nonanoate
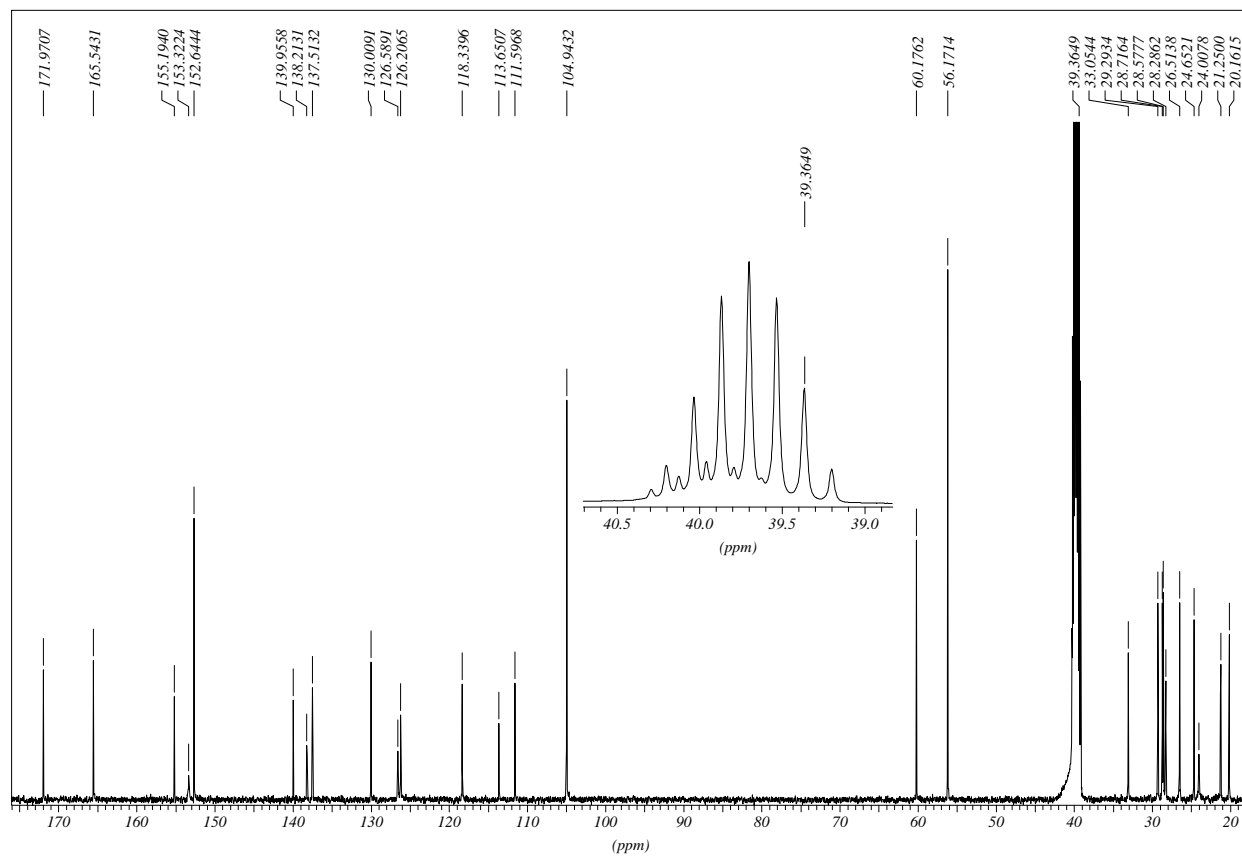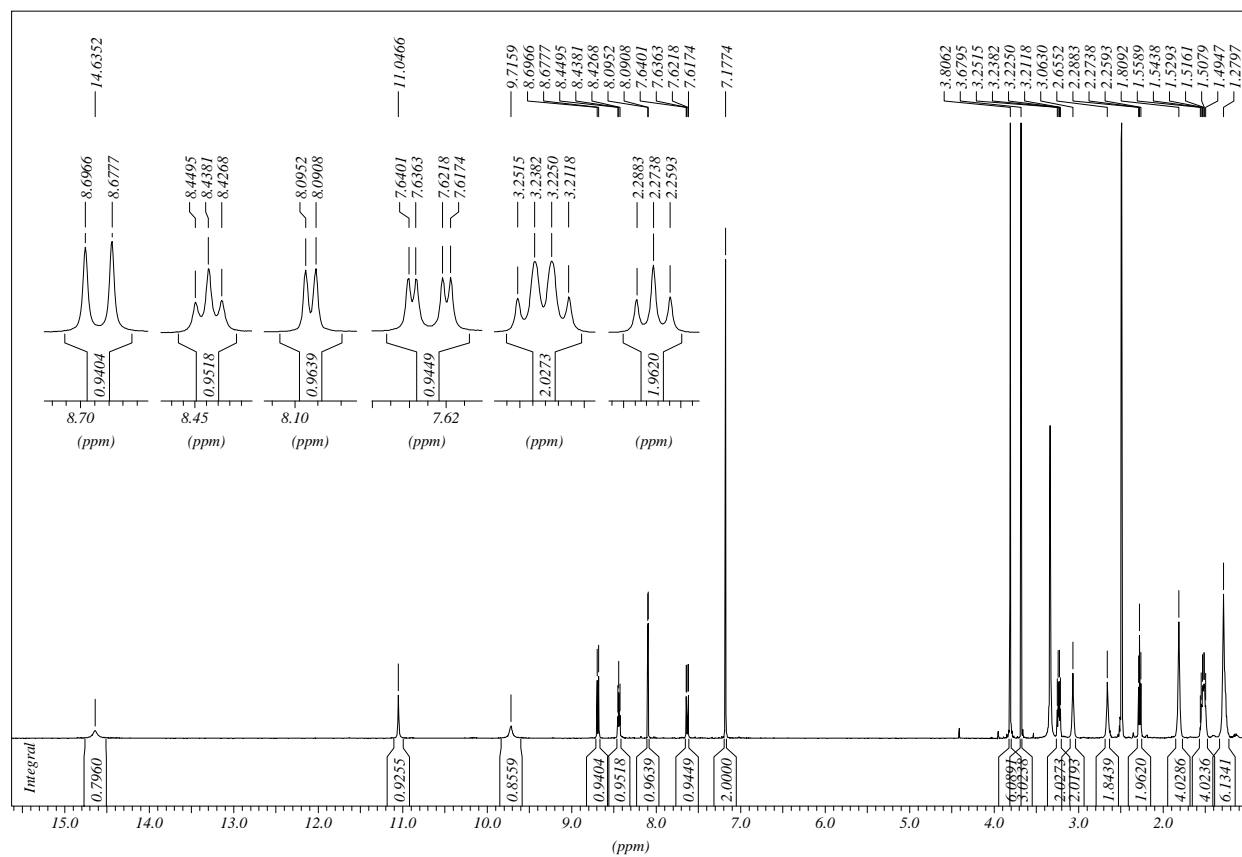
N-(9-Hydrazino-9-oxononyl)-3,4,5-trimethoxybenzamide
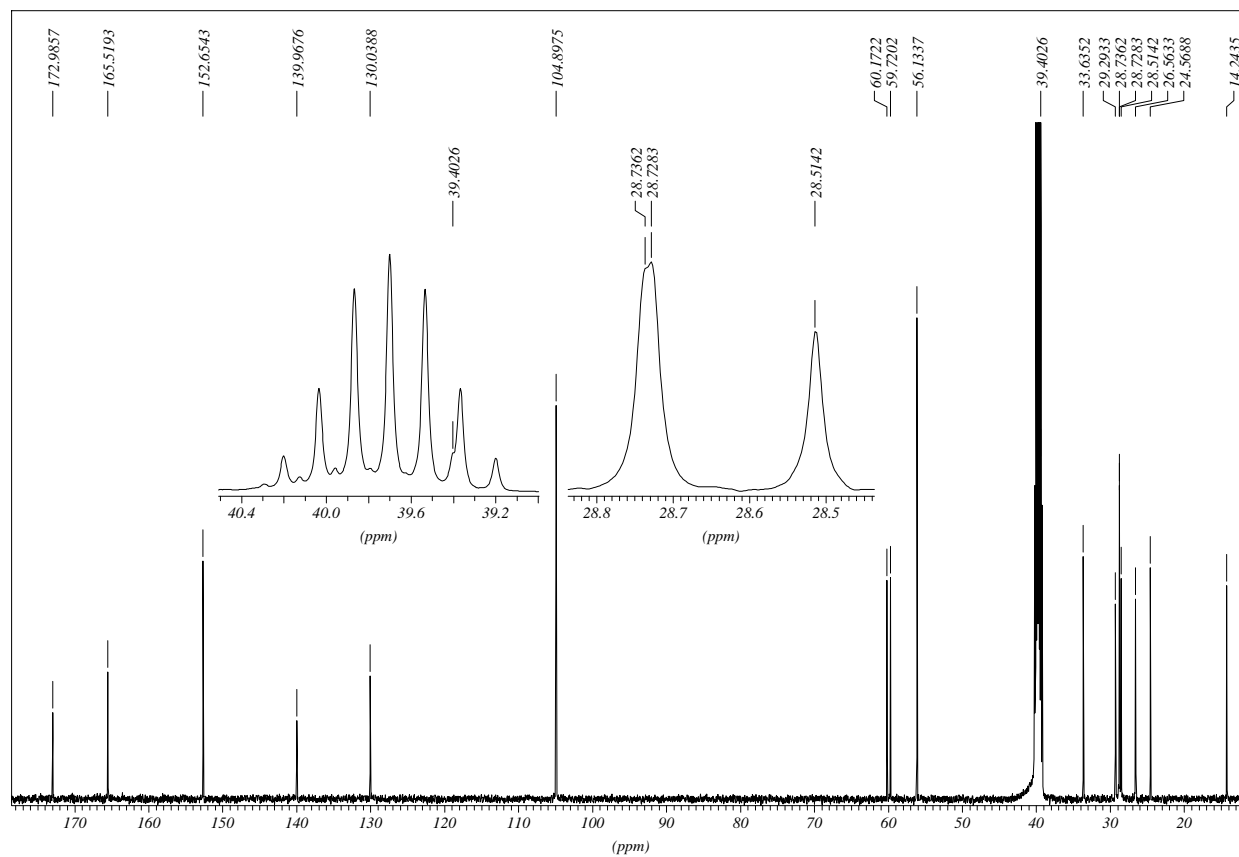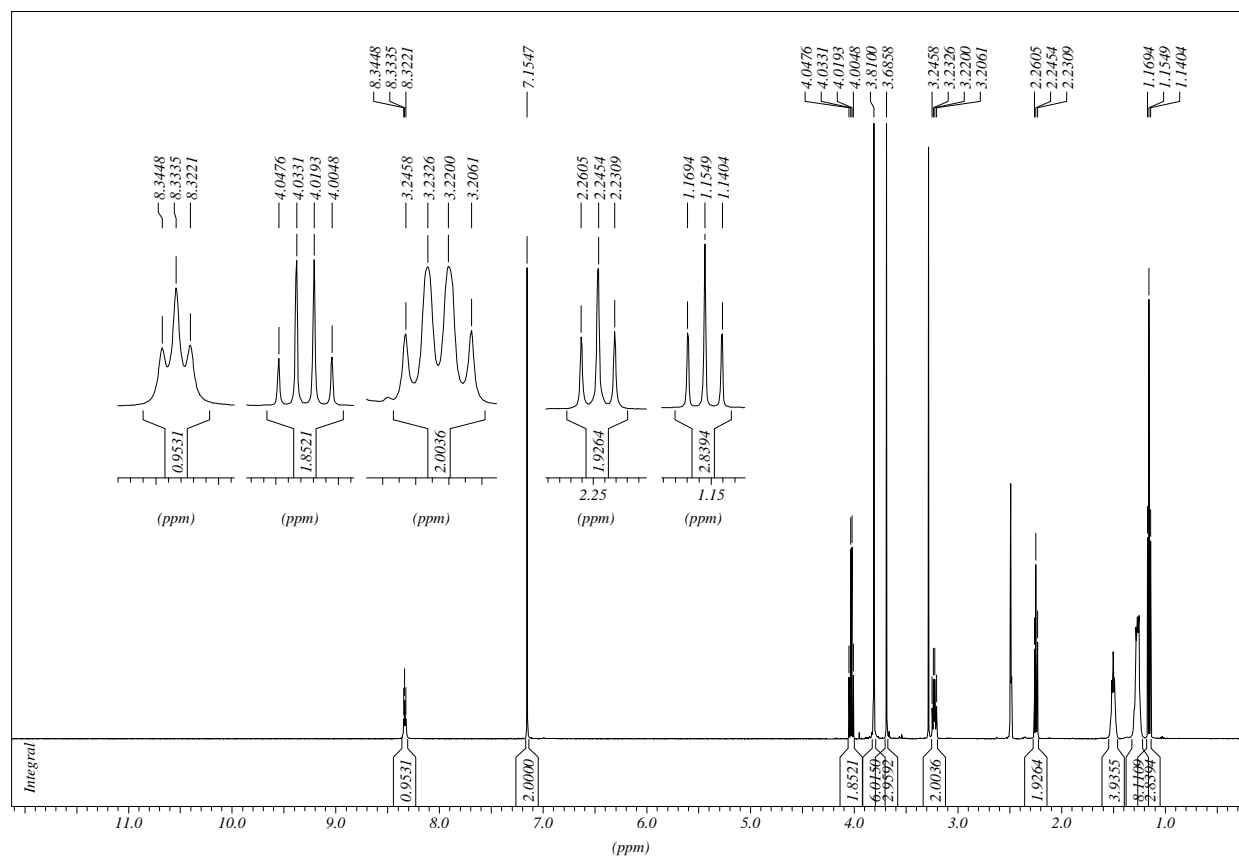
3,4,5-Trimethoxy-*N*-(9-oxo-9-(2-(1,2,3,4-tetrahydroacridin-9-yl)hydrazino)nonyl)benzamide
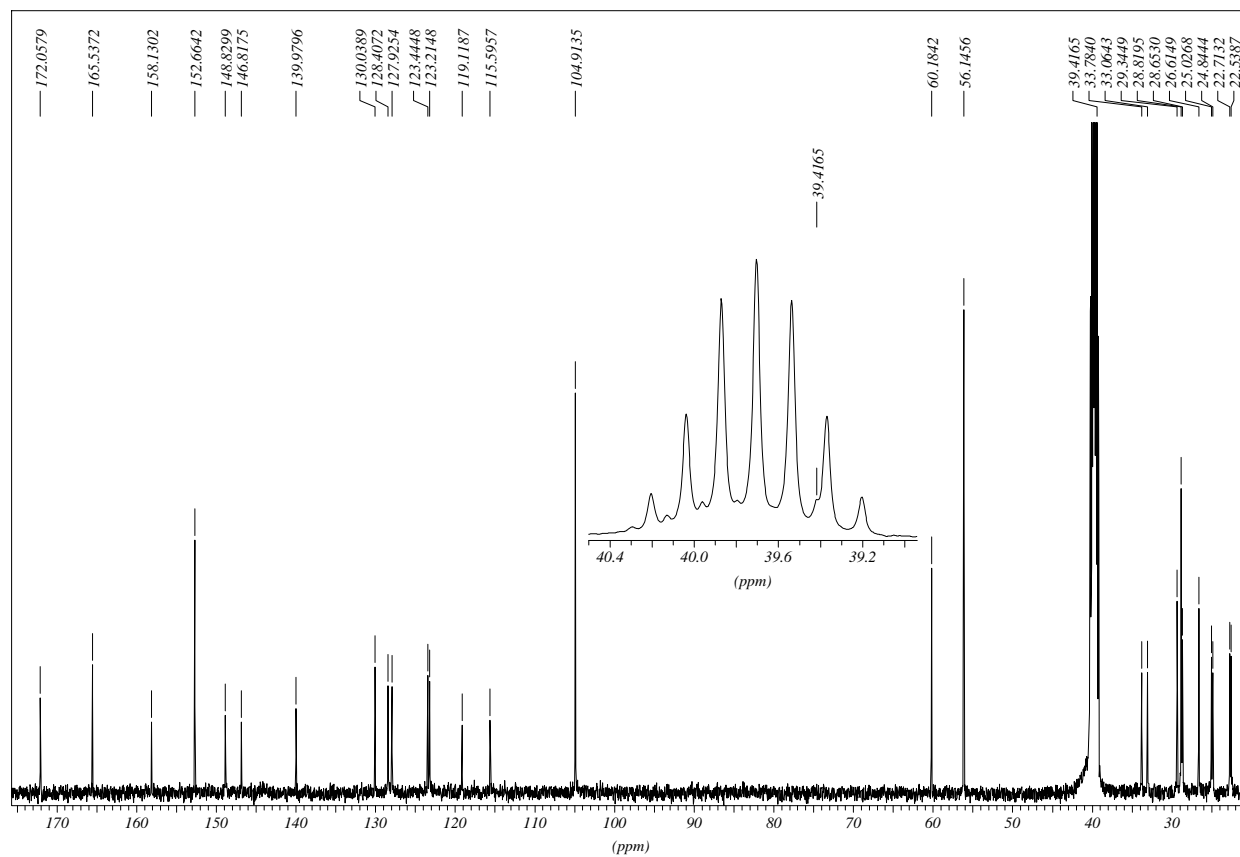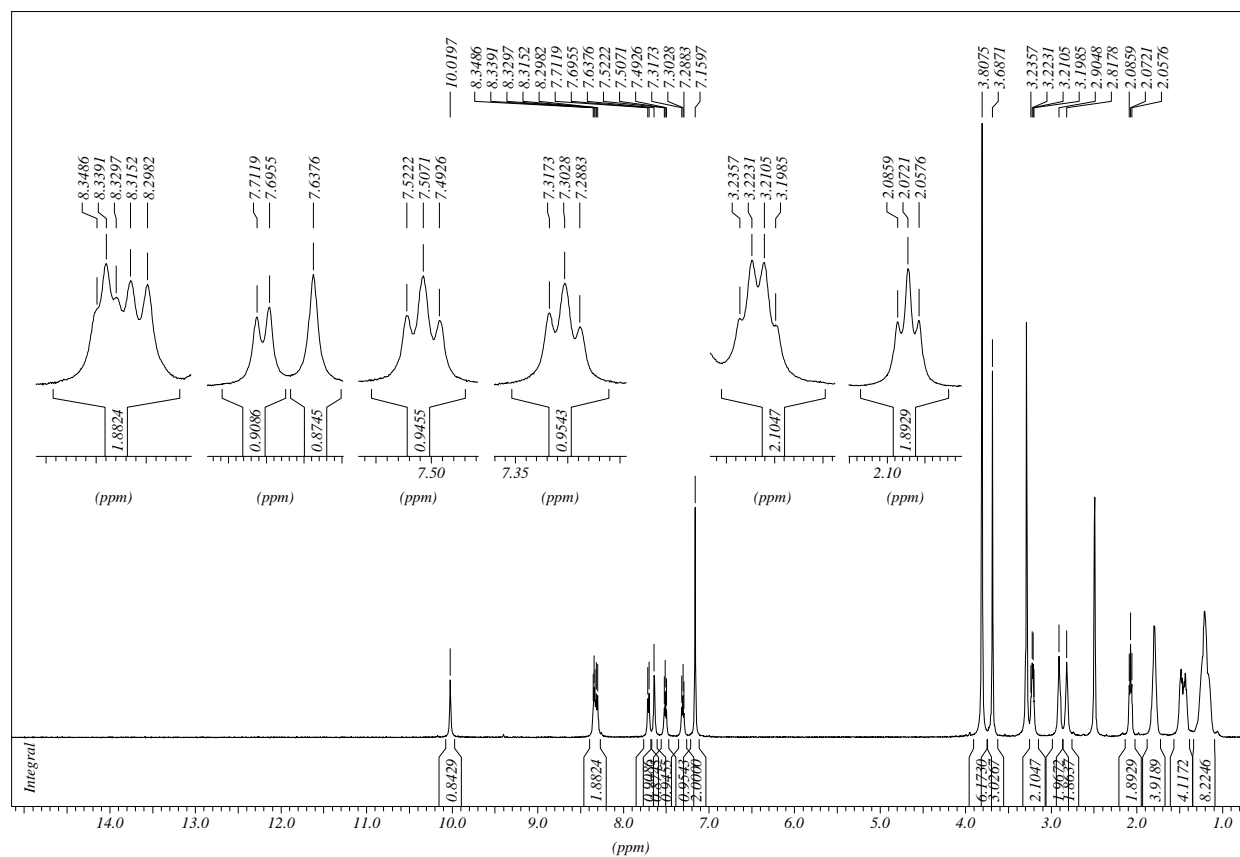
3,4,5-Trimethoxy-*N*-(9-oxo-9-(2-(6-chloro-1,2,3,4-tetrahydroacridin-9-yl)hydrazino)nonyl)-benzamide HCl
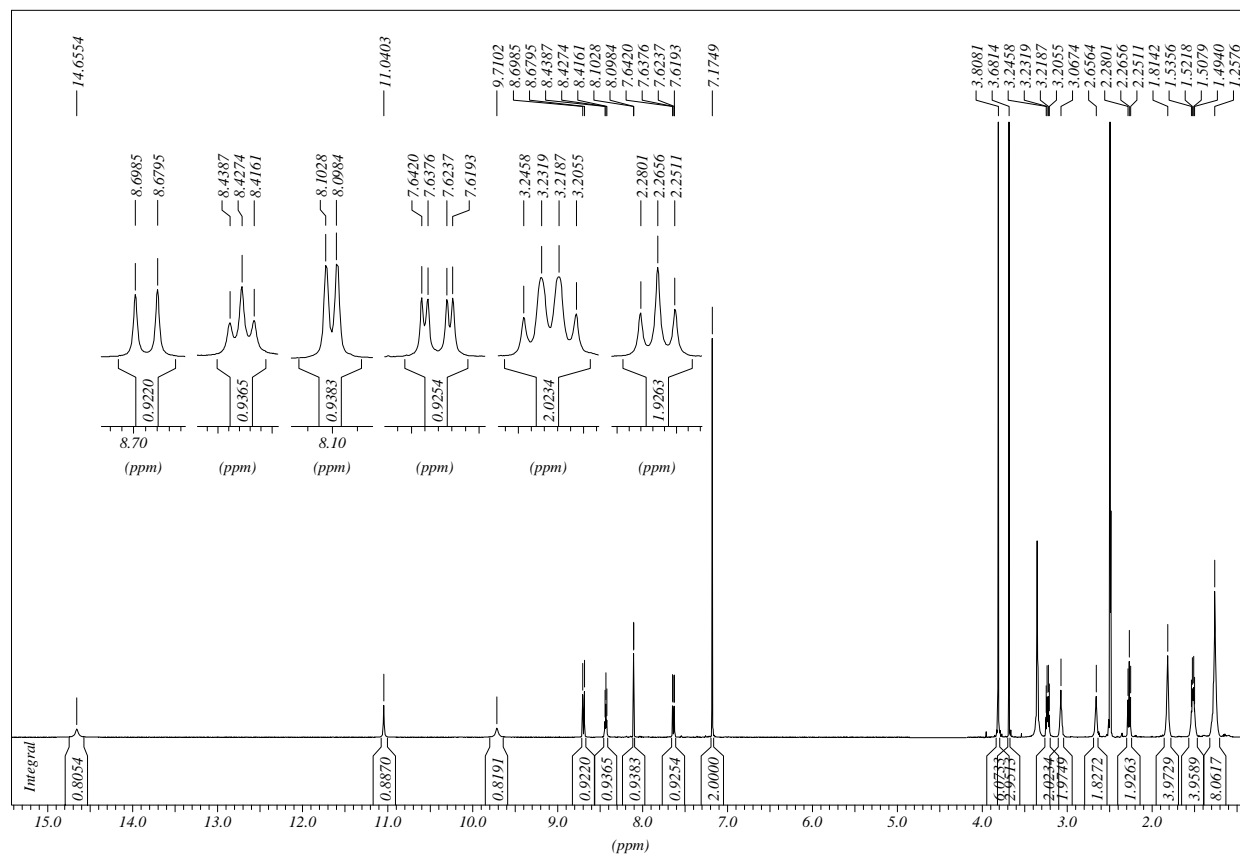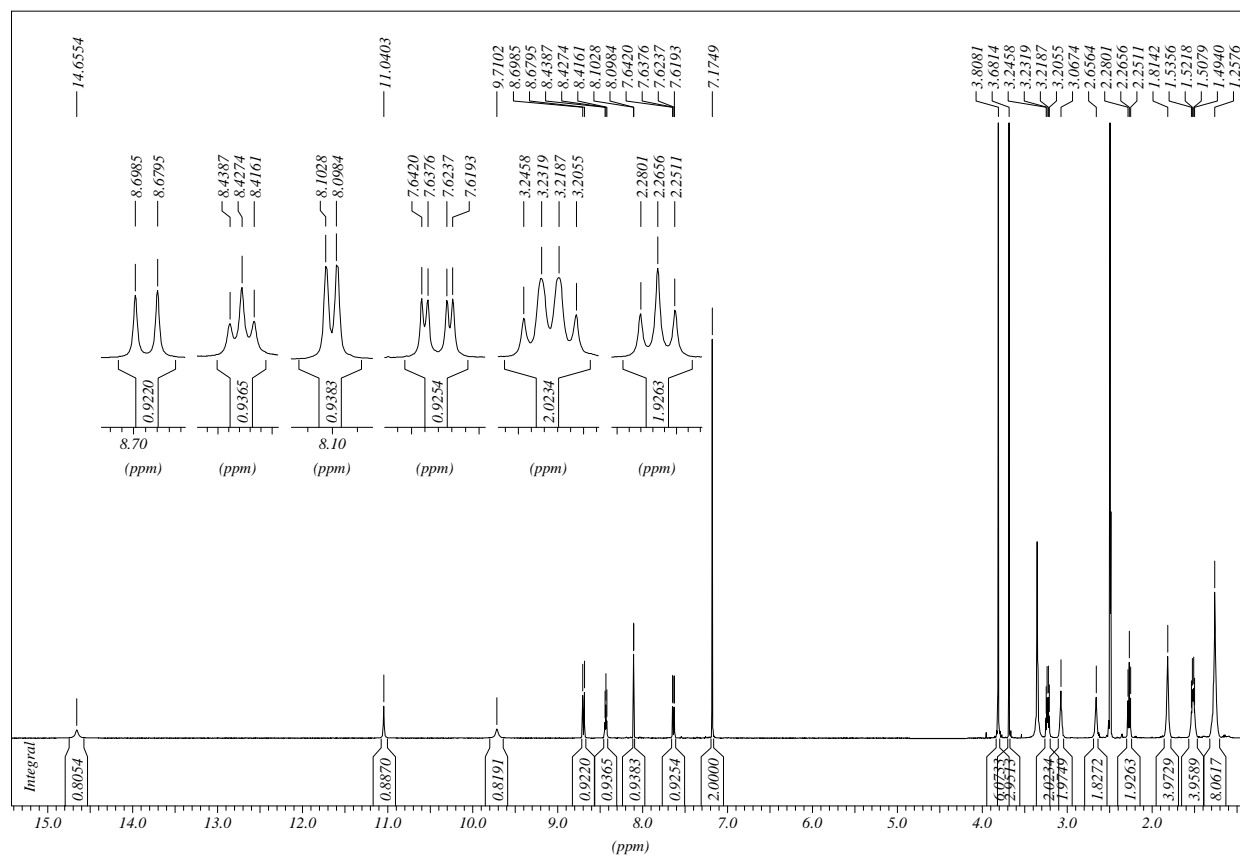
Methyl 3-(3,4,5-trimethoxyphenyl)propanoate
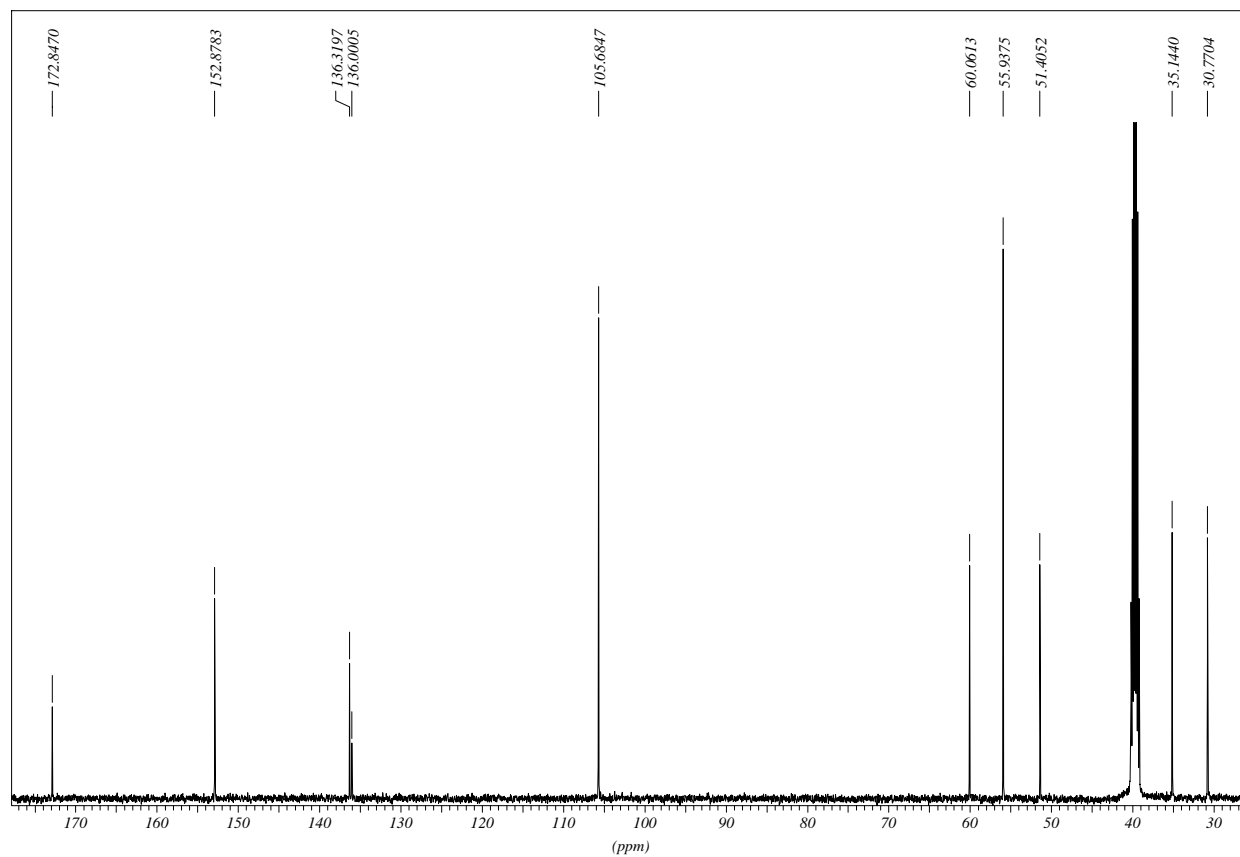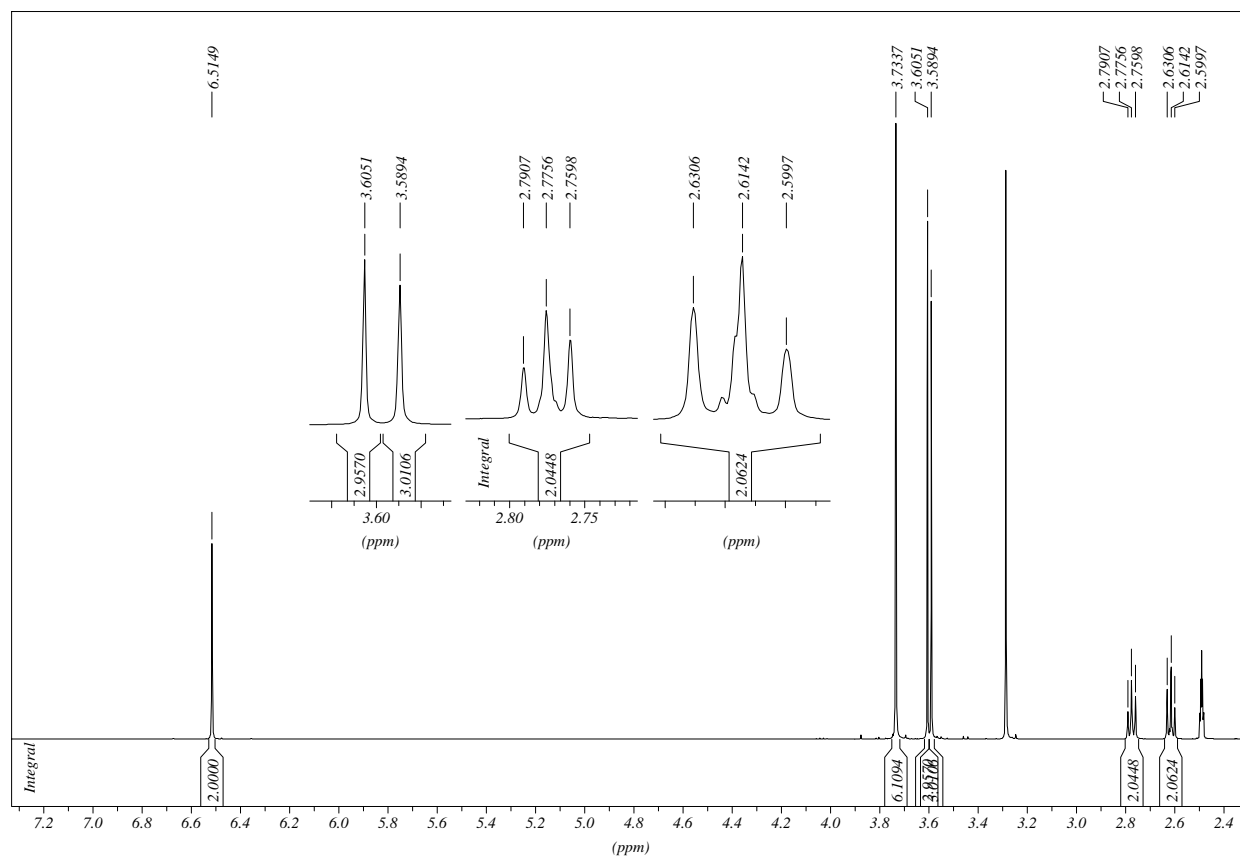
3-(3,4,5-Trimethoxyphenyl)propanohydrazide
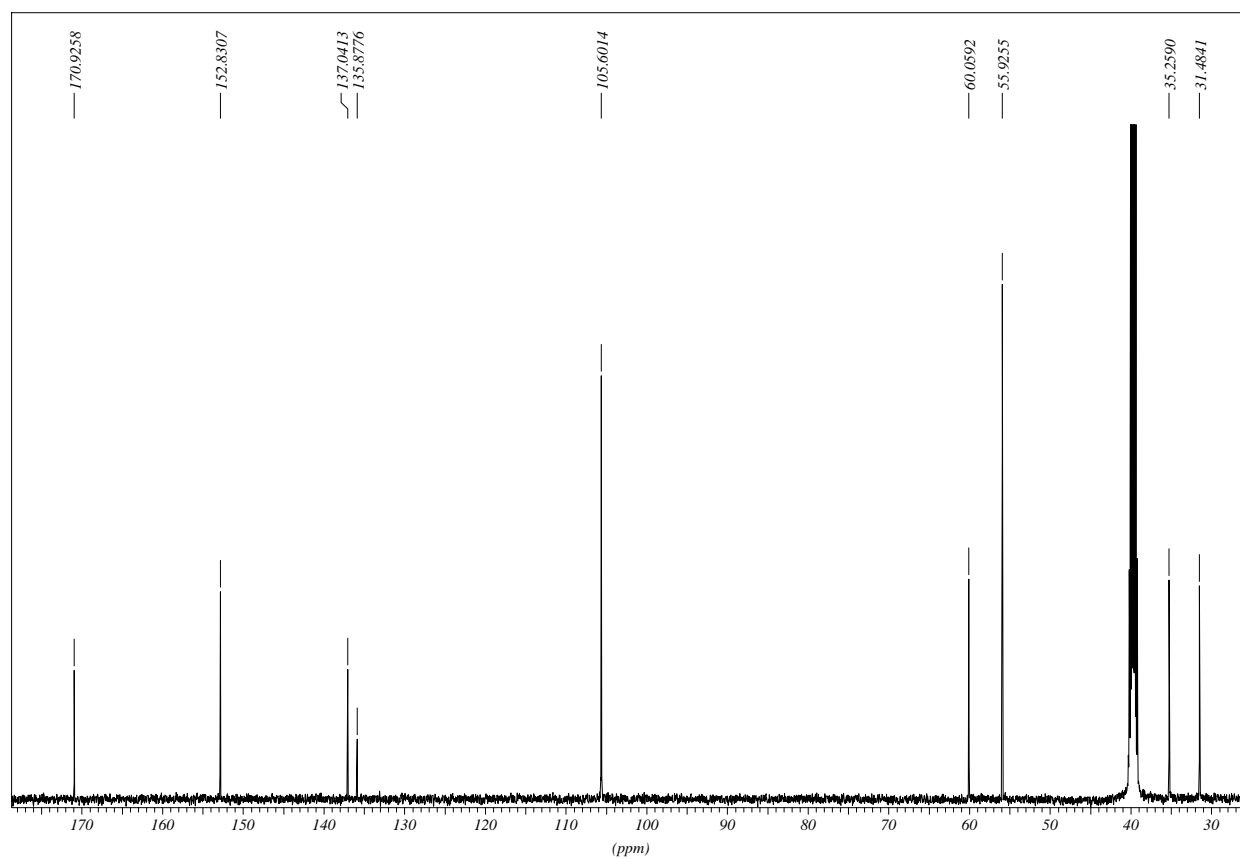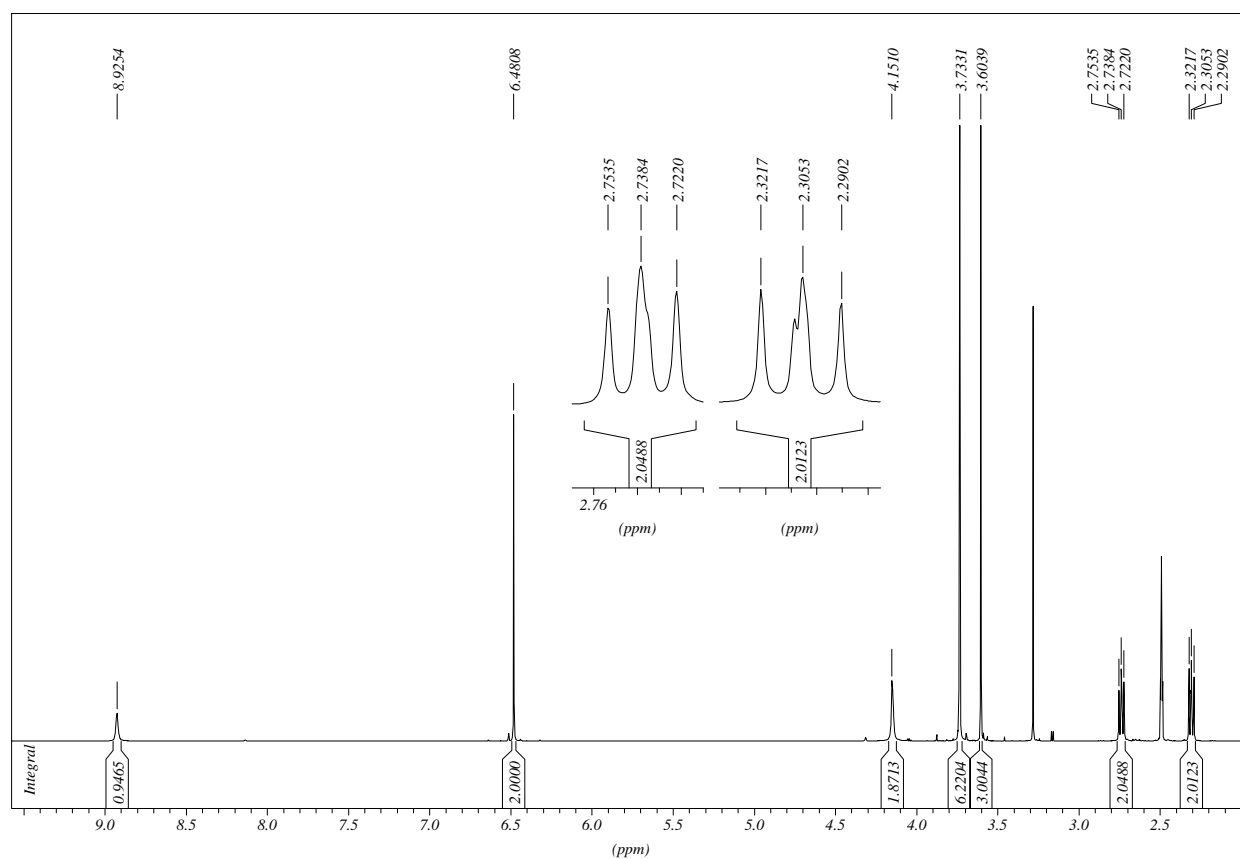
N'-1,2,3,4-Tetrahydroacridin-9-yl-3-(3,4,5-trimethoxyphenyl)propanohydrazide HCl
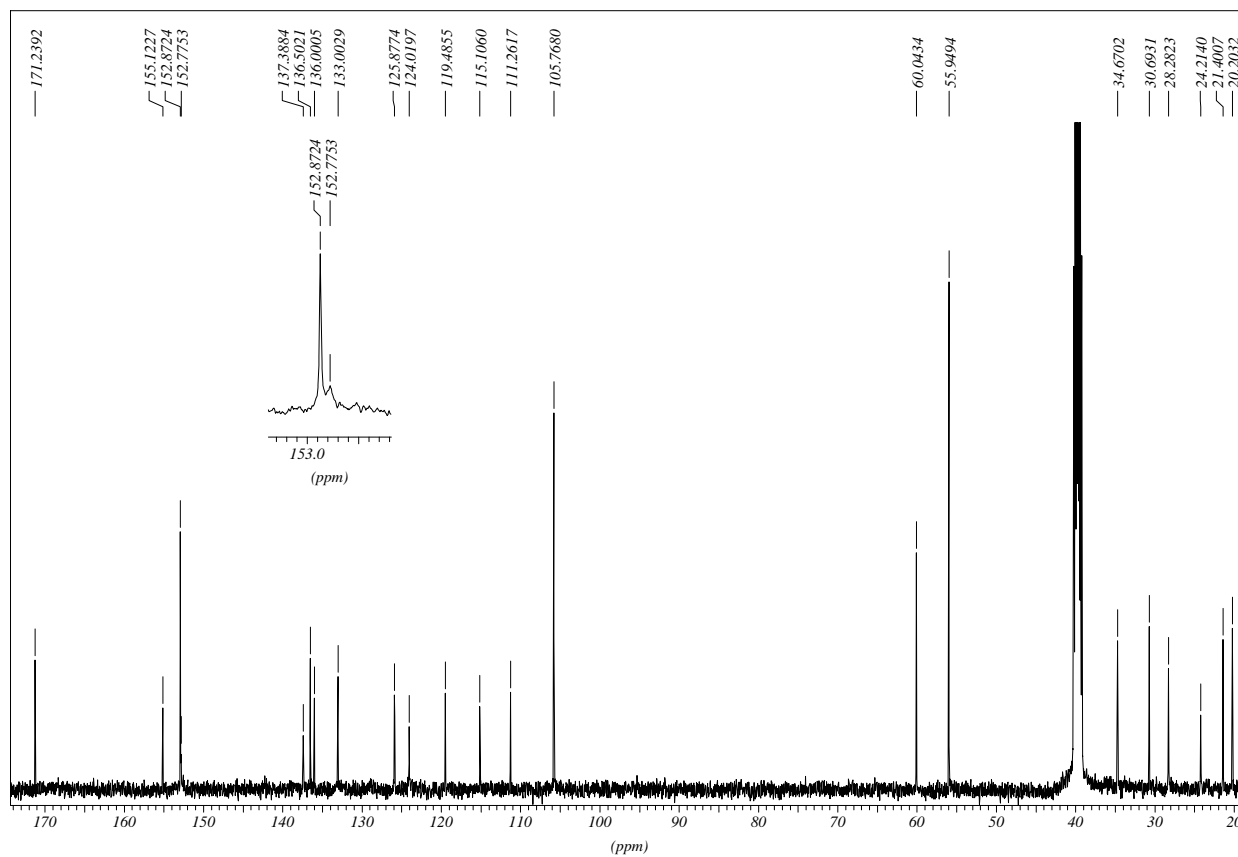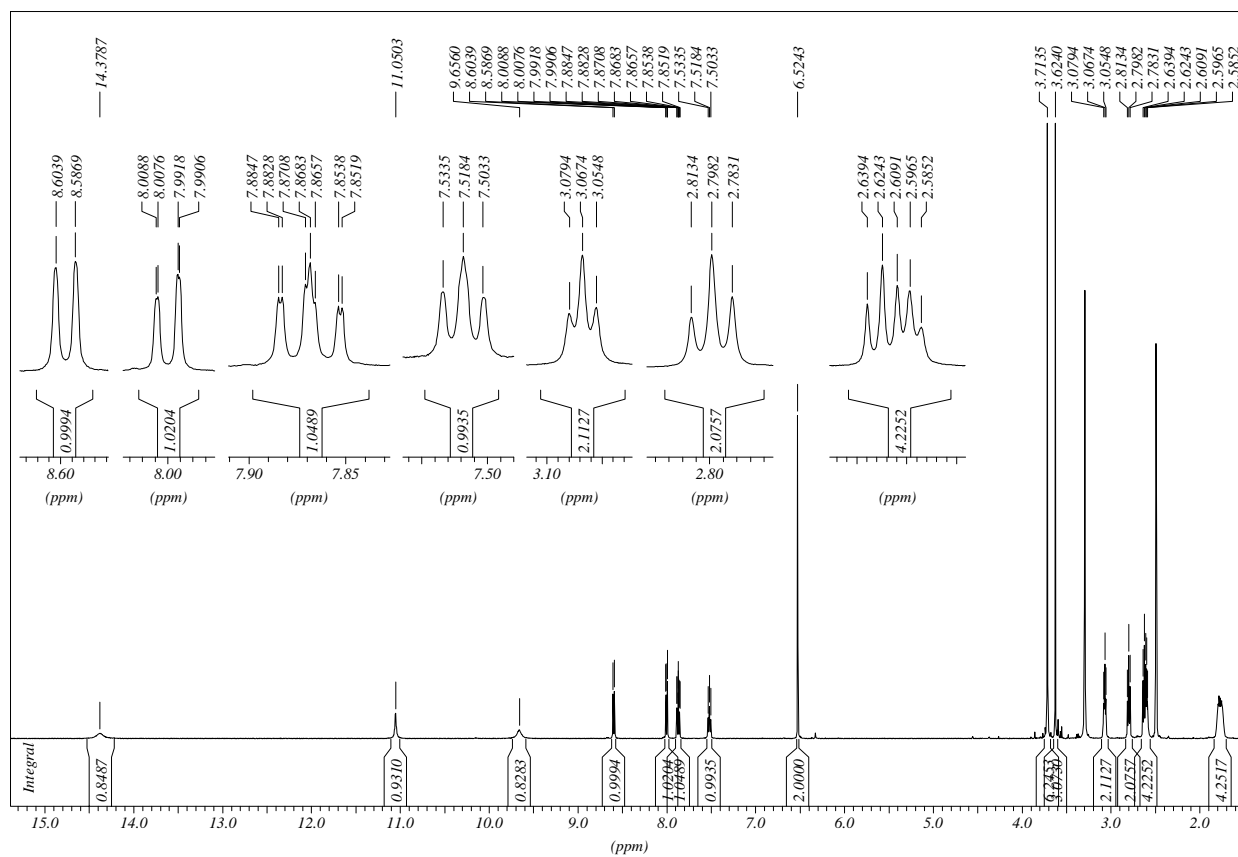
N′-1,2,3,4-Tetrahydroacridin-9-yl-3-(3,4,5-trimethoxyphenyl)propanohydrazide
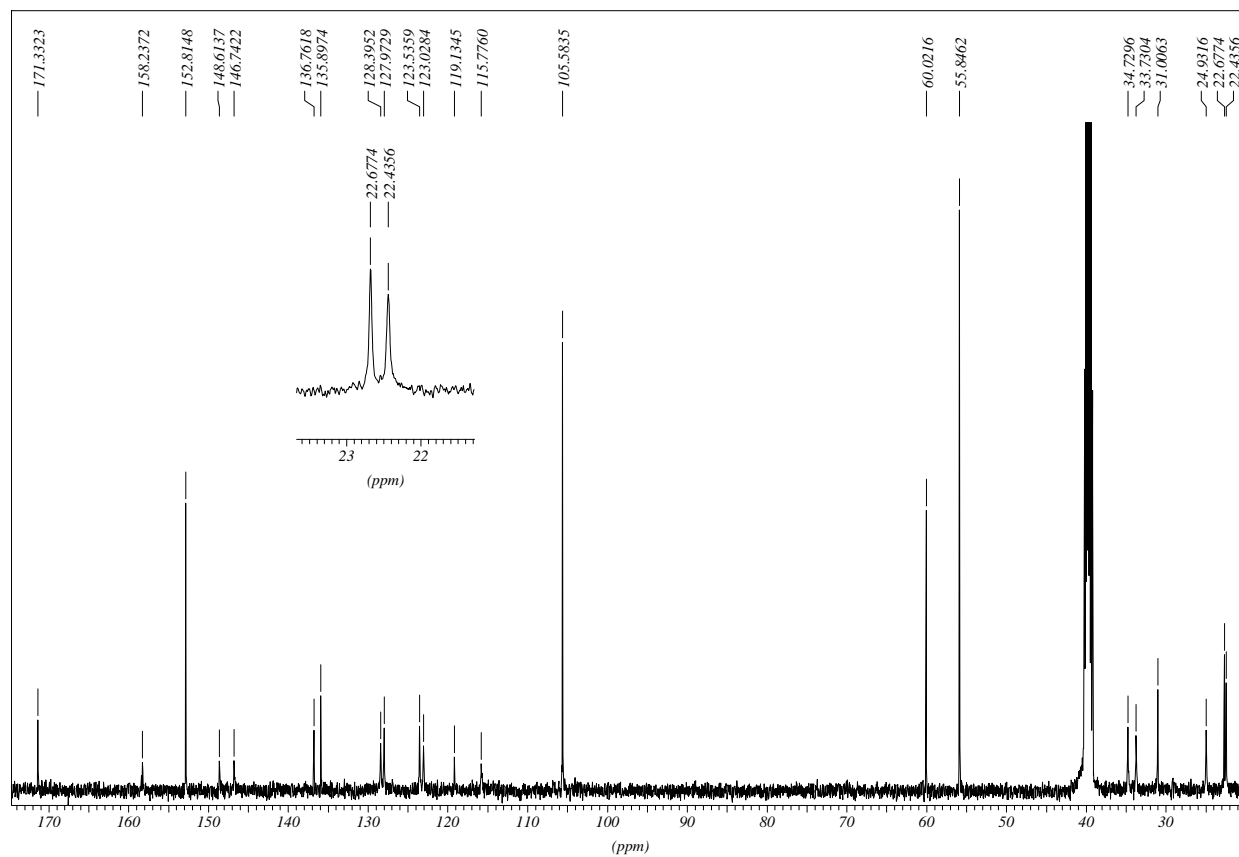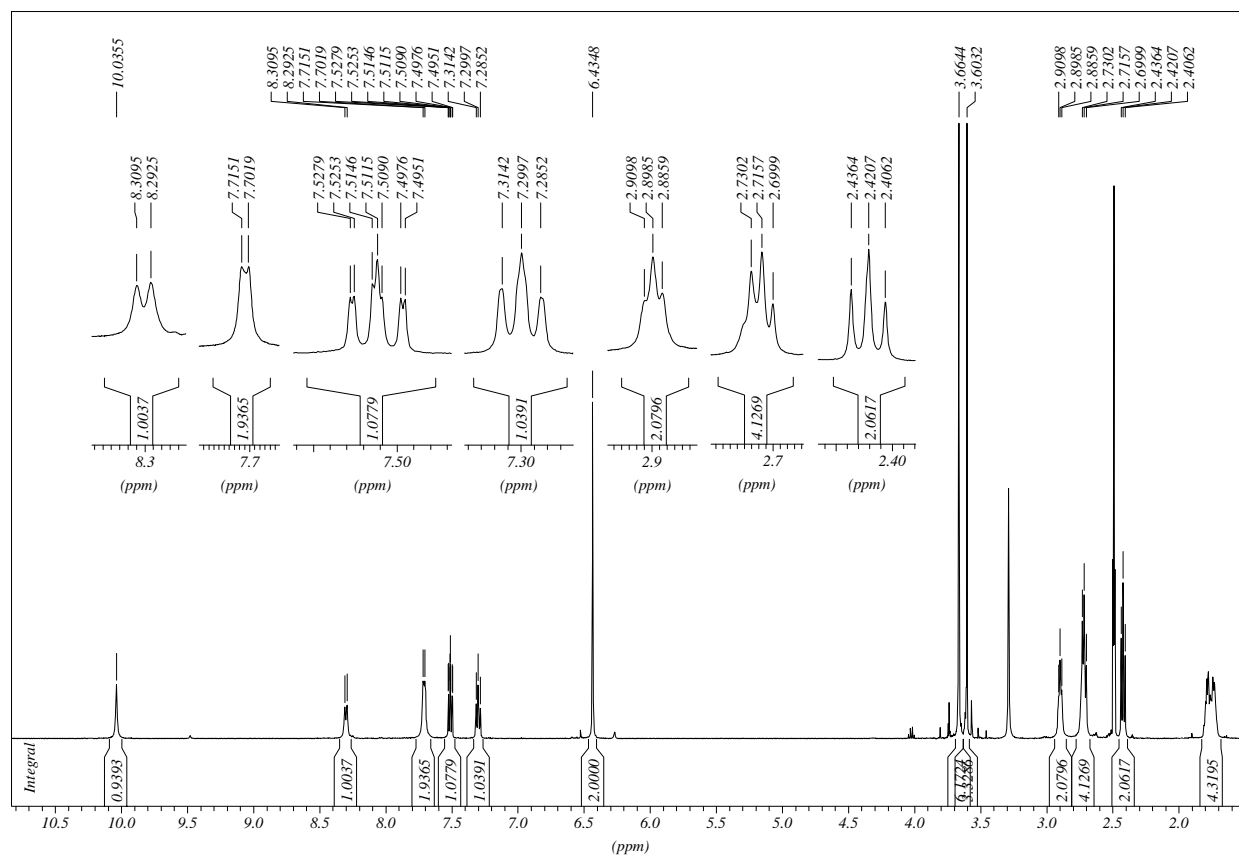
Ethyl ((2-(3,4,5-trimethoxyphenyl)propanoyl)amino)acetate
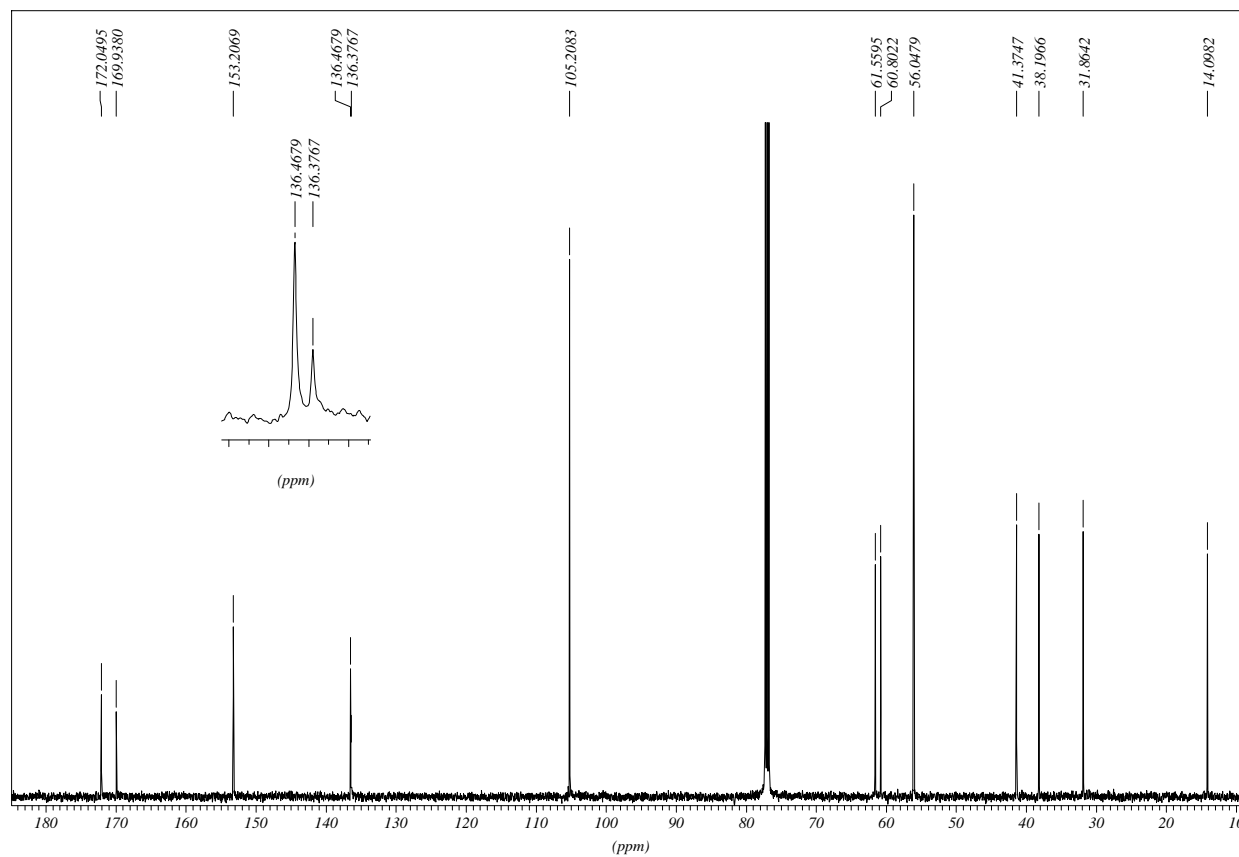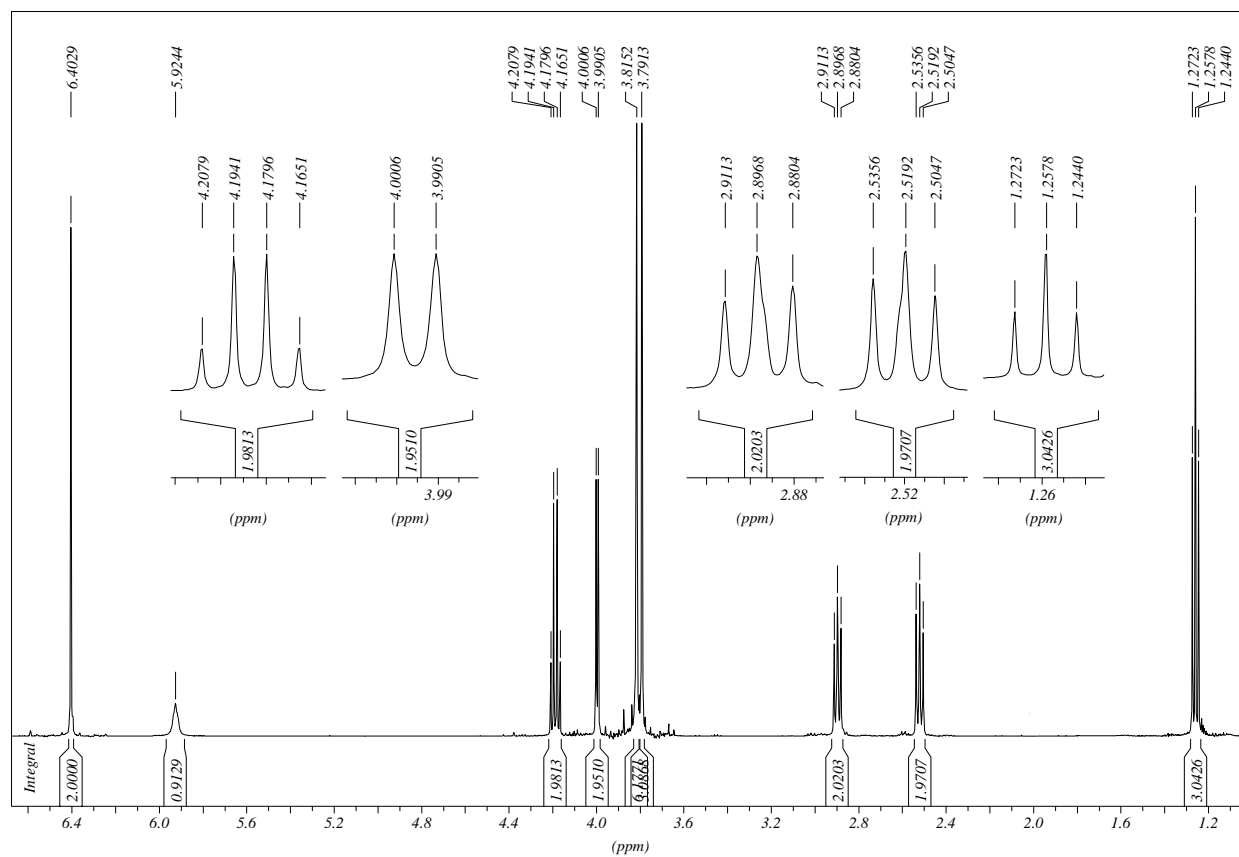
N-(2-Hydrazino-2-oxoethyl)-3-(3,4,5-trimethoxyphenyl)propanamide
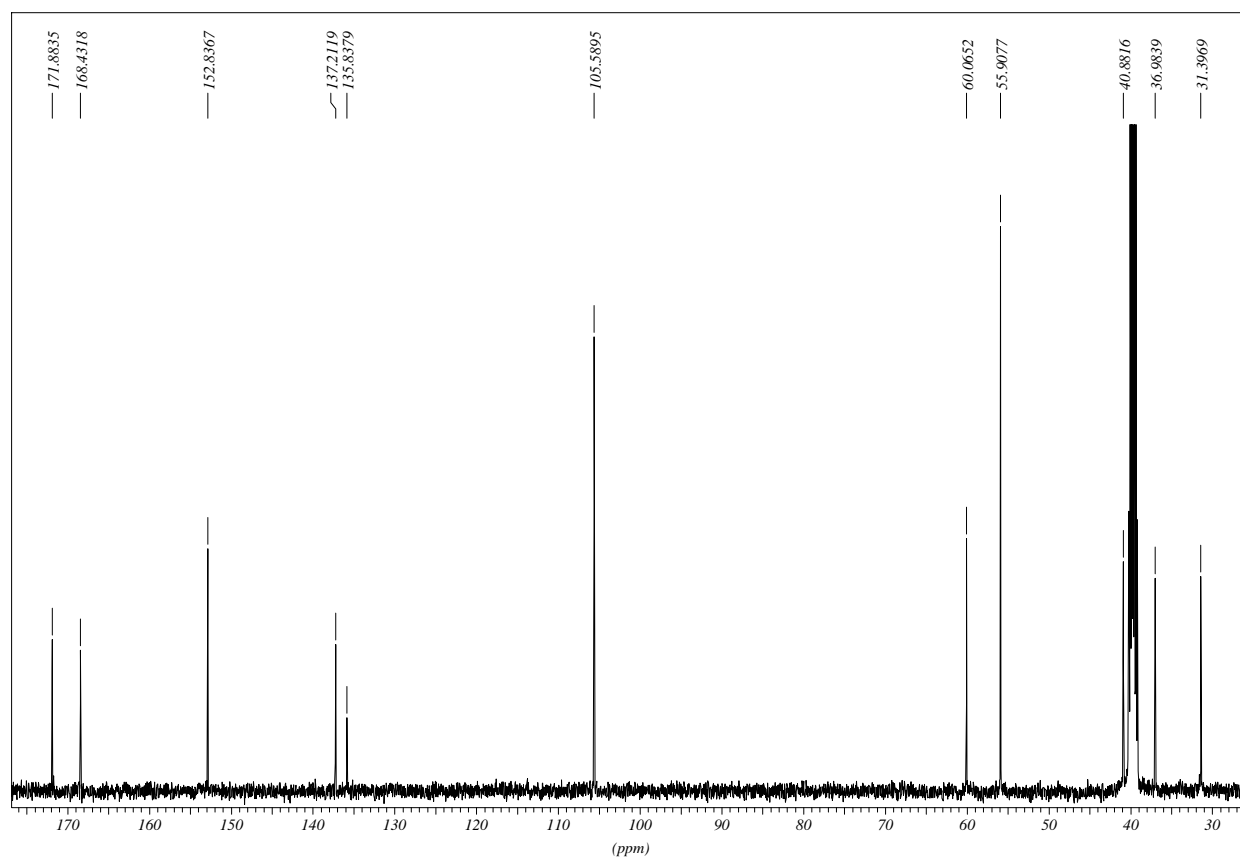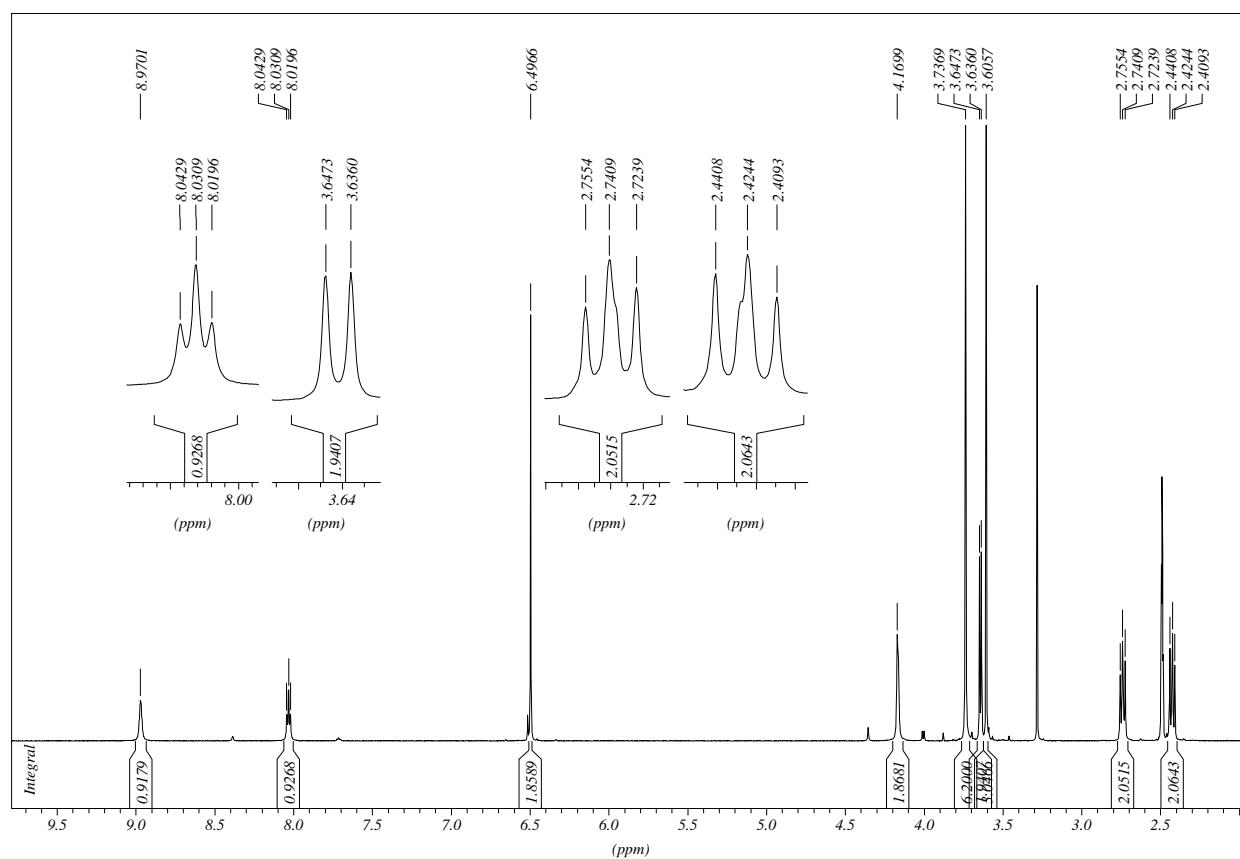
3-(3,4,5-Trimethoxyphenyl)-*N*-(2-oxo-2-(2-(1,2,3,4-tetrahydroacridin-9-yl)hydrazino)ethyl)-propanamide HCl
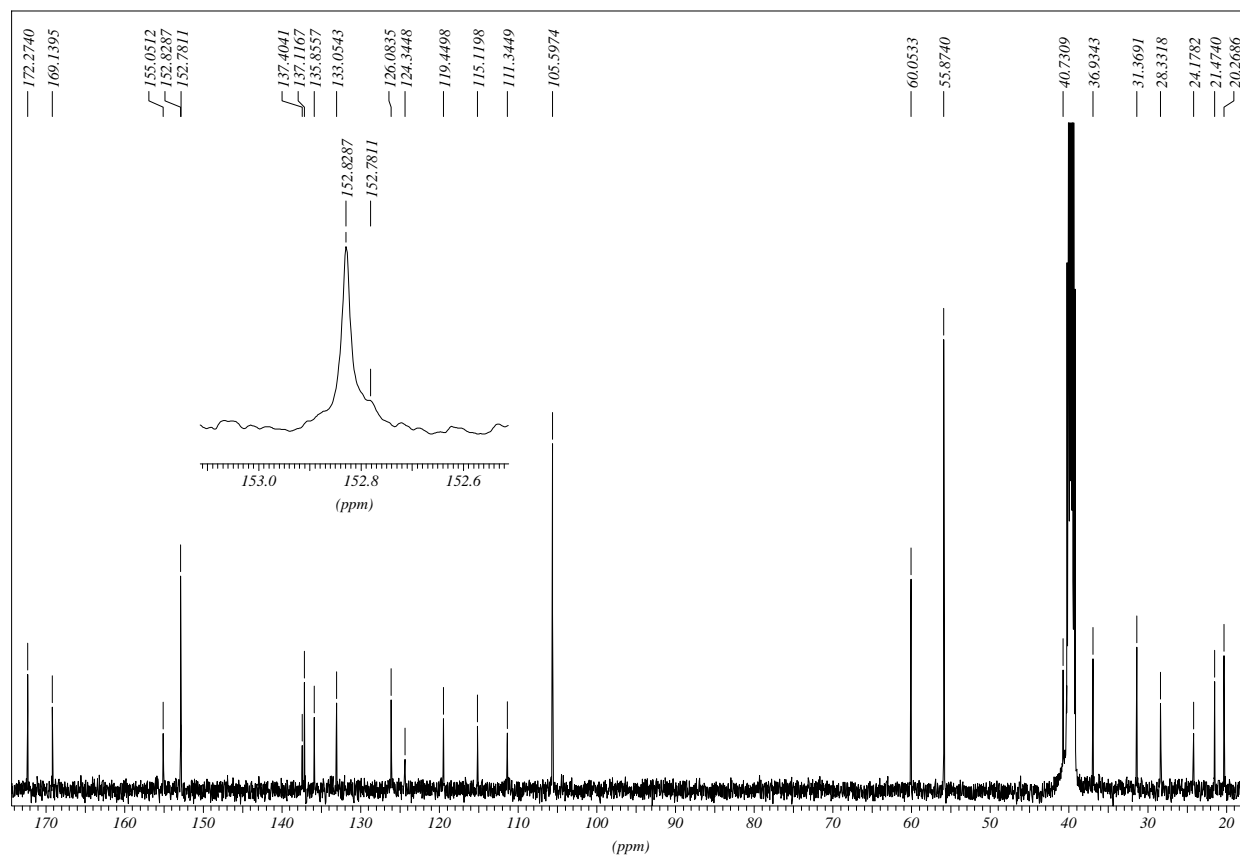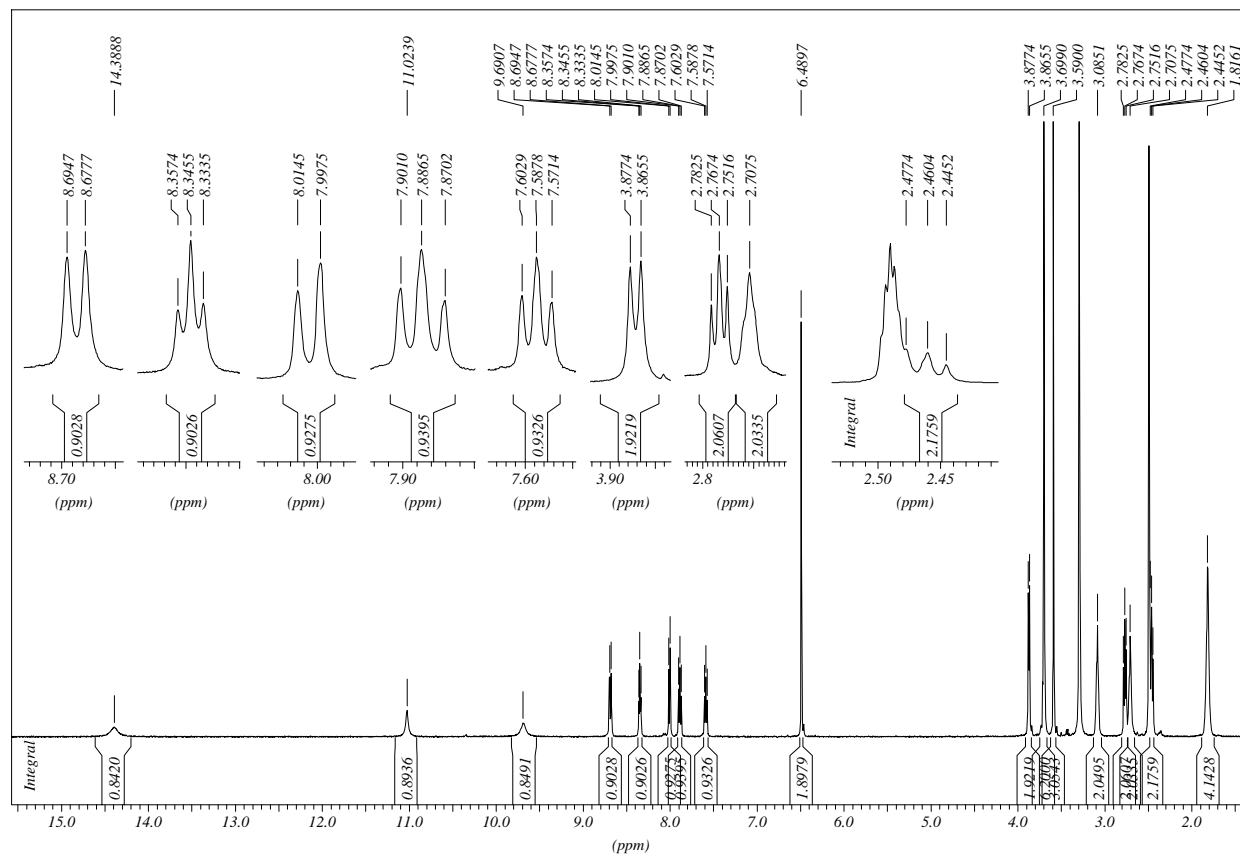
3-(3,4,5-Trimethoxyphenyl)-*N*-(2-oxo-2-(2-(1,2,3,4-tetrahydroacridin-9-yl)hydrazino)ethyl)-propanamide
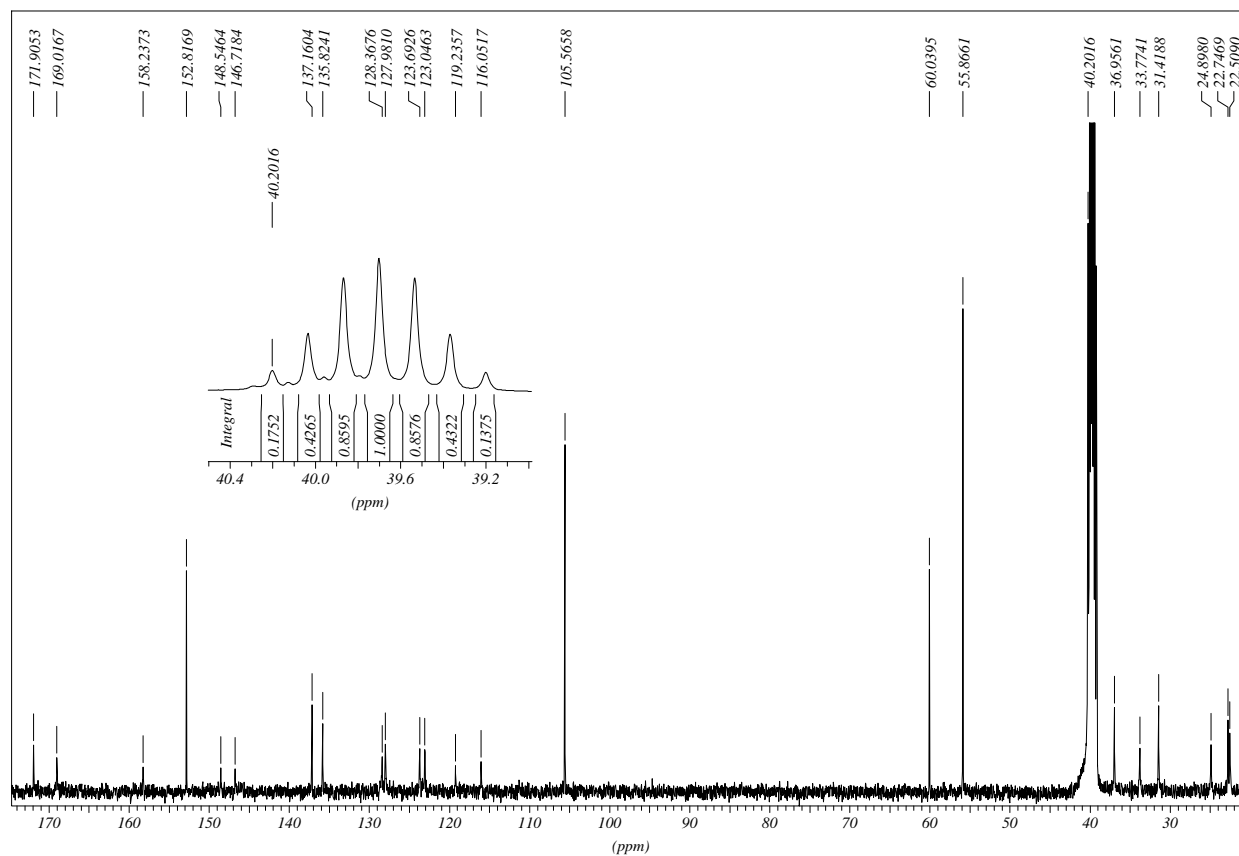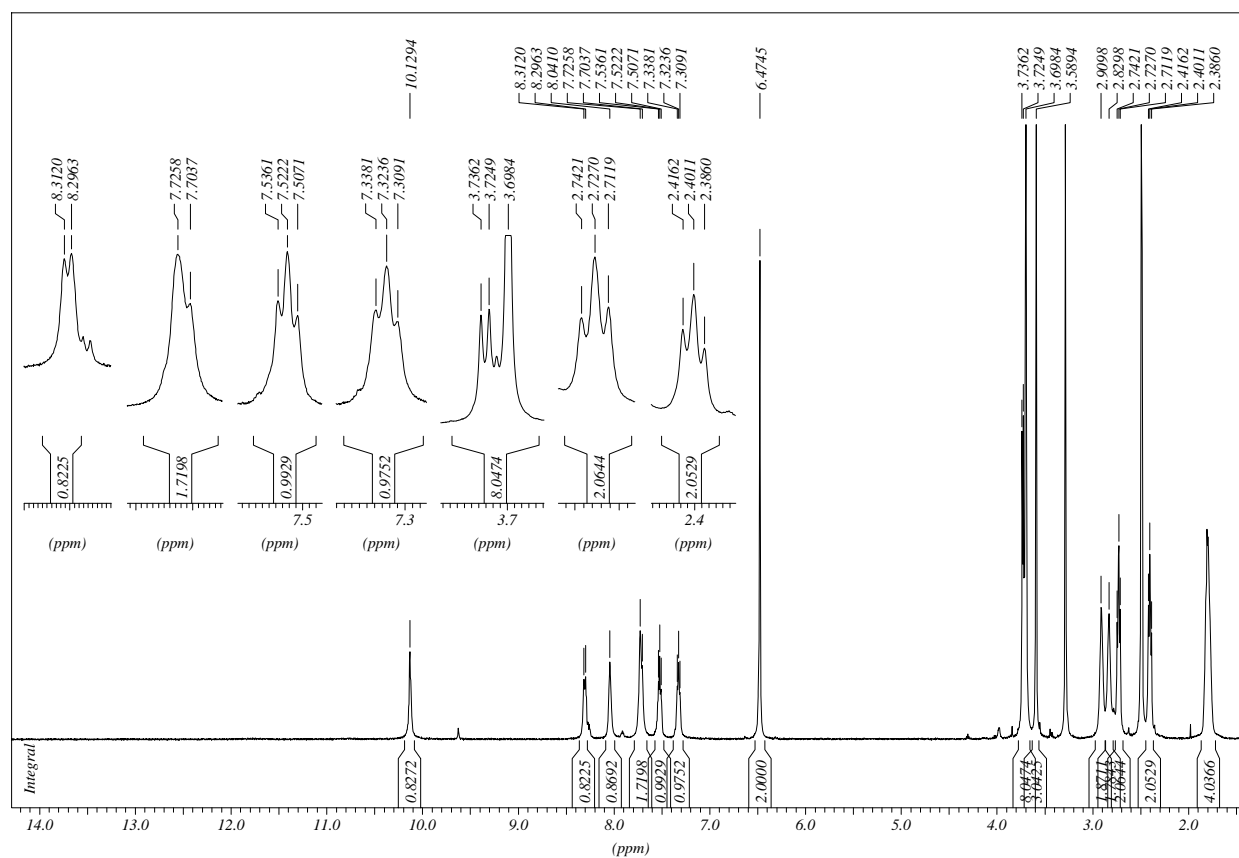
Ethyl 3-((3-(3,4,5-trimethoxyphenyl)propanoyl)amino)propanoate
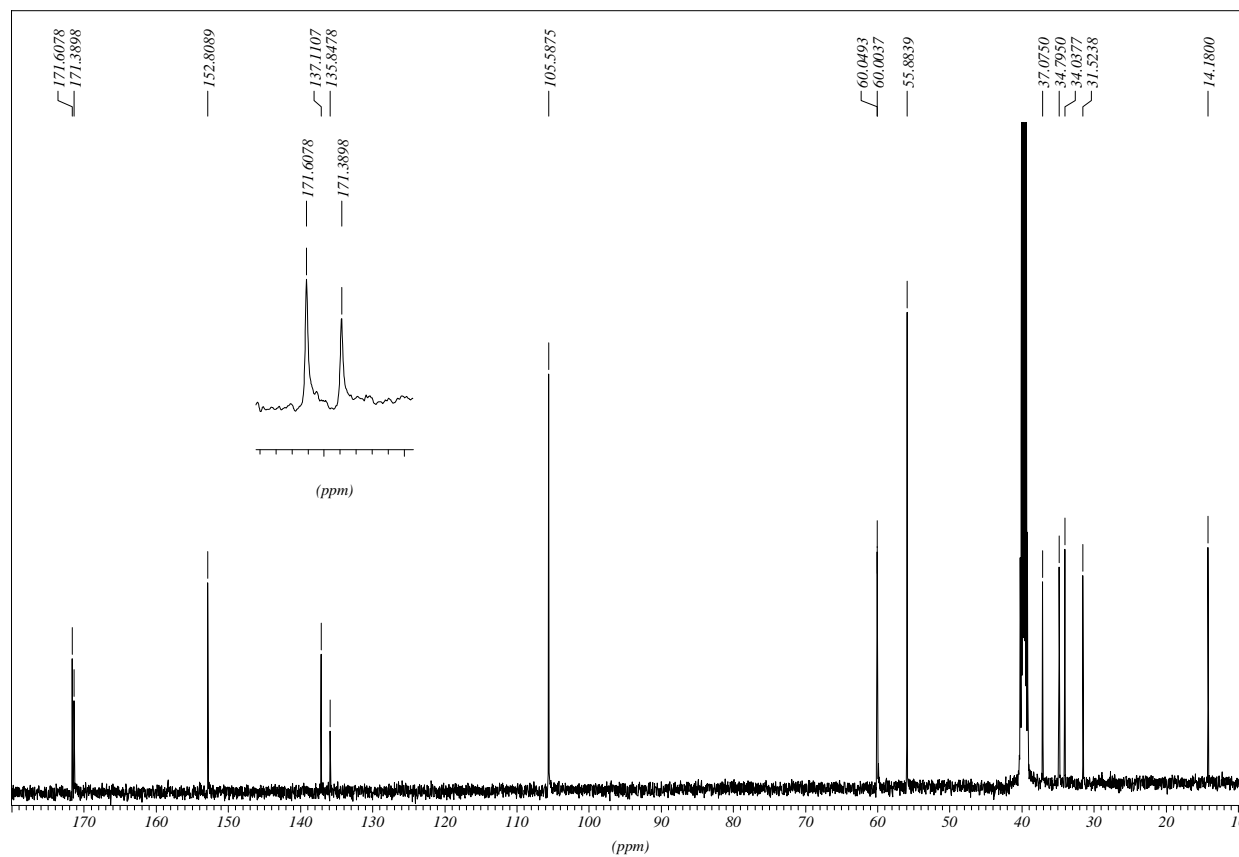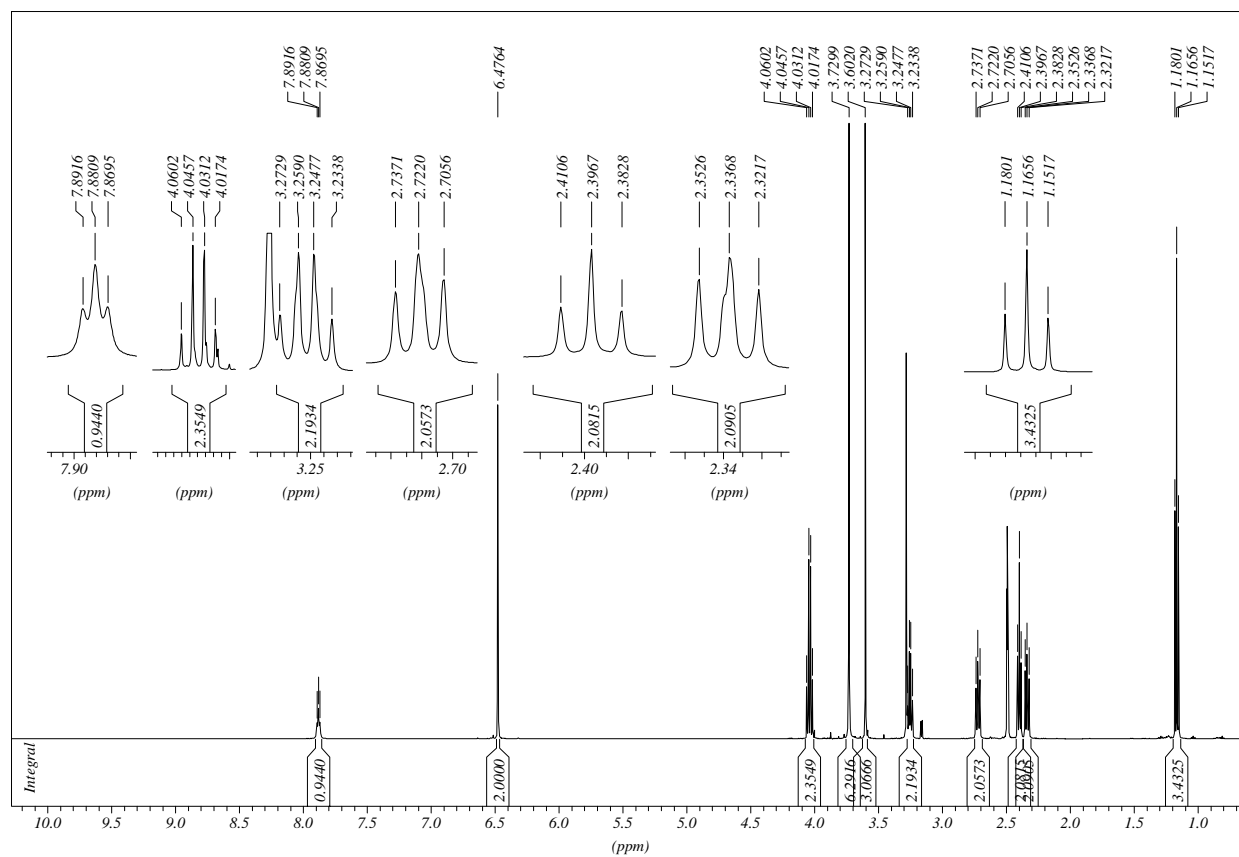
N-(3-Hydrazino-3-oxopropyl)-3-(3,4,5-trimethoxyphenyl)propanamide
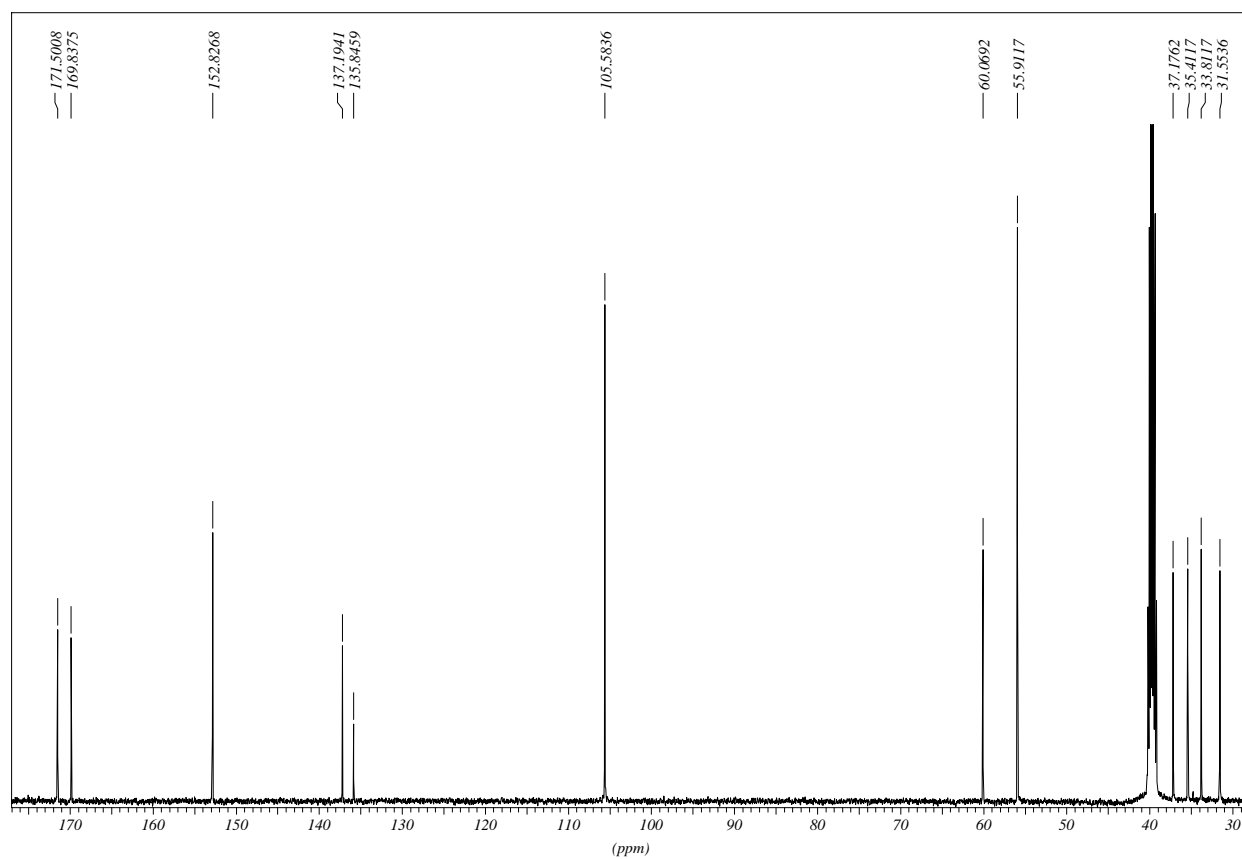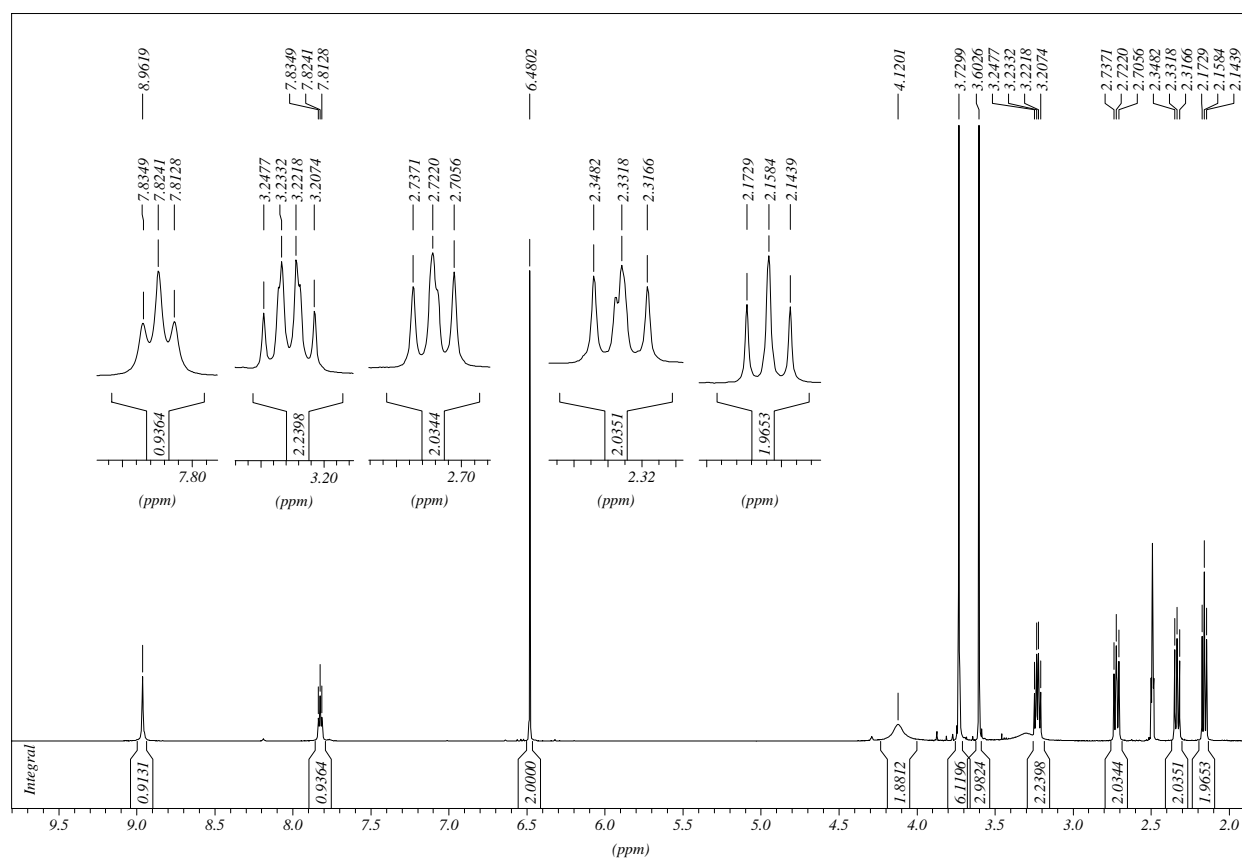
3-(3,4,5-Trimethoxyphenyl)-*N*-(3-oxo-3-(2-(1,2,3,4-tetrahydroacridin-9-yl)hydrazino)propyl)-propanamide HCl
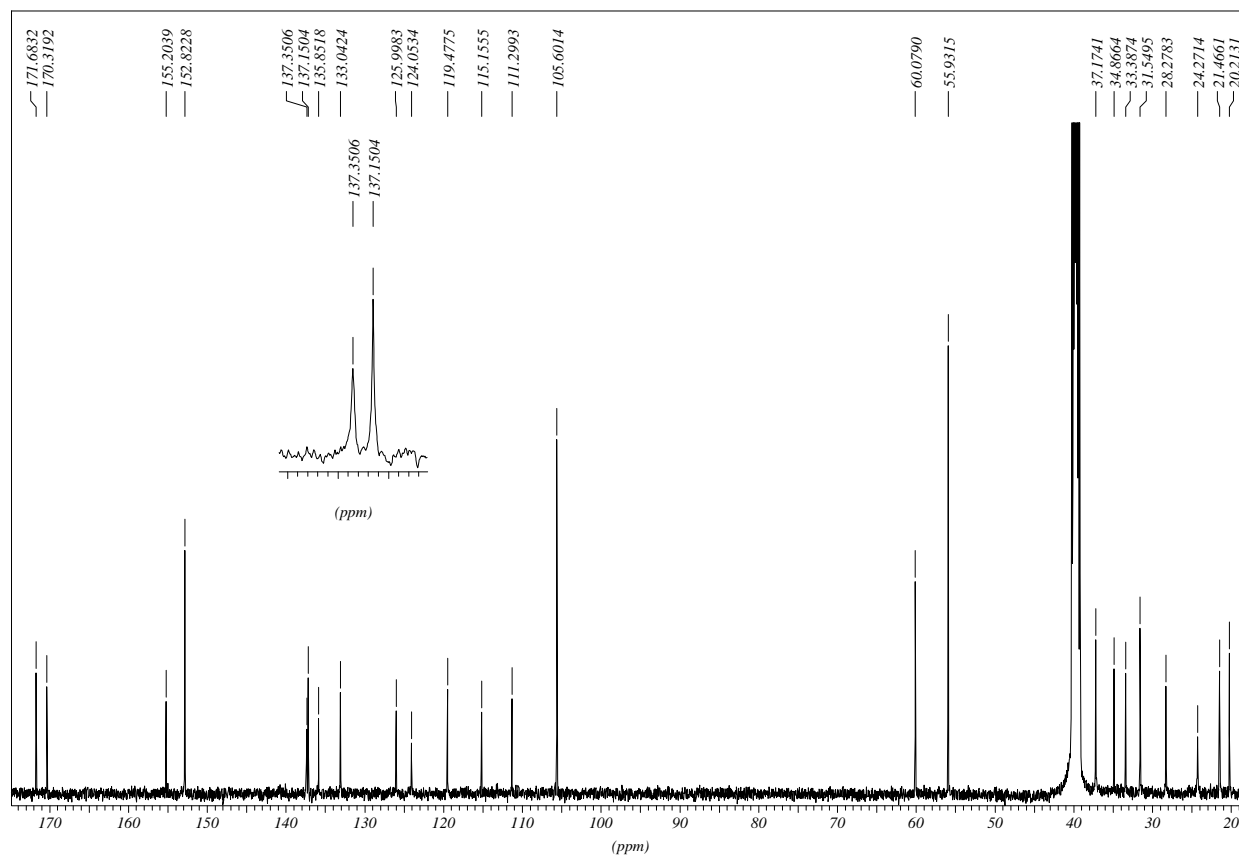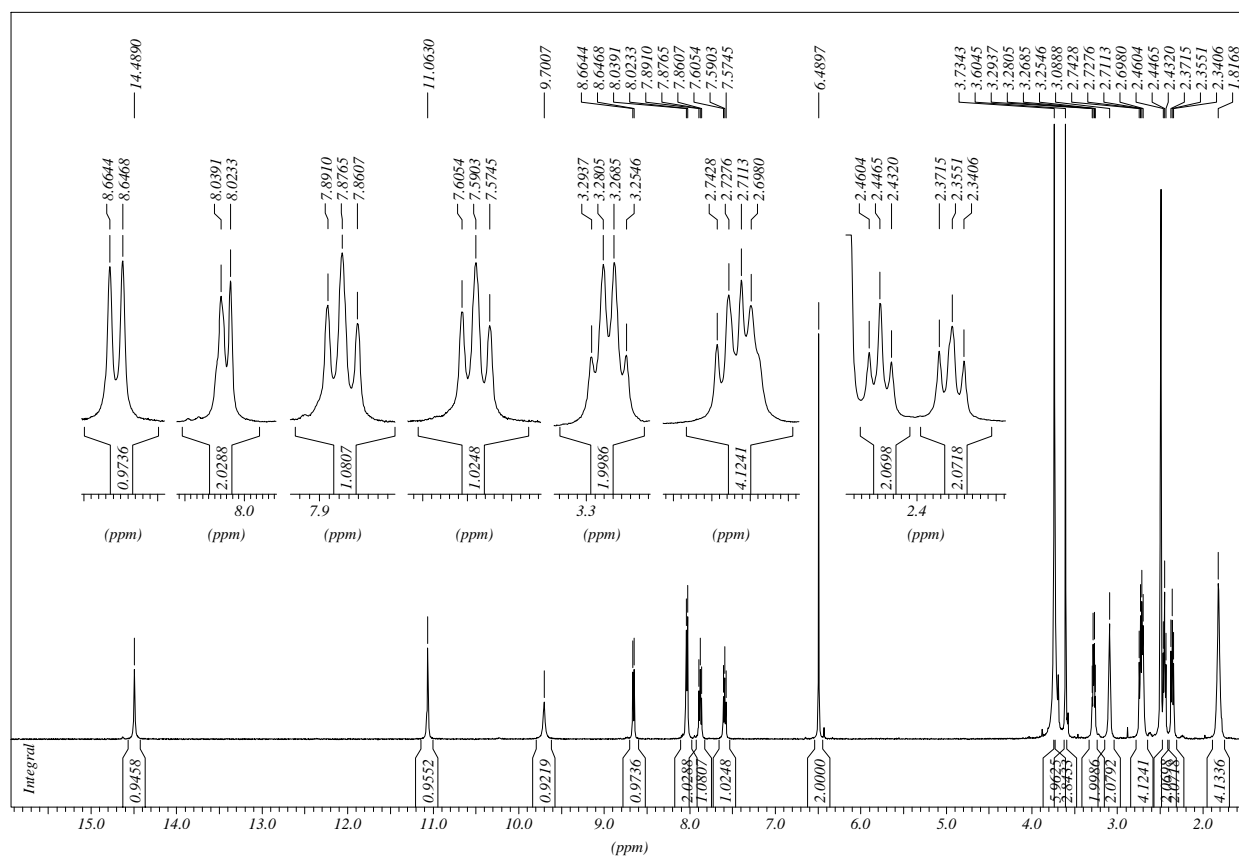
3-(3,4,5-Trimethoxyphenyl)-*N*-(3-oxo-3-(2-(1,2,3,4-tetrahydroacridin-9-yl)hydrazino)propyl)-propanamide
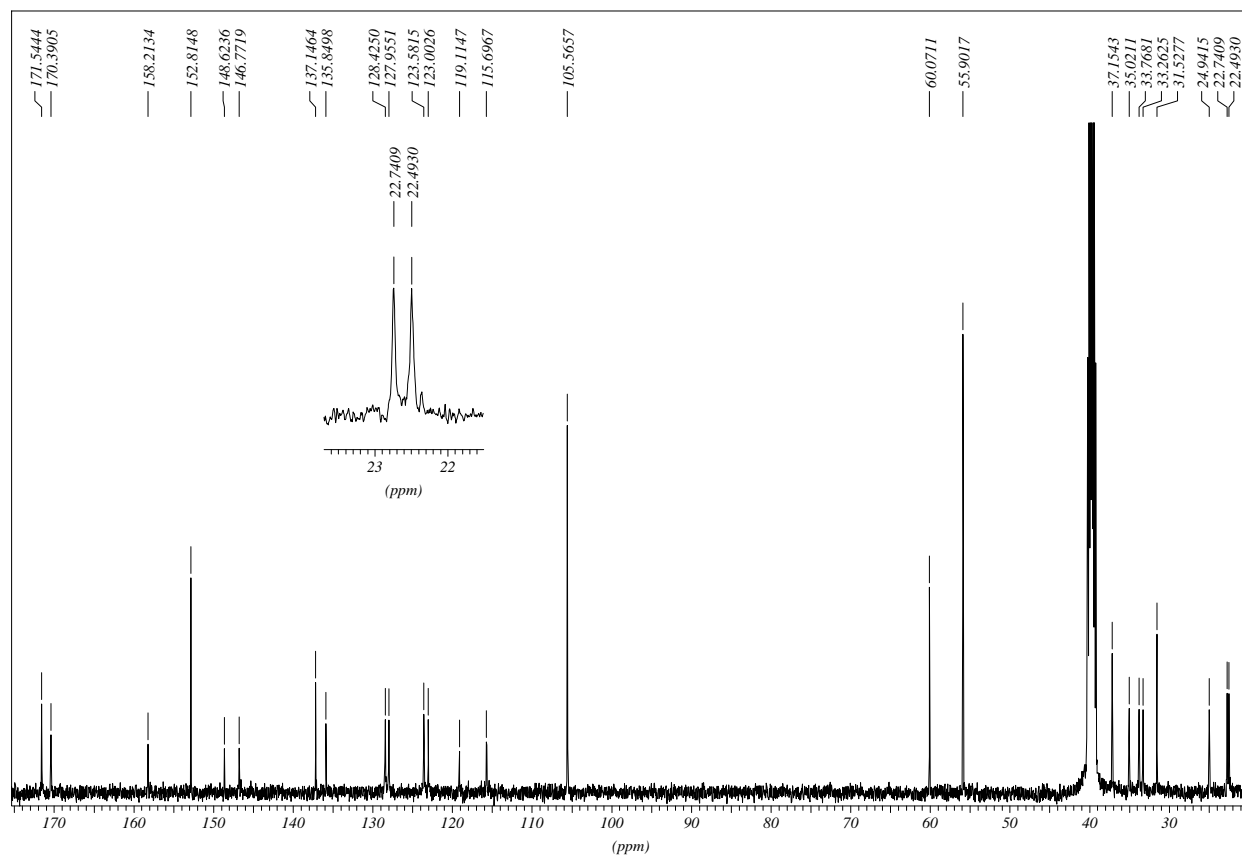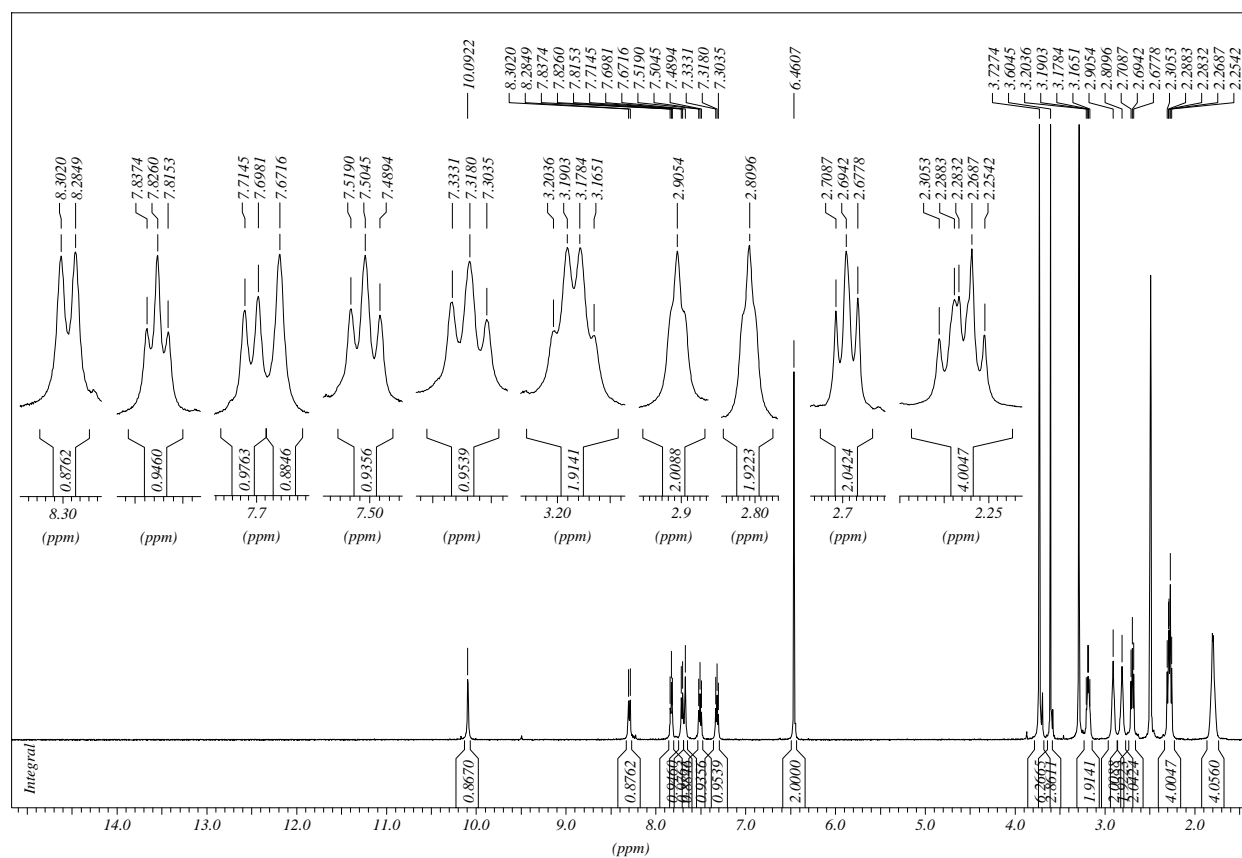
Ethyl 4-((3-(3,4,5-trimethoxyphenyl)propanoyl)amino)butanoate
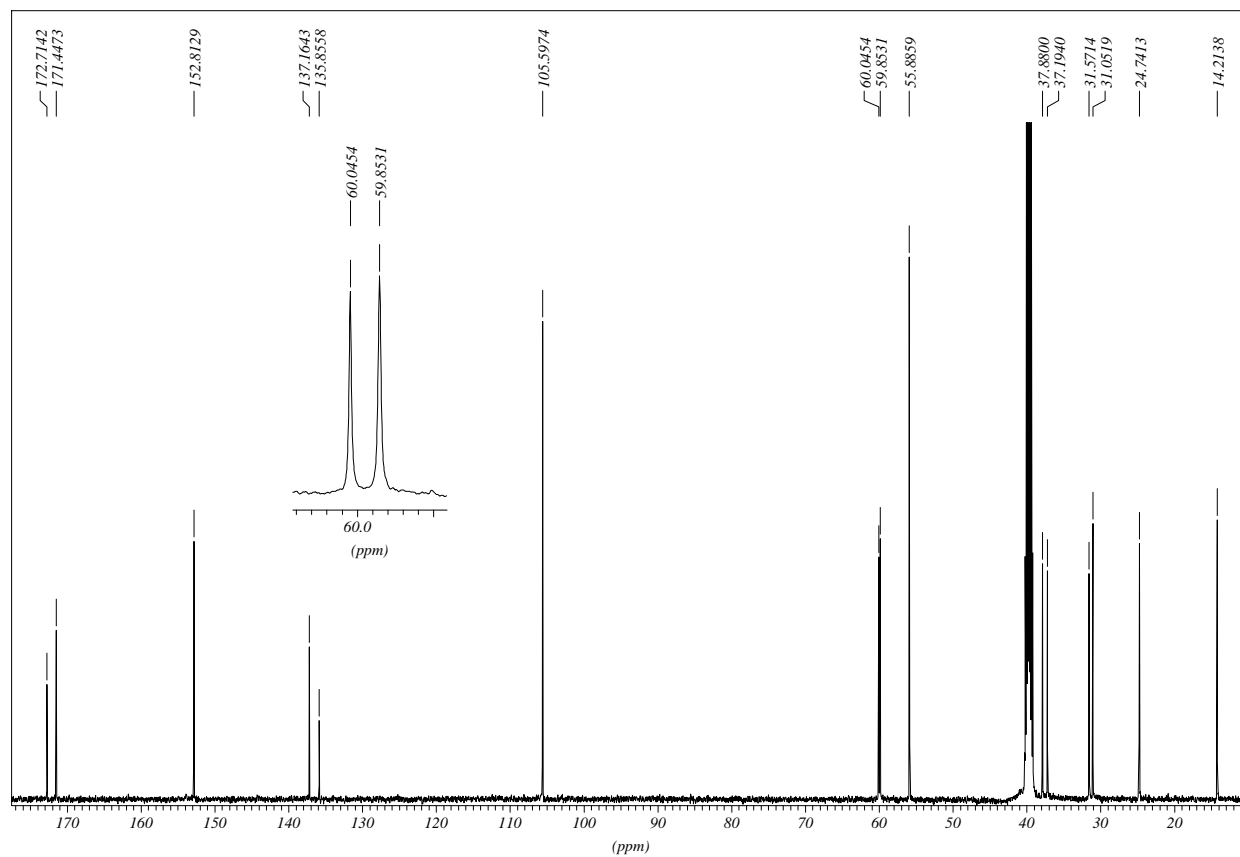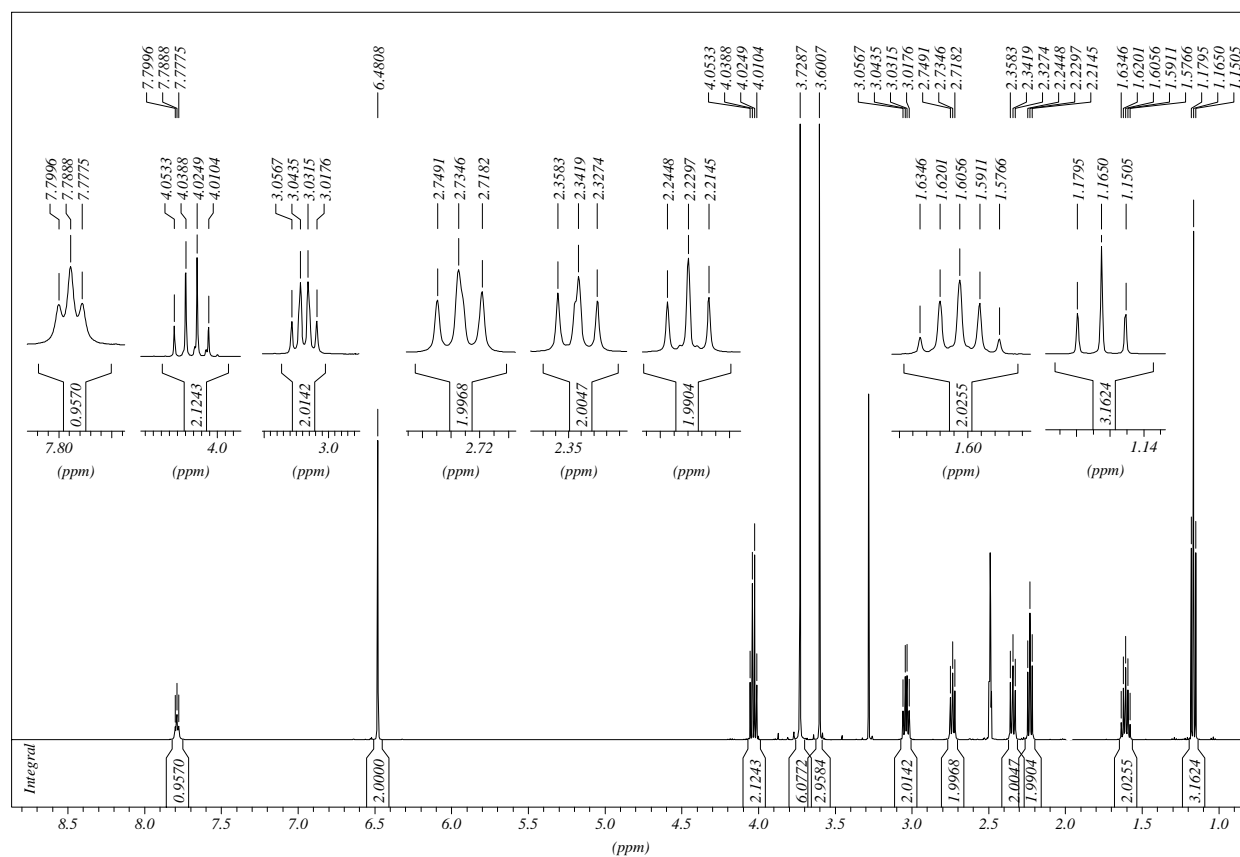
N-(4-Hydrazino-4-oxobutyl)-3-(3,4,5-trimethoxyphenyl)propanamide

3-(3,4,5-Trimethoxyphenyl)-*N*-(4-oxo-4-(2-(1,2,3,4-tetrahydroacridin-9-yl)hydrazino)butyl)-propanamide HCl

3-(3,4,5-Trimethoxyphenyl)-*N*-(4-oxo-4-(2-(1,2,3,4-tetrahydroacridin-9-yl)hydrazino)butyl)-propanamide

Ethyl 5-((3-(3,4,5-trimethoxyphenyl)propanoyl)amino)pentanoate

N-(5-Hydrazino-5-oxopentyl)-3-(3,4,5-trimethoxyphenyl)propanamide

3-(3,4,5-Trimethoxyphenyl)-*N*-(5-oxo-5-(2-(1,2,3,4-tetrahydroacridin-9-yl)hydrazino)pentyl)-propanamide HCl

3-(3,4,5-Trimethoxyphenyl)-*N*-(5-oxo-5-(2-(1,2,3,4-tetrahydroacridin-9-yl)hydrazino)pentyl)-propanamide

Ethyl 6-((3-(3,4,5-trimethoxyphenyl)propanoyl)amino)hexanoate
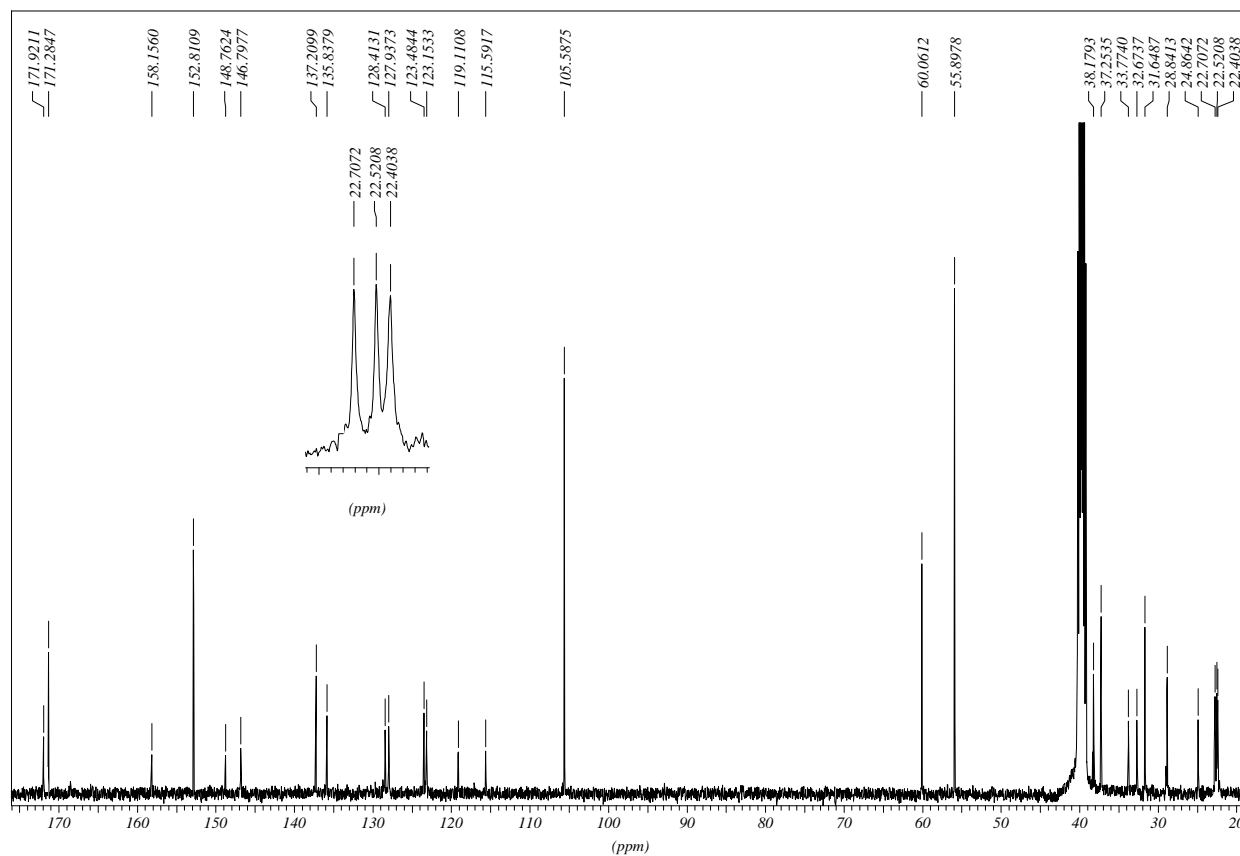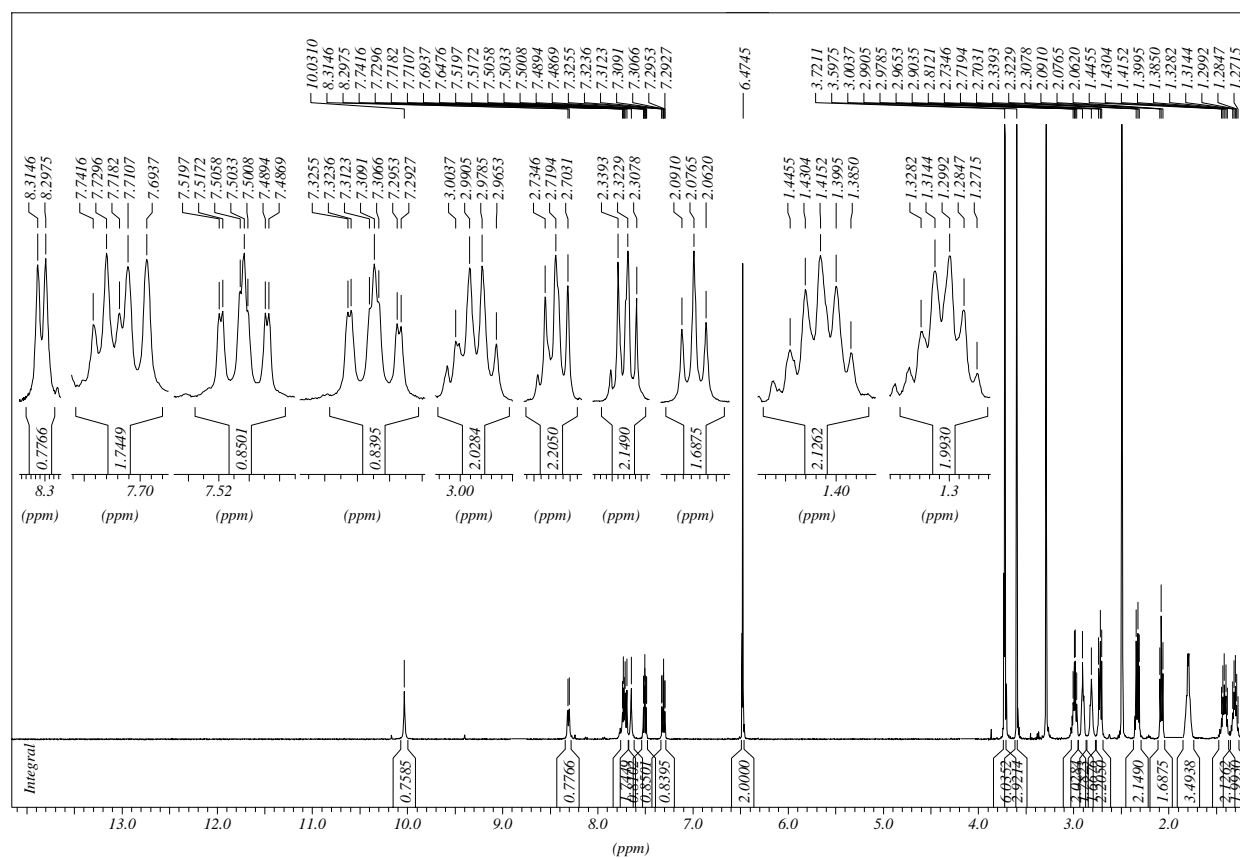
N-(6-Hydrazino-6-oxohexyl)-3-(3,4,5-trimethoxyphenyl)propanamide
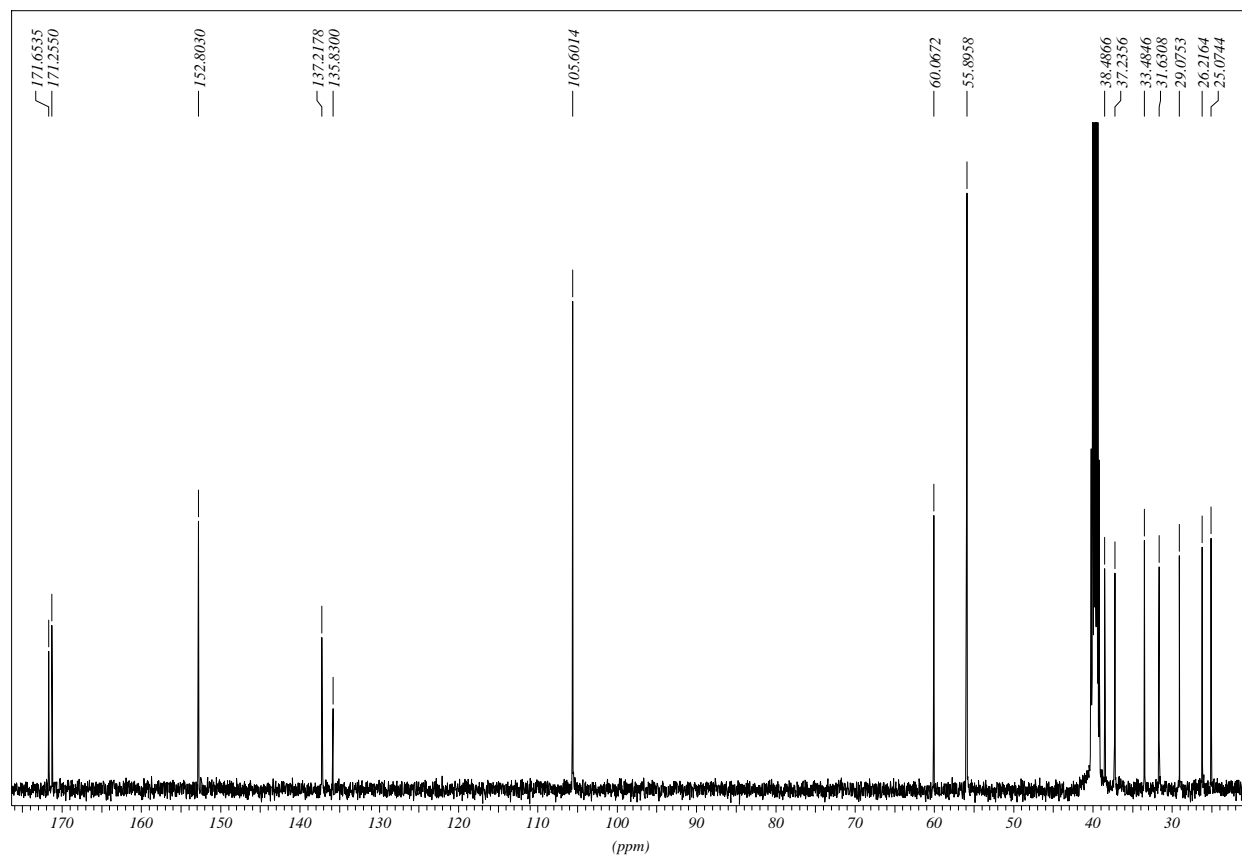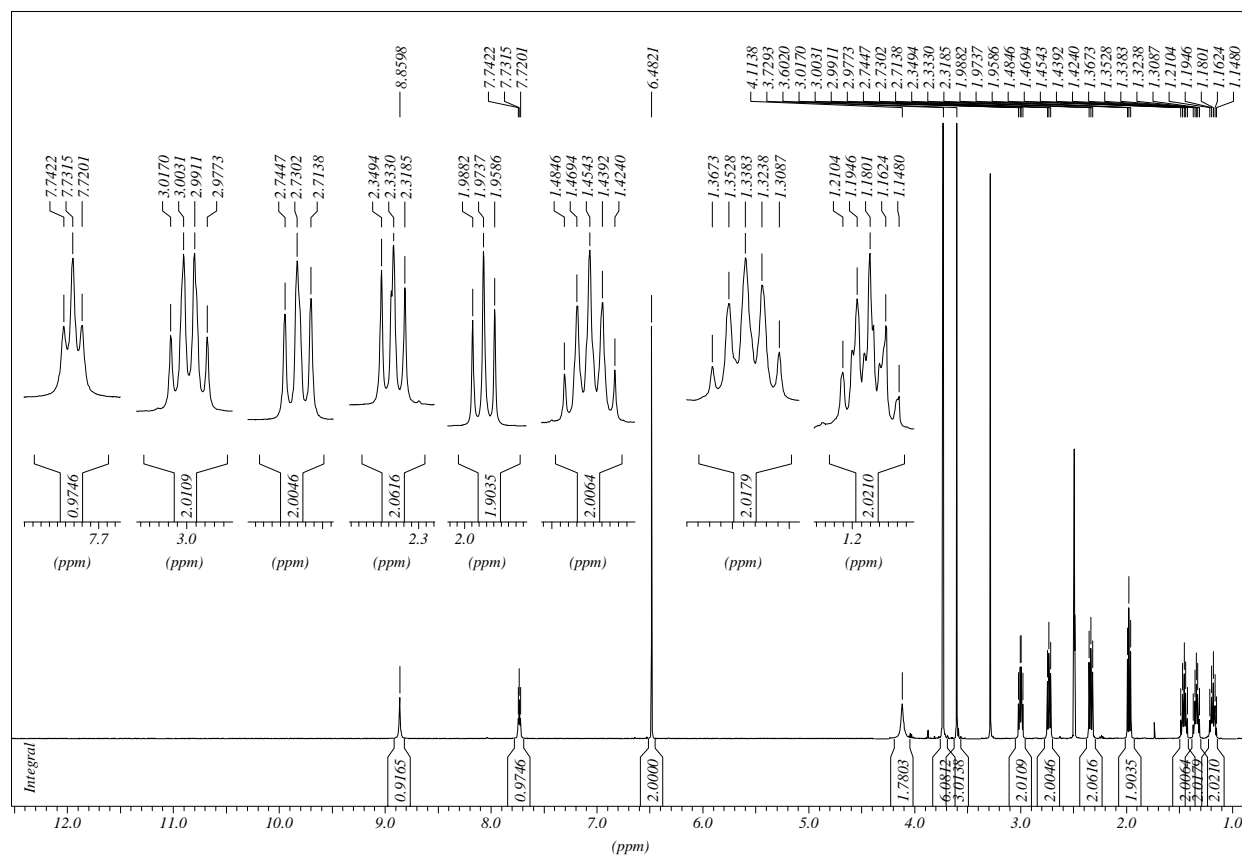
3-(3,4,5-Trimethoxyphenyl)-*N*-(6-oxo-6-(2-(1,2,3,4-tetrahydroacridin-9-yl)hydrazino)hexyl)-propanamide HCl
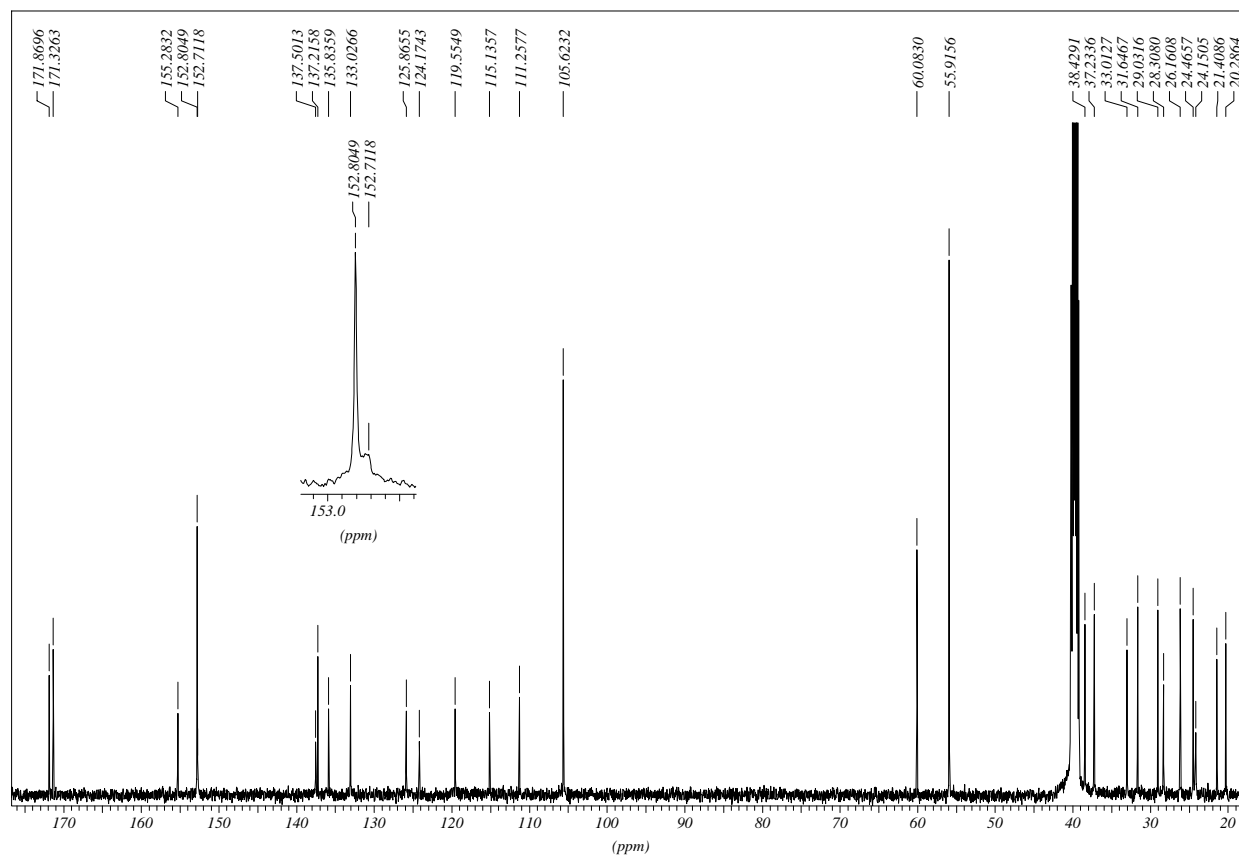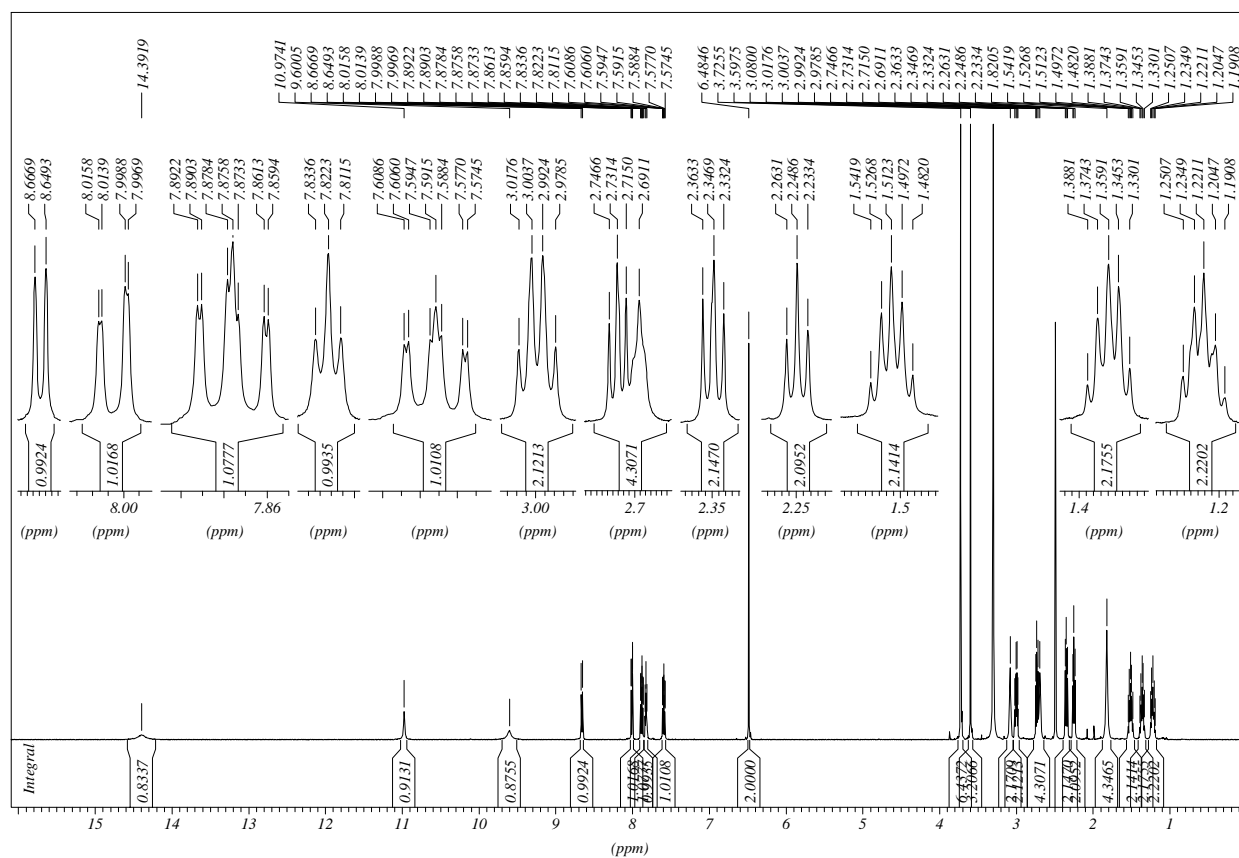
3-(3,4,5-Trimethoxyphenyl)-*N*-(6-oxo-6-(2-(1,2,3,4-tetrahydroacridin-9-yl)hydrazino)hexyl)-propanamide
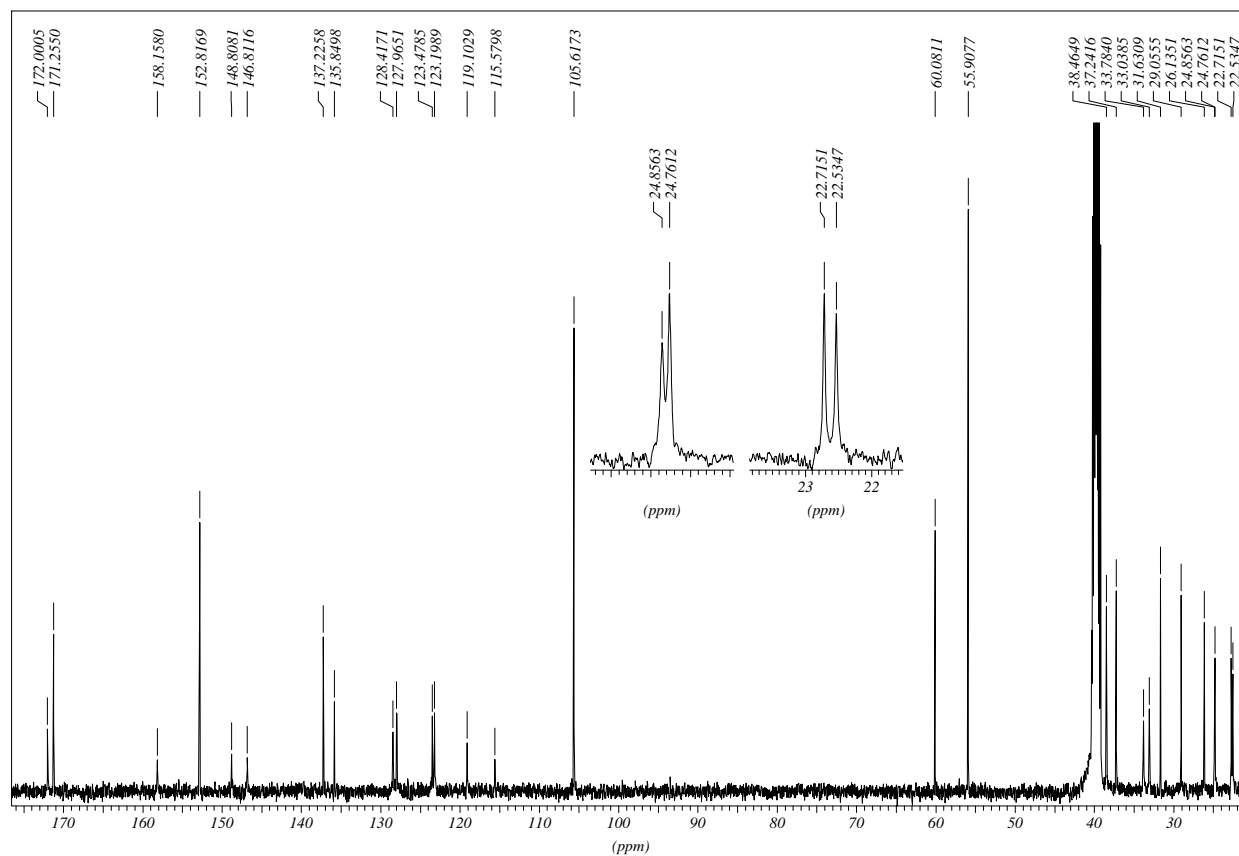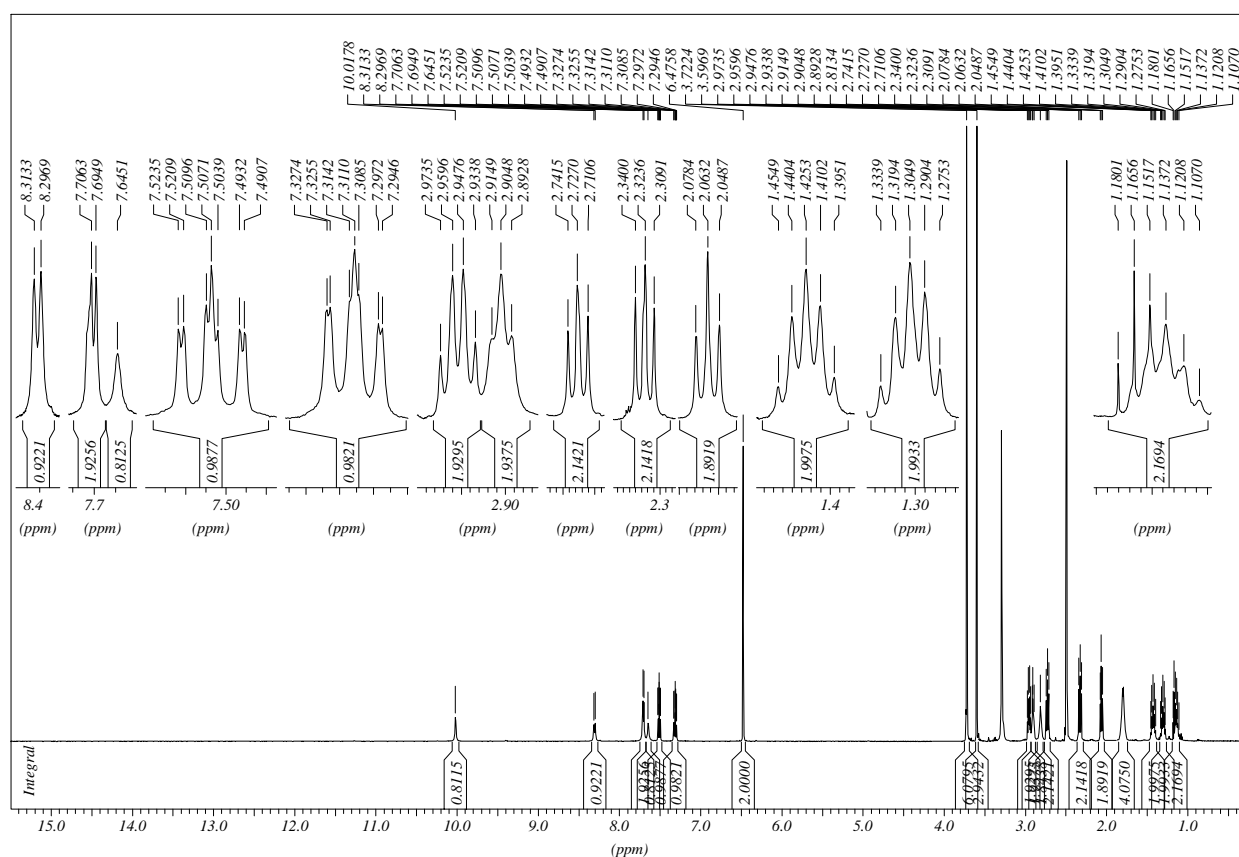
4-Acetyloxybenzoic acid
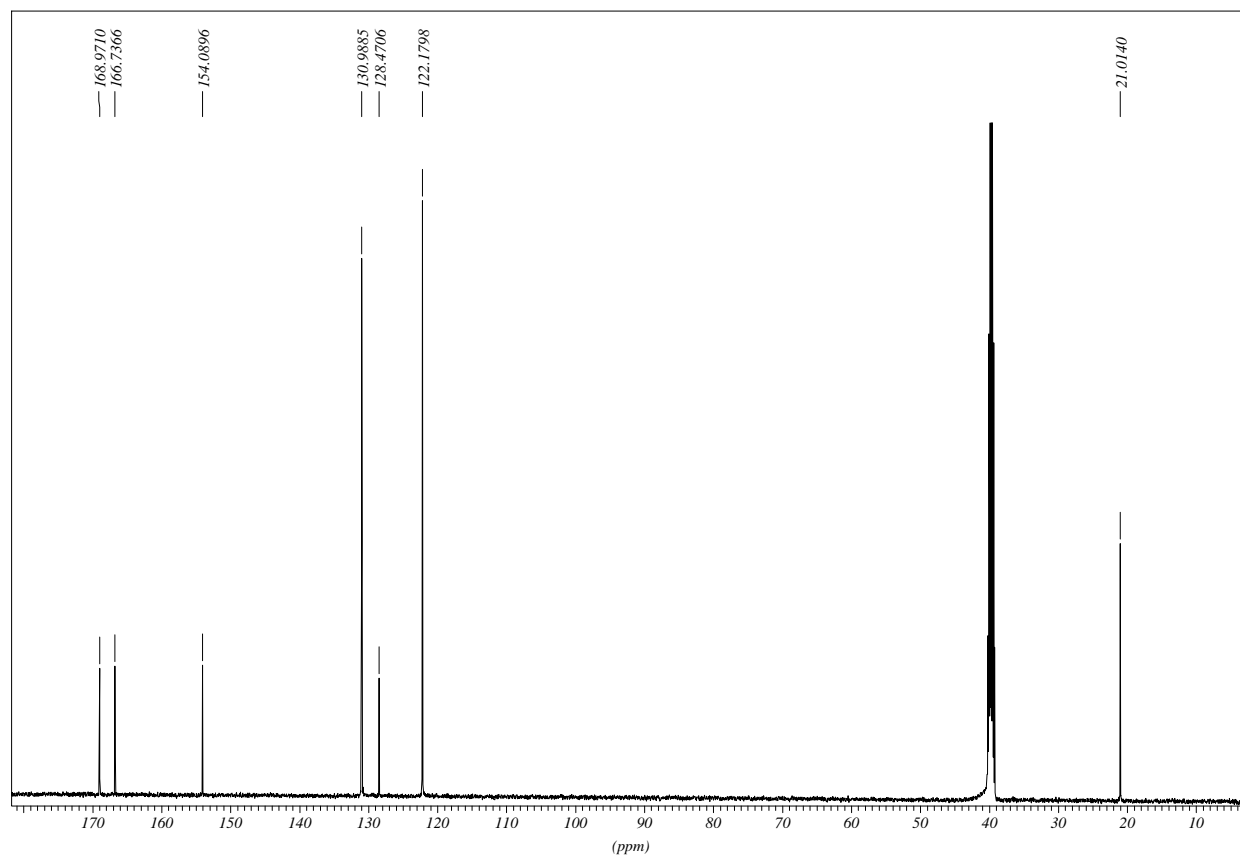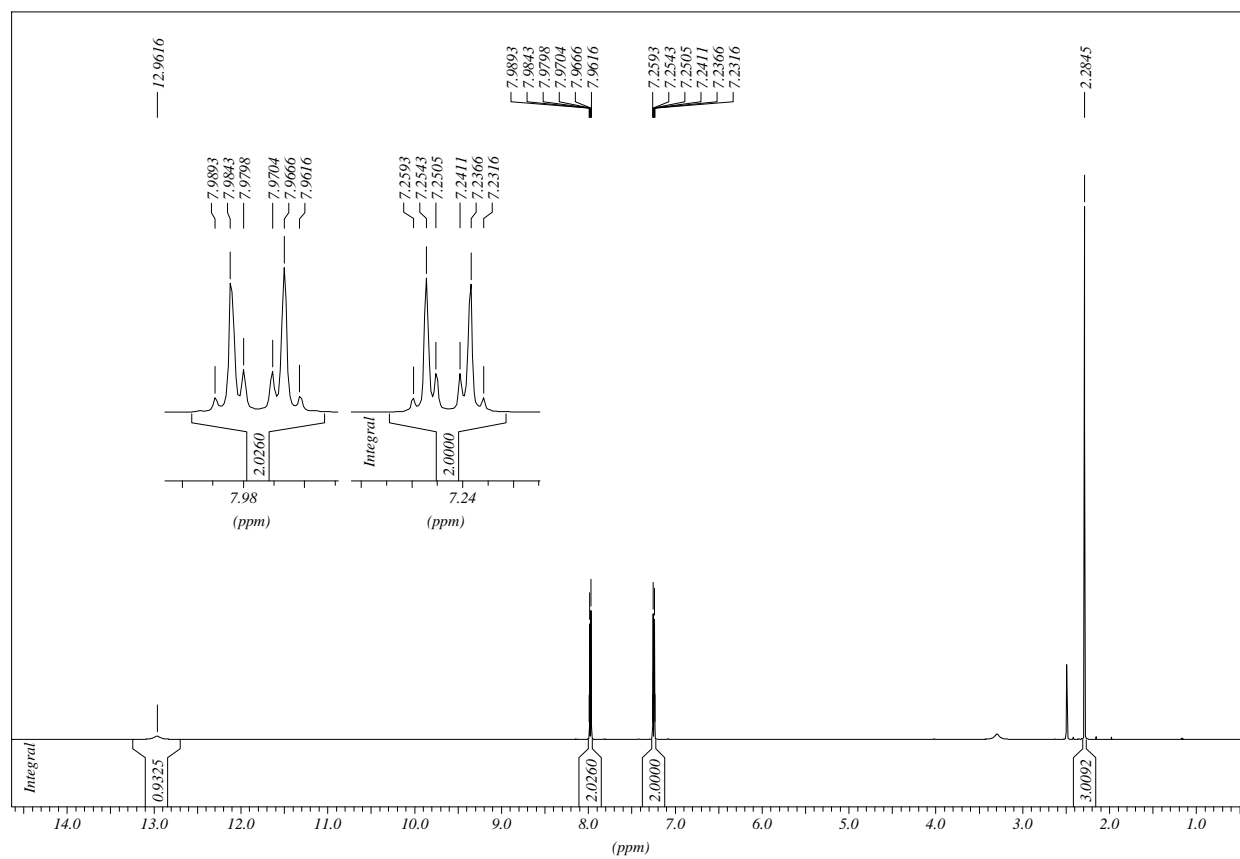
Ethyl 6-((4-hydroxybenzoyl)amino)hexanoate
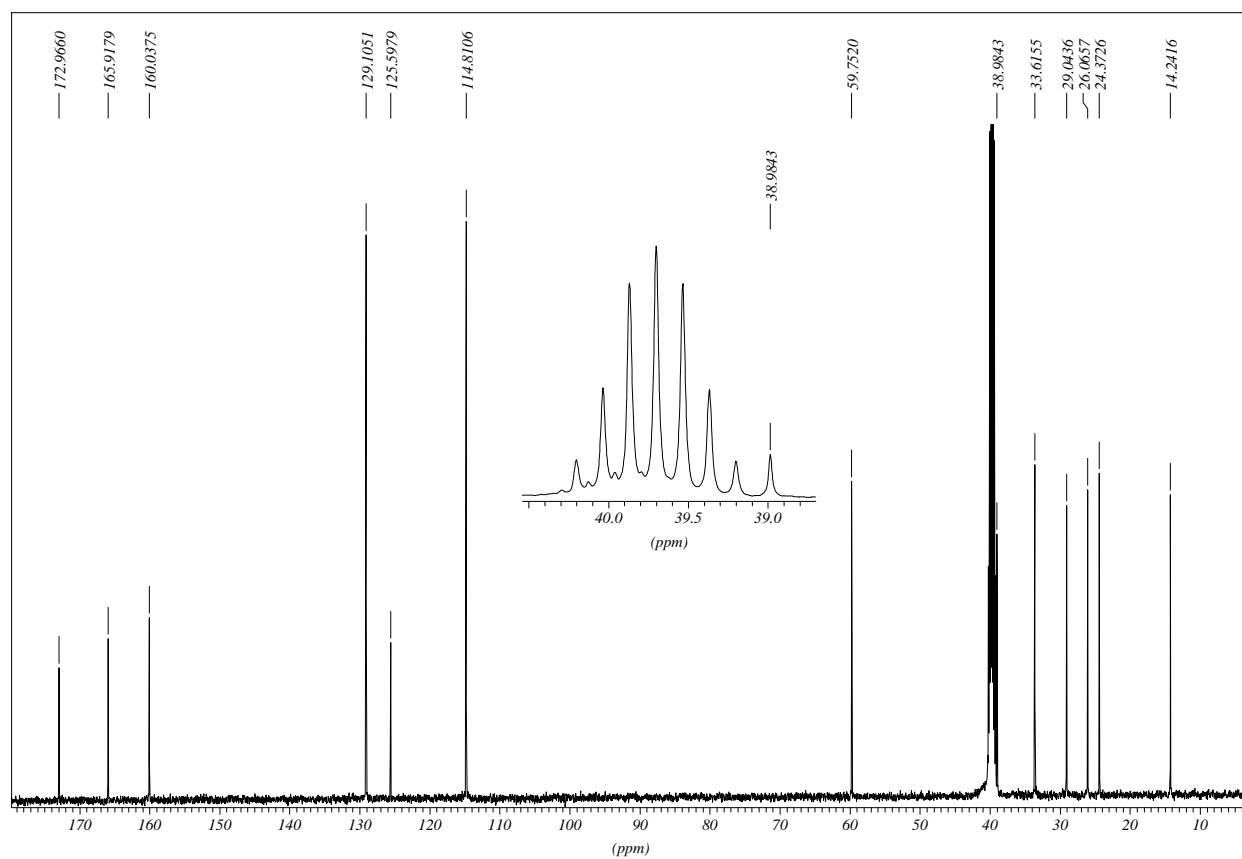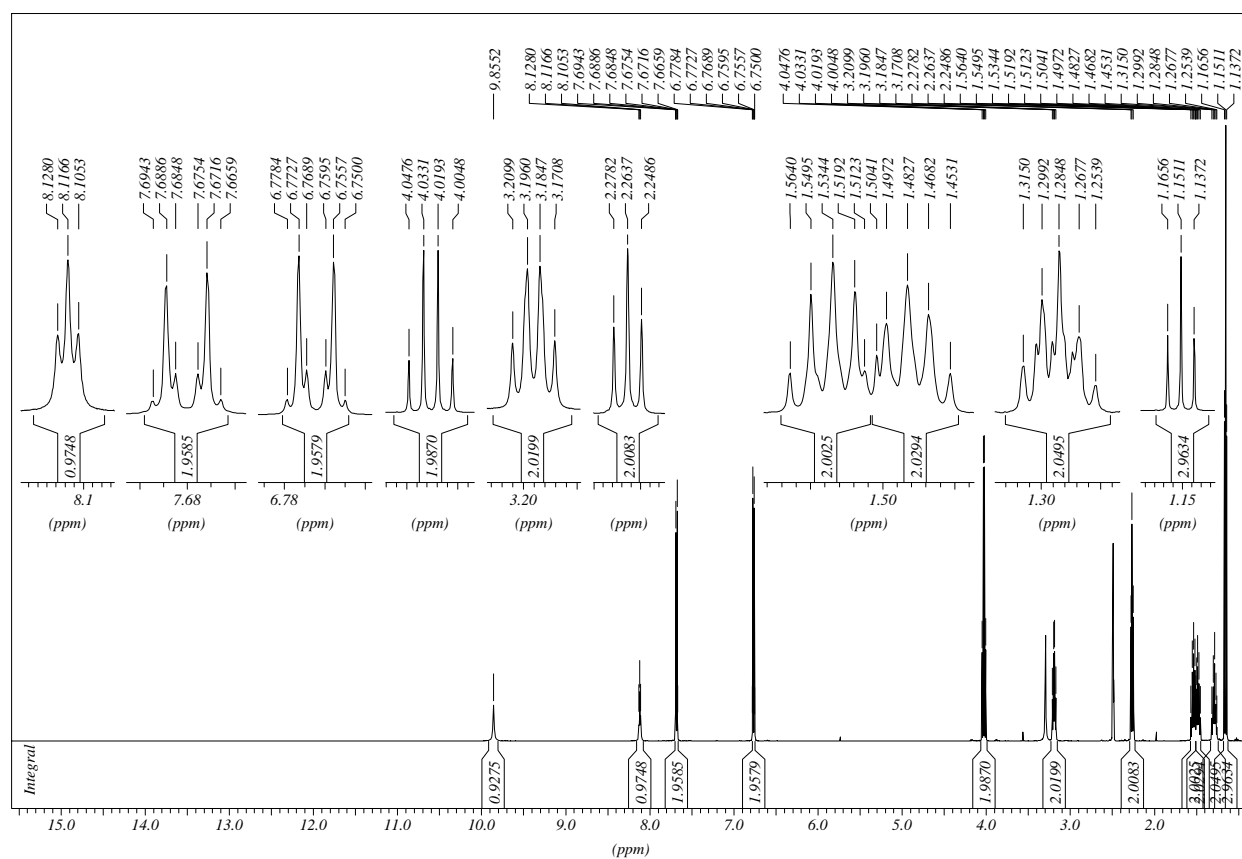
Ethyl 6-((4-(2-bromoethoxy)benzoyl)amino)hexanoate
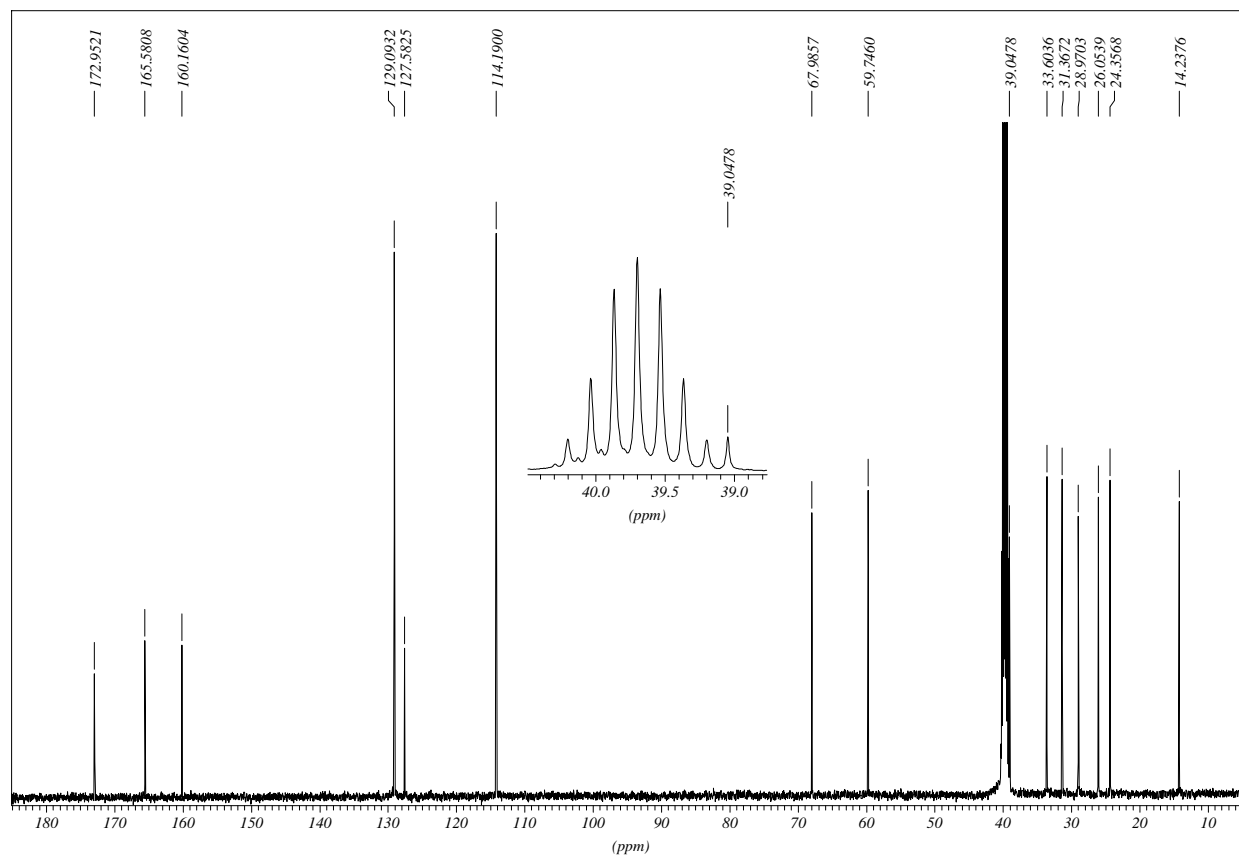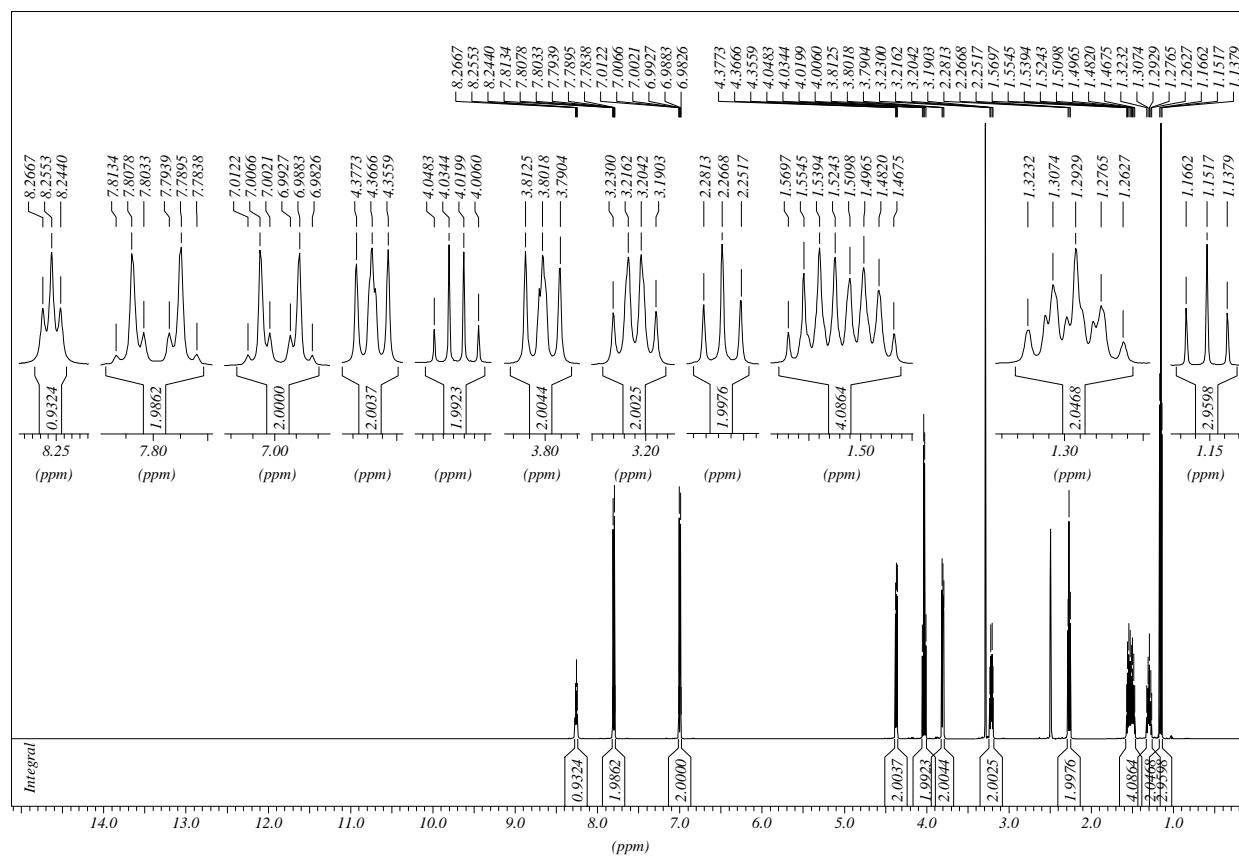
2-(4-(((6-Ethoxy-6-oxohexyl)amino)carbonyl)phenoxy)-*N,N,N*-triethylethanaminium bromide
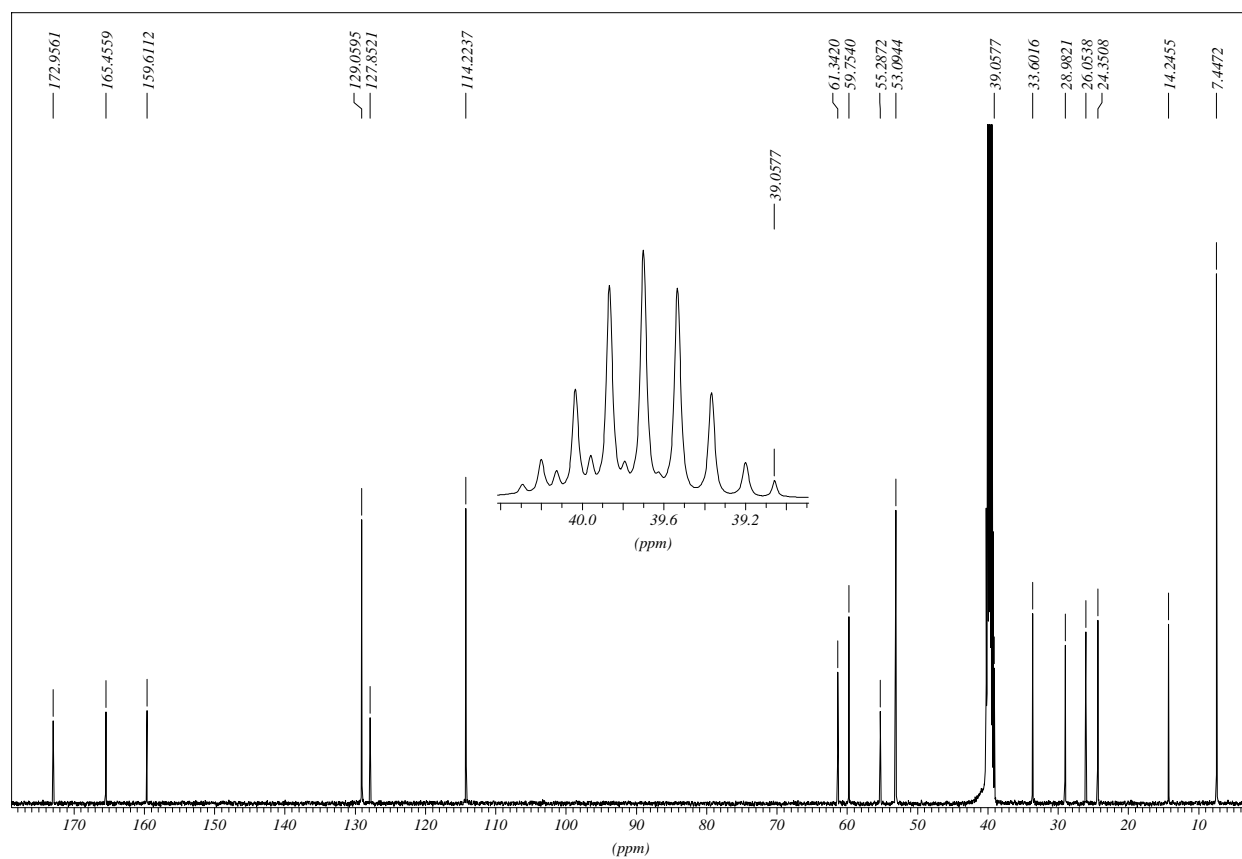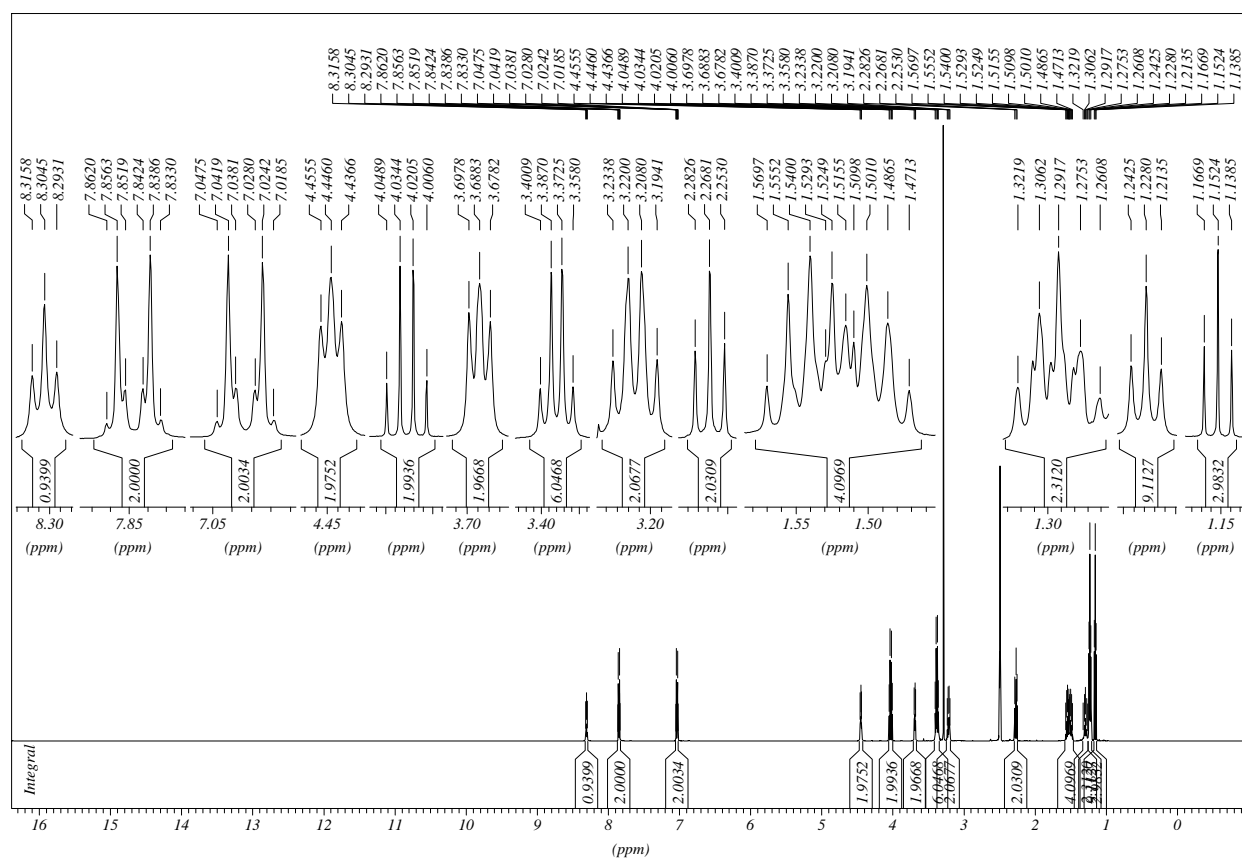
N,N,N-Triethyl-2-(4-(((6-hydrazino-6-oxohexyl)amino)carbonyl)phenoxy)ethanaminium bromide
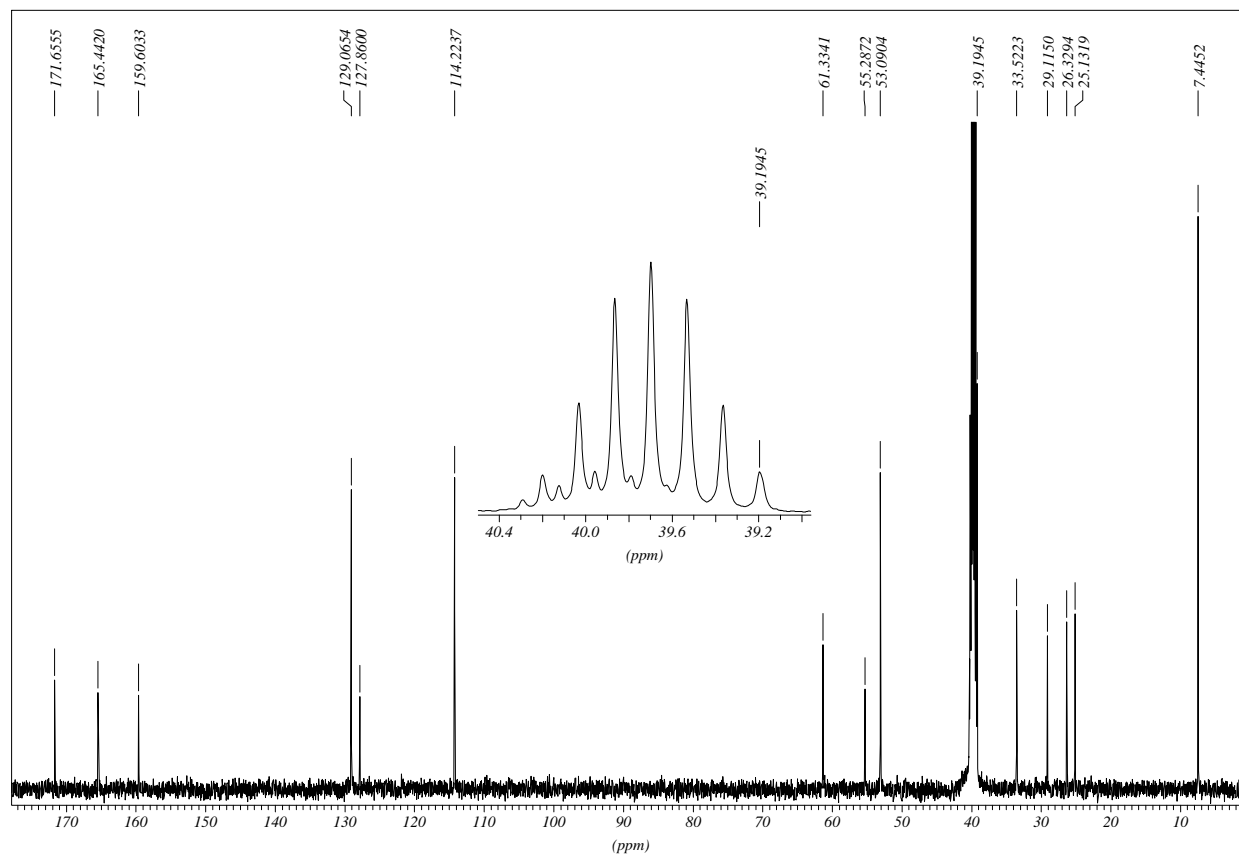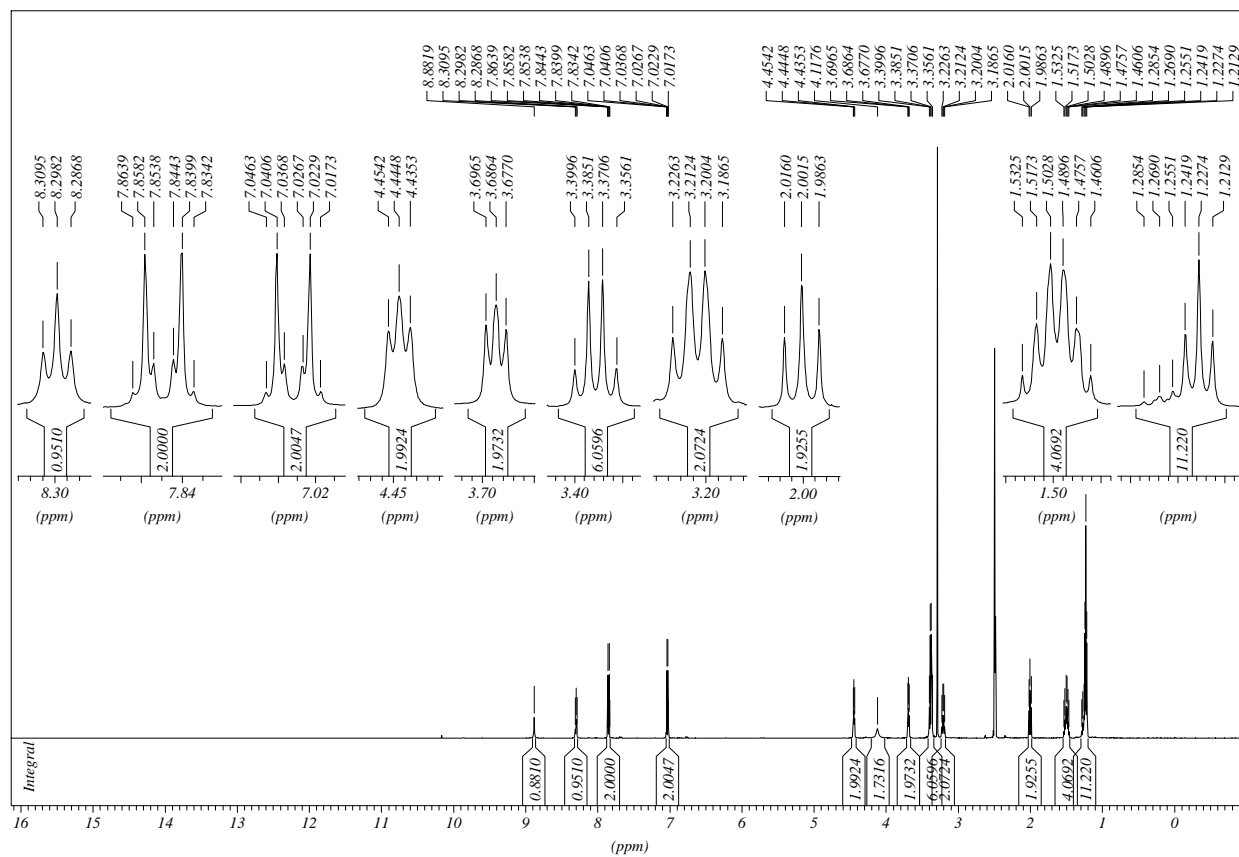
N,N,N-Triethyl-2-(4-(((6-(2-(1,2,3,4-tetrahydroacridin-9-yl)hydrazino)-6-oxohexyl)amino)-carbonyl)phenoxy)ethanaminium bromide HCl
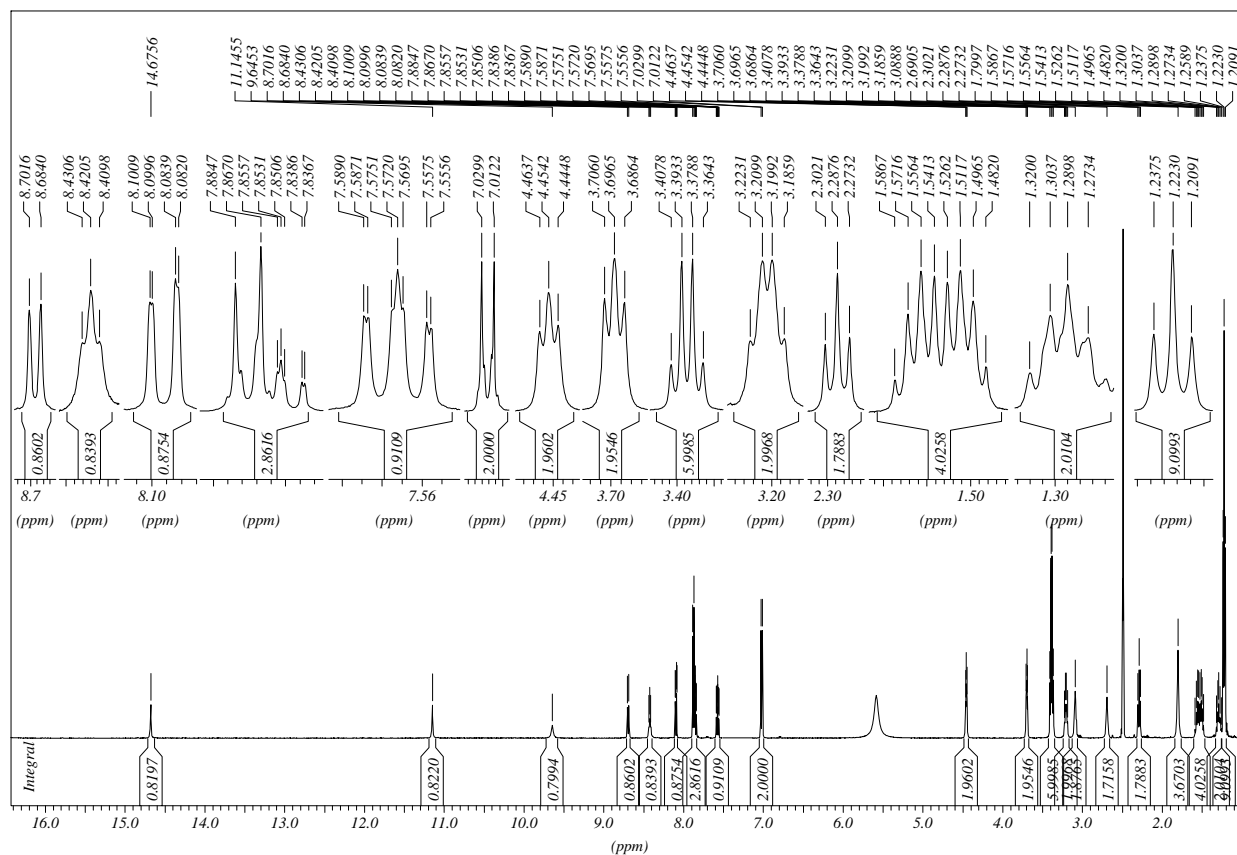
2-(4-(((6-(2-(6-Chloro-1,2,3,4-tetrahydroacridin-9-yl)hydrazino)-6-oxohexyl)amino)carbonyl)-phenoxy)-*N*,*N*,*N*-triethyl-ethanaminium bromide HCl
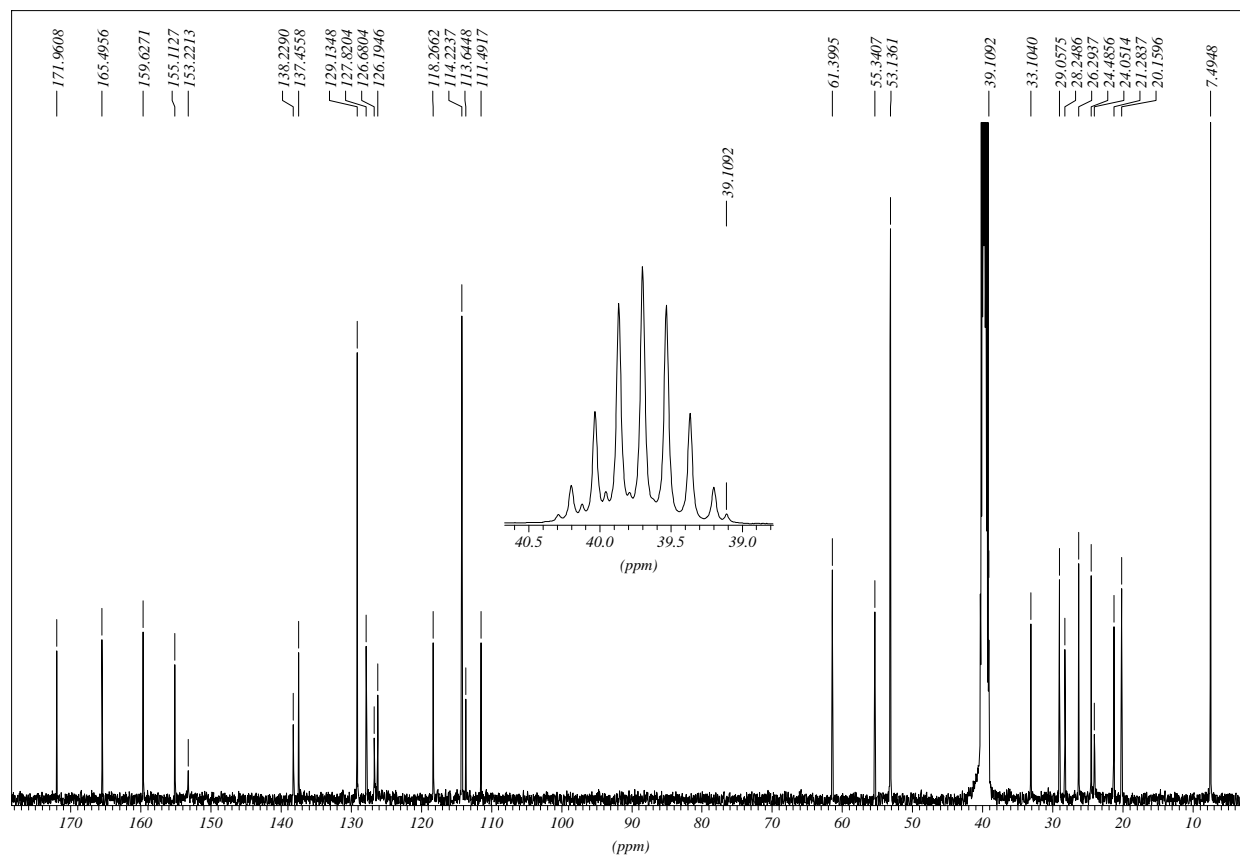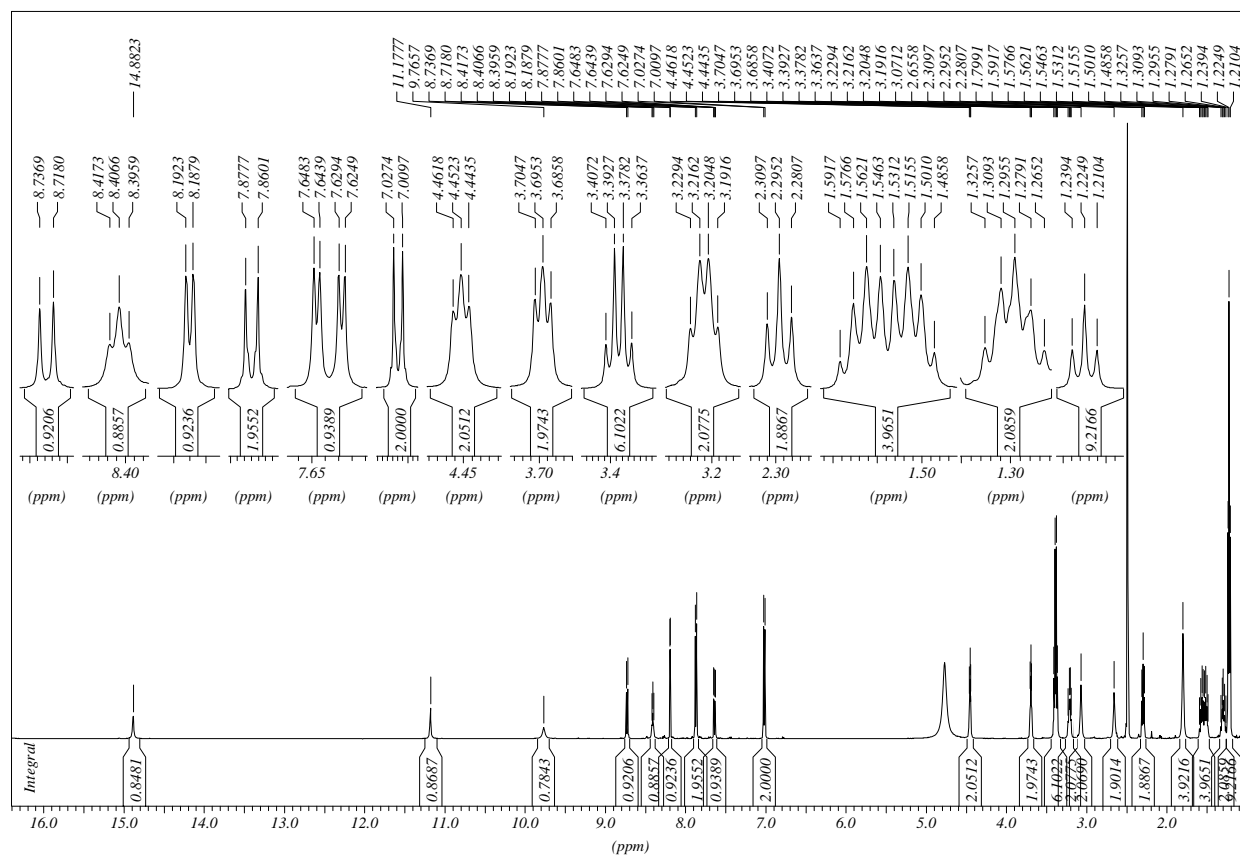
3,5-Bis(acetyloxy)benzoic acid

Ethyl 6-((3,5-dihydroxybenzoyl)amino)hexanoate
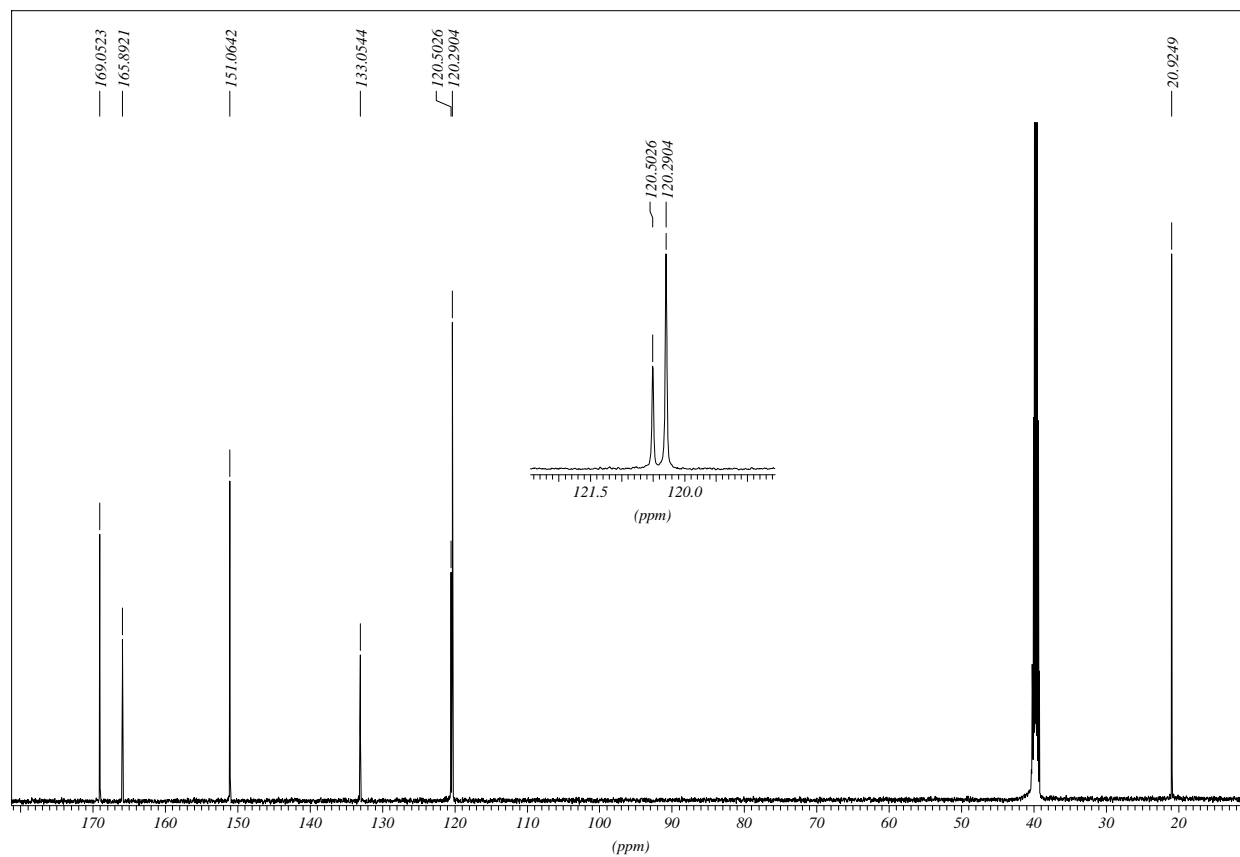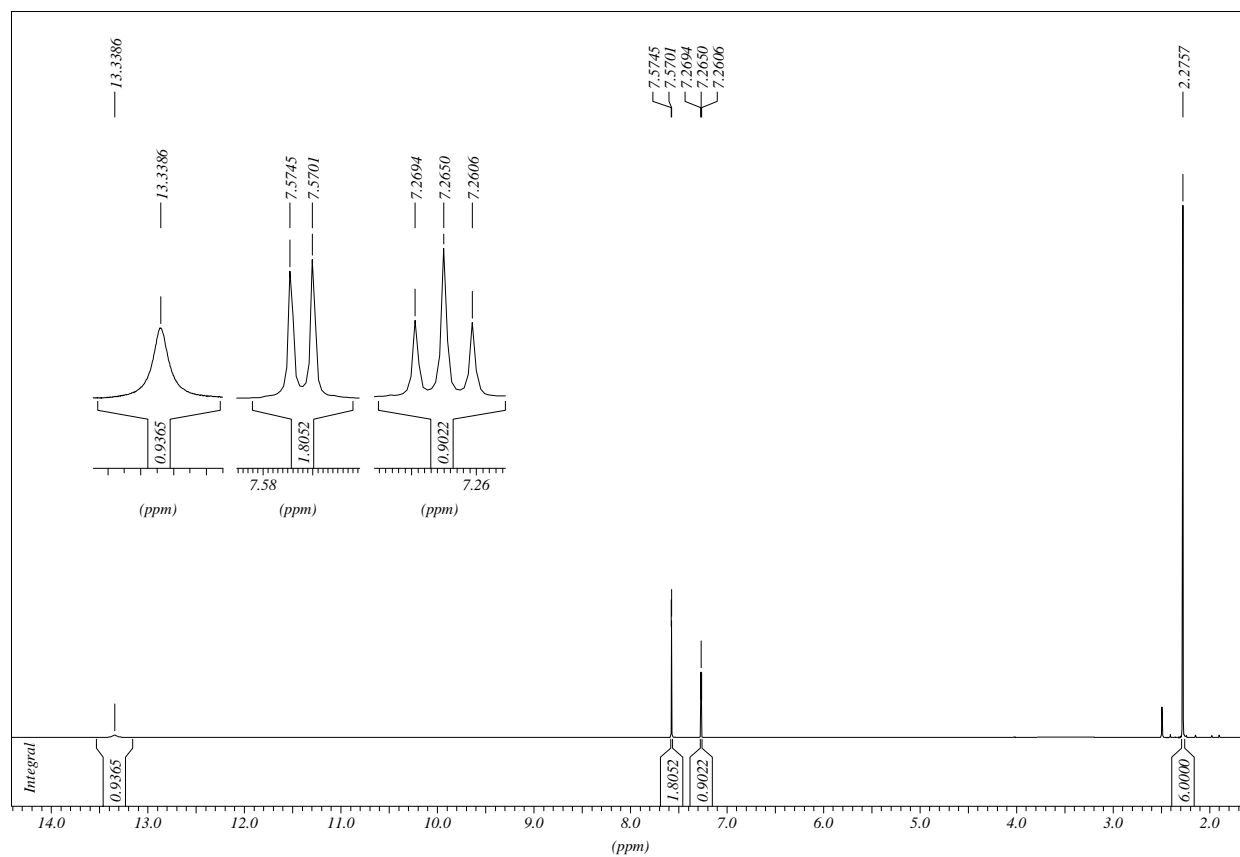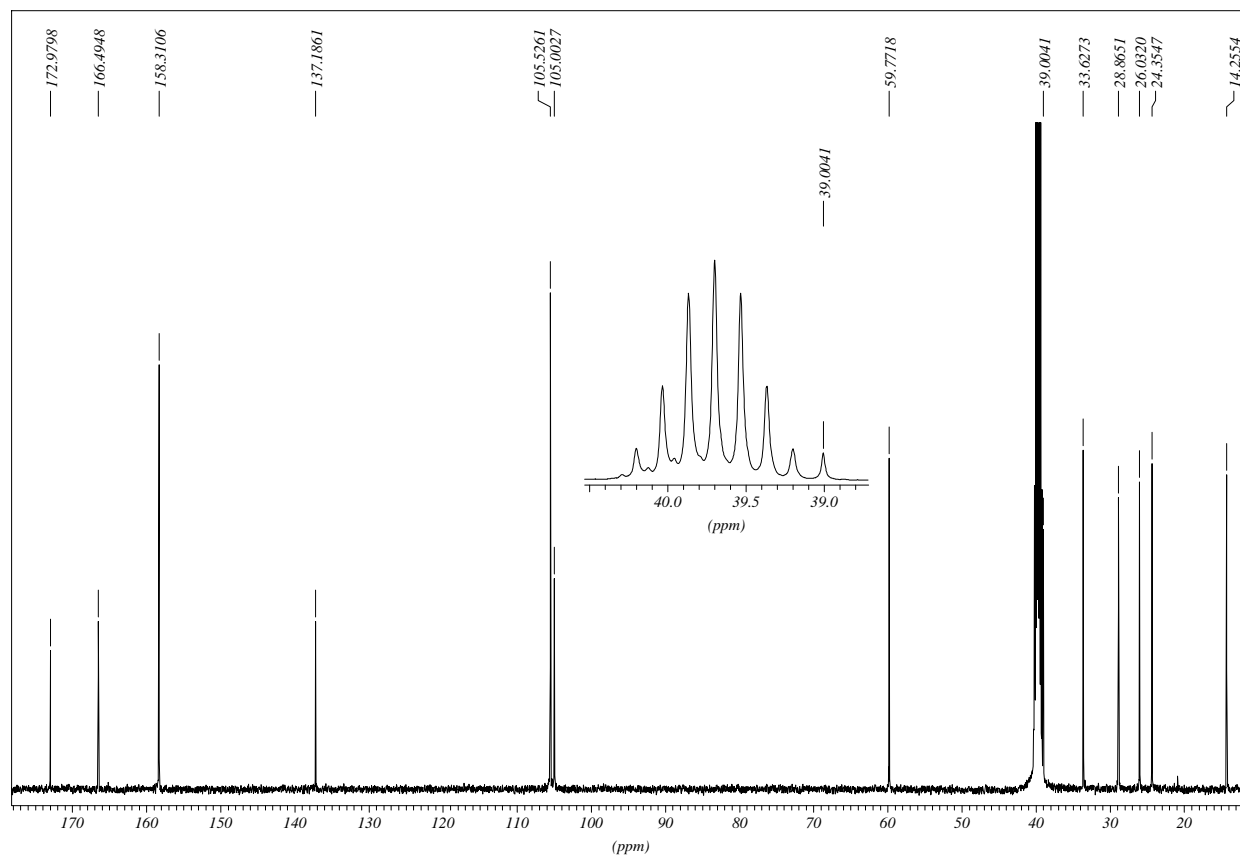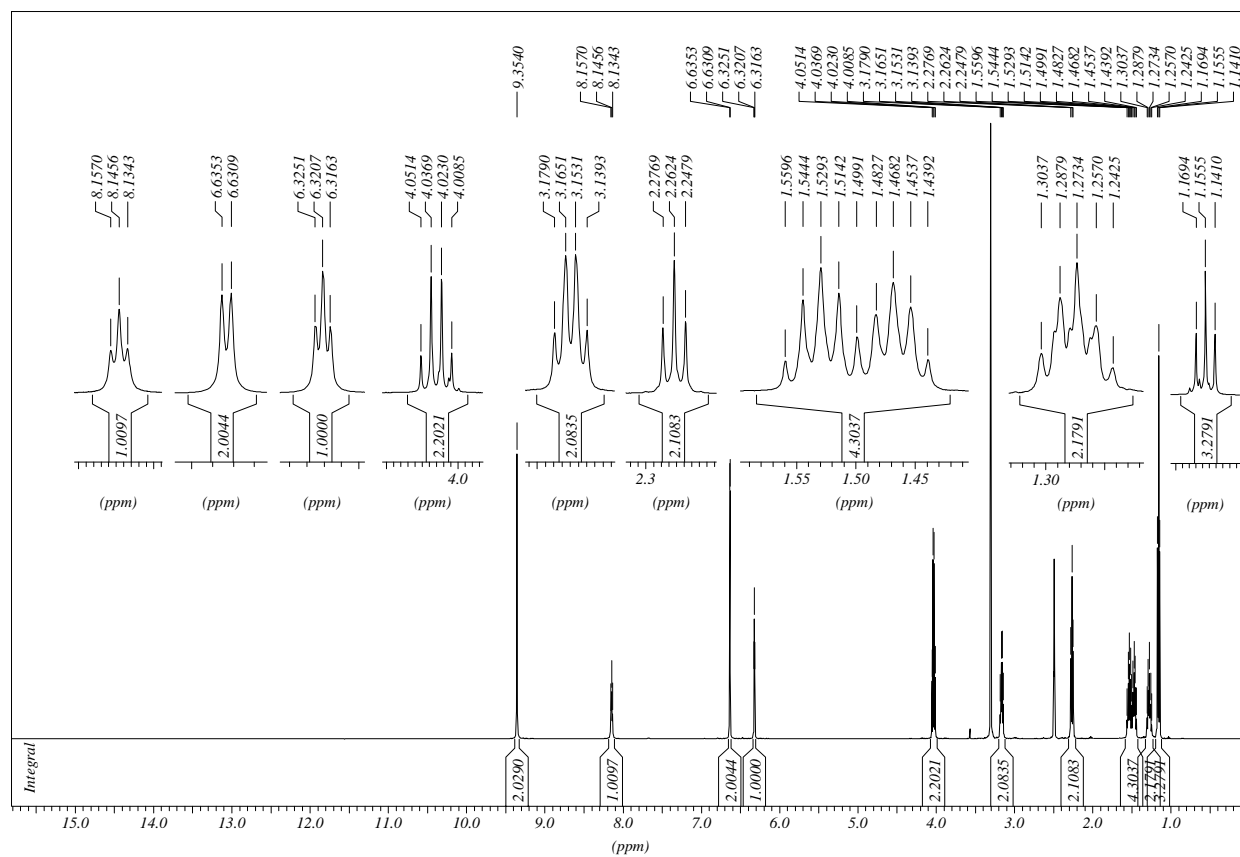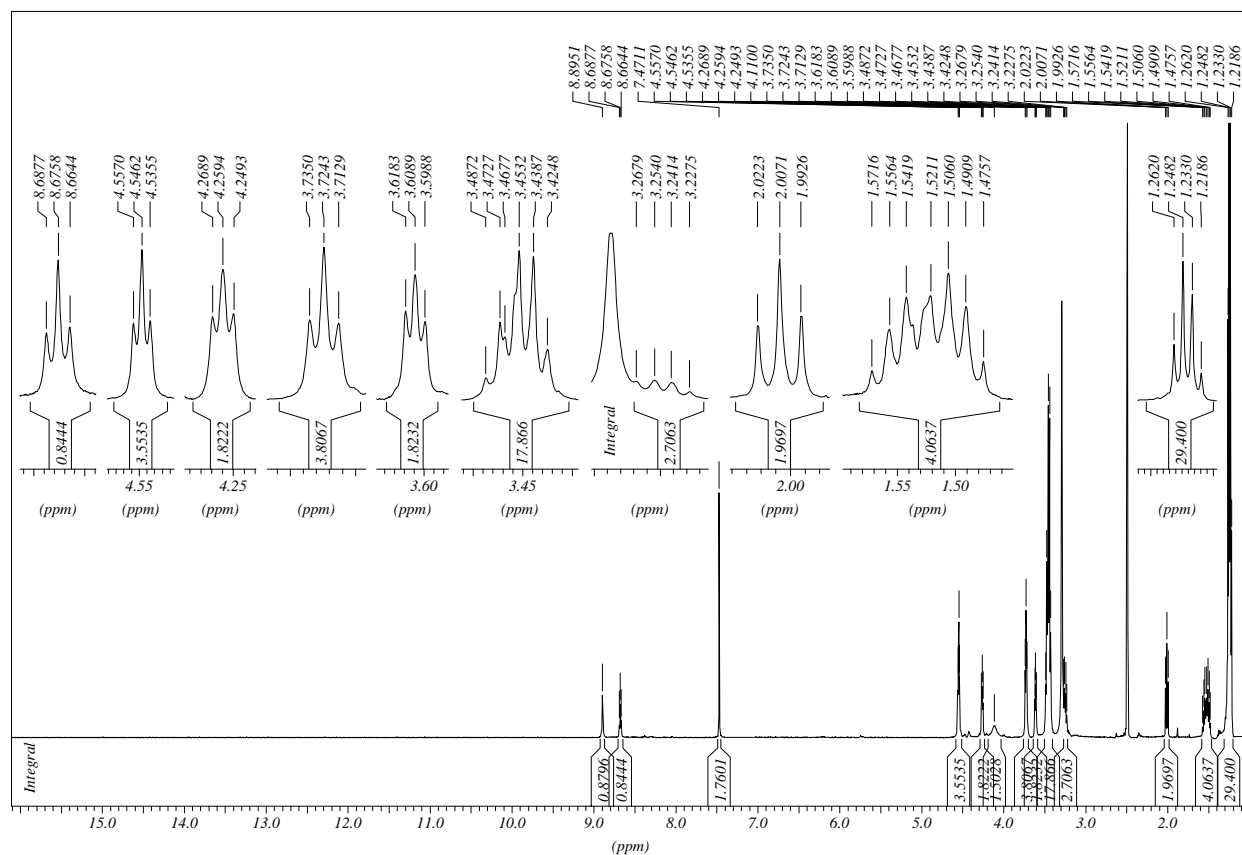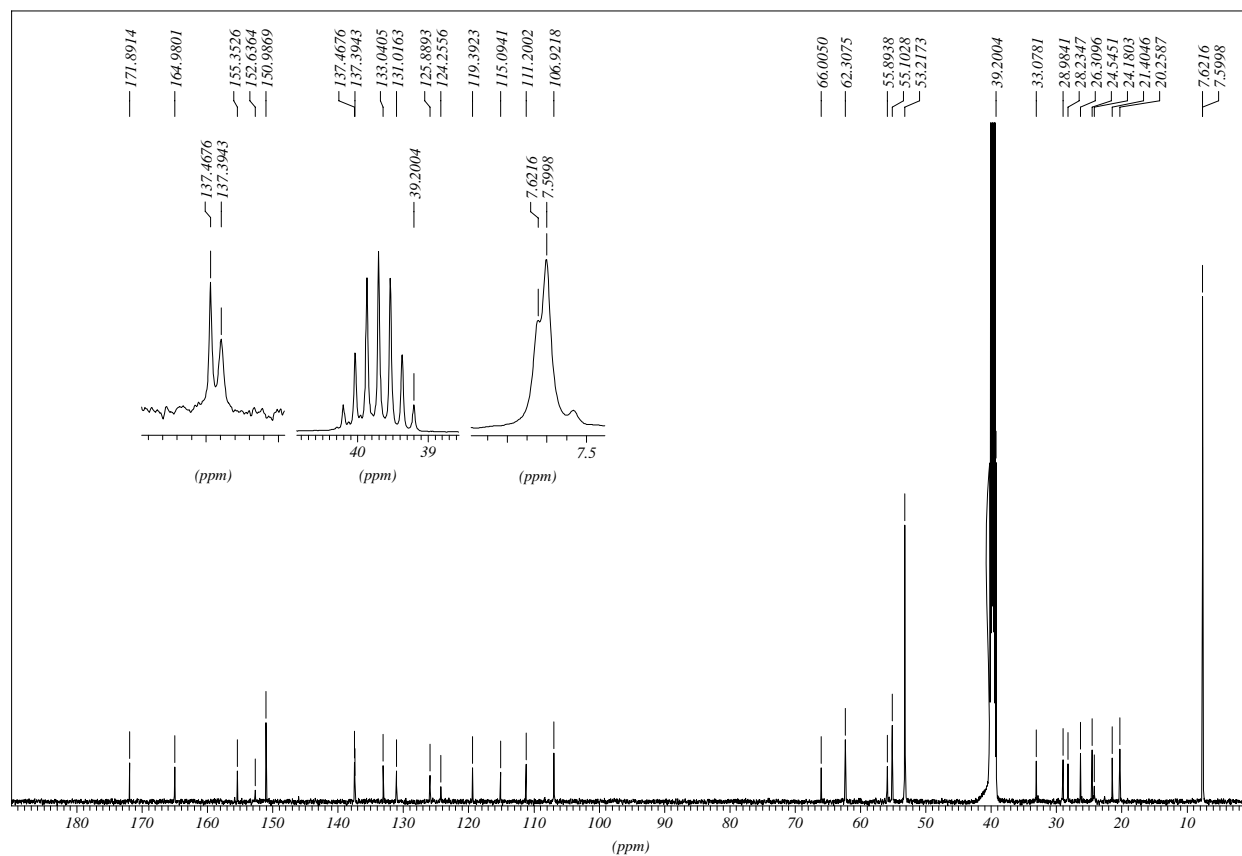
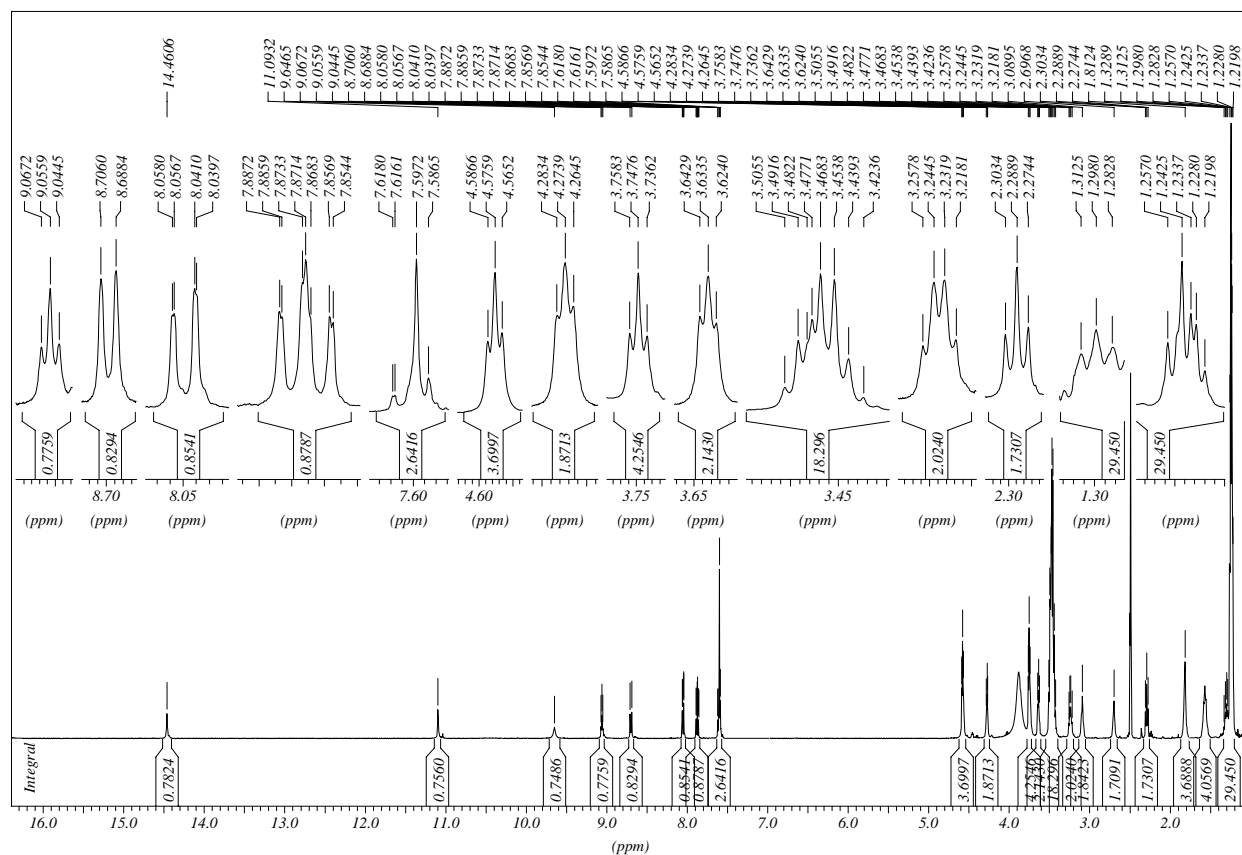## Ethyl 6-((3,5-bis(2-bromoethoxy)benzoyl)amino)hexanoate

## 2-(3-(((6-Ethoxy-6-oxohexyl)amino)carbonyl)-5-((2-triethylammonio)ethoxy)phenoxy)-*N,N,N*-triethylethanaminium dibromide
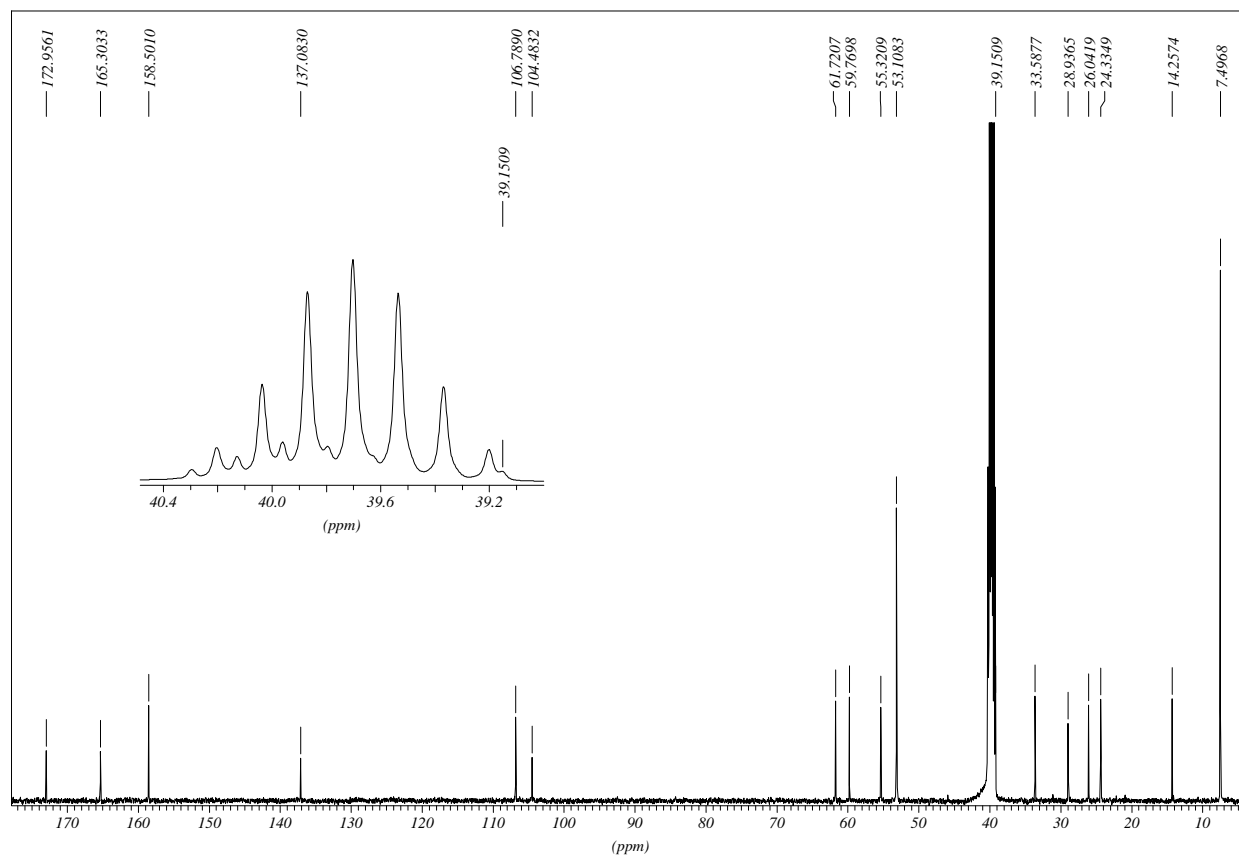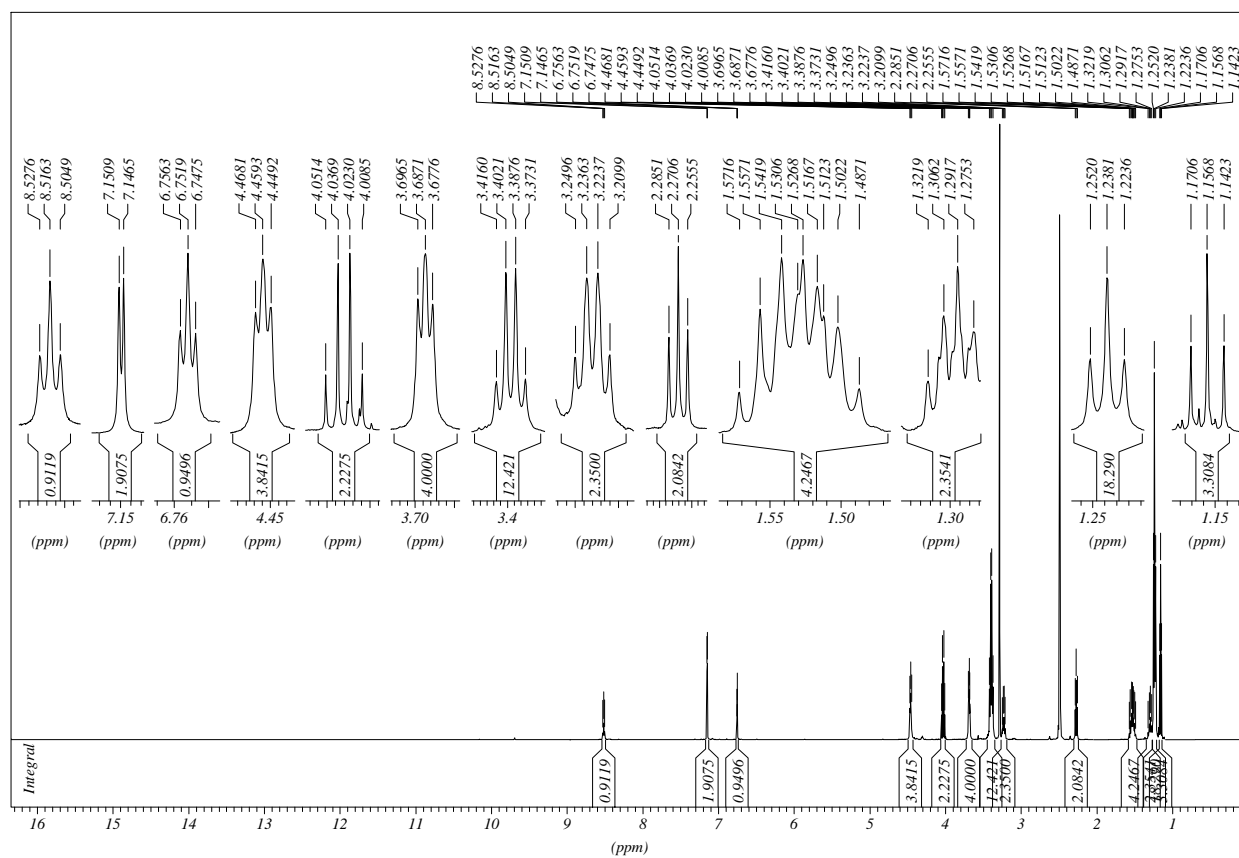
N,N,N-Triethyl-2-(3-(((6-hydrazino-6-oxohexyl)amino)carbonyl)-5-((2-triethylammonio)-ethoxy)phenoxy)ethanaminium dibromide
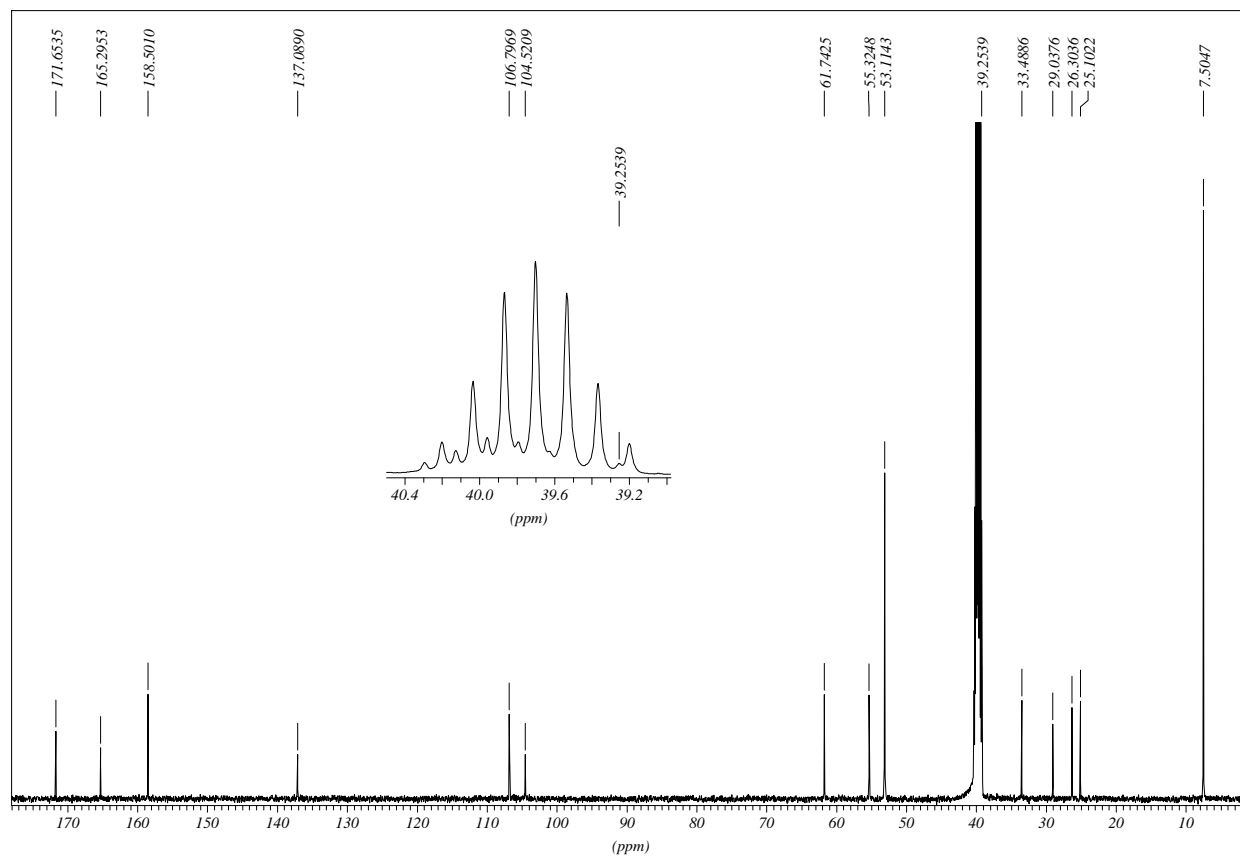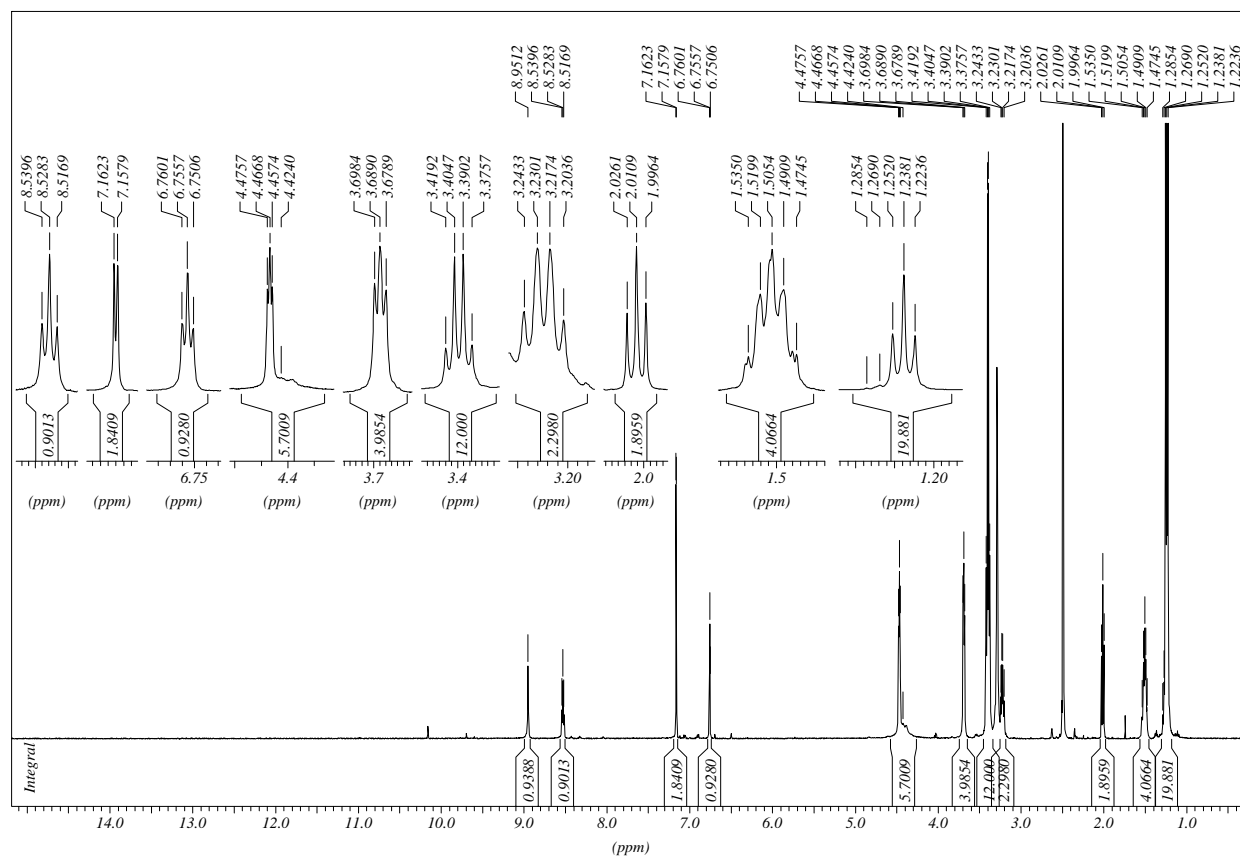
N,N,N-Triethyl-2-(3-(((6-(2-(1,2,3,4-tetrahydroacridin-9-yl)hydrazino)-6-oxohexyl)amino)-carbonyl)-5-((2-triethylammonio)ethoxy)phenoxy)ethanaminium dibromide HCl
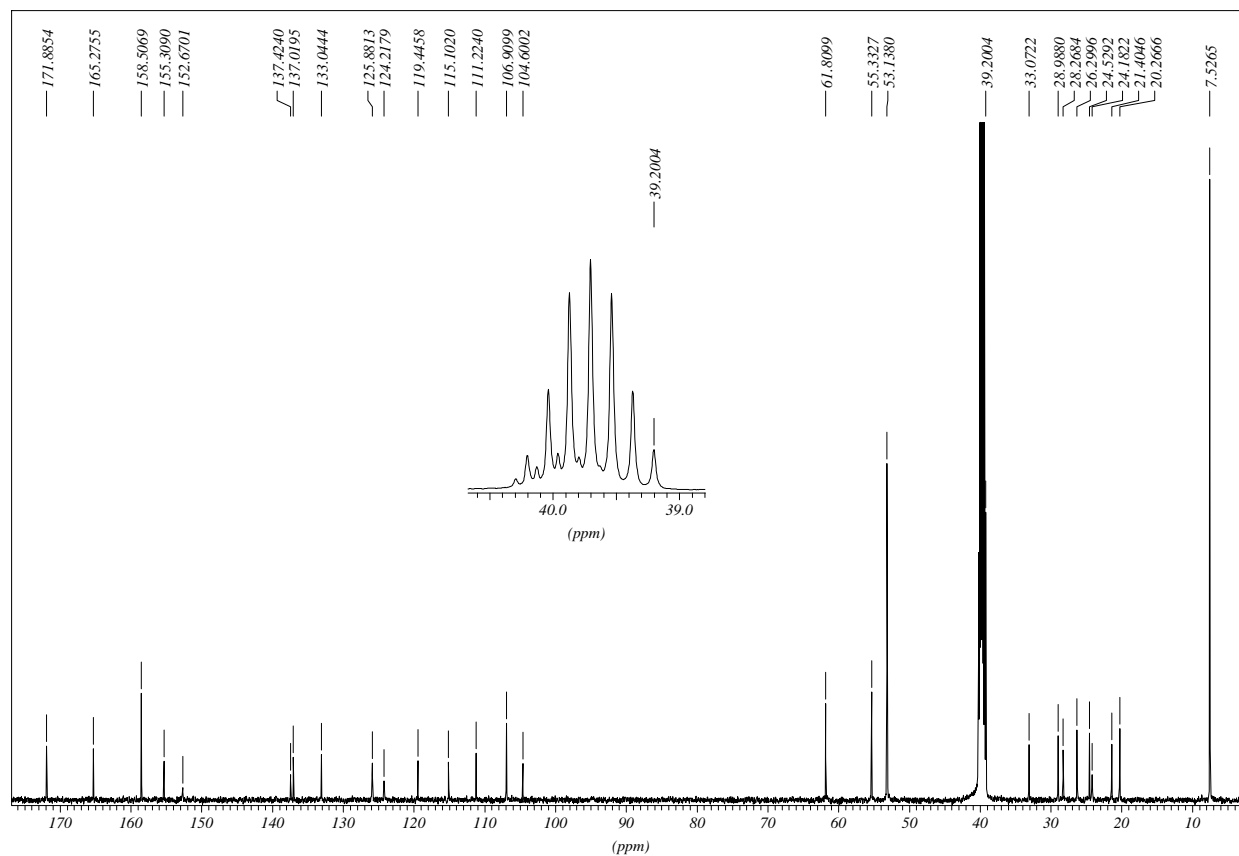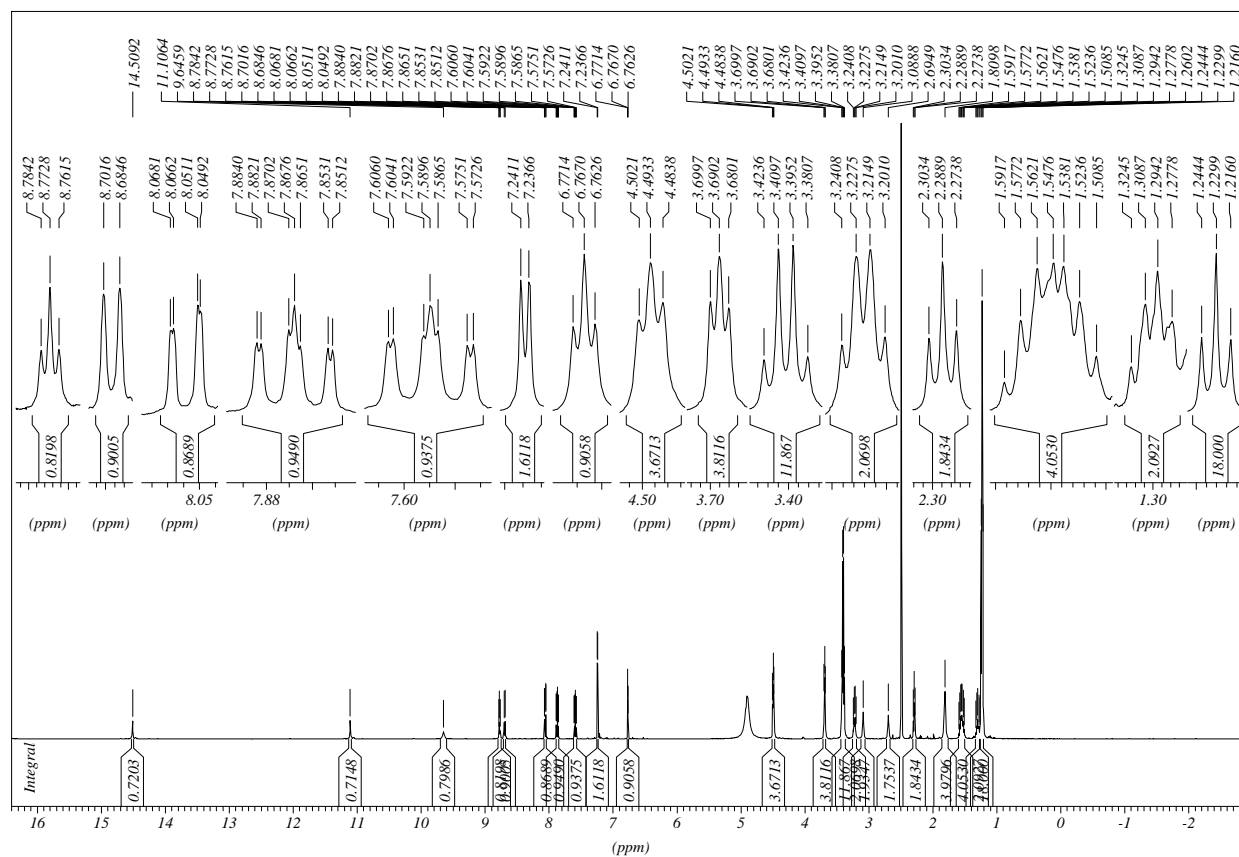
2-(3-(((6-(2-(6-Chloro-1,2,3,4-tetrahydroacridin-9-yl)hydrazino)-6-oxohexyl)amino)carbonyl)-5-((2-triethylammonio)ethoxy)phenoxy)-*N,N,N*-triethyl-ethanaminium dibromide HCl
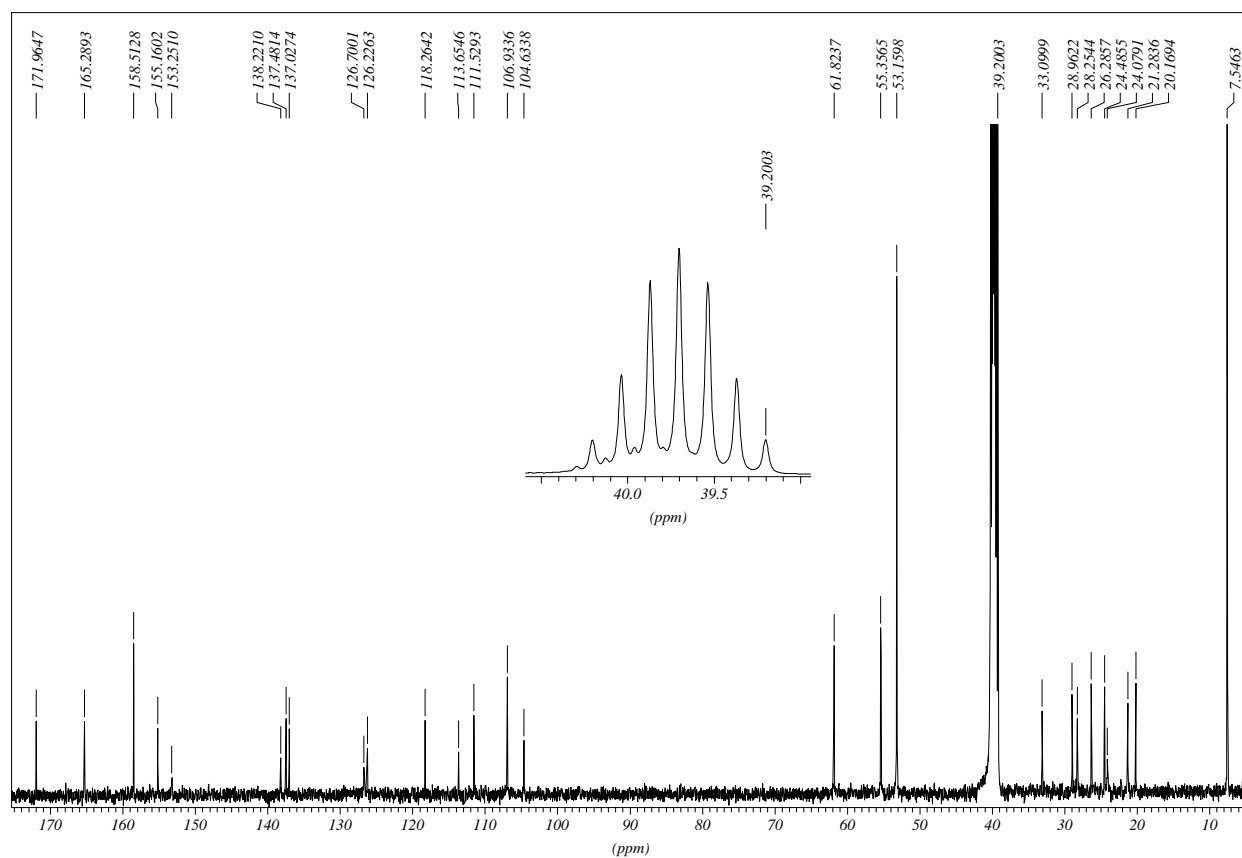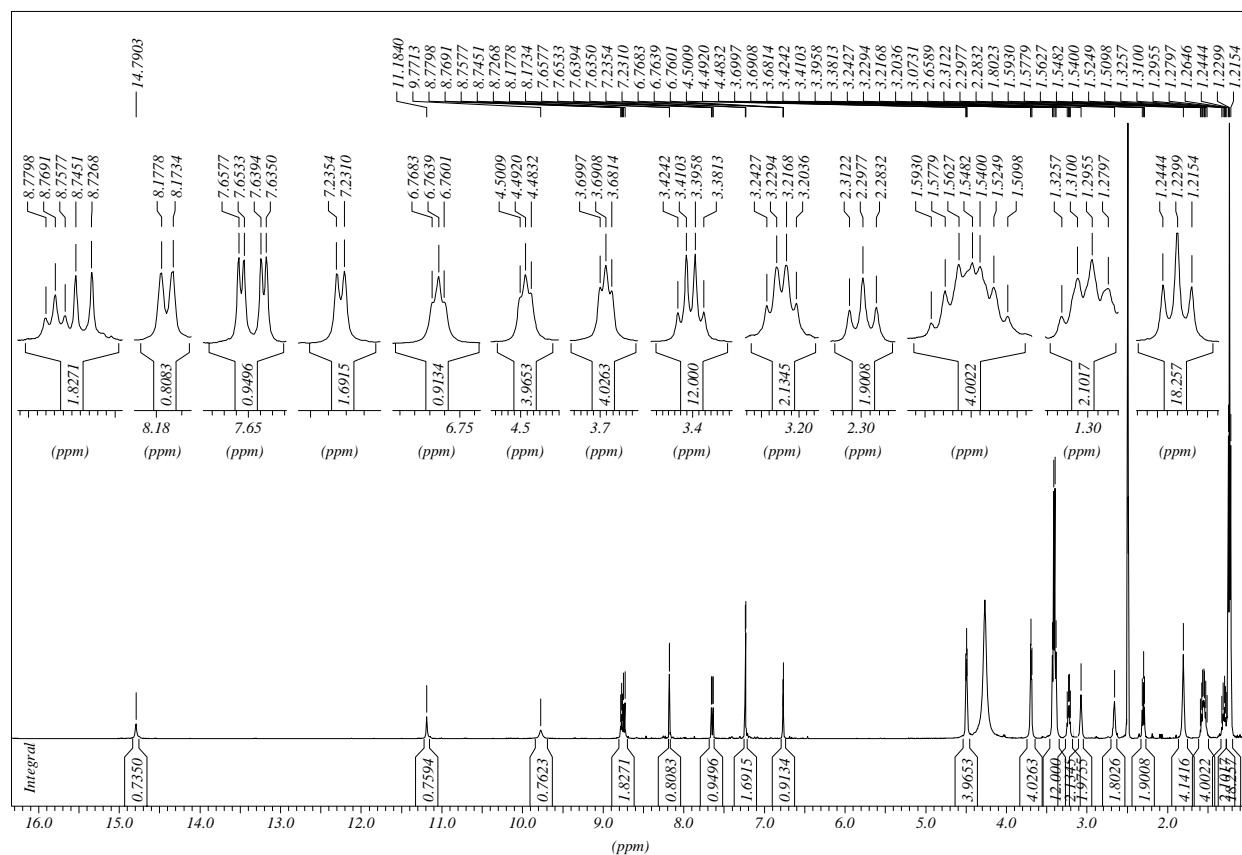
3,4,5-Tris(acetyloxy)benzoic acid
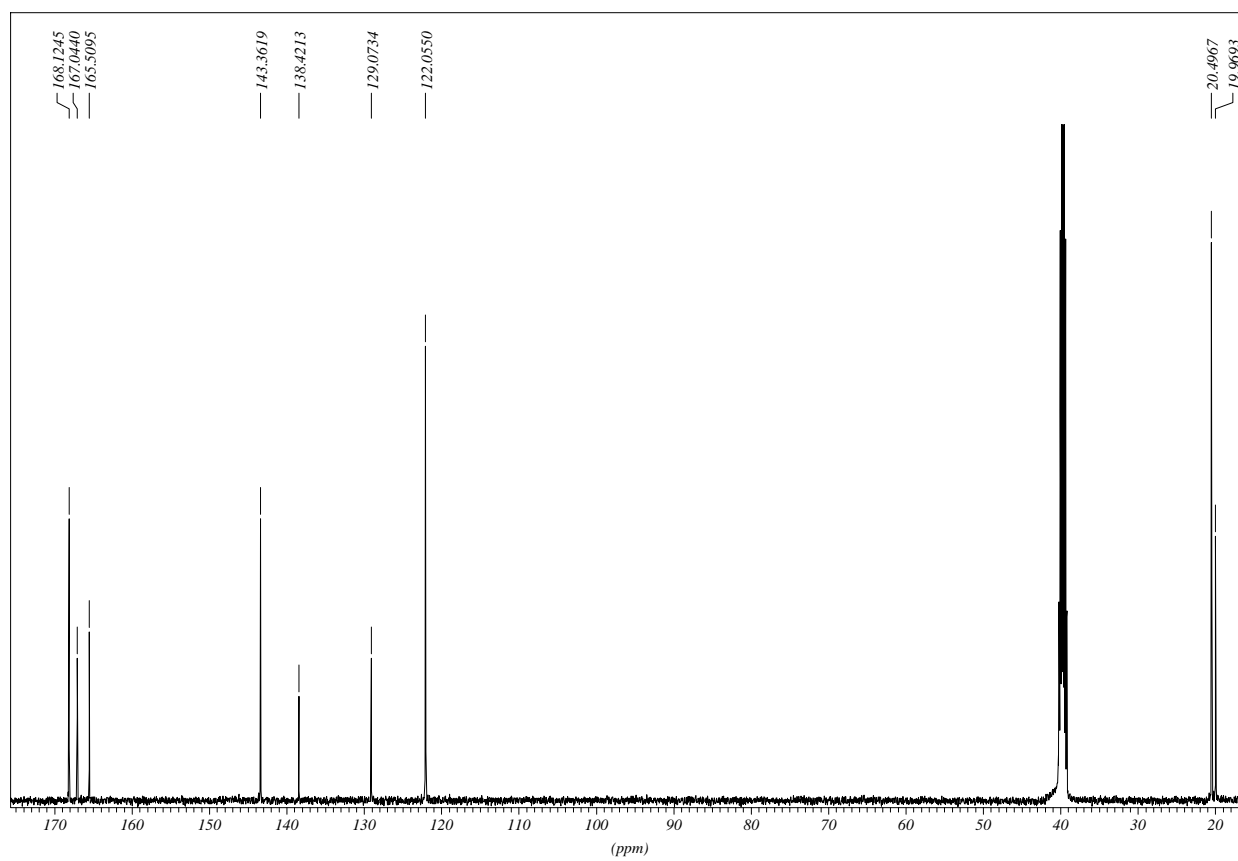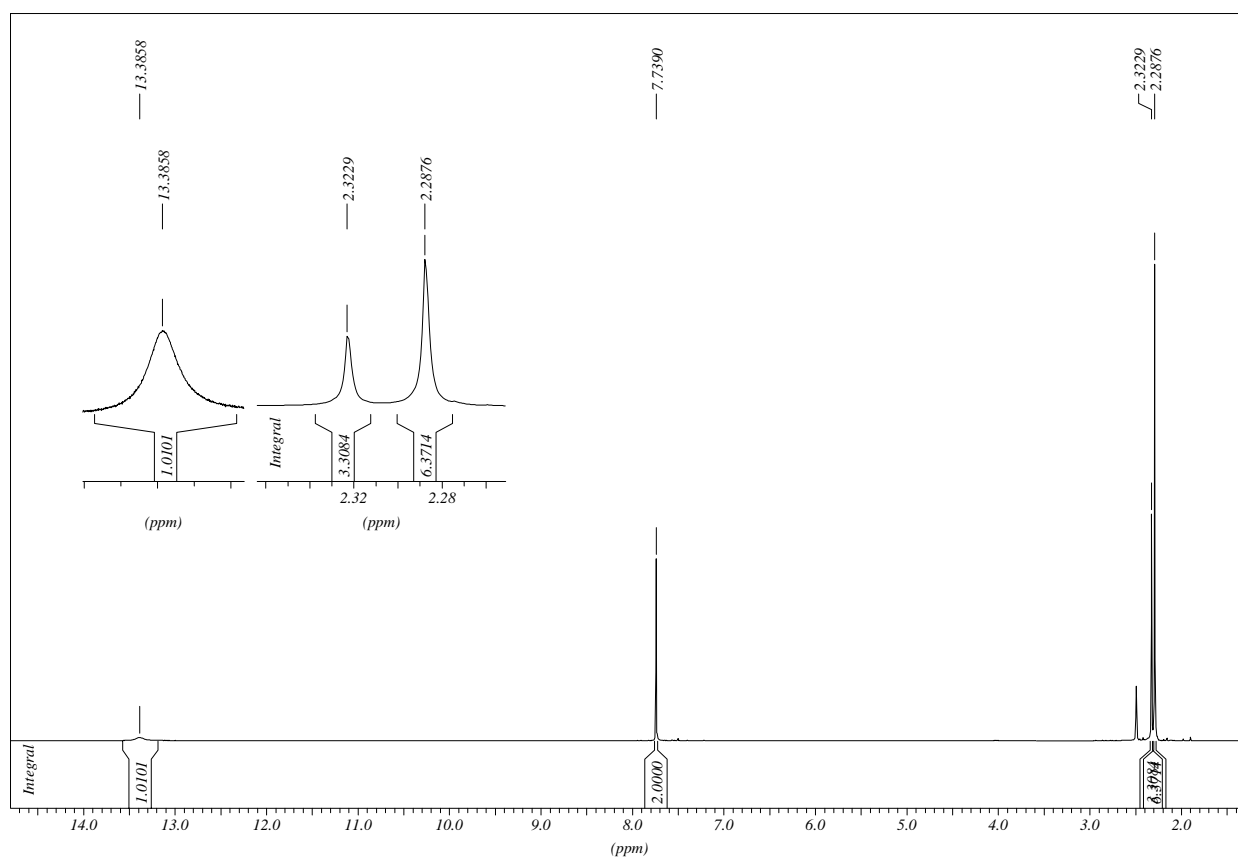
Ethyl 6-((4-benzyloxy-3,5-dihydroxybenzoyl)amino)hexanoate
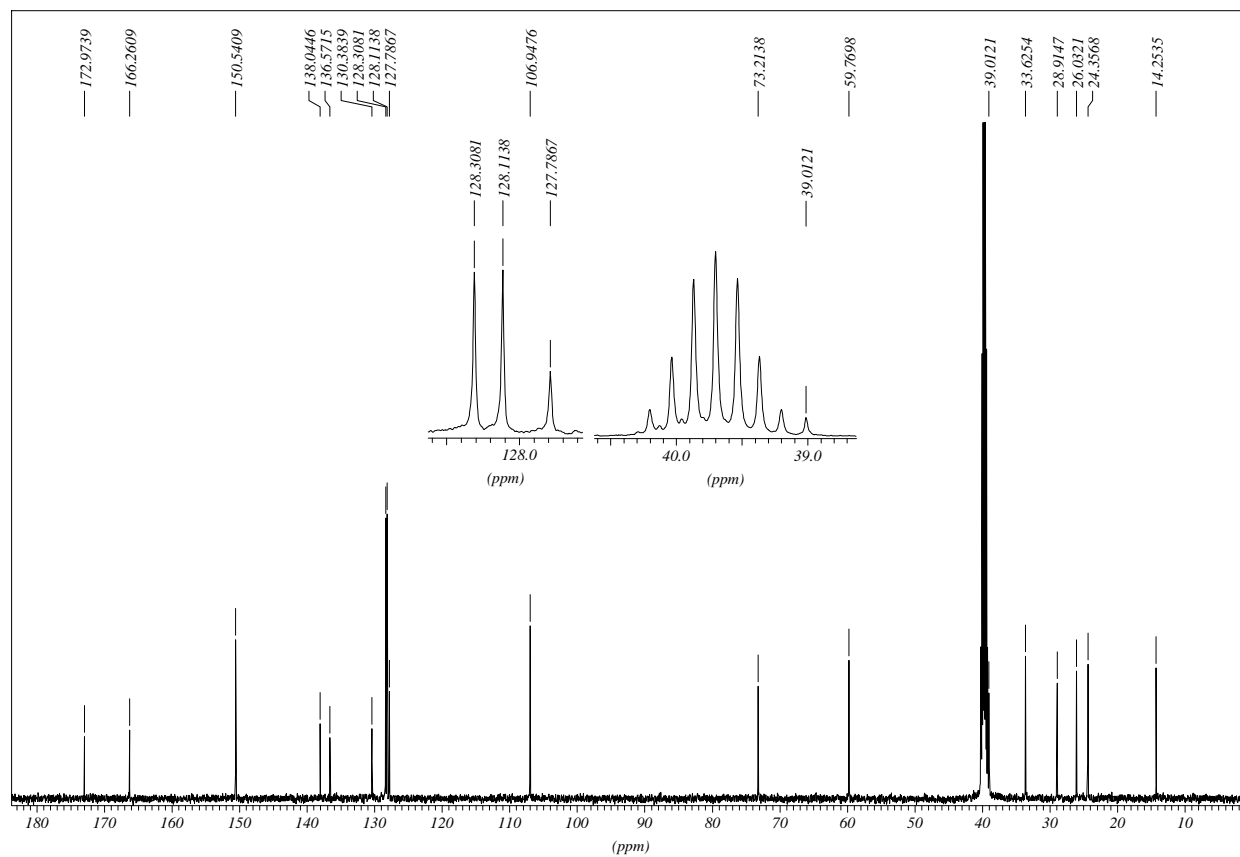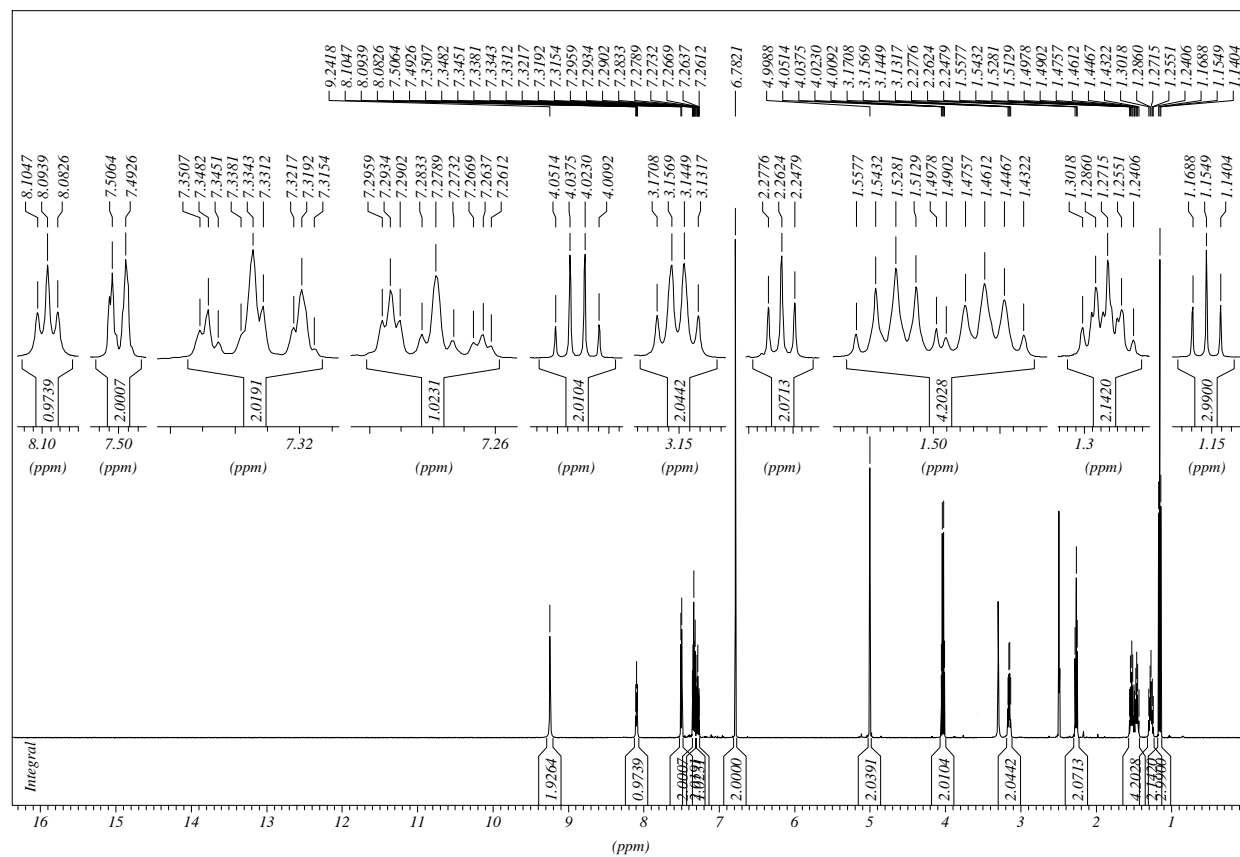
Ethyl 6-((4-benzyloxy-3,5-bis-(2-bromoethoxy)benzoyl)amino)hexanoate
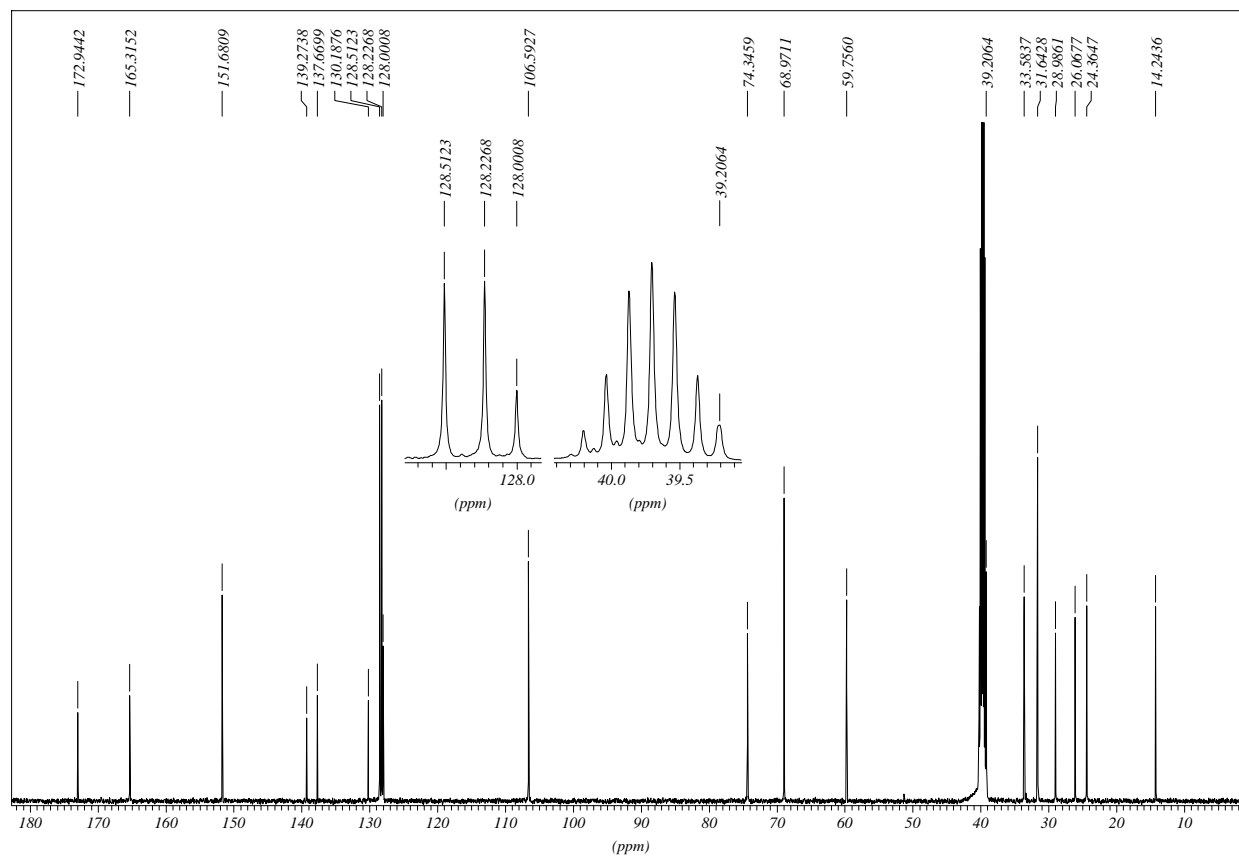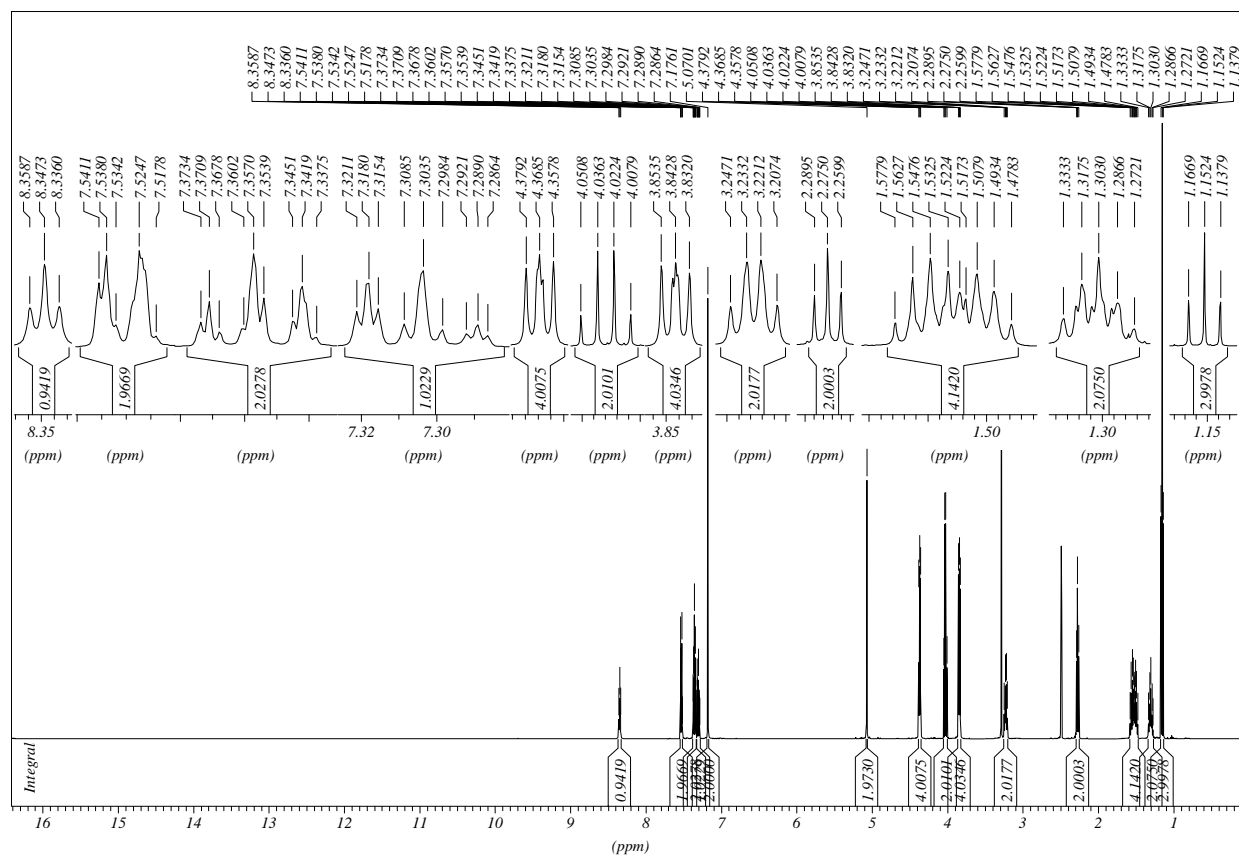
2-(5-(((6-Ethoxy-6-oxohexyl)amino)carbonyl)-2-(2-bromoethoxy)-3-((2-triethylammonio)-ethoxy)phenoxy)-*N,N,N*-triethylethanaminium dibromide
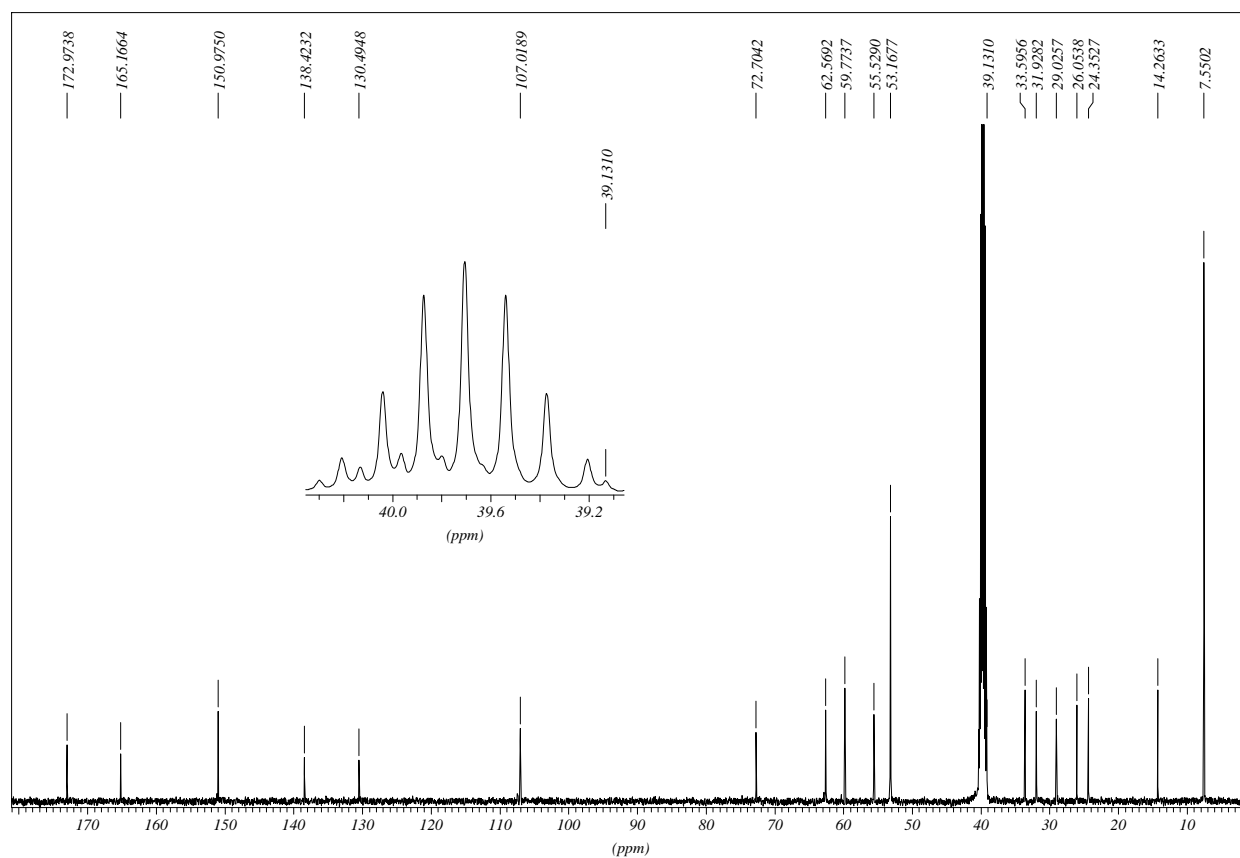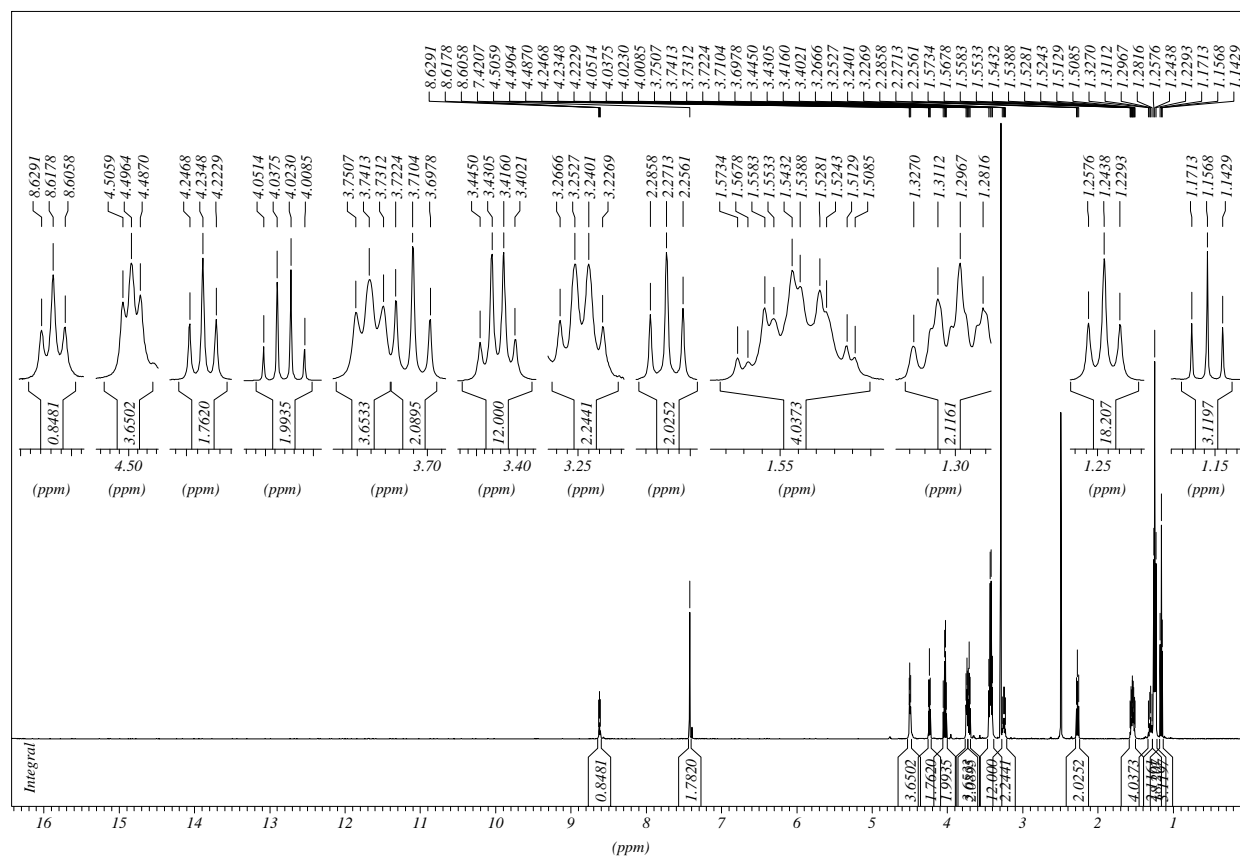
2-(5-(((6-Ethoxy-6-oxohexyl)amino)carbonyl)-2,3-bis((2-triethylammonio)ethoxy)phenoxy)-*N,N,N*-triethylethanaminium tribromide
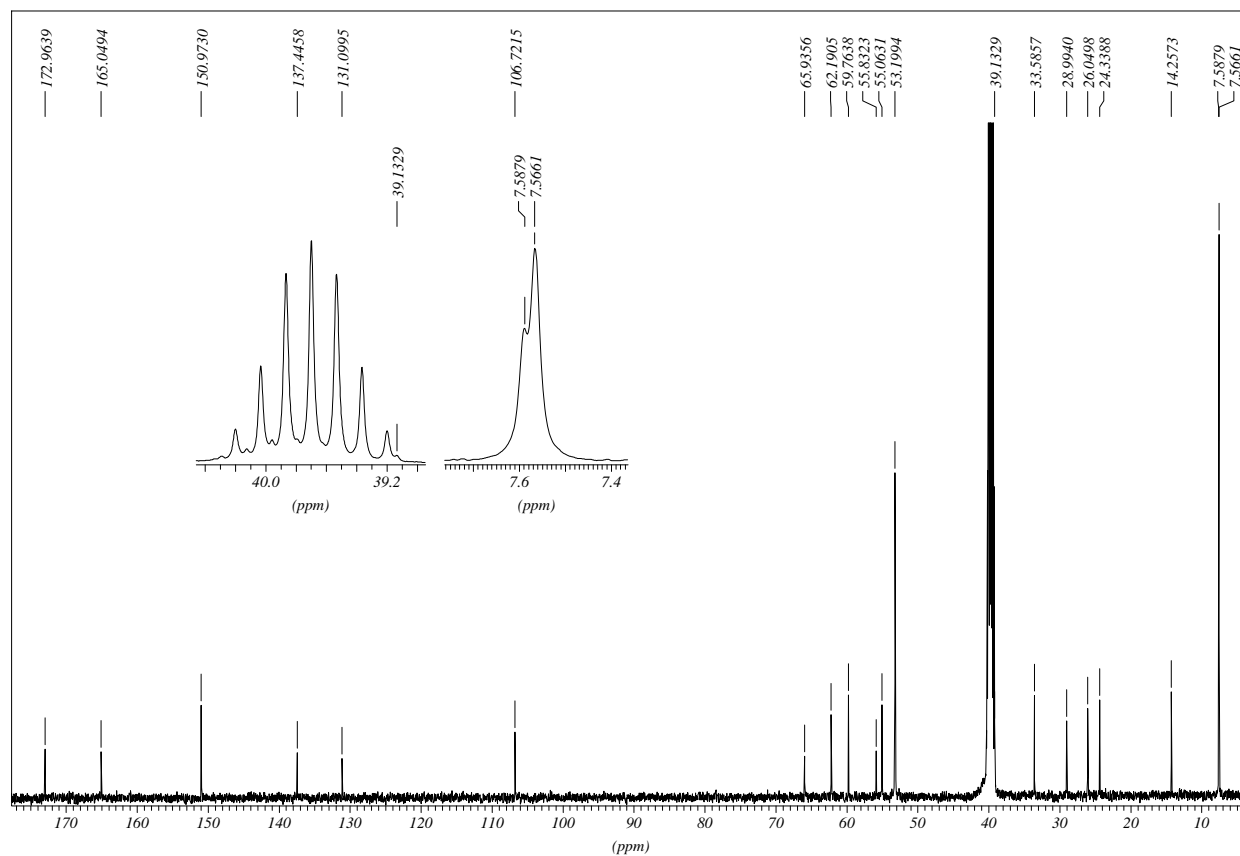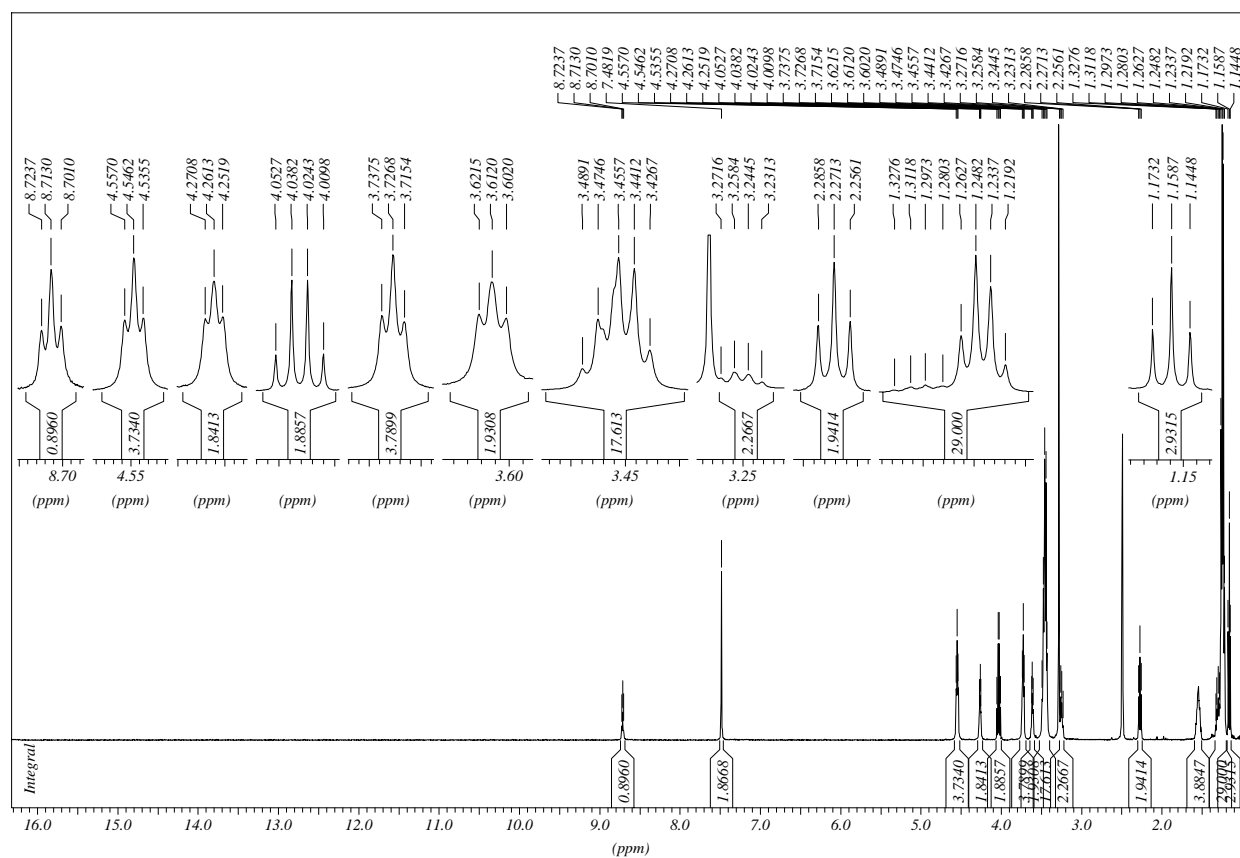
N,N,N-Triethyl-2-(5-(((6-hydrazino-6-oxohexyl)amino)carbonyl)-2,3-bis((2-triethylammonio)-ethoxy)phenoxy)ethanaminium tribromide
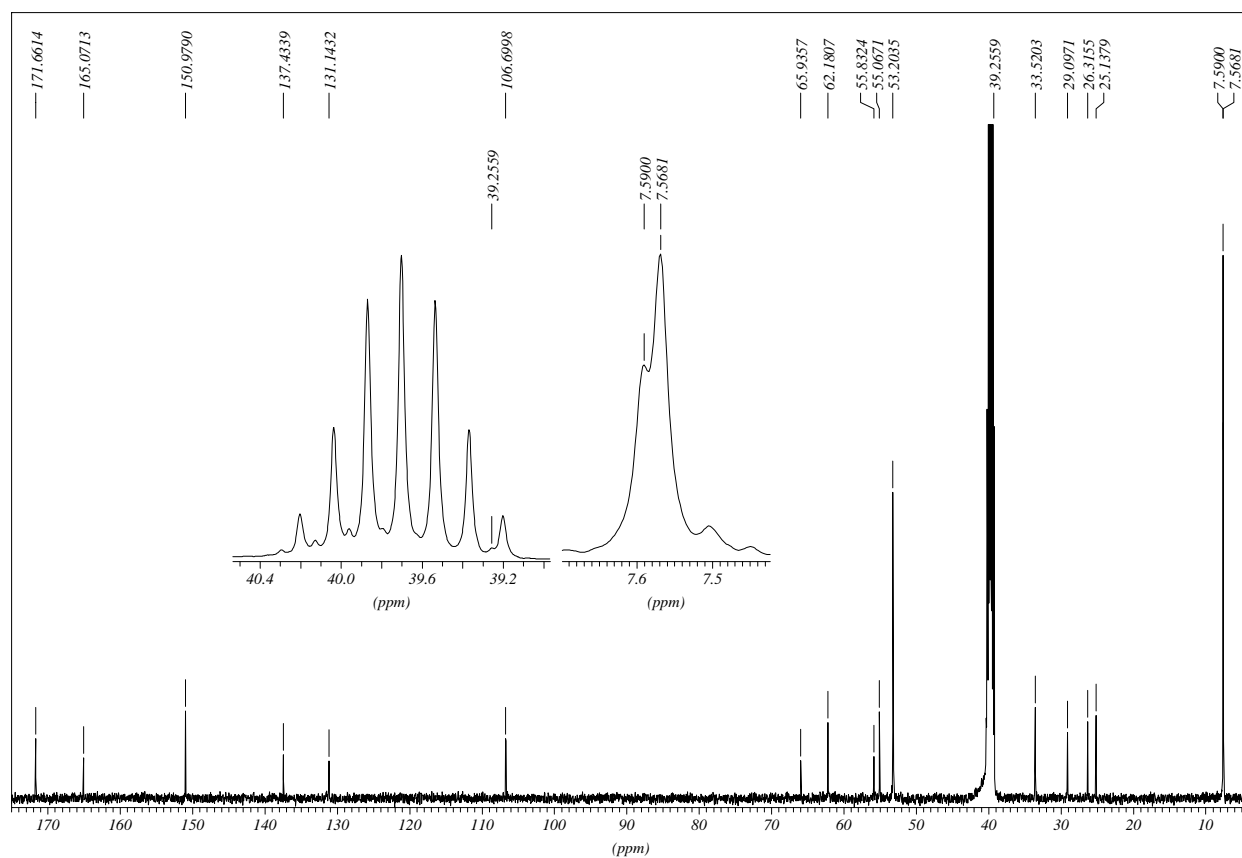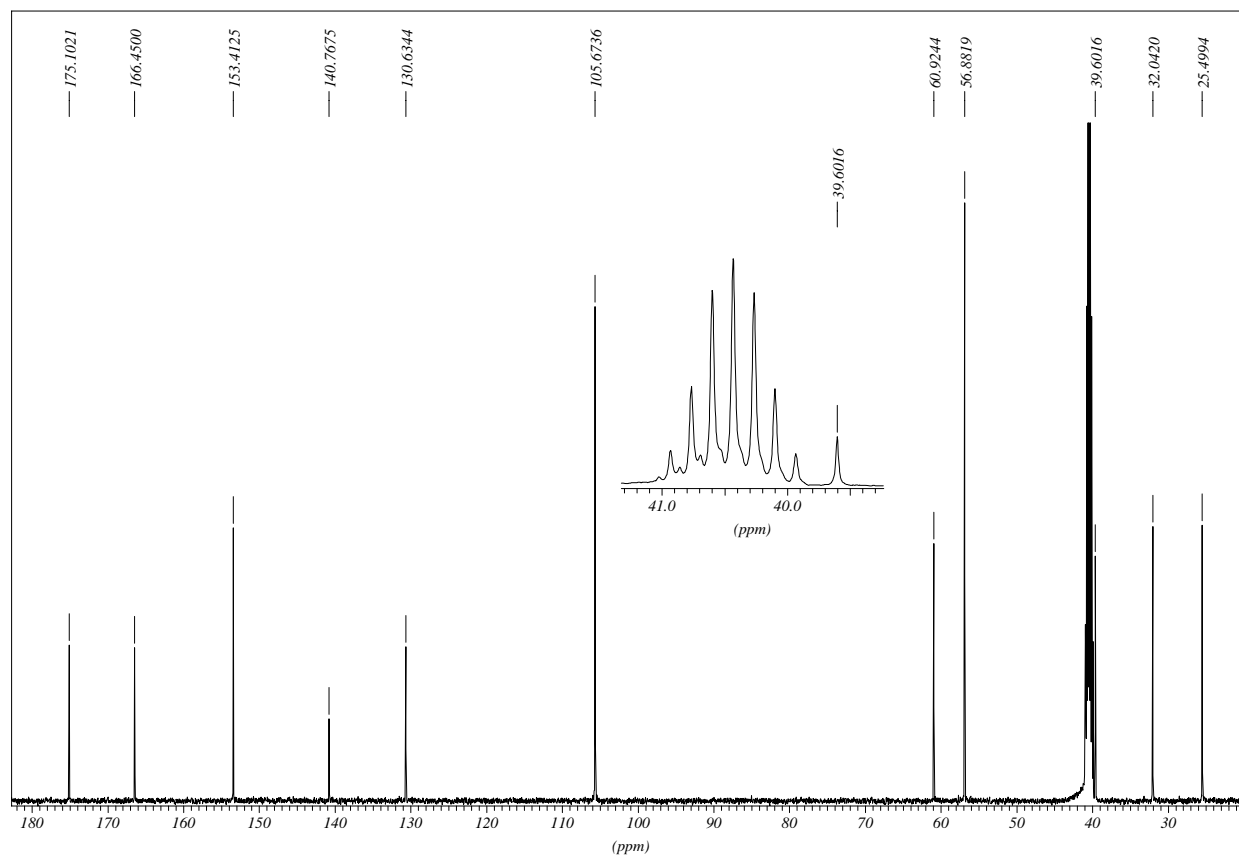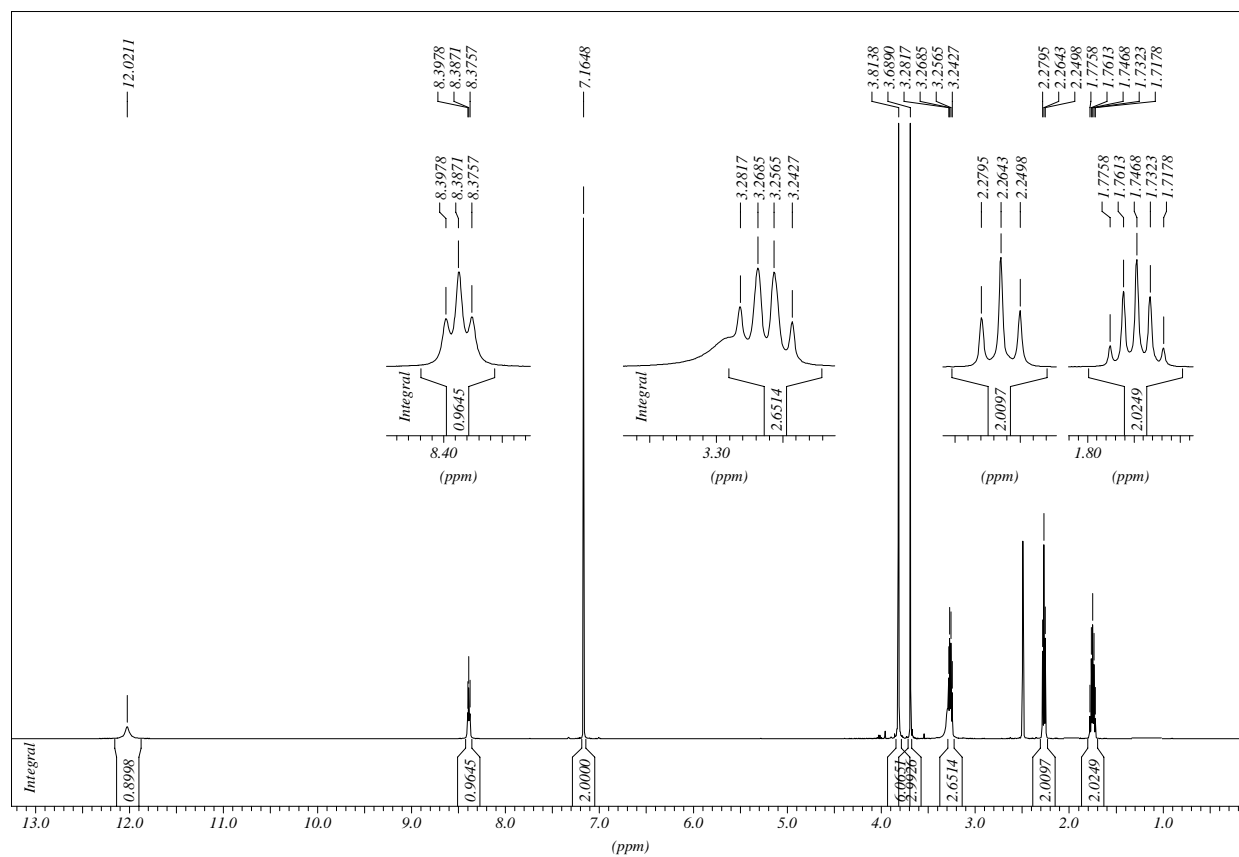
N,N,N-Triethyl-2-(5-(((6-(2-(1,2,3,4-tetrahydroacridin-9-yl)hydrazino)-6-oxohexyl)amino)-carbonyl)-2,3-bis((2-triethylammonio)ethoxy)phenoxy)ethanaminium tribromide HCl
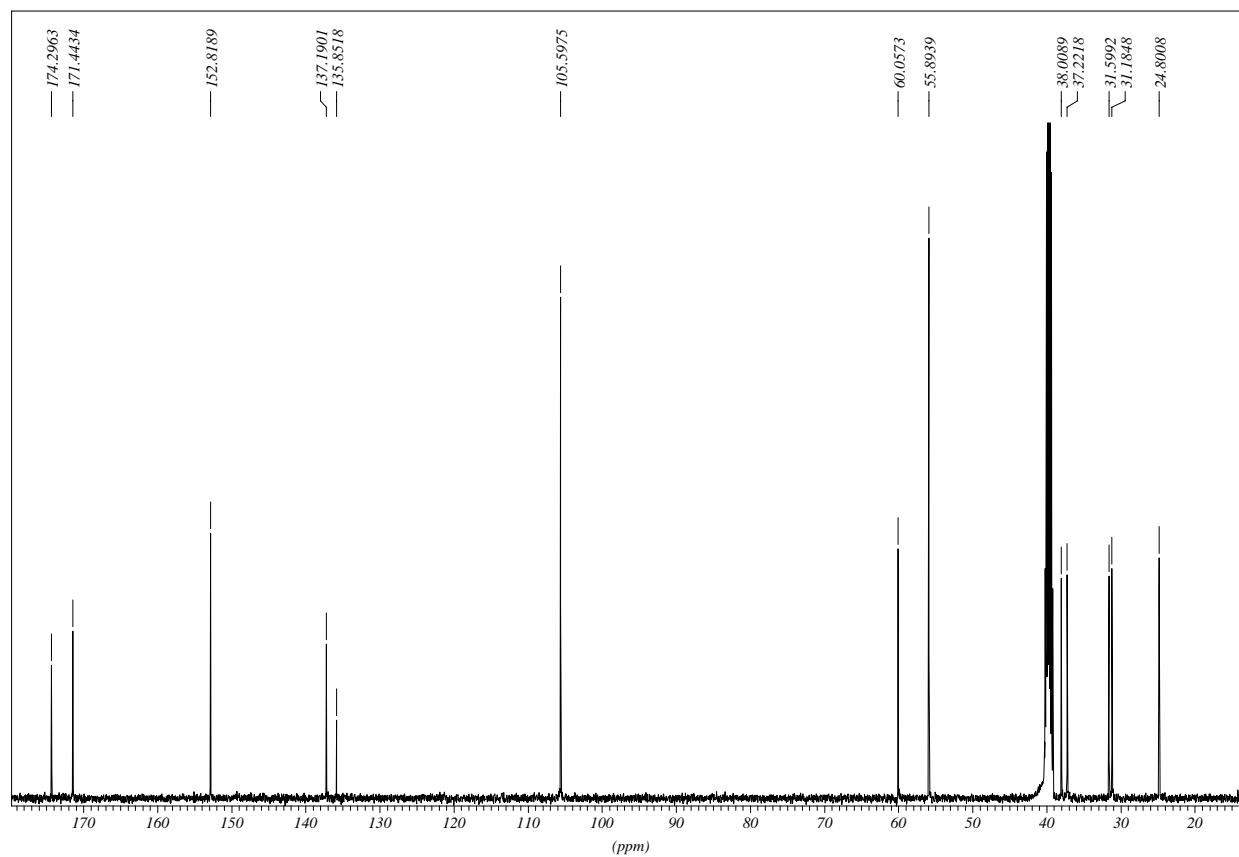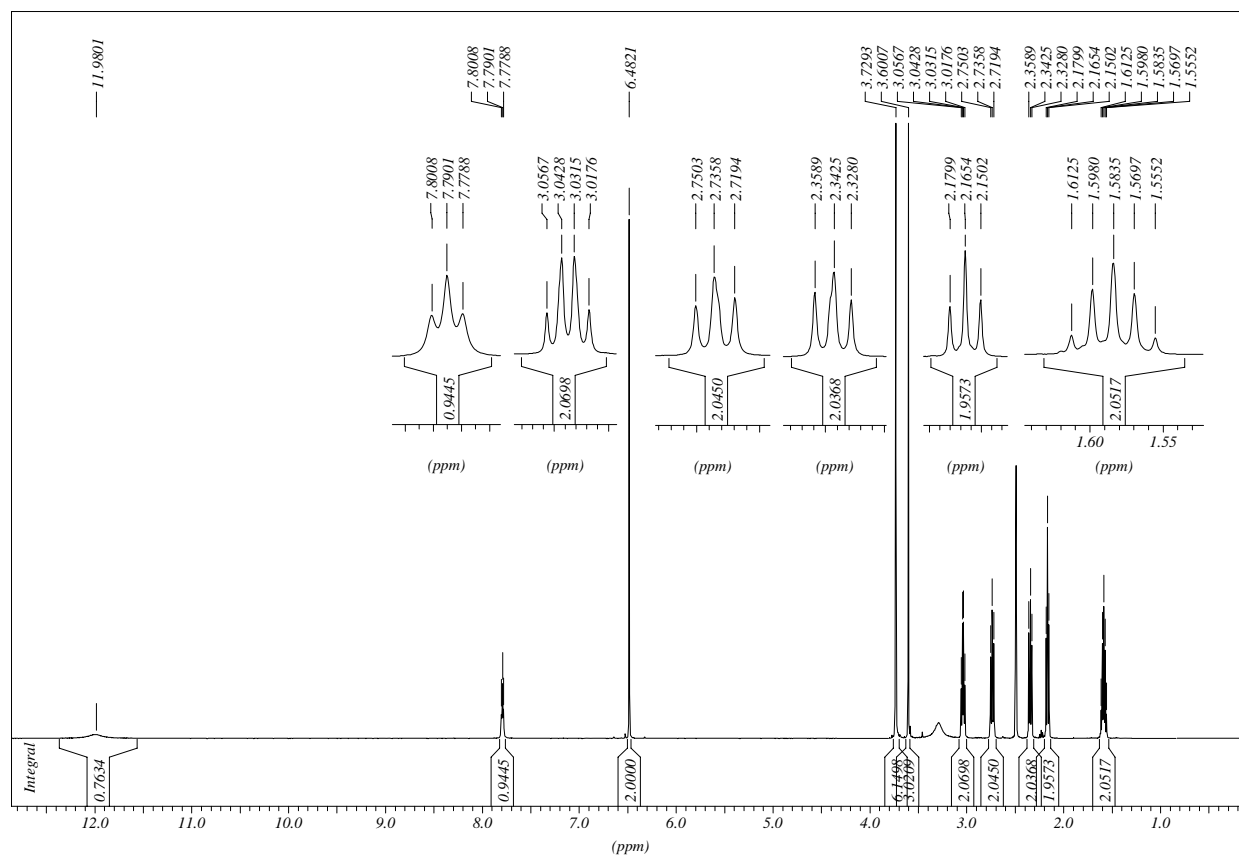
2-(5-(((6-(2-(6-Chloro-1,2,3,4-tetrahydroacridin-9-yl)hydrazino)-6-oxohexyl)amino)carbonyl)-2,3-bis((2-triethylammonio)ethoxy)phenoxy)-*N,N,N*-triethylethanaminium tribromide HCl
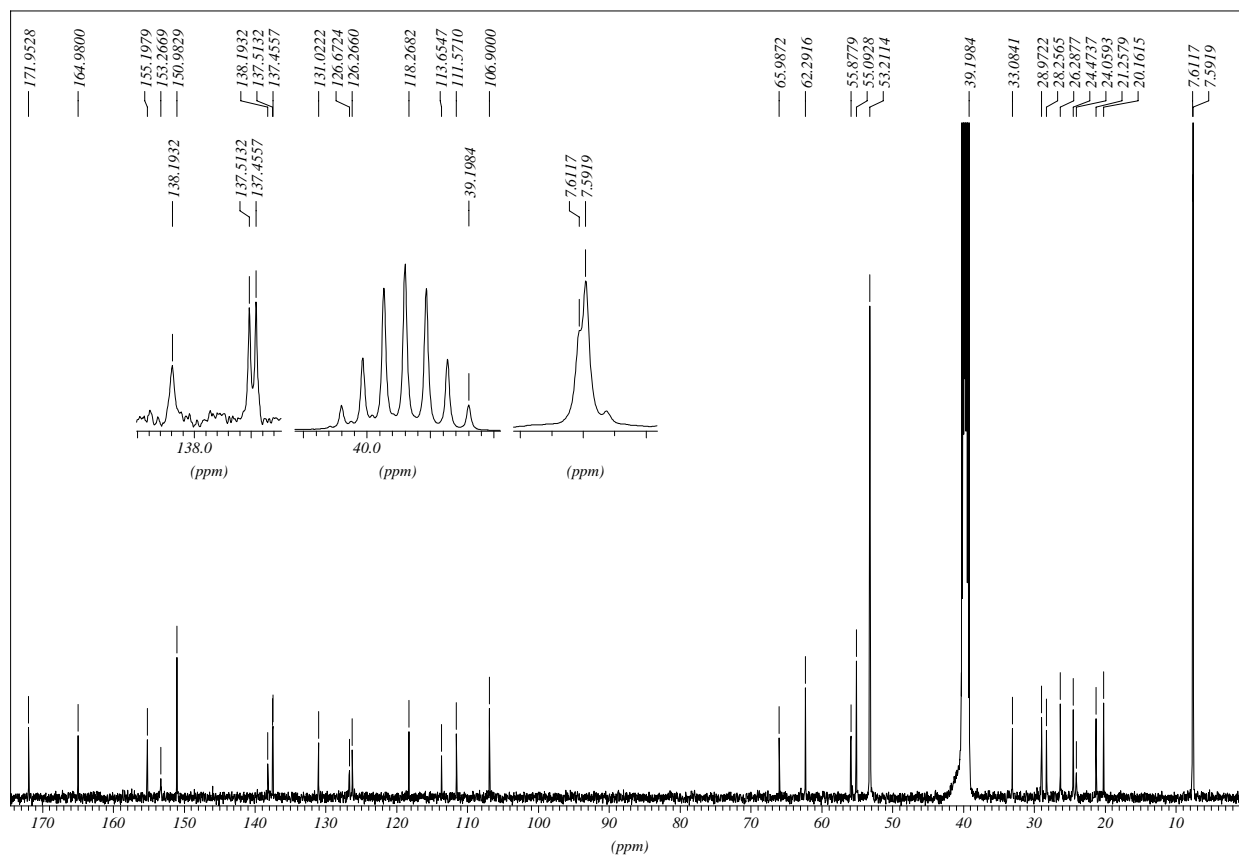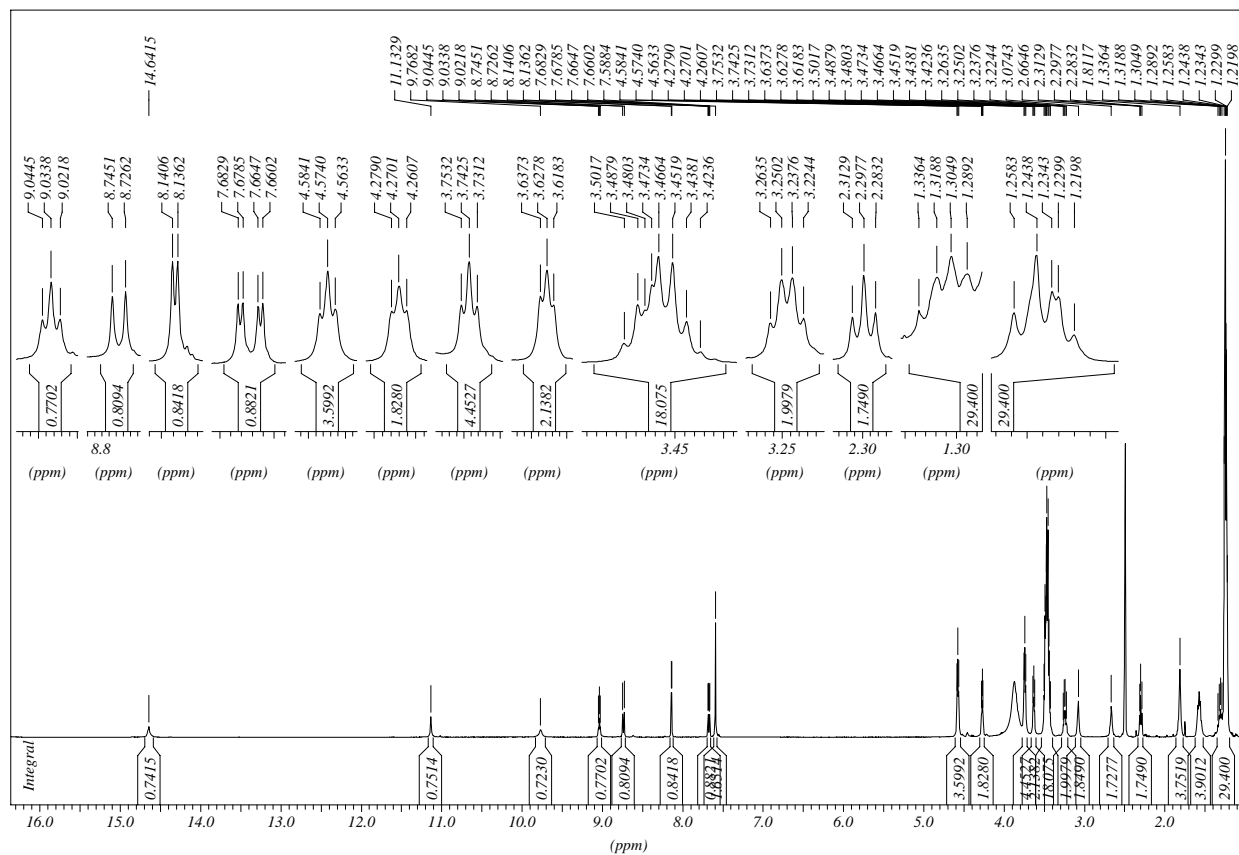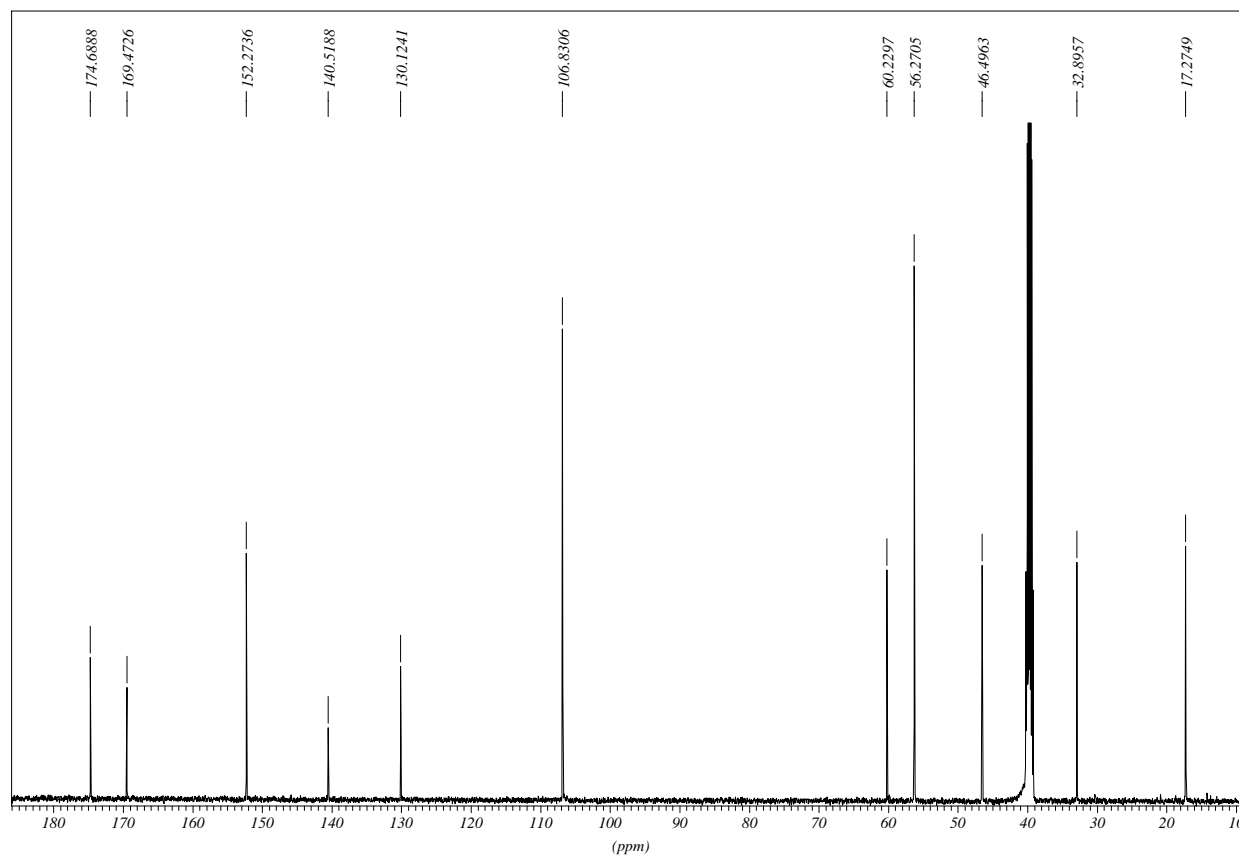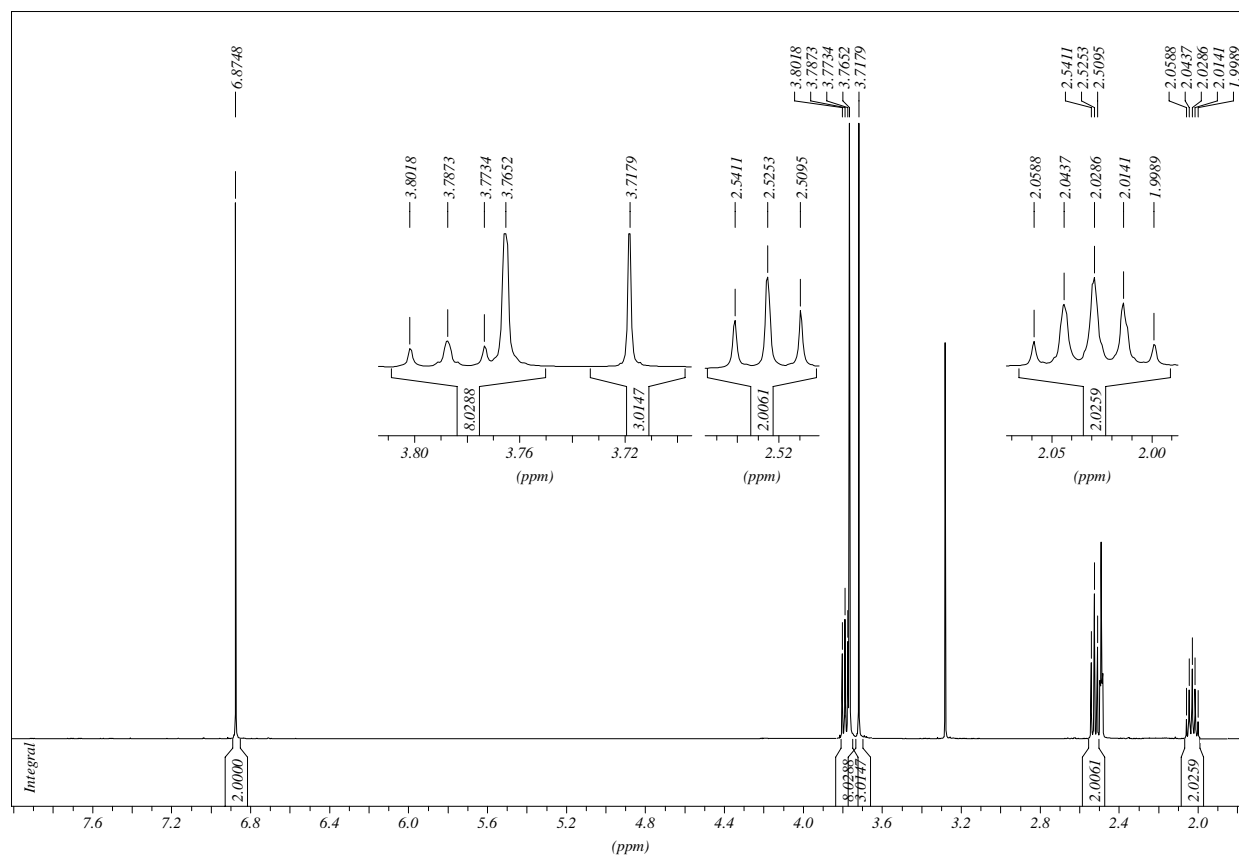
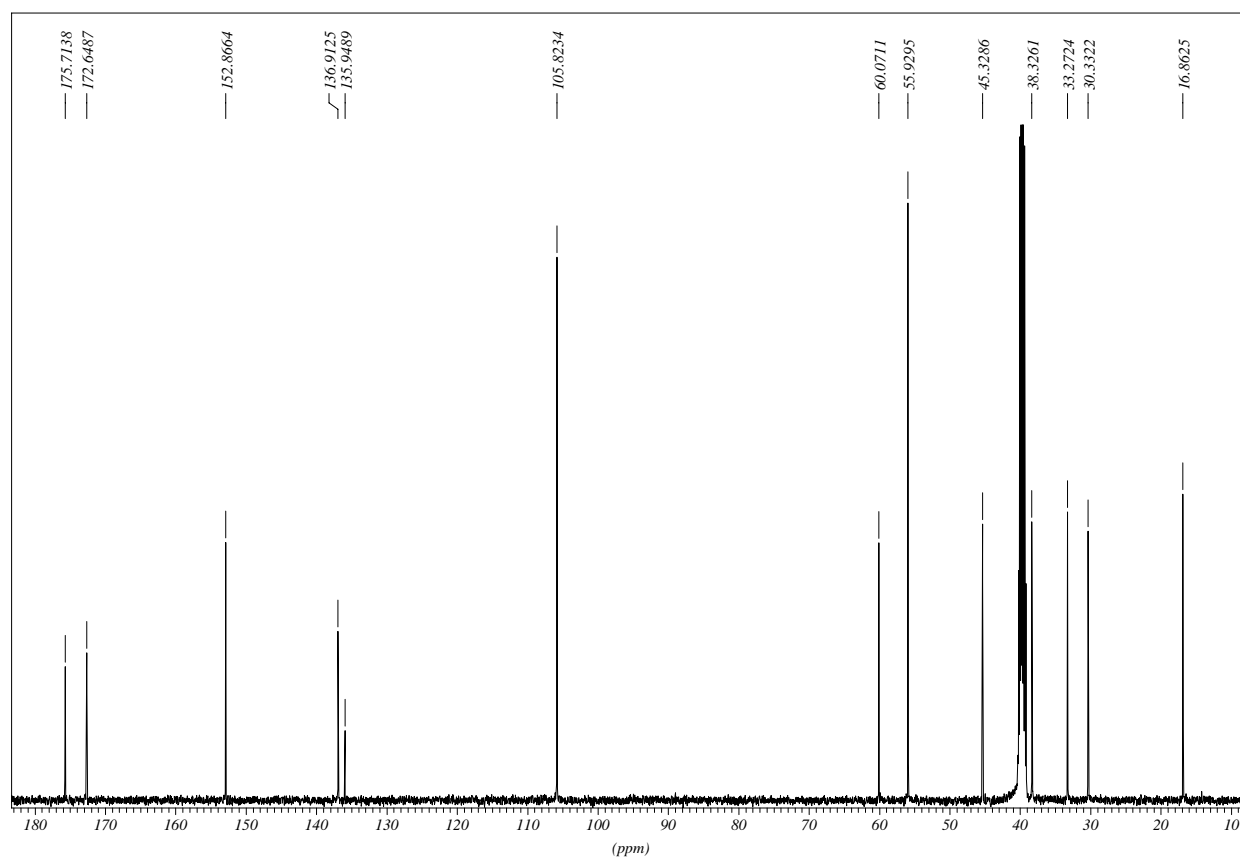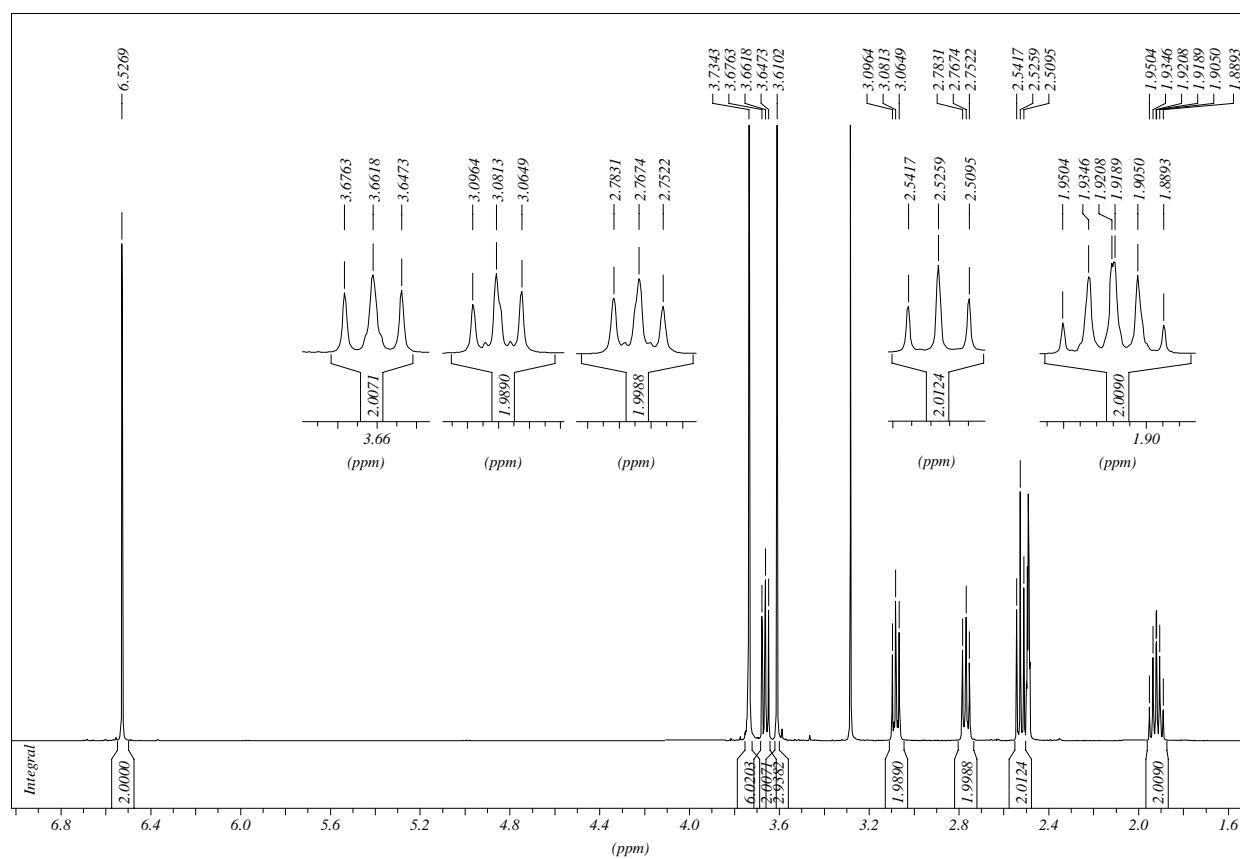# 4-((3,4,5-Trimethoxybenzoyl)amino)butanoic acid

4-((3-(3,4,5-Trimethoxyphenyl)propanoyl)amino)butanoic acid

^{1}H NMR spectrum

Peaks: 11.9801; 7.8008, 7.7901, 7.7788; 6.4821; 3.7293, 3.6007, 3.0567, 3.0428, 3.0315, 3.0176, 2.7503, 2.7358, 2.7194; 2.3589, 2.3425, 2.3280, 2.1799, 2.1654, 2.1502, 1.6125, 1.5980, 1.5835, 1.5697, 1.5552

Insets (ppm): 7.8008, 7.7901, 7.7788 — 0.9445; 3.0567, 3.0428, 3.0315, 3.0176 — 2.0698; 2.7503, 2.7358, 2.7194 — 2.0450; 2.3589, 2.3425, 2.3280 — 2.0368; 2.1799, 2.1654, 2.1502 — 1.9573; 1.6125, 1.5980, 1.5835, 1.5697, 1.5552 — 2.0517

Integral: 0.7634; 0.9445; 2.0000; 2.0698; 2.0450; 2.0368; 1.9573; 2.0517

^{13}C NMR spectrum

Peaks: 174.2963, 171.4434; 152.8189; 137.1901, 135.8518; 105.5975; 60.0573; 55.8939; 38.0089, 37.2218; 31.5902, 31.1848; 24.8008

1-(3,4,5-Trimethoxybenzoyl)pyrrolidin-2-one

1-(3-(3,4,5-Trimethoxyphenyl)propanoyl)pyrrolidin-2-one

Methyl 8-(2-bromoethoxy)-2,3-dihydrobenzo[*b*][1,4]dioxine-6-carboxylate